NISTIR 8271 DRAFT SUPPLEMENT

Face Recognition Vendor Test (FRVT)

Part 2: Identification

Patrick Grother
Mei Ngan
Kayee Hanaoka
Information Access Division
Information Technology Laboratory

This document is a draft supplement of NIST Interagency Report 8271

2020/02/26

National Institute of Standards and Technology
U.S. Department of Commerce

NISTIR 8271 DRAFT SUPPLEMENT

Face Recognition Vendor Test (FRVT)

Part 2: Identification

Patrick Grother
Mei Ngan
Kayee Hanaoka
Information Access Division
Information Technology Laboratory

This document is a draft supplement of NIST Interagency Report 8271

January 2020

U.S. Department of Commerce
Wilbur Ross, Secretary

National Institute of Standards and Technology
Walter Copan, Director

DISCLAIMER

Specific hardware and software products identified in this report were used in order to perform the evaluations described in this document. In no case does identification of any commercial product, trade name, or vendor, imply recommendation or endorsement by the National Institute of Standards and Technology, nor does it imply that the products and equipment identified are necessarily the best available for the purpose.

INSTITUTIONAL REVIEW BOARD

The National Institute of Standards and Technology's Research Protections Office reviewed the protocol for this project and determined it is not human subjects research as defined in Department of Commerce Regulations, 15 CFR 27, also known as the Common Rule for the Protection of Human Subjects (45 CFR 46, Subpart A).

Executive Summary

This report supplements the September 2019 report NIST Interagency Report 8271 that, in turn, replaced the NIST Interagency Report 8238. **This report adds partial results for algorithms submitted to NIST since those reports were prepared. This report will be updated on an approximately monthly basis with results from newly submitted algorithms. It will additionally be updated with results currently being computed in ongoing recognition tests, and with new results and analyses.**

The algorithms, which implement one-to-many identification of faces appearing in two-dimensional images, are prototypes from the research and development laboratories of mostly commercial suppliers, and are submitted to NIST as compiled black-box libraries implementing a NIST-specified C++ test interface. The report therefore does not describe how algorithms operate.

The evaluation used three datasets - frontal mugshots, profile views, and webcam photos - and the report lists accuracy results alongside developer names. It will therefore be useful for comparison of face recognition algorithms and assessment of absolute capability. The primary dataset is comprised of 26.6 million reasonably well-controlled live portrait photos of 12.3 million individuals. The three smaller datasets contain more unconstrained photos: 3.2 million webcam images; and 200 thousand side-view images. NIST Interagency Report 8271 includes results also for 2.5 million photojournalism and amateur photographer photos. These datasets are sequestered at NIST, meaning that developers do not have access to them for training or testing. The last dataset, however, consists of images drawn from the internet for testing purposes so while it is not truly sequestered, its composition is unknown to the developers.

The major result in NIST IRs 8238 and 8271 was that massive gains in accuracy have been achieved in the years 2013 to 2018 and these far exceed improvements made in the prior period, 2010 to 2013. While the industry gains were broad - at least 30 developers' algorithms outperformed the most accurate algorithm from late 2013 - there remains a wide range of capability. While this report shows accuracy gains only over the course of 2018, the most accurate algorithm reported here is substantially more accurate than anything reported in NIST IR 8238. This is evidence that face recognition development continues apace, and that FRVT reports are but a snapshot of contemporary capability.

From discussion with developers, the accuracy gains stem from the adoption of deep convolutional neural networks. As such, face recognition has undergone an industrial revolution, with algorithms increasingly tolerant of poorly illuminated and other low quality images, and poorly posed subjects. One related result is that a few algorithms correctly match side-view photographs to galleries of frontal photos, with search accuracy approaching that of the best c. 2010 algorithms executing frontal-frontal search. The capability to recognize under a 90-degree change in viewpoint - pose invariance - has been a long-sought milestone in face recognition research.

With good quality portrait photos, the most accurate algorithms will find matching entries, when present, in galleries containing 12 million individuals, with rank one miss rates of approaching 0.1%. The remaining errors are in large part attributable to long-run ageing, facial injury and poor image quality. Given this impressive achievement - close to perfect recognition - an advocate might claim that frontal face recognition is a solved problem, a statement that should be refuted with the following context and caveats:

- **Algorithm accuracy spectrum:** Many algorithms do not achieve the low error rates tabulated above, and while many of those may still be useful and valuable to end-users, only the most accurate excel on poor quality images and those collected long after the initial enrollment sample.

- **Versioning:** While results for up to seven algorithms from each developer are reported here, the intra-provider accuracy variations are usually smaller than the inter-provider variations. That said different versions give order of magnitude fewer misses. Some developers demonstrate speed-accuracy tradeoffs[1]. See Figs. 16, 17.

[1] NEC-0 prepares templates much faster than NEC-2 but gives twenty times more misses. Dermalog-5 executes a template search much more quickly than Dermalog-6 but is also much less accurate.

- ▷ **Quality:** The low error rates here are attained using mostly excellent cooperative live-capture mugshot images collected with an attendant present. Recognition in other circumstances, particularly those without a dedicated photographic environment and human or automated quality control checks, will lead to declines in accuracy. This is documented here for poorer quality webcam images and unconstrained "wild" images.

- ▷ **Low similarity scores:** In thousands of cases the correct gallery image is returned at rank 1 but its similarity score is nevertheless low, below some operationally required score threshold. This does not matter when face recognition is used for "lead generation" in investigational applications because human reviewers are specifically required to review potentially long candidate lists and the threshold is effectively 0. In applications where search volumes are higher and labor is not available to review the results from searches, a higher threshold can be applied. This reduces the length of candidate lists and false positive identification rates at the expense of increased false negative miss rates. The tradeoff between the two error rates is reported extensively later.

- ▷ **Population size:** As the number of enrolled subjects grows, some mates are displaced from rank one, decreasing accuracy. As tabulated later for N up to 12 million, false negative rates generally rise slowly with population size.

- ▷ **Database integrity:** An operational error rate should be added to all false negative rates in this report reflecting the proportion of images in a real database that are un-matchable. Such anomalies arise from images that: do not contain a face; include multiple persons; cannot be decoded; are rotated by 90° or 180°; depict a face on clothing; and others introduced by a long tail of various clerical errors. While the mugshot trials in this report have been constructed to minimize such effects, they are a real problem in actual operations.

Recognition accuracy is very strongly dependent on the algorithm and, more generally, on the developer of the algorithm. False negative error rates in a particular scenario range from a few tenths of one percent to beyond fifty percent. This is tabulated exhaustively later: For example Table 24 shows accuracy across datasets. Figure 1 here compares algorithms on mugshot searches in a consolidated gallery of 12 million subjects and 26.1 million photos. In positive or negative identification applications, a score threshold is set to limit the rate at which non-mate searches produce false positives. This has the consequence that some mated searches will report the mate below threshold, i.e. a miss, even if it is at rank 1. The utility of this is that many non-mated searches will usually not return any candidate identities at all. As the figure error-tradeoff characteristic shows, investigational miss rates on the right side are very low but then rise steadily (in the center region) as threshold is increased to support "lights-out" applications, and ultimately rise quickly (left side) as discussed below. Thus, if we demand that just one in one thousand non-mate searches produce any false positives, the most accurate algorithms there (Sensetime-003 and NEC-3) would fail on between 4 and 7% of mated searches. Even though the graph shows results for the most accurate algorithms, all but two would fail to find the mate in more than 10% of mated searches. While the NEC algorithm produces a relatively flat error tradeoff until the threshold is raised to limit false positives to about 1 in 400 non-mated searches[2]

Thereafter, as the threshold is raised to further reduce false positives, miss rates rise rapidly. This means that low false positive identification rates are inaccesible with these algorithms, a result that does not apply for ten-finger identification algorithms. The rapid rise occurs because the lower mate scores are mixed with very high non-mate scores, the low scores from poor image quality and ageing, the high non-mates from the presence of lookalikes persons (doppelgangers), twins (discussed next) and, ultimately, the presence of a few unconsolidated subjects i.e. persons present under multiple IDs.

▷ **False positives from twins:** By enrolling 640 000 mugshots, adding photos of one twin, and then searching photos

[2] The gallery size here is 12 million people, 26.1 million images. Given 331 254 non-mated searches, an exhaustive implementation of one-too-many search would execute 8.6 trillion comparisons. At a false positive identification rate of 0.0025 the number of false positives is, to first order, 828 corresponding to single-comparison false match rate of 828 / 8.6 trillion = 9.6 10^{-11} i.e. about 1 in 10 billion. Strictly this FMR computation is meaningful only for algorithms that implement 1:N search using N 1:1 comparisons, which is not always the case.

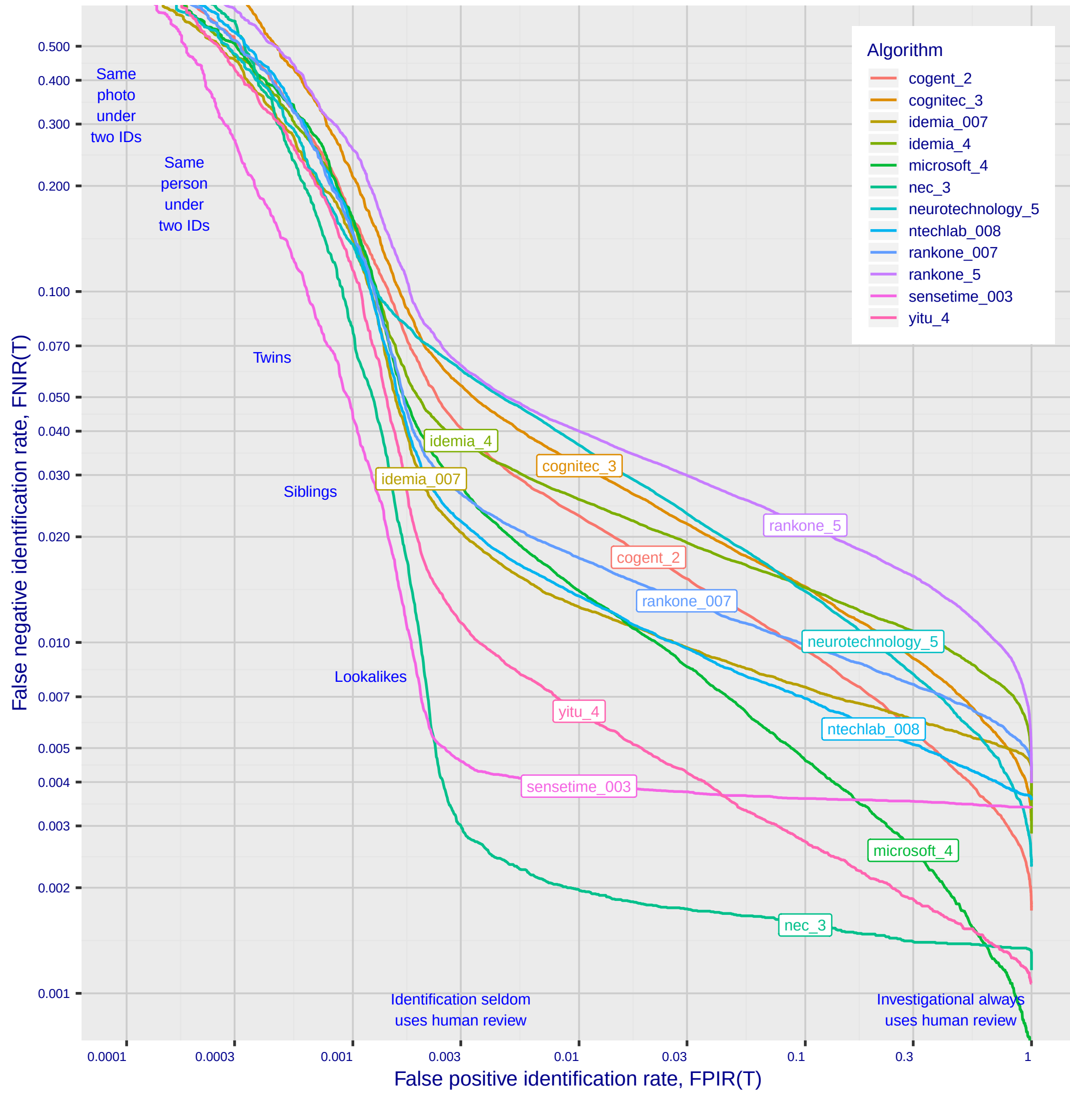

Figure 1: Identification Miss rates across the false positive range. N = 12 million individuals are enrolled with a total of 26.1 million images.

of those subjects and their twin the inset figure shows, for one typical algorithm, the similarity is generally greater when searching twins against themselves (A) than when searching twins against their sibling (B) but very often still above even stringent thresholds i.e. those corresponding to one in one thousand searches producing a false positive. Thus twins will very often produce a high-scoring non-match on a candidate list and a false alarm in an online identification system. The plot shows that some fraternal twins are correctly rejected at those thresholds - these are largely from different sex twins (at center). Figure 20 shows substantially similar behavior for all algorithms tested. In an investigative search, a twin would typically appear at rank 1, or rank 2 if their sibling happened to also be

Figure 2: Intra- and inter-twin scores

the gallery. Twins (and triplets etc.) constituted 3.3% of all live births [16] in recent years[3], and because that number is higher today than when the individuals in current adult databases were born, the false positives that arise from twins are now, and will increasingly be, an operational problem. Relative to the United States, twins are born with considerable regional variation. For example they are much less common in East Asia, and much more common in Sub-Saharan Africa [20]. The presence of twins in the mugshot database is inevitable given its size, around 12.3 million people. As this is not an insignificant sample of the domestic United States population, people with other familial ties will be present also. The data was collected over an extended period and because location information is not available, we are unable to estimate the proportion of the domestic population that is present in the dataset. However, if we assume twins are neither more or less disposed to arrest than the general population, we can estimate that hundreds of thousands of individuals in the dataset are twins. This will affect false positive rates because we randomly set aside 331 254 individuals for nonmate searches, and some proportion of those will be twins with siblings in the gallery.

From early 2020 this report is being updated continuously as new algorithms are submitted to FRVT, and run on new datasets. Participation in the one-to-many identification track requires a developer to first demonstrate high accuracy in the one-to-one verification track of FRVT.

[3]See the CDC's National Vital Statistics Report for 2017: https://www.cdc.gov/nchs/data/nvsr/nvsr67/nvsr67_08-508.pdf

Scope and Context

Audience: This report is intended for developers, integrators, end users, policy makers and others who have some familiarity with biometrics applications. The methods and metrics documented here will be of interest to organizations engaged in tests of face recognition algorithms. Some of these have been incorporated in the ISO/IEC 19795 Part 1 Biometric Testing and Reporting Framework standard, now under revision.

Prior benchmarks: Automated face recognition accuracy has improved massively in the two decades since initial commercialization of the various technologies. NIST has tracked that improvement through its conduct of regular independent, free, open, and public evaluations. These have fostered improvements in the state of the art. This report serves as an update to the NIST Interagency Report 8271 on performance of face identification algorithms, published in September 2019.

Demographics: In December 2019, NIST published a first report on demographic dependencies in face recognition, NIST Interagency Report 8280 that documented age, sex and race differentials in one-to-one and one-to-many false positive and false negative rates.

Scope: NIST IR 8271 documented recognition results for four databases containing in excess of 30.2 million still photographs of 14.4 million individuals. That constituted the largest public and independent evaluation of face recognition ever conducted. It includes results for accuracy, speed, investigative vs. identification applications, scalability to large populations, use of multiple images per person, images of cooperative and non-cooperative subjects.

The report also includes results for ageing, recognition of twins, and recognition of profile-view images against frontal galleries. It otherwise does not address causes of recognition failure, neither image-specific problems nor subject-specific factors including demographics. Separate reports on demographic dependencies in face recognition will be published in the future. Additionally out of scope are: performance of live human-in-the-loop transactional systems like automated border control gates; human recognition accuracy as used in forensic applications; and recognition of persons in video sequences (which NIST evaluated separately [8]). Some of those applications share core matching technologies that *are* tested in this report.

Images: Three kinds of images are employed. The primary dataset is a set of law enforcement mugshot images (Fig. 3) which are enrolled and then searched with three kinds of images: 1) other mugshots (i.e. within-domain); 2) profile-view photographs (90 degree cross-view); 3) lower quality webcam images (Fig. 4) collected in similar detention operations (cross-domain);

Participation and industry coverage: The report includes performance figures for prototype algorithms from the research laboratories of commercial developers and a few universities. This represents a substantial majority of the face recognition industry, but only a tiny minority of the academic community. Participation was open worldwide. While there is no charge for participation, developers incur some software engineering expense in implementing their algorithms behind the NIST application programming interface (API). The test is a black-box test where the function of the algorithm, and the intellectual property associated with it, is hidden inside pre-compiled libraries.

Recent technology development: Most face recognition research with deep convolutional neural networks (CNNs) has been aimed at achieving invariance to pose, illumination and expression variations that characterize photojournalism and social media images. The initial research [17, 21] employed large numbers of images of relatively few ($\sim 10^4$) individuals to learn invariance. Inevitably much larger populations ($\sim 10^7$) were employed for training [10, 19] but the benchmark, Labeled Faces in the Wild with (essentially) an equal error rate metric [11], represents an easy task, one-to-one verification at very high false match rates. While a larger scale identification benchmark duly followed, Megaface [14], its primary metric, rank one hit rate, contrasts with the high threshold discrimination task required in most large-population applications of face recognition, namely credential de-duplication, and background checks. There, identification in galleries containing up to 10^8 individuals must be performed using a) very few images per individual and b) stringent thresholds to afford very low false positive identification rates. This track of FRVT was launched to measure the capability of the new technologies, including in these two cases. FRVT has included open-set identification tests since 2002, reporting both false negative and positive identification rates [6].

Performance metrics for applications: This report documents the performance of one-to-many face recognition algorithms. The word ”performance” here refers to recognition accuracy and computational resource usage, as measured by executing those algorithms on massive sequestered datasets.

This report includes extensive tabulation of recognition error rates germane to the main use-cases for face search technology. The Figure below, inspired by the Figure 1 in [22] differentiates different applications of the technolgy. The last row directs readers to the main tables relevant to those applications, respectively threshold-based and rank-based metrics that are special cases of the metrics given in section 3. The terms negative identification and positive identification are taken from the ISO/IEC 2382-37:2017 standardized biometrics vocabulary.

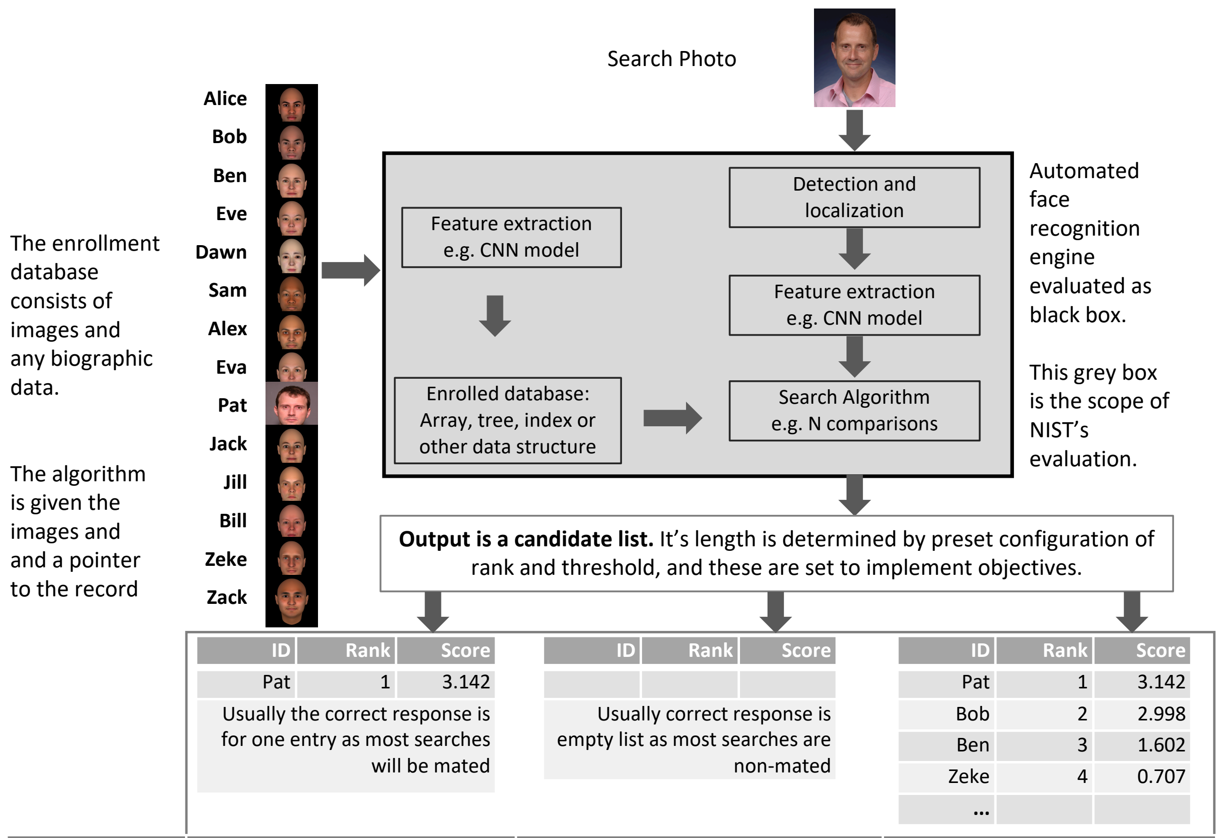

	Positive identification	Negative identification	Post-event investigation
Example	Access to a gym or cruise ship	Watchlist e.g. Detection of deportee or duplicate drivers license applications	Crime scene photos, or of detainee without ID documents.
Claim of identity	Implicit claim to be enrolled	Implicit claim to not be enrolled	No claim: Inquiry
Threshold	High, to implement security objective	High, to limit false positives	Zero
Num. candidates	1	0	L, set by request to algorithm
Human role	Review candidate to assist user in resolution of false negatives, or to detect impostor	Review candidate to determine false positive or correct hit	Review multiple candidates, refer possible hits to examiners see [26]
Intended human involvement frequency	Rare – approx. the false negative identification rate plus prior probability of impostor	Rare – approx. the false positive identification rate plus prior probability of an actual mate	Always
Performance metric of interest	**FNIR at low FPIR. See sec. 3.1, 3.2 and Tables 10, 19**	**FNIR at low FPIR. See sec. 3.1, 3.2 and Tables 10, 19**	**FNIR at ranks 1... 50, say. FPIR = 1. See sec. 3.2 and Table 12, 14, 16**

The algorithms are specifically configured for these applications by setting thresholds and candidate list lengths. Both rank-based metrics and threshold-based metrics include tradeoffs. In investigation, overall accuracy will be reduced if labor is only available to review a few candidates from the automated system. Note that when a fixed number of candidates are returned, the false positive identification rate of the automated face recognition engine will be 100%, because a probe image of anyone not enrolled will still return candidates. In identification applications where false positives must be limited to satisfy reviewer labor availability or a security objective, higher false negative rates are implied. This report includes extensive quantification of this threshold-based tradeoff. See Sec. 3

Template diversity: The FRVT is designed to evaluate black-box technologies with the consequence that the templates that hold features extracted from face images are entirely proprietary opaque binary data that embed considerable intellectual property of the developer. Despite migration to CNN-based technologies there is no consensus on the optimal feature vector dimension. This is evidenced by template sizes ranging from below 100 bytes to more than four kilobytes. This diversity of approaches, suggests there is no prospect of a standard template something that would require a common feature set to be extracted from faces. Interoperability in automated face recognition remains solidly based on images and documentary standards for those, in particular the ICAO portrait [26] specification deriving from the ISO/IEC 19794-5 Token frontal [23] standard, which are similar to certain ANSI/NIST Type 10 [25] formats.

Training: The algorithms submitted to NIST have been developed using image datasets that developers do not disclose. The development will often include application of machine learning techniques and will additionally involve iterative training and testing cycles. NIST itself does not perform any training and does not refine or alter the algorithm in any way. Thus the model, data files, and libraries that define an algorithm are fixed for the duration of the tests. This reflects typical operational reality where recognition software, once installed, is fixed and constant until upgraded. This situation persists because on-site training of algorithms on customer data is atypical essentially because training is not a turnkey process.

Automated search and human review: Virtually all applications using automated face search require human review of the outputs at some frequency: Always for investigational applications; rarely in positive identification applications, after rejection (false or otherwise); and rarely in negative identification applications, after an alarm (false or otherwise). The human role is usually to compare a reference image with the query image or the live-subject if present, to render either a definitive decision on “exclusion” (different subjects), or “identification” (same subject), or a declaration that one or both images have “no value” and that no decision can be made. Note that automated face recognition algorithms are not built to do exclusion - low scores from a face comparison arise from different faces *and* poor quality images of the same face.

Human reviewers make recognition errors [4, 18, 24] and are sensitive to image acquisition and quality. Accurate human review is supported by high resolution - as specified in the Type 50, 51 acquisition profiles of the ANSI/NIST Type 10 record [25], and by multiple non-frontal views as specified in the same standard. These often afford views of the ear. Organizations involved in image collection should consider supporting human adjudication by collecting high-resolution frontal and non-frontal views, preparing low resolution versions for automated face recognition [23], and retaining both for any subsequent resolution of candidate matches. Along these lines, the ISO/IEC Joint Technical Committee 1 subcommittee 37 on biometrics has just initiated projects on image quality assessment and face-aware capture.

Release Notes

FRVT Activities: Since February 2017, NIST has been evaluating one-to-one verification algorithms on an ongoing basis. NIST then restarted FRVT's one-to-many track in February 2018, inviting participants to send up to prototype algorithms. Both tracks allows developers to submit updated algorithms to NIST at any time but no more frequently than four calendar months. This more closely aligns development and evaluation schedules. Results are posted to the web within a few weeks of submission. Details and full report are linked from the Ongoing FRVT site.

FRVT Reports: The results of the FRVT appear in the series NIST Interagency Reports tabulated below. The reports were developed separately and released on different schedules. In prior years NIST has mostly reported FRVT results as a single report; this had the disadvantage that results from completed sub-studies were not published until all other studies were complete.

Date	Link	Title	No.
2014-03-20	PDF	FRVT Performance of Automated Age Estimation Algorithms	7995
2015-04-20	PDF	Face Recognition Vendor Test (FRVT) Performance of Automated Gender Classification Algorithms	8052
2014-05-21	PDF	FRVT Performance of face identification algorithms	8009
2017-03-07	PDF	Face In Video Evaluation (FIVE) Face Recognition of Non-Cooperative Subjects	8173
2017-11-23	PDF	The 2017 IARPA Face Recognition Prize Challenge (FRPC)	8197
2018-11-27	PDF	Face Recognition Vendor Test - Part 2: Identification	8271
2019-09-11	PDF	Face Recognition Vendor Test - Part 2: Identification	8271
2019-12-11	PDF	Face Recognition Vendor Test - Part 3: Demographic Effects	8280
2020-01-03	WWW	Face Recognition Vendor Test (FRVT) - Part 1 Verification	Draft

Details appear on pages linked from `https://www.nist.gov/programs-projects/face-projects`.

Appendices: This report is accompanied by appendices which present exhaustive results on a per-algorithm basis. These are machine-generated and are included because the authors believe that visualization of such data is broadly informative and vital to understanding the context of the report.

Typesetting: Virtually all of the tabulated content in this report was produced automatically. This involved the use of scripting tools to generate directly type-settable LaTeX content. This improves timeliness, flexibility, maintainability, and reduces transcription errors.

Graphics: Many of the Figures in this report were produced using the ggplot2 package running under R, the capabilities of which extend beyond those evident in this document.

Contents

1 Introduction

One-to-many identification represents the largest market for face recognition technology. Algorithms are used across the world in a diverse range of biometric applications: detection of duplicates in databases, detection of fraudulent applications for credentials such as passports and driving licenses, token-less access control, surveillance, social media tagging, lookalike discovery, criminal investigation, and forensic clustering.

This report contains a breadth of performance measurements relevant to many applications. Performance here refers to accuracy and resource consumption. In most applications, the core accuracy of a facial recognition algorithm is the most important performance variable. Resource consumption will be important also as it drives the amount of hardware, power, and cooling necessary to accommodate high volume workflows. Algorithms consume processing time, they require computer memory, and their static template data requires storage space. This report documents these variables.

1.1 Open-set searches

FRVT tested open-set identification algorithms. Real-world applications are almost always "open-set", meaning that some searches have an enrolled mate, but some do not. For example, some subjects have truly not been issued a visa or drivers license before; some law enforcement searches are from first-time arrestees[4]. In an "open-set" application, algorithms make no prior assumption about whether or not to return a high-scoring result, and for a mated search, the ideal behaviour is that the search produces the correct mate at high score and first rank. For a non-mate search, the ideal behavior is that the search produces zero high-scoring candidates.

Many academic benchmarks execute only closed-set searches. The proportion of mates found in the rank one position is the default accuracy metric. This hit rate metric ignores the score with which a mate is found; weak hits count as much as strong hits. This ignores the real-world imperative that in many applications it is necessary to elevate a threshold to reduce the number of false positives.

2 Evaluation datasets

This report documents accuracy for four kinds of images - mugshots, webcam, profiles and wild - as described in the following sections.

2.1 Mugshot images

The main mugshot dataset used is referred to as the FRVT 2018 set. This set was collected over the period 2002 to 2017 in routine United States law enforcement operations. This set has been extracted from a larger operational parent set by excluding non-face images, and setting aside webcam and profile-view images, for use in separate tests.

NIST Interagency Report 8238 includes a comparison of this set of mugshots with the smaller and easier sets of mugshots used in tests run in 2010 and 2014.

[4] Operationally closed-set applications are rare because it is usually not the case that all searches have an enrolled mate. One counter-example, however, is a cruise ship in which all passengers are enrolled and all searches should produce exactly one identity. Another example is forensic identification of dental records from an aircraft crash.

- ▷ **Mugshots**: Mugshots comprise about 86% of the database. They have reasonable compliance with the ANSI/NIST ITL1-2011 Type 10 standard's subject acquisition profiles levels 10-20 for frontal images [25]. The most common departure from the standard's requirements is the presence of mild pose variations around frontal - the images of Figure 3 are typical. The images vary in size, with many being 480x600 pixels with JPEG compression applied to produce filesizes of between 18 and 36KB with many images outside this range, implying that about 0.5 bits are being encoded per pixel.

- ▷ **Profile images**: Profile-view images have been collected in law enforcement for more than 100 years, as human capability is improved with orthogonal information. The profile images used in this report were collected during the same session as the frontal mugshot photograph, in the same standardized photographic setup. These would not therefore be used with automated face recognition. A small subset, 200 000 images, were set aside for testing.

- ▷ **Webcam images**: The remaining 14% of the images were collected using an inexpensive webcam attached to a flexible operator-directed mount. These images are all of size 240x240 pixels, that are in considerable violation of most quality-related clauses of all face recognition standards. As evident in the figure, the most common defects are non-frontal pose (associated with the rotational degrees of freedom of the camera mount), low contrast (due to varying and intense background lights), and poor spatial resolution (due to inexpensive camera optics) - see examples in Fig 4. The images are overly JPEG compressed, to between 4 and 7KB, implying that only 0.5 to 1 bits are being encoded per color pixel.

Example images are shown in Figures 3, 4 and 5 These are drawn from NIST Special Database 32 which may be downloaded here.

These images were partitioned in galleries and probesets for the various experiment listed in Table 1.

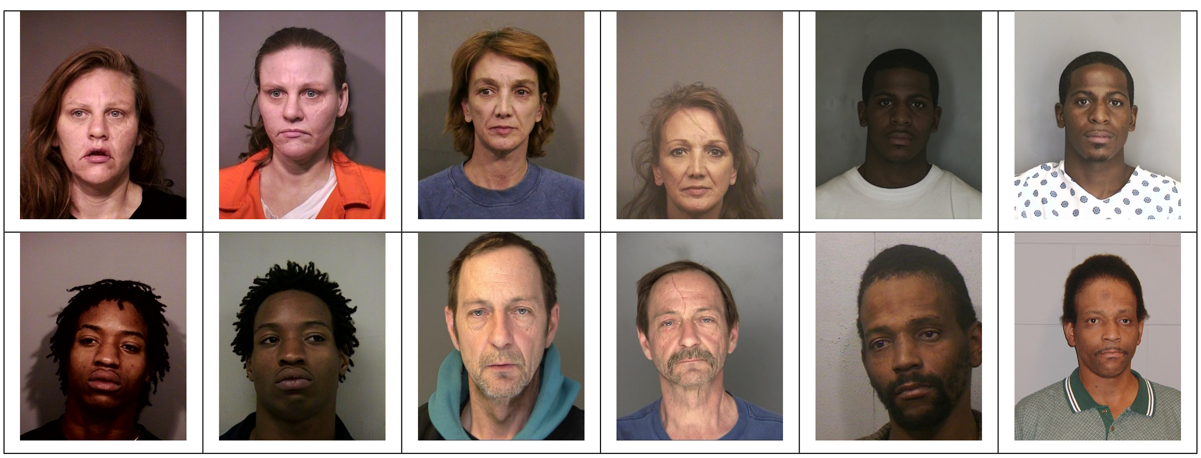

Figure 3: Six mated mugshot pairs representative of the FRVT-2014 (LEO) and FRVT-2018 datasets. The images are collected live, i.e. not scanned from paper. Image source: NIST Special Database 32 the Multiple Encounter Deceased Subjects dataset.

Figure 5: **[Profile views]** *The three images are a frontal enrollment, subsequent frontal probe, and same-session ninety degree profile view. While collection of both frontal and profile views has been typical in law enforcement for more than a century, the recognition of profile to frontal views has essentially been impossible. However, reasonbly high accuracy results is now possible - see section E.*

Figure 4: Twelve webcam images representative of probes against the FRVT-2018 mugshot gallery. The first eight images are four mated pairs. Such images present challenges to recognition including pose, non-uniform illumination, low contrast, compression, cropping, and low spatial sampling rate. Image source: NIST Special Database 32 the Multiple Encounter Deceased Subjects dataset.

2.2 Enrollment strategies

Many operational applications include collection and enrollment of biometric data from subjects on more than one occasion. This might be done on a regular basis, as might occur in credential (re-)issuance, or irregularly, as might happen in a criminal recidivist situation [3]. The number of images per person will depend on the application area. In civil identity credentialing (e.g. passports, driver's licenses), the images will be acquired approximately uniformly over time (e.g. ten years for a passport). While the distribution of dates for such images of a person might be assumed uniform, a number of factors might undermine this assumption[5]. In criminal applications, the number of images would depend on the number of arrests. The distribution of dates for arrest records for a person (i.e. the recidivism distribution) has been modeled using the exponential distribution but is recognized to be more complicated[6].

In any case, the 2010 NIST evaluation of face recognition showed that considerable accuracy benefits accrue with retention and use of *all* historical images [5].

[5]For example, a person might skip applying for a passport for one cycle, letting it expire. In addition, a person might submit identical images (from the same photography session) to consecutive passport applications at five year intervals.
[6]A number of distributions have been considered to model recidivism, see for example [2].

Image				
Encounter	1	...	$K_i - 1$	K_i
Capture Time	T_1	...	$T_{K_i - 1}$	T_{K_i}
Role RECENT	Not used	Not used	Enrolled	Search
Role LIFETIME	Enrolled	Enrolled	Enrolled	Search

Figure 6: Depiction of the "recent" and "lifetime" enrollment types. Image source: NIST Special Database 32

To this end, the FRVT API document provides $K \geq 1$ images of an individual to the enrollment software. The software is tasked with producing a single proprietary undocumented "black-box" template[7] from the K images. This affords the algorithm an ability to generate a *model* of the individual, rather than to simply extract features from each image on a sequential basis.

As depicted in Figure 6, the i-th individual in the FRVT 2018 dataset has K_i images. These are labelled as x_k for $k = 1 \ldots K_i$ in chronological order of capture date. To measure the utility of having multiple enrollment images, this report evaluates three kinds of enrollment:

- ▷ **Recent**: Only the second most recent image, $x_{K_i - 1}$ is enrolled. This strategy of enrollment mimics the operational policy of retaining the imagery from the most recent encounter. This might be done operationally to ameliorate the effects of face ageing. Obviously retaining only the most recent image should only be done if the identity of the person is trusted to be correct. For example, in an access control situation retention of the most recent successful *authentication* image would be hazardous if it could be a false positive.
- ▷ **Lifetime-consolidated**: All but the most recent image are enrolled, $x_1 \ldots x_{K_i - 1}$. This subject-centric strategy might be adopted if quality variations exist where an older image might be more suitable for matching, despite the ageing effect.
- ▷ **Lifetime-unconsolidated**: Again all but the most recent image are enrolled $x_1 \ldots x_{K_i - 1}$ but now separately, with different identifiers, such that the algorithm is not aware that the images are from the same face. This kind of event- or encounter-centric enrollment is very common when operational constraints preclude reliable consolidation of the historical encounters into a single identity. This aspect also prevents the recognition algorithm from a) building a holistic model of identity (as is common in speaker recognition systems) and b) implementing fusion, for example template-level fusion of feature vectors, or post-search score-level fusion. The result is that searches will typically yield more than one image of a person in the top ranks. This has consequences for appropriate metrics, as detailed in section 3.2.1

  NIST first evaluated this kind of enrollment in mid 2018, and the results tables include some comparison of accuracy available from all three enrollment styles.

In all cases, the most recent image, x_{K_i}, is reserved as the search image. For the 1.6 million subject enrollment partition of the FRVT 2018 data, $1 \leq K_i \leq 33$ with $K_i = 1$ in 80.1% of the individuals, $K_i = 2$ in 13.4%, $K_i = 3$ in 3.7%, $K_i = 4$ in

[7] There are no formal face template standards. Template standards only exist for fingerprint minutiae - see ISO/IEC 19794-2:2011.

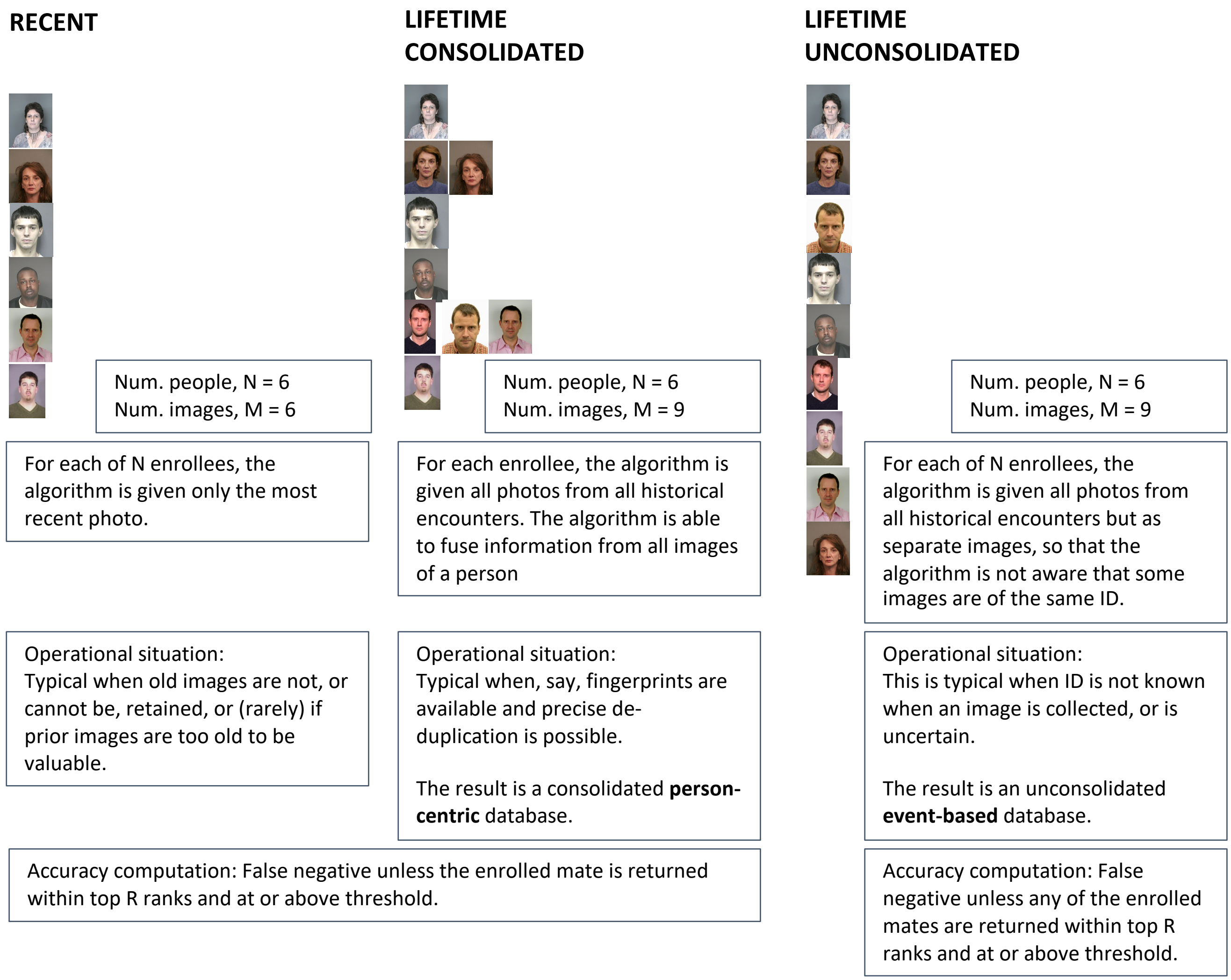

Figure 7: **Enrollment strategies**. *The figure shows the three kinds of enrollment databases examined in this report. Image source: NIST Special Database 32*

	ENROLLMENT				SEARCH			
	TYPE SEE	POPULATION			MATE		NON-MATE	
	SECTION 2.2	FILTER	N-SUBJECTS	N-IMAGES	N-SUBJECTS	N-IMAGES	N-SUBJECTS	N-IMAGES
Mugshot trials from enrollment of single images								
1	RECENT	NATURAL	640 000	640 000	154 549	154 549	331 254	331 254
2	RECENT	NATURAL	1 600 000	1 600 000				
3	RECENT	NATURAL	3 000 000	3 000 000				
4	RECENT	NATURAL	6 000 000	6 000 000				
5	RECENT	NATURAL	12 000 000	12 000 000				
Mugshot trials from enrollment of lifetime images								
6	CONSOL	NATURAL	640 000	1 247 331				
7	CONSOL	NATURAL	1 600 000	3 351 206				
8	CONSOL	NATURAL	3 000 000	6 417 057				
9	CONSOL	NATURAL	6 000 000	12 976 185				
10	CONSOL	NATURAL	12 000 000	26 107 917				
11	UN-CONSOL	NATURAL	640 000	1 247 331				
12	UN-CONSOL	NATURAL	1 600 000	3 351 206				
Cross-domain								
13	MUGSHOTS AS ON ROW 2				82 106 WEBCAM	82 106 WEBCAM	331 254 WEBCAM	331 254 WEBCAM
Cross-view								
14	MUGSHOTS AS ON ROW 2				100 000 PROFILE	100 000 PROFILE	100 000 PROFILE	100 000 PROFILE
Ageing								
17	OLDEST	NATURAL	3 068 801	3 068 801	2 853 221	10 951 064	0	0

Table 1: **Enrollment and search sets**. *Each row summarizes one identification trial. Unless stated otherwise, all entries refer to mugshot images. The term "natural" means that subjects were selected without heed to demographics, i.e. in the distribution native to this dataset. The probe images were collected in a different calendar year to the enrollment image. Missing values in rows 2-12 are the same as in row 1.*

1.4%, $K_i = 5$ in 0.6%, $K_i = 6$ in 0.3%, and $K_i > 6$ is 0.2% for everyone else. This distribution is substantially dependent on United States recidivism rates.

We did not evaluate the case of retaining only the highest quality image, since automated quality assessment is out of scope for this report. We do not anticipate that such strategies will prove beneficial when the quality assessment apparatus is imperfect and unvalidated.

3 Performance metrics

This section gives specific definitions for accuracy and timing metrics. Tests of open-set biometric algorithms must quantify frequency of two error conditions:

- **False positives**: Type I errors occur when search data from a person who has never been seen before is incorrectly associated with one or more enrollees' data.
- **Misses**: Type II errors arise when a search of an enrolled person's biometric does not return the correct identity.

Many practitioners prefer to talk about "hit rates" instead of "miss rates" - the first is simply one minus the other as detailed below. Sections 3.1 and 3.2 define metrics for the Type I and Type II performance variables.

Additionally, because recognition algorithms sometimes fail to produce a template from an image, or fail to execute a one-to-many search, the occurrence of such events must be recorded. Further because algorithms might elect to not produce a template from, for example, a poor quality image, these failure rates must be combined with the recognition error rates to support algorithm comparison. This is addressed in section 3.5.

Finally, section 3.7 discusses measurement of computation duration, and section 3.8 addresses the uncertainty associated with various measurements. Template size measurement is included with the results.

3.1 Quantifying false positives

It is typical for a search to be conducted into an enrolled population of N identities, and for the algorithm to be configured to return the closest L candidate identities. These candidates are ranked by their score, in descending order, with all scores required to be greater than or equal to zero. A human analyst might examine either all L candidates, or just the top $R \leq L$ identities, or only those with score greater than threshold, T. The workload associated with such examination is discussed later, in 3.6.

False alarm performance is quantified in two related ways. These express how many searches produces false positives, and then, how many false positives are produced in a search.

False positive identification rate: The first quantity, FPIR, is the proportion of non-mate searches that produce an adverse outcome:

$$\text{FPIR}(N,T) = \frac{\text{Num. non-mate searches where one or more enrolled candidates are returned with score at or above threshold}}{\text{Num. non-mate searches attempted.}} \tag{1}$$

Under this definition, FPIR can be computed from the highest non-mate candidate produced in a search - it is not necessary to consider candidates at rank 2 and above. FPIR is the primary measure of Type I errors in this report.

Selectivity: However, note that in any given search, several non-mate may be returned above threshold. In order to quantify such events, a second quantity, selectivity (SEL), is defined as the *number* of non-mates returned on a candidate list, averaged over all searches.

$$\text{SEL}(N,T) = \frac{\text{Num. non-mate enrolled candidates returned with score at or above threshold}}{\text{Num. non-mate searches attempted.}} \tag{2}$$

where $0 \leq$ SEL(N, T) $\leq$L. Both of these metrics are useful operationally. FPIR is useful for targeting how often an adverse false positive outcome can occur, while SEL as a number is related to workload associated with adjudicating candidate lists. The relationship between the two quantities is complicated - it depends on whether an algorithm concentrates the false alarms in the results of a few searches or whether it disburses them across many. This was detailed in FRVT 2014, NISTIR 8009. It has not yet been detailed in FRVT 2018.

3.2 Quantifying hits and misses

If L candidates are returned in a search, a shorter candidate list can be prepared by taking the top $R \leq L$ candidates for which the score is above some threshold, $T \geq 0$. This reduction of the candidate list is done because thresholds may be applied, and only short lists might be reviewed (according to policy or labor availability, for example). It is useful then to state accuracy in terms of R and T, so we define a "miss rate" with the general name **false negative identification**

rate (FNIR), as follows:

$$\text{FNIR}(N,R,T) = \frac{\text{Num. mate searches with enrolled mate found outside top R ranks or score below threshold}}{\text{Num. mate searches attempted.}} \quad (3)$$

This formulation is simple for evaluation in that it does not distinguish between causes of misses. Thus a mate that is not reported on a candidate list is treated the same as a miss arising from face finding failure, algorithm intolerance of poor quality, or software crashes. Thus if the algorithm fails to produce a candidate list, either because the search failed, or because a search template was not made, the result is regarded as a miss, adding to FNIR.

Hit rates, and true positive identification rates: While FNIR states the "miss rate" as how often the correct candidate is either not above threshold or not at good rank, many communities prefer to talk of "hit rates". This is simply the **true positive identification rate**(TPIR) which is the complement of FNIR giving a positive statement of how often mated searches are successful:

$$\text{TPIR}(N,R,T) = 1 - \text{FNIR}(N,R,T) \quad (4)$$

This report does not report true positive "hit" rates, preferring false negative miss rates for two reasons. First, costs rise linearly with error rates. For example, if we double FNIR in an access control system, then we double user inconvenience and delay. If we express that as decrease of TPIR from, say 98.5% to 97%, then we mentally have to invert the scale to see a doubling in costs. More subtly, readers don't perceive differences in numbers near 100% well, becoming inured to the "high nineties" effect where numbers close to 100 are perceived indifferently.

Reliability is a corresponding term, typically being identical to TPIR, and often cited in automated (fingerprint) identification system (AFIS) evaluations.

An important special case is the **cumulative match characteristic**(CMC) which summarizes accuracy of mated-searches only. It ignores similarity scores by relaxing the threshold requirement, and just reports the fraction of mated searches returning the mate at rank R or better.

$$\text{CMC}(N,R) = 1 - \text{FNIR}(N,R,0) \quad (5)$$

We primarily cite the complement of this quantity, FNIR$(N,R,0)$, the fraction of mates *not* in the top R ranks.

The **rank one hit rate** is the fraction of mated searches yielding the correct candidate at best rank, i.e. CMC(N, 1). While this quantity is the most common summary indicator of an algorithm's efficacy, it is not dependent on similarity scores, so it does not distinguish between strong (high scoring) and weak hits. It also ignores that an adjudicating reviewer is often willing to look at many candidates.

3.2.1 False negative rates for unconsolidated galleries

As detailed in section 2.2 a common type of gallery, here referred to as the lifetime unconsolidate type, is populated with all images of an individual without any association between them. That is, the gallery construction algorithm is not provided with any ID labels that would support processing of a person's images jointly. This constrasts with the lifetime consolidate type where an algorithm may explicitly fuse features from multiple images of a person, or select a best image. In such cases, where the number of enrolled images is a random variable, we define two false negative rates as follows.

The first demands that the algorithm place any of the K_i mates in the top $R \geq 1$ ranks. The proportion of searches for which this does not occur forms a false negative identification rate:

$$\text{FNIR}_{\text{any}}(N,R,T) = 1 - \frac{\text{Num. mate searches where any enrolled mate is found in the top R ranks and at-or-above threshold}}{\text{Num. mate searches attempted.}} \tag{6}$$

The second demands that the algorithm place all K_i mates in the top $R \geq K_i$ ranks. The proportion of searches for which this does not occur forms a false negative identification rate:

$$\text{FNIR}_{\text{all}}(N,R,T) = 1 - \frac{\text{Num. mate searches where all enrolled mates are found in the top R ranks and at-or-above threshold}}{\text{Num. mate searches attempted.}} \tag{7}$$

Placing all mates in the top ranks is a more difficult task than correctly retrieving any image, so it holds that: $\text{FNIR}_{\text{all}} \geq \text{FNIR}_{\text{any}}$. This is evident in the results presented for November 2018 algorithms in Tables starting at 28.

The information retrieval community might prefer to compute and plot *precision* and *recall*; this is a valid approach, but we advance the two metrics above because they relate to our normal definition of consolidated FNIR, and they cover the two extreme use-cases of wanting any hit vs. all hits.

3.3 DET interpretation

In biometrics, a false negative occurs when an algorithm fails to match two samples of one person a Type II error. Correspondingly, a false positive occurs when samples from two persons are improperly associated a Type I error.

Matches are declared by a biometric system when the native comparison score from the recognition algorithm meets some threshold. Comparison scores can be either similarity scores, in which case higher values indicate that the samples are more likely to come from the same person, or dissimilarity scores, in which case higher values indicate different people. Similarity scores are traditionally computed by fingerprint and face recognition algorithms, while dissimilarities are used in iris recognition. In some cases, the dissimilarity score is a distance possessing metric properties. In any case, scores can be either mate scores, coming from a comparison of one persons samples, or nonmate scores, coming from comparison of different persons samples.

The words ”genuine” or ”authentic” are synonyms for mate, and the word ”impostor” is used as a synonym for nonmate. The words ”mate” and ”nonmate” are traditionally used in identification applications (such as law enforcement search, or background checks) while genuine and impostor are used in verification applications (such as access control).

An error tradeoff characteristic represents the tradeoff between Type II and Type I classification errors. For identification this plots false negative vs. false positive identification rates i.e. FNIR vs. FPIR parametrically with T. Such plots are often called detection error tradeoff (DET) characteristics or receiver operating characteristic (ROC). These serve the same function $-$ to show error tradeoff $-$ but differ, for example, in plotting the complement of an error rate (e.g. TPIR = 1 $-$ FNIR) and in transforming the axes, most commonly using logarithms, to show multiple decades of FPIR. More rarely, the function might be the inverse of the Gaussian cumulative distribution function.

The slides of Figures 8 through 15 discuss presentation and interpretation of DETs used in this document for reporting face identification accuracy. Further detail is provided in formal biometrics testing standards, see the various parts of ISO/IEC 19795 Biometrics Testing and Reporting. More terms, including and beyond those to do with accuracy, appear in ISO/IEC 2382-37 Information technology – Vocabulary – Part 37: Harmonized biometric vocabulary.

FNIR(N, R, T) = False neg. identification rate
FPIR(N, T) = False pos. identification rate
N = Num. enrolled subjects
R = Num. candidates examined
T = Threshold
T = 0 → Investigation
T > 0 → Identification

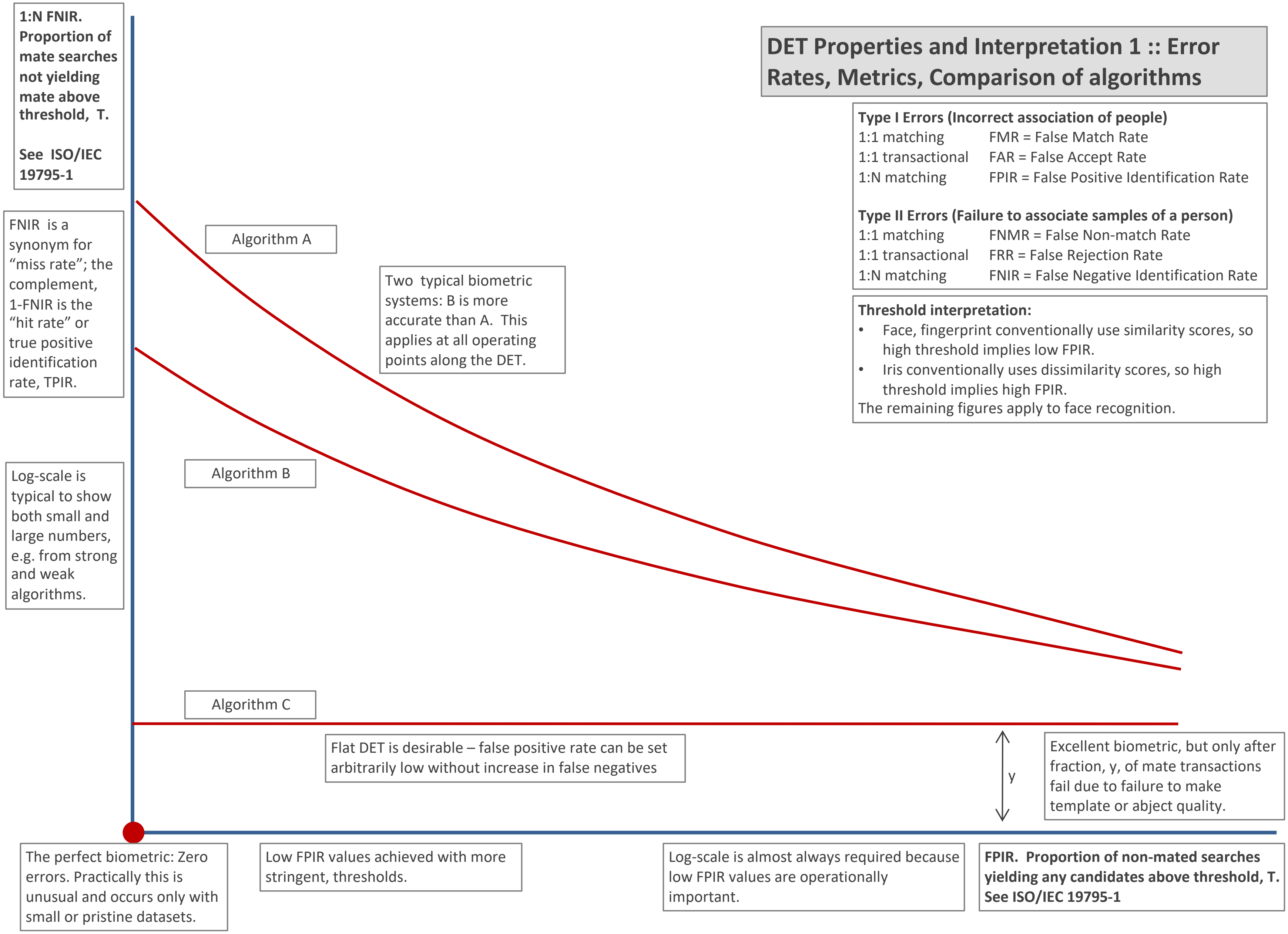

Figure 8: **DET as the primary performance reporting mechanism**.

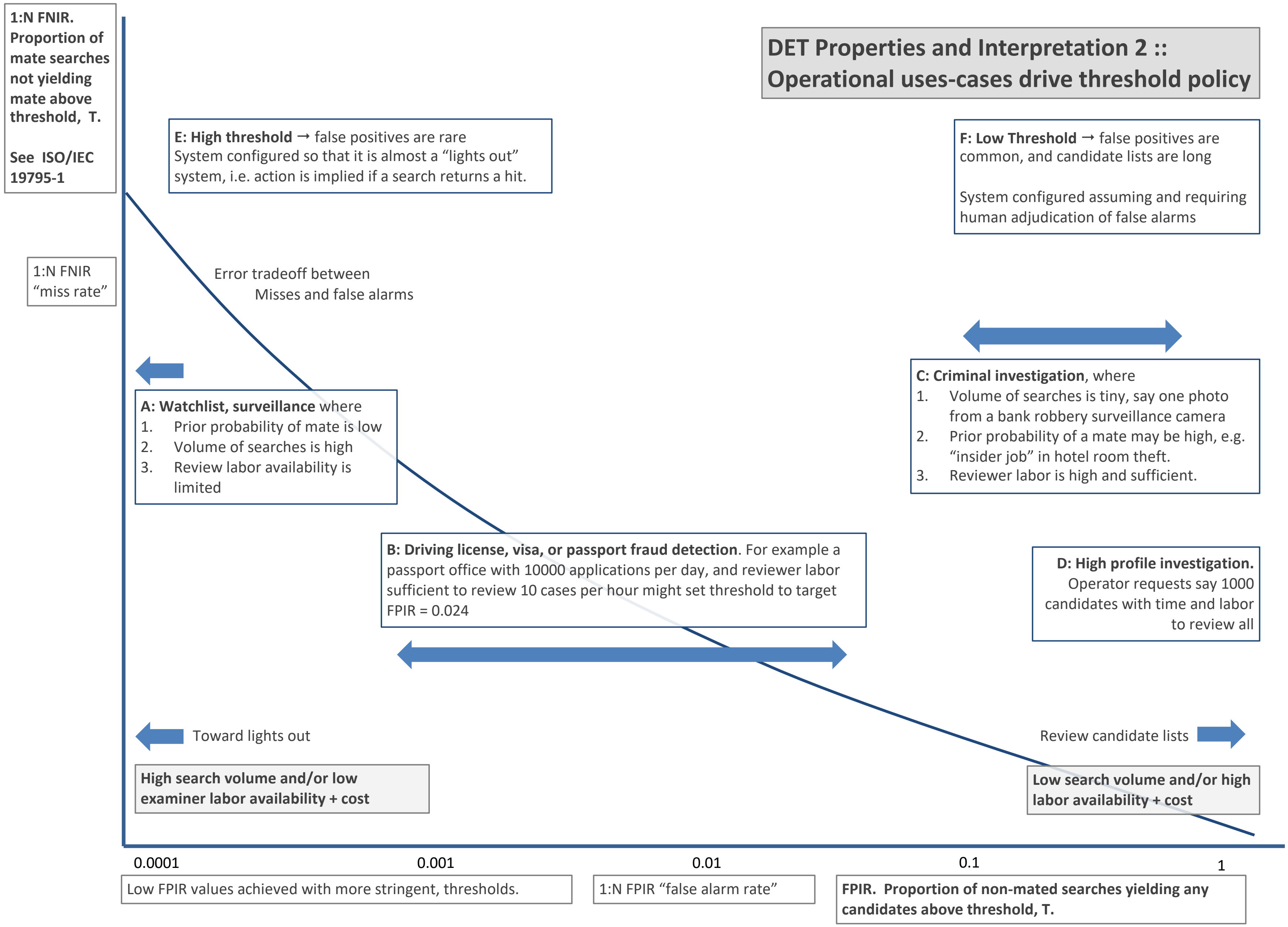

Figure 9: **DET as the primary performance reporting mechanism.**

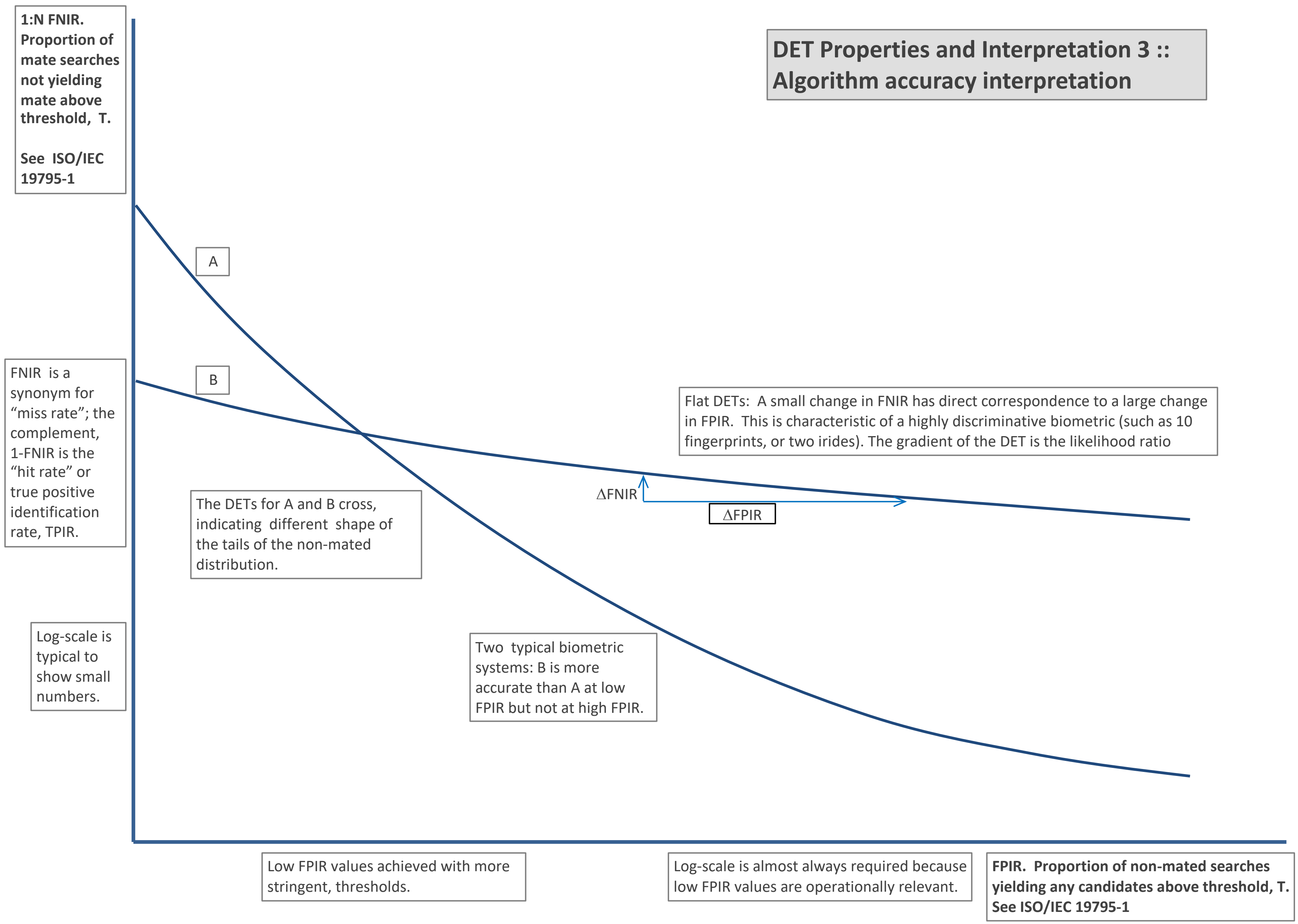

Figure 10: **DET as the primary performance reporting mechanism.**

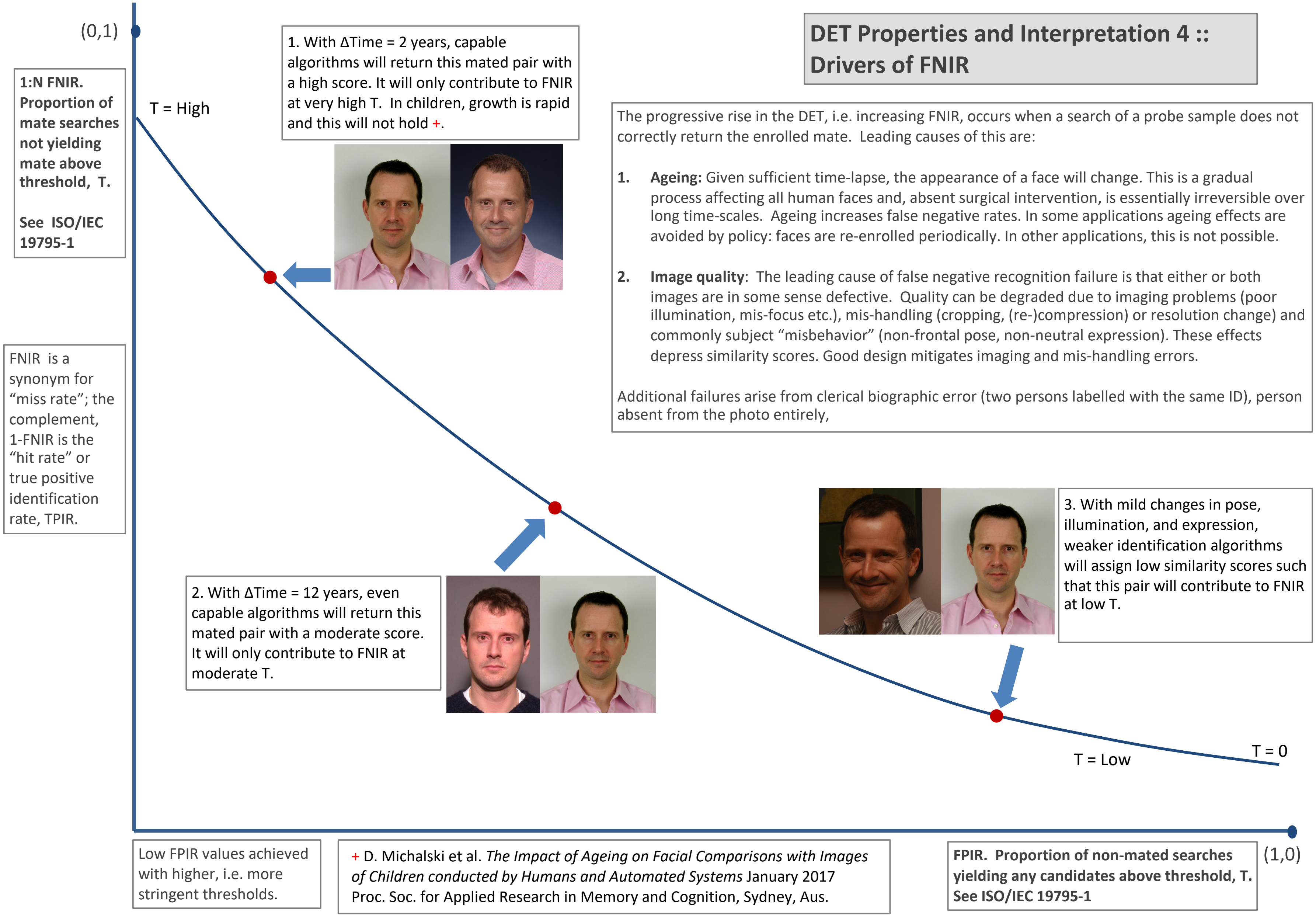

Figure 11: **DET as the primary performance reporting mechanism.**

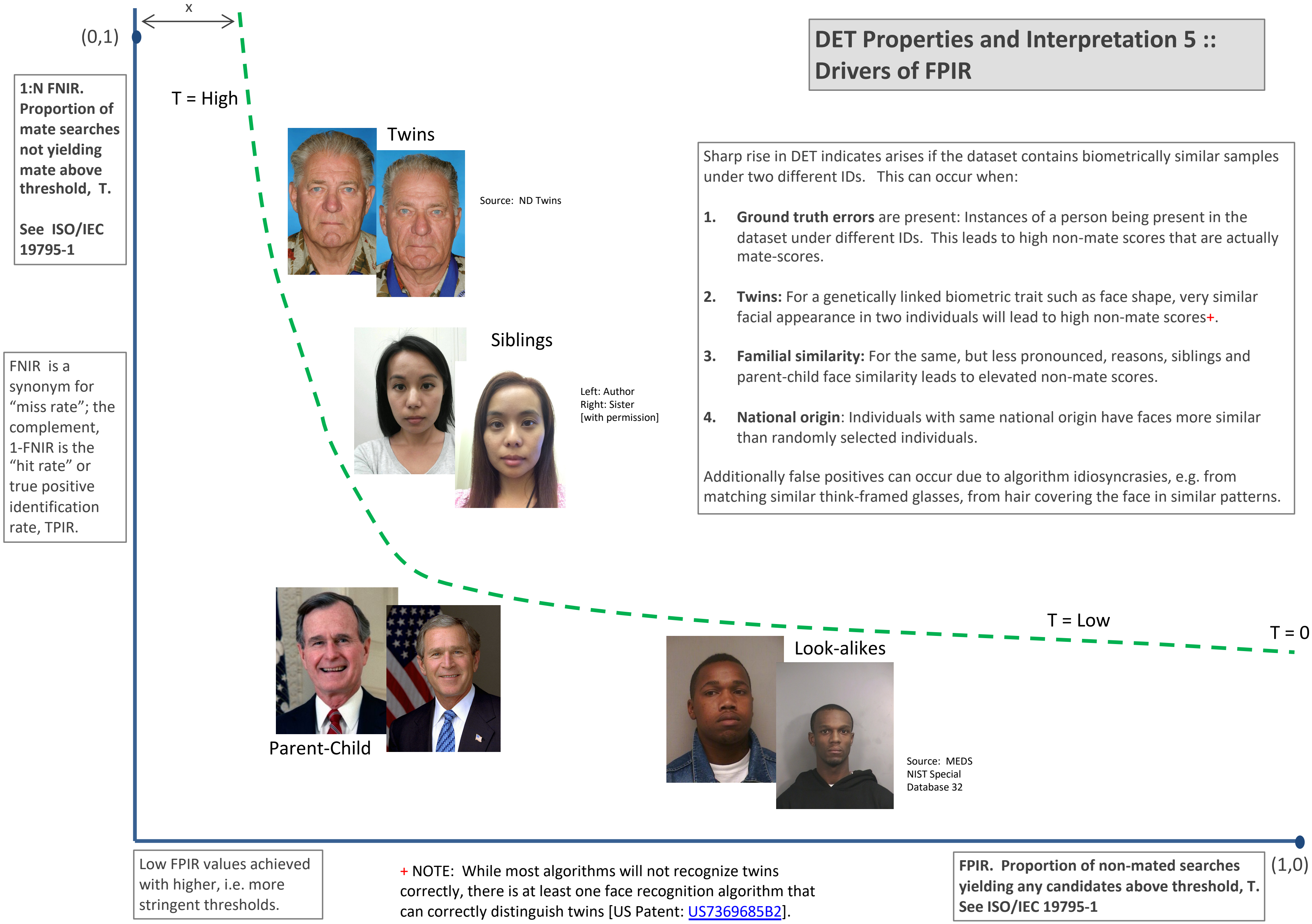

Figure 12: **DET as the primary performance reporting mechanism.**

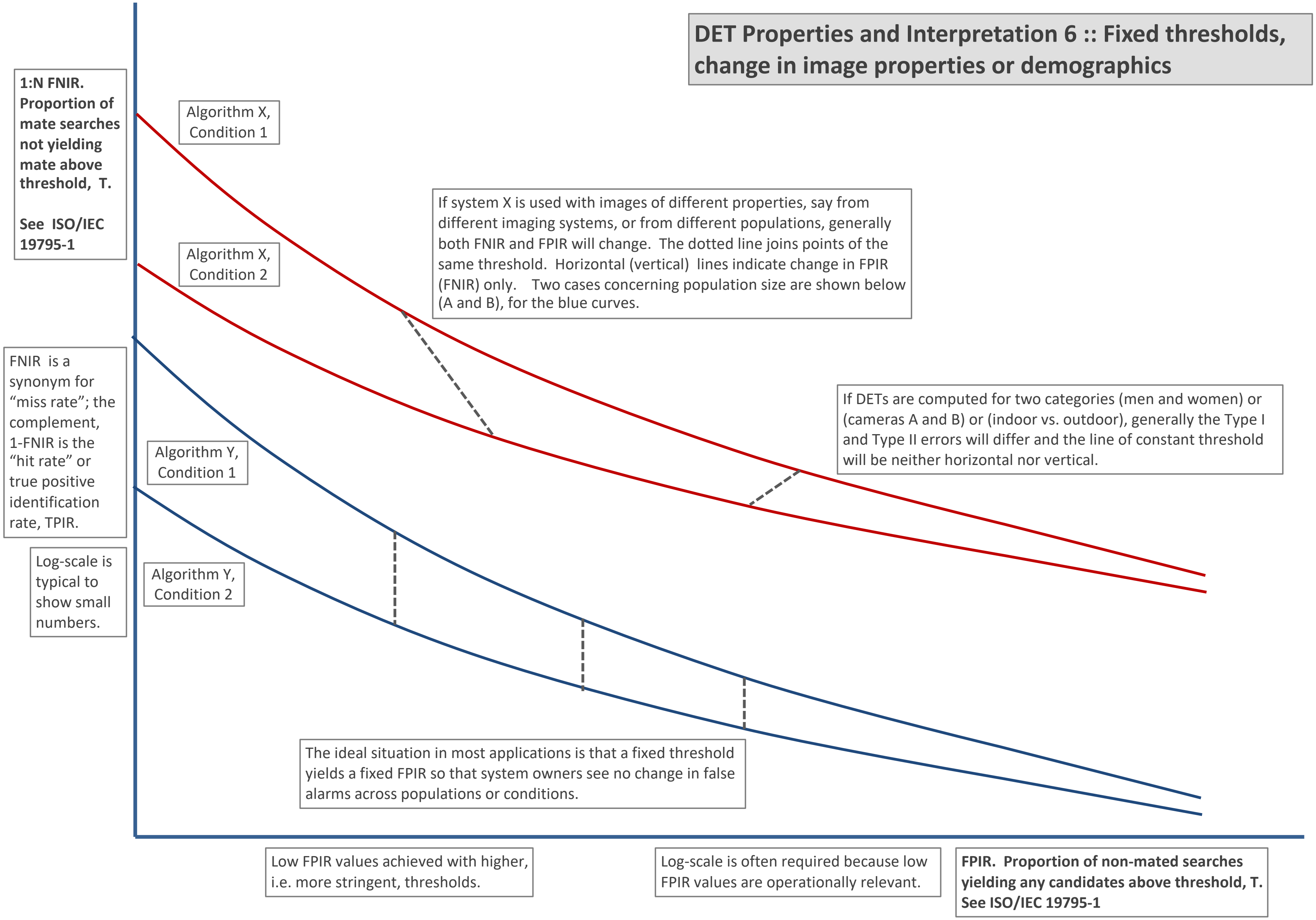

Figure 13: **DET as the primary performance reporting mechanism**.

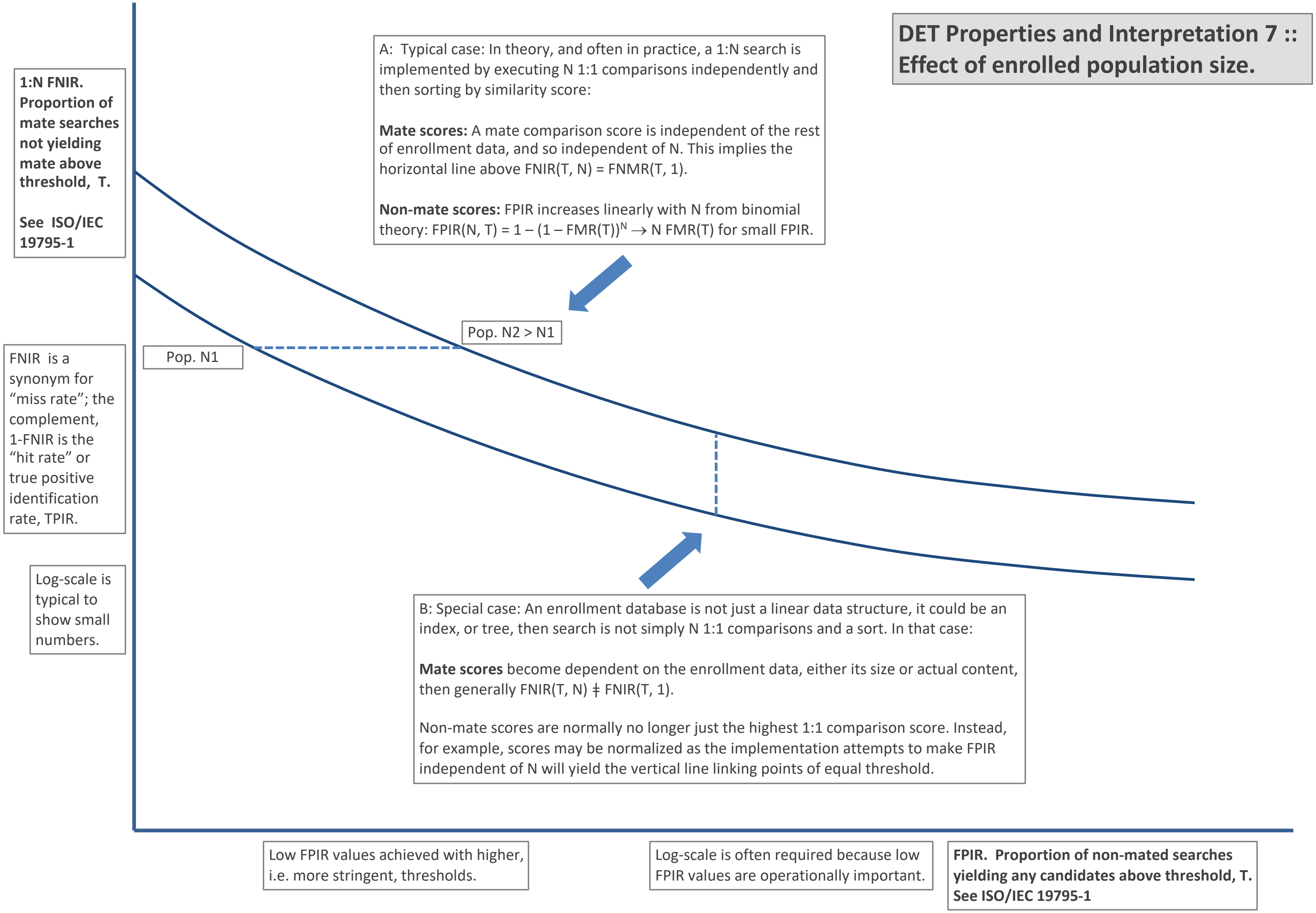

Figure 14: **DET as the primary performance reporting mechanism.**

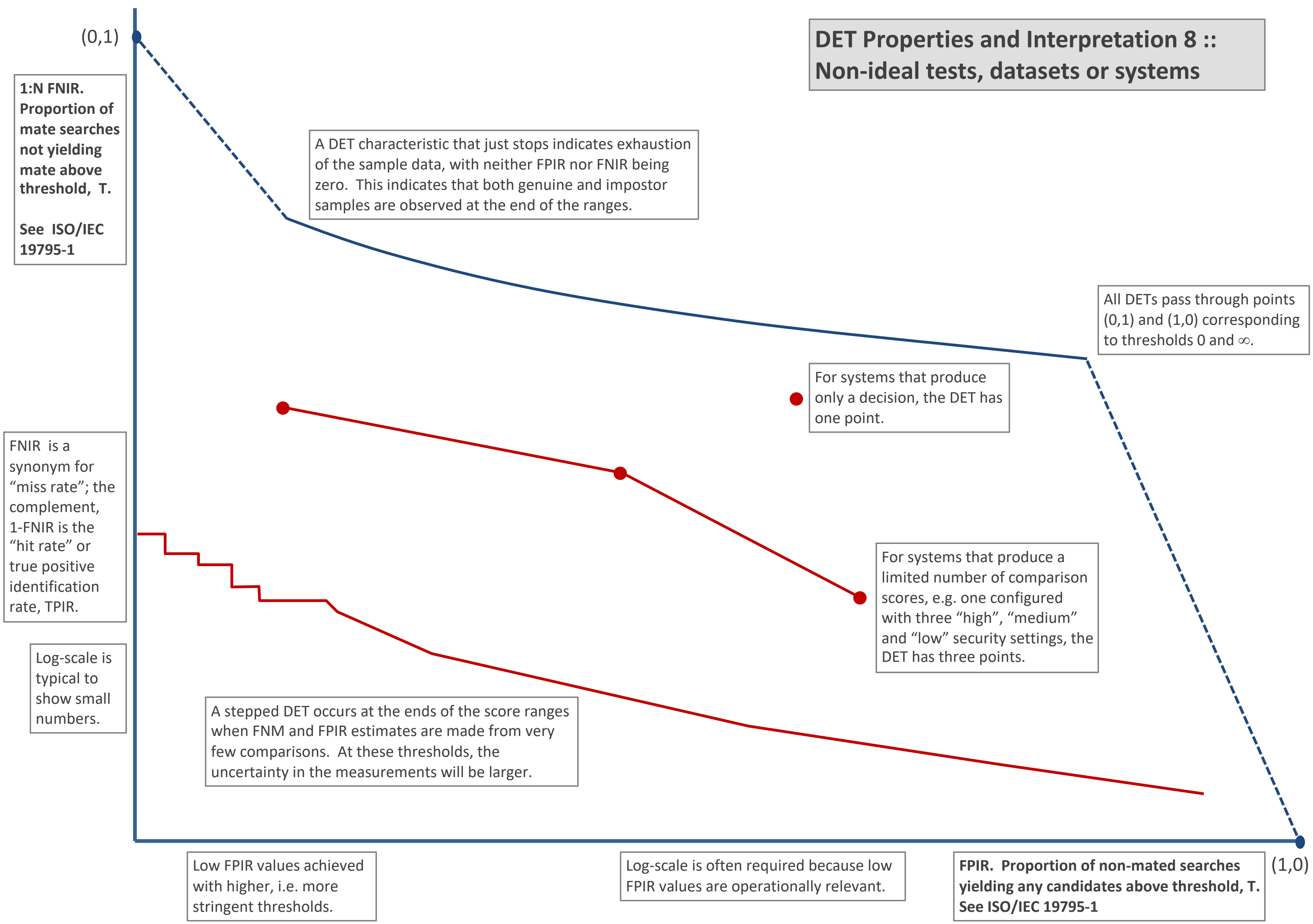

Figure 15: **DET as the primary performance reporting mechanism.**

3.4 Best practice testing requires execution of searches with and without mates

FRVT embeds 1:N searches of two kinds: Those for which there is an enrolled mate, and those for which there is not. The respective numbers for these types of searches appear in Table 1. However, it is common to conduct only mated searches[8]. The cumulative match characteristic is computed from candidate lists produced in mated searches. Even if the CMC is the only metric of interest, the actual trials executed in a test should nevertheless include searches for which no mate exists. As detailed in Table 1 the FRVT reserved disjoint populations of subjects for executing true non-mate searches.

3.5 Failure to extract features

During enrollment some algorithms fail to convert a face image to a template. The proportion of failures is the failure-to-enroll rate, denoted by FTE. Similarly, some search images are not converted to templates. The corresponding proportion is termed failure-to-extract, denoted by FTX.

We do not report FTX because we assume that the same underlying algorithm is used for template generation for enrollment and search.

Failure to extract rates are incorporated into FNIR and FPIR measurements as follows.

- ▷ **Enrollment templates**: Any failed enrollment is regarded as producing a zero length template. Algorithms are required by the API [9] to transparently process zero length templates. The effect of template generation failure on search accuracy depends on whether subsequent searches are mated, or non-mated: Mated searches will fail giving elevated FNIR; non-mated searches will not produce false positives so, to first order, FPIR will be reduced by a factor of $1-\mathrm{FTE}$.

- ▷ **Search templates and 1:N search**: In cases where the algorithm fails to produce a search template from input imagery, the result is taken to be a candidate list whose entries have no hypothesized identities and zero score. The effect of template generation failure on search accuracy depends on whether searches are mated, or non-mated: Mated searches will fail giving elevated FNIR; Non-mated searches will not produce false positives, so FPIR will be reduced. Thus given a measurement of false negative and positive rates made over only those where failures-to-extract did not occur, those rates - call them $\mathrm{FNIR}^{\dagger}$ and $\mathrm{FPIR}^{\dagger}$ - could be adjusted by an explicit measurement of FTX as follows

$$\mathrm{FNIR} = \mathrm{FTX} + (1 - \mathrm{FTX})\mathrm{FNIR}^{\dagger} \tag{8}$$

$$\mathrm{FPIR} = (1 - \mathrm{FTX})\mathrm{FPIR}^{\dagger} \tag{9}$$

This approach is the correct treatment for positive-identification applications such as access control where cooperative users are enrolled and make attempts at recognition. This approach is not appropriate to negative identification applications, such as visa fraud detection, in which hostile individuals may attempt to evade detection by submitting poor quality samples. In those cases, template generation failures should be investigated as though a false alarm had occurred.

[8] For example, the Megaface benchmark. This is bad practice for several reasons: First, if a developer knows, or can reasonably assume, that a mate always exists, then unrealistic gaming of the test is possible. A second reason is that it does not put FPIR on equal footing with FNIR and that matters because in most applications, not all searches have mates - not everyone has been previously enrolled in a driving license issuance or a criminal justice system - so addressing between-class separation becomes necessary.

3.6 Fixed length candidate lists, threshold independent workload

Suppose an automated face identification algorithm returns L candidates, and a human reviewer is retained to examine up to R candidates, where $R \leq L$ might be set by policy, preference or labor availability. For now, assume also that the reviewer is not provided with, or ignores, similarity scores, and thresholds are not applied. Given the algorithm typically places mates at low (good) ranks, the number of candidates a reviewer can be expected to review can be derived as follows. Note that the reviewer will:

- ▷ Always inspect the first ranked image — Frac. reviewed = 1
- ▷ Then inspect those candidates where mate not confirmed at rank 1 — Frac. reviewed = 1-CMC(1)
- ▷ Then inspect those candidates where mate not confirmed at rank 1 or 2 — Frac. reviewed = 1-CMC(2)

etc. Thus if the reviewer will stop after a maximum of R candidates, the expected number of candidate reviews is

$$M(R) = 1 + (1 - CMC(1)) + (1 - CMC(2)) + \ldots + (1 - CMC(R-1)) \tag{10}$$

$$= R - \sum_{r=1}^{R-1} CMC(r) \tag{11}$$

A recognition algorithm that front-loads the cumulative match characteristic will offer reduced workload for the reviewer. This workload is defined only over the searches for which a mate exists. In the cases where there truly is no mate, the reviewer would review all R candidates. Thus, if the proportion of searches for which a mate does exist is β, which in the law enforcement context would be the recidivism rate [2], the full expression for workload becomes:

$$M(R) = \beta \left(R - \sum_{r=1}^{R-1} CMC(r) \right) \quad + \quad (1-\beta)R \tag{12}$$

$$= R - \beta \sum_{r=1}^{R-1} CMC(r) \tag{13}$$

3.7 Timing measurement

Algorithms were submitted to NIST as implementations of the application programming interface(API) specified by NIST in the Evaluation Plan [9]. The API includes functions for initialization, template generation, finalization, search, gallery insert, and gallery delete. Two template generation functions are required, one for the preparation of an enrollment template, and one for a search template.

In NIST's test harness, all functions were wrapped by calls to the C++ std::chrono::high resolution clock which on the dedicated timing machine counts 1ns clock ticks. Precision is somewhat worse than that however.

3.8 Uncertainty estimation

3.8.1 Random error

This study leverages operational datasets for measurement of recognition error rates. This affords several advantages. First, large numbers of searches are conducted (see Table 1) giving precision to the measurements. Moreover, for the two mugshot datasets, these do not involve reuse of individuals so binomial statistics can be expected to apply to recognition error counts. In that case, an observed count of a particular recognition outcome (i.e. a false negative or false positive) in M trials will sustain 95% confidence that the actual error rate is no larger than some value.

As an example, the minimum number of mugshot searches conducted in this report is M =154 549, and for an observed FNIR around 0.002, the measurement supports a conclusion that the actual FNIR is no higher than 0.00228 at 99% confidence level. On the false positive side, we tabulate FNIR at FPIR values as low as 0.001. Given estimates based on 331 254 non-mate trials, the actual FPIR values will be below 0.00115 at 99% confidence. In conclusion, large scale evaluation, without reuse of subjects, supports tight uncertainty bounds on the measured error rates.

3.8.2 Systematic error

The FRVT 2018 dataset includes anomalies discovered as a result of inspecting images involved in recognition failures from the most accurate algorithms. Two kinds of failure occur: False negatives (which, for the purpose here, include failures to make templates) and false positives.

False negative errors: We reviewed 600 false negative pairs for which either or both of the leading two algorithms did not put the correct mate in the top 50 candidates. Given 154 549 searches, this number represents 0.39% of the total, resulting in FNIR ~ 0.0039. Of the 600 pairs:

- ▷ **A: Poor quality**: About 20% of the pairs included images of very low quality, often greyscale, low resolution, blurred, low contrast, partially cropped, interlaced, or noisy scans of paper images. Additionally, in a few cases, the face is injured or occluded by bandages or heavy cosmetics.
- ▷ **B: Ground truth identity label bugs**: About 15% of the pairs are not actually mated. We only assigned this outcome when a pair is clearly not mated.
- ▷ **C: Profile views**: About 35% included an image of a profile (side) view of the face, or, more rarely, an image that was rotated 90 degrees in-plane (roll).
- ▷ **D: Tattoos**: About 30% included an image of a tattoo that contained a face image. These arise from mis-labelling in the parent dataset metadata.
- ▷ **E: Ageing**: There is considerable time-lapse between the two captures.

All these estimates are approximate. Of these, the tattoo and mislabled images can never be matched. These constitute an accuracy floor in the sample implying that FNIR cannot be below 0.0018[9]. The profile-views, low-quality images, and images with considerable ageing can, in principle, be successfully matched - indeed some algorithms do so - so are not part of the accuracy floor.

[9] This value is the sum of two partial false negative rates: FNIR_B = 0.15 * 0.0039 plus FNIR_D = 0.3 * 0.0039

For the microsoft-4 algorithm the lowest miss rate from (recent entry in Table 16) is FNIR(640 000, 50, 0) = 0.0018. This is close to the value estimated from the inspection of misses. It is below the 0.0039 figure because the algorithm does match some profile and poor quality images, that the yitu-2 algorithm does not.

For many tables (e.g. Table 16), the FNIR values obtained for the FRVT-2018 mugshots could be corrected by reducing them by 0.0018. The best values would then be indistinct from zero. The results in this report *were not* adjusted to account for this systematic error.

False positive errors: As depicted in Figure 8 many of the DET characteristics in this report exhibit a pronounced turn upward at low false positive rates. The shape can be caused by identity labelling errors in the ground truth of a dataset, specifically persons present in the database under two IDs such that some proportion of non-mate pairs are actually mated. We merged the highest 1000 non-mate pairs produced by three different algorithms which resulted in 1839 unique pairs. This constitutes 0.56% of all non-mate searches. We assert that it is *very* difficult for human reviewers to assign the pairs into the following three categories: twins; doppelgangers; or ground-truth errors (instances of the same person under two IDs). Given this difficulty we made no attempt to correct any ground truth except by removing 57 pairs in the following categories:

- ▷ **A: Profile views**: Thirteen pairs included one or two profile-view images. As described in Figure 104, these can cause false positives.
- ▷ **B: Same-session photographs**: For twelve pairs, the images were identical or trivially altered (e.g. cropped) versions of the same photo. These were present under a different ID likely due to some clerical or procedural mistake.
- ▷ **C: Tattoos of faces**: There were fourteen instances of tattoo photographs that contained faces causing false matches.
- ▷ **D: T-shirt faces**: There were six instances of T-shirt photographs (of Bob Marley and Che Guevara) being detected instead of the face and causing false positives.
- ▷ **E: Background faces**: There were twelve instances of one subject appearing in the background of two otherwise correct portrait photos.

Note we did not remove any images where there was a chance that the pair was actually a different person.

In any case, the results in this report have not been adjusted for this systematic error.

4 Results

This section gives extensive results for algorithms submitted to FRVT 2018. Three page "report cards" for each algorithm are contained in a separate supplement. Performance metrics were described in section 3. The main results are summarized in tabular form with more exhaustive data included as DET, CMC and related graphs in appendices as follows:

▷ The three tables 2-4 list algorithms alongside full developer names, acceptance date, size of the provided configuration data, template size and generation time, and search duration data.

- The **template generation duration** is most important to applications that require fast response. For example, an eGate taking more than two seconds to produce a template might be unacceptable. Note that GPUs may be of utility in expediting this operation for some algorithms, though at additional expense. Two additional factors should be considered[10][11].
- The **search duration** is the time taken for a search of a search template into a gallery of N enrollment templates. This performance variable, together with the volume of searches, is influential on the amount of hardware needed to sustain an operational deployment. This is measured here with the algorithm running on a single core of a contemporary CPU. Search is most simply implemented as N computations of a distance metric followed by a sort operation to find the closest enrollments. However, considerable optimization of this process is possible, up to and including fast-search algorithms that, by various means, avoid computation of all N distances.
- The **template size** is the size of the extracted feature vector (or vectors) and any needed header information. Large template sizes may be influential on bus or network bandwidth, storage requirements, and on search duration. While the template itself is an opaque data blob, the feature dimensionality might be estimated by assuming a four-bytes-per-float encoding. There is a wide range of encodings. For the more accurate algorithm, sizes range from 256 bytes to about 2KB bytes, indicating essentially no consensus on face modeling and template design.
- The **template size multiplier** column shows how, given k input images, the size of the template grows. Most implementations internally extract features from each image and concatenate them, and implement some score-level fusion logic during search. Other implementations, including many of the most accurate algorithms, produce templates whose size does not grow with k. This could be achieved via selection of the best quality image - but this is not optimal in handling ageing where the oldest image could be the best quality. Another mechanism would be feature-level fusion where information is fused from all k inputs. In any case, as a black-box test, the fusion scheme is proprietary and unknown.
- The size of the **configuration data** is the total size of all files resident in a vendor-provided directory that contains arbitrary read-only files such as parameters, recognition models (e.g caffe). Generally a large value for this quantity may prohibit the use of the algorithm on a resource-constrained device.

[10] The FRVT 2018 API prohibited threading, so some gains from parallelism may be available on multiple-cores or multiple processors, if the feature extraction code could be distributed across them.

[11] Note also that factors of two or more may be realizable by exploiting modern vector processing instructions on CPUs. It is not clear in our measurements whether all developers exploited Intel's AVX2 instructions, for example. Our machine was so equipped, but we insisted that the same compiled library should also run on older machines lacking that instruction. The more sophisticated implementations may have detected AVX2 presence and branched accordingly. The less sophisticated may be defaulted to the reduced instruction set. Readers should see the FRVT 2018 API document for the specific chip details.

▷ Tables 16-17 report core rank-based accuracy for mugshot images. The population size is limited to N = 1.6 million identities because this is the largest gallery size on which all algorithms were executed. Notable observations from these tables are as follows:

– **Accuracy gains during 2018**: NIST Interagency Report 8238 documented massive gains over those reported in the FRVT 2014 report, NIST Interagency Report 8009.

Further gains are documented in this report. Comparing the most accurate algorithm in June 2018, Microsoft-4, with the most accurate in November 2018, NEC-2, the value of FNIR(N, 1, 0) reduced from 0.0031 to 0.0028 with N = 1.6 million recent images. For lifetime enrollments, Microsoft-4 remained the most accurate algorithm as the newer variants from Microsoft did not reduce this error rate.

We further note that the revolution is not over: Figure 18 shows that many developers have made great advances in the four months between Phases 1 and 2 of FRVT 2018, Feburary to June. Most developers saw a two-fold reduction in errors, with Neurotechnology seeing a five fold reduction.

– **Wide range in accuracy**: The rank-1 miss rates vary from FNIR(N, 1, 0) = 0.001 for nec-3 up to about 0.5 for the very fast but inaccurate microfocus-x algorithms. Among the developers who are superior to NEC in 2013, the range is from 0.002 to 0.035 for camvi-3. This large accuracy range is consistent with the buyer-beware maxim, and indicates that face recognition software is far from being commoditized.

▷ Tables 20-21 report threshold-based error rates, FNIR(N, L, T), for N = 1.6 million for mugshot-mugshot accuracy on FRVT 2014, FRVT 2018, and also (in pink) mugshot-webcam accuracy using FRVT 2018 enrollments. Notable observations from these tables are as follows:

– **Order of magnitude accuracy gains since 2014**: As with rank-based results, the gains in accuracy are substantial, though somewhat reduced. At FPIR = 0.01, the best improvement over NEC in 2014 is a 27 fold reduction in FNIR using the NEC_2 algorithm. At FPIR = 0.001, the largest gain is a six-fold reduction in FNIR via the NEC_3 algorithm.

– **Broad gains across the industry**: About 19 companies realize accuracy better than the NEC benchmark from 2014. This is somewhat lower than the 28 developers who succeeded on the rank-1 metric. This may be due to the ubiquity of, and emphasis on, the rank-1 metric in many published algorithm development papers.

– **Webcam images**: Searches of webcam images give FNIR(N, T) values around 2 to 3 times higher than mugshot searches. Notably the leading developers with mugshots are approximately the same with poorer quality webcams. But some developers e.g. Camvi, Megvii, TongYi, and Neurotechnology do improve their relative rankings on webcams, perhaps indicating their algorithms were tailored to less constrained images.

▷ Tables 7, 10, 11 and show, respectively, high-threshold, rank 1, nd rank 50 FNIR values for all algorithms performing searches into five different gallery sizes, N = 640 000, N = 1 600 000, N = 3 000 000, N = 6 000 000 and 12 000 000. The FPIR = 0.001 table is included to inform high-volume duplicate detection applications. The Rank-1 table is included as a primary accuracy indicator. The Rank-50 table is included to inform agencies who routinely produce 50 candidates for human-review. The notable results are:

– **Slow growth in rank-based miss rates:** FNIR(N, R) generally grows as a power law, aN^b. From the straight lines of many graphs of Figure 21 this is clearly a reasonable model for most, but not all, algorithms. The coefficient a can be interpreted as FNIR in a gallery of size 1. The more important coefficient b indicates scalability, and often, $b \ll 1$, implies very benign growth in FNIR. The coefficients of the models appear in the Tables 10 and 11.

– **Slow growth in threshold-based miss rates:** FNIR(N, T) also generally grows as a power law, aN^b except at the high threshold values corresponding to low FPIR values. This is visible in the plots of Figure 37 which show straight lines except for FPIR = 0.001, which increase more rapidly with N above 3 000 000. Each trace in those figures shows FNIR(N, T) at fixed FPIR with both N and T varying. Thus at large N, it is usually necessary to elevate T to maintain fixed FPIR. This causes increased FNIR. Why that would no-longer obey a power-law is not known. However, if we expect large galleries to contain individuals with familial relations to the non-mate search images - in the most extreme case, twins - then suppression of false positives becomes more difficult. This is discussed in the Figures starting at Fig. 8

▷ Figure 20 shows false positives from twins against their enrolled siblings, broken out by type of twin: fraternal or identical. The Figure is based on the enrollment of 104 single images on one of a pair of twins, and then the search of 2354 second images. Note that the dataset is heavily skewed towards identical twins which is not representative of the true population. There is also a skew towards same sex fraternal twin pairs compared to different sex fraternal twin pairs again not representative of the true population.

The notable results are:

– For all algorithms tested, the 1087 mated searches (Twin A vs. Twin A) produce scores almost always above typical operational thresholds, with (not shown) matches at rank 1. The images are of good quality, so this is the result expected from the rest of this report.

– For the 1066 identical twin searches (AB), almost all produce the twin at rank 1, with a few producing the mate at further down the candidate lists rank and low score.

– For the 169 fraternal searches (AB) from same sex pairs, most algorithms give a large number of very high scores, implying false positives at all thresholds. However, there there are long tails containing lower scores that are correctly below threshold. In general, scores that are higher in this distribution are all rank 1 whereas the lower scores have much higher ranks.

– (Not shown) Of the 169, there are 24 fraternal searches (AB) involving different sex twins. Here most algorithms correctly report scores well below the lowest threshold, and usually not on the candidate list at all.

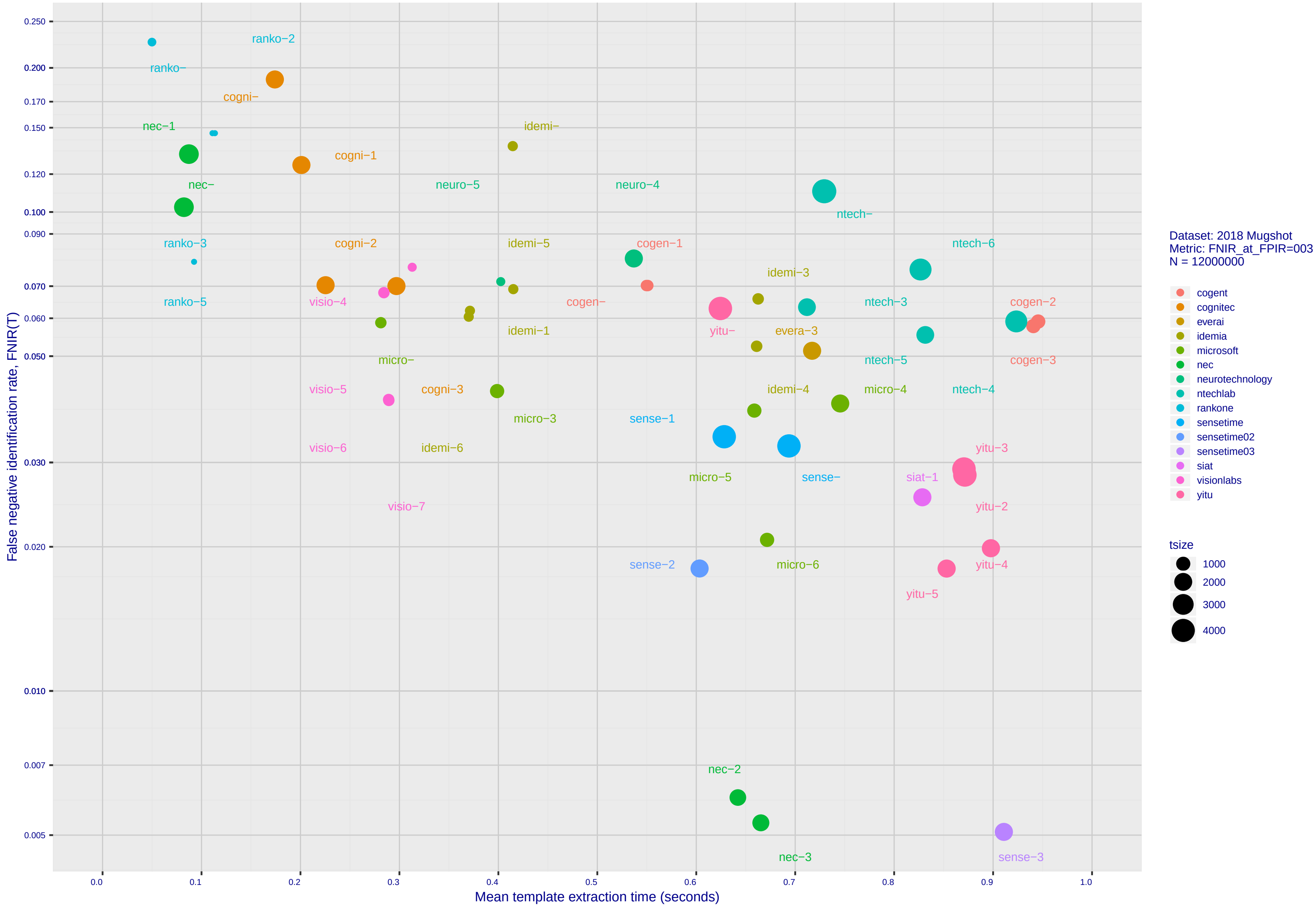

Figure 16: **[Mugshot Dataset] Speed-accuracy tradeoff**. *For developers of the more accurate algorithms the plot shows the tradeoff of high-threshold recognition miss-rates, FNIR(N, N, T) for FPIR(N, T) = 0.003, and template generation time. Developers are coded by color. Template size is encoded by the size of the circle. Some labels are quite distant from the respective point, to avoid superposing text. Without any other influences, the assumption would be that taking time to localize the face, and extract features, would lead to better accuracy. The most notable result, for NEC, is that their slower algorithms are much more accurate than the version that extract features in fewer than 90 milliseconds.*

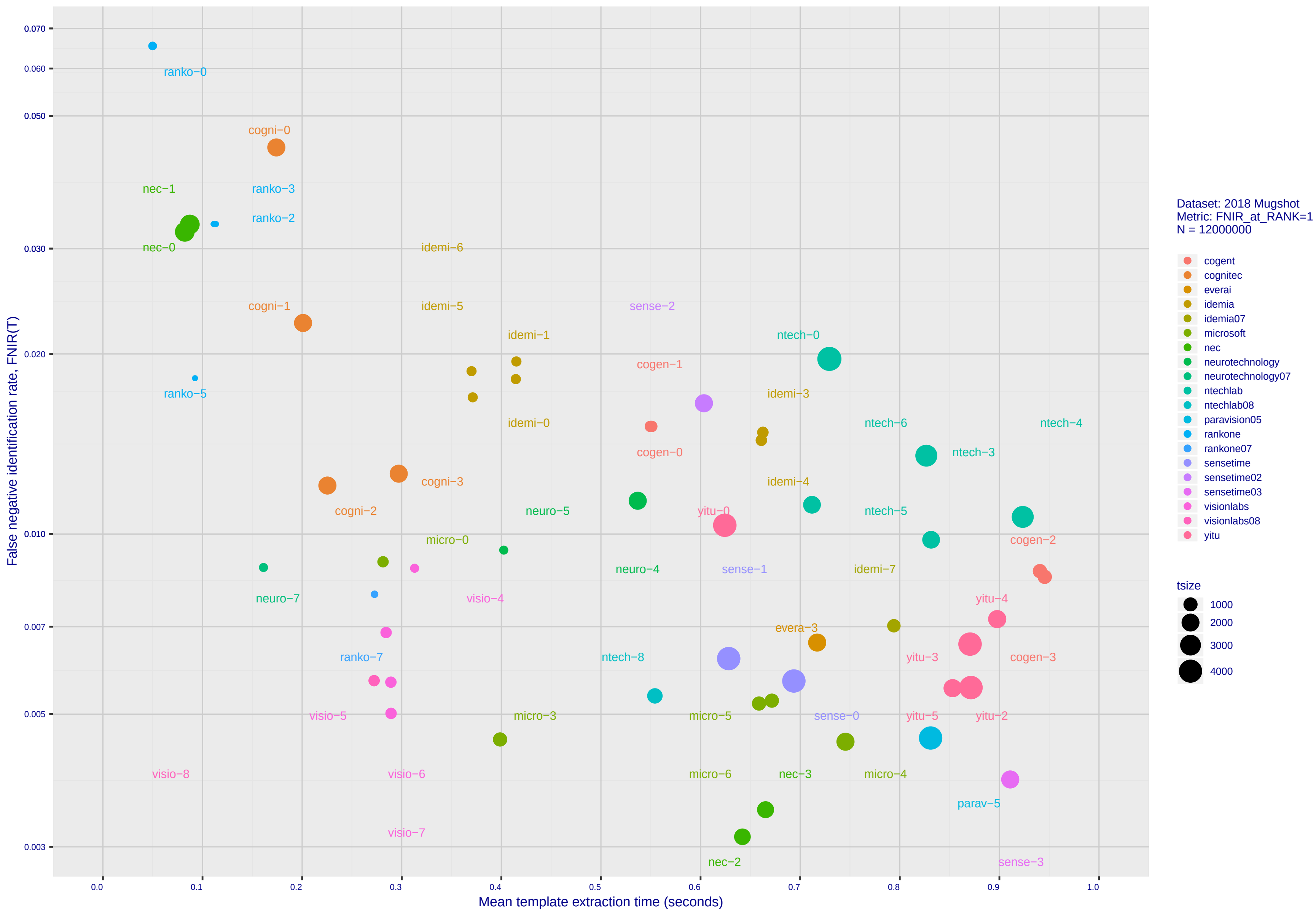

Figure 17: **[Mugshot Dataset] Speed-accuracy tradeoff**. *For developers of the more accurate algorithms the plot shows the tradeoff of rank-one recognition miss-rates, FNIR(N, 1, 0), and template generation time. Developers are coded by color. Template size is encoded by the size of the circle. Some labels are quite distant from the respective point, to avoid superposing text. Without any other influences, the assumption would be that taking time to localize the face, and extract features, would lead to better accuracy. This occurs for NEC with their slower algorithm being much accurate than the version that extract features in fewer than 90 milliseconds.*

FNIR(N, R, T) = False neg. identification rate
FPIR(N, T) = False pos. identification rate
N = Num. enrolled subjects
R = Num. candidates examined
T = Threshold
T = 0 → Investigation
T > 0 → Identification

	DEVELOPER	SHORT	SEQ.	VALIDATION	CONFIG[1]	TEMPLATE GENERATION			SEARCH DURATION[4] MILLISEC					
	FULL NAME	NAME	NUM.	DATE	DATA (MB)	SIZE (B)	MULT[2]	TIME (MS)[3]	L=1	L=50	L=50	L=50	L=50	POWER LAW
									N=1.6M	N=1.6M	N=3M	N=6M	N=12M	(μs)
1	3Divi	3divi	0	2018-02-09	186	[215]4096	k	[99]426	-	[120]553	-	-	-	
2	3Divi	3divi	1	2018-02-15	187	[228]4224	k	[103]428	-	[21]37	-	-	-	
3	3Divi	3divi	2	2018-02-15	187	[52]528	k	[101]428	-	[19]33	-	-	-	
4	3Divi	3divi	3	2018-06-19	165	[46]512	k	[145]625	[17]76	[25]76	-	-	-	
5	3Divi	3divi	4	2018-06-19	186	[211]4096	k	[146]628	[89]604	[145]801	-	-	-	
6	3Divi	3divi	5	2018-10-26	186	[209]4096	k	[155]653	[81]537	[117]537	[51]1376	[48]2612	[41]5524	[71]$0.07\ N^{1.1}$
7	3Divi	3divi	6	2018-10-26	187	[54]528	k	[157]653	[12]33	[17]33	-	-	-	
8	Alchera Inc	alchera	0	2018-06-30	168	[167]2048	k	[47]263	[150]3296	[224]5420	-	-	-	
9	Alchera Inc	alchera	1	2018-06-30	46	[141]2048	k	[8]66	[151]3516	[225]5489	-	-	-	
10	Alchera Inc	alchera	2	2018-10-30	7	[164]2048	k	[16]115	[147]2920	[208]2926	-	-	-	
11	Alchera Inc	alchera	3	2018-10-30	251	[125]2048	k	[131]548	[148]2952	[210]2953	[79]6540	[74]14998	[70]35227	[84]$0.10\ N^{1.2}$
12	AllGoVision	allgovision	000	2019-07-30	168	[154]2048	k	[98]425	[149]3217	[214]3203	-	-	-	
13	Anke Investments	anke	0	2018-10-30	779	[191]2072	k	[105]431	[91]675	[141]748	[53]1482	[50]2965	[43]6142	[58]$0.21\ N^{1.1}$
14	Anke Investments	anke	002	2019-06-27	341	[184]2056	k	[150]641	[90]624	[136]675	-	-	-	
15	Anke Investments	anke	1	2018-10-30	779	[190]2072	k	[106]433	[95]707	[143]769	-	-	-	
16	Aware	aware	0	2018-02-16	261	[108]1564	k	[156]653	-	[66]251	-	-	-	
17	Aware	aware	1	2018-02-16	232	[109]1564	k	[153]651	-	[67]251	-	-	-	
18	Aware	aware	2	2018-02-16	349	[193]2076	k	[229]912	-	[68]252	-	-	-	
19	Aware	aware	3	2018-06-22	350	[192]2076	k	[187]716	[143]2426	[203]2508	[74]4495	-	-	[41]$1.09\ N^{1.0}$
20	Aware	aware	4	2018-06-22	349	[2]92	k	[183]712	[114]1232	[165]1187	-	-	-	
21	Aware	aware	5	2018-10-30	368	[202]3100	k	[210]827	[20]94	[28]97	[13]202	[11]370	[9]251	[11]$4.13\ N^{0.7}$
22	Aware	aware	6	2018-10-30	368	[3]124	k	[203]818	[31]157	[43]162	-	-	-	
23	Ayonix	ayonix	0	2018-06-21	57	[84]1036	k	[1]10	[53]283	[81]298	-	-	-	
24	Ayonix	ayonix	1	2018-10-29	74	[88]1036	k	[3]12	[50]277	[76]277	-	-	-	
25	Ayonix	ayonix	2	2018-10-30	74	[86]1036	1	[2]11	[49]277	[75]274	[27]531	[25]1079	[22]2268	[50]$0.11\ N^{1.0}$
26	Camvi Technologies	camvitech	1	2018-02-16	94	[76]1024	1	[25]177	-	[13]23	-	-	-	
27	Camvi Technologies	camvitech	2	2018-02-16	442	[81]1024	1	[198]774	-	[12]20	-	-	-	
28	Camvi Technologies	camvitech	3	2018-06-30	233	[79]1024	1	[181]707	[8]10	[10]11	-	-	-	
29	Camvi Technologies	camvitech	4	2018-10-30	233	[73]1024	1	[189]718	[13]33	[16]32	[8]38	[6]40	[4]48	[2]$8492.66\ N^{0.1}$
30	Camvi Technologies	camvitech	5	2018-10-30	257	[68]1024	1	[196]769	[11]31	[15]30	-	-	-	
31	Thales	cogent	0	2018-06-20	533	[51]525	k	[132]551	[77]494	[123]558	[42]1047	[41]2060	[33]4141	[21]$0.46\ N^{1.0}$
32	Thales	cogent	1	2018-06-20	533	[50]525	k	[133]552	[78]498	[121]556	[43]1048	[42]2082	[35]4263	[26]$0.39\ N^{1.0}$
33	Thales	cogent	2	2018-10-30	681	[91]1043	k	[236]987	[137]2017	[195]2144	[73]4298	[69]8472	[65]16429	[37]$1.08\ N^{1.0}$
34	Thales	cogent	3	2018-10-30	681	[90]1043	k	[235]960	[113]1230	[171]1311	[63]2687	[60]5398	[55]10184	[39]$0.62\ N^{1.0}$
35	Cognitec Systems GmbH	cognitec	0	2018-06-21	364	[177]2052	k	[24]176	[129]1748	[183]1780	[68]3672	[64]7093	[63]15224	[55]$0.57\ N^{1.0}$
36	Cognitec Systems GmbH	cognitec	1	2018-06-21	412	[171]2052	k	[32]202	[132]1835	[185]1805	[71]3971	[67]7484	[64]16249	[60]$0.49\ N^{1.1}$
37	Cognitec Systems GmbH	cognitec	2	2018-10-30	463	[173]2052	k	[38]227	[128]1733	[182]1763	[67]3660	[66]7279	[59]13895	[40]$0.83\ N^{1.0}$
38	Cognitec Systems GmbH	cognitec	3	2018-10-30	465	[179]2052	k	[59]297	[127]1719	[184]1791	[66]3638	[65]7277	[61]14904	[52]$0.66\ N^{1.0}$
39	Cyberlink Corp	cyberlink	000	2019-06-12	217	[169]2052	1	[175]699	[93]694	[138]694	-	-	-	
40	Cyberlink Corp	cyberlink	001	2019-10-07	459	[180]2052	1	[107]433	[94]698	[139]697	-	-	-	
41	Dahua Technology Co Ltd	dahua	0	2018-10-29	276	[149]2048	k	[79]378	-	[71]256	-	-	-	
42	Dahua Technology Co Ltd	dahua	002	2019-12-02	607	[135]2048	k	[176]699	[46]243	[61]242	-	-	-	
43	Dahua Technology Co Ltd	dahua	1	2018-10-29	276	[127]2048	k	[75]371	-	[70]256	[33]601	[31]1199	[30]3001	[78]$0.02\ N^{1.2}$
44	Deepglint	deepglint	001	2019-10-25	448	[213]4096	1	[174]696	[76]484	[112]493	-	-	-	
45	Tencent Deepsea Lab	deepsea	001	2019-07-29	250	[129]2048	1	[200]780	[107]1021	[155]1017	-	-	-	
46	Dermalog	dermalog	0	2018-02-16	0	[5]128	1	[72]344	-	[98]404	-	-	-	
47	Dermalog	dermalog	1	2018-02-16	0	[8]128	1	[23]171	-	[102]407	-	-	-	
48	Dermalog	dermalog	2	2018-02-16	0	[20]256	k	[71]344	-	[134]640	-	-	-	
49	Dermalog	dermalog	3	2018-06-21	0	[7]128	1	[35]211	[19]92	[26]92	-	-	-	
50	Dermalog	dermalog	4	2018-06-21	0	[4]128	1	[33]208	[18]91	[27]93	-	-	-	
51	Dermalog	dermalog	5	2018-10-26	0	[6]128	1	[122]532	[3]0	[2]0	[1]0	[1]0	[1]0	[4]$66.21\ N^{0.2}$
52	Dermalog	dermalog	6	2018-10-26	0	[26]256	1	[117]514	[28]141	[38]143	[18]267	[16]527	[14]1285	[53]$0.05\ N^{1.0}$

Notes	
1	Configuration size does not capture static data present in libraries. Libraries are not counted because most implementations include common ancillary libraries for image processing (e.g. openCV) or numerical computation (e.g. blas).
2	This multiplier expresses the increase in template size when k images are passed to the template generation function.
3	All durations are measured on Intel®Xeon®CPU E5-2630 v4 @ 2.20GHz processors. Estimates are made by wrapping the API function call in calls to std::chrono::high_resolution_clock which on the machine in (3) counts 1ns clock ticks. Precision is somewhat worse than that however.
4	Search durations are measured as in the prior note. The power-law model in the final column mostly fits the empirical results in Figure 105. However in certain cases the model is not correct and should not be used numerically.

Table 2: Summary of algorithms and properties included in this report. The blue superscripts give ranking for the quantity in that column. Missing search durations, denoted by "-", are absent because those runs were not executed, usually because we did not run on the larger galleries. Caution: The power-law model is sometimes an incorrect model. It is included here only to show broad sublinear behavior, which is flagged in green. The models should not be used for prediction.

FNIR(N, R, T) = False neg. identification rate
FPIR(N, T) = False pos. identification rate
N = Num. enrolled subjects
R = Num. candidates examined
T = Threshold
T = 0 → Investigation
T > 0 → Identification

	DEVELOPER FULL NAME	SHORT NAME	SEQ. NUM.	VALIDATION DATE	CONFIG[1] DATA (MB)	TEMPLATE GENERATION SIZE (B)	MULT[2]	TIME (MS)[3]	SEARCH DURATION[4] MILLISEC L=1 N=1.6M	L=50 N=1.6M	L=50 N=3M	L=50 N=6M	L=50 N=12M	POWER LAW (μs)
53	Paravision (EverAI)	everai	0	2018-06-21	142	[161]2048	1	[109]438	[5]4	[6]3	[2]5	-	-	[9]42.41 $N^{0.3}$
54	Paravision (EverAI)	everai	1	2018-06-21	200	[122]2048	1	[140]590	[58]336	[89]356	[35]651	-	-	[74]0.03 $N^{1.1}$
55	Paravision (EverAI)	everai	2	2018-10-30	224	[150]2048	1	[78]377	[52]278	[78]283	-	-	-	
56	Paravision (EverAI)	everai	3	2018-10-30	438	[124]2048	1	[193]735	[51]278	[77]281	[30]572	[29]1146	[23]2278	[48]0.12 $N^{1.0}$
57	Paravision (EverAI)	everai-paravision	004	2019-06-19	527	[207]4096	1	[191]720	[84]559	[126]562	-	-	-	
58	Eyedea Recognition	eyedea	0	2018-02-16	644	[227]4152	k	[97]424	-	[135]640	-	-	-	
59	Eyedea Recognition	eyedea	1	2018-02-16	287	[89]1036	k	[63]311	-	[83]307	-	-	-	
60	Eyedea Recognition	eyedea	2	2018-02-16	287	[85]1036	k	[104]429	-	[82]305	-	-	-	
61	Eyedea Recognition	eyedea	3	2018-06-18	284	[87]1036	k	[80]385	[55]309	[85]311	-	-	-	
62	FarBar Inc	f8	001	2019-10-03	266	[134]2048	k	[218]851	[1]0	[1]0	-	-	-	
63	Glory Ltd	glory	0	2018-06-30	0	[37]418	k	[18]160	[86]575	[127]575	-	-	-	
64	Glory Ltd	glory	1	2018-06-30	0	[112]1726	k	[89]405	[133]1864	[188]1978	-	-	-	
65	Gorilla Technology	gorilla	0	2018-02-01	95	[235]8300	k	[100]427	-	[232]10426	-	-	-	
66	Gorilla Technology	gorilla	004	2020-01-06	182	[197]2192	k	[83]395	[54]286	[80]285	-	-	-	
67	Gorilla Technology	gorilla	1	2018-06-19	91	[196]2156	k	[21]169	[159]5254	[221]5156	-	-	-	
68	Gorilla Technology	gorilla	2	2018-10-29	91	[94]1132	k	[69]341	[29]145	[40]146	[19]293	[17]612	[17]1509	[66]0.02 $N^{1.1}$
69	Gorilla Technology	gorilla	3	2018-10-26	94	[195]2156	k	[139]563	[134]1934	[190]2047	-	-	-	
70	loginface Corp	hbinno	0	2018-02-01	88	[49]520	-	[48]265	-	[106]419	-	-	-	
71	Hikvision Research Institute	hikvision	0	2018-02-12	378	[114]1808	1	[225]875	-	[200]2360	-	-	-	
72	Hikvision Research Institute	hikvision	1	2018-02-12	378	[116]1808	1	[206]820	-	[201]2403	-	-	-	
73	Hikvision Research Institute	hikvision	2	2018-02-12	378	[115]1808	1	[204]820	-	[202]2408	-	-	-	
74	Hikvision Research Institute	hikvision	3	2018-06-30	408	[99]1408	1	[148]633	[104]904	[160]1108	[60]2377	[53]3785	[45]7570	[20]0.91 $N^{1.0}$
75	Hikvision Research Institute	hikvision	4	2018-06-30	334	[95]1152	1	[115]510	[99]784	[156]1024	[58]2094	[52]3254	[44]7117	[19]0.86 $N^{1.0}$
76	Hikvision Research Institute	hikvision	5	2018-10-29	593	[98]1408	1	[144]619	[103]883	[152]895	[55]1908	[54]3792	[52]9387	[72]0.10 $N^{1.1}$
77	Hikvision Research Institute	hikvision	6	2018-10-29	593	[97]1408	1	[141]610	[102]871	[151]877	-	-	-	
78	Idemia	idemia	0	2018-02-16	371	[36]364	1	[94]416	-	[31]133	[14]249	[12]502	-	[33]0.08 $N^{1.0}$
79	Idemia	idemia	007	2020-01-17	738	[65]860	1	[202]807	[30]151	[41]153	-	-	-	
80	Idemia	idemia	1	2018-02-16	371	[34]364	1	[95]417	-	[36]138	-	-	-	
81	Idemia	idemia	2	2018-02-16	371	[35]364	1	[96]417	-	[37]138	-	-	-	
82	Idemia	idemia	3	2018-06-21	472	[53]528	1	[168]689	[57]318	[90]361	[34]631	[28]1104	[24]2332	[12]5.03 $N^{0.8}$
83	Idemia	idemia	4	2018-06-21	472	[55]528	1	[165]669	[33]168	[58]211	[25]475	[23]995	[21]2225	[73]0.02 $N^{1.1}$
84	Idemia	idemia	5	2018-10-29	417	[32]352	1	[77]374	[23]137	[35]138	[23]437	[19]724	[19]1630	[82]0.01 $N^{1.2}$
85	Idemia	idemia	6	2018-10-29	417	[33]352	1	[76]373	[24]137	[34]138	[24]442	[22]827	[20]1646	[83]0.01 $N^{1.2}$
86	Institute of Information Technologies	iit	002	2019-12-04	253	[158]2048	k	[119]526	[121]1331	[174]1323	-	-	-	
87	Imagus Technology Pty Ltd	imagus	0	2018-02-14	35	[42]512	k	[5]43	-	[53]202	-	-	-	
88	Imagus Technology Pty Ltd	imagus	2	2018-06-21	35	[38]512	k	[9]76	[42]200	[57]208	-	-	-	
89	Imagus Technology Pty Ltd	imagus	3	2018-06-21	46	[44]512	k	[7]57	[43]201	[55]206	-	-	-	
90	Imperial College London	imperial	000	2019-08-28	461	[143]2048	1	[159]654	[60]360	[92]368	-	-	-	
91	Incode Technologies Inc	incode	0	2018-06-29	23	[82]1024	k	[30]190	[119]1293	[215]3510	-	-	-	
92	Incode Technologies Inc	incode	004	2019-06-24	254	[133]2048	1	[114]508	[61]365	[91]365	-	-	-	
93	Incode Technologies Inc	incode	1	2018-06-29	151	[165]2048	k	[170]690	[123]1542	[218]4497	-	-	-	
94	Incode Technologies Inc	incode	2	2018-10-29	71	[137]2048	1	[56]291	[71]411	[100]404	-	-	-	
95	Incode Technologies Inc	incode	3	2018-10-29	133	[160]2048	1	[179]704	[70]408	[105]412	[38]846	[35]1606	[36]4482	[69]0.05 $N^{1.1}$
96	Innovatrics	innovatrics	0	2018-02-16	0	[58]530	k	[110]455	-	[133]625	-	-	-	
97	Innovatrics	innovatrics	1	2018-02-16	0	[56]530	k	[65]316	-	[132]625	-	-	-	
98	Innovatrics	innovatrics	2	2018-06-21	0	[57]530	k	[44]255	[4]1	[4]2	-	-	-	
99	Innovatrics	innovatrics	3	2018-06-21	0	[59]530	k	[45]255	[138]2020	[186]1882	-	-	-	
100	Innovatrics	innovatrics	4	2018-10-30	0	[92]1076	k	[91]406	[7]8	[9]8	[4]11	[3]9	[2]13	[7]668.38 $N^{0.2}$
101	Lomonosov Moscow State University	intsysmsu	000	2019-08-19	375	[132]2048	1	[167]675	[72]430	[108]447	-	-	-	
102	Alivia / Innovation Sys	isystems	0	2018-02-14	262	[152]2048	1	[37]222	-	[95]393	-	-	-	
103	Alivia / Innovation Sys	isystems	1	2018-02-14	263	[70]1024	1	[36]222	-	[60]240	-	-	-	
104	Alivia / Innovation Sys	isystems	2	2018-06-25	268	[144]2048	1	[66]316	[66]385	[111]484	[50]1275	[39]1770	[31]3063	[16]0.68 $N^{0.9}$

Notes	
1	Configuration size does not capture static data present in libraries. Libraries are not counted because most implementations include common ancillary libraries for image processing (e.g. openCV) or numerical computation (e.g. blas).
2	This multiplier expresses the increase in template size when k images are passed to the template generation function.
3	All durations are measured on Intel®Xeon®CPU E5-2630 v4 @ 2.20GHz processors. Estimates are made by wrapping the API function call in calls to std::chrono::high_resolution_clock which on the machine in (3) counts 1ns clock ticks. Precision is somewhat worse than that however.
4	Search durations are measured as in the prior note. The power-law model in the final column mostly fits the empirical results in Figure 105. However in certain cases the model is not correct and should not be used numerically.

Table 3: Summary of algorithms and properties included in this report. The blue superscripts give ranking for the quantity in that column. Missing search durations, denoted by "-", are absent because those runs were not executed, usually because we did not run on the larger galleries. Caution: The power-law model is sometimes an incorrect model. It is included here only to show broad sublinear behavior, which is flagged in green. The models should not be used for prediction.

	DEVELOPER FULL NAME	SHORT NAME	SEQ. NUM.	VALIDATION DATE	CONFIG[1] DATA (MB)	TEMPLATE GENERATION SIZE (B)	MULT[2]	TIME (MS)[3]	SEARCH DURATION[4] MILLISEC L=1 N=1.6M	L=50 N=1.6M	L=50 N=3M	L=50 N=6M	L=50 N=12M	POWER LAW (μs)
105	Alivia / Innovation Sys	isystems	3	2018-10-30	350	[163] 2048	1	[219] 856	[65] 384	[94] 387	[41] 976	[40] 1817	[51] 9319	[86] $0.00\ N^{1.3}$
106	Kedacom International Pte	kedacom	001	2019-09-16	239	[30] 292	1	[126] 537	[97] 764	[142] 764	-	-	-	
107	Lookman Electroplast Industries	lookman	005	2019-09-16	239	[61] 548	1	[116] 514	[106] 1005	[154] 1010	-	-	-	
108	Lookman Electroplast Industries	lookman	3	2018-10-28	203	[29] 292	1	[70] 342	[96] 739	[140] 745	[52] 1394	[49] 2817	[46] 8286	[64] $0.13\ N^{1.1}$
109	Lookman Electroplast Industries	lookman	4	2018-10-28	184	[60] 548	1	[67] 325	[105] 981	[153] 998	-	-	-	
110	Megvii/Face++	megvii	0	2018-02-15	1327	[157] 2048	1	[201] 794	-	[79] 284	[26] 530	[24] 1060	-	[30] $0.18\ N^{1.0}$
111	Megvii/Face++	megvii	1	2018-10-28	1703	[216] 4096	1	[154] 652	[82] 551	[125] 560	[49] 1219	[45] 2316	[42] 5956	[68] $0.08\ N^{1.1}$
112	Megvii/Face++	megvii	2	2018-10-28	1735	[214] 4096	1	[160] 656	[83] 552	[122] 557	-	-	-	
113	MicroFocus	microfocus	0	2018-02-12	101	[23] 256	k	[118] 525	-	[47] 184	-	-	-	
114	MicroFocus	microfocus	1	2018-02-16	101	[15] 256	k	[120] 527	-	[22] 39	-	-	-	
115	MicroFocus	microfocus	2	2018-02-16	101	[24] 256	k	[121] 529	-	[5] 2	-	-	-	
116	MicroFocus	microfocus	3	2018-06-22	101	[16] 256	k	[51] 269	[38] 185	[50] 188	-	-	-	
117	MicroFocus	microfocus	4	2018-06-22	102	[22] 256	k	[52] 270	[39] 186	[51] 189	-	-	-	
118	MicroFocus	microfocus	5	2018-10-29	94	[28] 256	k	[50] 266	[36] 182	[49] 186	[20] 353	[18] 706	[15] 1422	[34] $0.11\ N^{1.0}$
119	MicroFocus	microfocus	6	2018-10-29	94	[21] 256	k	[49] 265	[37] 182	[48] 186	-	-	-	
120	Microsoft	microsoft	0	2018-01-30	126	[48] 512	1	[55] 283	-	[129] 593	[47] 1193	[46] 2395	[38] 4936	[51] $0.22\ N^{1.0}$
121	Microsoft	microsoft	1	2018-02-12	165	[75] 1024	1	[73] 349	-	[150] 869	-	-	-	
122	Microsoft	microsoft	2	2018-02-12	228	[80] 1024	1	[134] 555	-	[149] 869	-	-	-	
123	Microsoft	microsoft	3	2018-06-20	230	[72] 1024	1	[88] 404	[125] 1638	[177] 1603	[65] 3260	[63] 6730	[58] 13833	[56] $0.51\ N^{1.1}$
124	Microsoft	microsoft	4	2018-06-20	437	[145] 2048	1	[197] 773	[146] 2662	[206] 2691	[75] 5260	[71] 11070	[67] 22748	[57] $0.83\ N^{1.1}$
125	Microsoft	microsoft	5	2018-10-29	381	[77] 1024	1	[166] 673	[124] 1604	[179] 1671	[64] 3073	[61] 6296	[57] 13147	[38] $0.79\ N^{1.0}$
126	Microsoft	microsoft	6	2018-10-29	478	[69] 1024	1	[172] 695	[126] 1640	[178] 1617	[69] 3707	[62] 6394	[56] 12879	[47] $0.68\ N^{1.0}$
127	NEC	nec	0	2018-06-21	131	[201] 2592	k	[10] 82	[56] 317	[107] 426	[37] 738	[33] 1315	[27] 2737	[14] $0.73\ N^{0.9}$
128	NEC	nec	1	2018-06-29	131	[200] 2592	k	[11] 88	[41] 193	[56] 208	[22] 388	[20] 750	[18] 1577	[18] $0.21\ N^{1.0}$
129	NEC	nec	2	2018-10-30	705	[110] 1616	k	[158] 653	[69] 405	[104] 409	[44] 1072	[37] 1755	[34] 4255	[70] $0.06\ N^{1.1}$
130	NEC	nec	3	2018-10-30	774	[111] 1712	k	[169] 690	[6] 7	[8] 7	[5] 14	[5] 40	[6] 82	[80] $0.00\ N^{1.2}$
131	Neurotechnology	neurotech	0	2018-02-16	331	[230] 5214	k	[177] 702	-	[211] 3040	-	-	-	
132	Neurotechnology	neurotech	007	2019-10-03	57	[27] 256	k	[22] 169	[110] 1118	[161] 1119	-	-	-	
133	Neurotechnology	neurotech	1	2018-02-16	331	[231] 5214	k	[163] 661	-	[213] 3054	-	-	-	
134	Neurotechnology	neurotech	2	2018-02-16	331	[232] 5214	k	[162] 658	-	[212] 3051	-	-	-	
135	Neurotechnology	neurotech	3	2018-06-27	265	[128] 2048	k	[130] 547	[109] 1084	[157] 1059	[59] 2111	[57] 4779	[49] 8793	[31] $0.73\ N^{1.0}$
136	Neurotechnology	neurotech	4	2018-06-27	265	[166] 2048	k	[129] 543	[108] 1060	[158] 1061	[57] 2091	[56] 4263	[47] 8736	[17] $1.22\ N^{1.0}$
137	Neurotechnology	neurotech	5	2018-10-30	266	[19] 256	k	[92] 412	[100] 835	[147] 839	[54] 1690	[51] 3219	[50] 8955	[62] $0.19\ N^{1.1}$
138	Neurotechnology	neurotech	6	2018-10-30	564	[18] 256	k	[195] 746	[101] 839	[148] 842	-	-	-	
139	Newland Computer Co Ltd	newland	2	2018-10-30	96	[121] 2048	-	[222] 868	[166] 8653	[231] 8765	[86] 17713	[81] 38963	-	[67] $1.32\ N^{1.1}$
140	Noblis	noblis	1	2018-10-30	114	[146] 2048	1	[34] 211	[117] 1273	[168] 1272	-	-	-	
141	Noblis	noblis	2	2018-10-30	153	[233] 6144	1	[123] 535	[145] 2513	[204] 2522	[76] 5649	[72] 12432	[73] 44262	[85] $0.04\ N^{1.3}$
142	N-Tech Lab	ntech	0	2018-02-16	2124	[229] 4442	k	[192] 730	-	[93] 382	[36] 673	[34] 1344	-	[22] $0.27\ N^{1.0}$
143	N-Tech Lab	ntechlab	007	2019-06-25	2450	[203] 3348	k	[215] 834	[67] 393	[99] 404	-	-	-	
144	N-Tech Lab	ntechlab	008	2020-01-06	1111	[96] 1300	k	[138] 562	[35] 179	[46] 181	-	-	-	
145	N-Tech Lab	ntech	1	2018-02-16	851	[113] 1736	k	[90] 405	-	[42] 161	-	-	-	
146	N-Tech Lab	ntech	3	2018-06-21	3664	[204] 3484	k	[212] 831	[64] 384	[87] 326	[31] 596	[30] 1192	[25] 2411	[24] $0.24\ N^{1.0}$
147	N-Tech Lab	ntech	4	2018-06-21	3766	[205] 3484	k	[230] 929	[62] 378	[86] 312	[32] 597	[32] 1204	[26] 2416	[29] $0.21\ N^{1.0}$
148	N-Tech Lab	ntech	5	2018-10-30	1685	[119] 1940	k	[188] 717	[48] 243	[63] 246	[28] 538	[26] 1100	[28] 2867	[75] $0.02\ N^{1.1}$
149	N-Tech Lab	ntech	6	2018-10-30	1686	[120] 1940	k	[216] 841	[47] 243	[62] 246	[29] 546	[27] 1104	[29] 2873	[77] $0.02\ N^{1.1}$
150	Paravision (EverAI)	paravision	005	2019-12-11	543	[217] 4096	1	[220] 858	[85] 561	[124] 559	-	-	-	
151	Guangzhou Pixel Solutions Co Ltd	pixelall	002	2019-07-01	0	[198] 2560	k	[31] 198	[120] 1296	[173] 1322	-	-	-	
152	Guangzhou Pixel Solutions Co Ltd	pixelall	003	2019-11-05	0	[199] 2560	k	[190] 719	[116] 1273	[172] 1313	-	-	-	
153	Quantasoft	quantasoft	1	2018-10-30	276	[130] 2048	k	[84] 396	[167] 15422	[233] 14858	[85] 14717	-	[66] 18323	
154	Rank One Computing	rankone	0	2018-02-07	0	[14] 228	k	[6] 50	-	[24] 75	[11] 142	[10] 220	[10] 502	[15] $0.12\ N^{0.9}$
155	Rank One Computing	rankone	006	2019-06-03	0	[13] 165	k	[46] 261	-	-	-	-	-	
156	Rank One Computing	rankone	007	2019-11-12	0	[12] 165	k	[54] 278	[22] 116	[30] 115	-	-	-	

Notes	
1	Configuration size does not capture static data present in libraries. Libraries are not counted because most implementations include common ancillary libraries for image processing (e.g. openCV) or numerical computation (e.g. blas).
2	This multiplier expresses the increase in template size when k images are passed to the template generation function.
3	All durations are measured on Intel®Xeon®CPU E5-2630 v4 @ 2.20GHz processors. Estimates are made by wrapping the API function call in calls to std::chrono::high_resolution_clock which on the machine in (3) counts 1ns clock ticks. Precision is somewhat worse than that however.
4	Search durations are measured as in the prior note. The power-law model in the final column mostly fits the empirical results in Figure 105. However in certain cases the model is not correct and should not be used numerically.

Table 4: Summary of algorithms and properties included in this report. The blue superscripts give ranking for the quantity in that column. Missing search durations, denoted by "-", are absent because those runs were not executed, usually because we did not run on the larger galleries. Caution: The power-law model is sometimes an incorrect model. It is included here only to show broad sublinear behavior, which is flagged in green. The models should not be used for prediction.

	DEVELOPER	SHORT	SEQ.	VALIDATION	CONFIG[1]	TEMPLATE GENERATION			SEARCH DURATION[4] MILLISEC					
	FULL NAME	NAME	NUM.	DATE	DATA (MB)	SIZE (B)	MULT[2]	TIME (MS)[3]	L=1 N=1.6M	L=50 N=1.6M	L=50 N=3M	L=50 N=6M	L=50 N=12M	POWER LAW (μs)
157	Rank One Computing	rankone	1	2018-02-15	0	[31]324	k	[17]136	-	[45]169	-	-	-	
158	Rank One Computing	rankone	2	2018-06-19	0	[10]133	k	[14]113	[25]138	[32]137	[16]258	[14]517	[12]1029	[25]0.10 $N^{1.0}$
159	Rank One Computing	rankone	3	2018-06-19	0	[11]133	k	[15]114	[26]138	[33]137	[15]258	[13]515	[11]1027	[28]0.09 $N^{1.0}$
160	Rank One Computing	rankone	4	2018-10-09	0	[1]85	k	[4]36	[21]101	[29]101	[12]190	-	-	[27]0.07 $N^{1.0}$
161	Rank One Computing	rankone	5	2018-10-24	0	[9]133	k	[12]94	[27]140	[39]144	[17]266	[15]525	[13]1049	[23]0.11 $N^{1.0}$
162	Realnetworks Inc	realnetworks	0	2018-06-21	96	[218]4100	1	[42]244	[153]4257	[207]2740	-	-	-	
163	Realnetworks Inc	realnetworks	003	2019-06-12	93	[118]1848	k	[26]178	[112]1143	[163]1138	-	-	-	
164	Realnetworks Inc	realnetworks	004	2019-10-17	94	[117]1848	1	[27]185	[111]1142	[164]1145	-	-	-	
165	Realnetworks Inc	realnetworks	1	2018-06-21	105	[222]4104	k	[41]243	[152]3568	[193]2107	-	-	-	
166	Realnetworks Inc	realnetworks	2	2018-10-30	105	[220]4104	k	[43]245	[136]2006	[189]2046	[72]4190	[70]8633	[62]15020	[36]1.08 $N^{1.0}$
167	Remark Holdings	remarkai	0	2018-10-30	187	[147]2048	k	[142]615	[162]5685	[226]5723	-	-	-	
168	Remark Holdings	remarkai	000	2019-06-12	234	[123]2048	k	[171]691	[163]5776	[227]5748	-	-	-	
169	Remark Holdings	remarkai	1	2018-10-30	187	[126]2048	k	[108]434	[161]5680	[228]5761	[84]12475	[80]28726	[76]59618	[81]0.37 $N^{1.2}$
170	Scanovate Ltd	scanovate	000	2020-01-15	250	[159]2048	1	[184]712	[122]1419	[176]1417	-	-	-	
171	Sensetime Group	sensetime	0	2018-10-30	525	[219]4104	k	[186]715	[79]498	[113]501	[48]1212	[43]2281	[40]5032	[65]0.09 $N^{1.1}$
172	Sensetime Group	sensetime	002	2019-06-03	523	[183]2056	k	[152]650	[59]359	[88]350	-	-	-	
173	Sensetime Group	sensetime	003	2019-12-02	769	[182]2056	1	[234]940	[156]4885	[220]5001	-	-	-	
174	Sensetime Group	sensetime	1	2018-10-30	525	[221]4104	k	[161]656	[80]516	[114]502	[45]1146	[44]2301	[37]4765	[63]0.09 $N^{1.1}$
175	Shaman Software	shaman	0	2018-02-12	0	[212]4096	k	[127]538	-	[115]523	-	-	-	
176	Shaman Software	shaman	1	2018-02-12	0	[210]4096	k	[135]557	-	[116]524	-	-	-	
177	Shaman Software	shaman	2	2018-02-12	0	[234]8192	k	[136]557	-	[137]688	-	-	-	
178	Shaman Software	shaman	3	2018-06-30	0	[142]2048	k	[178]704	[92]692	[84]310	-	-	-	
179	Shaman Software	shaman	4	2018-06-30	0	[155]2048	k	[151]642	[74]434	[72]267	-	-	-	
180	Shaman Software	shaman	6	2018-10-26	0	[151]2048	k	[180]706	[88]594	[130]603	-	-	-	
181	Shaman Software	shaman	7	2018-10-26	0	[140]2048	k	[182]709	[87]593	[131]605	[46]1169	[47]2411	[39]5007	[49]0.25 $N^{1.0}$
182	Shenzhen Inst Adv Integrated Tech CAS	SIAT	0	2018-02-14	306	[93]1096	k	[74]358	-	[175]1343	-	-	-	
183	Shenzhen Inst Adv Integrated Tech CAS	SIAT	1	2018-06-30	521	[168]2052	1	[217]842	[155]4512	[216]4402	[81]9103	[76]18391	[71]38745	[44]2.06 $N^{1.0}$
184	Shenzhen Inst Adv Integrated Tech CAS	SIAT	2	2018-02-30	521	[175]2052	1	[227]906	[157]5101	[219]4884	[82]9556	[77]18834	[72]39717	[45]2.08 $N^{1.0}$
185	Smilart	smilart	0	2018-02-15	105	[71]1024	k	[20]168	-	[169]1285	-	-	-	
186	Smilart	smilart	1	2018-02-15	120	[78]1024	k	[164]662	-	[162]1135	-	-	-	
187	Smilart	smilart	2	2018-02-15	109	[74]1024	k	[137]560	-	[170]1302	-	-	-	
188	Smilart	smilart	4	2018-10-30	65	[40]512	k	[19]167	[168]15879	[234]15382	-	-	-	
189	Smilart	smilart	5	2018-10-30	562	[148]2048	k	[111]464	-	-	-	-	-	
190	Synesis	synesis	0	2018-02-15	332	[43]512	k	[40]237	-	[44]162	-	-	-	
191	Synesis	synesis	3	2018-10-30	237	[208]4096	k	[13]103	[98]784	[144]796	[56]1928	[55]3861	[48]8748	[76]0.07 $N^{1.1}$
192	Tech5 SA	tech5	001	2019-08-19	1394	[100]1536	k	[226]898	[63]383	[146]808	-	-	-	
193	Tevian	tevian	0	2018-02-16	666	[139]2048	1	[82]394	-	[101]405	-	-	-	
194	Tevian	tevian	1	2018-02-16	666	[156]2048	1	[87]398	-	[97]403	-	-	-	
195	Tevian	tevian	2	2018-02-16	666	[153]2048	1	[85]397	-	[96]402	-	-	-	
196	Tevian	tevian	3	2018-06-20	707	[131]2048	1	[61]300	[75]473	[119]539	-	-	-	
197	Tevian	tevian	4	2018-06-20	707	[162]2048	1	[60]299	[73]434	[118]537	-	-	-	
198	Tevian	tevian	5	2018-10-30	773	[138]2048	1	[93]416	[68]405	[103]407	[39]852	[36]1753	[32]3373	[54]0.14 $N^{1.0}$
199	TigerIT Americas LLC	tiger	0	2018-06-29	333	[174]2052	k	[102]428	[131]1822	[209]2942	-	-	-	
200	TigerIT Americas LLC	tiger	1	2018-06-27	333	[170]2052	k	[86]398	[2]0	[3]1	-	-	-	
201	TigerIT Americas LLC	tiger	2	2018-10-29	416	[178]2052	k	[113]464	[130]1814	[187]1919	[70]3829	[68]7519	[60]14805	[43]0.83 $N^{1.0}$
202	TigerIT Americas LLC	tiger	3	2018-10-30	416	[176]2052	k	[112]464	[40]191	[52]189	-	-	-	
203	TongYi Transportation Technology	tongyi	0	2018-06-29	1701	[189]2070	k	[29]190	[142]2256	[198]2272	-	-	-	
204	TongYi Transportation Technology	tongyi	1	2018-06-29	1701	[187]2070	1	[28]189	[141]2238	[197]2257	-	-	-	
205	Toshiba	toshiba	0	2018-10-30	961	[107]1548	k	[232]930	[165]6147	[229]6230	[83]12209	[79]25330	[75]49398	[79]0.36 $N^{1.2}$
206	Toshiba	toshiba	1	2018-10-30	961	[185]2060	k	[233]931	[164]6001	[230]6349	-	-	-	
207	Visidon	visidon	0	2018-06-20	208	[83]1028	k	[68]337	[135]2006	[205]2566	-	-	-	
208	Visidon	visidon	1	2018-10-30	166	[172]2052	k	[173]695	[154]4357	[217]4458	[80]8429	[75]17210	[69]34185	[35]2.40 $N^{1.0}$

Notes	
1	Configuration size does not capture static data present in libraries. Libraries are not counted because most implementations include common ancillary libraries for image processing (e.g. openCV) or numerical computation (e.g. blas).
2	This multiplier expresses the increase in template size when k images are passed to the template generation function.
3	All durations are measured on Intel®Xeon®CPU E5-2630 v4 @ 2.20GHz processors. Estimates are made by wrapping the API function call in calls to std::chrono::high_resolution_clock which on the machine in (3) counts 1ns clock ticks. Precision is somewhat worse than that however.
4	Search durations are measured as in the prior note. The power-law model in the final column mostly fits the empirical results in Figure 105. However in certain cases the model is not correct and should not be used numerically.

Table 5: Summary of algorithms and properties included in this report. The blue superscripts give ranking for the quantity in that column. Missing search durations, denoted by "-", are absent because those runs were not executed, usually because we did not run on the larger galleries. Caution: The power-law model is sometimes an incorrect model. It is included here only to show broad sublinear behavior, which is flagged in green. The models should not be used for prediction.

FNIR(N, R, T) = False neg. identification rate N = Num. enrolled subjects T = Threshold T = 0 → Investigation
FPIR(N, T) = False pos. identification rate R = Num. candidates examined T > 0 → Identification

	DEVELOPER	SHORT	SEQ.	VALIDATION	CONFIG[1]	TEMPLATE GENERATION			SEARCH DURATION[4] MILLISEC					
	FULL NAME	NAME	NUM.	DATE	DATA (MB)	SIZE (B)	MULT[2]	TIME (MS)[3]	L=1 N=1.6M	L=50 N=1.6M	L=50 N=3M	L=50 N=6M	L=50 N=12M	POWER LAW (μs)
209	Vigilant Solutions	vigilant	0	2018-02-08	335	^{104}1544	k	^{208}823	-	^{191}2058	-	-	-	
210	Vigilant Solutions	vigilant	1	2018-02-14	249	^{181}2056	k	^{194}739	-	^{192}2075	-	-	-	
211	Vigilant Solutions	vigilant	2	2018-02-14	335	^{106}1544	k	^{205}820	-	^{194}2121	-	-	-	
212	Vigilant Solutions	vigilant	3	2018-06-21	335	^{103}1544	k	^{213}832	^{144}2453	^{199}2307	-	-	-	
213	Vigilant Solutions	vigilant	4	2018-06-21	337	^{102}1544	k	^{211}830	^{139}2050	^{196}2251	-	-	-	
214	Vigilant Solutions	vigilant	5	2018-10-30	335	^{105}1544	k	^{199}778	-	^{181}1720	-	-	-	
215	Vigilant Solutions	vigilant	6	2018-10-30	337	^{101}1544	k	^{214}834	-	^{180}1713	-	-	-	
216	VisionLabs	visionlabs	008	2019-06-18	348	^{41}512	1	^{53}277	^{10}23	^{14}24	-	-	-	
217	VisionLabs	visionlabs	3	2018-02-16	624	^{17}256	1	^{39}228	-	^{7}5	^{3}5	^{2}6	-	^{6}417.37 $N^{0.2}$
218	VisionLabs	visionlabs	4	2018-06-22	299	^{25}256	1	^{64}315	^{9}19	^{11}17	^{6}20	^{4}26	^{3}29	^{3}2663.29 $N^{0.1}$
219	VisionLabs	visionlabs	5	2018-06-22	305	^{39}512	1	^{62}300	^{15}54	^{18}33	^{7}37	^{8}56	^{7}88	^{10}166.84 $N^{0.4}$
220	VisionLabs	visionlabs	6	2018-10-30	360	^{45}512	1	^{57}292	^{14}36	^{20}36	^{9}39	^{7}44	^{5}53	^{5}3211.93 $N^{0.2}$
221	VisionLabs	visionlabs	7	2018-10-30	360	^{47}512	1	^{58}293	^{16}63	^{23}63	^{10}72	^{9}80	^{8}115	^{8}2076.32 $N^{0.2}$
222	Vocord	vocord	0	2018-02-16	872	^{62}608	k	^{124}536	-	^{73}268	-	-	-	
223	Vocord	vocord	1	2018-02-16	872	^{63}608	k	^{125}536	-	^{74}268	-	-	-	
224	Vocord	vocord	2	2018-02-16	924	^{136}2048	k	^{149}635	-	^{65}248	-	-	-	
225	Vocord	vocord	3	2018-06-30	627	^{66}896	k	^{185}714	^{44}215	^{64}247	-	-	-	
226	Vocord	vocord	4	2018-06-30	627	^{67}896	k	^{128}538	^{45}216	^{69}253	-	-	-	
227	Vocord	vocord	5	2018-10-30	1035	^{64}768	k	^{207}822	^{32}158	^{54}204	^{21}383	^{21}767	^{16}1466	^{32}0.12 $N^{1.0}$
228	Vocord	vocord	6	2018-10-30	1035	^{236}10240	k	^{209}825	^{34}170	^{59}216	-	-	-	
229	Zhuhai Yisheng Electronics Technology	yisheng	0	2018-02-14	473	^{194}2108	k	^{143}615	-	^{128}587	-	-	-	
230	Zhuhai Yisheng Electronics Technology	yisheng	1	2018-06-19	474	^{206}3704	k	^{81}387	^{140}2228	^{159}1108	-	-	-	
231	Shanghai Yitu Technology	yitu	0	2018-02-12	1774	^{224}4136	1	^{147}633	-	^{110}464	^{40}868	^{38}1769	-	^{59}0.12 $N^{1.1}$
232	Shanghai Yitu Technology	yitu	1	2018-02-12	1944	^{223}4136	1	^{231}930	-	^{109}463	-	-	-	
233	Shanghai Yitu Technology	yitu	2	2018-06-21	2077	^{226}4138	1	^{223}870	^{160}5516	^{223}5417	^{77}6101	^{73}13264	^{68}33047	^{13}9.25 $N^{0.9}$
234	Shanghai Yitu Technology	yitu	3	2018-06-21	2077	^{225}4138	1	^{224}871	^{158}5248	^{222}5242	^{78}6286	^{78}19829	^{74}45621	^{61}1.08 $N^{1.1}$
235	Shanghai Yitu Technology	yitu	4	2018-10-30	2119	^{188}2070	1	^{228}910	^{118}1288	^{167}1203	^{61}2440	^{59}5241	^{54}9671	^{46}0.52 $N^{1.0}$
236	Shanghai Yitu Technology	yitu	5	2018-10-30	2043	^{186}2070	1	^{221}861	^{115}1235	^{166}1197	^{62}2508	^{58}5003	^{53}9601	^{42}0.55 $N^{1.0}$

Notes	
1	Configuration size does not capture static data present in libraries. Libraries are not counted because most implementations include common ancillary libraries for image processing (e.g. openCV) or numerical computation (e.g. blas).
2	This multiplier expresses the increase in template size when k images are passed to the template generation function.
3	All durations are measured on Intel®Xeon®CPU E5-2630 v4 @ 2.20GHz processors. Estimates are made by wrapping the API function call in calls to std::chrono::high_resolution_clock which on the machine in (3) counts 1ns clock ticks. Precision is somewhat worse than that however.
4	Search durations are measured as in the prior note. The power-law model in the final column mostly fits the empirical results in Figure 105. However in certain cases the model is not correct and should not be used numerically.

Table 6: Summary of algorithms and properties included in this report. The blue superscripts give ranking for the quantity in that column. Missing search durations, denoted by "-", are absent because those runs were not executed, usually because we did not run on the larger galleries. Caution: The power-law model is sometimes an incorrect model. It is included here only to show broad sublinear behavior, which is flagged in green. The models should not be used for prediction.

MISSES BELOW THRESHOLD, T		ENROL LIFETIME					ENROL MOST RECENT				
FNIR(N, T> 0, R >L)		DATASET: FRVT 2018					DATASET: FRVT 2018				
#	ALGORITHM	N=0.64M	N=1.6M	N=3.0M	N=6.0M	N=12.0M	N=0.64M	N=1.6M	N=3.0M	N=6.0M	N=12.0M
1	3DIVI-3	^{168}0.3000	^{153}0.3499	^{74}0.3859	^{70}0.4344		^{178}0.3550	^{175}0.4023			
2	3DIVI-5	^{123}0.1045	^{120}0.1339				^{133}0.1382	^{131}0.1691	^{101}0.1938	^{96}0.2392	^{92}0.3087
3	ALCHERA-0	^{111}0.0852	^{110}0.1105	^{62}0.1361	^{59}0.1913		^{124}0.1128	^{122}0.1405			
4	ALCHERA-3	^{120}0.1018	^{118}0.1296				^{126}0.1205	^{125}0.1590	^{99}0.1891	^{97}0.2467	^{99}0.3628
5	ALLGOVISION-000	^{92}0.0558	^{91}0.0736				^{98}0.0713	^{94}0.0905	^{79}0.1108	^{75}0.1412	^{67}0.2150
6	ANKE-0	^{105}0.0768	^{101}0.0989				^{113}0.0968	^{110}0.1199	^{91}0.1432	^{88}0.1811	^{85}0.2624
7	ANKE-002	^{29}0.0204	^{29}0.0278				^{31}0.0255	^{31}0.0344	^{31}0.0431	^{30}0.0630	^{26}0.1489
8	AWARE-3	^{110}0.0846	^{102}0.0991	^{59}0.1148	^{54}0.1459		^{123}0.1122	^{120}0.1306	^{92}0.1471	^{87}0.1793	^{77}0.2395
9	AWARE-5	^{161}0.2628	^{147}0.2984				^{176}0.3459	^{169}0.3729	^{109}0.4094	^{106}0.4615	^{88}0.2637
10	AYONIX-0	^{203}0.8262	^{170}0.8490	^{80}0.8640	^{75}0.8809		^{214}0.7795	^{210}0.8114			
11	AYONIX-2	^{199}0.7602	^{168}0.8038				^{215}0.7867	^{212}0.8246	^{114}0.8511	^{110}0.8708	^{108}0.8946
12	CAMVI-3	^{56}0.0281	^{69}0.0509	^{45}0.0680	^{58}0.1871		^{60}0.0413	^{80}0.0736			
13	CAMVI-4	^{47}0.0257	^{68}0.0505				^{57}0.0393	^{81}0.0741	^{74}0.1008	^{99}0.2532	^{89}0.2731
14	COGENT-0	^{73}0.0387	^{65}0.0434	^{39}0.0523	^{35}0.0784	^{21}0.1559	^{76}0.0455	^{62}0.0557	^{60}0.0734	^{64}0.1194	^{62}0.2029
15	COGENT-1	^{94}0.0598	^{70}0.0513				^{75}0.0455	^{61}0.0557	^{61}0.0734	^{63}0.1194	^{61}0.2029
16	COGENT-2	^{33}0.0220	^{31}0.0299	^{25}0.0390	^{34}0.0703	^{24}0.1595	^{42}0.0356	^{46}0.0475	^{47}0.0655	^{62}0.1185	^{70}0.2241
17	COGENT-3	^{48}0.0258	^{44}0.0341	^{34}0.0450	^{38}0.0842	^{35}0.1864	^{45}0.0361	^{53}0.0515	^{62}0.0771	^{72}0.1374	^{81}0.2488
18	COGNITEC-0	^{119}0.0989	^{116}0.1256				^{135}0.1400	^{128}0.1628	^{100}0.1892	^{92}0.2205	^{91}0.2859
19	COGNITEC-1	^{93}0.0597	^{92}0.0777	^{53}0.0946	^{51}0.1315	^{49}0.2552	^{106}0.0832	^{103}0.1045	^{84}0.1244	^{79}0.1561	^{75}0.2338
20	COGNITEC-2	^{60}0.0296	^{57}0.0401	^{38}0.0523	^{40}0.0852	^{45}0.2298	^{68}0.0433	^{63}0.0560	^{52}0.0695	^{50}0.0980	^{56}0.1967
21	COGNITEC-3	^{57}0.0288	^{56}0.0397	^{37}0.0505	^{37}0.0837	^{43}0.2140	^{64}0.0427	^{60}0.0555	^{48}0.0679	^{47}0.0938	^{49}0.1840
22	CYBERLINK-000	^{64}0.0312	^{63}0.0427				^{69}0.0440	^{69}0.0590	^{58}0.0732	^{57}0.1055	^{64}0.2071
23	CYBERLINK-001	^{58}0.0291	^{55}0.0396				^{61}0.0418	^{64}0.0561	^{56}0.0720	^{54}0.0997	^{47}0.1816
24	DAHUA-002	^{12}0.0099	^{10}0.0130	^{10}0.0159	^{8}0.0261	^{6}0.1116	^{12}0.0135	^{12}0.0177	^{12}0.0218	^{11}0.0317	^{13}0.1177
25	DAHUA-1	^{77}0.0410	^{71}0.0521				^{86}0.0596	^{83}0.0755	^{69}0.0905	^{61}0.1179	^{53}0.1910
26	DEEPSEA-001	^{40}0.0249	^{42}0.0325				^{49}0.0373	^{47}0.0488	^{42}0.0611	^{41}0.0827	^{44}0.1730
27	DERMALOG-4	^{172}0.3405	^{157}0.3892	^{76}0.4181	^{71}0.4533		^{186}0.4380	^{183}0.4813			
28	DERMALOG-5	^{87}0.0490	^{84}0.0649				^{102}0.0726	^{96}0.0909	^{80}0.1172	^{82}0.1618	^{84}0.2516
29	DERMALOG-6	^{54}0.0276	^{54}0.0383				^{62}0.0420	^{58}0.0542	^{51}0.0687	^{55}0.1004	^{46}0.1812
30	EVERAI-0	^{81}0.0460	^{88}0.0676				^{94}0.0681	^{99}0.0921	^{82}0.1223		
31	EVERAI-1	^{46}0.0255	^{51}0.0360				^{52}0.0383	^{54}0.0518	^{49}0.0686		
32	EVERAI-3	^{27}0.0191	^{27}0.0256	^{21}0.0338	^{16}0.0389		^{33}0.0282	^{32}0.0377	^{33}0.0473	^{32}0.0683	^{41}0.1653
33	EVERAI-PARAVISION-004	^{9}0.0079	^{8}0.0100	^{8}0.0130	^{7}0.0249	^{10}0.1234	^{7}0.0100	^{6}0.0127	^{6}0.0162	^{7}0.0293	^{17}0.1279
34	EYEDEA-3	^{167}0.2911	^{151}0.3283	^{73}0.3673	^{69}0.4154		^{177}0.3498	^{172}0.3893			
35	F8-001	^{189}0.5796	^{163}0.5949				^{125}0.1163	^{129}0.1681	^{96}0.1681	^{84}0.1681	^{43}0.1681
36	GLORY-1	^{153}0.2160	^{139}0.2447	^{68}0.2618	^{64}0.2884		^{168}0.2790	^{163}0.3067			
37	GORILLA-004	^{89}0.0513	^{85}0.0656	^{50}0.0793	^{48}0.1060	^{32}0.1765	^{101}0.0724	^{98}0.0917	^{77}0.1072	^{73}0.1393	^{57}0.1991
38	GORILLA-2	^{128}0.1088	^{125}0.1379				^{140}0.1561	^{138}0.1902	^{103}0.2210	^{100}0.2625	^{98}0.3426
39	HIK-2	^{129}0.1104	^{124}0.1363	^{63}0.1610	^{60}0.2061	^{52}0.3067	^{118}0.0985	^{115}0.1212			
40	HIK-3	^{112}0.0885	^{109}0.1097				^{107}0.0853	^{104}0.1054	^{83}0.1228	^{78}0.1552	^{82}0.2500
41	HIK-4	^{109}0.0839	^{107}0.1031	^{60}0.1225	^{57}0.1518	^{50}0.2618	^{105}0.0821	^{100}0.1013	^{81}0.1173	^{77}0.1498	^{83}0.2503
42	HIK-5	^{32}0.0218	^{35}0.0308	^{28}0.0397	^{31}0.0661		^{41}0.0339	^{43}0.0467	^{41}0.0593	^{49}0.0967	^{68}0.2164
43	IDEMIA-0	^{96}0.0645	^{93}0.0802	^{54}0.0986	^{50}0.1237	^{36}0.1872	^{110}0.0920	^{108}0.1135	^{87}0.1332	^{83}0.1628	^{69}0.2208
44	IDEMIA-007	^{17}0.0122	^{15}0.0155	^{13}0.0196	^{12}0.0309	^{14}0.1406	^{15}0.0162	^{15}0.0207	^{13}0.0254	^{15}0.0383	^{25}0.1425
45	IDEMIA-1	^{63}0.0304	^{53}0.0377	^{35}0.0465	^{27}0.0623	^{22}0.1578	^{70}0.0444	^{57}0.0540	^{45}0.0647	^{42}0.0856	^{37}0.1618
46	IDEMIA-2	^{80}0.0453	^{75}0.0564	^{43}0.0668	^{42}0.0896	^{29}0.1706	^{73}0.0449	^{59}0.0543			
47	IDEMIA-3	^{37}0.0238	^{34}0.0308				^{50}0.0373	^{48}0.0497	^{70}0.0927	^{102}0.2887	^{103}0.4442
48	IDEMIA-4	^{34}0.0223	^{28}0.0276	^{20}0.0338	^{19}0.0478	^{19}0.1556	^{37}0.0326	^{35}0.0399	^{32}0.0472	^{31}0.0644	^{42}0.1659
49	IDEMIA-5	^{51}0.0261	^{39}0.0319	^{27}0.0395	^{24}0.0588	^{31}0.1764	^{53}0.0385	^{42}0.0465	^{40}0.0562	^{40}0.0788	^{55}0.1951
50	IDEMIA-6	^{43}0.0253	^{38}0.0316	^{24}0.0383	^{23}0.0581	^{40}0.2046	^{51}0.0377	^{40}0.0458	^{38}0.0550	^{37}0.0760	^{71}0.2242
51	IMAGUS-2	^{195}0.6616	^{165}0.7143	^{78}0.7503	^{73}0.7867		^{209}0.7092	^{206}0.7510			
52	IMPERIAL-000	^{25}0.0157	^{24}0.0218	^{19}0.0288	^{72}0.6880	^{55}0.6198	^{28}0.0213	^{25}0.0285	^{29}0.0383	^{35}0.0758	^{48}0.1816
53	INCODE-004	^{61}0.0299	^{60}0.0408				^{65}0.0429	^{66}0.0564	^{50}0.0687	^{48}0.0942	^{39}0.1642
54	INCODE-1	^{136}0.1400	^{132}0.1796	^{66}0.2159	^{63}0.2741		^{146}0.1763	^{144}0.2143			
55	INCODE-3	^{117}0.0949	^{115}0.1227				^{132}0.1349	^{133}0.1703	^{102}0.1986	^{95}0.2378	^{94}0.3157
56	INNOVATRICS-4	^{108}0.0837	^{98}0.0928				^{122}0.1106	^{121}0.1340	^{90}0.1418	^{76}0.1418	^{24}0.1418
57	INTSYSMSU-000	^{219}0.9978	^{179}0.9981				^{232}0.9982	^{227}0.9984	^{118}0.9985	^{113}0.9987	^{110}0.9988
58	ISYSTEMS-0	^{85}0.0485	^{83}0.0633	^{51}0.0795	^{47}0.1057	^{41}0.2072	^{96}0.0707	^{97}0.0912			
59	ISYSTEMS-1	^{83}0.0480	^{82}0.0627	^{49}0.0784	^{46}0.1054	^{42}0.2081	^{95}0.0702	^{93}0.0903			
60	ISYSTEMS-2	^{74}0.0394	^{74}0.0545	^{44}0.0679			^{88}0.0612	^{86}0.0814	^{73}0.1006	^{74}0.1405	^{76}0.2374
61	ISYSTEMS-3	^{62}0.0301	^{59}0.0402	^{41}0.0557	^{41}0.0881	^{38}0.1992	^{78}0.0464	^{74}0.0620	^{67}0.0840	^{67}0.1324	^{79}0.2417
62	KEDACOM-001	^{28}0.0193	^{26}0.0228				^{24}0.0207	^{22}0.0253	^{17}0.0292	^{20}0.0448	^{22}0.1363
63	LOOKMAN-005	^{45}0.0254	^{37}0.0314				^{32}0.0266	^{30}0.0327	^{28}0.0382	^{24}0.0537	^{21}0.1357
64	LOOKMAN-3	^{68}0.0335	^{62}0.0425				^{48}0.0372	^{41}0.0463	^{35}0.0541	^{36}0.0758	^{40}0.1650
65	MEGVII-0	^{107}0.0822	^{106}0.1023	^{61}0.1228	^{55}0.1489	^{46}0.2348	^{109}0.0895	^{107}0.1086	^{86}0.1287	^{81}0.1606	^{73}0.2288
66	MEGVII-1						^{84}0.0586	^{82}0.0746	^{68}0.0896	^{68}0.1338	^{90}0.2761
67	MICROFOCUS-3	^{211}0.9002	^{174}0.9213	^{82}0.9342			^{220}0.9119	^{217}0.9310			
68	MICROFOCUS-5	^{214}0.9679	^{176}0.9835				^{227}0.9733	^{214}0.8361	^{115}0.8563	^{111}0.8760	^{109}0.8958
69	MICROSOFT-0	^{30}0.0208	^{30}0.0292	^{22}0.0361	^{21}0.0536	^{18}0.1502	^{38}0.0329	^{37}0.0443	^{36}0.0544	^{38}0.0767	^{45}0.1733
70	MICROSOFT-1	^{31}0.0214	^{32}0.0299	^{23}0.0373	^{22}0.0542	^{23}0.1585	^{40}0.0339	^{39}0.0449			
71	MICROSOFT-2	^{42}0.0252	^{46}0.0345	^{29}0.0425	^{25}0.0600	^{20}0.1558	^{54}0.0387	^{51}0.0503			
72	MICROSOFT-3	^{23}0.0133	^{22}0.0193				^{30}0.0223	^{29}0.0304	^{30}0.0384	^{28}0.0570	^{35}0.1603

Table 7: **Identification-mode: Effect of N on FNIR at high threshold.** *Values are threshold-based miss rates i.e. FNIR at FPIR = 0.001 for five enrollment population sizes, N. The left six columns apply for enrollment of a variable number of images per subject. The right six columns apply for enrollment of one image. Missing entries usually apply because another algorithm from the same developer was run instead. Some developers are missing because less accurate algorithms were not run on galleries with $N \geq 3\,000\,000$. Throughout blue superscripts indicate the rank of the algorithm for that column.*

MISSES BELOW THRESHOLD, T		ENROL LIFETIME					ENROL MOST RECENT				
FNIR(N, T> 0, R >L)		DATASET: FRVT 2018					DATASET: FRVT 2018				
#	ALGORITHM	N=0.64M	N=1.6M	N=3.0M	N=6.0M	N=12.0M	N=0.64M	N=1.6M	N=3.0M	N=6.0M	N=12.0M
73	MICROSOFT-4	[18]0.0128	[19]0.0179	[16]0.0241	[17]0.0405	[25]0.1628	[25]0.0209	[26]0.0288	[27]0.0360	[26]0.0550	[33]0.1576
74	MICROSOFT-5	[16]0.0119	[17]0.0171	[14]0.0218	[15]0.0387	[26]0.1654	[23]0.0201	[23]0.0279	[24]0.0347	[25]0.0545	[30]0.1549
75	MICROSOFT-6	[8]0.0058	[7]0.0080	[7]0.0110	[11]0.0284	[27]0.1664	[9]0.0109	[8]0.0141	[9]0.0183	[12]0.0343	[28]0.1544
76	NEC-0	[84]0.0483	[79]0.0604	[48]0.0726	[45]0.0989	[47]0.2378	[90]0.0662	[87]0.0815	[72]0.0961	[65]0.1199	[58]0.1994
77	NEC-1	[99]0.0711	[97]0.0899				[108]0.0889	[106]0.1081	[85]0.1276	[80]0.1565	[74]0.2311
78	NEC-2	[2]0.0018	[2]0.0024	[2]0.0038	[6]0.0211	[4]0.0991	[1]0.0040	[3]0.0047	[3]0.0057	[3]0.0190	[4]0.0723
79	NEC-3	[1]0.0018	[1]0.0021	[1]0.0026	[2]0.0113	[2]0.0788	[2]0.0040	[1]0.0044	[2]0.0049	[2]0.0095	[2]0.0580
80	NEUROTECHNOLOGY-007	[76]0.0405	[220]1.0000	[46]0.0698	[44]0.0976	[39]0.2035	[77]0.0461	[75]0.0648	[65]0.0827	[70]0.1344	[78]0.2414
81	NEUROTECHNOLOGY-3	[190]0.5809	[164]0.6390				[204]0.5959	[202]0.6649	[113]0.7217	[109]0.7852	[107]0.8336
82	NEUROTECHNOLOGY-4	[79]0.0427	[76]0.0575	[47]0.0711	[43]0.0954	[34]0.1845	[80]0.0493	[77]0.0656	[64]0.0810	[59]0.1167	[65]0.2138
83	NEUROTECHNOLOGY-5	[72]0.0384	[72]0.0527	[40]0.0546	[36]0.0811	[12]0.1366	[63]0.0422	[67]0.0564	[55]0.0705	[53]0.0988	[59]0.2014
84	NEWLAND-2						[182]0.4015	[180]0.4405	[110]0.4719	[107]0.5133	
85	NOBLIS-2	[217]0.9943	[178]0.9959				[231]0.9963	[226]0.9974	[117]0.9980	[112]0.9986	
86	NTECHLAB-0	[90]0.0518	[86]0.0666	[52]0.0850	[49]0.1158		[93]0.0677	[88]0.0830	[75]0.1029	[66]0.1306	[54]0.1948
87	NTECHLAB-007	[26]0.0170	[25]0.0223	[18]0.0287	[20]0.0479	[28]0.1680	[29]0.0214	[24]0.0282	[23]0.0343	[23]0.0520	[19]0.1329
88	NTECHLAB-008	[14]0.0112	[14]0.0151	[12]0.0189	[13]0.0310	[16]0.1489	[11]0.0133	[10]0.0171	[11]0.0214	[9]0.0312	[5]0.1019
89	NTECHLAB-1	[95]0.0634	[94]0.0818	[55]0.1006	[53]0.1337	[44]0.2162	[104]0.0803	[102]0.1021			
90	NTECHLAB-3	[66]0.0329	[64]0.0434				[71]0.0445	[65]0.0561	[53]0.0699	[46]0.0933	[36]0.1609
91	NTECHLAB-4	[44]0.0253	[43]0.0337	[30]0.0433	[33]0.0692	[33]0.1845	[39]0.0337	[36]0.0431	[37]0.0545	[34]0.0749	[27]0.1528
92	NTECHLAB-5	[53]0.0268	[48]0.0347				[44]0.0358	[38]0.0448	[39]0.0561	[39]0.0785	[32]0.1572
93	NTECHLAB-6	[35]0.0227	[33]0.0301	[26]0.0395	[30]0.0654	[37]0.1897	[34]0.0311	[33]0.0391	[34]0.0496	[33]0.0696	[29]0.1548
94	PARAVISION-005	[5]0.0049	[4]0.0056	[4]0.0067	[3]0.0148	[7]0.1147	[5]0.0059	[4]0.0068	[4]0.0083	[4]0.0201	[6]0.1061
95	PIXELALL-002	[113]0.0893	[114]0.1206				[103]0.0741	[105]0.1076	[94]0.1498	[98]0.2509	[101]0.3920
96	PIXELALL-003	[38]0.0240	[40]0.0320				[20]0.0184	[19]0.0244	[22]0.0314	[22]0.0499	[12]0.1162
97	QUANTASOFT-1	[216]0.9915	[177]0.9915				[205]0.6399	[200]0.6399	[112]0.6399		[105]0.6399
98	RANKONE-0	[137]0.1485	[131]0.1788	[67]0.2210	[65]0.3260	[54]0.4758	[148]0.1899	[145]0.2192	[107]0.2635	[103]0.2992	[102]0.4301
99	RANKONE-007	[24]0.0154	[23]0.0194	[15]0.0235	[14]0.0378	[15]0.1467	[22]0.0194	[21]0.0248	[18]0.0292	[17]0.0407	[11]0.1156
100	RANKONE-1	[131]0.1211	[129]0.1549	[65]0.1804	[62]0.2371	[53]0.3530	[139]0.1542	[130]0.1683			
101	RANKONE-2	[103]0.0744	[100]0.0943				[121]0.0998	[112]0.1200	[89]0.1382	[86]0.1744	[87]0.2636
102	RANKONE-3	[102]0.0744	[99]0.0943	[58]0.1120	[56]0.1490	[51]0.2946	[120]0.0998	[111]0.1200	[88]0.1382	[85]0.1744	[86]0.2636
103	RANKONE-4	[134]0.1265	[128]0.1545				[141]0.1631	[139]0.1951	[104]0.2211		
104	RANKONE-5	[70]0.0347	[66]0.0447	[42]0.0571	[39]0.0847	[48]0.2549	[81]0.0499	[72]0.0617	[57]0.0728	[52]0.0984	[63]0.2031
105	REALNETWORKS-0	[149]0.2098	[141]0.2476	[70]0.2837			[152]0.2003	[149]0.2362			
106	REALNETWORKS-003	[130]0.1117	[126]0.1405				[131]0.1323	[127]0.1617	[98]0.1880	[93]0.2267	[93]0.3095
107	REALNETWORKS-004	[116]0.0941	[113]0.1179				[130]0.1303	[126]0.1604	[97]0.1878	[94]0.2349	[95]0.3197
108	REALNETWORKS-2	[139]0.1688	[135]0.2049				[150]0.1974	[147]0.2341	[108]0.2691	[104]0.3186	[96]0.3261
109	REMARKAI-000	[67]0.0334	[67]0.0461				[67]0.0432	[68]0.0577	[54]0.0701	[56]0.1052	[60]0.2025
110	REMARKAI-2	[100]0.0731	[103]0.0991				[114]0.0971	[118]0.1264	[93]0.1495	[90]0.1928	
111	SCANOVATE-000	[200]0.7849	[167]0.7902	[79]0.7906	[74]0.7906	[56]0.7907	[82]0.0523	[78]0.0692	[66]0.0829	[58]0.1121	[10]0.1132
112	SENSETIME-0	[15]0.0118	[16]0.0165				[19]0.0184	[17]0.0234	[19]0.0296	[18]0.0427	[18]0.1287
113	SENSETIME-002	[22]0.0132	[12]0.0134	[9]0.0139	[9]0.0262	[3]0.0826	[17]0.0172	[11]0.0174	[8]0.0179	[5]0.0260	[3]0.0682
114	SENSETIME-003	[3]0.0038	[3]0.0040	[3]0.0043	[1]0.0067	[1]0.0454	[3]0.0042	[2]0.0045	[1]0.0048	[1]0.0080	[1]0.0477
115	SENSETIME-1	[19]0.0129	[18]0.0175				[21]0.0186	[20]0.0245	[21]0.0304	[21]0.0448	[20]0.1344
116	SHAMAN-3	[175]0.3506	[158]0.3921	[77]0.4295			[183]0.4179	[181]0.4527			
117	SHAMAN-7	[115]0.0924	[112]0.1112				[128]0.1236	[124]0.1436	[95]0.1610	[89]0.1901	[80]0.2480
118	SIAT-1	[162]0.2695	[145]0.2727	[69]0.2758			[14]0.0160	[13]0.0201	[15]0.0260	[13]0.0380	[7]0.1069
119	SIAT-2	[155]0.2198	[137]0.2239				[18]0.0179	[18]0.0242	[20]0.0301	[19]0.0434	[23]0.1377
120	SMILART-4	[204]0.8381	[175]0.9569				[224]0.9260	[221]0.9683	[116]0.9913		
121	SYNESIS-3	[184]0.4748	[161]0.5296				[196]0.5353	[194]0.5832	[111]0.6123	[108]0.6489	[106]0.6838
122	TECH5-001	[78]0.0426	[77]0.0590				[72]0.0446	[70]0.0599	[71]0.0935	[91]0.2127	[100]0.3742
123	TEVIAN-4	[98]0.0685	[96]0.0878	[57]0.1032			[112]0.0952	[113]0.1201			
124	TEVIAN-5	[91]0.0518	[87]0.0667				[99]0.0717	[92]0.0898	[78]0.1094	[69]0.1338	[50]0.1873
125	TIGER-0	[166]0.2859	[152]0.3361	[72]0.3659	[68]0.4139		[175]0.3452	[173]0.3921			
126	TIGER-2	[88]0.0511	[89]0.0698				[92]0.0671	[90]0.0888	[76]0.1065	[71]0.1361	[72]0.2284
127	TONGYITRANS-1	[97]0.0658	[95]0.0835	[56]0.1017	[52]0.1328		[83]0.0545	[79]0.0693			
128	TOSHIBA-0	[71]0.0374	[73]0.0529				[79]0.0488	[76]0.0648	[63]0.0809	[60]0.1170	[66]0.2140
129	VD-0	[208]0.8686	[173]0.9048	[81]0.9242	[76]0.9381		[218]0.8892	[216]0.9171			
130	VD-1	[135]0.1312	[130]0.1654				[142]0.1664	[143]0.2036	[106]0.2372	[101]0.2759	[97]0.3314
131	VIGILANTSOLUTIONS-3	[169]0.3061	[154]0.3568	[75]0.3861	[66]0.3861		[181]0.3648	[177]0.4097			
132	VISIONLABS-008	[10]0.0093	[9]0.0117				[10]0.0122	[9]0.0157	[10]0.0192	[10]0.0317	[16]0.1270
133	VISIONLABS-3	[49]0.0260	[47]0.0347	[33]0.0444	[32]0.0678		[58]0.0394	[52]0.0506	[44]0.0629	[45]0.0902	
134	VISIONLABS-4	[59]0.0294	[58]0.0402				[74]0.0452	[71]0.0604	[59]0.0733	[51]0.0982	[51]0.1893
135	VISIONLABS-5	[41]0.0250	[49]0.0353	[32]0.0441	[28]0.0628	[30]0.1727	[59]0.0396	[56]0.0531	[46]0.0654	[44]0.0878	[52]0.1894
136	VISIONLABS-6	[21]0.0131	[21]0.0185				[27]0.0211	[28]0.0289	[26]0.0359	[29]0.0571	[31]0.1572
137	VISIONLABS-7	[20]0.0131	[20]0.0185	[17]0.0242	[18]0.0412	[17]0.1495	[26]0.0211	[27]0.0289	[25]0.0359	[27]0.0569	[34]0.1576
138	VOCORD-3	[118]0.0969	[117]0.1295	[64]0.1627	[61]0.2361		[117]0.0973	[117]0.1258			
139	VOCORD-5	[101]0.0735	[108]0.1076				[129]0.1261	[132]0.1697	[105]0.2327	[105]0.3286	[104]0.4628
140	YISHENG-1	[160]0.2539	[148]0.3002	[71]0.3366	[67]0.3892		[170]0.3026	[166]0.3483			
141	YITU-0	[55]0.0279	[50]0.0358	[36]0.0468	[29]0.0636	[13]0.1389	[55]0.0388	[50]0.0502	[43]0.0622	[43]0.0862	[38]0.1621
142	YITU-1	[50]0.0261	[45]0.0341	[31]0.0434	[26]0.0611	[11]0.1361	[47]0.0366	[45]0.0472			
143	YITU-2	[11]0.0096	[11]0.0133	[11]0.0174	[10]0.0274	[9]0.1180	[13]0.0156	[14]0.0204	[14]0.0258	[14]0.0382	[14]0.1241
144	YITU-3	[13]0.0103	[13]0.0139				[16]0.0165	[16]0.0213	[16]0.0266	[16]0.0389	[15]0.1248

Table 8: **Identification-mode: Effect of N on FNIR at high threshold.** *Values are threshold-based miss rates i.e.* FNIR *at* FPIR *= 0.001 for five enrollment population sizes, N. The left six columns apply for enrollment of a variable number of images per subject. The right six columns apply for enrollment of one image. Missing entries usually apply because another algorithm from the same developer was run instead. Some developers are missing because less accurate algorithms were not run on galleries with $N \geq 3\,000\,000$. Throughout blue superscripts indicate the rank of the algorithm for that column.*

MISSES BELOW THRESHOLD, T		ENROL LIFETIME					ENROL MOST RECENT				
FNIR(N, T$>$ 0, R $>$L)		DATASET: FRVT 2018					DATASET: FRVT 2018				
#	ALGORITHM	N=0.64M	N=1.6M	N=3.0M	N=6.0M	N=12.0M	N=0.64M	N=1.6M	N=3.0M	N=6.0M	N=12.0M
145	YITU-4	^{6}0.0052	^{5}0.0074	^{5}0.0097	^{4}0.0187	^{8}0.1153	^{6}0.0093	^{5}0.0123	^{5}0.0159	^{6}0.0273	^{8}0.1107
146	YITU-5	^{7}0.0057	^{6}0.0076	^{6}0.0100	^{5}0.0188	^{5}0.1111	^{8}0.0101	^{7}0.0128	^{7}0.0163	^{8}0.0294	^{9}0.1118

Table 9: **Identification-mode: Effect of N on FNIR at high threshold.** *Values are threshold-based miss rates i.e.* FNIR *at* FPIR *= 0.001 for five enrollment population sizes, N. The left six columns apply for enrollment of a variable number of images per subject. The right six columns apply for enrollment of one image. Missing entries usually apply because another algorithm from the same developer was run instead. Some developers are missing because less accurate algorithms were not run on galleries with* $N \geq 3\,000\,000$*. Throughout blue superscripts indicate the rank of the algorithm for that column.*

MISSES NOT AT RANK 1		ENROL LIFETIME						ENROL MOST RECENT					
FNIR(N, T= 0, R =1)		DATASET: FRVT 2018						DATASET: FRVT 2018					
#	ALGORITHM	N=0.64M	N=1.6M	N=3.0M	N=6.0M	N=12.0M	aN^b	N=0.64M	N=1.6M	N=3.0M	N=6.0M	N=12.0M	aN^b
1	3DIVI-3	[169]0.0494	[150]0.0645	[73]0.0759	[68]0.0898		[106]$0.0014 N^{0.267}$[94]	[184]0.0680	[182]0.0857				[111]$0.0023 N^{0.252}$[126]
2	3DIVI-5	[109]0.0100	[111]0.0133				[46]$0.0002 N^{0.310}$[122]	[129]0.0163	[125]0.0202	[93]0.0236	[91]0.0279	[89]0.0327	[59]$0.0007 N^{0.239}$[117]
3	ALCHERA-0	[117]0.0106	[106]0.0121	[59]0.0135	[56]0.0170		[84]$0.0006 N^{0.207}$[71]	[130]0.0167	[120]0.0186				[120]$0.0035 N^{0.117}$[37]
4	ALCHERA-3	[121]0.0119	[116]0.0159				[51]$0.0002 N^{0.312}$[124]	[91]0.0101	[97]0.0127	[80]0.0146	[82]0.0171	[82]0.0204	[33]$0.0004 N^{0.236}$[112]
5	ALLGOVISION-000	[104]0.0095	[101]0.0106				[113]$0.0021 N^{0.113}$[35]	[112]0.0127	[107]0.0141	[83]0.0154	[83]0.0172	[79]0.0192	[106]$0.0019 N^{0.142}$[49]
6	ANKE-0	[94]0.0077	[93]0.0100				[47]$0.0002 N^{0.287}$[112]	[115]0.0128	[113]0.0158	[90]0.0181	[88]0.0214	[86]0.0251	[50]$0.0006 N^{0.231}$[110]
7	ANKE-002	[56]0.0045	[49]0.0048				[108]$0.0016 N^{0.078}$[21]	[35]0.0051	[30]0.0054	[30]0.0059	[30]0.0064	[26]0.0070	[86]$0.0011 N^{0.111}$[36]
8	AWARE-3	[136]0.0165	[127]0.0209	[64]0.0247	[61]0.0297		[78]$0.0005 N^{0.263}$[93]	[151]0.0264	[146]0.0332	[104]0.0387	[102]0.0456	[102]0.0532	[84]$0.0011 N^{0.239}$[118]
9	AWARE-5	[135]0.0163	[126]0.0208				[75]$0.0004 N^{0.270}$[96]	[153]0.0271	[147]0.0337	[105]0.0392	[103]0.0460	[93]0.0338	[130]$0.0070 N^{0.109}$[34]
10	AYONIX-0	[210]0.4198	[174]0.4649	[80]0.4969	[74]0.5318		[138]$0.1021 N^{0.106}$[32]	[226]0.4095	[222]0.4519				[143]$0.0973 N^{0.108}$[33]
11	AYONIX-2	[203]0.2192	[167]0.2606				[132]$0.0176 N^{0.189}$[57]	[220]0.2954	[217]0.3432	[116]0.3753	[112]0.4116	[109]0.4480	[140]$0.0449 N^{0.142}$[50]
12	CAMVI-3	[125]0.0144	[139]0.0368	[69]0.0528	[71]0.1791		[4]$0.0000 N^{1.076}$[142]	[146]0.0224	[170]0.0544				[2]$0.0000 N^{0.969}$[145]
13	CAMVI-4	[98]0.0082	[137]0.0326				[2]$0.0000 N^{1.500}$[143]	[120]0.0145	[167]0.0490	[110]0.0741	[111]0.2382	[108]0.2386	[1]$0.0000 N^{1.007}$[146]
14	COGENT-0	[114]0.0103	[100]0.0106	[52]0.0109	[46]0.0114	[41]0.0122	[120]$0.0047 N^{0.057}$[17]	[114]0.0127	[99]0.0131	[76]0.0136	[70]0.0141	[69]0.0151	[126]$0.0058 N^{0.058}$[13]
15	COGENT-1	[113]0.0103	[99]0.0106				[124]$0.0074 N^{0.025}$[11]	[113]0.0127	[98]0.0131	[75]0.0136	[69]0.0141	[68]0.0151	[125]$0.0058 N^{0.058}$[12]
16	COGENT-2	[20]0.0022	[20]0.0027	[14]0.0032	[13]0.0037	[14]0.0043	[33]$0.0001 N^{0.227}$[79]	[40]0.0054	[40]0.0062	[35]0.0067	[33]0.0075	[32]0.0085	[61]$0.0007 N^{0.150}$[55]
17	COGENT-3	[31]0.0032	[30]0.0037	[21]0.0042	[21]0.0048	[20]0.0056	[56]$0.0002 N^{0.192}$[59]	[45]0.0057	[42]0.0064	[39]0.0069	[37]0.0077	[34]0.0087	[72]$0.0008 N^{0.144}$[51]
18	COGNITEC-0	[126]0.0146	[121]0.0189				[64]$0.0003 N^{0.285}$[109]	[144]0.0221	[142]0.0278	[101]0.0323	[100]0.0378	[97]0.0443	[77]$0.0009 N^{0.236}$[113]
19	COGNITEC-1	[85]0.0069	[87]0.0089	[51]0.0106	[49]0.0128	[46]0.0154	[49]$0.0002 N^{0.275}$[100]	[105]0.0116	[109]0.0143	[88]0.0165	[86]0.0192	[84]0.0225	[49]$0.0006 N^{0.226}$[107]
20	COGNITEC-2	[36]0.0035	[40]0.0044	[32]0.0052	[31]0.0061	[30]0.0075	[40]$0.0001 N^{0.254}$[86]	[70]0.0074	[64]0.0083	[55]0.0093	[53]0.0105	[54]0.0121	[66]$0.0008 N^{0.166}$[69]
21	COGNITEC-3	[48]0.0040	[48]0.0048	[35]0.0055	[33]0.0064	[32]0.0078	[52]$0.0002 N^{0.226}$[77]	[74]0.0078	[67]0.0088	[58]0.0098	[57]0.0111	[58]0.0126	[74]$0.0009 N^{0.164}$[66]
22	CYBERLINK-000	[72]0.0052	[62]0.0056				[109]$0.0017 N^{0.085}$[23]	[55]0.0061	[45]0.0066	[41]0.0072	[39]0.0080	[38]0.0089	[80]$0.0010 N^{0.132}$[45]
23	CYBERLINK-001	[59]0.0047	[54]0.0051				[104]$0.0013 N^{0.094}$[25]	[44]0.0057	[41]0.0062	[37]0.0068	[35]0.0077	[35]0.0087	[63]$0.0008 N^{0.149}$[53]
24	DAHUA-002	[43]0.0039	[37]0.0040	[20]0.0041	[19]0.0043	[15]0.0046	[110]$0.0018 N^{0.058}$[18]	[21]0.0043	[19]0.0045	[18]0.0047	[15]0.0049	[13]0.0053	[102]$0.0017 N^{0.069}$[17]
25	DAHUA-1	[46]0.0040	[50]0.0049				[45]$0.0002 N^{0.242}$[84]	[69]0.0074	[69]0.0089	[59]0.0102	[61]0.0115	[60]0.0135	[40]$0.0005 N^{0.203}$[88]
26	DEEPSEA-001	[64]0.0048	[61]0.0055				[83]$0.0006 N^{0.152}$[43]	[52]0.0059	[52]0.0070	[48]0.0079	[48]0.0092	[49]0.0107	[30]$0.0004 N^{0.204}$[92]
27	DERMALOG-4	[172]0.0759	[153]0.0961	[76]0.1105	[70]0.1260		[119]$0.0037 N^{0.227}$[78]	[189]0.1040	[187]0.1274				[124]$0.0054 N^{0.221}$[104]
28	DERMALOG-5	[97]0.0081	[103]0.0113				[27]$0.0001 N^{0.353}$[137]	[118]0.0135	[117]0.0171	[91]0.0223	[96]0.0312	[100]0.0470	[5]$0.0000 N^{0.427}$[142]
29	DERMALOG-6	[75]0.0055	[66]0.0060				[107]$0.0015 N^{0.095}$[27]	[88]0.0095	[79]0.0102	[65]0.0107	[60]0.0115	[56]0.0125	[117]$0.0027 N^{0.092}$[26]
30	EVERAI-0	[83]0.0065	[118]0.0166				[3]$0.0000 N^{1.029}$[141]	[94]0.0102	[127]0.0209	[103]0.0348			[3]$0.0000 N^{0.795}$[144]
31	EVERAI-1	[21]0.0022	[21]0.0027				[39]$0.0001 N^{0.222}$[76]	[28]0.0047	[31]0.0056	[31]0.0061			[44]$0.0005 N^{0.166}$[67]
32	EVERAI-3	[16]0.0020	[16]0.0023	[11]0.0026	[11]0.0028		[54]$0.0002 N^{0.167}$[50]	[18]0.0041	[21]0.0047	[25]0.0052	[25]0.0059	[24]0.0066	[38]$0.0005 N^{0.160}$[64]
33	EVERAI-PARAVISION-004	[42]0.0038	[32]0.0039	[18]0.0039	[17]0.0041	[13]0.0042	[115]$0.0023 N^{0.036}$[14]	[20]0.0042	[15]0.0043	[14]0.0044	[14]0.0045	[7]0.0048	[110]$0.0023 N^{0.045}$[9]
34	EYEDEA-3	[168]0.0480	[149]0.0613	[72]0.0717	[67]0.0831		[111]$0.0018 N^{0.246}$[85]	[182]0.0663	[181]0.0824				[118]$0.0028 N^{0.238}$[115]
35	F8-001	[216]0.5361	[176]0.5364				[141]$0.5318 N^{0.001}$[6]	[119]0.0139	[110]0.0146	[81]0.0146	[73]0.0146	[65]0.0146	[134]$0.0116 N^{0.015}$[3]
36	GLORY-1	[178]0.0818	[152]0.0932	[74]0.1007	[69]0.1091		[131]$0.0147 N^{0.129}$[41]	[194]0.1154	[189]0.1291				[138]$0.0223 N^{0.123}$[40]
37	GORILLA-004	[81]0.0059	[76]0.0070	[42]0.0079	[38]0.0090	[35]0.0105	[74]$0.0004 N^{0.195}$[65]	[71]0.0075	[70]0.0089	[60]0.0102	[62]0.0118	[63]0.0140	[32]$0.0004 N^{0.214}$[98]
38	GORILLA-2	[111]0.0102	[112]0.0137				[43]$0.0001 N^{0.321}$[132]	[131]0.0170	[128]0.0220	[97]0.0261	[95]0.0311	[94]0.0375	[37]$0.0005 N^{0.269}$[135]
39	HIK-2	[132]0.0155	[119]0.0185	[62]0.0208	[59]0.0240	[53]0.0272	[102]$0.0012 N^{0.193}$[61]	[121]0.0147	[118]0.0172				[96]$0.0015 N^{0.173}$[73]
40	HIK-3	[100]0.0085	[102]0.0107				[59]$0.0003 N^{0.255}$[88]	[104]0.0115	[108]0.0141	[87]0.0164	[87]0.0194	[85]0.0228	[41]$0.0005 N^{0.235}$[111]
41	HIK-4	[99]0.0083	[97]0.0104	[55]0.0121	[52]0.0146	[47]0.0177	[57]$0.0003 N^{0.260}$[91]	[103]0.0112	[105]0.0138	[85]0.0159	[85]0.0188	[83]0.0220	[43]$0.0005 N^{0.230}$[109]
42	HIK-5	[26]0.0026	[25]0.0034	[19]0.0040	[22]0.0049		[25]$0.0001 N^{0.274}$[99]	[46]0.0057	[47]0.0067	[44]0.0075	[44]0.0087	[46]0.0103	[29]$0.0004 N^{0.202}$[86]
43	IDEMIA-0	[65]0.0048	[70]0.0063	[41]0.0076	[39]0.0095	[37]0.0116	[29]$0.0001 N^{0.304}$[117]	[86]0.0093	[86]0.0113	[73]0.0131	[74]0.0153	[75]0.0182	[34]$0.0004 N^{0.227}$[108]
44	IDEMIA-007	[50]0.0041	[42]0.0044	[27]0.0047	[24]0.0052	[22]0.0057	[91]$0.0009 N^{0.116}$[36]	[29]0.0048	[27]0.0052	[27]0.0056	[28]0.0063	[27]0.0070	[68]$0.0008 N^{0.133}$[47]
45	IDEMIA-1	[68]0.0049	[72]0.0065	[44]0.0080	[41]0.0100	[43]0.0124	[24]$0.0001 N^{0.320}$[131]	[89]0.0096	[90]0.0116	[74]0.0135	[78]0.0162	[80]0.0194	[28]$0.0004 N^{0.243}$[122]
46	IDEMIA-2	[93]0.0075	[91]0.0099	[54]0.0119	[54]0.0149	[50]0.0183	[41]$0.0001 N^{0.304}$[119]	[99]0.0105	[96]0.0126				[67]$0.0008 N^{0.194}$[81]
47	IDEMIA-3	[52]0.0041	[60]0.0054				[28]$0.0001 N^{0.294}$[115]	[75]0.0080	[77]0.0095	[67]0.0110	[67]0.0127	[66]0.0148	[36]$0.0005 N^{0.212}$[97]
48	IDEMIA-4	[53]0.0042	[57]0.0052	[37]0.0061	[35]0.0074	[34]0.0088	[42]$0.0001 N^{0.257}$[89]	[76]0.0080	[73]0.0092	[63]0.0106	[65]0.0124	[64]0.0143	[45]$0.0005 N^{0.202}$[87]
49	IDEMIA-5	[60]0.0047	[68]0.0062	[39]0.0073	[37]0.0089	[36]0.0107	[38]$0.0001 N^{0.280}$[103]	[84]0.0090	[83]0.0107	[71]0.0123	[71]0.0144	[73]0.0169	[39]$0.0005 N^{0.217}$[102]
50	IDEMIA-6	[76]0.0055	[77]0.0071	[45]0.0083	[42]0.0100	[40]0.0119	[48]$0.0002 N^{0.261}$[92]	[93]0.0102	[94]0.0122	[79]0.0139	[77]0.0161	[78]0.0187	[53]$0.0006 N^{0.209}$[96]
51	IMAGUS-2	[192]0.1470	[163]0.1833	[77]0.2086	[72]0.2379		[127]$0.0083 N^{0.215}$[73]	[209]0.1838	[208]0.2223				[133]$0.0115 N^{0.208}$[94]
52	IMPERIAL-000	[55]0.0043	[43]0.0044	[26]0.0046	[75]0.6835	[56]0.6087	[1]$0.0000 N^{2.035}$[144]	[31]0.0048	[26]0.0051	[26]0.0054	[24]0.0057	[21]0.0061	[101]$0.0016 N^{0.080}$[21]
53	INCODE-004	[62]0.0047	[58]0.0052				[100]$0.0011 N^{0.109}$[33]	[42]0.0056	[39]0.0062	[36]0.0068	[34]0.0076	[33]0.0086	[62]$0.0007 N^{0.149}$[54]
54	INCODE-1	[107]0.0098	[109]0.0131	[66]0.0286	[64]0.0466		[5]$0.0000 N^{0.729}$[140]	[124]0.0151	[121]0.0190				[46]$0.0005 N^{0.250}$[124]
55	INCODE-3	[84]0.0067	[86]0.0088				[37]$0.0001 N^{0.308}$[121]	[107]0.0121	[112]0.0153	[89]0.0178	[89]0.0215	[87]0.0258	[31]$0.0004 N^{0.257}$[127]
56	INNOVATRICS-4	[87]0.0070	[81]0.0081				[90]$0.0008 N^{0.162}$[47]	[106]0.0120	[111]0.0149	[84]0.0158	[75]0.0158	[70]0.0158	[121]$0.0040 N^{0.088}$[24]
57	INTSYSMSU-000	[186]0.1241	[157]0.1294				[135]$0.0673 N^{0.046}$[16]	[196]0.1418	[193]0.1480	[112]0.1520	[108]0.1566	[105]0.1614	[142]$0.0789 N^{0.044}$[8]
58	ISYSTEMS-0	[91]0.0074	[85]0.0085	[49]0.0095	[45]0.0105	[39]0.0118	[93]$0.0009 N^{0.160}$[46]	[109]0.0122	[102]0.0136				[113]$0.0025 N^{0.119}$[39]
59	ISYSTEMS-1	[92]0.0074	[84]0.0085	[48]0.0094	[44]0.0105	[38]0.0118	[94]$0.0009 N^{0.158}$[44]	[108]0.0122	[101]0.0136				[115]$0.0025 N^{0.118}$[38]
60	ISYSTEMS-2	[45]0.0039	[45]0.0046	[31]0.0052			[71]$0.0004 N^{0.175}$[53]	[73]0.0076	[66]0.0088	[57]0.0096	[55]0.0108	[55]0.0121	[78]$0.0009 N^{0.156}$[58]
61	ISYSTEMS-3	[34]0.0035	[35]0.0040	[25]0.0044	[23]0.0050	[21]0.0057	[68]$0.0004 N^{0.166}$[49]	[64]0.0069	[57]0.0075	[50]0.0081	[46]0.0090	[44]0.0100	[92]$0.0012 N^{0.129}$[43]
62	KEDACOM-001	[110]0.0101	[96]0.0102				[126]$0.0081 N^{0.017}$[8]	[95]0.0102	[81]0.0104	[64]0.0106	[56]0.0109	[51]0.0113	[129]$0.0064 N^{0.035}$[5]
63	LOOKMAN-005	[112]0.0103	[98]0.0105				[125]$0.0076 N^{0.022}$[10]	[97]0.0105	[84]0.0107	[66]0.0110	[58]0.0113	[53]0.0118	[127]$0.0060 N^{0.040}$[7]
64	LOOKMAN-3	[101]0.0086	[88]0.0089				[121]$0.0049 N^{0.042}$[15]	[101]0.0109	[87]0.0114	[69]0.0117	[64]0.0123	[59]0.0131	[122]$0.0049 N^{0.059}$[16]
65	MEGVII-0	[89]0.0072	[92]0.0099	[56]0.0123	[55]0.0150	[49]0.0182	[34]$0.0001 N^{0.317}$[129]	[72]0.0075	[74]0.0094	[68]0.0111	[68]0.0134	[71]0.0162	[15]$0.0002 N^{0.264}$[131]
66	MEGVII-1						-	[110]0.0124	[103]0.0137	[82]0.0148	[79]0.0163	[76]0.0182	[109]$0.0021 N^{0.131}$[44]
67	MICROFOCUS-3	[212]0.4791	[177]0.5389	[81]0.5771			[137]$0.0951 N^{0.121}$[38]	[228]0.5417	[225]0.5953				[144]$0.1370 N^{0.103}$[32]
68	MICROFOCUS-5	[207]0.3155	[171]0.3701				[133]$0.0307 N^{0.174}$[52]	[223]0.3716	[220]0.4257	[117]0.4624	[113]0.5013	[110]0.5404	[141]$0.0684 N^{0.127}$[42]
69	MICROSOFT-0	[18]0.0021	[19]0.0026	[13]0.0031	[15]0.0040	[17]0.0048	[17]$0.0000 N^{0.280}$[104]	[34]0.0051	[34]0.0058	[33]0.0066	[36]0.0077	[39]0.0090	[26]$0.0003 N^{0.199}$[83]
70	MICROSOFT-1	[17]0.0020	[18]0.0026	[12]0.0031	[14]0.0038	[16]0.0047	[15]$0.0000 N^{0.286}$[111]	[32]0.0049	[32]0.0056				[51]$0.0006 N^{0.158}$[61]
71	MICROSOFT-2	[22]0.0023	[23]0.0029	[16]0.0035	[18]0.0042	[19]0.0051	[21]$0.0001 N^{0.272}$[98]	[38]0.0052	[38]0.0061				[42]$0.0005 N^{0.174}$[74]
72	MICROSOFT-3	[2]0.0009	[4]0.0011				[13]$0.0000 N^{0.255}$[87]	[3]0.0028	[4]0.0032	[5]0.0035	[6]0.0039	[5]0.0045	[24]$0.0003 N^{0.166}$[68]

Table 10: **Investigation-mode: Effect of N on FNIR at rank 1** *For five enrollment population sizes, N, with T = 0 and FPIR = 1. The left five columns apply for consolidated enrollment of a variable number of lifetime images from each subject. The right five columns apply for enrollment of one recent image. Missing entries usually apply because another algorithm from the same developer was run instead. Some developers are missing because less accurate algorithms were not run on galleries with $N > 1\,600\,000$. Throughout blue superscripts indicate the rank of the algorithm for that column, and yellow highlighting indicates the most accurate value. Caution: The Power-low models are mostly intended to draw attention to the kind of behavior, not as a model to be used for prediction.*

MISSES NOT AT RANK 1		ENROL LIFETIME						ENROL MOST RECENT					
FNIR(N, T= 0, R =1)		DATASET: FRVT 2018						DATASET: FRVT 2018					
#	ALGORITHM	N=0.64M	N=1.6M	N=3.0M	N=6.0M	N=12.0M	aN^b	N=0.64M	N=1.6M	N=3.0M	N=6.0M	N=12.0M	aN^b
73	MICROSOFT-4	[1]0.0008	[1]0.0010	[3]0.0013	[4]0.0015	[4]0.0019	[10]0.0000 $N^{0.285}$ [108]	[2]0.0027	[2]0.0031	[3]0.0034	[4]0.0038	[4]0.0045	[18]0.0003 $N^{0.174}$ [75]
74	MICROSOFT-5	[4]0.0010	[5]0.0013	[5]0.0015	[6]0.0019	[7]0.0025	[9]0.0000 $N^{0.304}$ [118]	[4]0.0028	[5]0.0033	[8]0.0037	[10]0.0044	[11]0.0052	[9]0.0002 $N^{0.215}$ [100]
75	MICROSOFT-6	[5]0.0010	[7]0.0014	[7]0.0016	[8]0.0020	[9]0.0026	[7]0.0000 $N^{0.315}$ [127]	[5]0.0029	[8]0.0033	[9]0.0039	[12]0.0045	[12]0.0053	[13]0.0002 $N^{0.206}$ [93]
76	NEC-0	[106]0.0097	[108]0.0127	[60]0.0154	[57]0.0185	[51]0.0223	[55]0.0002 $N^{0.284}$ [106]	[125]0.0157	[122]0.0196	[92]0.0229	[90]0.0270	[88]0.0320	[52]0.0006 $N^{0.243}$ [121]
77	NEC-1	[124]0.0136	[117]0.0164				[96]0.0009 $N^{0.202}$ [69]	[139]0.0206	[134]0.0235	[96]0.0259	[94]0.0292	[90]0.0329	[112]0.0024 $N^{0.160}$ [65]
78	NEC-2	[6]0.0010	[3]0.0011	[1]0.0012	[1]0.0012	[1]0.0014	[60]0.0003 $N^{0.096}$ [30]	[1]0.0026	[1]0.0028	[1]0.0029	[1]0.0030	[1]0.0031	[91]0.0012 $N^{0.059}$ [15]
79	NEC-3	[7]0.0012	[6]0.0013	[4]0.0014	[3]0.0014	[2]0.0016	[73]0.0004 $N^{0.080}$ [22]	[8]0.0030	[3]0.0031	[2]0.0032	[2]0.0034	[2]0.0035	[100]0.0016 $N^{0.048}$ [10]
80	NEUROTECHNOLOGY-007	[71]0.0052	[220]1.0000	[36]0.0061	[34]0.0068	[31]0.0076	[144]21.1320 $N^{-0.477}$ [1]	[51]0.0058	[44]0.0066	[40]0.0071	[38]0.0079	[37]0.0088	[76]0.0009 $N^{0.139}$ [48]
81	NEUROTECHNOLOGY-3	[134]0.0161	[124]0.0199				[87]0.0007 $N^{0.234}$ [81]	[138]0.0204	[137]0.0250	[98]0.0288	[97]0.0331	[95]0.0386	[87]0.0011 $N^{0.216}$ [101]
82	NEUROTECHNOLOGY-4	[69]0.0049	[64]0.0058	[38]0.0065	[36]0.0075	[33]0.0087	[66]0.0004 $N^{0.195}$ [63]	[67]0.0072	[62]0.0082	[54]0.0090	[52]0.0100	[52]0.0114	[75]0.0009 $N^{0.156}$ [56]
83	NEUROTECHNOLOGY-5	[35]0.0035	[38]0.0042	[24]0.0043	[26]0.0053	[23]0.0061	[62]0.0003 $N^{0.184}$ [55]	[54]0.0061	[49]0.0068	[43]0.0074	[41]0.0082	[40]0.0094	[73]0.0008 $N^{0.149}$ [52]
84	NEWLAND-2						-	[183]0.0671	[180]0.0811	[111]0.0913	[107]0.1038		[123]0.0050 $N^{0.195}$ [82]
85	NOBLIS-2	[187]0.1261	[161]0.1565				[122]0.0054 $N^{0.236}$ [82]	[200]0.1509	[200]0.1816	[114]0.2040	[110]0.2377		[132]0.0102 $N^{0.201}$ [85]
86	NTECHLAB-0	[77]0.0056	[79]0.0077	[47]0.0094	[47]0.0114	[45]0.0139	[30]0.0001 $N^{0.310}$ [123]	[85]0.0092	[88]0.0115	[78]0.0137	[80]0.0164	[81]0.0196	[20]0.0003 $N^{0.261}$ [128]
87	NTECHLAB-007	[54]0.0043	[46]0.0047	[29]0.0050	[27]0.0055	[24]0.0062	[89]0.0008 $N^{0.126}$ [39]	[30]0.0048	[28]0.0053	[29]0.0057	[29]0.0064	[28]0.0071	[71]0.0008 $N^{0.132}$ [46]
88	NTECHLAB-008	[40]0.0038	[36]0.0040	[23]0.0042	[20]0.0045	[18]0.0049	[101]0.0011 $N^{0.089}$ [24]	[16]0.0041	[16]0.0044	[16]0.0046	[16]0.0050	[14]0.0054	[85]0.0011 $N^{0.096}$ [28]
89	NTECHLAB-1	[88]0.0070	[90]0.0097	[53]0.0119	[51]0.0146	[48]0.0179	[32]0.0001 $N^{0.317}$ [130]	[100]0.0108	[106]0.0139				[19]0.0003 $N^{0.278}$ [137]
90	NTECHLAB-3	[38]0.0037	[55]0.0051				[14]0.0000 $N^{0.351}$ [136]	[61]0.0065	[63]0.0082	[56]0.0096	[59]0.0115	[61]0.0135	[16]0.0002 $N^{0.251}$ [125]
91	NTECHLAB-4	[30]0.0030	[34]0.0040	[28]0.0049	[29]0.0060	[29]0.0075	[16]0.0000 $N^{0.315}$ [128]	[43]0.0056	[51]0.0068	[47]0.0078	[47]0.0092	[48]0.0107	[21]0.0003 $N^{0.220}$ [103]
92	NTECHLAB-5	[29]0.0028	[33]0.0039				[11]0.0000 $N^{0.365}$ [138]	[36]0.0051	[43]0.0064	[46]0.0076	[50]0.0092	[50]0.0112	[8]0.0001 $N^{0.266}$ [132]
93	NTECHLAB-6	[24]0.0024	[26]0.0034	[22]0.0042	[25]0.0052	[25]0.0066	[12]0.0000 $N^{0.346}$ [135]	[27]0.0047	[35]0.0059	[38]0.0069	[40]0.0081	[42]0.0098	[11]0.0002 $N^{0.250}$ [123]
94	PARAVISION-005	[39]0.0037	[31]0.0038	[17]0.0038	[16]0.0040	[12]0.0041	[114]0.0023 $N^{0.036}$ [13]	[17]0.0041	[14]0.0042	[13]0.0042	[9]0.0044	[6]0.0046	[114]0.0025 $N^{0.036}$ [6]
95	PIXELALL-002	[90]0.0072	[82]0.0084				[92]0.0009 $N^{0.159}$ [45]	[58]0.0064	[54]0.0072	[49]0.0079	[45]0.0089	[45]0.0101	[64]0.0008 $N^{0.158}$ [62]
96	PIXELALL-003	[63]0.0047	[51]0.0050				[112]0.0020 $N^{0.064}$ [19]	[23]0.0045	[23]0.0048	[24]0.0051	[23]0.0054	[20]0.0059	[94]0.0014 $N^{0.088}$ [23]
97	QUANTASOFT-1	[221]0.9857	[181]0.9857				[143]0.9857 $N^{-0.000}$ [2]	[215]0.2198	[207]0.2198	[115]0.2198		[106]0.2198	[145]0.2198 $N^{0.000}$ [1]
98	RANKONE-0	[151]0.0255	[135]0.0319	[67]0.0366	[63]0.0425	[55]0.0486	[105]0.0014 $N^{0.220}$ [75]	[169]0.0375	[163]0.0455	[109]0.0514	[105]0.0564	[104]0.0654	[119]0.0032 $N^{0.186}$ [77]
99	RANKONE-007	[61]0.0047	[56]0.0052	[34]0.0055	[30]0.0060	[26]0.0068	[97]0.0009 $N^{0.121}$ [37]	[41]0.0055	[36]0.0060	[32]0.0065	[31]0.0071	[30]0.0079	[81]0.0010 $N^{0.124}$ [41]
100	RANKONE-1	[130]0.0152	[123]0.0194	[63]0.0224	[60]0.0260	[54]0.0302	[85]0.0007 $N^{0.232}$ [80]	[147]0.0226	[136]0.0247				[128]0.0062 $N^{0.097}$ [29]
101	RANKONE-2	[120]0.0117	[114]0.0149				[65]0.0003 $N^{0.268}$ [95]	[136]0.0181	[130]0.0221	[95]0.0250	[93]0.0288	[92]0.0330	[89]0.0012 $N^{0.204}$ [91]
102	RANKONE-3	[119]0.0117	[113]0.0149	[61]0.0172	[58]0.0200	[52]0.0236	[79]0.0005 $N^{0.237}$ [83]	[135]0.0181	[129]0.0221	[94]0.0250	[92]0.0288	[91]0.0330	[88]0.0012 $N^{0.204}$ [90]
103	RANKONE-4	[148]0.0246	[134]0.0318				[81]0.0006 $N^{0.282}$ [105]	[164]0.0351	[162]0.0441	[108]0.0508			[95]0.0014 $N^{0.239}$ [119]
104	RANKONE-5	[80]0.0058	[78]0.0072	[46]0.0086	[43]0.0103	[42]0.0122	[50]0.0002 $N^{0.258}$ [90]	[92]0.0102	[93]0.0120	[77]0.0136	[76]0.0158	[77]0.0182	[60]0.0007 $N^{0.201}$ [84]
105	REALNETWORKS-0	[160]0.0337	[142]0.0443	[68]0.0527			[86]0.0007 $N^{0.290}$ [113]	[159]0.0330	[161]0.0426				[65]0.0008 $N^{0.280}$ [139]
106	REALNETWORKS-003	[138]0.0169	[128]0.0220				[70]0.0004 $N^{0.285}$ [107]	[141]0.0209	[140]0.0268	[100]0.0317	[99]0.0378	[99]0.0449	[56]0.0006 $N^{0.261}$ [129]
107	REALNETWORKS-004	[129]0.0149	[122]0.0192				[69]0.0004 $N^{0.276}$ [101]	[137]0.0202	[138]0.0262	[99]0.0310	[98]0.0373	[96]0.0442	[48]0.0006 $N^{0.268}$ [134]
108	REALNETWORKS-2	[146]0.0240	[136]0.0320				[67]0.0004 $N^{0.313}$ [125]	[157]0.0323	[155]0.0418	[107]0.0494	[106]0.0587	[103]0.0604	[103]0.0017 $N^{0.223}$ [105]
109	REMARKAI-000	[57]0.0046	[53]0.0051				[99]0.0011 $N^{0.109}$ [34]	[39]0.0054	[37]0.0060	[34]0.0067	[32]0.0075	[31]0.0085	[58]0.0007 $N^{0.156}$ [57]
110	REMARKAI-2	[58]0.0047	[69]0.0062				[26]0.0001 $N^{0.314}$ [126]	[81]0.0085	[82]0.0105	[70]0.0122	[72]0.0145		[27]0.0004 $N^{0.237}$ [114]
111	SCANOVATE-000	[217]0.7783	[178]0.7787	[82]0.7787	[76]0.7787	[57]0.7787	[142]0.7767 $N^{0.000}$ [3]	[59]0.0065	[60]0.0076	[52]0.0085	[51]0.0099	[43]0.0100	[69]0.0008 $N^{0.158}$ [63]
112	SENSETIME-0	[13]0.0016	[13]0.0018				[77]0.0005 $N^{0.095}$ [26]	[25]0.0046	[22]0.0048	[23]0.0050	[20]0.0053	[18]0.0057	[105]0.0018 $N^{0.071}$ [18]
113	SENSETIME-002	[122]0.0124	[107]0.0124	[57]0.0124	[48]0.0125	[44]0.0127	[130]0.0111 $N^{0.008}$ [7]	[128]0.0163	[115]0.0163	[86]0.0163	[81]0.0164	[72]0.0165	[136]0.0150 $N^{0.006}$ [2]
114	SENSETIME-003	[33]0.0034	[28]0.0034	[15]0.0034	[12]0.0035	[10]0.0036	[117]0.0026 $N^{0.020}$ [9]	[11]0.0036	[9]0.0036	[6]0.0037	[3]0.0038	[3]0.0039	[116]0.0026 $N^{0.025}$ [4]
115	SENSETIME-1	[12]0.0016	[11]0.0018				[76]0.0004 $N^{0.096}$ [29]	[24]0.0046	[24]0.0048	[21]0.0050	[21]0.0053	[22]0.0062	[93]0.0012 $N^{0.095}$ [27]
116	SHAMAN-3	[177]0.0808	[154]0.0969	[75]0.1091			[123]0.0060 $N^{0.195}$ [64]	[191]0.1074	[185]0.1266				[131]0.0097 $N^{0.180}$ [76]
117	SHAMAN-7	[154]0.0290	[132]0.0310				[129]0.0106 $N^{0.075}$ [20]	[171]0.0397	[158]0.0422	[106]0.0442	[104]0.0468	[101]0.0499	[135]0.0139 $N^{0.078}$ [19]
118	SIAT-1	[205]0.2638	[168]0.2639	[78]0.2640			[140]0.2618 $N^{0.001}$ [5]	[12]0.0037	[11]0.0039	[11]0.0041	[11]0.0044	[9]0.0049	[79]0.0010 $N^{0.098}$ [30]
119	SIAT-2	[202]0.2127	[166]0.2128				[139]0.2115 $N^{0.000}$ [4]	[13]0.0037	[12]0.0040	[12]0.0042	[13]0.0045	[8]0.0049	[82]0.0011 $N^{0.092}$ [25]
120	SMILART-4	[219]0.8189	[179]0.9531				[136]0.0894 $N^{0.166}$ [48]	[232]0.9176	[229]0.9649	[118]0.9908			[146]0.4706 $N^{0.050}$ [11]
121	SYNESIS-3	[183]0.1133	[159]0.1350				[128]0.0088 $N^{0.191}$ [58]	[199]0.1478	[198]0.1721	[113]0.1897	[109]0.2108	[107]0.2338	[137]0.0184 $N^{0.156}$ [59]
122	TECH5-001	[73]0.0052	[65]0.0059				[98]0.0009 $N^{0.128}$ [40]	[50]0.0058	[46]0.0066	[42]0.0074	[42]0.0083	[41]0.0097	[47]0.0006 $N^{0.173}$ [72]
123	TEVIAN-4	[79]0.0058	[80]0.0080	[50]0.0097			[20]0.0001 $N^{0.341}$ [134]	[98]0.0105	[100]0.0134				[25]0.0003 $N^{0.264}$ [130]
124	TEVIAN-5	[49]0.0040	[59]0.0053				[23]0.0001 $N^{0.307}$ [120]	[68]0.0074	[71]0.0092	[61]0.0104	[66]0.0125	[67]0.0151	[23]0.0003 $N^{0.240}$ [120]
125	TIGER-0	[163]0.0364	[144]0.0480	[70]0.0565	[66]0.0678		[95]0.0009 $N^{0.278}$ [102]	[175]0.0494	[174]0.0638				[90]0.0012 $N^{0.279}$ [138]
126	TIGER-2	[32]0.0034	[41]0.0044				[22]0.0001 $N^{0.295}$ [116]	[56]0.0063	[59]0.0075	[53]0.0088	[54]0.0107	[57]0.0126	[17]0.0003 $N^{0.239}$ [116]
127	TONGYITRANS-1	[105]0.0096	[104]0.0114	[58]0.0127	[53]0.0148		[88]0.0007 $N^{0.193}$ [60]	[77]0.0080	[75]0.0095				[54]0.0006 $N^{0.189}$ [80]
128	TOSHIBA-0	[25]0.0026	[24]0.0033				[19]0.0001 $N^{0.285}$ [110]	[49]0.0058	[50]0.0068	[45]0.0076	[43]0.0085	[74]0.0178	[6]0.0001 $N^{0.337}$ [141]
129	VD-0	[209]0.3583	[173]0.4303	[79]0.4776	[73]0.5281		[134]0.0355 $N^{0.174}$ [51]	[225]0.4073	[223]0.4751				[139]0.0431 $N^{0.168}$ [70]
130	VD-1	[142]0.0184	[129]0.0221				[103]0.0012 $N^{0.201}$ [68]	[150]0.0256	[145]0.0302	[102]0.0341	[101]0.0389	[98]0.0443	[107]0.0021 $N^{0.188}$ [79]
131	VIGILANTSOLUTIONS-3	[165]0.0410	[148]0.0549	[71]0.0654	[65]0.0654		[116]0.0023 $N^{0.219}$ [74]	[180]0.0561	[178]0.0719				[97]0.0015 $N^{0.271}$ [136]
132	VISIONLABS-008	[51]0.0041	[39]0.0042				[118]0.0028 $N^{0.029}$ [12]	[22]0.0045	[20]0.0046	[19]0.0048	[18]0.0052	[19]0.0057	[99]0.0015 $N^{0.079}$ [20]
133	VISIONLABS-3	[37]0.0037	[52]0.0050	[40]0.0076	[50]0.0130		[6]0.0000 $N^{0.563}$ [139]	[66]0.0070	[68]0.0089	[72]0.0124	[84]0.0185		[4]0.0000 $N^{0.434}$ [143]
134	VISIONLABS-4	[14]0.0016	[14]0.0020				[36]0.0001 $N^{0.203}$ [70]	[14]0.0037	[17]0.0044	[20]0.0049	[27]0.0062	[36]0.0088	[7]0.0001 $N^{0.282}$ [140]
135	VISIONLABS-5	[11]0.0015	[12]0.0018	[9]0.0020	[10]0.0028	[11]0.0040	[8]0.0000 $N^{0.332}$ [133]	[9]0.0035	[13]0.0041	[15]0.0046	[22]0.0054	[25]0.0068	[12]0.0002 $N^{0.223}$ [106]
136	VISIONLABS-6	[10]0.0013	[9]0.0015				[53]0.0002 $N^{0.142}$ [42]	[7]0.0030	[7]0.0033	[7]0.0037	[8]0.0044	[17]0.0057	[10]0.0002 $N^{0.214}$ [99]
137	VISIONLABS-7	[8]0.0013	[8]0.0014	[6]0.0016	[5]0.0018	[5]0.0022	[35]0.0001 $N^{0.183}$ [54]	[6]0.0030	[6]0.0033	[4]0.0035	[5]0.0039	[10]0.0050	[22]0.0003 $N^{0.169}$ [71]
138	VOCORD-3	[74]0.0053	[74]0.0067	[43]0.0080	[40]0.0096		[44]0.0001 $N^{0.271}$ [97]	[65]0.0070	[65]0.0085				[35]0.0005 $N^{0.204}$ [89]
139	VOCORD-5	[66]0.0048	[63]0.0057				[72]0.0004 $N^{0.187}$ [56]	[79]0.0081	[72]0.0092	[62]0.0104	[63]0.0120	[62]0.0140	[55]0.0006 $N^{0.188}$ [78]
140	YISHENG-1	[131]0.0155	[125]0.0208	[65]0.0248	[62]0.0298		[63]0.0003 $N^{0.294}$ [114]	[148]0.0227	[144]0.0290				[57]0.0006 $N^{0.266}$ [133]
141	YITU-0	[47]0.0040	[47]0.0047	[33]0.0053	[32]0.0061	[28]0.0071	[58]0.0003 $N^{0.200}$ [67]	[62]0.0066	[56]0.0074	[51]0.0082	[49]0.0092	[47]0.0103	[70]0.0008 $N^{0.156}$ [60]
142	YITU-1	[44]0.0039	[44]0.0046	[30]0.0051	[28]0.0059	[27]0.0069	[61]0.0003 $N^{0.194}$ [62]	[60]0.0065	[55]0.0072				[98]0.0015 $N^{0.110}$ [35]
143	YITU-2	[9]0.0013	[10]0.0015	[8]0.0017	[7]0.0019	[6]0.0023	[31]0.0001 $N^{0.196}$ [66]	[19]0.0041	[18]0.0044	[17]0.0047	[17]0.0050	[16]0.0055	[83]0.0011 $N^{0.099}$ [31]
144	YITU-3	[19]0.0021	[17]0.0023				[82]0.0006 $N^{0.098}$ [31]	[37]0.0052	[29]0.0054	[28]0.0057	[26]0.0061	[23]0.0065	[104]0.0017 $N^{0.081}$ [22]

Table 11: **Investigation-mode: Effect of N on FNIR at rank 1** *For five enrollment population sizes, N, with T = 0 and FPIR = 1. The left five columns apply for consolidated enrollment of a variable number of lifetime images from each subject. The right five columns apply for enrollment of one recent image. Missing entries usually apply because another algorithm from the same developer was run instead. Some developers are missing because less accurate algorithms were not run on galleries with $N > 1\,600\,000$. Throughout blue superscripts indicate the rank of the algorithm for that column, and yellow highlighting indicates the most accurate value. Caution: The Power-low models are mostly intended to draw attention to the kind of behavior, not as a model to be used for prediction.*

MISSES NOT AT RANK 1		ENROL LIFETIME						ENROL MOST RECENT					
FNIR(N, T= 0, R =1)		DATASET: FRVT 2018						DATASET: FRVT 2018					
#	ALGORITHM	N=0.64M	N=1.6M	N=3.0M	N=6.0M	N=12.0M	aN^b	N=0.64M	N=1.6M	N=3.0M	N=6.0M	N=12.0M	aN^b
145	YITU-4	[3] 0.0010	[2] 0.0011	[2] 0.0012	[2] 0.0014	[3] 0.0019	[18] 0.0001 $N^{0.211}$ [72]	[10] 0.0036	[10] 0.0037	[10] 0.0040	[7] 0.0042	[29] 0.0072	[14] 0.0002 $N^{0.208}$ [95]
146	YITU-5	[15] 0.0019	[15] 0.0020	[10] 0.0021	[9] 0.0023	[8] 0.0025	[80] 0.0005 $N^{0.096}$ [28]	[26] 0.0047	[25] 0.0048	[22] 0.0050	[19] 0.0052	[15] 0.0055	[108] 0.0021 $N^{0.058}$ [14]

Table 12: **Investigation-mode: Effect of N on FNIR at rank 1** *For five enrollment population sizes, N, with T = 0 and FPIR = 1. The left five columns apply for consolidated enrollment of a variable number of lifetime images from each subject. The right five columns apply for enrollment of one recent image. Missing entries usually apply because another algorithm from the same developer was run instead. Some developers are missing because less accurate algorithms were not run on galleries with $N >$ 1 600 000. Throughout blue superscripts indicate the rank of the algorithm for that column, and yellow highlighting indicates the most accurate value. Caution: The Power-low models are mostly intended to draw attention to the kind of behavior, not as a model to be used for prediction.*

MISSES NOT AT RANK 50		ENROL LIFETIME						ENROL MOST RECENT					
FNIR(N, T= 0, R =50)		DATASET: FRVT 2018						DATASET: FRVT 2018					
#	ALGORITHM	N=0.64M	N=1.6M	N=3.0M	N=6.0M	N=12.0M	aN^b	N=0.64M	N=1.6M	N=3.0M	N=6.0M	N=12.0M	aN^b
1	3DIVI-3	^{155}0.0103	^{143}0.0151	^{71}0.0192	^{66}0.0241		^{33}0.0001 $N^{0.382}$ ^{133}	^{167}0.0159	^{168}0.0217				^{12}0.0002 $N^{0.343}$ ^{135}
2	3DIVI-5	^{79}0.0030	^{85}0.0037				^{56}0.0001 $N^{0.237}$ ^{99}	^{116}0.0065	^{115}0.0074	^{84}0.0083	^{84}0.0094	^{84}0.0107	^{55}0.0007 $N^{0.169}$ ^{99}
3	ALCHERA-0	^{141}0.0073	^{123}0.0076	^{63}0.0079	^{59}0.0101		^{96}0.0012 $N^{0.133}$ ^{67}	^{159}0.0125	^{150}0.0129				^{134}0.0079 $N^{0.034}$ ^{26}
4	ALCHERA-3	^{78}0.0030	^{94}0.0040				^{24}0.0000 $N^{0.309}$ ^{116}	^{80}0.0047	^{87}0.0052	^{68}0.0056	^{71}0.0063	^{67}0.0070	^{64}0.0008 $N^{0.136}$ ^{88}
5	ALLGOVISION-000	^{138}0.0069	^{121}0.0073				^{122}0.0033 $N^{0.056}$ ^{39}	^{140}0.0089	^{131}0.0094	^{90}0.0097	^{88}0.0102	^{85}0.0108	^{124}0.0038 $N^{0.063}$ ^{54}
6	ANKE-0	^{65}0.0024	^{71}0.0030				^{51}0.0001 $N^{0.234}$ ^{97}	^{108}0.0057	^{104}0.0065	^{81}0.0072	^{79}0.0081	^{76}0.0092	^{51}0.0006 $N^{0.164}$ ^{96}
7	ANKE-002	^{107}0.0039	^{92}0.0039				^{114}0.0029 $N^{0.022}$ ^{23}	^{57}0.0042	^{53}0.0043	^{42}0.0044	^{41}0.0045	^{32}0.0046	^{113}0.0030 $N^{0.027}$ ^{17}
8	AWARE-3	^{108}0.0039	^{110}0.0050	^{59}0.0061	^{57}0.0077		^{40}0.0001 $N^{0.299}$ ^{113}	^{133}0.0081	^{141}0.0101	^{98}0.0118	^{97}0.0139	^{100}0.0170	^{28}0.0003 $N^{0.248}$ ^{124}
9	AWARE-5	^{114}0.0041	^{113}0.0053				^{55}0.0001 $N^{0.263}$ ^{107}	^{139}0.0088	^{143}0.0108	^{101}0.0127	^{100}0.0154	^{86}0.0115	^{83}0.0017 $N^{0.128}$ ^{82}
10	AYONIX-0	^{208}0.1723	^{173}0.2142	^{79}0.2467	^{74}0.2850		^{131}0.0085 $N^{0.225}$ ^{94}	^{226}0.1967	^{223}0.2402				^{138}0.0107 $N^{0.218}$ ^{115}
11	AYONIX-2	^{197}0.0646	^{162}0.0873				^{90}0.0008 $N^{0.329}$ ^{123}	^{218}0.0974	^{217}0.1298	^{116}0.1547	^{111}0.1850	^{108}0.2171	^{104}0.0026 $N^{0.273}$ ^{128}
12	CAMVI-3	^{163}0.0142	^{153}0.0367	^{75}0.0527	^{72}0.1789		^{5}0.0000 $N^{1.080}$ ^{140}	^{176}0.0221	^{190}0.0541				^{3}0.0000 $N^{0.980}$ ^{145}
13	CAMVI-4	^{148}0.0078	^{151}0.0323				^{2}0.0000 $N^{1.545}$ ^{143}	^{164}0.0137	^{187}0.0485	^{112}0.0736	^{112}0.2380	^{109}0.2383	^{1}0.0000 $N^{1.024}$ ^{146}
14	COGENT-0	^{55}0.0021	^{53}0.0024	^{31}0.0027	^{31}0.0031	^{41}0.0045	^{36}0.0001 $N^{0.253}$ ^{105}	^{83}0.0047	^{77}0.0050	^{63}0.0054	^{70}0.0062	^{88}0.0122	^{11}0.0001 $N^{0.288}$ ^{131}
15	COGENT-1	^{54}0.0021	^{52}0.0024				^{63}0.0002 $N^{0.189}$ ^{85}	^{82}0.0047	^{76}0.0050	^{62}0.0054	^{69}0.0062	^{87}0.0122	^{10}0.0001 $N^{0.288}$ ^{130}
16	COGENT-2	^{24}0.0011	^{27}0.0013	^{17}0.0014	^{17}0.0016	^{14}0.0017	^{60}0.0001 $N^{0.152}$ ^{70}	^{41}0.0038	^{44}0.0041	^{38}0.0042	^{37}0.0044	^{36}0.0047	^{78}0.0016 $N^{0.066}$ ^{58}
17	COGENT-3	^{35}0.0014	^{31}0.0016	^{19}0.0018	^{19}0.0020	^{17}0.0023	^{54}0.0001 $N^{0.181}$ ^{80}	^{47}0.0040	^{51}0.0042	^{46}0.0044	^{42}0.0046	^{40}0.0048	^{80}0.0017 $N^{0.065}$ ^{56}
18	COGNITEC-0	^{106}0.0039	^{108}0.0050				^{47}0.0001 $N^{0.281}$ ^{108}	^{127}0.0076	^{128}0.0092	^{96}0.0104	^{95}0.0123	^{96}0.0148	^{38}0.0004 $N^{0.227}$ ^{119}
19	COGNITEC-1	^{67}0.0024	^{66}0.0028	^{39}0.0032	^{41}0.0037	^{40}0.0044	^{64}0.0002 $N^{0.200}$ ^{86}	^{106}0.0056	^{99}0.0060	^{79}0.0066	^{77}0.0072	^{73}0.0081	^{67}0.0010 $N^{0.128}$ ^{83}
20	COGNITEC-2	^{49}0.0020	^{43}0.0021	^{24}0.0023	^{22}0.0025	^{19}0.0027	^{78}0.0004 $N^{0.113}$ ^{61}	^{93}0.0049	^{86}0.0052	^{64}0.0054	^{60}0.0056	^{57}0.0060	^{92}0.0021 $N^{0.063}$ ^{53}
21	COGNITEC-3	^{61}0.0023	^{54}0.0025	^{29}0.0026	^{26}0.0028	^{22}0.0031	^{85}0.0006 $N^{0.100}$ ^{58}	^{100}0.0053	^{94}0.0056	^{71}0.0057	^{64}0.0060	^{62}0.0063	^{103}0.0025 $N^{0.057}$ ^{48}
22	CYBERLINK-000	^{118}0.0043	^{102}0.0044				^{113}0.0028 $N^{0.031}$ ^{29}	^{84}0.0047	^{73}0.0049	^{57}0.0050	^{56}0.0052	^{50}0.0054	^{106}0.0026 $N^{0.043}$ ^{32}
23	CYBERLINK-001	^{104}0.0038	^{88}0.0039				^{116}0.0030 $N^{0.018}$ ^{19}	^{60}0.0042	^{58}0.0044	^{47}0.0044	^{46}0.0046	^{42}0.0049	^{98}0.0023 $N^{0.045}$ ^{34}
24	DAHUA-002	^{94}0.0036	^{83}0.0037	^{48}0.0037	^{44}0.0037	^{32}0.0038	^{118}0.0032 $N^{0.010}$ ^{13}	^{45}0.0039	^{42}0.0040	^{31}0.0040	^{29}0.0041	^{21}0.0041	^{115}0.0032 $N^{0.015}$ ^{10}
25	DAHUA-1	^{53}0.0021	^{48}0.0022				^{84}0.0005 $N^{0.099}$ ^{57}	^{78}0.0046	^{72}0.0049	^{59}0.0051	^{58}0.0054	^{54}0.0058	^{76}0.0015 $N^{0.085}$ ^{67}
26	DEEPSEA-001	^{90}0.0036	^{81}0.0036				^{111}0.0027 $N^{0.022}$ ^{22}	^{42}0.0039	^{43}0.0040	^{36}0.0042	^{35}0.0044	^{33}0.0046	^{84}0.0018 $N^{0.058}$ ^{50}
27	DERMALOG-4	^{168}0.0186	^{148}0.0272	^{73}0.0340	^{69}0.0427		^{58}0.0001 $N^{0.372}$ ^{131}	^{181}0.0262	^{183}0.0365				^{15}0.0002 $N^{0.363}$ ^{137}
28	DERMALOG-5	^{137}0.0066	^{131}0.0092				^{27}0.0001 $N^{0.362}$ ^{128}	^{155}0.0113	^{154}0.0142	^{107}0.0192	^{105}0.0275	^{104}0.0427	^{5}0.0000 $N^{0.457}$ ^{142}
29	DERMALOG-6	^{122}0.0046	^{104}0.0047				^{126}0.0035 $N^{0.020}$ ^{20}	^{132}0.0080	^{119}0.0081	^{85}0.0083	^{82}0.0085	^{74}0.0087	^{131}0.0053 $N^{0.030}$ ^{22}
30	EVERAI-0	^{127}0.0050	^{142}0.0150				^{4}0.0000 $N^{1.185}$ ^{141}	^{128}0.0077	^{165}0.0182	^{108}0.0317			^{2}0.0000 $N^{0.919}$ ^{144}
31	EVERAI-1	^{30}0.0013	^{29}0.0014				^{72}0.0004 $N^{0.096}$ ^{56}	^{25}0.0031	^{28}0.0033	^{21}0.0034			^{73}0.0012 $N^{0.070}$ ^{62}
32	EVERAI-3	^{28}0.0012	^{28}0.0013	^{16}0.0014	^{14}0.0014		^{76}0.0004 $N^{0.080}$ ^{50}	^{21}0.0029	^{16}0.0030	^{14}0.0032	^{15}0.0034	^{12}0.0035	^{72}0.0012 $N^{0.065}$ ^{57}
33	EVERAI-PARAVISION-004	^{91}0.0036	^{80}0.0036	^{47}0.0036	^{40}0.0037	^{31}0.0037	^{119}0.0032 $N^{0.008}$ ^{12}	^{43}0.0039	^{38}0.0039	^{29}0.0040	^{26}0.0040	^{20}0.0040	^{121}0.0036 $N^{0.007}$ ^{6}
34	EYEDEA-3	^{158}0.0113	^{144}0.0160	^{72}0.0209	^{67}0.0252		^{46}0.0001 $N^{0.364}$ ^{129}	^{172}0.0175	^{169}0.0236				^{20}0.0002 $N^{0.326}$ ^{133}
35	F8-001	^{216}0.5355	^{177}0.5355				^{141}0.5349 $N^{0.000}$ ^{4}	^{158}0.0124	^{148}0.0125	^{100}0.0125	^{96}0.0125	^{89}0.0125	^{140}0.0120 $N^{0.003}$ ^{3}
36	GLORY-1	^{187}0.0415	^{156}0.0490	^{76}0.0539	^{70}0.0600		^{128}0.0047 $N^{0.164}$ ^{73}	^{205}0.0604	^{201}0.0698				^{133}0.0073 $N^{0.158}$ ^{93}
37	GORILLA-004	^{102}0.0037	^{90}0.0039	^{52}0.0041	^{48}0.0043	^{44}0.0047	^{99}0.0013 $N^{0.077}$ ^{49}	^{56}0.0042	^{60}0.0044	^{54}0.0048	^{55}0.0051	^{51}0.0056	^{69}0.0011 $N^{0.098}$ ^{72}
38	GORILLA-2	^{59}0.0023	^{70}0.0029				^{22}0.0000 $N^{0.289}$ ^{110}	^{95}0.0050	^{100}0.0061	^{80}0.0070	^{80}0.0084	^{80}0.0102	^{16}0.0002 $N^{0.238}$ ^{122}
39	HIK-2	^{151}0.0084	^{130}0.0090	^{64}0.0097	^{60}0.0106	^{53}0.0118	^{103}0.0018 $N^{0.115}$ ^{62}	^{138}0.0087	^{129}0.0093				^{120}0.0035 $N^{0.068}$ ^{60}
40	HIK-3	^{58}0.0023	^{64}0.0028				^{50}0.0001 $N^{0.230}$ ^{96}	^{68}0.0044	^{80}0.0051	^{72}0.0058	^{73}0.0066	^{69}0.0076	^{36}0.0003 $N^{0.189}$ ^{106}
41	HIK-4	^{64}0.0023	^{68}0.0028	^{40}0.0033	^{45}0.0039	^{45}0.0048	^{45}0.0001 $N^{0.246}$ ^{101}	^{75}0.0045	^{81}0.0051	^{73}0.0058	^{72}0.0065	^{68}0.0076	^{41}0.0004 $N^{0.175}$ ^{101}
42	HIK-5	^{13}0.0009	^{17}0.0011	^{13}0.0012	^{15}0.0014		^{26}0.0001 $N^{0.210}$ ^{90}	^{23}0.0029	^{25}0.0033	^{22}0.0035	^{22}0.0038	^{23}0.0042	^{47}0.0006 $N^{0.122}$ ^{80}
43	IDEMIA-0	^{39}0.0016	^{42}0.0019	^{25}0.0023	^{24}0.0026	^{23}0.0031	^{43}0.0001 $N^{0.226}$ ^{95}	^{77}0.0045	^{78}0.0051	^{66}0.0055	^{66}0.0060	^{66}0.0067	^{63}0.0008 $N^{0.134}$ ^{86}
44	IDEMIA-007	^{88}0.0035	^{77}0.0036	^{44}0.0036	^{42}0.0037	^{33}0.0038	^{109}0.0024 $N^{0.027}$ ^{27}	^{37}0.0037	^{33}0.0038	^{27}0.0039	^{28}0.0040	^{22}0.0042	^{99}0.0023 $N^{0.036}$ ^{29}
45	IDEMIA-1	^{45}0.0019	^{51}0.0024	^{38}0.0029	^{38}0.0036	^{43}0.0046	^{17}0.0000 $N^{0.307}$ ^{115}	^{92}0.0049	^{97}0.0058	^{78}0.0065	^{78}0.0076	^{75}0.0089	^{34}0.0003 $N^{0.201}$ ^{111}
46	IDEMIA-2	^{82}0.0031	^{93}0.0040	^{54}0.0048	^{53}0.0058	^{50}0.0074	^{34}0.0001 $N^{0.290}$ ^{111}	^{115}0.0061	^{110}0.0069				^{68}0.0010 $N^{0.135}$ ^{87}
47	IDEMIA-3	^{46}0.0019	^{46}0.0022				^{66}0.0002 $N^{0.175}$ ^{77}	^{89}0.0049	^{88}0.0053	^{69}0.0057	^{68}0.0062	^{65}0.0067	^{70}0.0011 $N^{0.109}$ ^{77}
48	IDEMIA-4	^{37}0.0015	^{36}0.0017	^{21}0.0020	^{21}0.0023	^{20}0.0028	^{48}0.0001 $N^{0.207}$ ^{87}	^{65}0.0043	^{65}0.0046	^{58}0.0051	^{59}0.0055	^{61}0.0062	^{65}0.0008 $N^{0.121}$ ^{79}
49	IDEMIA-5	^{44}0.0018	^{49}0.0023	^{28}0.0026	^{34}0.0033	^{38}0.0042	^{19}0.0000 $N^{0.289}$ ^{109}	^{86}0.0048	^{93}0.0056	^{76}0.0062	^{76}0.0070	^{72}0.0080	^{42}0.0005 $N^{0.175}$ ^{100}
50	IDEMIA-6	^{57}0.0022	^{65}0.0028	^{42}0.0034	^{47}0.0043	^{46}0.0055	^{18}0.0000 $N^{0.312}$ ^{117}	^{101}0.0054	^{101}0.0062	^{82}0.0072	^{81}0.0084	^{81}0.0102	^{26}0.0003 $N^{0.220}$ ^{116}
51	IMAGUS-2	^{184}0.0348	^{157}0.0510	^{77}0.0641	^{71}0.0804		^{70}0.0002 $N^{0.375}$ ^{132}	^{198}0.0468	^{196}0.0657				^{33}0.0003 $N^{0.371}$ ^{138}
52	IMPERIAL-000	^{109}0.0039	^{95}0.0040	^{51}0.0040	^{75}0.6833	^{56}0.6083	^{1}0.0000 $N^{2.074}$ ^{144}	^{61}0.0043	^{55}0.0043	^{43}0.0044	^{39}0.0044	^{31}0.0045	^{119}0.0034 $N^{0.016}$ ^{12}
53	INCODE-004	^{110}0.0040	^{96}0.0040				^{124}0.0034 $N^{0.011}$ ^{14}	^{71}0.0044	^{61}0.0045	^{51}0.0046	^{48}0.0047	^{41}0.0049	^{110}0.0028 $N^{0.033}$ ^{24}
54	INCODE-1	^{71}0.0026	^{74}0.0033	^{70}0.0167	^{68}0.0323		^{3}0.0000 $N^{1.217}$ ^{142}	^{103}0.0055	^{102}0.0063				^{57}0.0007 $N^{0.153}$ ^{92}
55	INCODE-3	^{42}0.0017	^{44}0.0021				^{31}0.0001 $N^{0.251}$ ^{102}	^{70}0.0044	^{84}0.0052	^{70}0.0057	^{74}0.0067	^{71}0.0078	^{32}0.0003 $N^{0.194}$ ^{110}
56	INNOVATRICS-4	^{50}0.0020	^{47}0.0022				^{77}0.0004 $N^{0.118}$ ^{63}	^{97}0.0052	^{96}0.0058	^{75}0.0061	^{67}0.0061	^{60}0.0061	^{105}0.0026 $N^{0.054}$ ^{44}
57	INTSYSMSU-000	^{202}0.0965	^{164}0.1027				^{137}0.0391 $N^{0.068}$ ^{43}	^{220}0.1122	^{215}0.1187	^{115}0.1230	^{110}0.1275	^{107}0.1319	^{144}0.0539 $N^{0.055}$ ^{46}
58	ISYSTEMS-0	^{124}0.0048	^{109}0.0050	^{56}0.0053	^{52}0.0056	^{49}0.0060	^{101}0.0017 $N^{0.076}$ ^{47}	^{135}0.0086	^{127}0.0089				^{128}0.0048 $N^{0.044}$ ^{33}
59	ISYSTEMS-1	^{125}0.0048	^{111}0.0050	^{55}0.0053	^{51}0.0056	^{48}0.0060	^{102}0.0017 $N^{0.075}$ ^{46}	^{136}0.0086	^{126}0.0089				^{129}0.0049 $N^{0.041}$ ^{30}
60	ISYSTEMS-2	^{74}0.0026	^{62}0.0027	^{35}0.0029			^{95}0.0012 $N^{0.061}$ ^{41}	^{102}0.0054	^{95}0.0056	^{74}0.0058	^{65}0.0060	^{63}0.0063	^{107}0.0027 $N^{0.051}$ ^{42}
61	ISYSTEMS-3	^{69}0.0025	^{60}0.0026	^{30}0.0027	^{25}0.0028	^{21}0.0030	^{97}0.0012 $N^{0.053}$ ^{37}	^{98}0.0052	^{89}0.0054	^{65}0.0055	^{61}0.0057	^{55}0.0059	^{108}0.0028 $N^{0.046}$ ^{37}
62	KEDACOM-001	^{152}0.0097	^{133}0.0097				^{133}0.0092 $N^{0.004}$ ^{9}	^{146}0.0098	^{135}0.0098	^{93}0.0099	^{85}0.0099	^{77}0.0100	^{137}0.0090 $N^{0.007}$ ^{7}
63	LOOKMAN-005	^{153}0.0097	^{134}0.0098				^{132}0.0087 $N^{0.008}$ ^{11}	^{147}0.0098	^{138}0.0099	^{94}0.0099	^{86}0.0100	^{79}0.0101	^{136}0.0086 $N^{0.010}$ ^{9}
64	LOOKMAN-3	^{144}0.0075	^{124}0.0077				^{129}0.0060 $N^{0.017}$ ^{18}	^{149}0.0099	^{140}0.0100	^{95}0.0101	^{89}0.0102	^{82}0.0104	^{135}0.0079 $N^{0.016}$ ^{13}
65	MEGVII-0	^{27}0.0012	^{40}0.0019	^{26}0.0025	^{33}0.0032	^{37}0.0041	^{7}0.0000 $N^{0.422}$ ^{136}	^{12}0.0026	^{20}0.0031	^{20}0.0034	^{25}0.0039	^{37}0.0048	^{13}0.0002 $N^{0.204}$ ^{112}
66	MEGVII-1						-	^{144}0.0091	^{132}0.0094	^{88}0.0097	^{87}0.0101	^{83}0.0106	^{127}0.0044 $N^{0.053}$ ^{43}
67	MICROFOCUS-3	^{210}0.2047	^{175}0.2625	^{81}0.3017			^{130}0.0070 $N^{0.252}$ ^{103}	^{228}0.2518	^{225}0.3113				^{139}0.0114 $N^{0.232}$ ^{121}
68	MICROFOCUS-5	^{204}0.1040	^{168}0.1422				^{91}0.0011 $N^{0.341}$ ^{126}	^{223}0.1322	^{221}0.1744	^{117}0.2066	^{113}0.2445	^{110}0.2829	^{126}0.0042 $N^{0.260}$ ^{125}
69	MICROSOFT-0	^{8}0.0008	^{12}0.0010	^{11}0.0011	^{11}0.0012	^{10}0.0014	^{44}0.0001 $N^{0.174}$ ^{76}	^{18}0.0028	^{19}0.0031	^{15}0.0032	^{17}0.0035	^{15}0.0037	^{60}0.0007 $N^{0.101}$ ^{73}
70	MICROSOFT-1	^{9}0.0008	^{10}0.0009	^{10}0.0011	^{10}0.0012	^{11}0.0014	^{41}0.0001 $N^{0.177}$ ^{79}	^{15}0.0028	^{15}0.0030				^{62}0.0007 $N^{0.098}$ ^{70}
71	MICROSOFT-2	^{11}0.0008	^{11}0.0010	^{9}0.0011	^{12}0.0012	^{12}0.0014	^{39}0.0001 $N^{0.186}$ ^{83}	^{20}0.0029	^{21}0.0032				^{61}0.0007 $N^{0.101}$ ^{74}
72	MICROSOFT-3	^{2}0.0004	^{4}0.0004				^{25}0.0001 $N^{0.153}$ ^{71}	^{4}0.0018	^{4}0.0019	^{4}0.0021	^{4}0.0022	^{3}0.0023	^{54}0.0006 $N^{0.078}$ ^{65}

Table 13: **Investigation-mode: Effect of N on FNIR at rank 50** *For five enrollment population sizes, N, with T = 0 and FPIR = 1. The left five columns apply for consolidated enrollment of a variable number of lifetime images from each subject. The right five columns apply for enrollment of one recent image. Missing entries usually apply because another algorithm from the same developer was run instead. Some developers are missing because less accurate algorithms were not run on galleries with $N >$ 1 600 000. Throughout blue superscripts indicate the rank of the algorithm for that column, and yellow highlighting indicates the most accurate value. Caution: The Power-low models are mostly intended to draw attention to the kind of behavior, not as a model to be used for prediction.*

MISSES NOT AT RANK 50		ENROL LIFETIME					
FNIR(N, T= 0, R =50)		DATASET: FRVT 2018					
#	ALGORITHM	N=0.64M	N=1.6M	N=3.0M	N=6.0M	N=12.0M	aN^b
73	MICROSOFT-4	^{1}0.0004	^{1}0.0004	^{1}0.0005	^{1}0.0005	^{1}0.0006	^{30}0.0001 $N^{0.140}$ ^{69}
74	MICROSOFT-5	^{3}0.0004	^{3}0.0004	^{3}0.0005	^{2}0.0005	^{2}0.0006	^{37}0.0001 $N^{0.134}$ ^{68}
75	MICROSOFT-6	^{4}0.0004	^{2}0.0004	^{2}0.0005	^{3}0.0006	^{3}0.0006	^{20}0.0000 $N^{0.166}$ ^{74}
76	NEC-0	^{60}0.0023	^{73}0.0030	^{49}0.0038	^{50}0.0047	^{47}0.0059	^{15}0.0000 $N^{0.324}$ ^{119}
77	NEC-1	^{145}0.0076	^{126}0.0080				^{127}0.0038 $N^{0.051}$ ^{36}
78	NEC-2	^{10}0.0008	^{8}0.0008	^{6}0.0009	^{5}0.0009	^{4}0.0009	^{79}0.0004 $N^{0.046}$ ^{33}
79	NEC-3	^{22}0.0011	^{20}0.0011	^{12}0.0011	^{9}0.0011	^{8}0.0011	^{89}0.0008 $N^{0.022}$ ^{24}
80	NEUROTECHNOLOGY-007	^{116}0.0042	^{220}1.0000	^{53}0.0043	^{49}0.0045	^{42}0.0046	^{144}113.6663 $N^{-0.609}$ ^{1}
81	NEUROTECHNOLOGY-3	^{103}0.0038	^{112}0.0051				^{23}0.0000 $N^{0.326}$ ^{122}
82	NEUROTECHNOLOGY-4	^{51}0.0020	^{50}0.0024	^{32}0.0027	^{30}0.0031	^{28}0.0035	^{62}0.0002 $N^{0.189}$ ^{84}
83	NEUROTECHNOLOGY-5	^{40}0.0017	^{39}0.0018	^{20}0.0019	^{20}0.0021	^{16}0.0023	^{75}0.0004 $N^{0.105}$ ^{60}
84	NEWLAND-2						-
85	NOBLIS-2	^{185}0.0366	^{158}0.0520				^{68}0.0002 $N^{0.383}$ ^{134}
86	NTECHLAB-0	^{31}0.0013	^{32}0.0016	^{22}0.0021	^{23}0.0026	^{24}0.0032	^{11}0.0000 $N^{0.326}$ ^{121}
87	NTECHLAB-007	^{87}0.0035	^{78}0.0036	^{46}0.0036	^{43}0.0037	^{34}0.0038	^{107}0.0023 $N^{0.029}$ ^{28}
88	NTECHLAB-008	^{85}0.0034	^{76}0.0035	^{43}0.0035	^{37}0.0035	^{29}0.0036	^{112}0.0028 $N^{0.014}$ ^{16}
89	NTECHLAB-1	^{32}0.0013	^{38}0.0018	^{23}0.0022	^{27}0.0029	^{35}0.0038	^{9}0.0000 $N^{0.366}$ ^{130}
90	NTECHLAB-3	^{21}0.0010	^{23}0.0012				^{28}0.0001 $N^{0.219}$ ^{91}
91	NTECHLAB-4	^{15}0.0009	^{15}0.0010	^{14}0.0012	^{13}0.0014	^{13}0.0016	^{29}0.0001 $N^{0.208}$ ^{89}
92	NTECHLAB-5	^{6}0.0007	^{7}0.0008				^{14}0.0000 $N^{0.237}$ ^{98}
93	NTECHLAB-6	^{5}0.0006	^{5}0.0008	^{5}0.0008	^{7}0.0010	^{9}0.0012	^{13}0.0000 $N^{0.244}$ ^{100}
94	PARAVISION-005	^{92}0.0036	^{79}0.0036	^{45}0.0036	^{39}0.0036	^{30}0.0037	^{123}0.0033 $N^{0.006}$ ^{10}
95	PIXELALL-002	^{123}0.0046	^{107}0.0048				^{108}0.0024 $N^{0.049}$ ^{35}
96	PIXELALL-003	^{113}0.0040	^{99}0.0041				^{115}0.0029 $N^{0.024}$ ^{25}
97	QUANTASOFT-1	^{221}0.9843	^{181}0.9843				^{143}0.9843 $N^{0.000}$ ^{2}
98	RANKONE-0	^{142}0.0074	^{135}0.0100	^{66}0.0120	^{64}0.0146	^{55}0.0176	^{59}0.0001 $N^{0.297}$ ^{112}
99	RANKONE-007	^{101}0.0037	^{89}0.0039	^{50}0.0040	^{46}0.0041	^{39}0.0043	^{104}0.0020 $N^{0.047}$ ^{34}
100	RANKONE-1	^{117}0.0042	^{115}0.0055	^{62}0.0067	^{58}0.0082	^{52}0.0100	^{42}0.0001 $N^{0.300}$ ^{114}
101	RANKONE-2	^{100}0.0037	^{105}0.0047				^{57}0.0001 $N^{0.253}$ ^{104}
102	RANKONE-3	^{98}0.0037	^{103}0.0047	^{57}0.0055	^{54}0.0067	^{51}0.0079	^{53}0.0001 $N^{0.258}$ ^{106}
103	RANKONE-4	^{131}0.0058	^{125}0.0079				^{38}0.0001 $N^{0.335}$ ^{124}
104	RANKONE-5	^{56}0.0021	^{55}0.0025	^{36}0.0029	^{36}0.0034	^{36}0.0040	^{52}0.0001 $N^{0.220}$ ^{92}
105	REALNETWORKS-0	^{132}0.0059	^{128}0.0083	^{65}0.0108			^{16}0.0000 $N^{0.393}$ ^{135}
106	REALNETWORKS-003	^{133}0.0059	^{120}0.0070				^{83}0.0005 $N^{0.184}$ ^{81}
107	REALNETWORKS-004	^{129}0.0055	^{119}0.0062				^{94}0.0011 $N^{0.120}$ ^{64}
108	REALNETWORKS-2	^{115}0.0042	^{117}0.0061				^{10}0.0000 $N^{0.423}$ ^{137}
109	REMARKAI-000	^{96}0.0037	^{86}0.0038				^{110}0.0026 $N^{0.026}$ ^{26}
110	REMARKAI-2	^{34}0.0013	^{33}0.0016				^{35}0.0001 $N^{0.224}$ ^{93}
111	SCANOVATE-000	^{218}0.7781	^{178}0.7781	^{82}0.7781	^{76}0.7781	^{57}0.7781	^{142}0.7778 $N^{0.000}$ ^{3}
112	SENSETIME-0	^{29}0.0012	^{26}0.0013				^{82}0.0005 $N^{0.069}$ ^{44}
113	SENSETIME-002	^{161}0.0123	^{141}0.0123	^{67}0.0123	^{62}0.0123	^{54}0.0123	^{134}0.0123 $N^{0.000}$ ^{7}
114	SENSETIME-003	^{84}0.0034	^{75}0.0034	^{41}0.0034	^{35}0.0034	^{25}0.0034	^{121}0.0033 $N^{0.002}$ ^{8}
115	SENSETIME-1	^{26}0.0011	^{22}0.0012				^{86}0.0007 $N^{0.037}$ ^{32}
116	SHAMAN-3	^{181}0.0344	^{154}0.0404	^{74}0.0452			^{120}0.0032 $N^{0.177}$ ^{78}
117	SHAMAN-7	^{176}0.0243	^{147}0.0248				^{136}0.0183 $N^{0.021}$ ^{21}
118	SIAT-1	^{214}0.2635	^{176}0.2635	^{80}0.2636			^{140}0.2626 $N^{0.000}$ ^{5}
119	SIAT-2	^{212}0.2124	^{172}0.2124				^{139}0.2116 $N^{0.000}$ ^{6}
120	SMILART-4	^{219}0.8160	^{180}0.9522				^{138}0.0859 $N^{0.168}$ ^{75}
121	SYNESIS-3	^{194}0.0582	^{159}0.0632				^{135}0.0174 $N^{0.090}$ ^{55}
122	TECH5-001	^{99}0.0037	^{87}0.0038				^{106}0.0023 $N^{0.035}$ ^{30}
123	TEVIAN-4	^{47}0.0019	^{45}0.0022	^{27}0.0025			^{61}0.0002 $N^{0.185}$ ^{82}
124	TEVIAN-5	^{36}0.0014	^{34}0.0017				^{65}0.0002 $N^{0.160}$ ^{72}
125	TIGER-0	^{134}0.0061	^{132}0.0097	^{68}0.0125	^{65}0.0164		^{12}0.0000 $N^{0.444}$ ^{138}
126	TIGER-2	^{18}0.0010	^{21}0.0012				^{32}0.0001 $N^{0.208}$ ^{88}
127	TONGYITRANS-1	^{130}0.0057	^{116}0.0060	^{60}0.0062	^{55}0.0067		^{105}0.0020 $N^{0.076}$ ^{48}
128	TOSHIBA-0	^{23}0.0011	^{24}0.0012				^{67}0.0002 $N^{0.126}$ ^{66}
129	VD-0	^{203}0.1006	^{167}0.1421	^{78}0.1752	^{73}0.2147		^{92}0.0011 $N^{0.340}$ ^{125}
130	VD-1	^{154}0.0098	^{136}0.0105				^{117}0.0031 $N^{0.085}$ ^{51}
131	VIGILANTSOLUTIONS-3	^{140}0.0072	^{137}0.0110	^{69}0.0143	^{63}0.0143		^{49}0.0001 $N^{0.322}$ ^{118}
132	VISIONLABS-008	^{111}0.0040	^{97}0.0040				^{125}0.0034 $N^{0.011}$ ^{15}
133	VISIONLABS-3	^{80}0.0030	^{101}0.0042	^{61}0.0066	^{61}0.0119		^{6}0.0000 $N^{0.612}$ ^{139}
134	VISIONLABS-4	^{20}0.0010	^{19}0.0011				^{71}0.0002 $N^{0.103}$ ^{59}
135	VISIONLABS-5	^{17}0.0009	^{14}0.0010	^{15}0.0012	^{16}0.0016	^{18}0.0026	^{8}0.0000 $N^{0.341}$ ^{127}
136	VISIONLABS-6	^{19}0.0010	^{16}0.0010				^{81}0.0005 $N^{0.056}$ ^{40}
137	VISIONLABS-7	^{16}0.0009	^{13}0.0010	^{8}0.0010	^{8}0.0011	^{7}0.0011	^{73}0.0004 $N^{0.070}$ ^{45}
138	VOCORD-3	^{63}0.0023	^{56}0.0025	^{33}0.0028	^{28}0.0031		^{80}0.0004 $N^{0.123}$ ^{65}
139	VOCORD-5	^{75}0.0027	^{69}0.0029				^{98}0.0013 $N^{0.056}$ ^{38}
140	YISHENG-1	^{86}0.0035	^{106}0.0047	^{58}0.0058	^{56}0.0072		^{21}0.0000 $N^{0.325}$ ^{120}
141	YITU-0	^{72}0.0026	^{63}0.0027	^{37}0.0029	^{32}0.0031	^{27}0.0034	^{88}0.0008 $N^{0.090}$ ^{53}
142	YITU-1	^{70}0.0026	^{61}0.0027	^{34}0.0029	^{29}0.0031	^{26}0.0034	^{87}0.0008 $N^{0.090}$ ^{54}
143	YITU-2	^{12}0.0008	^{9}0.0009	^{7}0.0009	^{6}0.0010	^{5}0.0010	^{74}0.0004 $N^{0.063}$ ^{42}
144	YITU-3	^{43}0.0018	^{37}0.0018				^{93}0.0011 $N^{0.036}$ ^{31}

MISSES NOT AT RANK 50		ENROL MOST RECENT					
FNIR(N, T= 0, R =50)		DATASET: FRVT 2018					
#	ALGORITHM	N=0.64M	N=1.6M	N=3.0M	N=6.0M	N=12.0M	aN^b
73	MICROSOFT-4	^{3}0.0018	^{3}0.0019	^{3}0.0020	^{2}0.0021	^{2}0.0022	^{56}0.0007 $N^{0.070}$ ^{63}
74	MICROSOFT-5	^{2}0.0018	^{1}0.0018	^{1}0.0019	^{1}0.0020	^{1}0.0021	^{58}0.0007 $N^{0.067}$ ^{59}
75	MICROSOFT-6	^{1}0.0018	^{2}0.0019	^{2}0.0019	^{3}0.0021	^{4}0.0023	^{43}0.0005 $N^{0.091}$ ^{68}
76	NEC-0	^{104}0.0055	^{103}0.0064	^{83}0.0074	^{83}0.0085	^{78}0.0100	^{37}0.0003 $N^{0.205}$ ^{113}
77	NEC-1	^{162}0.0135	^{151}0.0138	^{102}0.0142	^{98}0.0147	^{97}0.0154	^{132}0.0073 $N^{0.046}$ ^{35}
78	NEC-2	^{7}0.0022	^{5}0.0023	^{5}0.0023	^{5}0.0024	^{5}0.0025	^{75}0.0014 $N^{0.034}$ ^{25}
79	NEC-3	^{13}0.0026	^{12}0.0027	^{10}0.0028	^{7}0.0028	^{6}0.0029	^{86}0.0019 $N^{0.026}$ ^{16}
80	NEUROTECHNOLOGY-007	^{79}0.0047	^{71}0.0048	^{56}0.0049	^{51}0.0050	^{47}0.0052	^{112}0.0029 $N^{0.036}$ ^{27}
81	NEUROTECHNOLOGY-3	^{120}0.0068	^{122}0.0083	^{89}0.0097	^{94}0.0116	^{95}0.0137	^{24}0.0003 $N^{0.243}$ ^{123}
82	NEUROTECHNOLOGY-4	^{85}0.0048	^{79}0.0051	^{61}0.0054	^{62}0.0057	^{59}0.0060	^{79}0.0016 $N^{0.081}$ ^{66}
83	NEUROTECHNOLOGY-5	^{73}0.0045	^{68}0.0047	^{55}0.0048	^{50}0.0050	^{48}0.0053	^{91}0.0021 $N^{0.055}$ ^{45}
84	NEWLAND-2	^{178}0.0235	^{174}0.0288	^{109}0.0332	^{107}0.0391		^{71}0.0011 $N^{0.227}$ ^{120}
85	NOBLIS-2	^{194}0.0403	^{192}0.0560	^{111}0.0682	^{108}0.0940		^{25}0.0003 $N^{0.372}$ ^{139}
86	NTECHLAB-0	^{29}0.0033	^{35}0.0039	^{39}0.0043	^{54}0.0051	^{53}0.0058	^{23}0.0002 $N^{0.193}$ ^{109}
87	NTECHLAB-007	^{39}0.0038	^{34}0.0038	^{28}0.0039	^{30}0.0041	^{24}0.0042	^{100}0.0023 $N^{0.036}$ ^{28}
88	NTECHLAB-008	^{35}0.0036	^{31}0.0037	^{26}0.0037	^{21}0.0038	^{16}0.0038	^{109}0.0028 $N^{0.019}$ ^{14}
89	NTECHLAB-1	^{31}0.0034	^{41}0.0040				^{31}0.0003 $N^{0.177}$ ^{102}
90	NTECHLAB-3	^{19}0.0028	^{23}0.0032	^{23}0.0035	^{24}0.0039	^{28}0.0044	^{40}0.0004 $N^{0.149}$ ^{91}
91	NTECHLAB-4	^{14}0.0027	^{13}0.0030	^{16}0.0032	^{16}0.0035	^{17}0.0039	^{45}0.0005 $N^{0.120}$ ^{78}
92	NTECHLAB-5	^{6}0.0021	^{8}0.0025	^{8}0.0027	^{9}0.0031	^{11}0.0035	^{21}0.0002 $N^{0.168}$ ^{97}
93	NTECHLAB-6	^{5}0.0021	^{6}0.0023	^{7}0.0026	^{8}0.0028	^{7}0.0032	^{27}0.0003 $N^{0.147}$ ^{90}
94	PARAVISION-005	^{46}0.0039	^{39}0.0040	^{30}0.0040	^{27}0.0040	^{19}0.0040	^{123}0.0037 $N^{0.005}$ ^{5}
95	PIXELALL-002	^{67}0.0044	^{62}0.0046	^{53}0.0047	^{52}0.0050	^{49}0.0054	^{82}0.0017 $N^{0.069}$ ^{61}
96	PIXELALL-003	^{50}0.0040	^{45}0.0041	^{33}0.0041	^{31}0.0041	^{25}0.0042	^{116}0.0032 $N^{0.016}$ ^{11}
97	QUANTASOFT-1	^{221}0.1140	^{214}0.1140	^{114}0.1140		^{106}0.1140	^{145}0.1140 $N^{0.000}$ ^{1}
98	RANKONE-0	^{161}0.0127	^{158}0.0159	^{106}0.0185	^{104}0.0206	^{102}0.0252	^{50}0.0006 $N^{0.226}$ ^{118}
99	RANKONE-007	^{55}0.0042	^{54}0.0043	^{49}0.0044	^{44}0.0046	^{38}0.0048	^{94}0.0021 $N^{0.049}$ ^{40}
100	RANKONE-1	^{131}0.0078	^{123}0.0086				^{89}0.0020 $N^{0.103}$ ^{76}
101	RANKONE-2	^{125}0.0075	^{125}0.0087	^{92}0.0098	^{93}0.0111	^{94}0.0128	^{53}0.0006 $N^{0.184}$ ^{105}
102	RANKONE-3	^{124}0.0075	^{124}0.0087	^{91}0.0098	^{92}0.0111	^{93}0.0128	^{52}0.0006 $N^{0.184}$ ^{104}
103	RANKONE-4	^{148}0.0099	^{149}0.0128	^{103}0.0153			^{19}0.0002 $N^{0.284}$ ^{129}
104	RANKONE-5	^{99}0.0053	^{98}0.0058	^{77}0.0063	^{75}0.0069	^{70}0.0077	^{66}0.0009 $N^{0.129}$ ^{84}
105	REALNETWORKS-0	^{130}0.0077	^{137}0.0098				^{18}0.0002 $N^{0.267}$ ^{127}
106	REALNETWORKS-003	^{119}0.0068	^{118}0.0080	^{87}0.0091	^{91}0.0107	^{92}0.0128	^{39}0.0004 $N^{0.216}$ ^{114}
107	REALNETWORKS-004	^{118}0.0066	^{117}0.0077	^{86}0.0088	^{90}0.0104	^{90}0.0125	^{35}0.0003 $N^{0.220}$ ^{117}
108	REALNETWORKS-2	^{126}0.0075	^{134}0.0098	^{99}0.0119	^{99}0.0149	^{98}0.0155	^{22}0.0002 $N^{0.262}$ ^{126}
109	REMARKAI-000	^{54}0.0041	^{49}0.0042	^{40}0.0043	^{40}0.0044	^{34}0.0046	^{101}0.0023 $N^{0.041}$ ^{31}
110	REMARKAI-2	^{40}0.0038	^{48}0.0042	^{50}0.0046	^{53}0.0050		^{59}0.0007 $N^{0.125}$ ^{81}
111	SCANOVATE-000	^{51}0.0040	^{50}0.0042	^{41}0.0044	^{47}0.0047	^{35}0.0047	^{88}0.0019 $N^{0.055}$ ^{47}
112	SENSETIME-0	^{52}0.0041	^{47}0.0041	^{37}0.0042	^{33}0.0043	^{27}0.0044	^{111}0.0028 $N^{0.026}$ ^{15}
113	SENSETIME-002	^{169}0.0162	^{159}0.0162	^{104}0.0162	^{101}0.0162	^{99}0.0162	^{141}0.0161 $N^{0.000}$ ^{2}
114	SENSETIME-003	^{34}0.0036	^{30}0.0036	^{25}0.0036	^{18}0.0036	^{13}0.0036	^{118}0.0034 $N^{0.003}$ ^{4}
115	SENSETIME-1	^{49}0.0040	^{46}0.0041	^{35}0.0041	^{32}0.0042	^{39}0.0048	^{85}0.0018 $N^{0.057}$ ^{49}
116	SHAMAN-3	^{199}0.0468	^{191}0.0544				^{130}0.0053 $N^{0.163}$ ^{95}
117	SHAMAN-7	^{192}0.0334	^{179}0.0339	^{110}0.0344	^{106}0.0352	^{103}0.0362	^{142}0.0230 $N^{0.028}$ ^{19}
118	SIAT-1	^{22}0.0029	^{14}0.0030	^{13}0.0031	^{11}0.0032	^{9}0.0033	^{77}0.0016 $N^{0.046}$ ^{36}
119	SIAT-2	^{26}0.0031	^{22}0.0032	^{17}0.0032	^{13}0.0033	^{10}0.0034	^{90}0.0020 $N^{0.032}$ ^{23}
120	SMILART-4	^{233}0.9159	^{230}0.9638	^{118}0.9906			^{146}0.4632 $N^{0.051}$ ^{41}
121	SYNESIS-3	^{211}0.0851	^{205}0.0891	^{113}0.0942	^{109}0.1020	^{105}0.1126	^{143}0.0231 $N^{0.096}$ ^{69}
122	TECH5-001	^{58}0.0042	^{56}0.0043	^{48}0.0044	^{43}0.0046	^{43}0.0049	^{95}0.0022 $N^{0.049}$ ^{39}
123	TEVIAN-4	^{53}0.0041	^{64}0.0046				^{49}0.0006 $N^{0.143}$ ^{89}
124	TEVIAN-5	^{30}0.0034	^{32}0.0037	^{32}0.0041	^{36}0.0044	^{46}0.0050	^{46}0.0006 $N^{0.134}$ ^{85}
125	TIGER-0	^{145}0.0098	^{152}0.0139				^{8}0.0001 $N^{0.384}$ ^{141}
126	TIGER-2	^{17}0.0028	^{18}0.0030	^{19}0.0034	^{20}0.0038	^{30}0.0045	^{30}0.0003 $N^{0.161}$ ^{94}
127	TONGYITRANS-1	^{90}0.0049	^{82}0.0052				^{96}0.0022 $N^{0.061}$ ^{52}
128	TOSHIBA-0	^{36}0.0037	^{37}0.0039	^{34}0.0041	^{34}0.0043	^{91}0.0127	^{6}0.0000 $N^{0.350}$ ^{136}
129	VD-0	^{222}0.1248	^{220}0.1699				^{74}0.0014 $N^{0.336}$ ^{134}
130	VD-1	^{165}0.0145	^{157}0.0155	^{105}0.0166	^{103}0.0179	^{101}0.0196	^{122}0.0036 $N^{0.103}$ ^{75}
131	VIGILANTSOLUTIONS-3	^{157}0.0118	^{161}0.0166				^{9}0.0001 $N^{0.373}$ ^{140}
132	VISIONLABS-008	^{64}0.0043	^{57}0.0043	^{44}0.0044	^{45}0.0046	^{45}0.0050	^{97}0.0022 $N^{0.048}$ ^{38}
133	VISIONLABS-3	^{112}0.0057	^{113}0.0073	^{97}0.0106	^{102}0.0166		^{4}0.0000 $N^{0.481}$ ^{143}
134	VISIONLABS-4	^{11}0.0025	^{11}0.0027	^{12}0.0030	^{23}0.0039	^{56}0.0059	^{7}0.0000 $N^{0.290}$ ^{132}
135	VISIONLABS-5	^{10}0.0025	^{10}0.0026	^{11}0.0029	^{14}0.0033	^{26}0.0044	^{14}0.0002 $N^{0.192}$ ^{108}
136	VISIONLABS-6	^{9}0.0023	^{9}0.0025	^{9}0.0027	^{10}0.0031	^{18}0.0040	^{17}0.0002 $N^{0.177}$ ^{103}
137	VISIONLABS-7	^{8}0.0023	^{7}0.0024	^{6}0.0025	^{6}0.0025	^{8}0.0032	^{48}0.0006 $N^{0.098}$ ^{71}
138	VOCORD-3	^{48}0.0040	^{52}0.0042				^{81}0.0017 $N^{0.063}$ ^{55}
139	VOCORD-5	^{96}0.0051	^{91}0.0054	^{67}0.0056	^{63}0.0060	^{64}0.0064	^{87}0.0019 $N^{0.074}$ ^{64}
140	YISHENG-1	^{122}0.0069	^{120}0.0082				^{44}0.0005 $N^{0.191}$ ^{107}
141	YITU-0	^{88}0.0048	^{75}0.0049	^{60}0.0052	^{57}0.0054	^{52}0.0057	^{93}0.0021 $N^{0.060}$ ^{51}
142	YITU-1	^{87}0.0048	^{74}0.0049				^{117}0.0033 $N^{0.029}$ ^{21}
143	YITU-2	^{32}0.0034	^{29}0.0035	^{24}0.0036	^{19}0.0036	^{14}0.0037	^{102}0.0024 $N^{0.027}$ ^{18}
144	YITU-3	^{76}0.0045	^{66}0.0047	^{52}0.0047	^{49}0.0048	^{44}0.0049	^{114}0.0031 $N^{0.029}$ ^{20}

Table 14: **Investigation-mode: Effect of N on FNIR at rank 50** *For five enrollment population sizes, N, with T = 0 and FPIR = 1. The left five columns apply for consolidated enrollment of a variable number of lifetime images from each subject. The right five columns apply for enrollment of one recent image. Missing entries usually apply because another algorithm from the same developer was run instead. Some developers are missing because less accurate algorithms were not run on galleries with $N >$ 1 600 000. Throughout blue superscripts indicate the rank of the algorithm for that column, and yellow highlighting indicates the most accurate value. Caution: The Power-low models are mostly intended to draw attention to the kind of behavior, not as a model to be used for prediction.*

MISSES NOT AT RANK 50		ENROL LIFETIME						ENROL MOST RECENT					
FNIR(N, T= 0, R =50)		DATASET: FRVT 2018						DATASET: FRVT 2018					
#	ALGORITHM	N=0.64M	N=1.6M	N=3.0M	N=6.0M	N=12.0M	aN^b	N=0.64M	N=1.6M	N=3.0M	N=6.0M	N=12.0M	aN^b
145	YITU-4	[7] 0.0008	[6] 0.0008	[4] 0.0008	[4] 0.0008	[6] 0.0011	[69] $0.0002\ N^{0.087}$ [52]	[28] 0.0032	[24] 0.0033	[18] 0.0033	[12] 0.0033	[58] 0.0060	[29] $0.0003\ N^{0.168}$ [98]
146	YITU-5	[41] 0.0017	[35] 0.0017	[18] 0.0017	[18] 0.0017	[15] 0.0018	[100] $0.0014\ N^{0.015}$ [17]	[66] 0.0044	[59] 0.0044	[45] 0.0044	[38] 0.0044	[29] 0.0045	[125] $0.0039\ N^{0.008}$ [8]

Table 15: **Investigation-mode: Effect of N on FNIR at rank 50** *For five enrollment population sizes, N, with T = 0 and FPIR = 1. The left five columns apply for consolidated enrollment of a variable number of lifetime images from each subject. The right five columns apply for enrollment of one recent image. Missing entries usually apply because another algorithm from the same developer was run instead. Some developers are missing because less accurate algorithms were not run on galleries with $N > 1\,600\,000$. Throughout blue superscripts indicate the rank of the algorithm for that column, and yellow highlighting indicates the most accurate value. Caution: The Power-low models are mostly intended to draw attention to the kind of behavior, not as a model to be used for prediction.*

MISSES OUTSIDE RANK R		RESOURCE USAGE		ENROLL LIFETIME CONSOLIDATED = 1.6M				ENROL MOST RECENT, N = 1.6M			
FNIR(N, T=0, R)		TEMPLATE		FRVT 2018 MUGSHOTS							
#	ALGORITHM	BYTES	MSEC	R=1	R=10	R=50	WORK-10	R=1	R=10	R=50	WORK-10
1	3DIVI-0	^{217}4096	^{99}426				^{232}10.000	^{148}0.0344	^{143}0.0156	^{142}0.0106	^{147}1.190
2	3DIVI-1	^{228}4224	^{103}428				^{221}10.000	^{149}0.0375	^{158}0.0213	^{164}0.0181	^{153}1.233
3	3DIVI-2	^{54}528	^{101}428				^{211}10.000	^{154}0.0404	^{162}0.0242	^{167}0.0212	^{159}1.259
4	3DIVI-3	^{47}512	^{145}625	^{150}0.0645	^{145}0.0269	^{143}0.0151	^{148}1.345	^{182}0.0857	^{175}0.0374	^{168}0.0217	^{178}1.469
5	3DIVI-4	^{207}4096	^{146}628	^{110}0.0133	^{102}0.0056	^{84}0.0037	^{103}1.069	^{124}0.0201	^{116}0.0100	^{114}0.0074	^{120}1.115
6	3DIVI-5	^{215}4096	^{156}653	^{111}0.0133	^{101}0.0056	^{85}0.0037	^{102}1.069	^{125}0.0202	^{111}0.0099	^{115}0.0074	^{121}1.116
7	3DIVI-6	^{53}528	^{155}653	^{120}0.0186	^{131}0.0126	^{139}0.0117	^{128}1.127	^{139}0.0265	^{150}0.0186	^{163}0.0173	^{145}1.186
8	ALCHERA-0	^{122}2048	^{47}263	^{106}0.0121	^{115}0.0085	^{123}0.0076	^{109}1.085	^{120}0.0186	^{139}0.0141	^{150}0.0129	^{131}1.138
9	ALCHERA-1	^{131}2048	^{8}66	^{180}0.9824	^{180}0.9647	^{179}0.9459	^{180}9.748	^{230}0.9869	^{230}0.9736	^{229}0.9591	^{230}9.812
10	ALCHERA-2	^{147}2048	^{16}115	^{151}0.0914	^{153}0.0469	^{150}0.0292	^{152}1.552	^{183}0.0973	^{180}0.0468	^{170}0.0279	^{182}1.567
11	ALCHERA-3	^{144}2048	^{131}548	^{116}0.0159	^{105}0.0068	^{94}0.0040	^{110}1.086	^{97}0.0127	^{89}0.0066	^{87}0.0052	^{89}1.074
12	ALLGOVISION-000	^{166}2048	^{98}425	^{101}0.0106	^{113}0.0080	^{121}0.0073	^{108}1.078	^{107}0.0141	^{122}0.0104	^{131}0.0094	^{113}1.103
13	ANKE-0	^{191}2072	^{105}431	^{93}0.0100	^{87}0.0045	^{71}0.0030	^{88}1.055	^{113}0.0158	^{103}0.0086	^{104}0.0065	^{105}1.095
14	ANKE-002	^{182}2056	^{150}641	^{49}0.0048	^{78}0.0041	^{92}0.0039	^{64}1.039	^{30}0.0054	^{46}0.0045	^{53}0.0043	^{37}1.043
15	ANKE-1	^{190}2072	^{106}433	^{94}0.0101	^{88}0.0045	^{72}0.0030	^{89}1.055	^{114}0.0158	^{104}0.0086	^{105}0.0066	^{107}1.096
16	AWARE-0	^{109}1564	^{157}653				^{225}10.000	^{175}0.0639	^{179}0.0422	^{182}0.0361	^{177}1.439
17	AWARE-1	^{108}1564	^{153}651				^{215}10.000	^{171}0.0587	^{172}0.0355	^{175}0.0290	^{173}1.382
18	AWARE-2	^{193}2076	^{229}912				^{216}10.000	^{172}0.0600	^{177}0.0404	^{181}0.0353	^{175}1.416
19	AWARE-3	^{192}2076	^{187}716	^{127}0.0209	^{117}0.0086	^{110}0.0050	^{124}1.110	^{146}0.0332	^{141}0.0153	^{141}0.0101	^{146}1.186
20	AWARE-4	^{2}92	^{183}712	^{146}0.0529	^{141}0.0211	^{138}0.0113	^{142}1.275	^{177}0.0704	^{167}0.0300	^{162}0.0171	^{171}1.378
21	AWARE-5	^{202}3100	^{210}827	^{126}0.0208	^{118}0.0086	^{113}0.0053	^{123}1.110	^{147}0.0337	^{144}0.0160	^{143}0.0108	^{148}1.191
22	AWARE-6	^{3}124	^{203}818	^{147}0.0538	^{142}0.0224	^{140}0.0122	^{144}1.286	^{179}0.0722	^{170}0.0313	^{166}0.0184	^{174}1.394
23	AYONIX-0	^{88}1036	^{1}10	^{174}0.4649	^{174}0.3062	^{173}0.2142	^{174}4.268	^{222}0.4519	^{223}0.3195	^{223}0.2402	^{223}4.304
24	AYONIX-1	^{89}1036	^{3}12	^{170}0.3364	^{168}0.1761	^{165}0.1043	^{169}3.073	^{218}0.3432	^{217}0.1998	^{216}0.1297	^{217}3.244
25	AYONIX-2	^{84}1036	^{2}11	^{167}0.2606	^{164}0.1395	^{162}0.0873	^{166}2.620	^{217}0.3432	^{218}0.1999	^{217}0.1298	^{218}3.244
26	CAMVI-1	^{69}1024	^{25}177				^{188}10.000	^{210}0.2267	^{204}0.1242	^{204}0.0856	^{207}2.419
27	CAMVI-2	^{78}1024	^{198}774				^{205}10.000	^{190}0.1292	^{190}0.0682	^{189}0.0502	^{189}1.781
28	CAMVI-3	^{80}1024	^{181}707	^{139}0.0368	^{149}0.0367	^{153}0.0367	^{146}1.330	^{170}0.0544	^{182}0.0541	^{190}0.0541	^{180}1.488
29	CAMVI-4	^{76}1024	^{189}718	^{137}0.0326	^{147}0.0323	^{151}0.0323	^{145}1.291	^{167}0.0490	^{181}0.0486	^{187}0.0485	^{176}1.438
30	CAMVI-5	^{73}1024	^{196}769	^{143}0.0458	^{151}0.0455	^{155}0.0455	^{150}1.410	^{176}0.0673	^{188}0.0668	^{199}0.0667	^{183}1.602
31	COGENT-0	^{51}525	^{132}551	^{100}0.0106	^{62}0.0034	^{53}0.0024	^{97}1.062	^{99}0.0131	^{131}0.0122	^{77}0.0050	^{117}1.111
32	COGENT-1	^{50}525	^{133}552	^{99}0.0106	^{61}0.0034	^{52}0.0024	^{98}1.062	^{98}0.0131	^{130}0.0122	^{76}0.0050	^{116}1.111
33	COGENT-2	^{91}1043	^{236}987	^{20}0.0027	^{27}0.0016	^{27}0.0013	^{22}1.017	^{40}0.0062	^{48}0.0045	^{44}0.0041	^{42}1.045
34	COGENT-3	^{90}1043	^{235}960	^{30}0.0037	^{33}0.0022	^{31}0.0016	^{32}1.024	^{42}0.0064	^{49}0.0047	^{51}0.0042	^{51}1.047
35	COGNITEC-0	^{176}2052	^{24}176	^{121}0.0189	^{114}0.0083	^{108}0.0050	^{117}1.103	^{142}0.0278	^{138}0.0134	^{128}0.0092	^{141}1.160
36	COGNITEC-1	^{171}2052	^{32}202	^{87}0.0089	^{72}0.0039	^{66}0.0028	^{84}1.048	^{109}0.0143	^{98}0.0077	^{99}0.0060	^{99}1.086
37	COGNITEC-2	^{179}2052	^{38}227	^{40}0.0044	^{38}0.0026	^{43}0.0021	^{35}1.027	^{64}0.0083	^{70}0.0058	^{86}0.0052	^{69}1.059
38	COGNITEC-3	^{169}2052	^{59}297	^{48}0.0048	^{45}0.0029	^{54}0.0025	^{41}1.031	^{67}0.0088	^{79}0.0061	^{94}0.0056	^{75}1.062
39	CYBERLINK-000	^{173}2052	^{175}699	^{62}0.0056	^{93}0.0047	^{102}0.0044	^{78}1.044	^{45}0.0066	^{62}0.0052	^{73}0.0049	^{57}1.051
40	CYBERLINK-001	^{180}2052	^{107}433	^{54}0.0051	^{76}0.0041	^{88}0.0039	^{68}1.040	^{41}0.0062	^{51}0.0047	^{58}0.0044	^{48}1.046
41	DAHUA-0	^{162}2048	^{79}378	^{75}0.0070	^{89}0.0046	^{98}0.0040	^{82}1.047	^{89}0.0115	^{101}0.0081	^{112}0.0073	^{96}1.082
42	DAHUA-002	^{161}2048	^{176}699	^{37}0.0040	^{69}0.0037	^{83}0.0037	^{53}1.034	^{19}0.0045	^{32}0.0041	^{42}0.0040	^{23}1.038
43	DAHUA-1	^{150}2048	^{75}371	^{50}0.0049	^{39}0.0027	^{48}0.0022	^{39}1.030	^{69}0.0089	^{69}0.0056	^{72}0.0049	^{68}1.058
44	DEEPGLINT-001	^{212}4096	^{174}696	^{160}0.1425	^{165}0.1425	^{169}0.1424	^{163}2.282				^{232}10.000
45	DEEPSEA-001	^{140}2048	^{200}780	^{61}0.0055	^{71}0.0039	^{81}0.0036	^{66}1.039	^{52}0.0070	^{44}0.0045	^{43}0.0040	^{47}1.046
46	DERMALOG-0	^{5}128	^{71}344				^{202}10.000	^{191}0.1309	^{187}0.0652	^{185}0.0397	^{188}1.778
47	DERMALOG-1	^{7}128	^{23}171				^{233}10.000	^{194}0.1563	^{192}0.0800	^{188}0.0499	^{193}1.945
48	DERMALOG-2	^{25}256	^{72}344				^{207}10.000	^{192}0.1377	^{189}0.0680	^{186}0.0414	^{191}1.817
49	DERMALOG-3	^{8}128	^{35}211	^{155}0.0970	^{154}0.0470	^{149}0.0275	^{154}1.566	^{188}0.1281	^{186}0.0626	^{184}0.0369	^{187}1.752
50	DERMALOG-4	^{4}128	^{33}208	^{153}0.0961	^{152}0.0467	^{148}0.0272	^{153}1.561	^{187}0.1274	^{185}0.0621	^{183}0.0365	^{186}1.748
51	DERMALOG-5	^{6}128	^{122}532	^{103}0.0113	^{122}0.0095	^{131}0.0092	^{114}1.089	^{117}0.0171	^{140}0.0146	^{154}0.0142	^{130}1.137
52	DERMALOG-6	^{17}256	^{117}514	^{66}0.0060	^{96}0.0049	^{104}0.0047	^{83}1.047	^{79}0.0102	^{102}0.0085	^{119}0.0081	^{95}1.081
53	EVERAI-0	^{135}2048	^{109}438	^{118}0.0166	^{134}0.0153	^{142}0.0150	^{130}1.141	^{127}0.0209	^{151}0.0186	^{165}0.0182	^{142}1.174
54	EVERAI-1	^{126}2048	^{140}590	^{21}0.0027	^{25}0.0016	^{29}0.0014	^{21}1.017	^{31}0.0056	^{22}0.0037	^{28}0.0033	^{24}1.038
55	EVERAI-2	^{155}2048	^{78}377	^{22}0.0029	^{28}0.0017	^{30}0.0014	^{26}1.018	^{33}0.0058	^{24}0.0038	^{27}0.0033	^{27}1.039
56	EVERAI-3	^{121}2048	^{193}735	^{16}0.0023	^{21}0.0015	^{28}0.0013	^{17}1.015	^{21}0.0047	^{16}0.0034	^{16}0.0030	^{15}1.034
57	EVERAI-PARAVISION-004	^{210}4096	^{191}720	^{32}0.0039	^{67}0.0037	^{80}0.0036	^{49}1.033	^{15}0.0043	^{28}0.0040	^{38}0.0039	^{20}1.037
58	EYEDEA-0	^{227}4152	^{97}424				^{186}10.000	^{215}0.3000	^{215}0.1599	^{208}0.0975	^{215}2.864
59	EYEDEA-1	^{87}1036	^{63}311				^{217}10.000	^{203}0.1981	^{200}0.1052	^{195}0.0647	^{202}2.226
60	EYEDEA-2	^{85}1036	^{104}429				^{194}10.000	^{204}0.2000	^{202}0.1072	^{200}0.0671	^{203}2.246
61	EYEDEA-3	^{86}1036	^{80}385	^{149}0.0613	^{146}0.0278	^{144}0.0160	^{147}1.343	^{181}0.0824	^{176}0.0387	^{169}0.0236	^{179}1.470
62	F8-001	^{156}2048	^{218}851	^{176}0.5364	^{177}0.5357	^{177}0.5355	^{177}5.823	^{110}0.0146	^{137}0.0128	^{148}0.0125	^{124}1.120
63	GLORY-0	^{37}418	^{18}160	^{158}0.1335	^{160}0.0936	^{161}0.0738	^{158}1.965	^{199}0.1803	^{206}0.1289	^{210}0.1031	^{204}2.318
64	GLORY-1	^{112}1726	^{89}405	^{152}0.0932	^{156}0.0630	^{156}0.0490	^{156}1.656	^{189}0.1291	^{193}0.0894	^{201}0.0698	^{192}1.925
65	GORILLA-0	^{235}8300	^{100}427				^{204}10.000				^{231}10.000
66	GORILLA-004	^{197}2192	^{83}395	^{76}0.0070	^{86}0.0045	^{90}0.0039	^{81}1.047	^{70}0.0089	^{64}0.0053	^{60}0.0044	^{65}1.057
67	GORILLA-1	^{196}2156	^{21}169	^{141}0.0414	^{136}0.0157	^{127}0.0081	^{137}1.211	^{173}0.0627	^{163}0.0255	^{153}0.0142	^{166}1.331
68	GORILLA-2	^{94}1132	^{69}341	^{112}0.0137	^{98}0.0051	^{70}0.0029	^{101}1.067	^{128}0.0220	^{106}0.0092	^{100}0.0061	^{122}1.116
69	GORILLA-3	^{195}2156	^{139}563	^{130}0.0245	^{109}0.0076	^{91}0.0039	^{122}1.110	^{151}0.0384	^{136}0.0126	^{111}0.0073	^{144}1.178
70	HBINNO-0	^{49}520	^{48}265				^{196}10.000	^{214}0.2746	^{212}0.1522	^{209}0.0980	^{214}2.743
71	HIK-0	^{114}1808	^{225}875				^{183}10.000	^{135}0.0236	^{149}0.0178	^{160}0.0164	^{143}1.176
72	HIK-1	^{116}1808	^{206}820				^{229}10.000	^{119}0.0173	^{124}0.0111	^{133}0.0096	^{123}1.116

Table 16: **Rank-based accuracy for the FRVT 2018 mugshot sets**. *In columns 3 and 4 are template size and template generation duration. Thereafter values are rank-based FNIR with T = 0 and FPIR = 1. This is appropriate to investigational uses but not those with higher volumes where candidates from all searches would need review. Columns 5 - 9 show FRVT 2018 accuracy for various ranks for galleries unenrolled with all lifetime images. Column 10 is a workload statistic, a small value shows an algorithm front-loads mates into the first 10 candidates. The last four columns gives analogous results for enrollment only of the most recent image - see Figure 7. Throughout, blue superscripts indicate the rank of the algorithm for that column, and the best value is highlighted in yellow.*

MISSES OUTSIDE RANK R		RESOURCE USAGE		ENROLL LIFETIME CONSOLIDATED = 1.6M				ENROL MOST RECENT, N = 1.6M			
FNIR(N, T=0, R)		TEMPLATE		FRVT 2018 MUGSHOTS							
#	ALGORITHM	BYTES	MSEC	R=1	R=10	R=50	WORK-10	R=1	R=10	R=50	WORK-10
73	HIK-2	^{115}1808	^{204}820	^{119}0.0185	^{127}0.0111	^{130}0.0090	^{126}1.119	^{118}0.0172	^{123}0.0110	^{129}0.0093	^{119}1.115
74	HIK-3	^{98}1408	^{147}633	^{102}0.0107	^{85}0.0045	^{64}0.0028	^{92}1.057	^{108}0.0141	^{91}0.0070	^{80}0.0051	^{97}1.082
75	HIK-4	^{95}1152	^{115}510	^{97}0.0104	^{83}0.0043	^{68}0.0028	^{90}1.055	^{105}0.0138	^{92}0.0071	^{81}0.0051	^{93}1.081
76	HIK-5	^{97}1408	^{144}619	^{25}0.0034	^{22}0.0015	^{17}0.0011	^{25}1.018	^{47}0.0067	^{26}0.0040	^{25}0.0033	^{38}1.043
77	HIK-6	^{99}1408	^{141}610	^{27}0.0034	^{23}0.0015	^{18}0.0011	^{24}1.018	^{48}0.0067	^{27}0.0040	^{26}0.0033	^{39}1.043
78	IDEMIA-0	^{35}364	^{93}416	^{70}0.0063	^{43}0.0028	^{42}0.0019	^{51}1.034	^{86}0.0113	^{84}0.0064	^{78}0.0051	^{84}1.070
79	IDEMIA-007	^{65}860	^{202}807	^{42}0.0044	^{68}0.0037	^{77}0.0036	^{54}1.035	^{27}0.0052	^{30}0.0041	^{33}0.0038	^{28}1.039
80	IDEMIA-1	^{36}364	^{96}417	^{72}0.0065	^{46}0.0030	^{51}0.0024	^{55}1.035	^{90}0.0116	^{88}0.0066	^{97}0.0058	^{86}1.072
81	IDEMIA-2	^{34}364	^{95}417	^{91}0.0099	^{94}0.0048	^{93}0.0040	^{91}1.056	^{96}0.0126	^{95}0.0076	^{110}0.0069	^{94}1.081
82	IDEMIA-3	^{55}528	^{168}689	^{60}0.0054	^{48}0.0030	^{46}0.0022	^{46}1.033	^{77}0.0095	^{86}0.0065	^{88}0.0053	^{80}1.066
83	IDEMIA-4	^{52}528	^{165}669	^{57}0.0052	^{37}0.0025	^{36}0.0017	^{38}1.029	^{73}0.0092	^{72}0.0058	^{65}0.0046	^{72}1.061
84	IDEMIA-5	^{33}352	^{77}374	^{68}0.0062	^{42}0.0028	^{49}0.0023	^{50}1.034	^{83}0.0107	^{82}0.0062	^{93}0.0056	^{81}1.068
85	IDEMIA-6	^{32}352	^{76}373	^{77}0.0071	^{54}0.0033	^{65}0.0028	^{67}1.039	^{94}0.0122	^{90}0.0068	^{101}0.0062	^{90}1.075
86	IIT-002	^{139}2048	^{119}526	^{162}0.1652	^{166}0.1647	^{171}0.1646	^{165}2.484				^{233}10.000
87	IMAGUS-0	^{48}512	^{5}43				^{231}10.000	^{216}0.3054	^{216}0.1750	^{212}0.1136	^{216}2.977
88	IMAGUS-2	^{41}512	^{9}76	^{163}0.1833	^{159}0.0880	^{157}0.0510	^{161}2.070	^{208}0.2223	^{203}0.1113	^{196}0.0657	^{205}2.329
89	IMAGUS-3	^{46}512	^{7}57	^{169}0.3008	^{167}0.1735	^{166}0.1124	^{168}2.951	^{219}0.3576	^{219}0.2153	^{218}0.1420	^{219}3.380
90	IMPERIAL-000	^{138}2048	^{159}654	^{43}0.0044	^{75}0.0041	^{95}0.0040	^{62}1.038	^{26}0.0051	^{43}0.0045	^{55}0.0043	^{36}1.041
91	INCODE-0	^{74}1024	^{29}190	^{140}0.0376	^{137}0.0158	^{129}0.0089	^{136}1.201	^{169}0.0515	^{159}0.0229	^{155}0.0142	^{162}1.285
92	INCODE-004	^{143}2048	^{114}508	^{58}0.0052	^{80}0.0042	^{96}0.0040	^{70}1.040	^{39}0.0062	^{55}0.0048	^{61}0.0045	^{49}1.046
93	INCODE-1	^{142}2048	^{170}690	^{109}0.0131	^{97}0.0051	^{74}0.0033	^{99}1.066	^{121}0.0190	^{105}0.0088	^{102}0.0063	^{114}1.106
94	INCODE-2	^{133}2048	^{56}291	^{105}0.0120	^{90}0.0046	^{67}0.0028	^{96}1.060	^{126}0.0203	^{108}0.0094	^{106}0.0066	^{118}1.113
95	INCODE-3	^{128}2048	^{178}704	^{86}0.0088	^{60}0.0034	^{44}0.0021	^{77}1.044	^{112}0.0153	^{93}0.0072	^{84}0.0052	^{98}1.086
96	INNOVATRICS-0	^{59}530	^{110}455				^{218}10.000	^{157}0.0421	^{154}0.0191	^{147}0.0124	^{155}1.234
97	INNOVATRICS-1	^{57}530	^{65}316				^{214}10.000	^{156}0.0421	^{153}0.0191	^{146}0.0124	^{154}1.234
98	INNOVATRICS-2	^{58}530	^{45}255	^{145}0.0499	^{148}0.0354	^{152}0.0325	^{149}1.354	^{166}0.0475	^{171}0.0346	^{176}0.0320	^{170}1.343
99	INNOVATRICS-3	^{56}530	^{44}255	^{131}0.0301	^{126}0.0106	^{114}0.0055	^{131}1.147	^{143}0.0287	^{127}0.0118	^{116}0.0076	^{138}1.151
100	INNOVATRICS-4	^{92}1076	^{91}406	^{81}0.0081	^{52}0.0032	^{47}0.0022	^{76}1.042	^{111}0.0149	^{96}0.0077	^{96}0.0058	^{100}1.087
101	INTSYSMSU-000	^{137}2048	^{167}675	^{157}0.1294	^{162}0.1129	^{164}0.1027	^{160}2.069	^{193}0.1480	^{207}0.1295	^{215}0.1187	^{201}2.224
102	ISYSTEMS-0	^{158}2048	^{37}222	^{85}0.0085	^{104}0.0057	^{109}0.0050	^{95}1.059	^{102}0.0136	^{110}0.0099	^{127}0.0089	^{108}1.098
103	ISYSTEMS-1	^{71}1024	^{36}222	^{84}0.0085	^{103}0.0057	^{111}0.0050	^{94}1.058	^{101}0.0136	^{109}0.0098	^{126}0.0089	^{109}1.098
104	ISYSTEMS-2	^{153}2048	^{66}316	^{45}0.0046	^{50}0.0031	^{62}0.0027	^{45}1.032	^{66}0.0088	^{81}0.0062	^{95}0.0056	^{76}1.062
105	ISYSTEMS-3	^{124}2048	^{219}856	^{35}0.0040	^{44}0.0029	^{60}0.0026	^{37}1.029	^{57}0.0075	^{73}0.0058	^{89}0.0054	^{66}1.057
106	KEDACOM-001	^{30}292	^{126}537	^{96}0.0102	^{124}0.0098	^{133}0.0097	^{113}1.089	^{81}0.0104	^{113}0.0100	^{135}0.0098	^{101}1.091
107	LOOKMAN-005	^{60}548	^{116}514	^{98}0.0105	^{125}0.0100	^{134}0.0098	^{115}1.091	^{84}0.0107	^{117}0.0101	^{138}0.0099	^{102}1.092
108	LOOKMAN-3	^{29}292	^{70}342	^{88}0.0089	^{111}0.0079	^{124}0.0077	^{106}1.074	^{87}0.0114	^{119}0.0103	^{140}0.0100	^{104}1.095
109	LOOKMAN-4	^{61}548	^{67}325	^{89}0.0091	^{110}0.0078	^{122}0.0075	^{107}1.074	^{91}0.0117	^{118}0.0103	^{139}0.0100	^{106}1.096
110	MEGVII-0	^{129}2048	^{201}794	^{92}0.0099	^{63}0.0035	^{40}0.0019	^{85}1.048	^{74}0.0094	^{38}0.0043	^{20}0.0031	^{60}1.052
111	MEGVII-1	^{208}4096	^{154}652				^{191}10.000	^{103}0.0137	^{120}0.0103	^{132}0.0094	^{111}1.102
112	MEGVII-2	^{213}4096	^{161}656				^{208}10.000	^{104}0.0137	^{121}0.0103	^{130}0.0094	^{112}1.102
113	MICROFOCUS-0	^{20}256	^{118}525				^{200}10.000	^{226}0.5972	^{226}0.4252	^{226}0.3156	^{226}5.397
114	MICROFOCUS-1	^{26}256	^{120}527				^{212}10.000	^{227}0.5972	^{227}0.4254	^{227}0.3160	^{227}5.398
115	MICROFOCUS-2	^{24}256	^{121}529				^{206}10.000	^{228}0.6272	^{228}0.4877	^{228}0.4095	^{228}5.839
116	MICROFOCUS-3	^{23}256	^{51}269	^{177}0.5389	^{176}0.3651	^{175}0.2625	^{176}4.849	^{225}0.5953	^{225}0.4220	^{225}0.3113	^{225}5.373
117	MICROFOCUS-4	^{22}256	^{52}270	^{175}0.5191	^{175}0.3485	^{174}0.2490	^{175}4.688	^{224}0.5775	^{224}0.4042	^{224}0.2975	^{224}5.212
118	MICROFOCUS-5	^{18}256	^{50}266	^{171}0.3701	^{170}0.2184	^{168}0.1422	^{171}3.437	^{220}0.4257	^{220}0.2626	^{221}0.1744	^{220}3.877
119	MICROFOCUS-6	^{19}256	^{49}265	^{172}0.3732	^{171}0.2198	^{170}0.1441	^{172}3.453	^{221}0.4283	^{221}0.2643	^{222}0.1767	^{221}3.897
120	MICROSOFT-0	^{40}512	^{55}283	^{19}0.0026	^{15}0.0013	^{12}0.0010	^{16}1.015	^{34}0.0058	^{17}0.0036	^{19}0.0031	^{25}1.038
121	MICROSOFT-1	^{81}1024	^{73}349	^{18}0.0026	^{14}0.0012	^{10}0.0009	^{15}1.015	^{32}0.0056	^{18}0.0036	^{15}0.0030	^{22}1.038
122	MICROSOFT-2	^{70}1024	^{134}555	^{23}0.0029	^{17}0.0014	^{11}0.0010	^{20}1.016	^{38}0.0061	^{25}0.0039	^{21}0.0032	^{34}1.041
123	MICROSOFT-3	^{79}1024	^{88}404	^{4}0.0011	^{3}0.0006	^{4}0.0004	^{2}1.007	^{4}0.0032	^{4}0.0022	^{4}0.0019	^{3}1.022
124	MICROSOFT-4	^{134}2048	^{197}773	^{1}0.0010	^{1}0.0006	^{1}0.0004	^{1}1.006	^{2}0.0031	^{2}0.0021	^{3}0.0019	^{2}1.022
125	MICROSOFT-5	^{77}1024	^{166}673	^{5}0.0013	^{2}0.0006	^{3}0.0004	^{3}1.007	^{5}0.0033	^{1}0.0021	^{1}0.0018	^{1}1.021
126	MICROSOFT-6	^{75}1024	^{172}695	^{7}0.0014	^{4}0.0006	^{2}0.0004	^{4}1.007	^{8}0.0033	^{3}0.0022	^{2}0.0019	^{4}1.023
127	NEC-0	^{201}2592	^{10}82	^{108}0.0127	^{99}0.0052	^{73}0.0030	^{100}1.066	^{122}0.0196	^{107}0.0092	^{103}0.0064	^{115}1.110
128	NEC-1	^{200}2592	^{11}88	^{117}0.0164	^{121}0.0094	^{126}0.0080	^{116}1.101	^{130}0.0235	^{142}0.0154	^{151}0.0138	^{140}1.158
129	NEC-2	^{110}1616	^{158}653	^{3}0.0011	^{6}0.0009	^{8}0.0008	^{6}1.009	^{1}0.0028	^{5}0.0024	^{5}0.0023	^{5}1.023
130	NEC-3	^{111}1712	^{169}690	^{6}0.0013	^{10}0.0011	^{20}0.0011	^{9}1.011	^{3}0.0031	^{8}0.0028	^{12}0.0027	^{8}1.026
131	NEUROTECHNOLOGY-0	^{230}5214	^{177}702				^{203}10.000	^{168}0.0497	^{160}0.0230	^{156}0.0147	^{161}1.278
132	NEUROTECHNOLOGY-007	^{28}256	^{22}169	^{220}1.0000	^{220}1.0000	^{220}1.0000	^{220}10.000	^{44}0.0066	^{58}0.0051	^{71}0.0048	^{54}1.050
133	NEUROTECHNOLOGY-1	^{232}5214	^{163}661				^{228}10.000	^{165}0.0467	^{156}0.0197	^{145}0.0117	^{158}1.250
134	NEUROTECHNOLOGY-2	^{231}5214	^{162}658				^{226}10.000	^{164}0.0465	^{155}0.0197	^{144}0.0116	^{157}1.249
135	NEUROTECHNOLOGY-3	^{152}2048	^{130}547	^{124}0.0199	^{116}0.0086	^{112}0.0051	^{120}1.108	^{137}0.0250	^{134}0.0125	^{122}0.0083	^{136}1.148
136	NEUROTECHNOLOGY-4	^{159}2048	^{129}543	^{64}0.0058	^{57}0.0033	^{50}0.0024	^{60}1.037	^{62}0.0082	^{74}0.0058	^{79}0.0051	^{67}1.058
137	NEUROTECHNOLOGY-5	^{21}256	^{92}412	^{38}0.0042	^{35}0.0023	^{39}0.0018	^{34}1.026	^{49}0.0068	^{59}0.0051	^{68}0.0047	^{56}1.050
138	NEUROTECHNOLOGY-6	^{15}256	^{195}746	^{115}0.0153	^{95}0.0048	^{59}0.0026	^{104}1.070	^{123}0.0201	^{100}0.0079	^{85}0.0052	^{110}1.102
139	NEWLAND-2	^{127}2048	^{222}868				^{189}10.000	^{180}0.0811	^{178}0.0422	^{174}0.0288	^{181}1.491
140	NOBLIS-1	^{157}2048	^{34}211	^{165}0.2049	^{163}0.1293	^{163}0.0951	^{164}2.390	^{212}0.2512	^{214}0.1565	^{213}0.1136	^{212}2.698
141	NOBLIS-2	^{233}6144	^{123}535	^{161}0.1565	^{158}0.0835	^{158}0.0520	^{159}1.967	^{200}0.1816	^{194}0.0928	^{192}0.0560	^{196}2.098
142	NTECHLAB-0	^{229}4442	^{192}730	^{79}0.0077	^{41}0.0028	^{32}0.0016	^{61}1.038	^{88}0.0115	^{68}0.0054	^{35}0.0039	^{78}1.064
143	NTECHLAB-007	^{203}3348	^{214}834	^{46}0.0047	^{70}0.0037	^{78}0.0036	^{57}1.036	^{28}0.0053	^{31}0.0041	^{34}0.0038	^{29}1.040
144	NTECHLAB-008	^{96}1300	^{138}562	^{36}0.0040	^{64}0.0035	^{76}0.0035	^{47}1.033	^{16}0.0044	^{23}0.0038	^{31}0.0037	^{18}1.035

Table 17: **Rank-based accuracy for the FRVT 2018 mugshot sets**. *In columns 3 and 4 are template size and template generation duration. Thereafter values are rank-based FNIR with T = 0 and FPIR = 1. This is appropriate to investigational uses but not those with higher volumes where candidates from all searches would need review. Columns 5 - 9 show FRVT 2018 accuracy for various ranks for galleries unenrolled with all lifetime images. Column 10 is a workload statistic, a small value shows an algorithm front-loads mates into the first 10 candidates. The last four columns gives analogous results for enrollment only of the most recent image - see Figure 7. Throughout, blue superscripts indicate the rank of the algorithm for that column, and the best value is highlighted in yellow.*

MISSES OUTSIDE RANK R		RESOURCE USAGE		ENROLL LIFETIME CONSOLIDATED = 1.6M				ENROL MOST RECENT, N = 1.6M			
FNIR(N, T=0, R)		TEMPLATE		FRVT 2018 MUGSHOTS							
#	ALGORITHM	BYTES	MSEC	R=1	R=10	R=50	WORK-10	R=1	R=10	R=50	WORK-10
145	NTECHLAB-1	[113] 1736	[90] 405	[90] 0.0097	[53] 0.0032	[38] 0.0018	[79] 1.046	[106] 0.0139	[77] 0.0060	[41] 0.0040	[88] 1.074
146	NTECHLAB-3	[204] 3484	[212] 831	[55] 0.0051	[32] 0.0019	[23] 0.0012	[33] 1.024	[63] 0.0082	[33] 0.0041	[23] 0.0032	[50] 1.047
147	NTECHLAB-4	[205] 3484	[230] 929	[34] 0.0040	[20] 0.0015	[15] 0.0010	[29] 1.019	[51] 0.0068	[20] 0.0036	[13] 0.0030	[33] 1.041
148	NTECHLAB-5	[119] 1940	[188] 717	[33] 0.0039	[16] 0.0013	[7] 0.0008	[27] 1.018	[43] 0.0064	[13] 0.0033	[8] 0.0025	[21] 1.037
149	NTECHLAB-6	[120] 1940	[216] 841	[26] 0.0034	[11] 0.0011	[5] 0.0008	[18] 1.015	[35] 0.0059	[11] 0.0030	[6] 0.0023	[16] 1.034
150	PARAVISION-005	[211] 4096	[220] 858	[31] 0.0038	[65] 0.0036	[79] 0.0036	[48] 1.033	[14] 0.0042	[29] 0.0040	[39] 0.0040	[19] 1.036
151	PIXELALL-002	[199] 2560	[31] 198	[82] 0.0084	[100] 0.0055	[107] 0.0048	[93] 1.057	[54] 0.0072	[60] 0.0051	[62] 0.0046	[58] 1.052
152	PIXELALL-003	[198] 2560	[190] 719	[51] 0.0050	[82] 0.0043	[99] 0.0041	[71] 1.040	[23] 0.0048	[36] 0.0042	[45] 0.0041	[26] 1.039
153	QUANTASOFT-1	[136] 2048	[84] 396	[181] 0.9857	[181] 0.9848	[181] 0.9843	[181] 9.866	[207] 0.2198	[210] 0.1491	[214] 0.1140	[211] 2.559
154	RANKONE-0	[14] 228	[6] 50	[135] 0.0319	[135] 0.0157	[135] 0.0100	[135] 1.188	[163] 0.0455	[161] 0.0238	[158] 0.0159	[160] 1.275
155	RANKONE-006	[13] 165	[46] 261	[71] 0.0065	[92] 0.0046	[100] 0.0042	[80] 1.046	[61] 0.0077	[66] 0.0053	[70] 0.0047	[63] 1.054
156	RANKONE-007	[12] 165	[54] 278	[56] 0.0052	[79] 0.0042	[89] 0.0039	[69] 1.040	[36] 0.0060	[53] 0.0047	[54] 0.0043	[44] 1.046
157	RANKONE-1	[31] 324	[17] 136	[123] 0.0194	[120] 0.0089	[115] 0.0055	[121] 1.109	[136] 0.0247	[133] 0.0123	[123] 0.0086	[134] 1.145
158	RANKONE-2	[11] 133	[14] 113	[114] 0.0149	[108] 0.0072	[105] 0.0047	[112] 1.086	[130] 0.0221	[129] 0.0119	[125] 0.0087	[129] 1.135
159	RANKONE-3	[9] 133	[15] 114	[113] 0.0149	[107] 0.0072	[103] 0.0047	[111] 1.086	[129] 0.0221	[128] 0.0119	[124] 0.0087	[128] 1.135
160	RANKONE-4	[1] 85	[4] 36	[134] 0.0318	[133] 0.0135	[125] 0.0079	[134] 1.171	[162] 0.0441	[157] 0.0204	[149] 0.0128	[156] 1.249
161	RANKONE-5	[10] 133	[12] 94	[78] 0.0072	[66] 0.0036	[55] 0.0025	[75] 1.042	[93] 0.0120	[94] 0.0073	[98] 0.0058	[92] 1.078
162	REALNETWORKS-0	[218] 4100	[42] 244	[142] 0.0443	[138] 0.0163	[128] 0.0083	[138] 1.222	[161] 0.0426	[148] 0.0172	[137] 0.0098	[152] 1.222
163	REALNETWORKS-003	[117] 1848	[26] 178	[128] 0.0220	[123] 0.0098	[120] 0.0070	[127] 1.120	[140] 0.0268	[126] 0.0116	[118] 0.0080	[133] 1.144
164	REALNETWORKS-004	[118] 1848	[27] 185	[122] 0.0192	[119] 0.0089	[119] 0.0062	[119] 1.107	[138] 0.0262	[125] 0.0113	[117] 0.0077	[132] 1.140
165	REALNETWORKS-1	[219] 4104	[41] 243	[138] 0.0329	[129] 0.0120	[118] 0.0062	[133] 1.163	[160] 0.0426	[147] 0.0172	[136] 0.0098	[151] 1.222
166	REALNETWORKS-2	[222] 4104	[43] 245	[136] 0.0320	[128] 0.0117	[117] 0.0061	[132] 1.159	[155] 0.0418	[146] 0.0165	[134] 0.0098	[150] 1.217
167	REMARKAI-0	[151] 2048	[143] 615	[73] 0.0065	[40] 0.0028	[41] 0.0019	[52] 1.034	[85] 0.0109	[71] 0.0058	[63] 0.0046	[79] 1.065
168	REMARKAI-000	[163] 2048	[171] 691	[53] 0.0051	[73] 0.0040	[86] 0.0038	[65] 1.039	[37] 0.0060	[47] 0.0045	[49] 0.0042	[40] 1.044
169	REMARKAI-2	[160] 2048	[108] 434	[69] 0.0062	[36] 0.0025	[33] 0.0016	[43] 1.031	[82] 0.0105	[65] 0.0053	[48] 0.0042	[71] 1.061
170	SCANOVATE-000	[165] 2048	[184] 712	[178] 0.7787	[178] 0.7782	[178] 0.7781	[178] 8.005	[60] 0.0076	[56] 0.0049	[50] 0.0042	[55] 1.050
171	SENSETIME-0	[221] 4104	[186] 715	[13] 0.0018	[19] 0.0014	[26] 0.0013	[14] 1.014	[22] 0.0048	[39] 0.0043	[47] 0.0041	[31] 1.040
172	SENSETIME-002	[181] 2056	[152] 650	[107] 0.0124	[130] 0.0123	[141] 0.0123	[125] 1.111	[115] 0.0163	[145] 0.0162	[159] 0.0162	[135] 1.146
173	SENSETIME-003	[183] 2056	[234] 940	[28] 0.0034	[59] 0.0034	[75] 0.0034	[40] 1.030	[9] 0.0036	[19] 0.0036	[30] 0.0036	[14] 1.032
174	SENSETIME-1	[220] 4104	[160] 656	[11] 0.0018	[18] 0.0014	[22] 0.0012	[13] 1.013	[24] 0.0048	[37] 0.0043	[46] 0.0041	[30] 1.040
175	SHAMAN-0	[209] 4096	[127] 538				[193] 10.000	[196] 0.1707	[196] 0.0982	[202] 0.0704	[195] 2.092
176	SHAMAN-1	[216] 4096	[135] 557				[223] 10.000	[197] 0.1718	[195] 0.0950	[197] 0.0666	[194] 2.078
177	SHAMAN-2	[234] 8192	[136] 557				[227] 10.000	[213] 0.2620	[213] 0.1540	[211] 0.1058	[213] 2.710
178	SHAMAN-3	[132] 2048	[179] 704	[154] 0.0969	[155] 0.0551	[154] 0.0404	[155] 1.613	[185] 0.1266	[191] 0.0732	[191] 0.0544	[190] 1.811
179	SHAMAN-4	[146] 2048	[151] 642	[164] 0.1867	[161] 0.1015	[160] 0.0675	[162] 2.163	[209] 0.2242	[205] 0.1265	[203] 0.0850	[208] 2.431
180	SHAMAN-6	[164] 2048	[180] 706	[133] 0.0312	[144] 0.0262	[146] 0.0248	[141] 1.249	[159] 0.0424	[174] 0.0357	[180] 0.0340	[169] 1.339
181	SHAMAN-7	[125] 2048	[182] 709	[132] 0.0310	[143] 0.0262	[147] 0.0248	[140] 1.248	[158] 0.0422	[173] 0.0357	[179] 0.0339	[168] 1.337
182	SIAT-0	[93] 1096	[74] 358				[230] 10.000	[78] 0.0101	[61] 0.0052	[40] 0.0040	[70] 1.059
183	SIAT-1	[170] 2052	[217] 842	[168] 0.2639	[173] 0.2636	[176] 0.2635	[170] 3.373	[11] 0.0039	[12] 0.0033	[14] 0.0030	[11] 1.031
184	SIAT-2	[175] 2052	[227] 906	[166] 0.2128	[169] 0.2125	[172] 0.2124	[167] 2.913	[12] 0.0040	[15] 0.0034	[22] 0.0032	[13] 1.032
185	SMILART-0	[82] 1024	[20] 168				[224] 10.000	[201] 0.1931	[199] 0.1045	[198] 0.0667	[199] 2.204
186	SMILART-1	[72] 1024	[164] 662				[197] 10.000	[206] 0.2188	[208] 0.1300	[206] 0.0932	[209] 2.435
187	SMILART-2	[68] 1024	[137] 560				[187] 10.000	[202] 0.1946	[198] 0.1019	[194] 0.0637	[198] 2.196
188	SMILART-4	[42] 512	[19] 167	[179] 0.9531	[179] 0.9523	[180] 0.9522	[179] 9.573	[229] 0.9649	[229] 0.9641	[230] 0.9638	[229] 9.679
189	SMILART-5	[141] 2048	[113] 464				[210] 10.000				[234] 10.000
190	SYNESIS-0	[39] 512	[40] 237				[184] 10.000	[195] 0.1621	[211] 0.1513	[219] 0.1509	[206] 2.380
191	SYNESIS-3	[214] 4096	[13] 103	[159] 0.1350	[157] 0.0791	[159] 0.0632	[157] 1.868	[198] 0.1721	[201] 0.1070	[205] 0.0891	[197] 2.140
192	TECH5-001	[100] 1536	[226] 898	[65] 0.0059	[81] 0.0042	[87] 0.0038	[74] 1.042	[46] 0.0066	[52] 0.0047	[56] 0.0043	[53] 1.047
193	TEVIAN-0	[123] 2048	[82] 394				[185] 10.000	[132] 0.0225	[114] 0.0100	[108] 0.0068	[126] 1.122
194	TEVIAN-1	[167] 2048	[87] 398				[236] 10.000	[133] 0.0225	[115] 0.0100	[109] 0.0068	[127] 1.122
195	TEVIAN-2	[130] 2048	[85] 397				[199] 10.000	[131] 0.0224	[112] 0.0100	[107] 0.0068	[125] 1.121
196	TEVIAN-3	[145] 2048	[62] 300	[95] 0.0102	[77] 0.0041	[57] 0.0026	[87] 1.052	[116] 0.0169	[99] 0.0078	[90] 0.0054	[103] 1.093
197	TEVIAN-4	[154] 2048	[60] 299	[80] 0.0080	[55] 0.0033	[45] 0.0022	[72] 1.041	[100] 0.0134	[87] 0.0065	[64] 0.0046	[91] 1.076
198	TEVIAN-5	[148] 2048	[94] 416	[59] 0.0053	[34] 0.0023	[34] 0.0017	[36] 1.028	[71] 0.0092	[50] 0.0047	[32] 0.0037	[62] 1.054
199	TIGER-0	[177] 2052	[102] 428	[144] 0.0480	[139] 0.0185	[132] 0.0097	[139] 1.247	[174] 0.0638	[164] 0.0257	[152] 0.0139	[167] 1.334
200	TIGER-1	[178] 2052	[86] 398				[222] 10.000				[235] 10.000
201	TIGER-2	[174] 2052	[112] 464	[41] 0.0044	[30] 0.0018	[21] 0.0012	[31] 1.023	[59] 0.0075	[35] 0.0041	[18] 0.0030	[45] 1.046
202	TIGER-3	[168] 2052	[111] 464				[190] 10.000	[58] 0.0075	[34] 0.0041	[17] 0.0030	[46] 1.046
203	TONGYITRANS-0	[188] 2070	[30] 190	[67] 0.0060	[51] 0.0032	[58] 0.0026	[56] 1.036	[76] 0.0095	[76] 0.0059	[83] 0.0052	[73] 1.062
204	TONGYITRANS-1	[186] 2070	[28] 189	[104] 0.0114	[106] 0.0069	[116] 0.0060	[105] 1.073	[75] 0.0095	[75] 0.0058	[82] 0.0052	[74] 1.062
205	TOSHIBA-0	[107] 1548	[231] 930	[24] 0.0033	[24] 0.0016	[24] 0.0012	[28] 1.018	[50] 0.0068	[40] 0.0044	[37] 0.0039	[43] 1.046
206	TOSHIBA-1	[185] 2060	[233] 931	[29] 0.0035	[26] 0.0016	[25] 0.0012	[30] 1.019	[53] 0.0071	[45] 0.0045	[36] 0.0039	[52] 1.047
207	VD-0	[83] 1028	[68] 337	[173] 0.4303	[172] 0.2334	[167] 0.1421	[173] 3.703	[223] 0.4751	[222] 0.2714	[220] 0.1699	[222] 4.074
208	VD-1	[172] 2052	[173] 695	[129] 0.0221	[132] 0.0129	[136] 0.0105	[129] 1.140	[145] 0.0302	[152] 0.0187	[157] 0.0155	[149] 1.197
209	VIGILANTSOLUTIONS-0	[102] 1544	[208] 823				[198] 10.000	[184] 0.1254	[183] 0.0578	[178] 0.0331	[184] 1.712
210	VIGILANTSOLUTIONS-1	[184] 2056	[194] 739				[235] 10.000	[205] 0.2038	[197] 0.1004	[193] 0.0586	[200] 2.210
211	VIGILANTSOLUTIONS-2	[104] 1544	[205] 820				[209] 10.000	[211] 0.2387	[209] 0.1392	[207] 0.0940	[210] 2.555
212	VIGILANTSOLUTIONS-3	[106] 1544	[213] 832	[148] 0.0549	[140] 0.0210	[137] 0.0110	[143] 1.280	[178] 0.0719	[165] 0.0288	[161] 0.0166	[172] 1.378
213	VIGILANTSOLUTIONS-4	[101] 1544	[211] 830	[156] 0.0993	[150] 0.0434	[145] 0.0238	[151] 1.549	[186] 0.1272	[184] 0.0582	[177] 0.0330	[185] 1.721
214	VIGILANTSOLUTIONS-5	[103] 1544	[199] 778				[201] 10.000	[92] 0.0118	[80] 0.0062	[67] 0.0047	[83] 1.069
215	VIGILANTSOLUTIONS-6	[105] 1544	[215] 834				[213] 10.000	[95] 0.0125	[83] 0.0064	[69] 0.0047	[87] 1.072
216	VISIONLABS-008	[45] 512	[53] 277	[39] 0.0042	[74] 0.0040	[97] 0.0040	[59] 1.037	[20] 0.0046	[41] 0.0044	[57] 0.0043	[32] 1.040

Table 18: **Rank-based accuracy for the FRVT 2018 mugshot sets**. *In columns 3 and 4 are template size and template generation duration. Thereafter values are rank-based FNIR with T = 0 and FPIR = 1. This is appropriate to investigational uses but not those with higher volumes where candidates from all searches would need review. Columns 5 - 9 show FRVT 2018 accuracy for various ranks for galleries unenrolled with all lifetime images. Column 10 is a workload statistic, a small value shows an algorithm front-loads mates into the first 10 candidates. The last four columns gives analogous results for enrollment only of the most recent image - see Figure 7. Throughout, blue superscripts indicate the rank of the algorithm for that column, and the best value is highlighted in yellow.*

MISSES OUTSIDE RANK R		RESOURCE USAGE		ENROLL LIFETIME CONSOLIDATED = 1.6M				ENROL MOST RECENT, N = 1.6M			
FNIR(N, T=0, R)		TEMPLATE		FRVT 2018 MUGSHOTS							
#	ALGORITHM	BYTES	MSEC	R=1	R=10	R=50	WORK-10	R=1	R=10	R=50	WORK-10
217	VISIONLABS-3	[16] 256	[39] 228	[52] 0.0050	[84] 0.0044	[101] 0.0042	[73] 1.041	[68] 0.0089	[97] 0.0077	[113] 0.0073	[85] 1.072
218	VISIONLABS-4	[27] 256	[64] 315	[14] 0.0020	[13] 0.0012	[19] 0.0011	[12] 1.013	[17] 0.0044	[10] 0.0030	[11] 0.0027	[10] 1.031
219	VISIONLABS-5	[38] 512	[61] 300	[12] 0.0018	[12] 0.0012	[14] 0.0010	[11] 1.012	[13] 0.0041	[9] 0.0029	[10] 0.0026	[9] 1.029
220	VISIONLABS-6	[44] 512	[57] 292	[9] 0.0015	[9] 0.0011	[16] 0.0010	[10] 1.011	[7] 0.0033	[7] 0.0026	[9] 0.0025	[7] 1.025
221	VISIONLABS-7	[43] 512	[58] 293	[8] 0.0014	[8] 0.0011	[13] 0.0010	[8] 1.010	[6] 0.0033	[6] 0.0025	[7] 0.0024	[6] 1.025
222	VOCORD-0	[63] 608	[125] 536				[192] 10.000	[153] 0.0403	[169] 0.0306	[173] 0.0284	[165] 1.301
223	VOCORD-1	[62] 608	[124] 536				[182] 10.000	[152] 0.0402	[168] 0.0305	[172] 0.0282	[164] 1.299
224	VOCORD-2	[149] 2048	[149] 635				[219] 10.000	[150] 0.0382	[166] 0.0298	[171] 0.0280	[163] 1.290
225	VOCORD-3	[67] 896	[185] 714	[74] 0.0067	[56] 0.0033	[56] 0.0025	[63] 1.038	[65] 0.0085	[57] 0.0050	[52] 0.0042	[64] 1.054
226	VOCORD-4	[66] 896	[128] 538	[83] 0.0084	[91] 0.0046	[82] 0.0036	[86] 1.051	[80] 0.0102	[85] 0.0064	[92] 0.0054	[82] 1.068
227	VOCORD-5	[64] 768	[207] 822	[63] 0.0057	[58] 0.0034	[69] 0.0029	[58] 1.036	[72] 0.0092	[78] 0.0061	[91] 0.0054	[77] 1.063
228	VOCORD-6	[236] 10240	[209] 825				[234] 10.000	[236] 1.0000	[236] 1.0000	[231] 1.0000	[236] 10.000
229	YISHENG-0	[194] 2108	[142] 615				[195] 10.000	[141] 0.0268	[132] 0.0123	[121] 0.0083	[137] 1.149
230	YISHENG-1	[206] 3704	[81] 387	[125] 0.0208	[112] 0.0080	[106] 0.0047	[118] 1.105	[144] 0.0290	[135] 0.0125	[120] 0.0082	[139] 1.156
231	YITU-0	[224] 4136	[148] 633	[47] 0.0047	[49] 0.0031	[63] 0.0027	[44] 1.031	[56] 0.0074	[67] 0.0053	[75] 0.0049	[61] 1.053
232	YITU-1	[223] 4136	[232] 930	[44] 0.0046	[47] 0.0030	[61] 0.0027	[42] 1.031	[55] 0.0072	[63] 0.0053	[74] 0.0049	[59] 1.052
233	YITU-2	[226] 4138	[223] 870	[10] 0.0015	[7] 0.0010	[9] 0.0009	[7] 1.010	[18] 0.0044	[21] 0.0037	[29] 0.0035	[17] 1.035
234	YITU-3	[225] 4138	[224] 871	[17] 0.0023	[31] 0.0018	[37] 0.0018	[23] 1.018	[29] 0.0054	[54] 0.0048	[66] 0.0047	[41] 1.044
235	YITU-4	[189] 2070	[228] 910	[2] 0.0011	[5] 0.0008	[6] 0.0008	[5] 1.008	[10] 0.0037	[14] 0.0033	[24] 0.0033	[12] 1.031
236	YITU-5	[187] 2070	[221] 861	[15] 0.0020	[29] 0.0017	[35] 0.0017	[19] 1.016	[25] 0.0048	[42] 0.0044	[59] 0.0044	[35] 1.041

Table 19: **Rank-based accuracy for the FRVT 2018 mugshot sets**. *In columns 3 and 4 are template size and template generation duration. Thereafter values are rank-based FNIR with T = 0 and FPIR = 1. This is appropriate to investigational uses but not those with higher volumes where candidates from all searches would need review. Columns 5 - 9 show FRVT 2018 accuracy for various ranks for galleries unenrolled with all lifetime images. Column 10 is a workload statistic, a small value shows an algorithm front-loads mates into the first 10 candidates. The last four columns gives analogous results for enrollment only of the most recent image - see Figure 7. Throughout, blue superscripts indicate the rank of the algorithm for that column, and the best value is highlighted in yellow.*

MISSES BELOW THRESHOLD, T		ENROL MOST RECENT MUGSHOT, N = 1.6M								
FNIR(N, T> 0, R >L)		DATASET: FRVT 2018 MUGSHOTS			DATASET: WEBCAM PROBES			DATASET: PROFILE PROBES		
#	ALGORITHM	FPIR=0.001	FPIR=0.01	FPIR=0.1	FPIR=0.001	FPIR=0.01	FPIR=0.1	FPIR=0.001	FPIR=0.01	FPIR=0.1
1	3DIVI-0	[156] 0.256	[164] 0.160	[165] 0.086	[143] 0.425	[145] 0.302	[144] 0.180			
2	3DIVI-1	[155] 0.256	[165] 0.160	[166] 0.087						
3	3DIVI-2	[151] 0.255	[166] 0.164	[167] 0.089						
4	3DIVI-3	[175] 0.402	[182] 0.284	[182] 0.168	[159] 0.626	[162] 0.497	[158] 0.343			
5	3DIVI-4	[135] 0.171	[137] 0.096	[129] 0.047	[134] 0.343	[136] 0.237	[138] 0.138			
6	3DIVI-5	[131] 0.169	[136] 0.095	[130] 0.047	[132] 0.339	[135] 0.234	[137] 0.137	[81] 0.996	[84] 0.990	[99] 0.974
7	3DIVI-6	[134] 0.170	[140] 0.098	[137] 0.051	[133] 0.342	[137] 0.238	[139] 0.142			
8	ALCHERA-0	[122] 0.140	[122] 0.073	[119] 0.035	[100] 0.216	[103] 0.146	[106] 0.087	[98] 0.999	[117] 0.996	[106] 0.979
9	ALCHERA-1	[229] 0.999	[229] 0.999	[230] 0.995	[199] 1.000	[199] 1.000	[191] 1.000			
10	ALCHERA-2	[186] 0.490	[185] 0.304	[184] 0.184	[156] 0.591	[156] 0.442	[155] 0.295	[123] 1.000	[137] 0.999	[145] 0.997
11	ALCHERA-3	[125] 0.159	[123] 0.073	[112] 0.030	[107] 0.239	[108] 0.152	[101] 0.081	[111] 0.999	[122] 0.997	[95] 0.969
12	ALLGOVISION-000	[94] 0.091	[101] 0.048	[102] 0.024	[88] 0.166	[93] 0.106	[90] 0.062	[55] 0.990	[69] 0.982	[88] 0.962
13	ANKE-0	[110] 0.120	[117] 0.065	[115] 0.033	[102] 0.220	[106] 0.151	[109] 0.088	[65] 0.994	[82] 0.990	[119] 0.982
14	ANKE-002	[31] 0.034	[29] 0.016	[28] 0.008	[24] 0.079	[23] 0.050	[26] 0.028	[21] 0.948	[21] 0.795	[28] 0.657
15	ANKE-1	[116] 0.122	[116] 0.065	[116] 0.033	[101] 0.220	[107] 0.151	[108] 0.088	[69] 0.994	[93] 0.992	[127] 0.984
16	AWARE-0	[224] 0.983	[156] 0.128	[163] 0.085	[171] 0.817	[139] 0.253	[143] 0.178	[153] 1.000	[132] 0.998	[115] 0.981
17	AWARE-1	[225] 0.996	[155] 0.127	[162] 0.081				[148] 1.000	[139] 0.999	[113] 0.980
18	AWARE-2	[222] 0.977	[152] 0.120	[160] 0.078				[149] 1.000	[125] 0.998	[110] 0.980
19	AWARE-3	[120] 0.131	[128] 0.085	[138] 0.051	[125] 0.298	[128] 0.204	[136] 0.132	[46] 0.984	[62] 0.977	[91] 0.965
20	AWARE-4	[157] 0.271	[169] 0.177	[174] 0.107	[151] 0.509	[153] 0.375	[153] 0.253	[126] 1.000	[138] 0.999	[108] 0.979
21	AWARE-5	[169] 0.373	[131] 0.088	[135] 0.050	[111] 0.253	[111] 0.163	[114] 0.099	[130] 1.000	[140] 0.999	[147] 0.998
22	AWARE-6	[158] 0.278	[170] 0.178	[176] 0.109	[139] 0.398	[143] 0.283	[145] 0.188	[120] 0.999	[135] 0.999	[144] 0.996
23	AYONIX-0	[210] 0.811	[217] 0.725	[220] 0.598	[181] 0.939	[183] 0.892	[185] 0.802	[91] 0.998	[114] 0.995	[139] 0.991
24	AYONIX-1	[213] 0.825	[215] 0.702	[218] 0.526	[176] 0.920	[179] 0.845	[181] 0.703	[117] 0.999	[119] 0.996	[124] 0.984
25	AYONIX-2	[212] 0.825	[216] 0.702	[217] 0.526	[177] 0.920	[178] 0.845	[180] 0.702	[114] 0.999	[118] 0.996	[123] 0.984
26	CAMVI-1	[203] 0.684	[208] 0.549	[208] 0.375	[168] 0.770	[173] 0.648	[174] 0.488	[64] 0.994	[72] 0.984	[86] 0.961
27	CAMVI-2	[190] 0.537	[194] 0.402	[191] 0.242				[50] 0.989	[54] 0.973	[64] 0.931
28	CAMVI-3	[80] 0.074	[111] 0.060	[145] 0.055	[66] 0.132	[94] 0.108	[112] 0.094	[26] 0.970	[36] 0.940	[57] 0.914
29	CAMVI-4	[81] 0.074	[107] 0.056	[134] 0.050	[68] 0.136	[81] 0.100	[102] 0.083	[112] 0.999	[126] 0.998	[60] 0.915
30	CAMVI-5	[101] 0.102	[127] 0.078	[153] 0.069	[96] 0.179	[100] 0.132	[123] 0.110	[121] 1.000	[133] 0.998	[56] 0.904
31	COGENT-0	[62] 0.056	[75] 0.032	[88] 0.020	[71] 0.140	[85] 0.100	[97] 0.069	[75] 0.995	[91] 0.991	[126] 0.984
32	COGENT-1	[61] 0.056	[74] 0.032	[87] 0.020	[70] 0.140	[84] 0.100	[96] 0.069	[74] 0.995	[90] 0.991	[125] 0.984
33	COGENT-2	[46] 0.047	[34] 0.020	[33] 0.010	[39] 0.098	[41] 0.063	[44] 0.036	[86] 0.998	[98] 0.994	[129] 0.986
34	COGENT-3	[53] 0.051	[32] 0.018	[31] 0.009	[35] 0.095	[39] 0.061	[47] 0.037	[90] 0.998	[112] 0.995	[133] 0.988
35	COGNITEC-0	[128] 0.163	[138] 0.098	[141] 0.053	[126] 0.303	[126] 0.200	[126] 0.115	[58] 0.992	[48] 0.971	[77] 0.953
36	COGNITEC-1	[103] 0.105	[105] 0.055	[106] 0.027	[105] 0.230	[102] 0.135	[98] 0.071	[184] 1.000	[43] 0.965	[72] 0.947
37	COGNITEC-2	[63] 0.056	[65] 0.027	[61] 0.014	[95] 0.178	[88] 0.101	[77] 0.050	[133] 1.000	[40] 0.956	[70] 0.941
38	COGNITEC-3	[60] 0.055	[67] 0.028	[65] 0.014	[86] 0.162	[82] 0.100	[75] 0.050	[134] 1.000	[37] 0.946	[62] 0.924
39	CYBERLINK-000	[69] 0.059	[56] 0.025	[46] 0.011	[53] 0.116	[53] 0.070	[51] 0.038	[78] 0.995	[68] 0.981	[55] 0.900
40	CYBERLINK-001	[64] 0.056	[54] 0.025	[43] 0.011	[48] 0.109	[48] 0.067	[41] 0.036	[73] 0.995	[71] 0.984	[67] 0.934
41	DAHUA-0	[91] 0.089	[97] 0.047	[95] 0.022	[67] 0.135	[70] 0.083	[68] 0.046			
42	DAHUA-002	[12] 0.018	[10] 0.009	[12] 0.005	[11] 0.046	[11] 0.029	[11] 0.017	[6] 0.638	[9] 0.522	[10] 0.394
43	DAHUA-1	[83] 0.075	[84] 0.039	[80] 0.018	[61] 0.122	[62] 0.075	[60] 0.042	[39] 0.980	[33] 0.933	[37] 0.790
44	DEEPGLINT-001				[207] 1.000	[207] 1.000	[208] 1.000	[200] 1.000	[201] 1.000	[202] 1.000
45	DEEPSEA-001	[47] 0.049	[51] 0.024	[49] 0.012	[41] 0.101	[35] 0.059	[31] 0.031	[47] 0.985	[55] 0.973	[71] 0.942
46	DERMALOG-0	[185] 0.488	[189] 0.364	[190] 0.233	[163] 0.657	[168] 0.528	[163] 0.362	[77] 0.995	[85] 0.991	[105] 0.978
47	DERMALOG-1	[188] 0.528	[195] 0.405	[195] 0.268				[56] 0.990	[70] 0.983	[89] 0.964
48	DERMALOG-2	[187] 0.503	[191] 0.378	[192] 0.244				[52] 0.990	[66] 0.981	[85] 0.960
49	DERMALOG-3	[184] 0.484	[188] 0.362	[188] 0.231	[161] 0.655	[167] 0.526	[162] 0.361			
50	DERMALOG-4	[183] 0.481	[187] 0.360	[187] 0.230	[162] 0.657	[165] 0.526	[161] 0.359	[79] 0.995	[92] 0.991	[112] 0.980
51	DERMALOG-5	[96] 0.091	[90] 0.045	[101] 0.024	[77] 0.154	[79] 0.096	[83] 0.057	[54] 0.990	[39] 0.950	[40] 0.816
52	DERMALOG-6	[58] 0.054	[68] 0.028	[68] 0.015	[43] 0.105	[46] 0.067	[54] 0.039	[40] 0.981	[34] 0.933	[36] 0.758
53	EVERAI-0	[99] 0.092	[100] 0.047	[108] 0.028	[89] 0.170	[83] 0.100	[86] 0.060	[109] 0.999	[121] 0.997	[31] 0.702
54	EVERAI-1	[54] 0.052	[44] 0.023	[34] 0.010	[63] 0.128	[58] 0.074	[53] 0.039	[99] 0.999	[99] 0.994	[21] 0.530
55	EVERAI-2	[55] 0.053	[53] 0.025	[40] 0.011	[58] 0.119	[63] 0.076	[57] 0.041	[45] 0.983	[19] 0.748	[16] 0.495
56	EVERAI-3	[32] 0.038	[31] 0.018	[27] 0.008	[36] 0.096	[36] 0.060	[36] 0.034	[68] 0.994	[14] 0.733	[11] 0.395
57	EVERAI-PARAVISION-004	[6] 0.013	[6] 0.007	[7] 0.005	[9] 0.038	[8] 0.024	[6] 0.015	[141] 1.000	[23] 0.797	[2] 0.170
58	EYEDEA-0	[211] 0.812	[214] 0.679	[214] 0.484	[175] 0.914	[176] 0.783	[177] 0.619	[84] 0.998	[88] 0.991	[107] 0.979
59	EYEDEA-1	[198] 0.632	[199] 0.480	[202] 0.335				[105] 0.999	[102] 0.994	[104] 0.978
60	EYEDEA-2	[208] 0.794	[202] 0.490	[204] 0.338				[115] 0.999	[116] 0.996	[109] 0.980
61	EYEDEA-3	[172] 0.389	[180] 0.267	[180] 0.160	[153] 0.543	[155] 0.404	[154] 0.264	[70] 0.994	[81] 0.990	[114] 0.981
62	F8-001	[129] 0.168	[82] 0.038	[85] 0.020				[97] 0.998	[115] 0.995	[69] 0.935
63	GLORY-0	[168] 0.369	[184] 0.297	[189] 0.233	[154] 0.547	[159] 0.470	[168] 0.390	[72] 0.995	[96] 0.993	[140] 0.991
64	GLORY-1	[163] 0.307	[177] 0.238	[183] 0.179	[152] 0.537	[157] 0.448	[159] 0.352	[62] 0.993	[87] 0.991	[135] 0.989
65	GORILLA-0									
66	GORILLA-004	[98] 0.092	[91] 0.046	[86] 0.020	[84] 0.160	[86] 0.101	[81] 0.053	[22] 0.959	[28] 0.903	[38] 0.796
67	GORILLA-1	[176] 0.408	[178] 0.248	[177] 0.136	[146] 0.453	[147] 0.314	[147] 0.191	[139] 1.000	[153] 1.000	[141] 0.993
68	GORILLA-2	[138] 0.190	[144] 0.108	[136] 0.051	[118] 0.268	[117] 0.170	[111] 0.093	[150] 1.000	[97] 0.993	[59] 0.915
69	GORILLA-3	[165] 0.326	[163] 0.160	[154] 0.074	[145] 0.434	[138] 0.247	[134] 0.131	[170] 1.000	[148] 1.000	[111] 0.980
70	HBINNO-0	[207] 0.766	[212] 0.632	[213] 0.458				[135] 1.000	[145] 1.000	[149] 0.998
71	HIK-0	[109] 0.114	[121] 0.070	[123] 0.040	[78] 0.155	[90] 0.103	[89] 0.061	[41] 0.981	[49] 0.971	[74] 0.949
72	HIK-1	[114] 0.120	[119] 0.067	[118] 0.034				[53] 0.990	[67] 0.981	[87] 0.961

Table 20: **Threshold-based accuracy**. *Values are FNIR(N, T, L) with N = 1.6 million with thresholds set to produce FPIR = 0.001, 0.01, and 0.1 in non-mate searches. Columns 3-5 apply to FRVT-2018 mugshots: Columns 6-8 show the corresponding FNIR values for webcam images searched against the FRVT-2018 mugshot gallery. Finally, the three rightmost columns show FNIR for profile view images searched against the FRVT-2018 frontal gallery. Throughout blue superscripts indicate the rank of the algorithm for that column. Caution: The Power-low models are mostly intended to draw attention to the kind of behavior, not as a model to be used for prediction.*

MISSES BELOW THRESHOLD, T		ENROL MOST RECENT MUGSHOT, N = 1.6M								
FNIR(N, T> 0, R >L)		DATASET: FRVT 2018 MUGSHOTS			DATASET: WEBCAM PROBES			DATASET: PROFILE PROBES		
#	ALGORITHM	FPIR=0.001	FPIR=0.01	FPIR=0.1	FPIR=0.001	FPIR=0.01	FPIR=0.1	FPIR=0.001	FPIR=0.01	FPIR=0.1
73	HIK-2	[115] 0.121	[120] 0.067	[117] 0.034				[59] 0.992	[73] 0.985	[93] 0.966
74	HIK-3	[104] 0.105	[110] 0.060	[113] 0.030	[80] 0.158	[91] 0.105	[88] 0.061	[25] 0.969	[31] 0.925	[43] 0.835
75	HIK-4	[100] 0.101	[108] 0.056	[110] 0.029	[76] 0.153	[87] 0.101	[84] 0.059	[31] 0.976	[38] 0.947	[49] 0.879
76	HIK-5	[43] 0.047	[39] 0.022	[47] 0.011	[23] 0.077	[22] 0.048	[28] 0.028	[118] 0.999	[128] 0.998	[42] 0.831
77	HIK-6	[49] 0.050	[43] 0.022	[45] 0.011	[26] 0.086	[26] 0.052	[29] 0.029	[152] 1.000	[141] 0.999	[41] 0.819
78	IDEMIA-0	[108] 0.114	[113] 0.062	[109] 0.029	[108] 0.240	[109] 0.156	[105] 0.085	[51] 0.990	[74] 0.986	[101] 0.976
79	IDEMIA-007	[15] 0.021	[15] 0.011	[21] 0.007	[15] 0.055	[14] 0.033	[14] 0.021	[193] 1.000	[194] 1.000	[195] 1.000
80	IDEMIA-1	[57] 0.054	[73] 0.031	[79] 0.018				[28] 0.971	[42] 0.964	[80] 0.955
81	IDEMIA-2	[59] 0.054	[76] 0.032	[81] 0.019				[27] 0.970	[44] 0.965	[75] 0.952
82	IDEMIA-3	[48] 0.050	[49] 0.024	[62] 0.014	[87] 0.165	[65] 0.079	[78] 0.050		[219] 1.000	[143] 0.996
83	IDEMIA-4	[35] 0.040	[48] 0.024	[66] 0.014	[57] 0.118	[64] 0.079	[76] 0.050	[30] 0.973	[45] 0.968	[83] 0.960
84	IDEMIA-5	[42] 0.047	[69] 0.028	[73] 0.017	[75] 0.150	[89] 0.102	[95] 0.065	[35] 0.978	[53] 0.973	[94] 0.967
85	IDEMIA-6	[40] 0.046	[66] 0.028	[76] 0.018	[104] 0.226	[110] 0.161	[122] 0.108	[42] 0.982	[65] 0.980	[102] 0.976
86	IIT-002				[140] 0.403	[154] 0.382	[164] 0.367	[119] 0.999	[17] 0.743	[22] 0.581
87	IMAGUS-0	[205] 0.734	[211] 0.608	[212] 0.453	[173] 0.872	[175] 0.779	[178] 0.635	[127] 1.000	[143] 1.000	[150] 0.999
88	IMAGUS-2	[206] 0.751	[209] 0.566	[209] 0.377	[170] 0.816	[172] 0.645	[172] 0.460	[142] 1.000	[149] 1.000	[154] 0.999
89	IMAGUS-3	[209] 0.808	[213] 0.670	[216] 0.512	[174] 0.909	[177] 0.809	[179] 0.667	[136] 1.000	[146] 1.000	[153] 0.999
90	IMPERIAL-000	[25] 0.029	[19] 0.012	[22] 0.007	[19] 0.068	[18] 0.041	[18] 0.024	[101] 0.999	[103] 0.995	[12] 0.441
91	INCODE-0	[164] 0.313	[174] 0.201	[173] 0.107	[142] 0.420	[146] 0.304	[146] 0.191	[94] 0.998	[100] 0.994	[122] 0.984
92	INCODE-004	[66] 0.056	[59] 0.026	[44] 0.011	[60] 0.120	[54] 0.070	[45] 0.036	[71] 0.995	[32] 0.929	[25] 0.630
93	INCODE-1	[144] 0.214	[145] 0.114	[132] 0.050	[122] 0.296	[124] 0.198	[124] 0.110	[144] 1.000	[144] 1.000	[52] 0.885
94	INCODE-2	[137] 0.186	[142] 0.102	[128] 0.046	[119] 0.269	[119] 0.176	[115] 0.100	[63] 0.993	[61] 0.976	[61] 0.918
95	INCODE-3	[133] 0.170	[129] 0.086	[122] 0.037	[115] 0.264	[113] 0.164	[107] 0.087	[116] 0.999	[120] 0.996	[54] 0.899
96	INNOVATRICS-0	[154] 0.255	[168] 0.165	[169] 0.089	[135] 0.361	[140] 0.258	[142] 0.159	[44] 0.983	[60] 0.975	[79] 0.953
97	INNOVATRICS-1	[153] 0.255	[167] 0.165	[168] 0.089				[43] 0.983	[59] 0.975	[78] 0.953
98	INNOVATRICS-2	[150] 0.237	[162] 0.142	[161] 0.079	[127] 0.310	[130] 0.209	[130] 0.126	[147] 1.000	[142] 0.999	[118] 0.982
99	INNOVATRICS-3	[146] 0.224	[158] 0.134	[152] 0.068	[123] 0.297	[127] 0.203	[127] 0.116	[124] 1.000	[131] 0.998	[66] 0.933
100	INNOVATRICS-4	[121] 0.134	[126] 0.076	[121] 0.035	[103] 0.222	[104] 0.149	[104] 0.085	[38] 0.980	[51] 0.973	[82] 0.957
101	INTSYSMSU-000	[227] 0.998	[227] 0.990	[227] 0.921	[188] 1.000	[188] 0.998	[50] 0.038	[125] 1.000	[127] 0.998	[32] 0.705
102	ISYSTEMS-0	[97] 0.091	[96] 0.047	[99] 0.023	[92] 0.173	[95] 0.110	[93] 0.065	[61] 0.993	[80] 0.989	[117] 0.981
103	ISYSTEMS-1	[93] 0.090	[94] 0.047	[98] 0.023				[60] 0.993	[79] 0.989	[116] 0.981
104	ISYSTEMS-2	[86] 0.081	[80] 0.035	[70] 0.015	[62] 0.126	[67] 0.080	[70] 0.046	[83] 0.998	[95] 0.993	[90] 0.965
105	ISYSTEMS-3	[74] 0.062	[63] 0.027	[56] 0.012	[46] 0.107	[50] 0.068	[52] 0.039	[129] 1.000	[124] 0.997	[76] 0.953
106	KEDACOM-001	[22] 0.025	[28] 0.016	[54] 0.012	[21] 0.072	[28] 0.054	[61] 0.042	[49] 0.986	[56] 0.973	[97] 0.972
107	LOOKMAN-005	[30] 0.033	[33] 0.020	[59] 0.013	[25] 0.086	[42] 0.063	[69] 0.046	[34] 0.978	[52] 0.973	[96] 0.971
108	LOOKMAN-3	[41] 0.046	[64] 0.027	[74] 0.017	[50] 0.112	[68] 0.082	[82] 0.057			
109	LOOKMAN-4	[44] 0.047	[62] 0.027	[71] 0.016	[45] 0.105	[60] 0.075	[80] 0.052	[32] 0.977	[57] 0.974	[98] 0.972
110	MEGVII-0	[107] 0.109	[109] 0.058	[105] 0.025	[52] 0.116	[47] 0.067	[37] 0.034			
111	MEGVII-1	[82] 0.075	[83] 0.039	[94] 0.022	[38] 0.097	[37] 0.061	[35] 0.033			
112	MEGVII-2	[85] 0.080	[85] 0.039	[92] 0.022	[37] 0.096	[34] 0.059	[34] 0.033	[96] 0.998	[27] 0.872	[27] 0.644
113	MICROFOCUS-0	[218] 0.933	[222] 0.867	[224] 0.749	[187] 0.985	[186] 0.950	[188] 0.877			
114	MICROFOCUS-1	[219] 0.933	[223] 0.867	[225] 0.749						
115	MICROFOCUS-2	[220] 0.934	[224] 0.870	[226] 0.758						
116	MICROFOCUS-3	[217] 0.931	[221] 0.866	[223] 0.748	[186] 0.979	[185] 0.948	[187] 0.876			
117	MICROFOCUS-4	[228] 0.999	[230] 0.999	[229] 0.994	[184] 0.975	[184] 0.940	[186] 0.862			
118	MICROFOCUS-5	[214] 0.836	[219] 0.736	[219] 0.588	[179] 0.928	[181] 0.865	[184] 0.748			
119	MICROFOCUS-6	[223] 0.978	[225] 0.963	[221] 0.641	[178] 0.923	[180] 0.858	[183] 0.739			
120	MICROSOFT-0	[37] 0.044	[38] 0.022	[38] 0.010	[51] 0.115	[55] 0.071	[55] 0.040			
121	MICROSOFT-1	[39] 0.045	[40] 0.022	[39] 0.011						
122	MICROSOFT-2	[51] 0.050	[58] 0.026	[53] 0.012						
123	MICROSOFT-3	[29] 0.030	[25] 0.014	[18] 0.006	[31] 0.091	[32] 0.056	[27] 0.028			
124	MICROSOFT-4	[26] 0.029	[24] 0.013	[15] 0.005	[27] 0.087	[27] 0.053	[24] 0.026			
125	MICROSOFT-5	[23] 0.028	[21] 0.012	[10] 0.005	[20] 0.070	[19] 0.041	[13] 0.021	[5] 0.587	[5] 0.354	[6] 0.222
126	MICROSOFT-6	[8] 0.014	[8] 0.008	[5] 0.004	[8] 0.037	[9] 0.024	[7] 0.016	[1] 0.386	[2] 0.281	[3] 0.198
127	NEC-0	[87] 0.082	[102] 0.049	[111] 0.029	[72] 0.140	[75] 0.093	[85] 0.059	[36] 0.979	[47] 0.969	[81] 0.956
128	NEC-1	[106] 0.108	[115] 0.063	[120] 0.035	[98] 0.197	[101] 0.133	[103] 0.083	[48] 0.986	[50] 0.972	[84] 0.960
129	NEC-2	[3] 0.005	[1] 0.004	[1] 0.003	[3] 0.020	[3] 0.013	[2] 0.010	[113] 0.999	[106] 0.995	[14] 0.474
130	NEC-3	[1] 0.004	[2] 0.004	[2] 0.003	[2] 0.017	[2] 0.013	[3] 0.011	[12] 0.824	[10] 0.628	[13] 0.450
131	NEUROTECHNOLOGY-0	[159] 0.295	[173] 0.196	[175] 0.108	[147] 0.465	[148] 0.317	[149] 0.196	[104] 0.999	[113] 0.995	[100] 0.974
132	NEUROTECHNOLOGY-007	[75] 0.065	[50] 0.024	[42] 0.011	[91] 0.173	[49] 0.068	[48] 0.038	[132] 1.000	[123] 0.997	[103] 0.977
133	NEUROTECHNOLOGY-1	[161] 0.299	[172] 0.195	[172] 0.105				[87] 0.998	[108] 0.995	[134] 0.989
134	NEUROTECHNOLOGY-2	[162] 0.299	[171] 0.195	[171] 0.105				[85] 0.998	[111] 0.995	[136] 0.989
135	NEUROTECHNOLOGY-3	[202] 0.665	[141] 0.101	[140] 0.052	[117] 0.266	[112] 0.164	[110] 0.088	[221] 1.000	[221] 1.000	[221] 1.000
136	NEUROTECHNOLOGY-4	[77] 0.066	[71] 0.030	[67] 0.014	[54] 0.117	[56] 0.073	[56] 0.040	[67] 0.994	[83] 0.990	[128] 0.984
137	NEUROTECHNOLOGY-5	[67] 0.056	[55] 0.025	[52] 0.012	[64] 0.130	[59] 0.074	[62] 0.042	[89] 0.998	[78] 0.989	[92] 0.965
138	NEUROTECHNOLOGY-6	[152] 0.255	[153] 0.124	[139] 0.051	[141] 0.418	[129] 0.206	[117] 0.103			
139	NEWLAND-2	[180] 0.441	[183] 0.296	[179] 0.157	[148] 0.466	[150] 0.335	[151] 0.213	[106] 0.999	[130] 0.998	[130] 0.986
140	NOBLIS-1	[230] 1.000	[228] 0.992	[210] 0.419	[231] 1.000	[231] 1.000	[190] 1.000	[154] 1.000	[158] 1.000	[159] 1.000
141	NOBLIS-2	[226] 0.997	[203] 0.490	[199] 0.309	[196] 1.000	[196] 1.000	[176] 0.565	[140] 1.000	[154] 1.000	[157] 1.000
142	NTECHLAB-0	[88] 0.083	[99] 0.047	[96] 0.023	[85] 0.162	[92] 0.105	[87] 0.061	[18] 0.900	[25] 0.826	[33] 0.720
143	NTECHLAB-007	[24] 0.028	[27] 0.015	[26] 0.008	[18] 0.067	[17] 0.041	[17] 0.023	[9] 0.750	[12] 0.642	[17] 0.498
144	NTECHLAB-008	[10] 0.017	[12] 0.009	[17] 0.006	[10] 0.045	[12] 0.029	[9] 0.017	[4] 0.529	[6] 0.391	[7] 0.252

Table 21: **Threshold-based accuracy**. *Values are FNIR(N, T, L) with N = 1.6 million with thresholds set to produce FPIR = 0.001, 0.01, and 0.1 in non-mate searches. Columns 3-5 apply to FRVT-2018 mugshots: Columns 6-8 show the corresponding FNIR values for webcam images searched against the FRVT-2018 mugshot gallery. Finally, the three rightmost columns show FNIR for profile view images searched against the FRVT-2018 frontal gallery. Throughout blue superscripts indicate the rank of the algorithm for that column. Caution: The Power-low models are mostly intended to draw attention to the kind of behavior, not as a model to be used for prediction.*

MISSES BELOW THRESHOLD, T		ENROL MOST RECENT MUGSHOT, N = 1.6M								
FNIR(N, T> 0, R >L)		DATASET: FRVT 2018 MUGSHOTS			DATASET: WEBCAM PROBES			DATASET: PROFILE PROBES		
#	ALGORITHM	FPIR=0.001	FPIR=0.01	FPIR=0.1	FPIR=0.001	FPIR=0.01	FPIR=0.1	FPIR=0.001	FPIR=0.01	FPIR=0.1
145	NTECHLAB-1	^{102}0.102	^{106}0.056	^{107}0.027				^{19}0.909	^{26}0.842	^{35}0.734
146	NTECHLAB-3	^{65}0.056	^{72}0.030	^{69}0.015	^{55}0.118	^{61}0.075	^{63}0.043	^{14}0.837	^{20}0.752	^{23}0.628
147	NTECHLAB-4	^{36}0.043	^{46}0.024	^{51}0.012	^{44}0.105	^{45}0.065	^{43}0.036	^{13}0.833	^{18}0.746	^{24}0.629
148	NTECHLAB-5	^{38}0.045	^{47}0.024	^{50}0.012	^{42}0.102	^{43}0.063	^{39}0.034	^{11}0.771	^{13}0.661	^{19}0.516
149	NTECHLAB-6	^{33}0.039	^{36}0.021	^{35}0.010	^{33}0.094	^{33}0.059	^{32}0.032	^{10}0.754	^{11}0.635	^{15}0.490
150	PARAVISION-005	^{4}0.007	^{4}0.005	^{4}0.004	^{4}0.024	^{4}0.016	^{5}0.012	^{37}0.980	^{1}0.181	^{1}0.109
151	PIXELALL-002	^{105}0.108	^{77}0.032	^{63}0.014	^{137}0.388	^{69}0.083	^{65}0.044	^{145}1.000	^{150}1.000	^{146}0.997
152	PIXELALL-003	^{19}0.024	^{17}0.012	^{20}0.006	^{22}0.073	^{21}0.043	^{19}0.024	^{122}1.000	^{129}0.998	^{34}0.720
153	QUANTASOFT-1	^{200}0.640	^{205}0.494	^{203}0.335						
154	RANKONE-0	^{145}0.219	^{157}0.129	^{159}0.078	^{138}0.391	^{144}0.291	^{148}0.195			
155	RANKONE-006	^{34}0.040	^{41}0.022	^{57}0.012				^{33}0.977	^{35}0.937	^{48}0.870
156	RANKONE-007	^{21}0.025	^{26}0.014	^{30}0.009	^{34}0.095	^{38}0.061	^{42}0.036	^{24}0.967	^{30}0.924	^{45}0.850
157	RANKONE-1	^{130}0.168	^{130}0.087	^{126}0.043						
158	RANKONE-2	^{112}0.120	^{125}0.073	^{125}0.042	^{113}0.261	^{123}0.190	^{129}0.126			
159	RANKONE-3	^{111}0.120	^{124}0.073	^{124}0.042	^{112}0.255	^{121}0.187	^{128}0.122			
160	RANKONE-4	^{139}0.195	^{154}0.126	^{155}0.076	^{144}0.426	^{149}0.324	^{152}0.221			
161	RANKONE-5	^{72}0.062	^{81}0.036	^{89}0.021	^{93}0.173	^{97}0.119	^{100}0.074	^{92}0.998	^{101}0.994	^{137}0.990
162	REALNETWORKS-0	^{149}0.236	^{161}0.140	^{158}0.077	^{130}0.319	^{132}0.209	^{132}0.129			
163	REALNETWORKS-003	^{127}0.162	^{133}0.093	^{133}0.050	^{116}0.266	^{118}0.172	^{116}0.102	^{95}0.998	^{75}0.987	^{58}0.914
164	REALNETWORKS-004	^{126}0.160	^{132}0.092	^{131}0.049	^{114}0.263	^{115}0.169	^{113}0.099	^{110}0.999	^{94}0.992	^{68}0.935
165	REALNETWORKS-1	^{148}0.236	^{160}0.140	^{157}0.077	^{129}0.319	^{131}0.209	^{131}0.129			
166	REALNETWORKS-2	^{147}0.234	^{159}0.139	^{156}0.077	^{128}0.315	^{133}0.209	^{133}0.129			
167	REMARKAI-0	^{119}0.130	^{114}0.062	^{104}0.025	^{99}0.203	^{99}0.123	^{92}0.064			
168	REMARKAI-000	^{68}0.058	^{57}0.025	^{41}0.011	^{59}0.120	^{52}0.070	^{46}0.037	^{108}0.999	^{105}0.995	^{50}0.880
169	REMARKAI-2	^{118}0.126	^{112}0.061	^{103}0.024	^{97}0.196	^{98}0.122	^{91}0.063	^{57}0.991	^{64}0.980	^{65}0.932
170	SCANOVATE-000	^{78}0.069	^{78}0.033	^{64}0.014	^{110}0.240	^{105}0.150	^{99}0.073	^{17}0.893	^{24}0.803	^{30}0.683
171	SENSETIME-0	^{17}0.023	^{18}0.012	^{23}0.007	^{16}0.063	^{16}0.040	^{20}0.025	^{203}1.000	^{76}0.988	^{47}0.869
172	SENSETIME-002	^{11}0.017	^{30}0.017	^{75}0.017	^{6}0.028	^{7}0.023	^{16}0.021	^{66}0.994	^{63}0.979	^{44}0.842
173	SENSETIME-003	^{2}0.004	^{3}0.004	^{3}0.004	^{1}0.012	^{1}0.009	^{1}0.007	^{2}0.477	^{3}0.311	^{5}0.212
174	SENSETIME-1	^{20}0.025	^{20}0.012	^{24}0.007	^{17}0.064	^{20}0.041	^{22}0.025			
175	SHAMAN-0	^{182}0.474	^{190}0.370	^{194}0.259	^{158}0.621	^{163}0.507	^{166}0.375			
176	SHAMAN-1	^{189}0.532	^{196}0.406	^{197}0.274						
177	SHAMAN-2	^{204}0.700	^{210}0.582	^{211}0.424						
178	SHAMAN-3	^{181}0.453	^{186}0.348	^{186}0.225	^{157}0.597	^{160}0.472	^{156}0.317			
179	SHAMAN-4	^{195}0.616	^{201}0.490	^{206}0.344	^{167}0.754	^{171}0.639	^{173}0.480			
180	SHAMAN-6	^{123}0.143	^{135}0.095	^{149}0.060	^{106}0.237	^{114}0.168	^{121}0.108	^{29}0.972	^{41}0.960	^{63}0.931
181	SHAMAN-7	^{124}0.144	^{134}0.094	^{148}0.060	^{109}0.240	^{116}0.169	^{119}0.107			
182	SIAT-0	^{95}0.091	^{95}0.047	^{91}0.022	^{47}0.107	^{44}0.064	^{40}0.035			
183	SIAT-1	^{13}0.020	^{11}0.009	^{9}0.005	^{136}0.365	^{151}0.348	^{157}0.337			
184	SIAT-2	^{18}0.024	^{13}0.009	^{8}0.005	^{149}0.478	^{158}0.460	^{171}0.451			
185	SMILART-0	^{196}0.620	^{200}0.486	^{200}0.322						
186	SMILART-1	^{201}0.641	^{207}0.505	^{205}0.342						
187	SMILART-2	^{197}0.629	^{204}0.492	^{201}0.325						
188	SMILART-4	^{221}0.968	^{226}0.965	^{228}0.964	^{185}0.976	^{187}0.973	^{189}0.973			
189	SMILART-5									
190	SYNESIS-0	^{193}0.554	^{192}0.378	^{185}0.213	^{166}0.734	^{170}0.598	^{170}0.431			
191	SYNESIS-3	^{194}0.583	^{198}0.444	^{198}0.294	^{160}0.646	^{164}0.524	^{165}0.372			
192	TECH5-001	^{70}0.060	^{35}0.021	^{36}0.010	^{180}0.935	^{31}0.055	^{25}0.027	^{155}1.000	^{147}1.000	^{151}0.999
193	TEVIAN-0	^{141}0.203	^{147}0.114	^{143}0.054	^{131}0.331	^{134}0.227	^{135}0.132			
194	TEVIAN-1	^{142}0.203	^{148}0.114	^{144}0.054						
195	TEVIAN-2	^{140}0.202	^{146}0.114	^{142}0.054						
196	TEVIAN-3	^{136}0.180	^{139}0.098	^{127}0.044	^{124}0.298	^{125}0.198	^{125}0.113			
197	TEVIAN-4	^{113}0.120	^{118}0.066	^{114}0.031	^{94}0.176	^{96}0.115	^{94}0.065			
198	TEVIAN-5	^{92}0.090	^{98}0.047	^{93}0.022	^{73}0.144	^{72}0.089	^{74}0.049	^{23}0.962	^{22}0.796	^{26}0.634
199	TIGER-0	^{173}0.392	^{179}0.263	^{178}0.142	^{150}0.500	^{152}0.366	^{150}0.211			
200	TIGER-1				^{155}0.580	^{161}0.487	^{169}0.396			
201	TIGER-2	^{90}0.089	^{87}0.042	^{78}0.018	^{82}0.158	^{78}0.095	^{73}0.048	^{103}0.999	^{58}0.975	^{29}0.678
202	TIGER-3	^{89}0.089	^{88}0.042	^{77}0.018	^{81}0.158	^{77}0.095	^{72}0.048			
203	TONGYITRANS-0	^{84}0.077	^{86}0.041	^{82}0.019	^{49}0.112	^{51}0.069	^{49}0.038			
204	TONGYITRANS-1	^{79}0.069	^{79}0.035	^{72}0.016	^{40}0.101	^{40}0.062	^{38}0.034			
205	TOSHIBA-0	^{76}0.065	^{70}0.029	^{58}0.013	^{56}0.118	^{57}0.074	^{59}0.041	^{76}0.995	^{77}0.988	^{73}0.949
206	TOSHIBA-1	^{73}0.062	^{37}0.021	^{37}0.010	^{32}0.092	^{29}0.054	^{33}0.032			
207	VD-0	^{216}0.917	^{220}0.828	^{222}0.668	^{182}0.946	^{182}0.871	^{182}0.725			
208	VD-1	^{143}0.204	^{151}0.118	^{147}0.059	^{120}0.281	^{122}0.188	^{118}0.106			
209	VIGILANTSOLUTIONS-0	^{191}0.539	^{193}0.394	^{193}0.247	^{165}0.695	^{169}0.557	^{167}0.389	^{88}0.998	^{104}0.995	^{138}0.990
210	VIGILANTSOLUTIONS-1	^{199}0.637	^{206}0.502	^{207}0.348				^{128}1.000	^{134}0.998	^{142}0.995
211	VIGILANTSOLUTIONS-2	^{215}0.876	^{218}0.731	^{215}0.489				^{102}0.999	^{109}0.995	^{132}0.987
212	VIGILANTSOLUTIONS-3	^{177}0.410	^{181}0.283	^{181}0.163	^{164}0.660	^{166}0.526	^{160}0.356	^{100}0.999	^{107}0.995	^{131}0.986
213	VIGILANTSOLUTIONS-4	^{192}0.550	^{197}0.424	^{196}0.268	^{172}0.817	^{174}0.709	^{175}0.523	^{80}0.996	^{89}0.991	^{121}0.984
214	VIGILANTSOLUTIONS-5	^{179}0.433	^{89}0.045	^{97}0.023				^{143}1.000	^{155}1.000	^{152}0.999
215	VIGILANTSOLUTIONS-6	^{178}0.426	^{92}0.046	^{100}0.023				^{146}1.000	^{156}1.000	^{148}0.998
216	VISIONLABS-008	^{9}0.016	^{9}0.008	^{13}0.005	^{13}0.051	^{13}0.032	^{12}0.019	^{3}0.481	^{4}0.317	^{4}0.203

Table 22: **Threshold-based accuracy**. *Values are FNIR(N, T, L) with N = 1.6 million with thresholds set to produce FPIR = 0.001, 0.01, and 0.1 in non-mate searches. Columns 3-5 apply to FRVT-2018 mugshots: Columns 6-8 show the corresponding FNIR values for webcam images searched against the FRVT-2018 mugshot gallery. Finally, the three rightmost columns show FNIR for profile view images searched against the FRVT-2018 frontal gallery. Throughout blue superscripts indicate the rank of the algorithm for that column. Caution: The Power-low models are mostly intended to draw attention to the kind of behavior, not as a model to be used for prediction.*

MISSES BELOW THRESHOLD, T		ENROL MOST RECENT MUGSHOT, N = 1.6M								
FNIR(N, T> 0, R >L)		DATASET: FRVT 2018 MUGSHOTS			DATASET: WEBCAM PROBES			DATASET: PROFILE PROBES		
#	ALGORITHM	FPIR=0.001	FPIR=0.01	FPIR=0.1	FPIR=0.001	FPIR=0.01	FPIR=0.1	FPIR=0.001	FPIR=0.01	FPIR=0.1
217	VISIONLABS-3	^{52}0.051	^{60}0.026	^{60}0.013	^{69}0.137	^{73}0.091	^{79}0.051	^{107}0.999	^{110}0.995	^{39}0.811
218	VISIONLABS-4	^{71}0.060	^{61}0.026	^{32}0.010	^{83}0.159	^{80}0.097	^{66}0.045	^{16}0.890	^{16}0.742	^{20}0.525
219	VISIONLABS-5	^{56}0.053	^{42}0.022	^{29}0.008	^{74}0.147	^{71}0.087	^{58}0.041	^{15}0.888	^{15}0.736	^{18}0.514
220	VISIONLABS-6	^{28}0.029	^{23}0.012	^{16}0.005	^{30}0.090	^{25}0.051	^{23}0.025	^{7}0.672	^{8}0.511	^{9}0.328
221	VISIONLABS-7	^{27}0.029	^{22}0.012	^{14}0.005	^{29}0.090	^{24}0.051	^{21}0.025	^{8}0.672	^{7}0.511	^{8}0.328
222	VOCORD-0	^{174}0.399	^{150}0.116	^{151}0.062	^{121}0.285	^{120}0.181	^{120}0.108	^{138}1.000	^{152}1.000	^{156}1.000
223	VOCORD-1	^{160}0.299	^{149}0.116	^{150}0.062				^{137}1.000	^{151}1.000	^{155}1.000
224	VOCORD-2	^{167}0.366	^{143}0.107	^{146}0.057				^{151}1.000	^{157}1.000	^{158}1.000
225	VOCORD-3	^{117}0.126	^{103}0.050	^{84}0.020	^{79}0.155	^{76}0.093	^{71}0.048	^{93}0.998	^{86}0.991	^{53}0.891
226	VOCORD-4	^{170}0.378	^{104}0.054	^{90}0.021	^{90}0.173	^{74}0.093	^{67}0.046	^{131}1.000	^{136}0.999	^{120}0.982
227	VOCORD-5	^{132}0.170	^{93}0.046	^{83}0.019	^{65}0.130	^{66}0.080	^{64}0.043	^{82}0.997	^{46}0.968	^{46}0.865
228	VOCORD-6	^{236}1.000	^{236}1.000	^{236}1.000	^{233}1.000	^{233}1.000	^{233}1.000	^{232}1.000	^{232}1.000	^{232}1.000
229	YISHENG-0	^{171}0.380	^{176}0.209	^{164}0.086	^{183}0.974	^{142}0.275	^{141}0.146			
230	YISHENG-1	^{166}0.348	^{175}0.208	^{170}0.090	^{169}0.808	^{141}0.269	^{140}0.144			
231	YITU-0	^{50}0.050	^{52}0.025	^{55}0.012	^{28}0.090	^{30}0.054	^{30}0.030			
232	YITU-1	^{45}0.047	^{45}0.023	^{48}0.011						
233	YITU-2	^{14}0.020	^{14}0.011	^{19}0.006	^{12}0.049	^{10}0.028	^{8}0.016			
234	YITU-3	^{16}0.021	^{16}0.011	^{25}0.007	^{14}0.052	^{15}0.033	^{15}0.021			
235	YITU-4	^{5}0.012	^{5}0.007	^{6}0.004	^{5}0.027	^{5}0.017	^{4}0.011	^{20}0.936	^{29}0.913	^{51}0.880
236	YITU-5	^{7}0.013	^{7}0.007	^{11}0.005	^{7}0.032	^{6}0.023	^{10}0.017			

Table 23: **Threshold-based accuracy**. *Values are FNIR(N, T, L) with N = 1.6 million with thresholds set to produce FPIR = 0.001, 0.01, and 0.1 in non-mate searches. Columns 3-5 apply to FRVT-2018 mugshots: Columns 6-8 show the corresponding FNIR values for webcam images searched against the FRVT-2018 mugshot gallery. Finally, the three rightmost columns show FNIR for profile view images searched against the FRVT-2018 frontal gallery. Throughout blue superscripts indicate the rank of the algorithm for that column. Caution: The Power-low models are mostly intended to draw attention to the kind of behavior, not as a model to be used for prediction.*

		INVESTIGATION MODE				IDENTIFICATION MODE				FAILURE TO EXTRACT			
		RANK ONE MISS RATE, FNIR(N, 0, 1)				HIGH T → FPIR = 0.01, FNIR(N, T, L)				FEATURES			
		N=1.6M	N=1.6M	N=1.6M	N=1.1M	N=1.6M	N=1.6M	N=1.6M	N=1.1M	N=1.6M	N=1.6M	N=1.6M	N=1.1M
#	ALGORITHM	FRVT-18	WEBCAM	PROFILE	WILD	FRVT-18	WEBCAM	PROFILE	WILD^{+}	FRVT-18	WEBCAM	PROFILE	WILD
1	3DIVI-0	^{148}0.034	^{140}0.086		^{59}0.071	^{164}0.160	^{145}0.302		^{63}0.095	0.003	0.007		0.013
2	3DIVI-1	^{149}0.038			^{62}0.074	^{165}0.160			^{64}0.095	0.003			0.013
3	3DIVI-2	^{154}0.040			^{64}0.076	^{166}0.164			^{65}0.096	0.003			0.013
4	3DIVI-3	^{182}0.086	^{158}0.206		^{81}0.094	^{182}0.284	^{162}0.497		^{85}0.136	0.002	0.005		0.009
5	3DIVI-4	^{124}0.020	^{125}0.062			^{137}0.096	^{136}0.237			0.002	0.005		
6	3DIVI-5	^{125}0.020	^{124}0.062	^{89}0.930	^{32}0.052	^{136}0.095	^{135}0.234	^{84}0.990	^{42}0.069	0.002	0.005	0.442	0.004
7	3DIVI-6	^{139}0.027	^{134}0.074		^{38}0.060	^{140}0.098	^{137}0.238		^{45}0.072	0.002	0.005		0.004
8	ALCHERA-0	^{120}0.019	^{111}0.047	^{80}0.870	^{77}0.092	^{122}0.073	^{103}0.146	^{117}0.996	^{55}0.089	0.006	0.014	0.328	0.030
9	ALCHERA-1	^{230}0.987	^{194}1.000			^{229}0.999	^{199}1.000			0.006	0.013	0.324	
10	ALCHERA-2	^{183}0.097	^{155}0.166	^{113}0.954	^{84}0.098	^{185}0.304	^{156}0.442	^{137}0.999	^{84}0.135	0.001	0.002	0.106	0.012
11	ALCHERA-3	^{97}0.013	^{88}0.035	^{52}0.741	^{46}0.064	^{123}0.073	^{108}0.152	^{122}0.997	^{40}0.067	0.001	0.002	0.106	0.012
12	ALLGOVISION-000	^{107}0.014	^{84}0.033	^{82}0.894		^{101}0.048	^{93}0.106	^{69}0.982		0.002	0.003	0.122	
13	ANKE-0	^{113}0.016	^{93}0.038	^{93}0.931	^{112}0.289	^{117}0.065	^{106}0.151	^{82}0.990		0.000	0.001	0.080	0.001
14	ANKE-002	^{30}0.005	^{26}0.016	^{31}0.522		^{29}0.016	^{23}0.050	^{21}0.795		0.001	0.001	0.049	
15	ANKE-1	^{114}0.016	^{92}0.038	^{106}0.946	^{111}0.284	^{116}0.065	^{107}0.151	^{93}0.992		0.000	0.001	0.080	0.001
16	AWARE-0	^{175}0.064	^{151}0.138	^{147}0.978	^{125}0.588	^{156}0.128	^{139}0.253	^{132}0.998	^{123}0.587	0.006	0.054	0.829	0.143
17	AWARE-1	^{171}0.059		^{146}0.977	^{124}0.580	^{155}0.127		^{139}0.999	^{121}0.580	0.006		0.829	0.143
18	AWARE-2	^{172}0.060		^{145}0.977		^{152}0.120		^{125}0.998		0.006		0.829	0.143
19	AWARE-3	^{146}0.033	^{141}0.090	^{131}0.966	^{122}0.503	^{128}0.085	^{128}0.204	^{62}0.977	^{118}0.505	0.004	0.003	0.874	0.014
20	AWARE-4	^{177}0.070	^{157}0.176	^{144}0.976		^{169}0.177	^{153}0.375	^{138}0.999		0.003	0.003	0.776	
21	AWARE-5	^{147}0.034	^{127}0.067	^{148}0.978	^{123}0.509	^{131}0.088	^{111}0.163	^{140}0.999	^{119}0.508	0.001	0.002	0.189	0.002
22	AWARE-6	^{179}0.072	^{150}0.128	^{151}0.983		^{170}0.178	^{143}0.283	^{135}0.999		0.001	0.002	0.189	
23	AYONIX-0	^{222}0.452	^{187}0.685	^{162}0.996	^{120}0.400	^{217}0.725	^{183}0.892	^{114}0.995	^{122}0.586	0.010	0.031	0.939	0.068
24	AYONIX-1	^{218}0.343	^{182}0.527	^{157}0.993	^{117}0.334	^{215}0.702	^{179}0.845	^{119}0.996	^{120}0.555	0.010	0.031	0.939	0.066
25	AYONIX-2	^{217}0.343	^{183}0.527	^{156}0.993		^{216}0.702	^{178}0.845	^{118}0.996		0.010	0.031	0.939	
26	CAMVI-1	^{210}0.227	^{172}0.337	^{111}0.953	^{96}0.148	^{208}0.549	^{173}0.648	^{72}0.984	^{95}0.196	0.005	0.009	0.598	0.058
27	CAMVI-2	^{190}0.129		^{84}0.915	^{91}0.130	^{194}0.402		^{54}0.973	^{90}0.157	0.005		0.598	0.058
28	CAMVI-3	^{170}0.054	^{142}0.090	^{83}0.911	^{94}0.139	^{111}0.060	^{94}0.108	^{36}0.940	^{77}0.130	0.006	0.013	0.675	0.074
29	CAMVI-4	^{167}0.049	^{136}0.077	^{54}0.744	^{136}1.000	^{107}0.056	^{81}0.100	^{126}0.998	^{134}1.000	0.000	0.000	0.000	0.000
30	CAMVI-5	^{176}0.067	^{146}0.103	^{55}0.746	^{162}1.000	^{127}0.078	^{100}0.132	^{133}0.998	^{161}1.000	0.000	0.000	0.000	0.001
31	COGENT-0	^{99}0.013	^{109}0.046	^{128}0.965	^{78}0.093	^{75}0.032	^{85}0.100	^{91}0.991	^{72}0.110	0.000	0.000	0.000	0.000
32	COGENT-1	^{98}0.013	^{108}0.046	^{127}0.965		^{74}0.032	^{84}0.100	^{90}0.991		0.000	0.000	0.000	
33	COGENT-2	^{40}0.006	^{46}0.020	^{87}0.925	^{21}0.045	^{34}0.020	^{41}0.063	^{98}0.994	^{23}0.051	0.000	0.000	0.000	0.000
34	COGENT-3	^{42}0.006	^{53}0.021	^{104}0.939	^{33}0.053	^{32}0.018	^{39}0.061	^{112}0.995	^{32}0.063	0.000	0.000	0.000	0.000
35	COGNITEC-0	^{142}0.028	^{120}0.059	^{123}0.964		^{138}0.098	^{126}0.200	^{48}0.971		0.003	0.002	0.924	
36	COGNITEC-1	^{109}0.014	^{86}0.034	^{117}0.958	^{61}0.074	^{105}0.055	^{102}0.135	^{43}0.965	^{46}0.072	0.003	0.002	0.924	0.025
37	COGNITEC-2	^{64}0.008	^{72}0.025	^{108}0.949	^{50}0.065	^{65}0.027	^{88}0.101	^{40}0.956	^{28}0.061	0.003	0.002	0.924	0.021
38	COGNITEC-3	^{67}0.009	^{71}0.025	^{92}0.930	^{29}0.051	^{67}0.028	^{82}0.100	^{37}0.946	^{19}0.049	0.004	0.002	0.878	0.012
39	CYBERLINK-000	^{45}0.007	^{45}0.020	^{50}0.717		^{56}0.025	^{53}0.070	^{68}0.981		0.001	0.001	0.063	
40	CYBERLINK-001	^{41}0.006	^{35}0.018	^{51}0.731		^{54}0.025	^{48}0.067	^{71}0.984		0.000	0.000	0.040	
41	DAHUA-0	^{89}0.012	^{74}0.026			^{97}0.047	^{70}0.083			0.004	0.003		
42	DAHUA-002	^{19}0.004	^{11}0.012	^{12}0.304		^{10}0.009	^{11}0.029	^{9}0.522		0.001	0.000	0.099	
43	DAHUA-1	^{69}0.009	^{66}0.024	^{49}0.703	^{4}0.038	^{84}0.039	^{62}0.075	^{33}0.933	^{8}0.043	0.002	0.002	0.346	0.001
44	DEEPGLINT-001		^{192}0.909	^{64}0.796			^{207}1.000	^{201}1.000		0.000	0.000	0.038	
45	DEEPSEA-001	^{52}0.007	^{24}0.016	^{72}0.814		^{51}0.024	^{35}0.059	^{55}0.973		0.000	0.001	0.047	
46	DERMALOG-0	^{191}0.131	^{162}0.218	^{91}0.930	^{63}0.075	^{189}0.364	^{168}0.528	^{85}0.991	^{69}0.104	0.003	0.002	0.133	0.020
47	DERMALOG-1	^{194}0.156		^{105}0.941	^{75}0.089	^{195}0.405		^{70}0.983	^{81}0.131	0.003		0.133	0.020
48	DERMALOG-2	^{192}0.138		^{94}0.933	^{66}0.076	^{191}0.378		^{66}0.981	^{70}0.105	0.003		0.133	0.020
49	DERMALOG-3	^{188}0.128	^{161}0.217			^{188}0.362	^{167}0.526			0.002	0.002	0.103	
50	DERMALOG-4	^{187}0.127	^{160}0.215	^{90}0.930	^{53}0.066	^{187}0.360	^{165}0.526	^{92}0.991	^{61}0.095	0.001	0.002	0.107	0.013
51	DERMALOG-5	^{117}0.017	^{91}0.037	^{48}0.701	^{52}0.066	^{90}0.045	^{79}0.096	^{39}0.950	^{38}0.066	0.001	0.002	0.102	0.013
52	DERMALOG-6	^{79}0.010	^{70}0.024	^{41}0.619	^{35}0.056	^{68}0.028	^{46}0.067	^{34}0.933	^{26}0.054	0.003	0.006	0.181	0.014
53	EVERAI-0	^{127}0.021	^{95}0.038	^{33}0.534		^{100}0.047	^{83}0.100	^{121}0.997		0.000	0.000	0.000	
54	EVERAI-1	^{31}0.006	^{47}0.020	^{14}0.329	^{129}0.928	^{44}0.023	^{58}0.074	^{99}0.994	^{127}0.927	0.000	0.000	0.000	0.000
55	EVERAI-2	^{33}0.006	^{55}0.022	^{16}0.335	^{113}0.302	^{53}0.025	^{63}0.076	^{19}0.748	^{108}0.308	0.000	0.000	0.032	0.001
56	EVERAI-3	^{21}0.005	^{41}0.019	^{10}0.252	^{5}0.038	^{31}0.018	^{36}0.060	^{14}0.733	^{11}0.044	0.000	0.000	0.032	0.001
57	EVERAI-PARAVISION-004	^{15}0.004	^{8}0.010	^{2}0.104		^{6}0.007	^{8}0.024	^{23}0.797		0.000	0.000	0.032	
58	EYEDEA-0	^{215}0.300	^{177}0.443	^{142}0.974	^{92}0.131	^{214}0.679	^{176}0.783	^{88}0.991	^{103}0.249	0.001	0.003	0.161	0.008
59	EYEDEA-1	^{203}0.198		^{99}0.937	^{60}0.072	^{199}0.480		^{102}0.994	^{80}0.131	0.001		0.161	0.008
60	EYEDEA-2	^{204}0.200		^{95}0.934	^{57}0.070	^{202}0.490		^{116}0.996	^{78}0.130	0.000		0.079	0.005
61	EYEDEA-3	^{181}0.082	^{153}0.148	^{121}0.960	^{48}0.064	^{180}0.267	^{155}0.404	^{81}0.990	^{56}0.091	0.001	0.003	0.161	0.008
62	F8-001	^{110}0.015		^{45}0.669		^{82}0.038		^{115}0.995		0.004	1.000	0.158	
63	GLORY-0	^{199}0.180	^{169}0.320	^{160}0.994		^{184}0.297	^{159}0.470	^{96}0.993		0.011	0.013	0.985	
64	GLORY-1	^{189}0.129	^{166}0.267	^{155}0.992	^{114}0.315	^{177}0.238	^{157}0.448	^{87}0.991	^{110}0.353	0.011	0.013	0.988	0.114
65	GORILLA-0				^{133}0.994				^{131}0.994	0.001		0.069	0.008
66	GORILLA-004	^{70}0.009	^{67}0.024	^{47}0.697		^{91}0.046	^{86}0.101	^{28}0.903		0.000	0.001	0.042	
67	GORILLA-1	^{173}0.063	^{143}0.095	^{98}0.936	^{37}0.057	^{178}0.248	^{147}0.314	^{153}1.000	^{48}0.076	0.001	0.001	0.069	0.007
68	GORILLA-2	^{128}0.022	^{105}0.044	^{56}0.753	^{19}0.045	^{144}0.108	^{117}0.170	^{97}0.993	^{20}0.049	0.001	0.001	0.069	0.006
69	GORILLA-3	^{151}0.038	^{130}0.070	^{73}0.821	^{56}0.069	^{163}0.160	^{138}0.247	^{148}1.000	^{51}0.080	0.001	0.001	0.069	0.007
70	HBINNO-0	^{214}0.275		^{154}0.990	^{118}0.335	^{212}0.632		^{145}1.000	^{112}0.411	0.007		0.288	0.151
71	HIK-0	^{135}0.024	^{83}0.033	^{115}0.957	^{97}0.153	^{121}0.070	^{90}0.103	^{49}0.971	^{89}0.155	0.010	0.004	0.896	0.027
72	HIK-1	^{119}0.017		^{110}0.952	^{101}0.162	^{119}0.067		^{67}0.981	^{92}0.166	0.003		0.791	0.013

Table 24: **Miss rates by dataset:** *At left, rank 1 miss rates relevant to investigations; at right, with threshold set to target FPIR = 0.01 for higher volume, low prior, uses. $^{+}$For the WILD set, FPIR = 0.1 Yellow indicates most accurate algorithm. Throughout blue superscripts indicate the rank of the algorithm for that column.*

		INVESTIGATION MODE				IDENTIFICATION MODE				FAILURE TO EXTRACT			
		RANK ONE MISS RATE, FNIR(N, 0, 1)				HIGH T $\rightarrow$ FPIR = 0.01, FNIR(N, T, L)				FEATURES			
		N=1.6M	N=1.6M	N=1.6M	N=1.1M	N=1.6M	N=1.6M	N=1.6M	N=1.1M	N=1.6M	N=1.6M	N=1.6M	N=1.1M
#	ALGORITHM	FRVT-18	WEBCAM	PROFILE	WILD	FRVT-18	WEBCAM	PROFILE	WILD$^+$	FRVT-18	WEBCAM	PROFILE	WILD
73	HIK-2	[118]0.017		[78]0.857	[83]0.094	[120]0.067		[73]0.985	[68]0.103	0.001		0.058	0.008
74	HIK-3	[108]0.014	[76]0.027	[46]0.689		[110]0.060	[91]0.105	[31]0.925		0.000	0.000	0.048	
75	HIK-4	[105]0.014	[75]0.027	[53]0.743	[42]0.062	[108]0.056	[87]0.101	[38]0.947	[47]0.075	0.000	0.000	0.048	0.008
76	HIK-5	[47]0.007	[28]0.017	[34]0.535		[39]0.022	[22]0.048	[128]0.998		0.000	0.000	0.000	0.001
77	HIK-6	[48]0.007	[27]0.017	[35]0.535	[135]1.000	[43]0.022	[26]0.052	[141]0.999	[133]1.000	0.000	0.000	0.000	0.001
78	IDEMIA-0	[86]0.011	[87]0.034	[96]0.935	[104]0.166	[113]0.062	[109]0.156	[74]0.986	[107]0.288	0.003	0.000	0.172	0.002
79	IDEMIA-007	[27]0.005	[21]0.015	[197]1.000		[15]0.011	[14]0.033	[194]1.000		0.000	0.000	0.040	
80	IDEMIA-1	[90]0.012		[100]0.937	[99]0.157	[73]0.031		[42]0.964	[97]0.205	0.003		0.172	0.002
81	IDEMIA-2	[96]0.013		[114]0.956	[107]0.198	[76]0.032		[44]0.965	[100]0.242	0.005		0.906	0.031
82	IDEMIA-3	[77]0.010	[85]0.034	[116]0.958		[49]0.024	[65]0.079	[219]1.000		0.000	0.000	0.041	
83	IDEMIA-4	[73]0.009	[82]0.032	[107]0.947	[27]0.051	[48]0.024	[64]0.079	[45]0.968	[35]0.064	0.000	0.000	0.041	0.003
84	IDEMIA-5	[83]0.011	[98]0.039	[112]0.954	[16]0.044	[69]0.028	[89]0.102	[53]0.973	[27]0.055	0.000	0.000	0.041	0.000
85	IDEMIA-6	[94]0.012	[132]0.072	[134]0.969	[31]0.052	[66]0.028	[110]0.161	[65]0.980	[39]0.067	0.000	0.000	0.041	0.000
86	IIT-002		[174]0.359	[23]0.438			[154]0.382	[17]0.743		0.001	0.005	0.051	
87	IMAGUS-0	[216]0.305	[179]0.482	[161]0.994	[109]0.222	[211]0.608	[175]0.779	[143]1.000	[109]0.311	0.009	0.013	0.727	0.049
88	IMAGUS-2	[208]0.222	[167]0.301	[153]0.988	[98]0.154	[209]0.566	[172]0.645	[149]1.000	[105]0.252	0.004	0.008	0.550	0.023
89	IMAGUS-3	[219]0.358	[180]0.513	[158]0.993		[213]0.670	[177]0.809	[146]1.000		0.004	0.008	0.550	
90	IMPERIAL-000	[26]0.005	[18]0.015	[11]0.280		[19]0.012	[18]0.041	[103]0.995		0.000	0.000	0.000	
91	INCODE-0	[169]0.051	[145]0.100	[109]0.951		[174]0.201	[146]0.304	[100]0.994		0.001	0.004	0.173	
92	INCODE-004	[39]0.006	[33]0.017	[26]0.475		[59]0.026	[54]0.070	[32]0.929		0.000	0.001	0.066	
93	INCODE-1	[121]0.019	[110]0.046	[57]0.762	[30]0.052	[145]0.114	[124]0.198	[144]1.000	[30]0.062	0.001	0.004	0.173	0.009
94	INCODE-2	[126]0.020	[112]0.048	[74]0.843	[8]0.039	[142]0.102	[119]0.176	[61]0.976	[13]0.045	0.000	0.001	0.066	0.001
95	INCODE-3	[112]0.015	[100]0.040	[58]0.764	[10]0.039	[129]0.086	[113]0.164	[120]0.996	[12]0.044	0.000	0.001	0.066	0.001
96	INNOVATRICS-0	[157]0.042	[135]0.076	[125]0.964	[105]0.188	[168]0.165	[140]0.258	[60]0.975	[101]0.245	0.002	0.008	0.592	0.093
97	INNOVATRICS-1	[156]0.042		[124]0.964	[106]0.193	[167]0.165		[59]0.975	[99]0.221	0.002		0.592	0.093
98	INNOVATRICS-2	[166]0.048	[133]0.074	[77]0.853		[162]0.142	[130]0.209	[142]0.999		0.000	0.001	0.046	
99	INNOVATRICS-3	[143]0.029	[115]0.055	[76]0.845	[58]0.071	[158]0.134	[127]0.203	[131]0.998	[52]0.081	0.000	0.001	0.046	0.007
100	INNOVATRICS-4	[111]0.015	[101]0.040	[118]0.958	[55]0.067	[126]0.076	[104]0.149	[51]0.973	[43]0.071	0.000	0.001	0.046	0.013
101	INTSYSMSU-000	[193]0.148	[65]0.023	[37]0.562		[227]0.990	[188]0.998	[127]0.998		0.000	0.000	0.050	
102	ISYSTEMS-0	[102]0.014	[97]0.038	[136]0.969	[103]0.163	[96]0.047	[95]0.110	[80]0.989	[94]0.169	0.003	0.013	0.529	0.065
103	ISYSTEMS-1	[101]0.014		[135]0.969	[102]0.162	[94]0.047		[79]0.989	[93]0.169	0.003		0.529	0.065
104	ISYSTEMS-2	[66]0.009	[73]0.026	[75]0.844	[24]0.049	[80]0.035	[67]0.080	[95]0.993	[22]0.051	0.002	0.002	0.142	0.009
105	ISYSTEMS-3	[57]0.007	[63]0.023	[61]0.791	[15]0.043	[63]0.027	[50]0.068	[124]0.997	[10]0.044	0.002	0.002	0.142	0.003
106	KEDACOM-001	[81]0.010	[89]0.036	[139]0.972		[28]0.016	[28]0.054	[56]0.973		0.000	0.000	0.000	
107	LOOKMAN-005	[84]0.011	[90]0.036	[140]0.972		[33]0.020	[42]0.063	[52]0.973		0.000	0.000	0.000	
108	LOOKMAN-3	[87]0.011	[96]0.038		[203]1.000	[64]0.027	[68]0.082			0.000	0.000		0.000
109	LOOKMAN-4	[91]0.012	[99]0.039	[141]0.973	[206]1.000	[62]0.027	[60]0.075	[57]0.974		0.000	0.000	0.000	0.000
110	MEGVII-0	[74]0.009	[31]0.017		[41]0.061	[109]0.058	[47]0.067		[60]0.094	0.000	0.000		0.005
111	MEGVII-1	[103]0.014	[32]0.017			[83]0.039	[37]0.061			0.002	0.000		
112	MEGVII-2	[104]0.014	[34]0.017	[24]0.450		[85]0.039	[34]0.059	[27]0.872		0.002	0.000	0.033	
113	MICROFOCUS-0	[226]0.597	[191]0.782		[115]0.316	[222]0.867	[186]0.950		[115]0.434	0.005	0.030		0.065
114	MICROFOCUS-1	[227]0.597			[116]0.316	[223]0.867			[116]0.434	0.005			0.065
115	MICROFOCUS-2	[228]0.627			[119]0.342	[224]0.870			[117]0.447	0.005			0.065
116	MICROFOCUS-3	[225]0.595	[190]0.781		[110]0.279	[221]0.866	[185]0.948		[113]0.412	0.001	0.005		0.014
117	MICROFOCUS-4	[224]0.577	[189]0.758			[230]0.999	[184]0.940			0.001	0.005		
118	MICROFOCUS-5	[220]0.426	[186]0.601		[100]0.158	[219]0.736	[181]0.865		[106]0.261	0.001	0.005		0.011
119	MICROFOCUS-6	[221]0.428	[185]0.583		[95]0.146	[225]0.963	[180]0.858		[102]0.246	0.001	0.005		0.011
120	MICROSOFT-0	[34]0.006	[49]0.021		[49]0.065	[38]0.022	[55]0.071		[37]0.065	0.000	0.001		0.019
121	MICROSOFT-1	[32]0.006			[44]0.062	[40]0.022			[29]0.061	0.000			0.019
122	MICROSOFT-2	[38]0.006			[45]0.063	[58]0.026			[34]0.063	0.000			0.019
123	MICROSOFT-3	[4]0.003	[13]0.012			[25]0.014	[32]0.056			0.000	0.001		
124	MICROSOFT-4	[2]0.003	[12]0.012		[9]0.039	[24]0.013	[27]0.053		[9]0.043	0.000	0.001		0.004
125	MICROSOFT-5	[5]0.003	[9]0.011	[4]0.144	[2]0.033	[21]0.012	[19]0.041	[5]0.354	[4]0.041	0.000	0.001	0.049	0.000
126	MICROSOFT-6	[8]0.003	[10]0.011	[6]0.150		[8]0.008	[9]0.024	[2]0.281		0.000	0.001	0.049	
127	NEC-0	[122]0.020	[103]0.041	[120]0.959	[134]0.999	[102]0.049	[75]0.093	[47]0.969	[132]0.999	0.001	0.002	0.890	0.064
128	NEC-1	[134]0.024	[116]0.056	[133]0.967		[115]0.063	[101]0.133	[50]0.972		0.005	0.003	0.934	
129	NEC-2	[1]0.003	[3]0.009	[20]0.363	[80]0.093	[1]0.004	[3]0.013	[106]0.995	[71]0.107	0.000	0.001	0.041	0.025
130	NEC-3	[3]0.003	[6]0.010	[19]0.352	[74]0.088	[2]0.004	[2]0.013	[10]0.628	[58]0.092	0.000	0.001	0.041	0.025
131	NEUROTECHNOLOGY-0	[168]0.050	[147]0.104	[138]0.972	[137]1.000	[173]0.196	[148]0.317	[113]0.995	[135]1.000	0.004	0.022	0.822	0.091
132	NEUROTECHNOLOGY-007	[44]0.007	[52]0.021	[65]0.796		[50]0.024	[49]0.068	[123]0.997		0.001	0.001	0.041	
133	NEUROTECHNOLOGY-1	[165]0.047		[130]0.966	[130]0.954	[172]0.195		[108]0.995	[128]0.953	0.001		0.281	0.028
134	NEUROTECHNOLOGY-2	[164]0.047		[129]0.966	[131]0.983	[171]0.195		[111]0.995	[129]0.983	0.001		0.233	0.028
135	NEUROTECHNOLOGY-3	[137]0.025	[104]0.042	[122]0.961		[141]0.101	[112]0.164	[221]1.000		0.000	0.001	0.131	
136	NEUROTECHNOLOGY-4	[62]0.008	[44]0.020	[137]0.970	[76]0.090	[71]0.030	[56]0.073	[83]0.990	[74]0.122	0.000	0.001	0.131	0.007
137	NEUROTECHNOLOGY-5	[49]0.007	[69]0.024	[81]0.893	[121]0.408	[55]0.025	[59]0.074	[78]0.989	[114]0.415	0.000	0.000	0.030	0.000
138	NEUROTECHNOLOGY-6	[123]0.020	[107]0.045	[40]0.606	[25]0.050	[153]0.124	[129]0.206		[36]0.065	0.000	0.000		0.001
139	NEWLAND-2	[180]0.081	[148]0.117	[97]0.936		[183]0.296	[150]0.335	[130]0.998		0.007	0.012	0.200	
140	NOBLIS-1	[212]0.251	[181]0.522	[159]0.993	[127]0.734	[228]0.992	[231]1.000	[158]1.000	[124]0.744	0.000	0.000	0.000	0.000
141	NOBLIS-2	[200]0.182	[176]0.392	[150]0.982		[203]0.490	[196]1.000	[154]1.000		0.000	0.000	0.000	
142	NTECHLAB-0	[88]0.012	[81]0.031	[39]0.595	[12]0.041	[99]0.047	[92]0.105	[25]0.826	[7]0.043	0.000	0.001	0.043	0.005
143	NTECHLAB-007	[28]0.005	[14]0.012	[13]0.326		[27]0.015	[17]0.041	[12]0.642		0.000	0.000	0.042	
144	NTECHLAB-008	[16]0.004	[4]0.010	[7]0.157		[12]0.009	[12]0.029	[6]0.391		0.000	0.000	0.044	

Table 25: **Miss rates by dataset:** *At left, rank 1 miss rates relevant to investigations; at right, with threshold set to target FPIR = 0.01 for higher volume, low prior, uses. $^+$For the WILD set, FPIR = 0.1 Yellow indicates most accurate algorithm. Throughout blue superscripts indicate the rank of the algorithm for that column.*

		INVESTIGATION MODE RANK ONE MISS RATE, FNIR(N, 0, 1)				IDENTIFICATION MODE HIGH T → FPIR = 0.01, FNIR(N, T, L)				FAILURE TO EXTRACT FEATURES			
		N=1.6M	N=1.6M	N=1.6M	N=1.1M	N=1.6M	N=1.6M	N=1.6M	N=1.1M	N=1.6M	N=1.6M	N=1.6M	N=1.1M
#	ALGORITHM	FRVT-18	WEBCAM	PROFILE	WILD	FRVT-18	WEBCAM	PROFILE	WILD+	FRVT-18	WEBCAM	PROFILE	WILD
145	NTECHLAB-1	[106] 0.014		[42] 0.630	[20] 0.045	[106] 0.056		[26] 0.842	[21] 0.049	0.000		0.043	0.005
146	NTECHLAB-3	[63] 0.008	[60] 0.023	[27] 0.504		[72] 0.030	[61] 0.075	[20] 0.752		0.000	0.000	0.040	
147	NTECHLAB-4	[51] 0.007	[40] 0.019	[28] 0.506	[14] 0.043	[46] 0.024	[45] 0.065	[18] 0.746	[18] 0.048	0.000	0.000	0.040	0.003
148	NTECHLAB-5	[43] 0.006	[36] 0.018	[21] 0.367	[7] 0.038	[47] 0.024	[43] 0.063	[13] 0.661	[6] 0.042	0.000	0.000	0.040	0.000
149	NTECHLAB-6	[35] 0.006	[30] 0.017	[18] 0.347	[6] 0.038	[36] 0.021	[33] 0.059	[11] 0.635	[5] 0.042	0.000	0.000	0.040	0.000
150	PARAVISION-005	[14] 0.004	[5] 0.010	[1] 0.079		[4] 0.005	[4] 0.016	[1] 0.181		0.000	0.000	0.038	
151	PIXELALL-002	[54] 0.007	[57] 0.022	[70] 0.810		[77] 0.032	[69] 0.083	[150] 1.000		0.000	0.000	0.000	
152	PIXELALL-003	[23] 0.005	[16] 0.014	[30] 0.515		[17] 0.012	[21] 0.043	[129] 0.998		0.000	0.000	0.000	
153	QUANTASOFT-1	[207] 0.220	[188] 0.727		[126] 0.620	[205] 0.494			[125] 0.760	0.000	0.000		0.000
154	RANKONE-0	[163] 0.045	[149] 0.117		[89] 0.114	[157] 0.129	[144] 0.291		[91] 0.161	0.000	0.000		0.000
155	RANKONE-006	[61] 0.008		[67] 0.797		[41] 0.022		[35] 0.937		0.002		0.167	
156	RANKONE-007	[36] 0.006	[39] 0.019	[63] 0.796		[26] 0.014	[38] 0.061	[30] 0.924		0.001	0.001	0.102	
157	RANKONE-1	[136] 0.025			[68] 0.077	[130] 0.087			[67] 0.102	0.000			0.000
158	RANKONE-2	[130] 0.022	[131] 0.071			[125] 0.073	[123] 0.190			0.000	0.000		
159	RANKONE-3	[129] 0.022	[128] 0.068		[69] 0.078	[124] 0.073	[121] 0.187		[62] 0.095	0.000	0.000		0.000
160	RANKONE-4	[162] 0.044	[152] 0.141		[82] 0.094	[154] 0.126	[149] 0.324		[75] 0.126	0.000	0.000		0.000
161	RANKONE-5	[93] 0.012	[102] 0.041	[152] 0.986	[39] 0.061	[81] 0.036	[97] 0.119	[101] 0.994	[41] 0.068	0.000	0.000	0.489	0.000
162	REALNETWORKS-0	[161] 0.043	[139] 0.078		[65] 0.076	[161] 0.140	[132] 0.209		[53] 0.084	0.001	0.000		0.004
163	REALNETWORKS-003	[140] 0.027	[123] 0.062	[60] 0.771		[133] 0.093	[118] 0.172	[75] 0.987		0.001	0.000	0.009	
164	REALNETWORKS-004	[138] 0.026	[119] 0.059	[66] 0.797		[132] 0.092	[115] 0.169	[94] 0.992		0.001	0.000	0.009	
165	REALNETWORKS-1	[160] 0.043	[138] 0.078			[160] 0.140	[131] 0.209			0.001	0.000		
166	REALNETWORKS-2	[155] 0.042	[137] 0.078		[132] 0.992	[159] 0.139	[133] 0.209		[130] 0.992	0.001	0.000		0.000
167	REMARKAI-0	[85] 0.011	[80] 0.030			[114] 0.062	[99] 0.123			0.000	0.001		
168	REMARKAI-000	[37] 0.006	[37] 0.018	[44] 0.660		[57] 0.025	[52] 0.070	[105] 0.995		0.000	0.000	0.000	
169	REMARKAI-2	[82] 0.010	[78] 0.029	[68] 0.802	[23] 0.046	[112] 0.061	[98] 0.122	[64] 0.980	[25] 0.052	0.000	0.001	0.017	0.000
170	SCANOVATE-000	[60] 0.008	[106] 0.045	[36] 0.560		[78] 0.033	[105] 0.150	[24] 0.803		0.000	0.001	0.057	
171	SENSETIME-0	[22] 0.005	[23] 0.016	[32] 0.528		[18] 0.012	[16] 0.040	[76] 0.988		0.004	0.000	0.042	0.000
172	SENSETIME-002	[115] 0.016	[42] 0.020	[22] 0.384		[30] 0.017	[7] 0.023	[63] 0.979		0.009	0.000	0.040	
173	SENSETIME-003	[9] 0.004	[1] 0.007	[5] 0.150		[3] 0.004	[1] 0.009	[3] 0.311		0.000	0.000	0.041	
174	SENSETIME-1	[24] 0.005	[22] 0.016		[3] 0.038	[20] 0.012	[20] 0.041		[1] -0.796	0.004	0.000		0.000
175	SHAMAN-0	[196] 0.171	[165] 0.262		[90] 0.115	[190] 0.370	[163] 0.507		[86] 0.146	0.020	0.011		0.043
176	SHAMAN-1	[197] 0.172			[88] 0.113	[196] 0.406			[88] 0.153	0.020			0.043
177	SHAMAN-2	[213] 0.262			[93] 0.132	[210] 0.582			[96] 0.201	0.020			0.043
178	SHAMAN-3	[185] 0.127	[156] 0.172		[86] 0.109	[186] 0.348	[160] 0.472		[82] 0.132	0.020	0.011		0.043
179	SHAMAN-4	[209] 0.224	[168] 0.319			[201] 0.490	[171] 0.639			0.020	0.011		
180	SHAMAN-6	[159] 0.042	[118] 0.058	[103] 0.938		[135] 0.095	[114] 0.168	[41] 0.960		0.020	0.011	0.869	
181	SHAMAN-7	[158] 0.042	[117] 0.057		[70] 0.078	[134] 0.094	[116] 0.169		[50] 0.079	0.020	0.010		0.029
182	SIAT-0	[78] 0.010	[51] 0.021		[71] 0.078	[95] 0.047	[44] 0.064		[104] 0.250	0.000	0.000		0.008
183	SIAT-1	[11] 0.004	[171] 0.333		[11] 0.040	[11] 0.009	[151] 0.348		[3] 0.041	0.000	0.000		0.003
184	SIAT-2	[12] 0.004	[178] 0.446			[13] 0.009	[158] 0.460			0.000	0.000		
185	SMILART-0	[201] 0.193	[170] 0.325		[221] 1.000	[200] 0.486			[221] 1.000	0.008			0.121
186	SMILART-1	[206] 0.219			[157] 1.000	[207] 0.505			[156] 1.000	0.021			0.006
187	SMILART-2	[202] 0.195			[146] 1.000	[204] 0.492			[145] 1.000	0.000			0.048
188	SMILART-4	[229] 0.965	[193] 0.974		[128] 0.834	[226] 0.965	[187] 0.973		[126] 0.833	0.011	0.013		0.039
189	SMILART-5									0.011	0.013		
190	SYNESIS-0	[195] 0.162	[175] 0.361			[192] 0.378	[170] 0.598			0.002	0.009		0.081
191	SYNESIS-3	[198] 0.172	[163] 0.235			[198] 0.444	[164] 0.524			0.006	0.015		0.042
192	TECH5-001	[46] 0.007	[29] 0.017	[38] 0.584		[35] 0.021	[31] 0.055	[147] 1.000		0.000	0.000	0.006	
193	TEVIAN-0	[132] 0.022	[126] 0.066		[34] 0.054	[147] 0.114	[134] 0.227		[44] 0.072	0.002	0.005		0.007
194	TEVIAN-1	[133] 0.022			[43] 0.062	[148] 0.114			[49] 0.078	0.002			0.007
195	TEVIAN-2	[131] 0.022			[79] 0.093	[146] 0.114			[73] 0.118	0.002			0.008
196	TEVIAN-3	[116] 0.017	[113] 0.052			[139] 0.098	[125] 0.198			0.001	0.002		
197	TEVIAN-4	[100] 0.013	[94] 0.038		[26] 0.050	[118] 0.066	[96] 0.115		[33] 0.063	0.001	0.002		0.005
198	TEVIAN-5	[71] 0.009	[77] 0.028	[25] 0.467		[98] 0.047	[72] 0.089	[22] 0.796		0.001	0.002	0.116	
199	TIGER-0	[174] 0.064	[144] 0.095		[209] 1.000	[179] 0.263	[152] 0.366		[208] 1.000	0.000	0.000		0.005
200	TIGER-1		[173] 0.351				[161] 0.487			0.000	0.000		
201	TIGER-2	[59] 0.008	[62] 0.023	[29] 0.514		[87] 0.042	[78] 0.095	[58] 0.975		0.000	0.000	0.056	
202	TIGER-3	[58] 0.008	[61] 0.023			[88] 0.042	[77] 0.095			0.000	0.000		
203	TONGYITRANS-0	[76] 0.010	[59] 0.022			[86] 0.041	[51] 0.069			0.003	0.001		
204	TONGYITRANS-1	[75] 0.010	[58] 0.022		[87] 0.112	[79] 0.035	[40] 0.062		[83] 0.134	0.003	0.001		0.009
205	TOSHIBA-0	[50] 0.007	[54] 0.022	[59] 0.766		[70] 0.029	[57] 0.074	[77] 0.988		0.000	0.000	0.070	0.002
206	TOSHIBA-1	[53] 0.007	[56] 0.022			[37] 0.021	[29] 0.054			0.000	0.000		
207	VD-0	[223] 0.475	[184] 0.551		[108] 0.217	[220] 0.828	[182] 0.871		[111] 0.362	0.011	0.013		0.026
208	VD-1	[145] 0.030	[114] 0.053			[151] 0.118	[122] 0.188			0.005	0.001		0.017
209	VIGILANTSOLUTIONS-0	[184] 0.125	[159] 0.212	[149] 0.980	[67] 0.076	[193] 0.394	[169] 0.557	[104] 0.995	[87] 0.152	0.000	0.001	0.127	0.003
210	VIGILANTSOLUTIONS-1	[205] 0.204		[143] 0.975	[85] 0.103	[206] 0.502		[134] 0.998	[98] 0.209	0.000		0.127	0.003
211	VIGILANTSOLUTIONS-2	[211] 0.239		[132] 0.966	[47] 0.064	[218] 0.731		[109] 0.995	[76] 0.129	0.000		0.127	0.003
212	VIGILANTSOLUTIONS-3	[178] 0.072	[154] 0.151	[119] 0.958	[51] 0.065	[181] 0.283	[166] 0.526	[107] 0.995	[79] 0.131	0.000	0.001	0.127	0.003
213	VIGILANTSOLUTIONS-4	[186] 0.127	[164] 0.244	[126] 0.965		[197] 0.424	[174] 0.709	[89] 0.991		0.000	0.001	0.127	
214	VIGILANTSOLUTIONS-5	[92] 0.012		[85] 0.920		[89] 0.045		[155] 1.000		0.000	0.001	0.127	
215	VIGILANTSOLUTIONS-6	[95] 0.013		[86] 0.921		[92] 0.046		[156] 1.000		0.000	0.001	0.127	
216	VISIONLABS-008	[20] 0.005	[15] 0.014	[3] 0.141		[9] 0.008	[13] 0.032	[4] 0.317		0.001	0.000	0.075	

Table 26: **Miss rates by dataset:** *At left, rank 1 miss rates relevant to investigations; at right, with threshold set to target FPIR = 0.01 for higher volume, low prior, uses. +For the WILD set, FPIR = 0.1 Yellow indicates most accurate algorithm. Throughout blue superscripts indicate the rank of the algorithm for that column.*

FNIR(N, R, T) =	False neg. identification rate	N = Num. enrolled subjects	T = Threshold	T = 0 → Investigation
FPIR(N, T) =	False pos. identification rate	R = Num. candidates examined		T > 0 → Identification

		INVESTIGATION MODE				IDENTIFICATION MODE				FAILURE TO EXTRACT			
		RANK ONE MISS RATE, FNIR(N, 0, 1)				HIGH T $\longrightarrow$ FPIR = 0.01, FNIR(N, T, L)				FEATURES			
		N=1.6M	N=1.6M	N=1.6M	N=1.1M	N=1.6M	N=1.6M	N=1.6M	N=1.1M	N=1.6M	N=1.6M	N=1.6M	N=1.1M
#	ALGORITHM	FRVT-18	WEBCAM	PROFILE	WILD	FRVT-18	WEBCAM	PROFILE	WILD^{+}	FRVT-18	WEBCAM	PROFILE	WILD
217	VISIONLABS-3	^{68}0.009	^{79}0.030	^{43}0.640	^{28}0.051	^{60}0.026	^{73}0.091	^{110}0.995	^{15}0.046	0.002	0.003	0.181	0.014
218	VISIONLABS-4	^{17}0.004	^{43}0.020	^{17}0.343		^{61}0.026	^{80}0.097	^{16}0.742		0.001	0.001	0.046	
219	VISIONLABS-5	^{13}0.004	^{38}0.019	^{15}0.334	^{13}0.043	^{42}0.022	^{71}0.087	^{15}0.736	^{16}0.046	0.001	0.001	0.046	0.006
220	VISIONLABS-6	^{7}0.003	^{20}0.015	^{9}0.211		^{23}0.012	^{25}0.051	^{8}0.511		0.001	0.001	0.051	
221	VISIONLABS-7	^{6}0.003	^{19}0.015	^{8}0.211	^{1}0.033	^{22}0.012	^{24}0.051	^{7}0.511	^{2}0.035	0.001	0.001	0.051	0.001
222	VOCORD-0	^{153}0.040	^{129}0.068	^{102}0.937		^{150}0.116	^{120}0.181	^{152}1.000		0.015	0.025	0.164	0.019
223	VOCORD-1	^{152}0.040		^{101}0.937		^{149}0.116		^{151}1.000		0.015		0.192	0.018
224	VOCORD-2	^{150}0.038		^{88}0.929		^{143}0.107		^{157}1.000		0.015		0.194	0.015
225	VOCORD-3	^{65}0.008	^{68}0.024	^{69}0.804	^{36}0.057	^{103}0.050	^{76}0.093	^{86}0.991	^{31}0.062	0.001	0.011	0.425	0.006
226	VOCORD-4	^{80}0.010	^{50}0.021	^{62}0.792		^{104}0.054	^{74}0.093	^{136}0.999		0.000	0.000	0.000	
227	VOCORD-5	^{72}0.009	^{64}0.023	^{71}0.812	^{17}0.044	^{93}0.046	^{66}0.080	^{46}0.968	^{14}0.045	0.001	0.009	0.554	0.003
228	VOCORD-6	^{236}1.000	^{233}1.000	^{232}1.000		^{236}1.000	^{233}1.000	^{232}1.000		0.001	0.009	0.554	
229	YISHENG-0	^{141}0.027	^{121}0.060		^{54}0.067	^{176}0.209	^{142}0.275		^{66}0.100	0.002	0.005		0.014
230	YISHENG-1	^{144}0.029	^{122}0.060		^{40}0.061	^{175}0.208	^{141}0.269		^{54}0.087	0.002	0.005		0.014
231	YITU-0	^{56}0.007	^{48}0.020		^{73}0.086	^{52}0.025	^{30}0.054		^{59}0.094	0.003	0.001		0.026
232	YITU-1	^{55}0.007			^{72}0.086	^{45}0.023			^{57}0.092	0.003			0.026
233	YITU-2	^{18}0.004	^{7}0.010		^{22}0.046	^{14}0.011	^{10}0.028		^{24}0.051	0.000	0.000		0.000
234	YITU-3	^{29}0.005	^{25}0.016			^{16}0.011	^{15}0.033			0.003	0.001		
235	YITU-4	^{10}0.004	^{2}0.008	^{79}0.866	^{18}0.044	^{5}0.007	^{5}0.017	^{29}0.913	^{17}0.047	0.000	0.000	0.000	0.006
236	YITU-5	^{25}0.005	^{17}0.014			^{7}0.007	^{6}0.023			0.003	0.001		

Table 27: **Miss rates by dataset:** *At left, rank 1 miss rates relevant to investigations; at right, with threshold set to target FPIR = 0.01 for higher volume, low prior, uses.* $^{+}$*For the WILD set, FPIR = 0.1 Yellow indicates most accurate algorithm. Throughout blue superscripts indicate the rank of the algorithm for that column.*

MISSES OUTSIDE RANK R		MUGSHOT SEARCHES, N = 1.6M IDENTITIES							
		INVESTIGATION MODE, T = 0				IDENTIFICATION MODE, T > 0 FOR FPIR = 0.001			
FNIR(N, T, R)		PROPORTION MATED SEARCHES				PROPORTION MATED SEARCHES			
GALLERY		WITHOUT THE MATE AT RANK 1		WITH NO MATE AT RANK 1	WITH K-TH MATE NOT IN TOP K	WITH THE MATE BELOW THRESHOLD		WITHOUT ANY MATE ABOVE THRESH	WITHOUT ALL MATES ABOVE THRESH
		RECENT	CONSOLIDATED	UNCONSOLIDATED		RECENT	CONSOLIDATED	UNCONSOLIDATED	
1	3DIVI-0	[144] 0.0344				[152] 0.2565			
2	3DIVI-1	[145] 0.0375				[151] 0.2562			
3	3DIVI-2	[150] 0.0404				[147] 0.2554			
4	3DIVI-3	[178] 0.0857	[146] 0.0645			[171] 0.4023	[149] 0.3499		
5	3DIVI-4	[120] 0.0201	[107] 0.0133			[131] 0.1711	[118] 0.1349		
6	3DIVI-5	[121] 0.0202	[108] 0.0133	[70] 0.0133	[72] 0.0449	[127] 0.1691	[116] 0.1339	[71] 0.1339	[73] 0.3186
7	3DIVI-6	[135] 0.0265	[116] 0.0186	[75] 0.0172	[71] 0.0410	[130] 0.1705	[117] 0.1345	[72] 0.1350	[72] 0.3160
8	ALCHERA-0	[116] 0.0186	[103] 0.0121			[119] 0.1405	[107] 0.1105		
9	ALCHERA-1	[227] 0.9869	[175] 0.9824			[225] 0.9995	[175] 0.9993		
10	ALCHERA-2	[179] 0.0973	[147] 0.0914	[89] 0.0734	[91] 0.1876	[182] 0.4899	[151] 0.3736	[90] 0.4418	[90] 0.6820
11	ALLGOVISION-000	[103] 0.0141	[98] 0.0106	[67] 0.0105	[60] 0.0233	[92] 0.0905	[88] 0.0736	[59] 0.0736	[58] 0.1995
12	ANKE-0	[109] 0.0158	[90] 0.0100	[64] 0.0100	[69] 0.0338	[107] 0.1199	[98] 0.0989	[65] 0.0989	[66] 0.2558
13	ANKE-002	[28] 0.0054	[47] 0.0048	[34] 0.0048	[20] 0.0087	[29] 0.0344	[27] 0.0278	[23] 0.0278	[23] 0.0901
14	ANKE-1	[110] 0.0158	[91] 0.0101	[65] 0.0101	[68] 0.0337	[113] 0.1218	[101] 0.1001	[67] 0.1001	[67] 0.2581
15	AWARE-0	[171] 0.0639				[220] 0.9826			
16	AWARE-1	[167] 0.0587				[221] 0.9965			
17	AWARE-2	[168] 0.0600				[218] 0.9772			
18	AWARE-3	[142] 0.0332	[123] 0.0209			[117] 0.1306	[99] 0.0991		
19	AWARE-4	[173] 0.0704	[142] 0.0529			[153] 0.2709	[132] 0.2233		
20	AWARE-5	[143] 0.0337	[122] 0.0208	[79] 0.0230	[83] 0.0740	[165] 0.3729	[143] 0.2984	[87] 0.3777	[88] 0.6534
21	AWARE-6	[175] 0.0722	[143] 0.0538	[86] 0.0538	[88] 0.1551	[154] 0.2779	[134] 0.2419	[85] 0.2465	[85] 0.5140
22	AYONIX-0	[218] 0.4519	[170] 0.4649			[206] 0.8114	[165] 0.8490		
23	AYONIX-1	[214] 0.3432	[166] 0.3364	[95] 0.2841	[96] 0.4764	[209] 0.8247	[166] 0.8533	[93] 0.7935	[93] 0.9037
24	AYONIX-2	[213] 0.3432	[163] 0.2606	[96] 0.2841	[95] 0.4763	[208] 0.8246	[163] 0.8038	[92] 0.7933	[92] 0.9036
25	CAMVI-1	[206] 0.2267				[199] 0.6845			
26	CAMVI-2	[186] 0.1292				[186] 0.5369			
27	CAMVI-3	[166] 0.0544	[135] 0.0368			[78] 0.0736	[67] 0.0509		
28	CAMVI-4	[163] 0.0490	[133] 0.0326	[85] 0.0469	[73] 0.0475	[79] 0.0741	[66] 0.0505	[55] 0.0661	[30] 0.1105
29	CAMVI-5	[172] 0.0673	[139] 0.0458	[88] 0.0633	[80] 0.0638	[98] 0.1020	[87] 0.0727	[62] 0.0922	[48] 0.1513
30	COGENT-0	[95] 0.0131	[97] 0.0106			[61] 0.0557	[63] 0.0434		
31	COGENT-1	[94] 0.0131	[96] 0.0106			[60] 0.0557	[68] 0.0513		
32	COGENT-2	[39] 0.0062	[20] 0.0027	[12] 0.0027	[19] 0.0086	[45] 0.0475	[29] 0.0299	[34] 0.0391	[35] 0.1275
33	COGENT-3	[41] 0.0064	[30] 0.0037	[13] 0.0029	[21] 0.0091	[52] 0.0515	[42] 0.0341	[42] 0.0450	[47] 0.1448
34	COGNITEC-0	[138] 0.0278	[117] 0.0189			[124] 0.1628	[113] 0.1256		
35	COGNITEC-1	[105] 0.0143	[84] 0.0089			[100] 0.1045	[89] 0.0777		
36	COGNITEC-2	[62] 0.0083	[39] 0.0044	[29] 0.0043	[44] 0.0145	[62] 0.0560	[55] 0.0401	[37] 0.0400	[40] 0.1342
37	COGNITEC-3	[65] 0.0088	[46] 0.0048	[35] 0.0048	[45] 0.0148	[59] 0.0555	[54] 0.0397	[36] 0.0397	[39] 0.1322
38	CYBERLINK-000	[44] 0.0066	[60] 0.0056	[44] 0.0056	[35] 0.0116	[68] 0.0590	[61] 0.0427	[45] 0.0467	[46] 0.1415
39	CYBERLINK-001	[40] 0.0062	[52] 0.0051	[39] 0.0053	[31] 0.0111	[63] 0.0561	[53] 0.0396	[46] 0.0468	[45] 0.1415
40	DAHUA-0	[86] 0.0115	[73] 0.0070	[55] 0.0072	[57] 0.0204	[89] 0.0891	[79] 0.0624	[56] 0.0691	[57] 0.1967
41	DAHUA-002	[18] 0.0045	[36] 0.0040	[25] 0.0040	[15] 0.0063	[11] 0.0177	[10] 0.0130	[10] 0.0139	[10] 0.0481
42	DAHUA-1	[67] 0.0089	[48] 0.0049	[37] 0.0052	[49] 0.0173	[81] 0.0755	[69] 0.0521	[51] 0.0577	[54] 0.1738
43	DEEPGLINT-001	[225] 0.7953	[156] 0.1425	[99] 0.9269	[99] 0.9243	[227] 1.0000	[123] 0.1432	[165] 1.0000	[165] 1.0000
44	DEEPSEA-001	[51] 0.0070	[59] 0.0055	[46] 0.0059	[48] 0.0157	[46] 0.0488	[40] 0.0325	[33] 0.0390	[34] 0.1263
45	DERMALOG-0	[187] 0.1309				[181] 0.4876			
46	DERMALOG-1	[190] 0.1563				[184] 0.5285			
47	DERMALOG-2	[188] 0.1377				[183] 0.5033			
48	DERMALOG-3	[184] 0.1281	[151] 0.0970			[180] 0.4837	[152] 0.3884		
49	DERMALOG-4	[183] 0.1274	[149] 0.0961			[179] 0.4813	[153] 0.3892		
50	DERMALOG-5	[113] 0.0171	[100] 0.0113	[72] 0.0139	[65] 0.0254	[94] 0.0909	[82] 0.0649	[60] 0.0767	[61] 0.2072
51	DERMALOG-6	[76] 0.0102	[64] 0.0060	[48] 0.0061	[36] 0.0119	[57] 0.0542	[52] 0.0383	[39] 0.0416	[36] 0.1280
52	EVERAI-0	[123] 0.0209	[114] 0.0166			[96] 0.0921	[85] 0.0676		
53	EVERAI-1	[29] 0.0056	[21] 0.0027			[53] 0.0518	[49] 0.0360		
54	EVERAI-2	[31] 0.0058	[22] 0.0029	[15] 0.0032	[23] 0.0099	[54] 0.0526	[50] 0.0370	[38] 0.0410	[38] 0.1312
55	EVERAI-3	[20] 0.0047	[16] 0.0023	[11] 0.0024	[17] 0.0073	[31] 0.0377	[25] 0.0256	[24] 0.0285	[25] 0.0978
56	EVERAI-PARAVISION-004	[15] 0.0043	[32] 0.0039	[23] 0.0039	[11] 0.0050	[6] 0.0127	[8] 0.0100	[7] 0.0107	[7] 0.0345
57	EYEDEA-0	[211] 0.3000				[207] 0.8123			
58	EYEDEA-1	[199] 0.1981				[194] 0.6322			
59	EYEDEA-2	[200] 0.2000				[204] 0.7942			
60	EYEDEA-3	[177] 0.0824	[145] 0.0613			[168] 0.3893	[147] 0.3283		
61	F8-001	[106] 0.0146	[172] 0.5364	[68] 0.0115	[53] 0.0181	[125] 0.1681	[159] 0.5949	[79] 0.1559	[78] 0.3507
62	GLORY-0	[195] 0.1803	[154] 0.1335			[164] 0.3687	[145] 0.3020		
63	GLORY-1	[185] 0.1291	[148] 0.0932			[159] 0.3067	[135] 0.2447		
64	GORILLA-1	[169] 0.0627	[137] 0.0414			[172] 0.4080	[146] 0.3116		
65	GORILLA-2	[124] 0.0220	[109] 0.0137	[74] 0.0153	[79] 0.0570	[134] 0.1902	[121] 0.1379	[77] 0.1537	[79] 0.3589
66	GORILLA-3	[147] 0.0384	[126] 0.0245	[81] 0.0283	[86] 0.1032	[161] 0.3260	[142] 0.2730	[86] 0.3043	[86] 0.5786
67	HBINNO-0	[210] 0.2746				[203] 0.7655			
68	HIK-0	[131] 0.0236				[106] 0.1141			
69	HIK-1	[115] 0.0173				[111] 0.1202			
70	HIK-2	[114] 0.0172	[115] 0.0185			[112] 0.1212	[120] 0.1363		
71	HIK-3	[104] 0.0141	[99] 0.0107			[101] 0.1054	[106] 0.1097		
72	HIK-4	[101] 0.0138	[94] 0.0104			[97] 0.1013	[104] 0.1031		
73	HIK-5	[46] 0.0067	[25] 0.0034	[21] 0.0037	[41] 0.0140	[42] 0.0467	[33] 0.0308	[32] 0.0364	[32] 0.1228
74	HIK-6	[47] 0.0067	[27] 0.0034	[20] 0.0037	[40] 0.0140	[48] 0.0500	[39] 0.0324	[35] 0.0392	[37] 0.1310

Table 28: **Comparing enrollment styles for the FRVT 2018 mugshot sets**. *Consolidated refers to enrollment of all lifetime images in one template Unconsolidated refers to enrollment of those images separately under different identifiers. Columns 3 - 6 values are FNIR at rank 1 and with T = 0. Columns 7 - 10 values are high threshold FNIR. Throughout, blue superscripts indicate the rank of the algorithm for that column, and the best three values are highlighted in yellow and green.*

MISSES OUTSIDE RANK R		MUGSHOT SEARCHES, N = 1.6M IDENTITIES							
		INVESTIGATION MODE, $T = 0$				IDENTIFICATION MODE, $T > 0$ FOR FPIR = 0.001			
FNIR(N, T, R)		PROPORTION MATED SEARCHES				PROPORTION MATED SEARCHES			
GALLERY		WITHOUT THE MATE AT RANK 1		WITH NO MATE AT RANK 1	WITH K-TH MATE NOT IN TOP K	WITH THE MATE BELOW THRESHOLD		WITHOUT ANY MATE ABOVE THRESH	WITHOUT ALL MATES ABOVE THRESH
		RECENT	CONSOLIDATED	UNCONSOLIDATED		RECENT	CONSOLIDATED	UNCONSOLIDATED	
75	IDEMIA-0	^{83}0.0113	^{68}0.0063			^{105}0.1135	^{90}0.0802		
76	IDEMIA-1	^{87}0.0116	^{70}0.0065			^{56}0.0540	^{51}0.0377		
77	IDEMIA-2	^{93}0.0126	^{88}0.0099			^{58}0.0543	^{73}0.0564		
78	IDEMIA-3	^{74}0.0095	^{58}0.0054			^{47}0.0497	^{32}0.0308		
79	IDEMIA-4	^{70}0.0092	^{55}0.0052			^{34}0.0399	^{26}0.0276		
80	IDEMIA-5	^{80}0.0107	^{66}0.0062	^{50}0.0064	^{56}0.0192	^{41}0.0465	^{37}0.0319	^{31}0.0348	^{31}0.1125
81	IDEMIA-6	^{91}0.0122	^{74}0.0071	^{57}0.0076	^{55}0.0188	^{39}0.0458	^{36}0.0316	^{28}0.0342	^{27}0.1032
82	IIT-002	^{34}0.0060	^{158}0.1652	^{92}0.1605	^{90}0.1631	^{30}0.0366	^{129}0.1810	^{82}0.1763	^{63}0.2218
83	IMAGUS-0	^{212}0.3054				^{201}0.7344			
84	IMAGUS-2	^{204}0.2223	^{159}0.1833			^{202}0.7510	^{161}0.7143		
85	IMAGUS-3	^{215}0.3576	^{165}0.3008			^{205}0.8076	^{162}0.7731		
86	IMPERIAL-000	^{25}0.0051	^{41}0.0044	^{32}0.0045	^{18}0.0076	^{23}0.0285	^{22}0.0218	^{21}0.0244	^{22}0.0802
87	INCODE-0	^{165}0.0515	^{136}0.0376			^{160}0.3127	^{139}0.2644		
88	INCODE-004	^{38}0.0062	^{56}0.0052	^{40}0.0054	^{33}0.0113	^{65}0.0564	^{58}0.0408	^{43}0.0457	^{42}0.1395
89	INCODE-1	^{117}0.0190	^{106}0.0131			^{140}0.2143	^{128}0.1796		
90	INCODE-2	^{122}0.0203	^{102}0.0120	^{71}0.0137	^{74}0.0480	^{133}0.1861	^{119}0.1360	^{76}0.1507	^{77}0.3500
91	INCODE-3	^{108}0.0153	^{83}0.0088	^{66}0.0103	^{70}0.0368	^{129}0.1703	^{112}0.1227	^{74}0.1388	^{75}0.3290
92	INNOVATRICS-0	^{153}0.0421				^{150}0.2555			
93	INNOVATRICS-1	^{152}0.0421				^{149}0.2555			
94	INNOVATRICS-2	^{162}0.0475	^{141}0.0499			^{146}0.2366	^{138}0.2575		
95	INNOVATRICS-3	^{139}0.0287	^{127}0.0301			^{142}0.2236	^{136}0.2474		
96	INNOVATRICS-4	^{107}0.0149	^{78}0.0081	^{59}0.0081	^{67}0.0293	^{118}0.1340	^{95}0.0928	^{63}0.0927	^{65}0.2479
97	INTSYSMSU-000	^{189}0.1480	^{153}0.1294	^{90}0.1074	^{87}0.1458	^{223}0.9984	^{174}0.9981	^{99}0.9976	^{98}0.9987
98	ISYSTEMS-0	^{98}0.0136	^{82}0.0085			^{95}0.0912	^{81}0.0633		
99	ISYSTEMS-1	^{97}0.0136	^{81}0.0085			^{91}0.0903	^{80}0.0627		
100	ISYSTEMS-2	^{64}0.0088	^{43}0.0046			^{84}0.0814	^{72}0.0545		
101	ISYSTEMS-3	^{56}0.0075	^{35}0.0040	^{26}0.0041	^{27}0.0106	^{73}0.0620	^{57}0.0402	^{47}0.0500	^{49}0.1519
102	KEDACOM-001	^{78}0.0104	^{93}0.0102	^{60}0.0085	^{26}0.0105	^{20}0.0253	^{24}0.0228	^{15}0.0198	^{11}0.0545
103	LOOKMAN-005	^{81}0.0107	^{95}0.0105	^{61}0.0088	^{34}0.0114	^{28}0.0327	^{35}0.0314	^{22}0.0255	^{18}0.0738
104	LOOKMAN-3	^{84}0.0114	^{85}0.0089	^{53}0.0067	^{28}0.0109	^{40}0.0463	^{60}0.0425	^{27}0.0338	^{26}0.1015
105	LOOKMAN-4	^{88}0.0117	^{86}0.0091	^{54}0.0072	^{39}0.0134	^{43}0.0472	^{59}0.0417	^{29}0.0346	^{28}0.1086
106	MEGVII-0	^{71}0.0094	^{89}0.0099			^{104}0.1086	^{103}0.1023		
107	MEGVII-1	^{99}0.0137		^{62}0.0096	^{59}0.0231	^{80}0.0746		^{52}0.0577	^{53}0.1688
108	MEGVII-2	^{100}0.0137		^{63}0.0097	^{62}0.0236	^{83}0.0796		^{54}0.0623	^{55}0.1810
109	MICROFOCUS-0	^{222}0.5972				^{214}0.9335			
110	MICROFOCUS-1	^{223}0.5972				^{215}0.9335			
111	MICROFOCUS-2	^{224}0.6272				^{216}0.9340			
112	MICROFOCUS-3	^{221}0.5953	^{173}0.5389			^{213}0.9310	^{169}0.9213		
113	MICROFOCUS-4	^{220}0.5775	^{171}0.5191			^{224}0.9994	^{167}0.9015		
114	MICROFOCUS-5	^{216}0.4257	^{167}0.3701	^{97}0.3701	^{97}0.5522	^{210}0.8361	^{171}0.9835	^{94}0.8139	^{94}0.9189
115	MICROFOCUS-6	^{217}0.4283	^{168}0.3732	^{98}0.3732	^{98}0.5566	^{219}0.9780	^{164}0.8195	^{95}0.8195	^{95}0.9215
116	MICROSOFT-0	^{32}0.0058	^{19}0.0026			^{36}0.0443	^{28}0.0292		
117	MICROSOFT-1	^{30}0.0056	^{18}0.0026			^{38}0.0449	^{30}0.0299		
118	MICROSOFT-2	^{37}0.0061	^{23}0.0029			^{50}0.0503	^{44}0.0345		
119	MICROSOFT-3	^{4}0.0032	^{4}0.0011			^{27}0.0304	^{20}0.0193		
120	MICROSOFT-4	^{2}0.0031	^{1}0.0010			^{24}0.0288	^{17}0.0179		
121	MICROSOFT-5	^{5}0.0033	^{5}0.0013	^{6}0.0015	^{14}0.0062	^{21}0.0279	^{15}0.0171	^{13}0.0193	^{19}0.0755
122	MICROSOFT-6	^{8}0.0033	^{7}0.0014	^{7}0.0015	^{13}0.0060	^{8}0.0141	^{7}0.0080	^{19}0.0213	^{20}0.0772
123	NEC-0	^{118}0.0196	^{105}0.0127			^{85}0.0815	^{77}0.0604		
124	NEC-1	^{130}0.0235	^{113}0.0164			^{103}0.1081	^{94}0.0899		
125	NEC-2	^{1}0.0028	^{3}0.0011	^{1}0.0008	^{1}0.0019	^{3}0.0047	^{2}0.0024	^{1}0.0021	^{3}0.0086
126	NEC-3	^{3}0.0031	^{6}0.0013	^{2}0.0010	^{2}0.0019	^{1}0.0044	^{1}0.0021	^{2}0.0022	^{2}0.0080
127	NEUROTECHNOLOGY-0	^{164}0.0497				^{155}0.2948			
128	NEUROTECHNOLOGY-007	^{43}0.0066	^{213}1.0000	^{41}0.0054	^{30}0.0110	^{74}0.0648	^{213}1.0000	^{50}0.0551	^{51}0.1614
129	NEUROTECHNOLOGY-1	^{161}0.0467				^{157}0.2992			
130	NEUROTECHNOLOGY-2	^{160}0.0465				^{158}0.2993			
131	NEUROTECHNOLOGY-3	^{133}0.0250	^{120}0.0199			^{198}0.6649	^{160}0.6390		
132	NEUROTECHNOLOGY-4	^{60}0.0082	^{62}0.0058			^{76}0.0656	^{74}0.0575		
133	NEUROTECHNOLOGY-5	^{48}0.0068	^{37}0.0042	^{14}0.0032	^{22}0.0094	^{66}0.0564	^{70}0.0527	^{40}0.0438	^{41}0.1364
134	NEUROTECHNOLOGY-6	^{119}0.0201	^{112}0.0153	^{73}0.0142	^{76}0.0534	^{148}0.2555	^{140}0.2695	^{84}0.2125	^{84}0.4458
135	NEWLAND-2	^{176}0.0811		^{87}0.0599	^{89}0.1562	^{176}0.4405		^{88}0.3790	^{87}0.6252
136	NOBLIS-1	^{208}0.2512	^{161}0.2049	^{93}0.2032	^{93}0.3631	^{226}0.9996	^{176}0.9998	^{100}0.9994	^{100}0.9997
137	NOBLIS-2	^{196}0.1816	^{157}0.1565	^{94}0.2517	^{94}0.3944	^{222}0.9974	^{173}0.9959	^{98}0.9967	^{99}0.9987
138	NTECHLAB-0	^{85}0.0115	^{76}0.0077			^{86}0.0830	^{83}0.0666		
139	NTECHLAB-007	^{26}0.0053	^{44}0.0047	^{33}0.0047	^{25}0.0103	^{22}0.0282	^{23}0.0223	^{20}0.0223	^{21}0.0776
140	NTECHLAB-1	^{102}0.0139	^{87}0.0097			^{99}0.1021	^{91}0.0818		
141	NTECHLAB-3	^{61}0.0082	^{53}0.0051			^{64}0.0561	^{62}0.0434		
142	NTECHLAB-4	^{50}0.0068	^{34}0.0040			^{35}0.0431	^{41}0.0337		
143	NTECHLAB-5	^{42}0.0064	^{33}0.0039	^{24}0.0039	^{52}0.0179	^{37}0.0448	^{46}0.0347	^{30}0.0347	^{33}0.1235
144	NTECHLAB-6	^{33}0.0059	^{26}0.0034	^{17}0.0034	^{47}0.0154	^{32}0.0391	^{31}0.0301	^{25}0.0301	^{29}0.1088
145	PARAVISION-005	^{14}0.0042	^{31}0.0038	^{22}0.0038	^{10}0.0046	^{4}0.0068	^{4}0.0056	^{4}0.0060	^{4}0.0158
146	PIXELALL-002	^{53}0.0072	^{79}0.0084	^{47}0.0060	^{42}0.0142	^{102}0.1076	^{111}0.1206	^{64}0.0949	^{64}0.2475
147	PIXELALL-003	^{22}0.0048	^{49}0.0050	^{27}0.0042	^{16}0.0067	^{17}0.0244	^{38}0.0320	^{18}0.0202	^{15}0.0658
148	QUANTASOFT-1	^{203}0.2198	^{176}0.9857	^{100}0.9426	^{100}0.9502	^{196}0.6399	^{172}0.9915	^{96}0.9640	^{97}0.9801

Table 29: **Comparing enrollment styles for the FRVT 2018 mugshot sets**. *Consolidated refers to enrollment of all lifetime images in one template Unconsolidated refers to enrollment of those images separately under different identifiers. Columns 3 - 6 values are FNIR at rank 1 and with $T = 0$. Columns 7 - 10 values are high threshold FNIR. Throughout, blue superscripts indicate the rank of the algorithm for that column, and the best three values are highlighted in yellow and green.*

MISSES OUTSIDE RANK R		MUGSHOT SEARCHES, N = 1.6M IDENTITIES							
		INVESTIGATION MODE, T $= 0$				IDENTIFICATION MODE, T > 0 FOR FPIR = 0.001			
FNIR(N, T, R)		PROPORTION MATED SEARCHES				PROPORTION MATED SEARCHES			
GALLERY		WITHOUT THE MATE AT RANK 1		WITH NO MATE AT RANK 1	WITH K-TH MATE NOT IN TOP K	WITH THE MATE BELOW THRESHOLD		WITHOUT ANY MATE ABOVE THRESH	WITHOUT ALL MATES ABOVE THRESH
		RECENT	CONSOLIDATED	UNCONSOLIDATED		RECENT	CONSOLIDATED	UNCONSOLIDATED	
149	RANKONE-0	^{159}0.0455	^{131}0.0319			^{141}0.2192	^{127}0.1788		
150	RANKONE-006	^{59}0.0077	^{69}0.0065	^{51}0.0065	^{46}0.0149	^{33}0.0397	^{34}0.0310	^{26}0.0310	^{24}0.0967
151	RANKONE-007	^{35}0.0060	^{54}0.0052	^{38}0.0052	^{24}0.0101	^{19}0.0248	^{21}0.0194	^{14}0.0194	^{13}0.0622
152	RANKONE-1	^{132}0.0247	^{119}0.0194			^{126}0.1683	^{125}0.1549		
153	RANKONE-2	^{126}0.0221	^{111}0.0149			^{109}0.1200	^{97}0.0943		
154	RANKONE-3	^{125}0.0221	^{110}0.0149			^{108}0.1200	^{96}0.0943		
155	RANKONE-4	^{158}0.0441	^{130}0.0318	^{84}0.0318	^{85}0.0945	^{135}0.1951	^{124}0.1545	^{78}0.1545	^{80}0.3590
156	RANKONE-5	^{90}0.0120	^{75}0.0072	^{56}0.0072	^{63}0.0237	^{71}0.0617	^{64}0.0447	^{41}0.0447	^{44}0.1404
157	REALNETWORKS-0	^{157}0.0426	^{138}0.0443			^{145}0.2362	^{137}0.2476		
158	REALNETWORKS-003	^{136}0.0268	^{124}0.0220	^{78}0.0224	^{82}0.0722	^{123}0.1617	^{122}0.1405	^{75}0.1415	^{76}0.3368
159	REALNETWORKS-004	^{134}0.0262	^{118}0.0192	^{77}0.0222	^{81}0.0713	^{122}0.1604	^{110}0.1179	^{73}0.1360	^{74}0.3288
160	REALNETWORKS-1	^{156}0.0426	^{134}0.0329			^{144}0.2362	^{130}0.2045		
161	REALNETWORKS-2	^{151}0.0418	^{132}0.0320	^{80}0.0268	^{84}0.0903	^{143}0.2341	^{131}0.2049	^{83}0.1775	^{83}0.3949
162	REMARKAI-0	^{82}0.0109	^{71}0.0065	^{52}0.0065	^{64}0.0238	^{116}0.1301	^{102}0.1020	^{68}0.1020	^{71}0.2671
163	REMARKAI-000	^{36}0.0060	^{51}0.0051	^{36}0.0051	^{32}0.0111	^{67}0.0577	^{65}0.0461	^{44}0.0461	^{43}0.1399
164	REMARKAI-2	^{79}0.0105	^{67}0.0062	^{49}0.0062	^{61}0.0235	^{115}0.1264	^{100}0.0991	^{66}0.0991	^{68}0.2615
165	SENSETIME-0	^{21}0.0048	^{13}0.0018	^{9}0.0018	^{4}0.0037	^{15}0.0234	^{14}0.0165	^{11}0.0168	^{12}0.0603
166	SENSETIME-002	^{111}0.0163	^{104}0.0124	^{69}0.0124	^{38}0.0127	^{10}0.0174	^{12}0.0134	^{9}0.0134	^{5}0.0160
167	SENSETIME-003	^{9}0.0036	^{28}0.0034	^{18}0.0034	^{5}0.0039	^{2}0.0045	^{3}0.0040	^{3}0.0041	^{1}0.0078
168	SENSETIME-1	^{23}0.0048	^{11}0.0018	^{8}0.0018	^{8}0.0041	^{18}0.0245	^{16}0.0175	^{12}0.0177	^{14}0.0628
169	SHAMAN-0	^{192}0.1707				^{178}0.4744			
170	SHAMAN-1	^{193}0.1718				^{185}0.5316			
171	SHAMAN-2	^{209}0.2620				^{200}0.6998			
172	SHAMAN-3	^{181}0.1266	^{150}0.0969			^{177}0.4527	^{154}0.3921		
173	SHAMAN-4	^{205}0.2242	^{160}0.1867			^{191}0.6164	^{158}0.5907		
174	SHAMAN-6	^{155}0.0424	^{129}0.0312	^{83}0.0312	^{77}0.0542	^{120}0.1432	^{108}0.1109	^{69}0.1109	^{70}0.2629
175	SHAMAN-7	^{154}0.0422	^{128}0.0310	^{82}0.0310	^{75}0.0529	^{121}0.1436	^{109}0.1112	^{70}0.1112	^{69}0.2624
176	SIAT-0	^{75}0.0101				^{93}0.0906			
177	SIAT-1	^{11}0.0039	^{164}0.2639			^{12}0.0201	^{141}0.2727		
178	SIAT-2	^{12}0.0040	^{162}0.2128			^{16}0.0242	^{133}0.2239		
179	SMILART-0	^{197}0.1931				^{192}0.6202			
180	SMILART-1	^{202}0.2188				^{197}0.6411			
181	SMILART-2	^{198}0.1946				^{193}0.6290			
182	SMILART-4	^{226}0.9649	^{174}0.9531	^{101}0.9722	^{101}0.9738	^{217}0.9683	^{170}0.9569	^{97}0.9740	^{96}0.9781
183	SYNESIS-0	^{191}0.1621				^{189}0.5538			
184	SYNESIS-3	^{194}0.1721	^{155}0.1350	^{91}0.1350	^{92}0.2571	^{190}0.5832	^{157}0.5296	^{91}0.5295	^{91}0.7459
185	TECH5-001	^{45}0.0066	^{63}0.0059	^{43}0.0056	^{43}0.0144	^{69}0.0599	^{75}0.0590	^{49}0.0537	^{52}0.1641
186	TEVIAN-0	^{128}0.0225				^{137}0.2028			
187	TEVIAN-1	^{129}0.0225				^{138}0.2028			
188	TEVIAN-2	^{127}0.0224				^{136}0.2024			
189	TEVIAN-3	^{112}0.0169	^{92}0.0102			^{132}0.1798	^{115}0.1316		
190	TEVIAN-4	^{96}0.0134	^{77}0.0080			^{110}0.1201	^{93}0.0878		
191	TEVIAN-5	^{68}0.0092	^{57}0.0053	^{45}0.0058	^{58}0.0213	^{90}0.0898	^{84}0.0667	^{61}0.0770	^{62}0.2079
192	TIGER-0	^{170}0.0638	^{140}0.0480			^{169}0.3921	^{148}0.3361		
193	TIGER-2	^{58}0.0075	^{40}0.0044	^{31}0.0044	^{51}0.0177	^{88}0.0888	^{86}0.0698	^{57}0.0698	^{60}0.2016
194	TIGER-3	^{57}0.0075		^{30}0.0044	^{50}0.0177	^{87}0.0888		^{58}0.0698	^{59}0.2015
195	TONGYITRANS-0	^{73}0.0095	^{65}0.0060			^{82}0.0769	^{78}0.0607		
196	TONGYITRANS-1	^{72}0.0095	^{101}0.0114			^{77}0.0693	^{92}0.0835		
197	TOSHIBA-0	^{49}0.0068	^{24}0.0033	^{16}0.0033	^{29}0.0110	^{75}0.0648	^{71}0.0529	^{48}0.0529	^{50}0.1599
198	TOSHIBA-1	^{52}0.0071	^{29}0.0035	^{19}0.0035	^{37}0.0120	^{72}0.0618	^{76}0.0596	^{53}0.0585	^{56}0.1819
199	VD-0	^{219}0.4751	^{169}0.4303			^{212}0.9171	^{168}0.9048		
200	VD-1	^{141}0.0302	^{125}0.0221	^{76}0.0221	^{78}0.0560	^{139}0.2036	^{126}0.1654	^{80}0.1658	^{81}0.3657
201	VIGILANTSOLUTIONS-0	^{180}0.1254				^{187}0.5387			
202	VIGILANTSOLUTIONS-1	^{201}0.2038				^{195}0.6374			
203	VIGILANTSOLUTIONS-2	^{207}0.2387				^{211}0.8760			
204	VIGILANTSOLUTIONS-3	^{174}0.0719	^{144}0.0549			^{173}0.4097	^{150}0.3568		
205	VIGILANTSOLUTIONS-4	^{182}0.1272	^{152}0.0993			^{188}0.5504	^{156}0.4914		
206	VIGILANTSOLUTIONS-5	^{89}0.0118				^{175}0.4327			
207	VIGILANTSOLUTIONS-6	^{92}0.0125		^{58}0.0077	^{66}0.0258	^{174}0.4260		^{89}0.4155	^{89}0.6577
208	VISIONLABS-008	^{19}0.0046	^{38}0.0042	^{28}0.0043	^{12}0.0055	^{9}0.0157	^{9}0.0117	^{8}0.0129	^{9}0.0424
209	VISIONLABS-3	^{66}0.0089	^{50}0.0050			^{51}0.0506	^{45}0.0347		
210	VISIONLABS-4	^{16}0.0044	^{14}0.0020			^{70}0.0604	^{56}0.0402		
211	VISIONLABS-5	^{13}0.0041	^{12}0.0018			^{55}0.0531	^{47}0.0353		
212	VISIONLABS-6	^{7}0.0033	^{9}0.0015	^{5}0.0015	^{7}0.0040	^{26}0.0289	^{19}0.0185	^{17}0.0201	^{17}0.0737
213	VISIONLABS-7	^{6}0.0033	^{8}0.0014	^{4}0.0014	^{6}0.0039	^{25}0.0289	^{18}0.0185	^{16}0.0201	^{16}0.0737
214	VOCORD-0	^{149}0.0403				^{170}0.3994			
215	VOCORD-1	^{148}0.0402				^{156}0.2991			
216	VOCORD-2	^{146}0.0382				^{163}0.3663			
217	VOCORD-3	^{63}0.0085	^{72}0.0067			^{114}0.1258	^{114}0.1295		
218	VOCORD-4	^{77}0.0102	^{80}0.0084			^{166}0.3784	^{155}0.4055		
219	VOCORD-5	^{69}0.0092	^{61}0.0057	^{42}0.0054	^{54}0.0182	^{128}0.1697	^{105}0.1076	^{81}0.1717	^{82}0.3775
220	YISHENG-0	^{137}0.0268				^{167}0.3804			
221	YISHENG-1	^{140}0.0290	^{121}0.0208			^{162}0.3483	^{144}0.3002		
222	YITU-0	^{55}0.0074	^{45}0.0047			^{49}0.0502	^{48}0.0358		

Table 30: **Comparing enrollment styles for the FRVT 2018 mugshot sets**. *Consolidated refers to enrollment of all lifetime images in one template Unconsolidated refers to enrollment of those images separately under different identifiers. Columns 3 - 6 values are FNIR at rank 1 and with* T *= 0. Columns 7 - 10 values are high threshold FNIR. Throughout, blue superscripts indicate the rank of the algorithm for that column, and the best three values are highlighted in yellow and green.*

MISSES OUTSIDE RANK R		MUGSHOT SEARCHES, N = 1.6M IDENTITIES							
		INVESTIGATION MODE, T = 0				IDENTIFICATION MODE, T > 0 FOR FPIR = 0.001			
FNIR(N, T, R)		PROPORTION MATED SEARCHES				PROPORTION MATED SEARCHES			
GALLERY		WITHOUT THE MATE AT RANK 1		WITH NO MATE AT RANK 1	WITH K-TH MATE NOT IN TOP K	WITH THE MATE BELOW THRESHOLD		WITHOUT ANY MATE ABOVE THRESH	WITHOUT ALL MATES ABOVE THRESH
		RECENT	CONSOLIDATED	UNCONSOLIDATED		RECENT	CONSOLIDATED	UNCONSOLIDATED	
223	YITU-1	[54]0.0072	[42]0.0046			[44]0.0472	[43]0.0341		
224	YITU-2	[17]0.0044	[10]0.0015			[13]0.0204	[11]0.0133		
225	YITU-3	[27]0.0054	[17]0.0023			[14]0.0213	[13]0.0139		
226	YITU-4	[10]0.0037	[2]0.0011	[3]0.0012	[3]0.0033	[5]0.0123	[5]0.0074	[5]0.0080	[6]0.0337
227	YITU-5	[24]0.0048	[15]0.0020	[10]0.0020	[9]0.0041	[7]0.0128	[6]0.0076	[6]0.0088	[8]0.0350

Table 31: **Comparing enrollment styles for the FRVT 2018 mugshot sets**. *Consolidated refers to enrollment of all lifetime images in one template Unconsolidated refers to enrollment of those images separately under different identifiers. Columns 3 - 6 values are FNIR at rank 1 and with* T *= 0. Columns 7 - 10 values are high threshold FNIR. Throughout, blue superscripts indicate the rank of the algorithm for that column, and the best three values are highlighted in yellow and green.*

2020/02/26	FNIR(N, R, T) =	False neg. identification rate	N = Num. enrolled subjects	T = Threshold	$T = 0 \rightarrow$ Investigation
13:34:01	FPIR(N, T) =	False pos. identification rate	R = Num. candidates examined		$T > 0 \rightarrow$ Identification

FNIR(N, R, T) = False neg. identification rate
FPIR(N, T) = False pos. identification rate
N = Num. enrolled subjects
R = Num. candidates examined
T = Threshold
T = 0 → Investigation
T > 0 → Identification

Figure 18: **[Mugshot Dataset] Error rate reductions in 2018**. *For each* FRVT*2018 participant, the plot shows accuracy gains between Phase 1 (Feb 2018), Phase 2 (Jun 2018) and Phase 3 (Nov 2018) according to two metrics: rank one miss rate, FNIR(N, 1, 0), and high threshold, FNIR(N, L, T), with T set to achieve FPIR = 0.003. The text "Red=" gives the best reduction multiplier for the given metric on the recent enrollment strategy - a smaller value is better.*

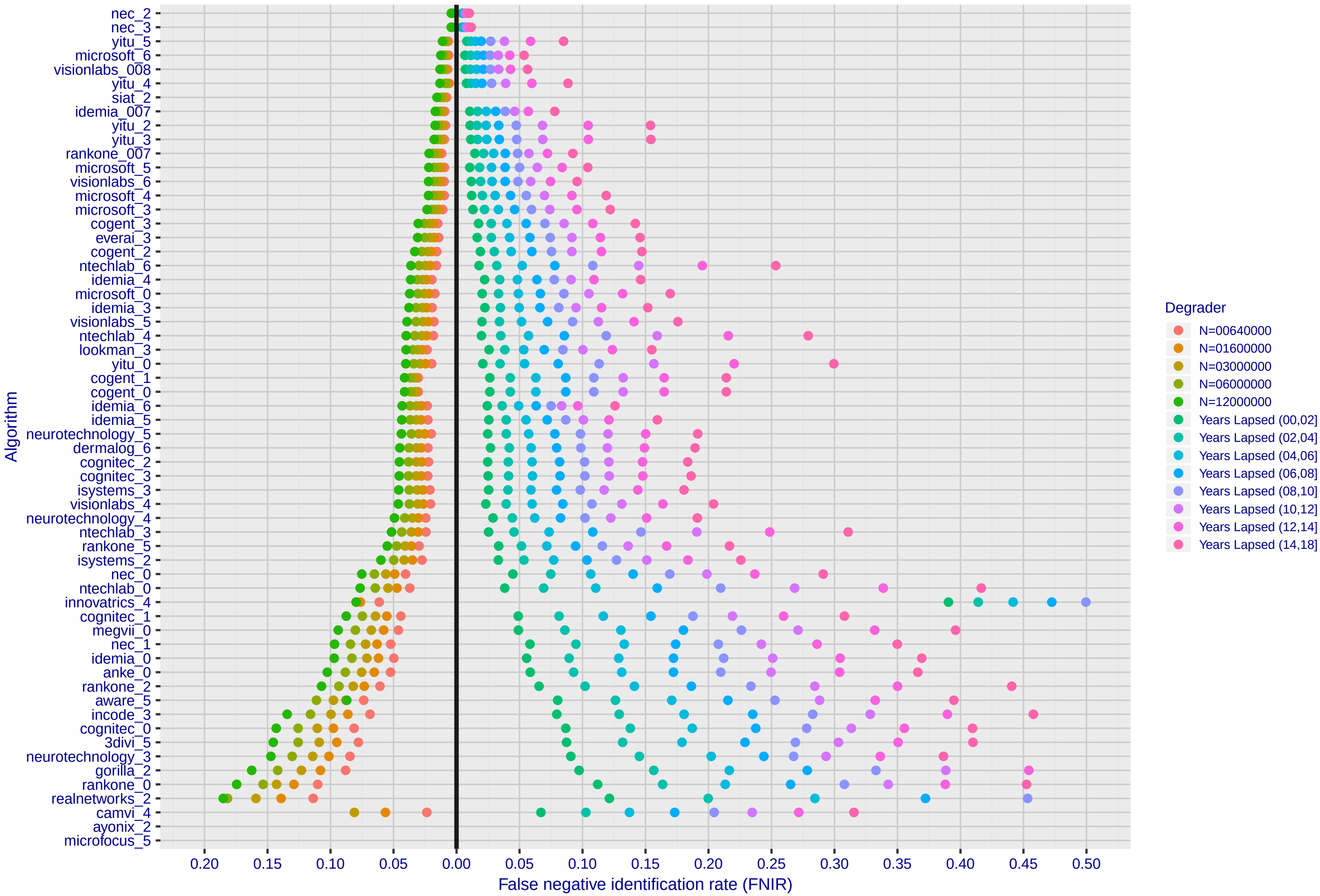

Figure 19: **[FRVT-2018 Mugshot Ageing Dataset] Contrast of ageing and population size dependency.** *The Figure shows, at left, the dependence FNIR(N) for the FRVT-2018, as tabulated in Table 10. At right, is FNIR(N = 3 000 000, ΔT) from Figure 61. Ageing miss rates are computed over all searches binned by number of years between search and initial enrollment. In all cases, FPIR = 0.01.*

This publication is available free of charge from: https://doi.org/10.6028/NIST.IR.8271

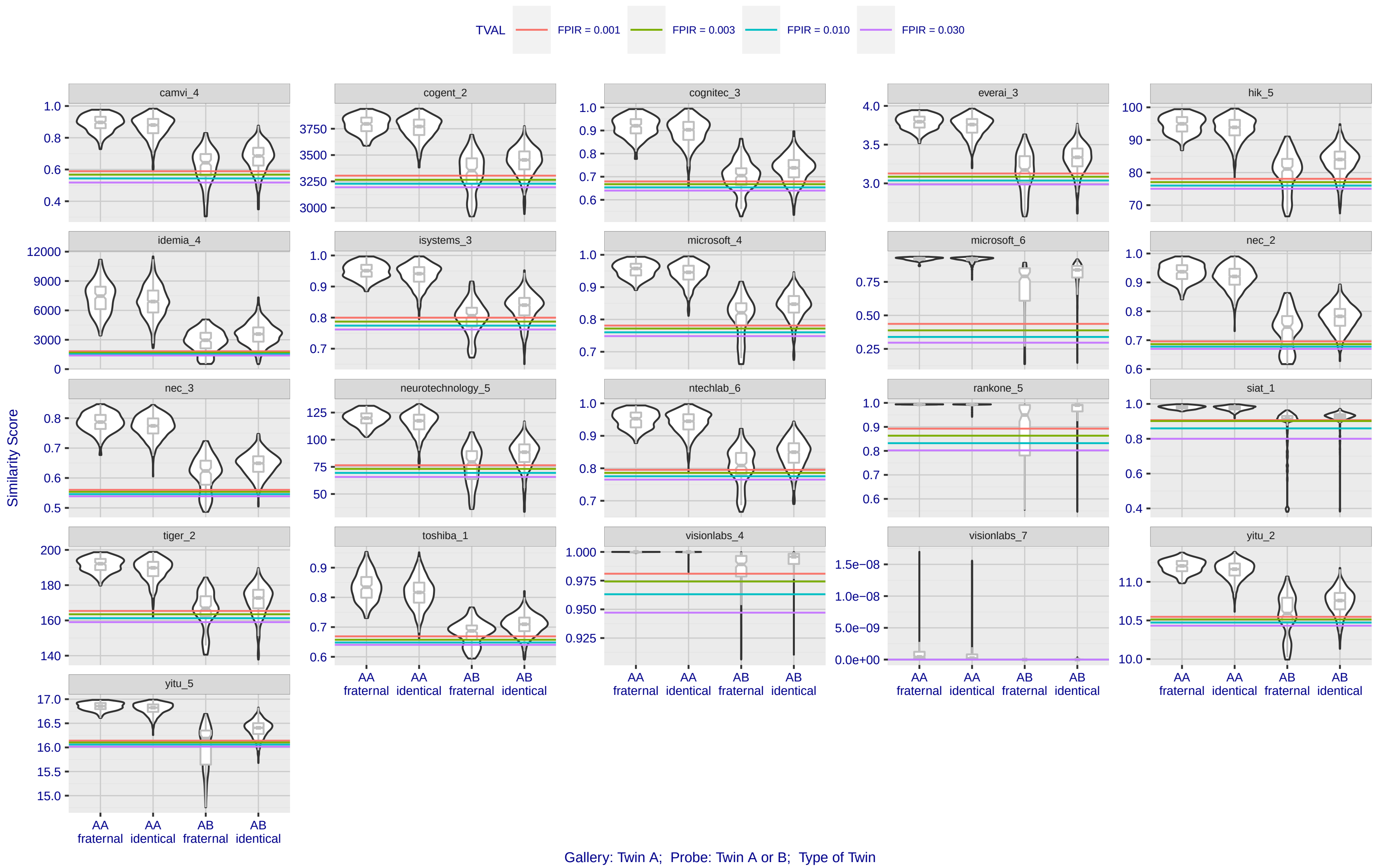

Figure 20: **[Twins Dataset] High scores from twins.** *The Figure shows native similarity scores from searches into a dataset of N = 640 000 background mugshot images plus 104 portrait images, one from each of one of a pair of twins. Two distributions of scores are plotted for each of monozygotic (identical) and dizygotic (fraternal) twins. The first distribution ("AA") shows the mate score from Twin A against their own enrollment. The second ("AB") shows scores from searches of Twin B against the Twin A enrollment: As these are non-mate scores they should be below the various thresholds shown as horizontal lines. That they usually are not is an indication that twins produce very high non-mate scores. Note in theory half of dizygotic (fraternal) twins are different sex. In the sample used here some fraternal twins are correctly rejected.*

Appendices

Appendix A Accuracy on large-population FRVT 2018 mugshots

This publication is available free of charge from: https://doi.org/10.6028/NIST.IR.8271

FNIR(N, R, T) = False neg. identification rate
FPIR(N, T) = False pos. identification rate
N = Num. enrolled subjects
R = Num. candidates examined
T = Threshold
T = 0 → Investigation
T > 0 → Identification

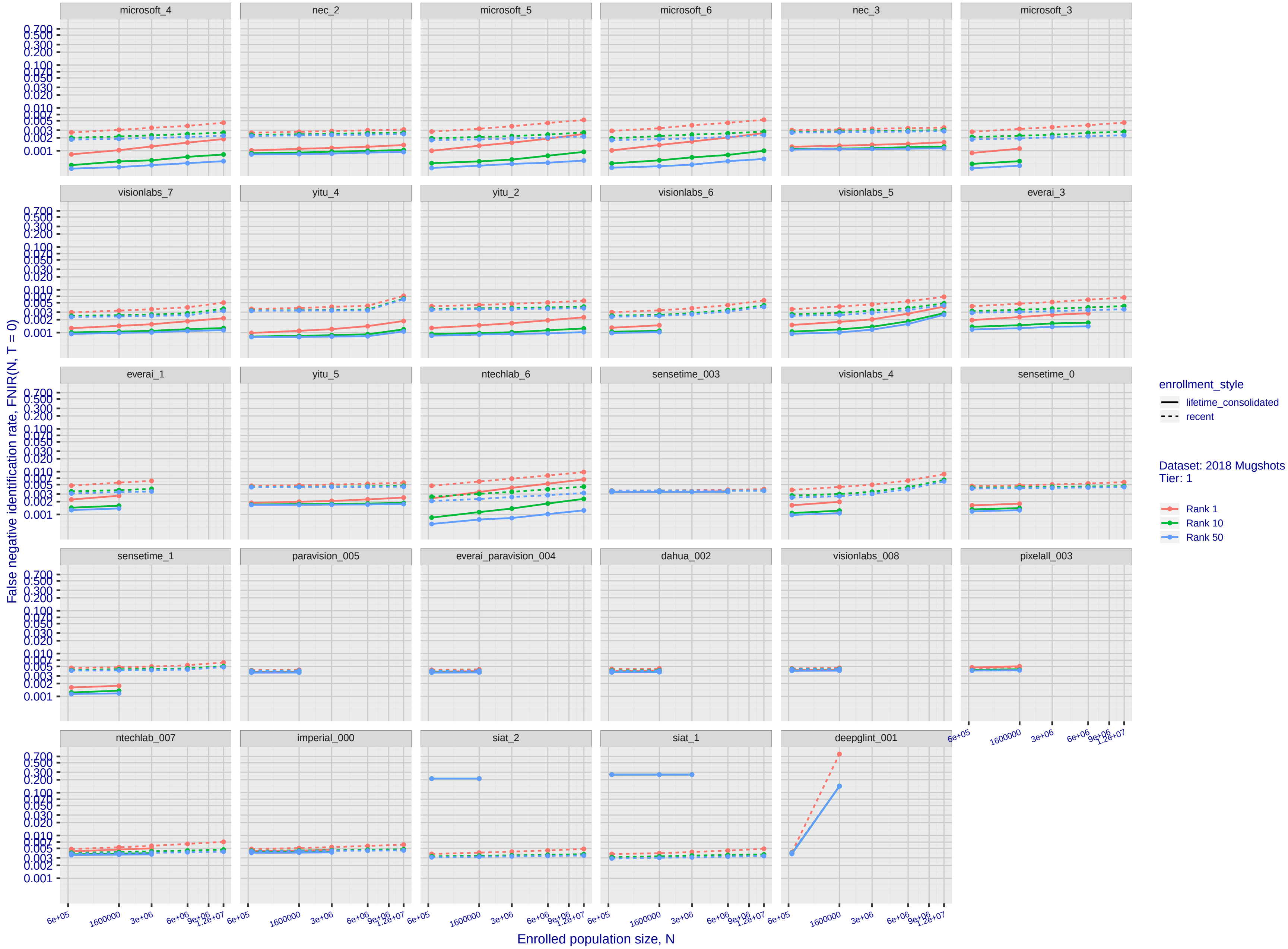

Figure 21: **[FRVT-2018 Mugshot Dataset] Rank-based identification miss rates vs. number of enrolled subjects**. *The figure shows false negative identification rates, FNIR(N, R), across various gallery sizes and ranks 1, 10 and 50. The threshold is set to zero, so this metric rewards even weak scoring rank 1 mates. This also means FPIR = 1, so any search without an enrolled mate will return non-mated candidates. For clarity, results are sorted and reported into tiers spanning multiple pages, the tiering criteria being rank 1 hit rate on a gallery size of 640 000.*

FNIR(N, R, T) = False neg. identification rate
FPIR(N, T) = False pos. identification rate
N = Num. enrolled subjects
R = Num. candidates examined
T = Threshold
T = 0 → Investigation
T > 0 → Identification

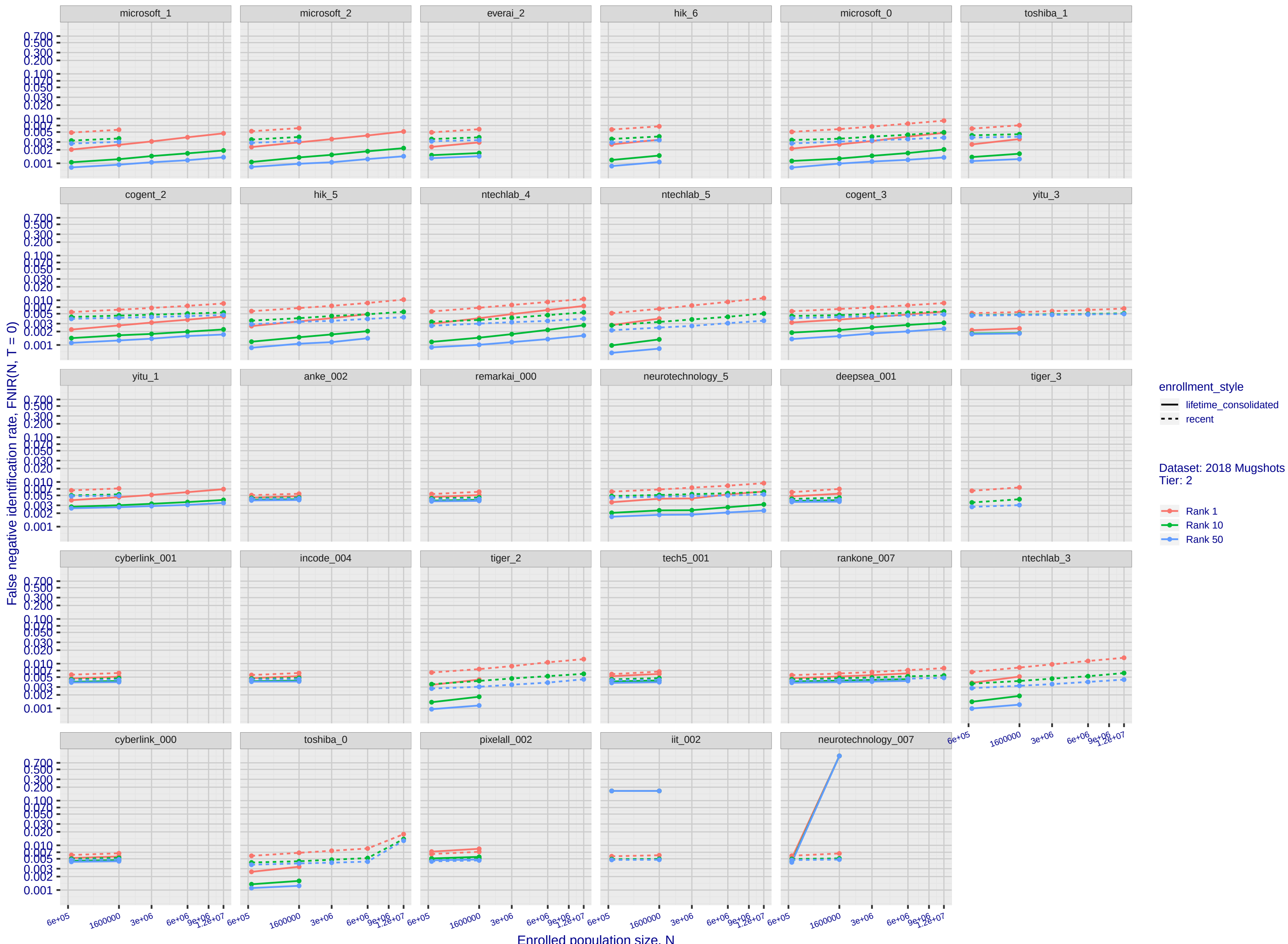

Figure 22: **[FRVT-2018 Mugshot Dataset] Rank-based identification miss rates vs. number of enrolled subjects**. *The figure shows false negative identification rates, FNIR(N, R), across various gallery sizes and ranks 1, 10 and 50. The threshold is set to zero, so this metric rewards even weak scoring rank 1 mates. This also means FPIR = 1, so any search without an enrolled mate will return non-mated candidates. For clarity, results are sorted and reported into tiers spanning multiple pages, the tiering criteria being rank 1 hit rate on a gallery size of 640 000.*

FNIR(N, R, T) = False neg. identification rate
FPIR(N, T) = False pos. identification rate
N = Num. enrolled subjects
R = Num. candidates examined
T = Threshold
T = 0 → Investigation
T > 0 → Identification

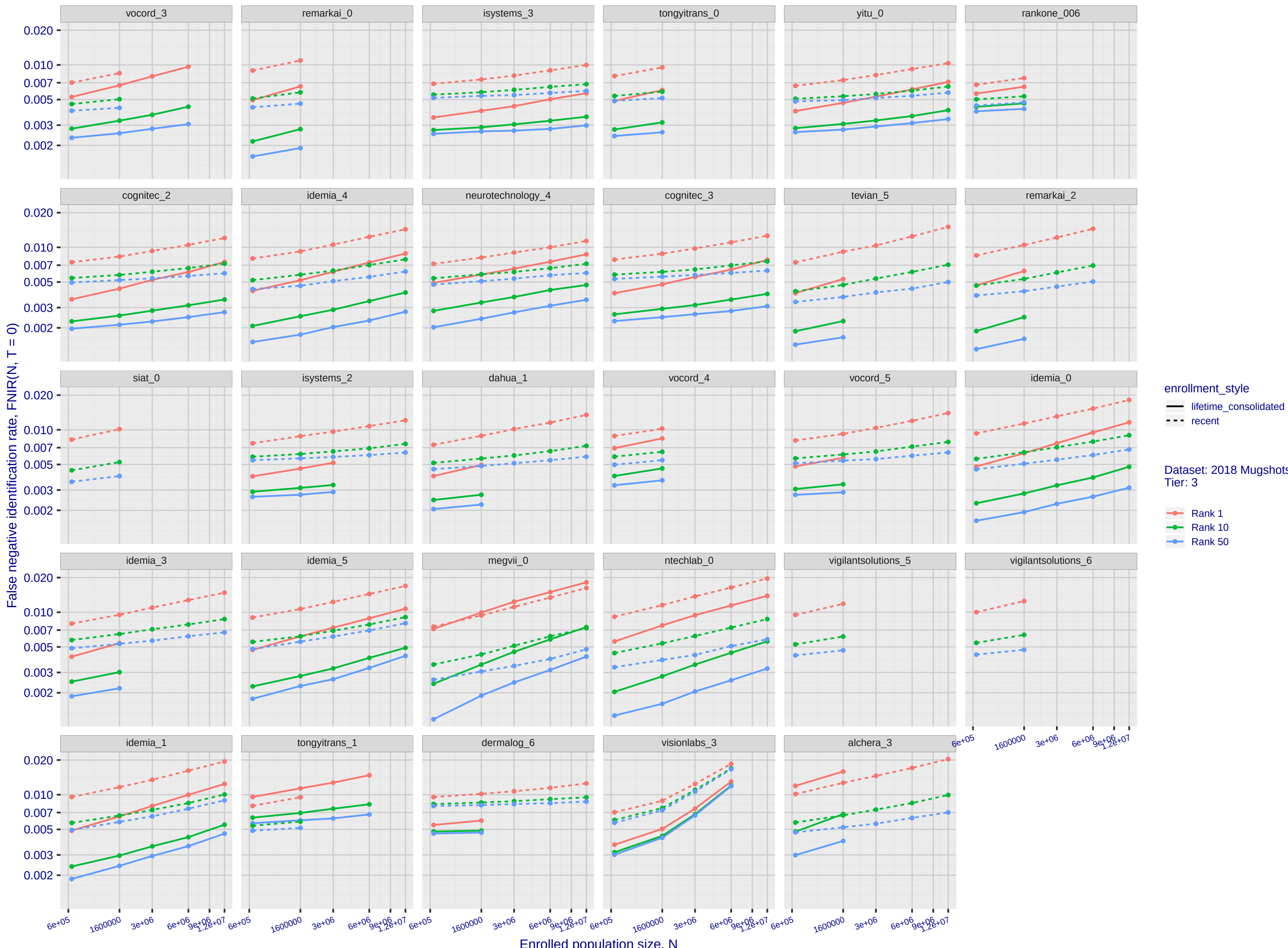

Figure 23: **[FRVT-2018 Mugshot Dataset] Rank-based identification miss rates vs. number of enrolled subjects**. *The figure shows false negative identification rates, FNIR(N, R), across various gallery sizes and ranks 1, 10 and 50. The threshold is set to zero, so this metric rewards even weak scoring rank 1 mates. This also means FPIR = 1, so any search without an enrolled mate will return non-mated candidates. For clarity, results are sorted and reported into tiers spanning multiple pages, the tiering criteria being rank 1 hit rate on a gallery size of 640 000.*

FNIR(N, R, T) = False neg. identification rate
FPIR(N, T) = False pos. identification rate

N = Num. enrolled subjects
R = Num. candidates examined

T = Threshold

T = 0 → Investigation
T > 0 → Identification

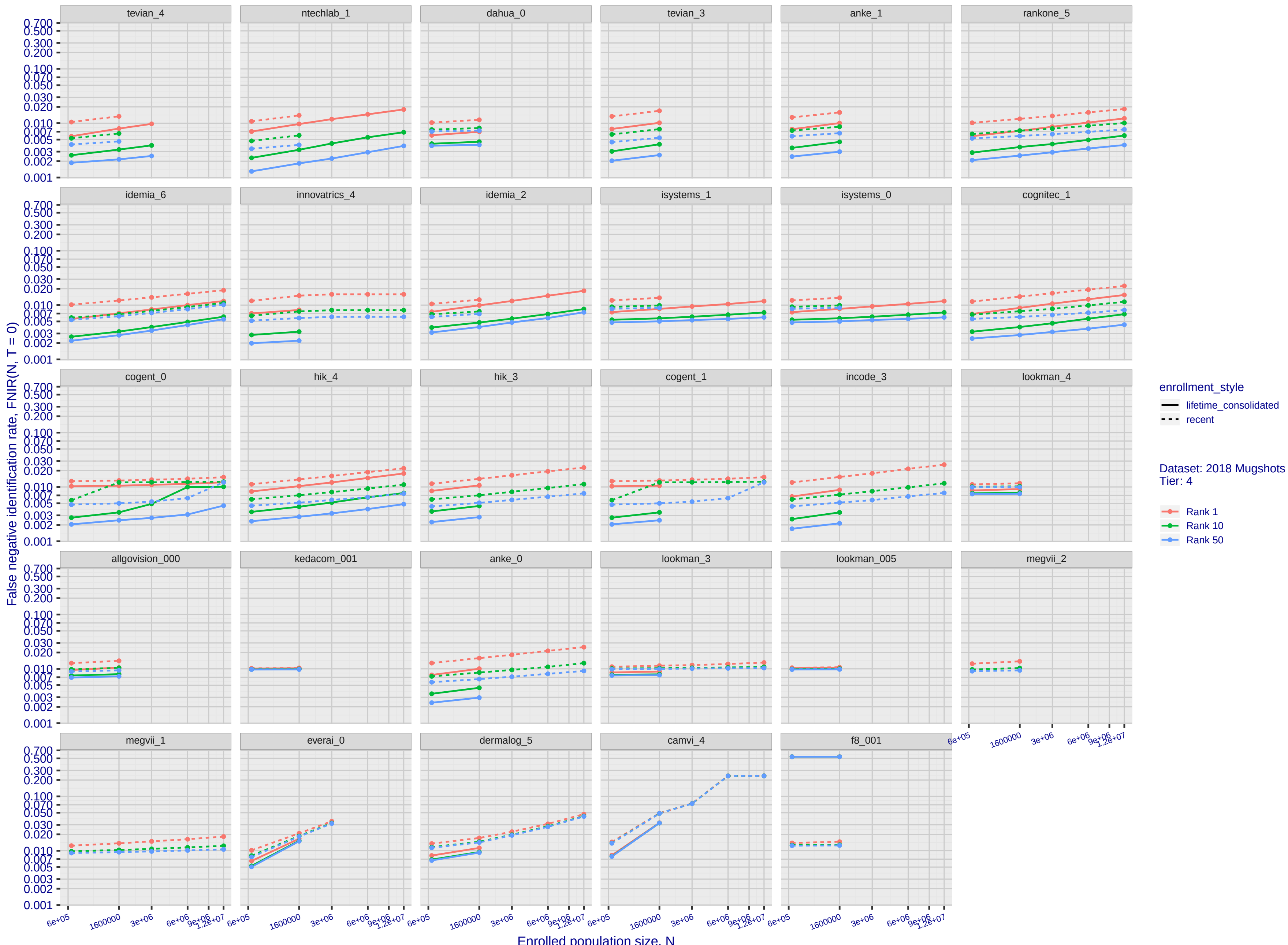

Figure 24: **[FRVT-2018 Mugshot Dataset] Rank-based identification miss rates vs. number of enrolled subjects**. *The figure shows false negative identification rates, FNIR(N, R), across various gallery sizes and ranks 1, 10 and 50. The threshold is set to zero, so this metric rewards even weak scoring rank 1 mates. This also means FPIR = 1, so any search without an enrolled mate will return non-mated candidates. For clarity, results are sorted and reported into tiers spanning multiple pages, the tiering criteria being rank 1 hit rate on a gallery size of 640 000.*

This publication is available free of charge from: https://doi.org/10.6028/NIST.IR.8271

2020/02/26
13:34:01

FNIR(N, R, T) = False neg. identification rate
FPIR(N, T) = False pos. identification rate
N = Num. enrolled subjects
R = Num. candidates examined
T = Threshold
T = 0 → Investigation
T > 0 → Identification

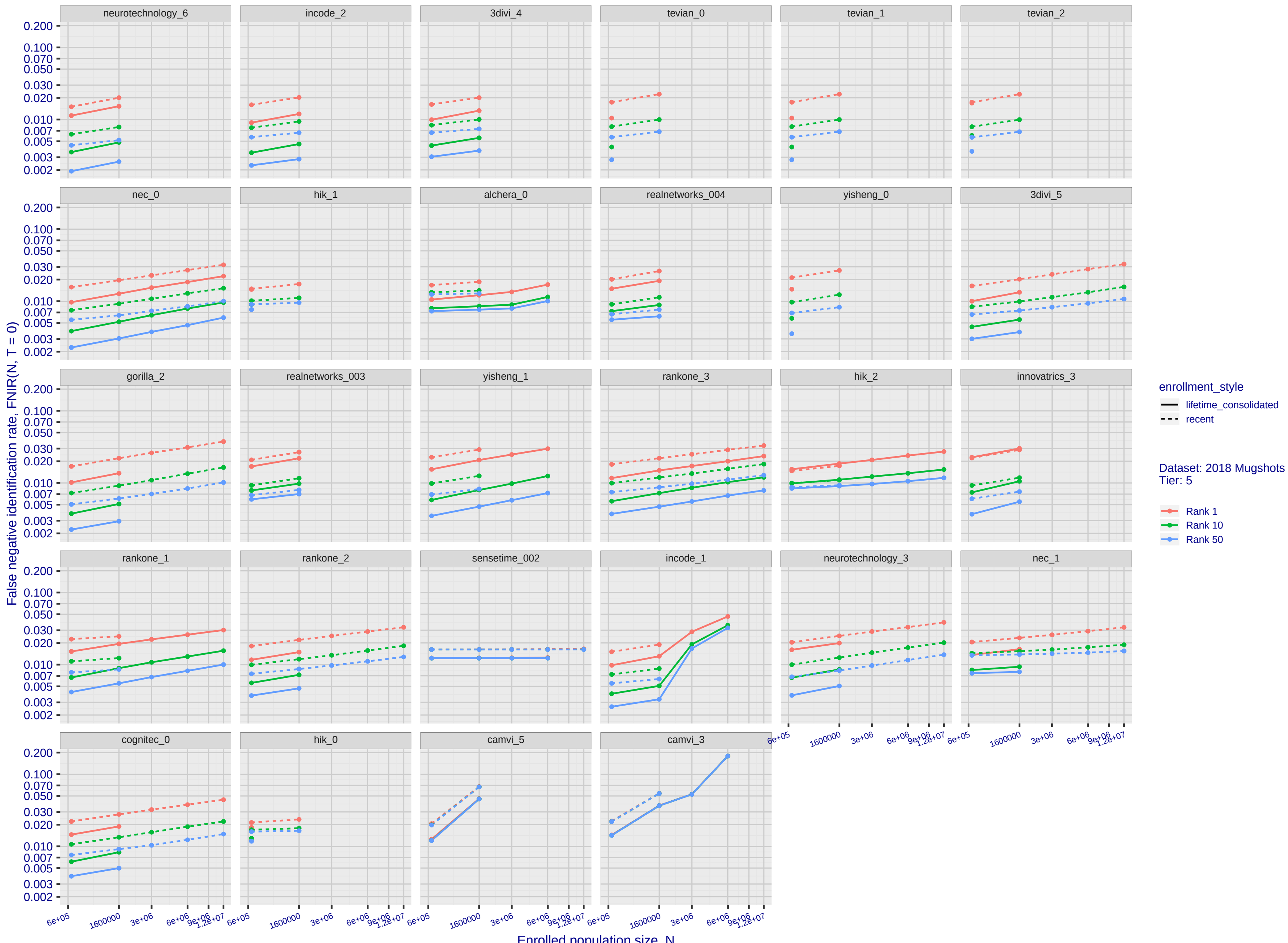

Figure 25: **[FRVT-2018 Mugshot Dataset] Rank-based identification miss rates vs. number of enrolled subjects**. *The figure shows false negative identification rates, FNIR(N, R), across various gallery sizes and ranks 1, 10 and 50. The threshold is set to zero, so this metric rewards even weak scoring rank 1 mates. This also means FPIR = 1, so any search without an enrolled mate will return non-mated candidates. For clarity, results are sorted and reported into tiers spanning multiple pages, the tiering criteria being rank 1 hit rate on a gallery size of 640 000.*

FNIR(N, R, T) = False neg. identification rate
FPIR(N, T) = False pos. identification rate
N = Num. enrolled subjects
R = Num. candidates examined
T = Threshold
T = 0 → Investigation
T > 0 → Identification

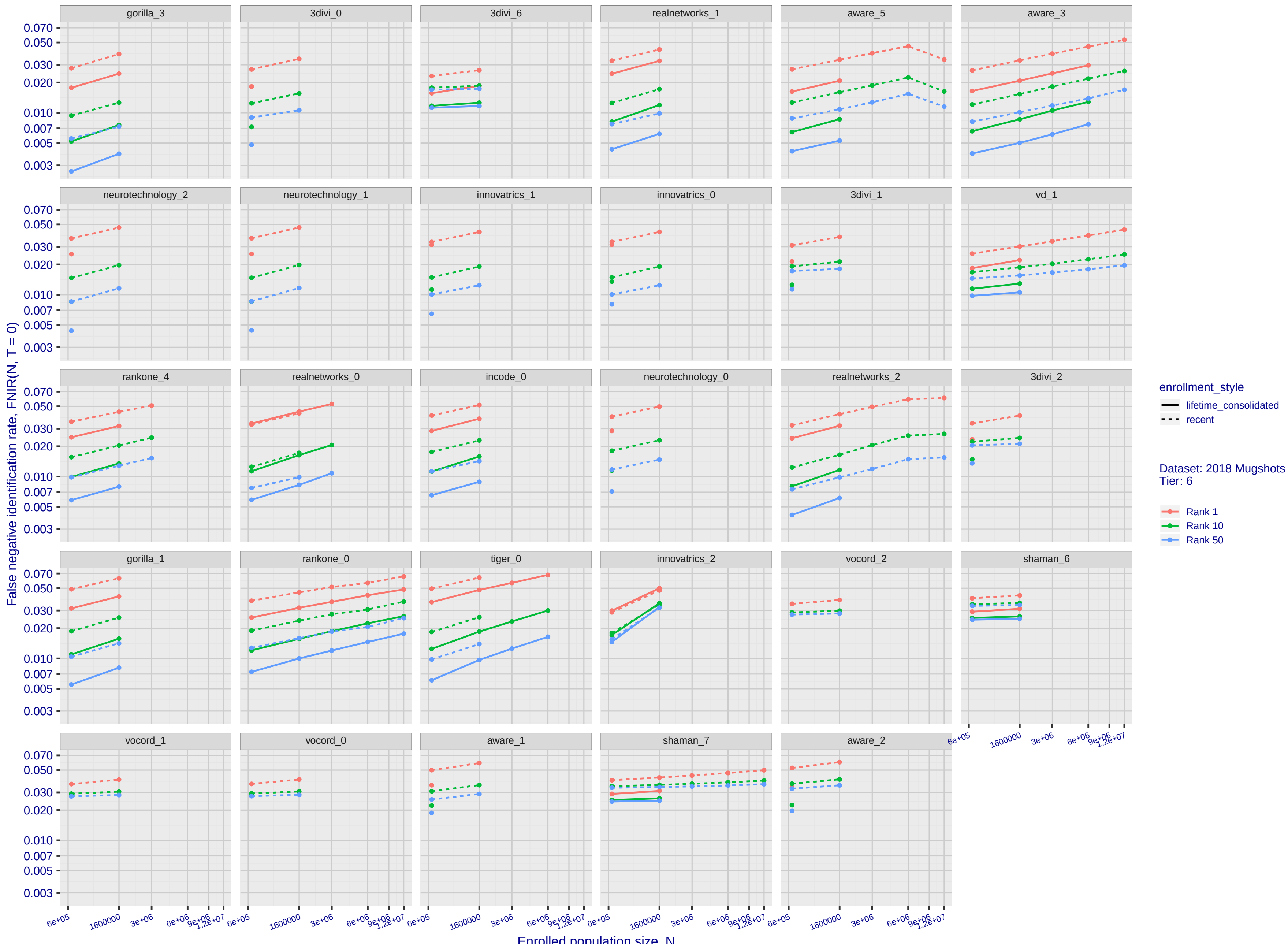

Figure 26: **[FRVT-2018 Mugshot Dataset] Rank-based identification miss rates vs. number of enrolled subjects**. *The figure shows false negative identification rates, FNIR(N, R), across various gallery sizes and ranks 1, 10 and 50. The threshold is set to zero, so this metric rewards even weak scoring rank 1 mates. This also means FPIR = 1, so any search without an enrolled mate will return non-mated candidates. For clarity, results are sorted and reported into tiers spanning multiple pages, the tiering criteria being rank 1 hit rate on a gallery size of 640 000.*

FNIR(N, R, T) = False neg. identification rate
FPIR(N, T) = False pos. identification rate
N = Num. enrolled subjects
R = Num. candidates examined
T = Threshold
T = 0 → Investigation
T > 0 → Identification

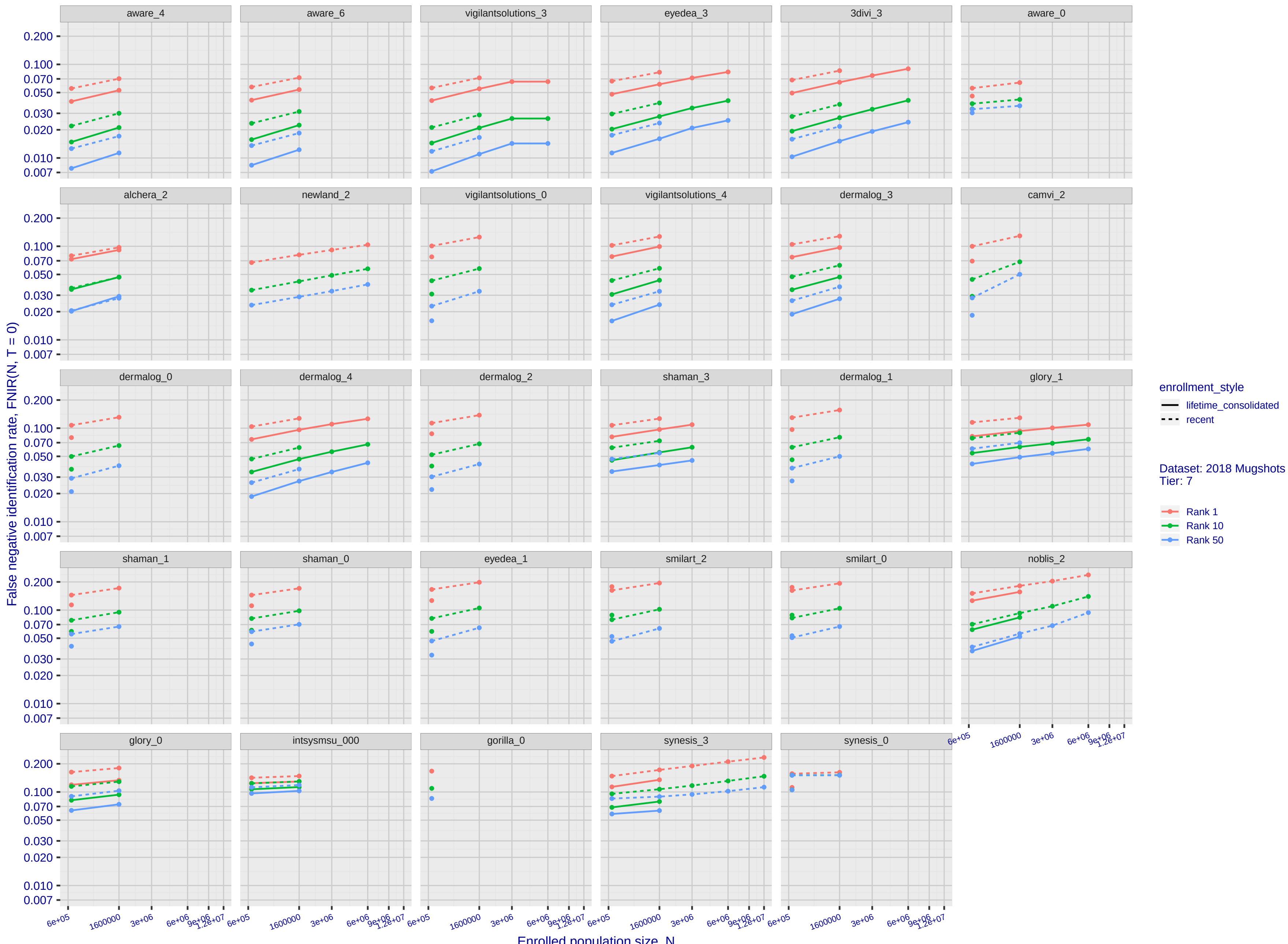

Figure 27: **[FRVT-2018 Mugshot Dataset] Rank-based identification miss rates vs. number of enrolled subjects**. *The figure shows false negative identification rates, FNIR(N, R), across various gallery sizes and ranks 1, 10 and 50. The threshold is set to zero, so this metric rewards even weak scoring rank 1 mates. This also means FPIR = 1, so any search without an enrolled mate will return non-mated candidates. For clarity, results are sorted and reported into tiers spanning multiple pages, the tiering criteria being rank 1 hit rate on a gallery size of 640 000.*

This publication is available free of charge from: https://doi.org/10.6028/NIST.IR.8271

2020/02/26 13:34:01

FNIR(N, R, T) = False neg. identification rate
FPIR(N, T) = False pos. identification rate
N = Num. enrolled subjects
R = Num. candidates examined
T = Threshold
T = 0 → Investigation
T > 0 → Identification

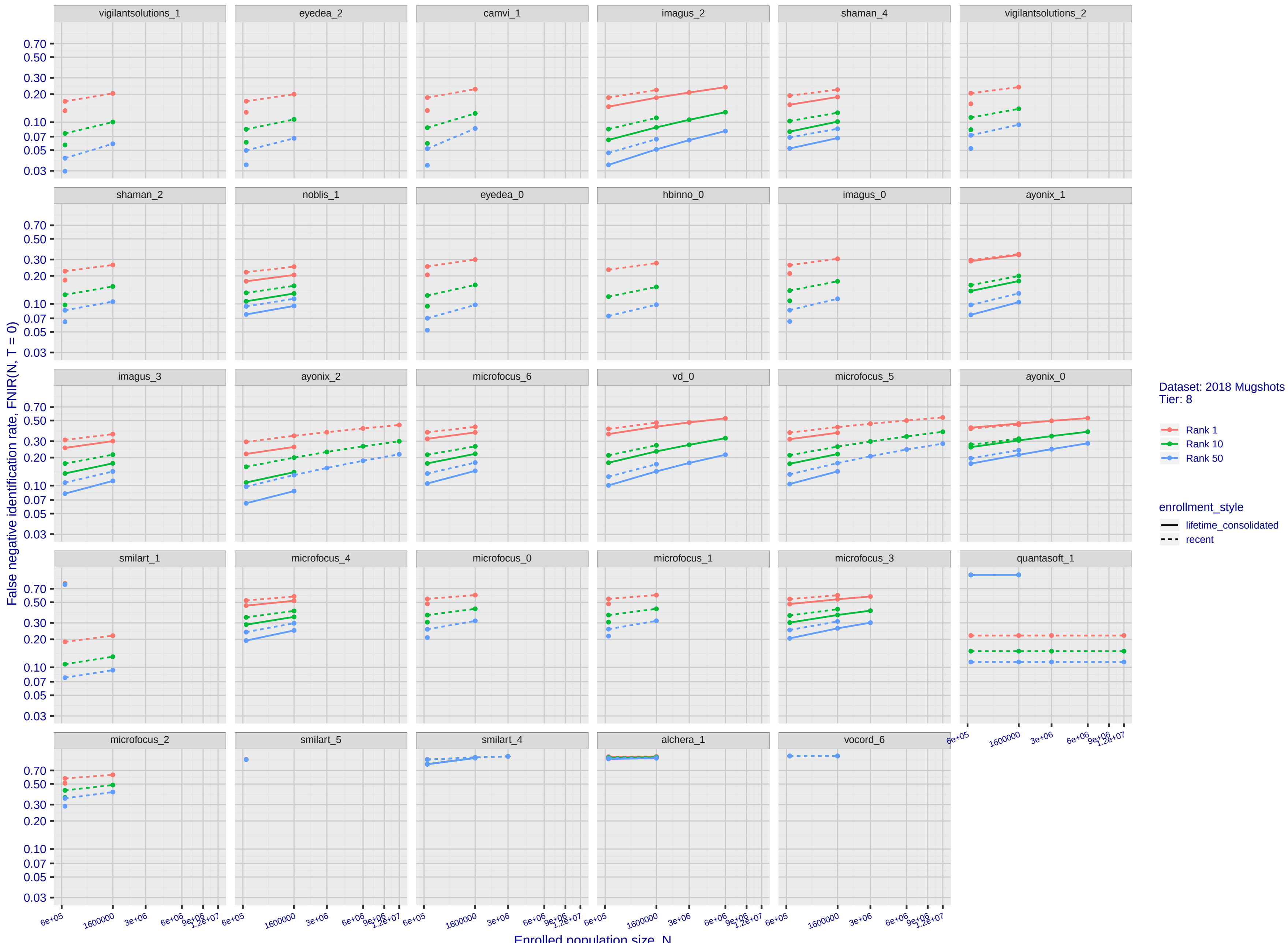

Figure 28: **[FRVT-2018 Mugshot Dataset] Rank-based identification miss rates vs. number of enrolled subjects**. *The figure shows false negative identification rates, FNIR(N, R), across various gallery sizes and ranks 1, 10 and 50. The threshold is set to zero, so this metric rewards even weak scoring rank 1 mates. This also means FPIR = 1, so any search without an enrolled mate will return non-mated candidates. For clarity, results are sorted and reported into tiers spanning multiple pages, the tiering criteria being rank 1 hit rate on a gallery size of 640 000.*

2020/02/26	FNIR(N, R, T) =	False neg. identification rate	N = Num. enrolled subjects	T = Threshold	$T = 0 \rightarrow$ Investigation
13:34:01	FPIR(N, T) =	False pos. identification rate	R = Num. candidates examined		$T > 0 \rightarrow$ Identification

FNIR(N, R, T) = False neg. identification rate
FPIR(N, T) = False pos. identification rate
N = Num. enrolled subjects
R = Num. candidates examined
T = Threshold
T = 0 → Investigation
T > 0 → Identification

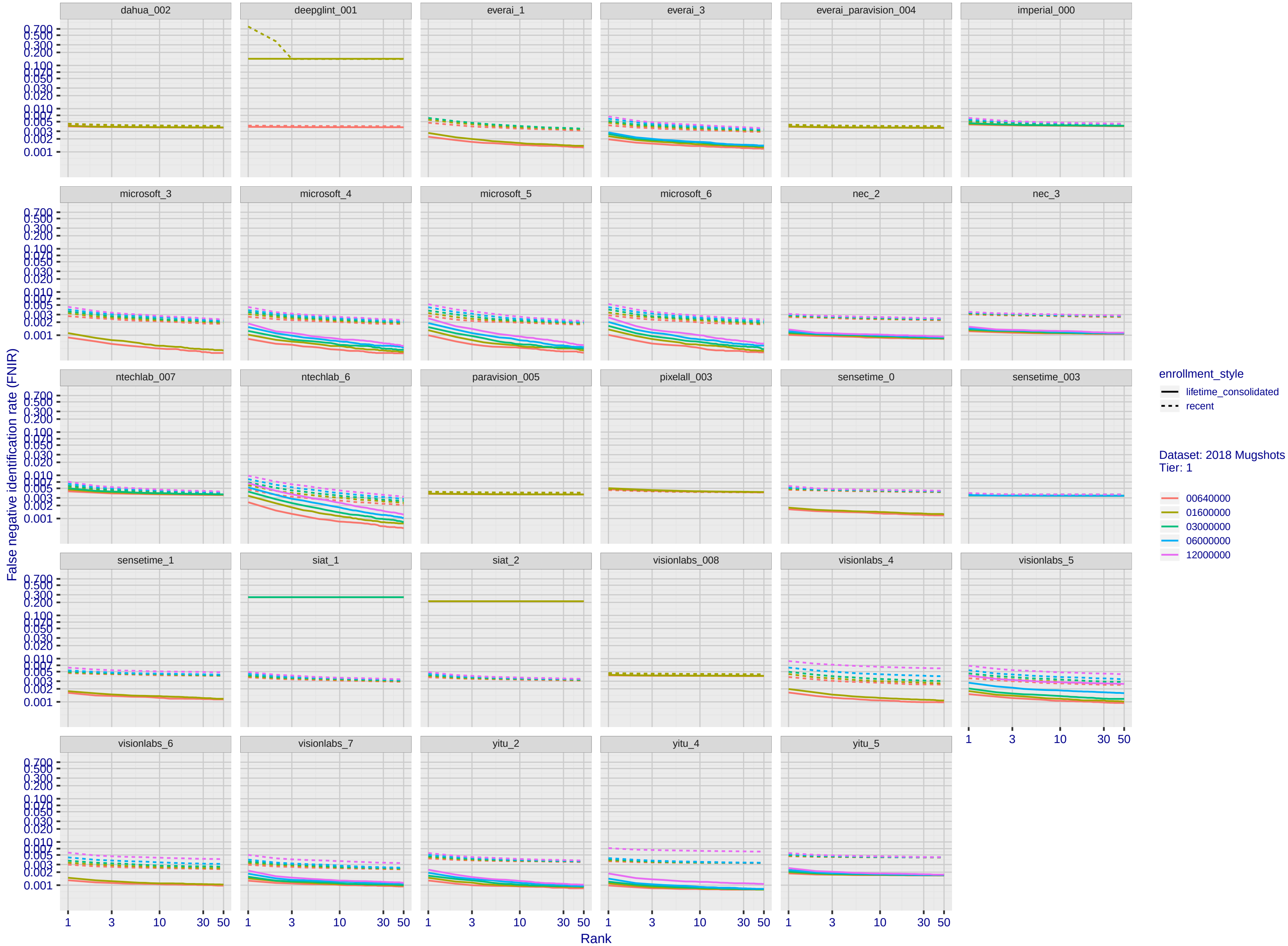

Figure 29: **[FRVT-2018 Mugshot Dataset] Rank-based identification miss rates vs. rank**. *The figure shows false negative identification rates (FNIR) for ranks up to 50. This metric is appropriate to investigational applications where human reviewers will adjudicate sorted candidate lists. Note that with threshold set to zero, FPIR = 1, i.e. any search without an enrolled mate will return non-mated candidates. Results are sorted and reported into tiers for clarity, with the tiering criteria being rank 1 hit rate on a gallery size of N = 640 000 subjects.*

FNIR(N, R, T) = False neg. identification rate
FPIR(N, T) = False pos. identification rate
N = Num. enrolled subjects
R = Num. candidates examined
T = Threshold
T = 0 → Investigation
T > 0 → Identification

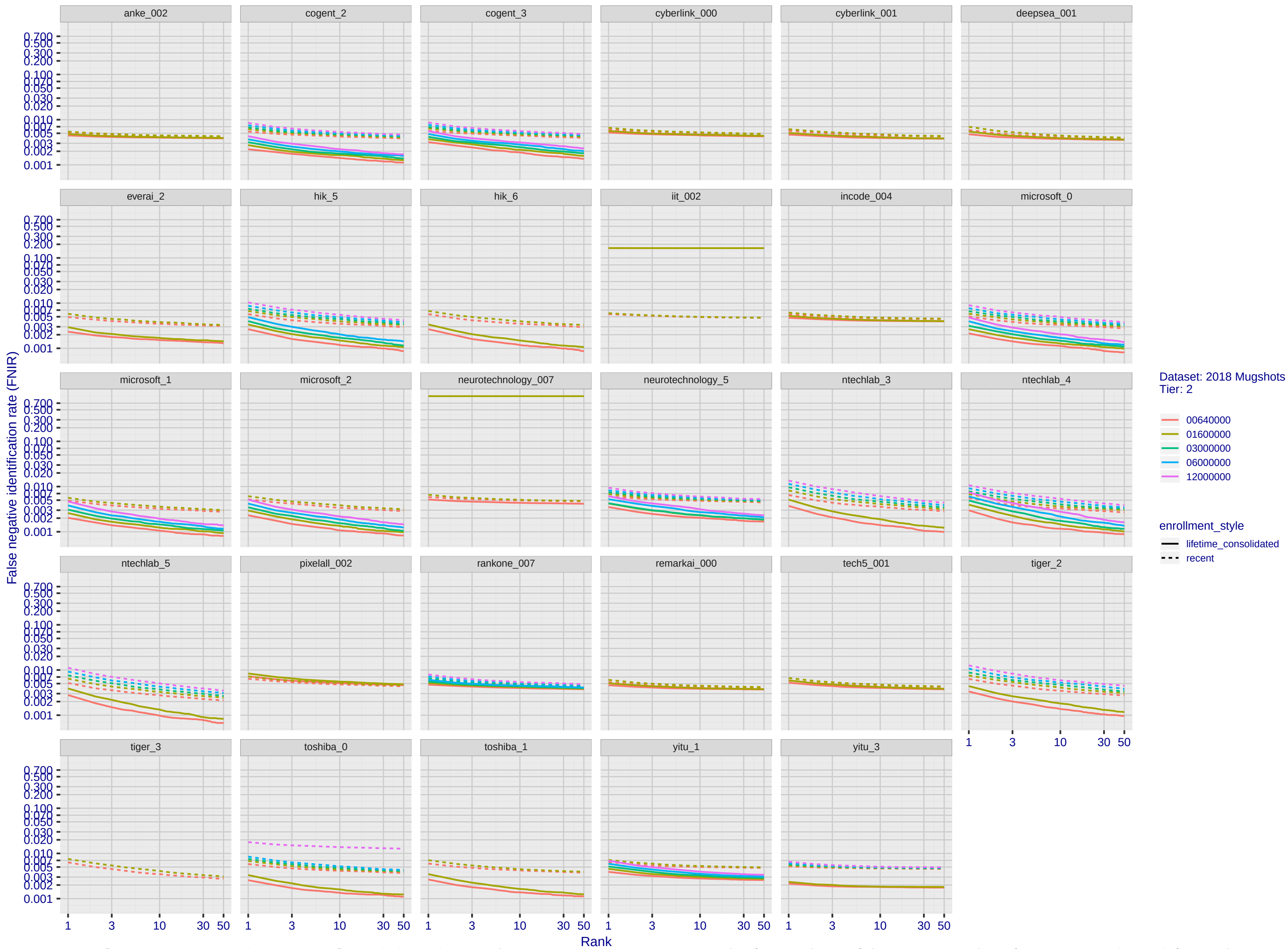

Figure 30: **[FRVT-2018 Mugshot Dataset] Rank-based identification miss rates vs. rank**. *The figure shows false negative identification rates (FNIR) for ranks up to 50. This metric is appropriate to investigational applications where human reviewers will adjudicate sorted candidate lists. Note that with threshold set to zero, FPIR = 1, i.e. any search without an enrolled mate will return non-mated candidates. Results are sorted and reported into tiers for clarity, with the tiering criteria being rank 1 hit rate on a gallery size of N = 640 000 subjects.*

This publication is available free of charge from: https://doi.org/10.6028/NIST.IR.8271

FNIR(N, R, T) = False neg. identification rate
FPIR(N, T) = False pos. identification rate
N = Num. enrolled subjects
R = Num. candidates examined
T = Threshold
T = 0 → Investigation
T > 0 → Identification

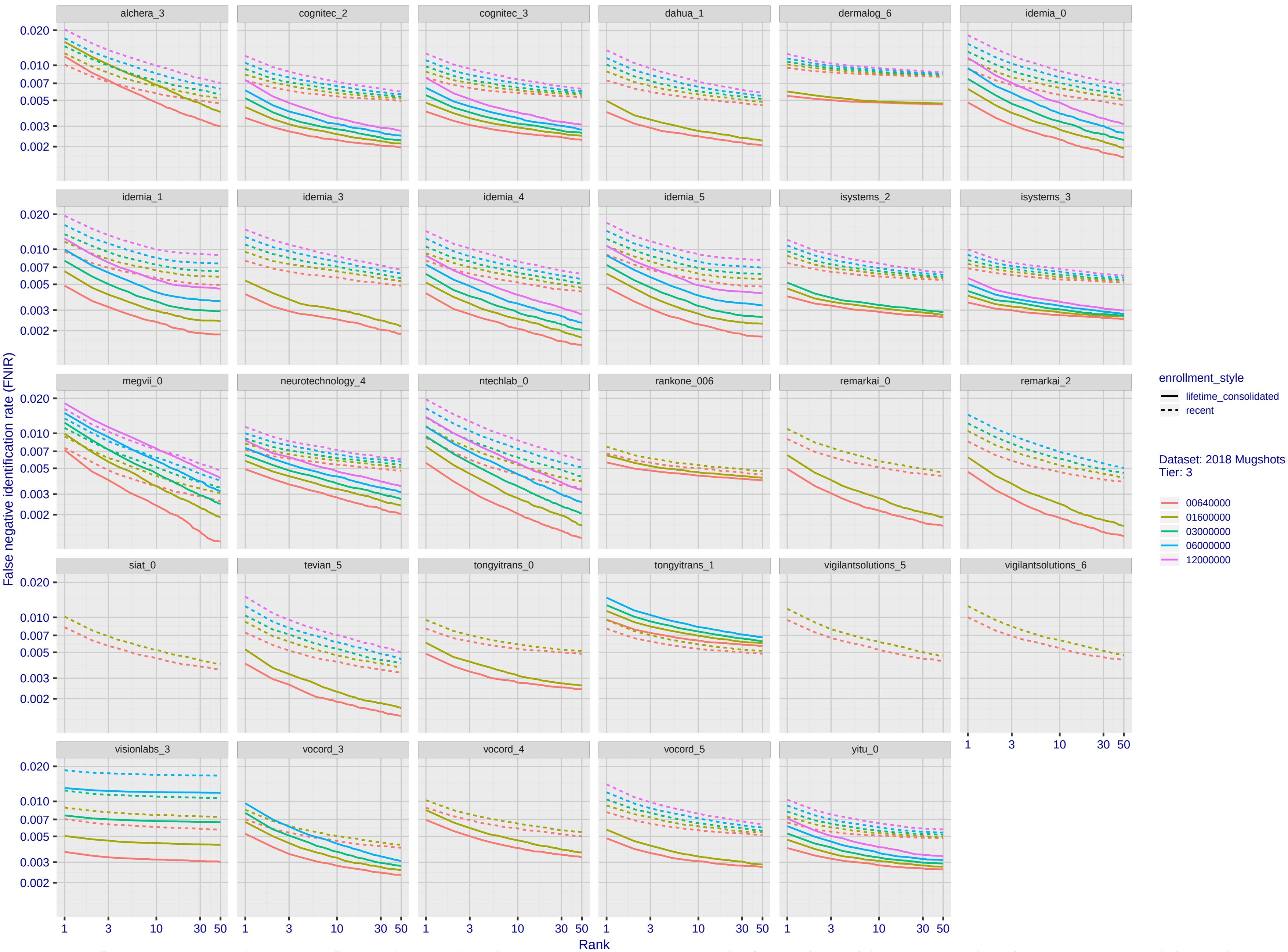

Figure 31: **[FRVT-2018 Mugshot Dataset] Rank-based identification miss rates vs. rank**. *The figure shows false negative identification rates (FNIR) for ranks up to 50. This metric is appropriate to investigational applications where human reviewers will adjudicate sorted candidate lists. Note that with threshold set to zero, FPIR = 1, i.e. any search without an enrolled mate will return non-mated candidates. Results are sorted and reported into tiers for clarity, with the tiering criteria being rank 1 hit rate on a gallery size of N = 640 000 subjects.*

This publication is available free of charge from: https://doi.org/10.6028/NIST.IR.8271

FNIR(N, R, T) = False neg. identification rate
FPIR(N, T) = False pos. identification rate
N = Num. enrolled subjects
R = Num. candidates examined
T = Threshold
T = 0 → Investigation
T > 0 → Identification

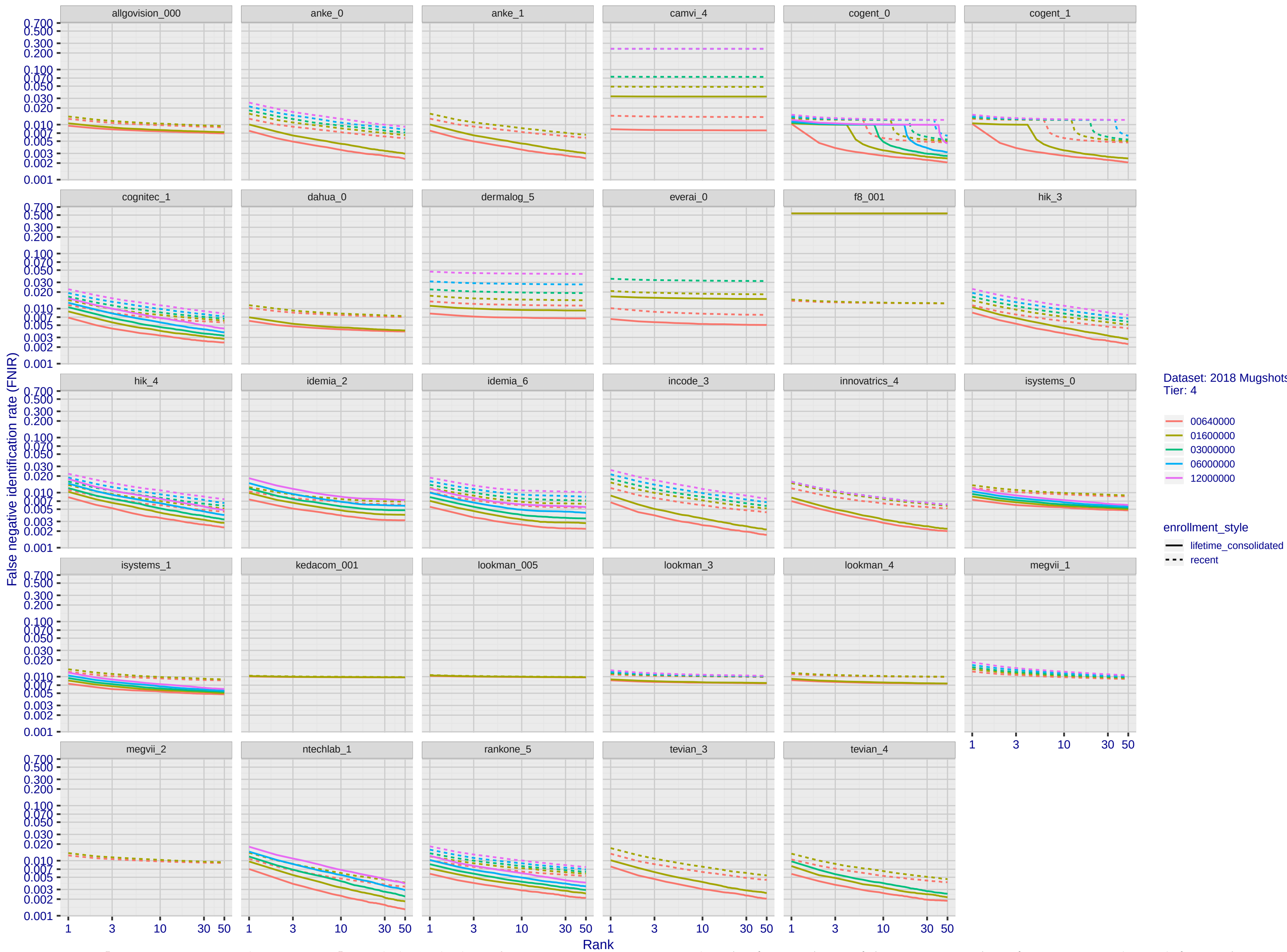

Figure 32: **[FRVT-2018 Mugshot Dataset] Rank-based identification miss rates vs. rank**. *The figure shows false negative identification rates (FNIR) for ranks up to 50. This metric is appropriate to investigational applications where human reviewers will adjudicate sorted candidate lists. Note that with threshold set to zero, FPIR = 1, i.e. any search without an enrolled mate will return non-mated candidates. Results are sorted and reported into tiers for clarity, with the tiering criteria being rank 1 hit rate on a gallery size of N = 640 000 subjects.*

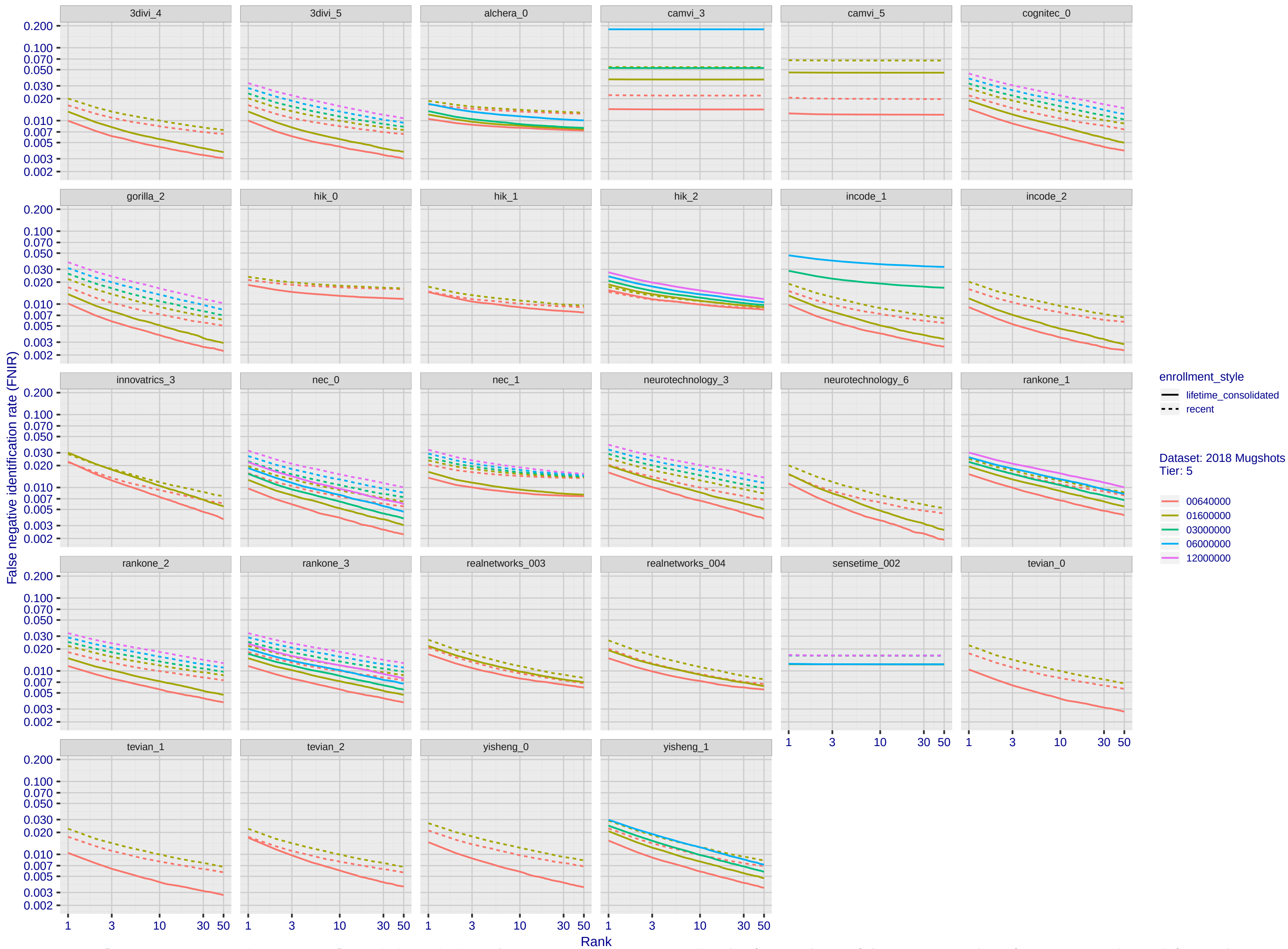

Figure 33: **[FRVT-2018 Mugshot Dataset] Rank-based identification miss rates vs. rank**. *The figure shows false negative identification rates (FNIR) for ranks up to 50. This metric is appropriate to investigational applications where human reviewers will adjudicate sorted candidate lists. Note that with threshold set to zero, FPIR = 1, i.e. any search without an enrolled mate will return non-mated candidates. Results are sorted and reported into tiers for clarity, with the tiering criteria being rank 1 hit rate on a gallery size of N = 640 000 subjects.*

This publication is available free of charge from: https://doi.org/10.6028/NIST.IR.8271

FNIR(N, R, T) = False neg. identification rate
FPIR(N, T) = False pos. identification rate
N = Num. enrolled subjects
R = Num. candidates examined
T = Threshold
T = 0 → Investigation
T > 0 → Identification

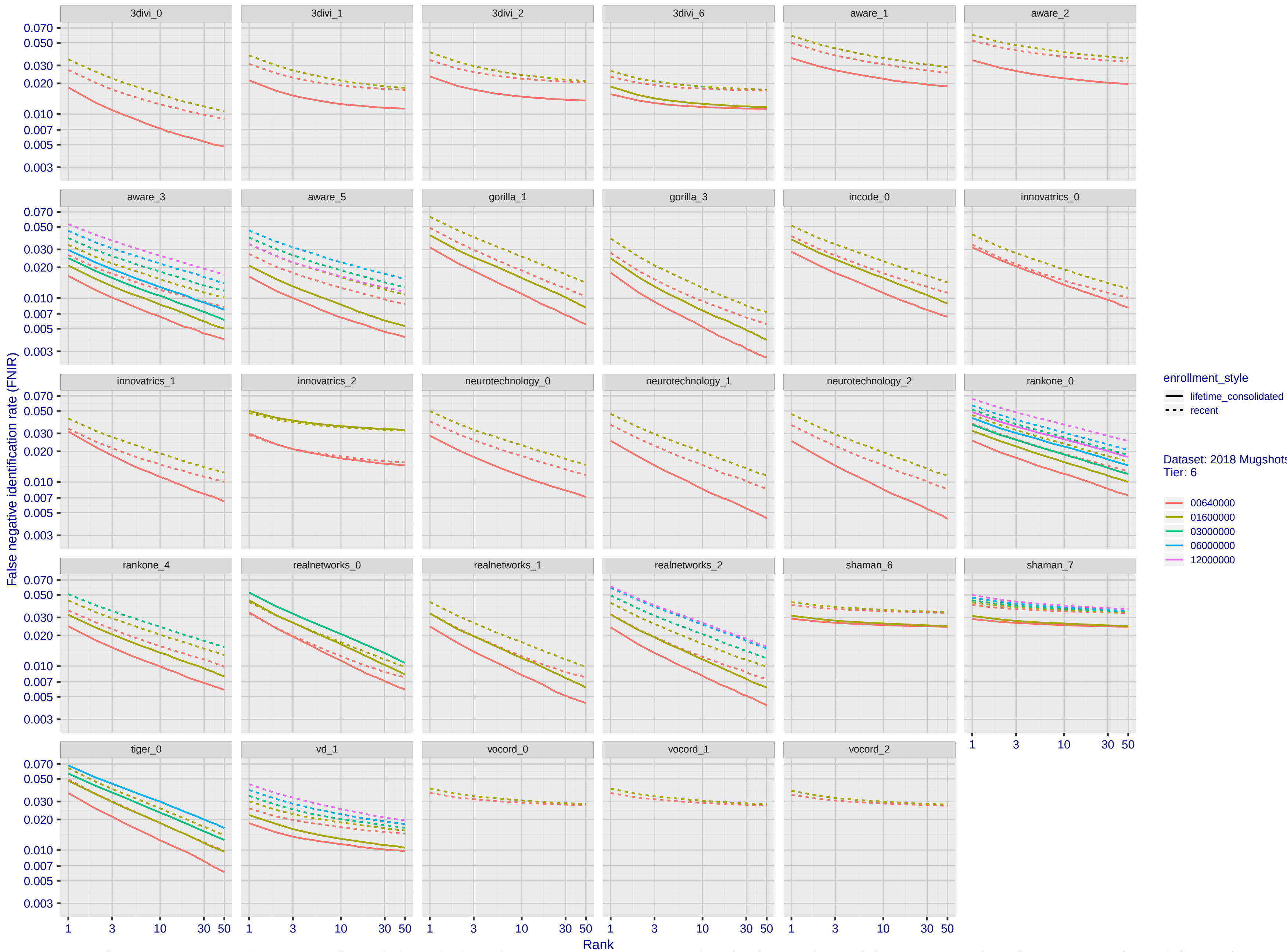

Figure 34: **[FRVT-2018 Mugshot Dataset] Rank-based identification miss rates vs. rank**. *The figure shows false negative identification rates (FNIR) for ranks up to 50. This metric is appropriate to investigational applications where human reviewers will adjudicate sorted candidate lists. Note that with threshold set to zero, FPIR = 1, i.e. any search without an enrolled mate will return non-mated candidates. Results are sorted and reported into tiers for clarity, with the tiering criteria being rank 1 hit rate on a gallery size of N = 640 000 subjects.*

This publication is available free of charge from: https://doi.org/10.6028/NIST.IR.8271

FNIR(N, R, T) = False neg. identification rate
FPIR(N, T) = False pos. identification rate
N = Num. enrolled subjects
R = Num. candidates examined
T = Threshold
T = 0 → Investigation
T > 0 → Identification

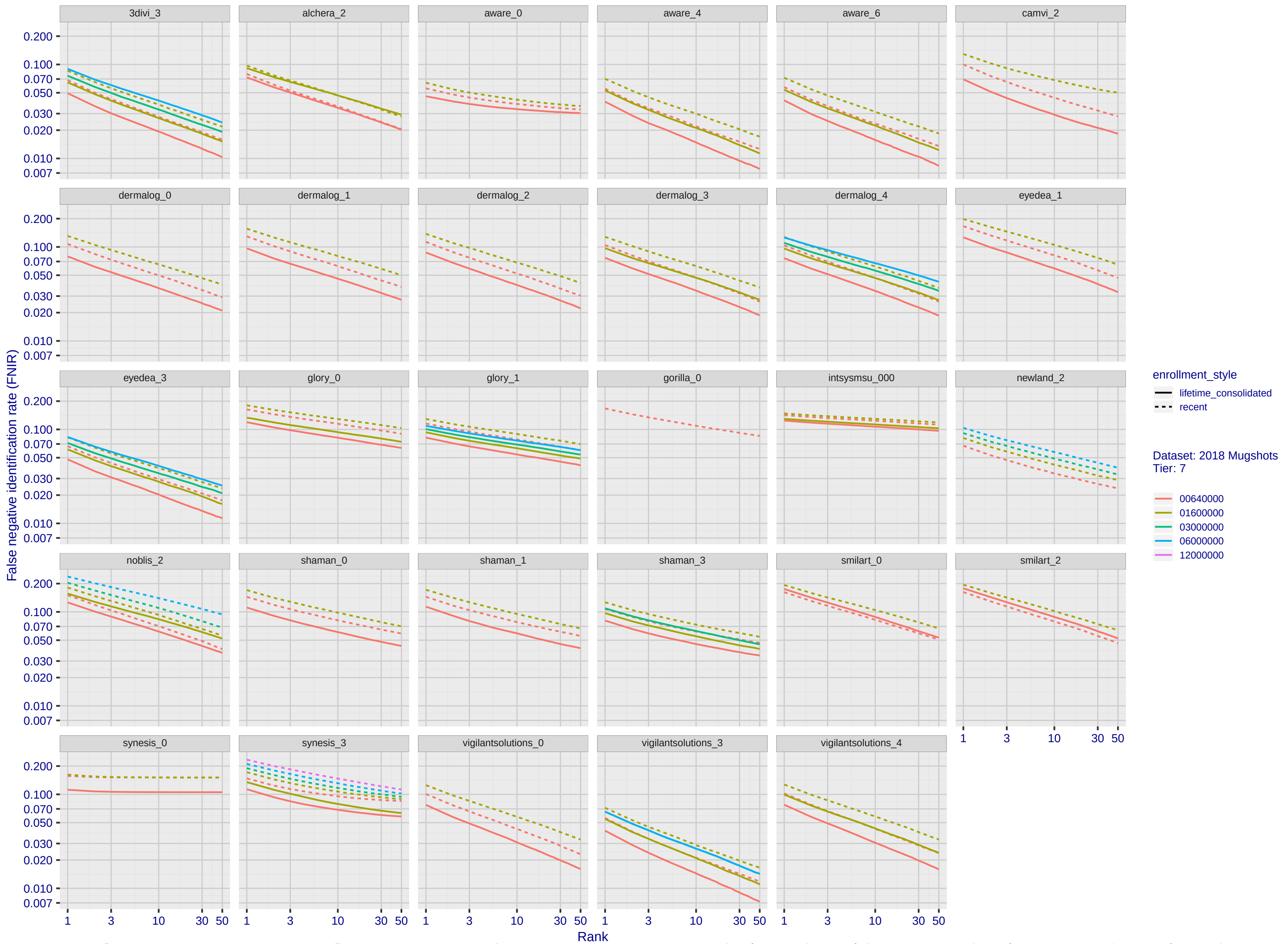

Figure 35: **[FRVT-2018 Mugshot Dataset] Rank-based identification miss rates vs. rank**. *The figure shows false negative identification rates (FNIR) for ranks up to 50. This metric is appropriate to investigational applications where human reviewers will adjudicate sorted candidate lists. Note that with threshold set to zero, FPIR = 1, i.e. any search without an enrolled mate will return non-mated candidates. Results are sorted and reported into tiers for clarity, with the tiering criteria being rank 1 hit rate on a gallery size of N = 640 000 subjects.*

FNIR(N, R, T) = False neg. identification rate
FPIR(N, T) = False pos. identification rate
N = Num. enrolled subjects
R = Num. candidates examined
T = Threshold
T = 0 → Investigation
T > 0 → Identification

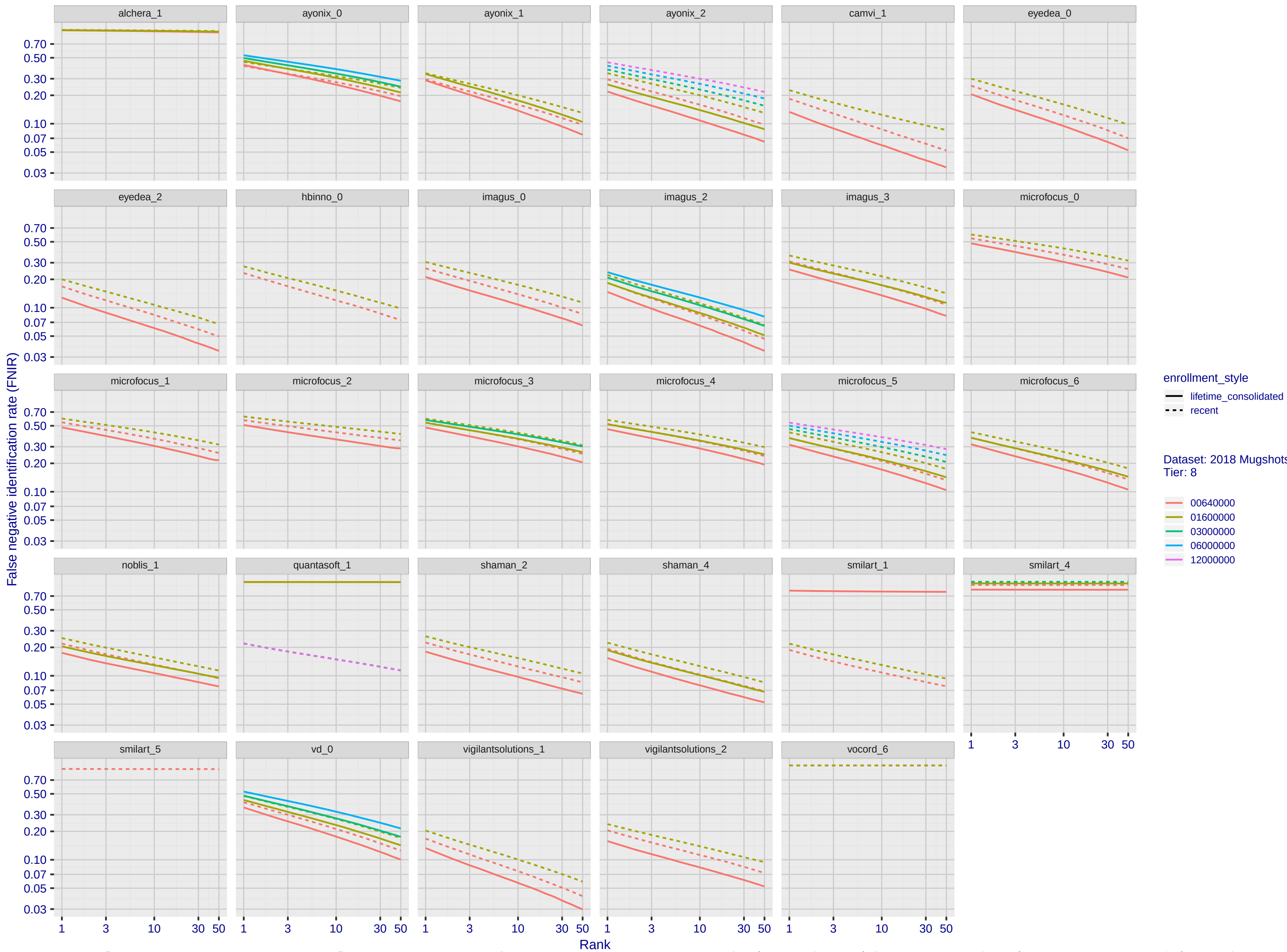

Figure 36: **[FRVT-2018 Mugshot Dataset] Rank-based identification miss rates vs. rank**. *The figure shows false negative identification rates (FNIR) for ranks up to 50. This metric is appropriate to investigational applications where human reviewers will adjudicate sorted candidate lists. Note that with threshold set to zero, FPIR = 1, i.e. any search without an enrolled mate will return non-mated candidates. Results are sorted and reported into tiers for clarity, with the tiering criteria being rank 1 hit rate on a gallery size of N = 640 000 subjects.*

2020/02/26	FNIR(N, R, T) =	False neg. identification rate	N = Num. enrolled subjects	T = Threshold	$T = 0 \rightarrow$ Investigation
13:34:01	FPIR(N, T) =	False pos. identification rate	R = Num. candidates examined		$T > 0 \rightarrow$ Identification

FNIR(N, R, T) = False neg. identification rate
FPIR(N, T) = False pos. identification rate
N = Num. enrolled subjects
R = Num. candidates examined
T = Threshold
T = 0 → Investigation
T > 0 → Identification

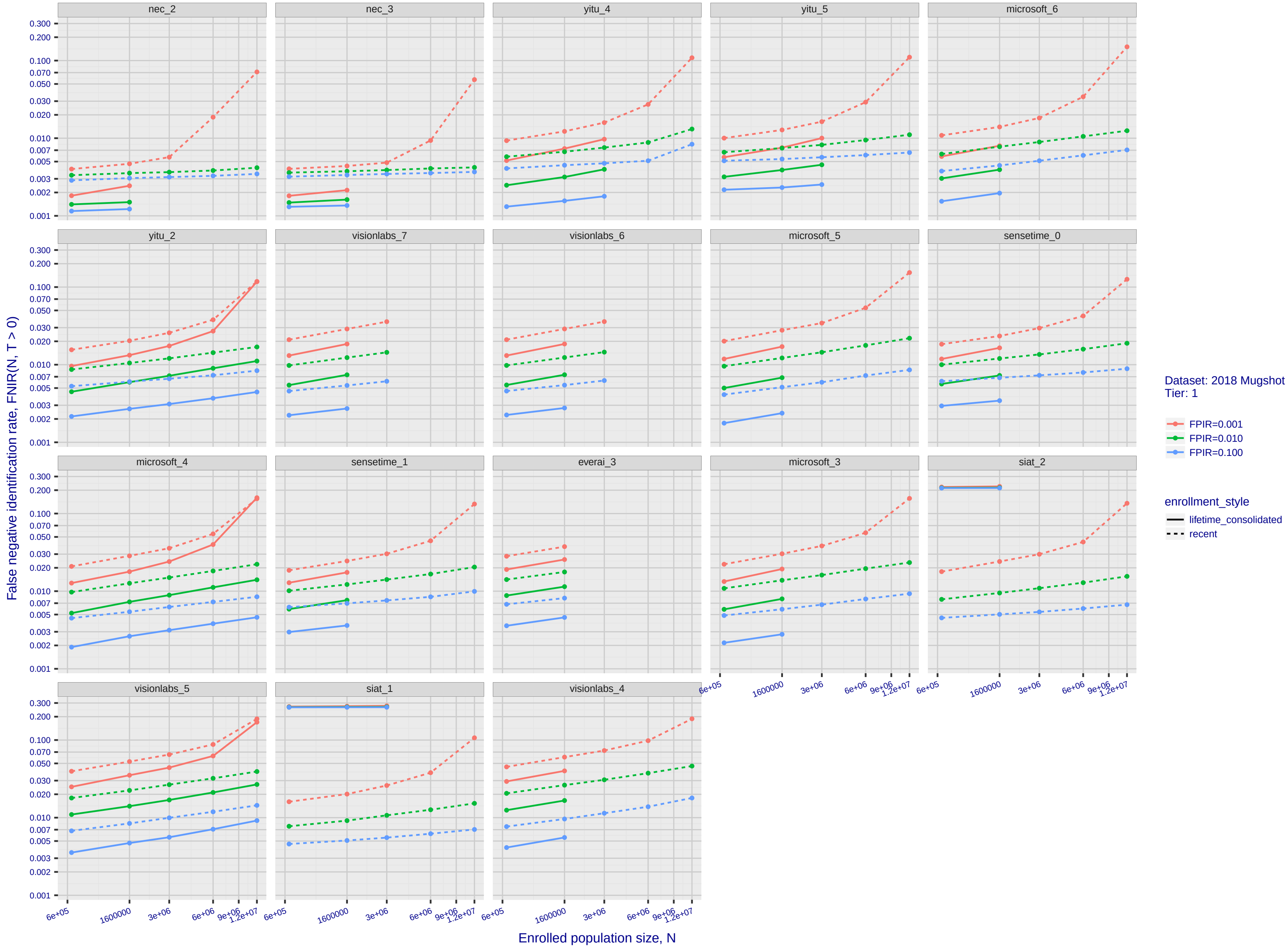

Figure 37: **[FRVT-2018 Mugshot Dataset] Threshold-based identification miss rates vs. number of enrolled subjects**. *The figure shows FNIR(N, T) across various gallery sizes when the threshold is set to achieve the given FPIRs. The rank criterion is irrelevant at high thresholds as mates are always at rank 1. The results are computed from the trials listed in rows 1-10 of Table 1. Less accurate algorithms were not run on large N, so results are missing. For clarity, results are sorted and reported into tiers spanning multiple pages. The tiering criteria is complicated: First paging by FNIR(N_b, 1, 0), then sorting by median FNIR(N_b, T), N_b = 640 000.*

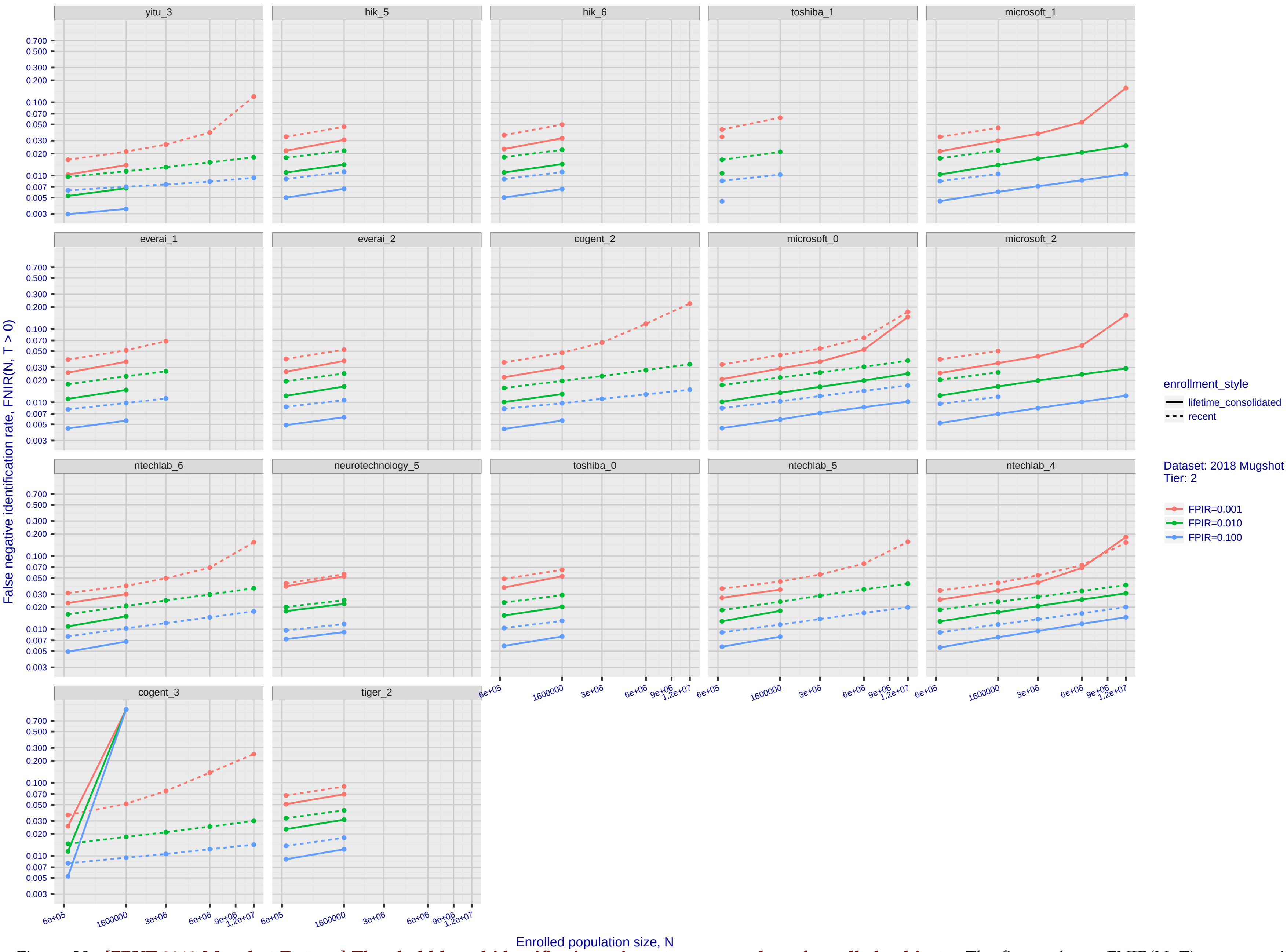

Figure 38: **[FRVT-2018 Mugshot Dataset] Threshold-based identification miss rates vs. number of enrolled subjects**. *The figure shows FNIR(N, T) across various gallery sizes when the threshold is set to achieve the given FPIRs. The rank criterion is irrelevant at high thresholds as mates are always at rank 1. The results are computed from the trials listed in rows 1-10 of Table 1. Less accurate algorithms were not run on large N, so results are missing. For clarity, results are sorted and reported into tiers spanning multiple pages. The tiering criteria is complicated: First paging by FNIR(N_b, 1, 0), then sorting by median FNIR(N_b, T), N_b = 640 000.*

FNIR(N, R, T) = False neg. identification rate
FPIR(N, T) = False pos. identification rate
N = Num. enrolled subjects
R = Num. candidates examined
T = Threshold
T = 0 → Investigation
T > 0 → Identification

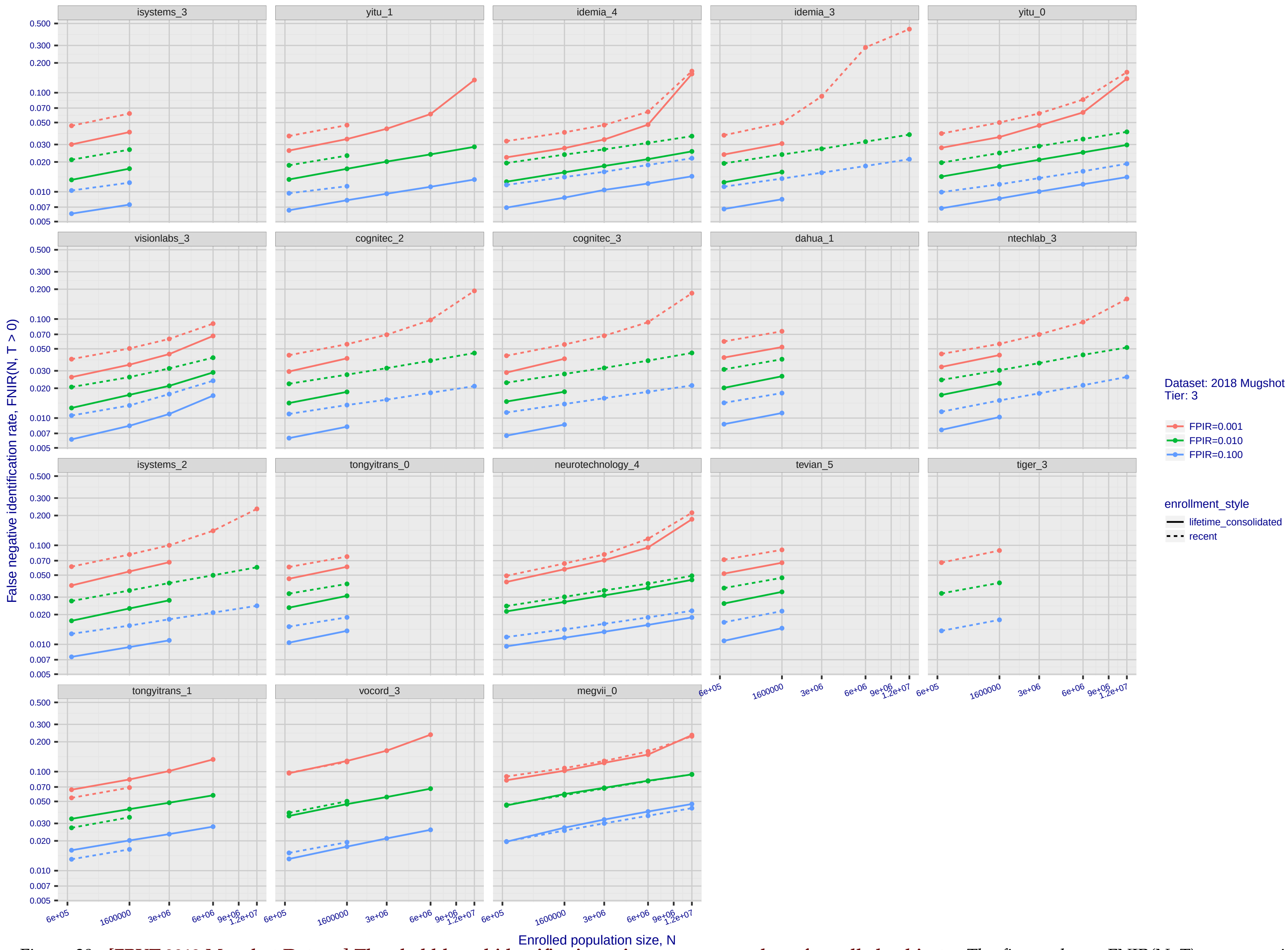

Figure 39: **[FRVT-2018 Mugshot Dataset] Threshold-based identification miss rates vs. number of enrolled subjects**. *The figure shows FNIR(N, T) across various gallery sizes when the threshold is set to achieve the given FPIRs. The rank criterion is irrelevant at high thresholds as mates are always at rank 1. The results are computed from the trials listed in rows 1-10 of Table 1. Less accurate algorithms were not run on large N, so results are missing. For clarity, results are sorted and reported into tiers spanning multiple pages. The tiering criteria is complicated: First paging by FNIR(N_b, 1, 0), then sorting by median FNIR(N_b, T), N_b = 640 000.*

This publication is available free of charge from: https://doi.org/10.6028/NIST.IR.8271

FNIR(N, R, T) = False neg. identification rate
FPIR(N, T) = False pos. identification rate
N = Num. enrolled subjects
R = Num. candidates examined
T = Threshold
T = 0 → Investigation
T > 0 → Identification

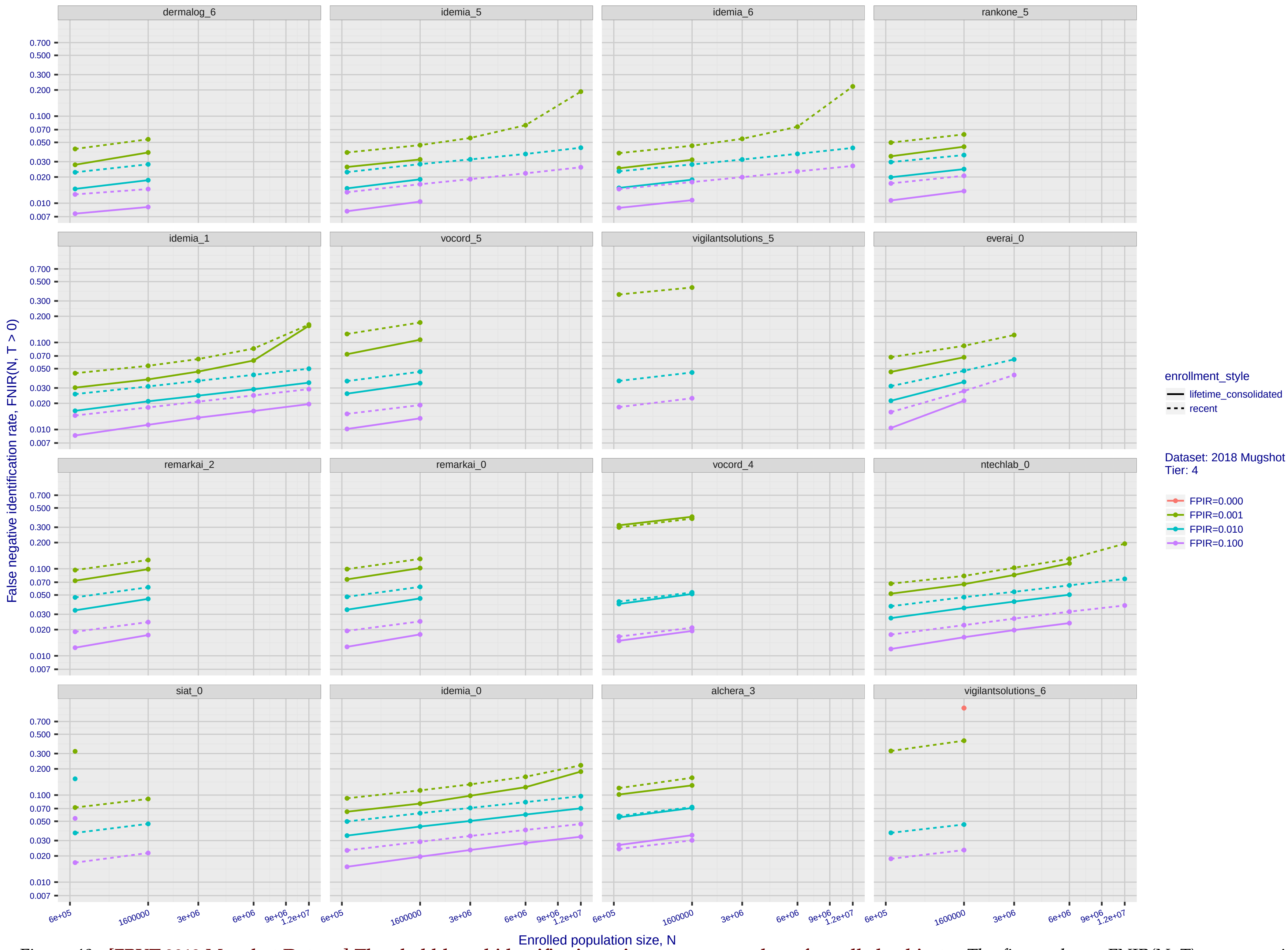

Figure 40: **[FRVT-2018 Mugshot Dataset] Threshold-based identification miss rates vs. number of enrolled subjects**. *The figure shows FNIR(N, T) across various gallery sizes when the threshold is set to achieve the given FPIRs. The rank criterion is irrelevant at high thresholds as mates are always at rank 1. The results are computed from the trials listed in rows 1-10 of Table 1. Less accurate algorithms were not run on large N, so results are missing. For clarity, results are sorted and reported into tiers spanning multiple pages. The tiering criteria is complicated: First paging by FNIR(N_b, 1, 0), then sorting by median FNIR(N_b, T), N_b = 640 000.*

FNIR(N, R, T) = False neg. identification rate
FPIR(N, T) = False pos. identification rate
N = Num. enrolled subjects
R = Num. candidates examined
T = Threshold
T = 0 → Investigation
T > 0 → Identification

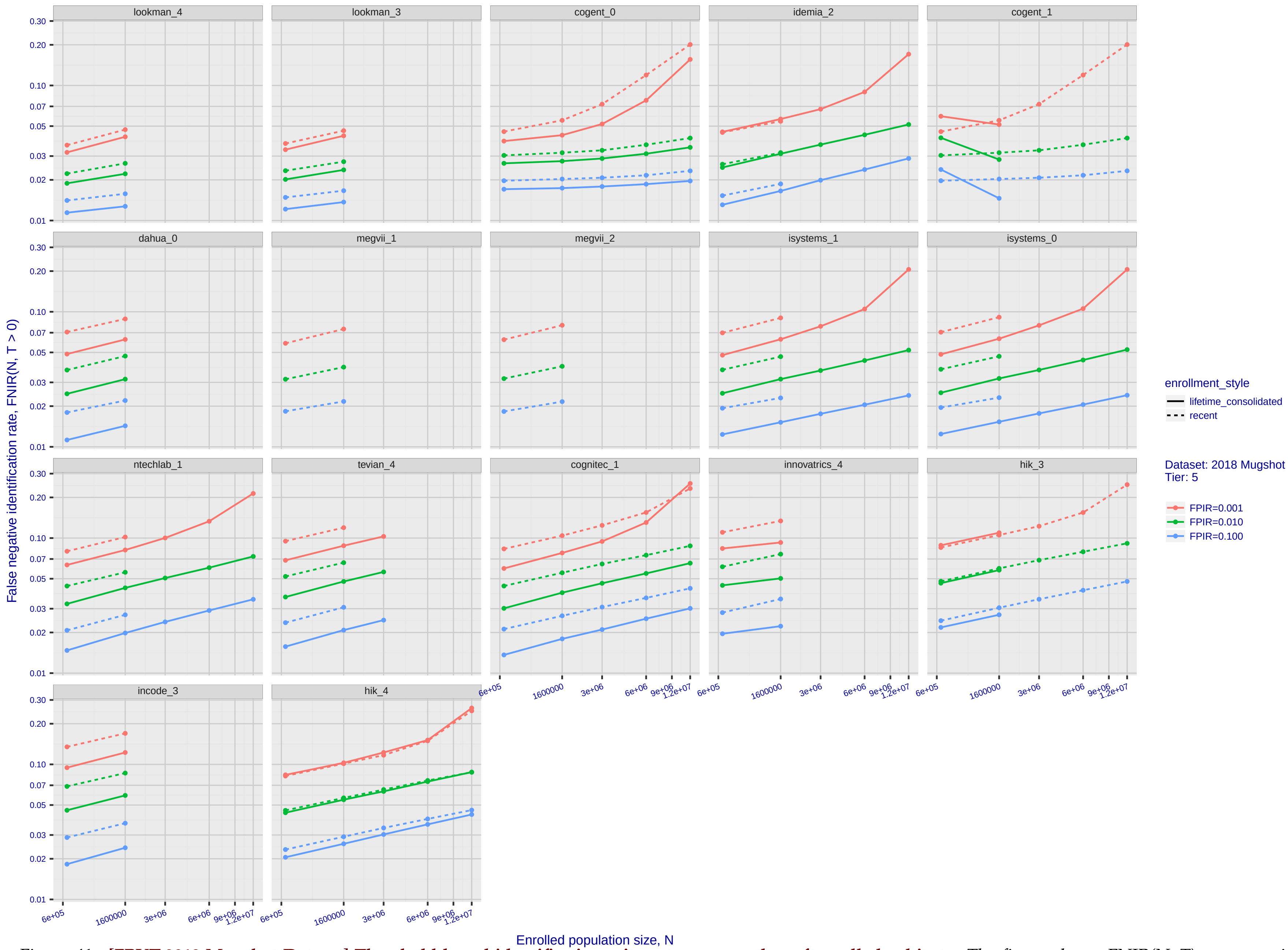

Figure 41: **[FRVT-2018 Mugshot Dataset] Threshold-based identification miss rates vs. number of enrolled subjects**. *The figure shows FNIR(N, T) across various gallery sizes when the threshold is set to achieve the given FPIRs. The rank criterion is irrelevant at high thresholds as mates are always at rank 1. The results are computed from the trials listed in rows 1-10 of Table 1. Less accurate algorithms were not run on large N, so results are missing. For clarity, results are sorted and reported into tiers spanning multiple pages. The tiering criteria is complicated: First paging by FNIR(N_b, 1, 0), then sorting by median FNIR(N_b, T), N_b = 640 000.*

2020/02/26
13:34:01

FNIR(N, R, T) = False neg. identification rate
FPIR(N, T) = False pos. identification rate
N = Num. enrolled subjects
R = Num. candidates examined
T = Threshold
T = 0 → Investigation
T > 0 → Identification

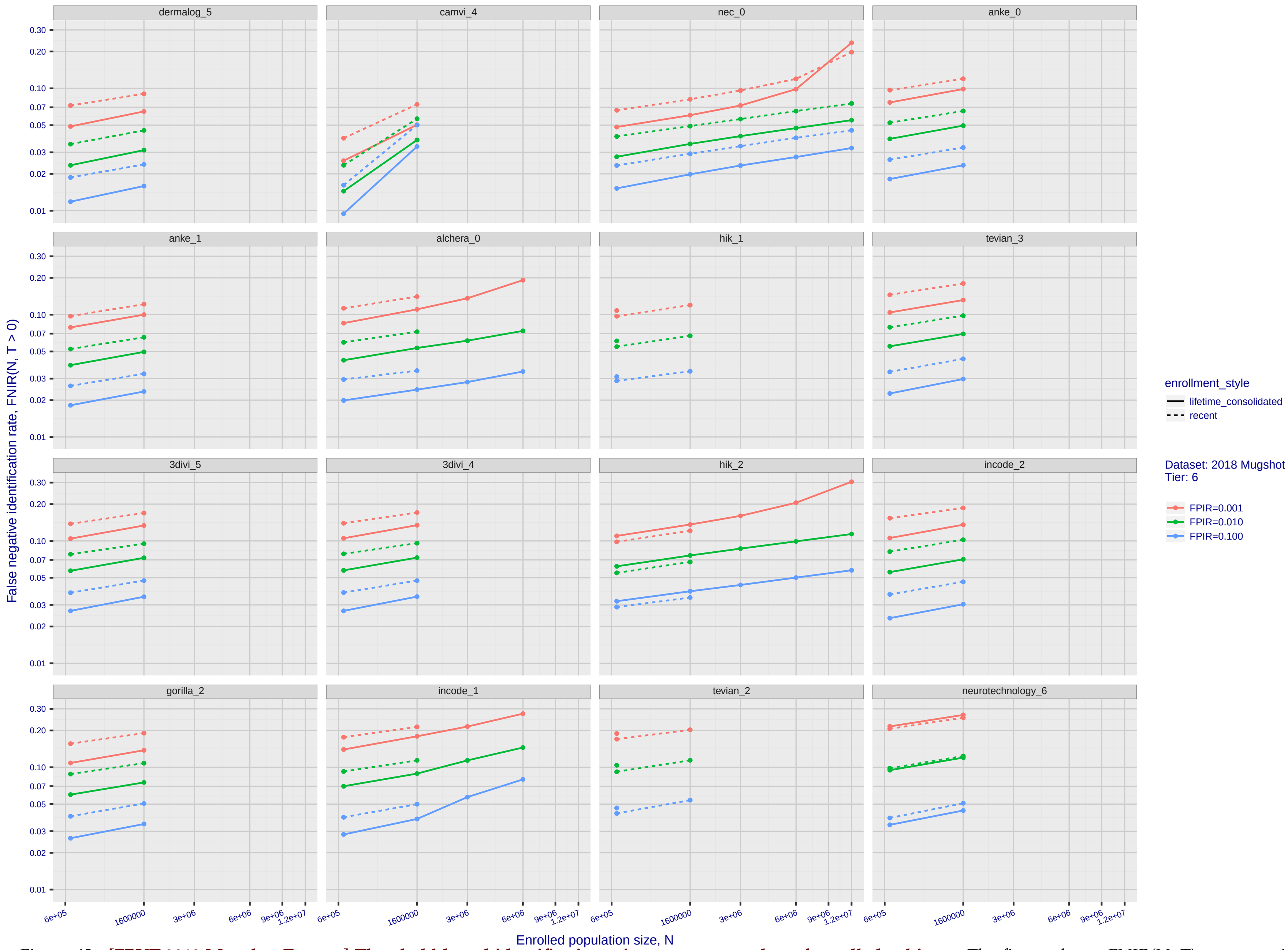

Figure 42: **[FRVT-2018 Mugshot Dataset] Threshold-based identification miss rates vs. number of enrolled subjects**. *The figure shows FNIR(N, T) across various gallery sizes when the threshold is set to achieve the given FPIRs. The rank criterion is irrelevant at high thresholds as mates are always at rank 1. The results are computed from the trials listed in rows 1-10 of Table 1. Less accurate algorithms were not run on large N, so results are missing. For clarity, results are sorted and reported into tiers spanning multiple pages. The tiering criteria is complicated: First paging by FNIR(N_b, 1, 0), then sorting by median FNIR(N_b, T), N_b = 640 000.*

FNIR(N, R, T) = False neg. identification rate
FPIR(N, T) = False pos. identification rate
N = Num. enrolled subjects
R = Num. candidates examined
T = Threshold
T = 0 → Investigation
T > 0 → Identification

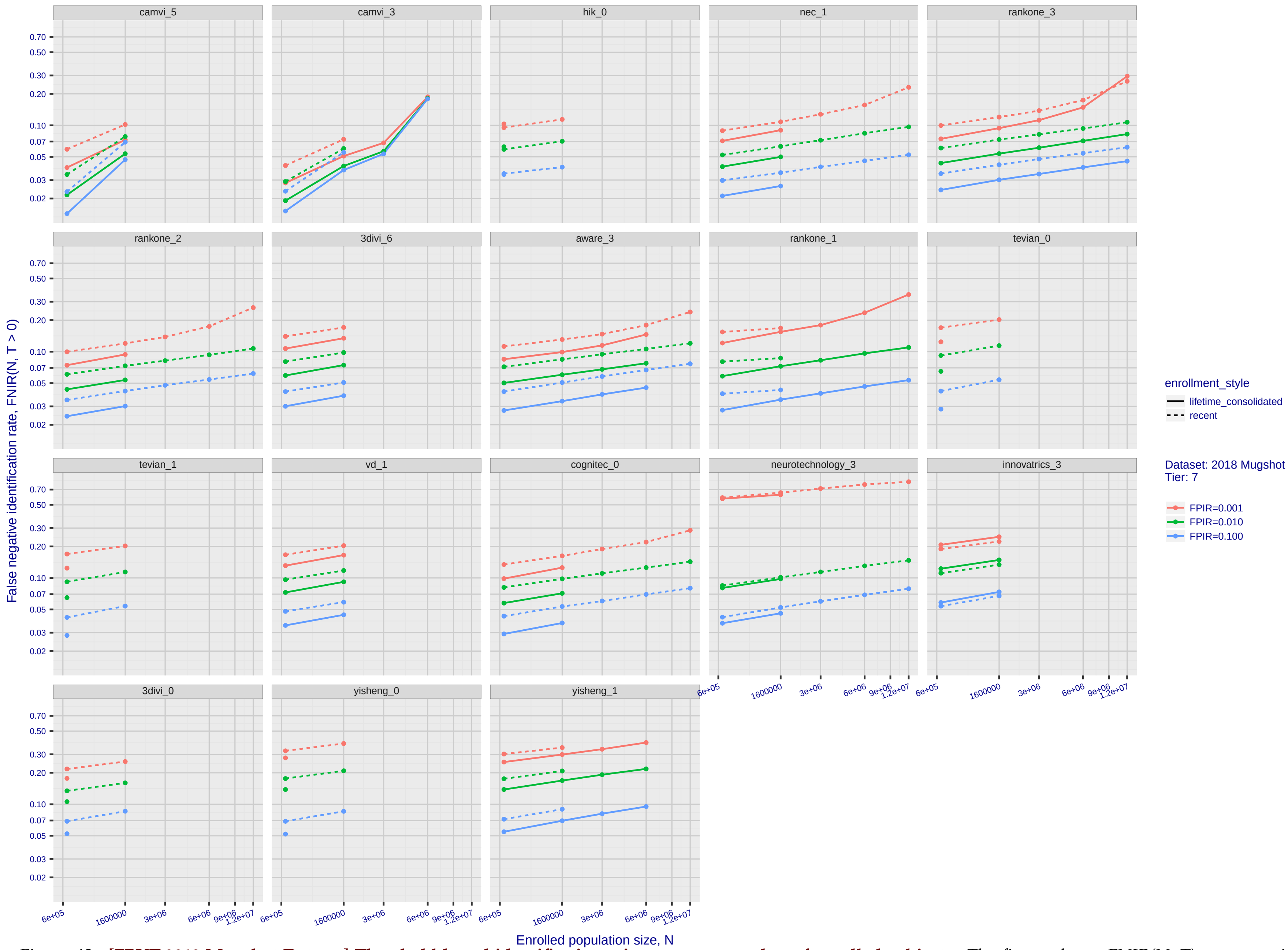

Figure 43: **[FRVT-2018 Mugshot Dataset] Threshold-based identification miss rates vs. number of enrolled subjects**. *The figure shows FNIR(N, T) across various gallery sizes when the threshold is set to achieve the given FPIRs. The rank criterion is irrelevant at high thresholds as mates are always at rank 1. The results are computed from the trials listed in rows 1-10 of Table 1. Less accurate algorithms were not run on large N, so results are missing. For clarity, results are sorted and reported into tiers spanning multiple pages. The tiering criteria is complicated: First paging by FNIR(N_b, 1, 0), then sorting by median FNIR(N_b, T), N_b = 640 000.*

This publication is available free of charge from: https://doi.org/10.6028/NIST.IR.8271

2020/02/26 13:34:01

FNIR(N, R, T) = False neg. identification rate
FPIR(N, T) = False pos. identification rate
N = Num. enrolled subjects
R = Num. candidates examined
T = Threshold
T = 0 → Investigation
T > 0 → Identification

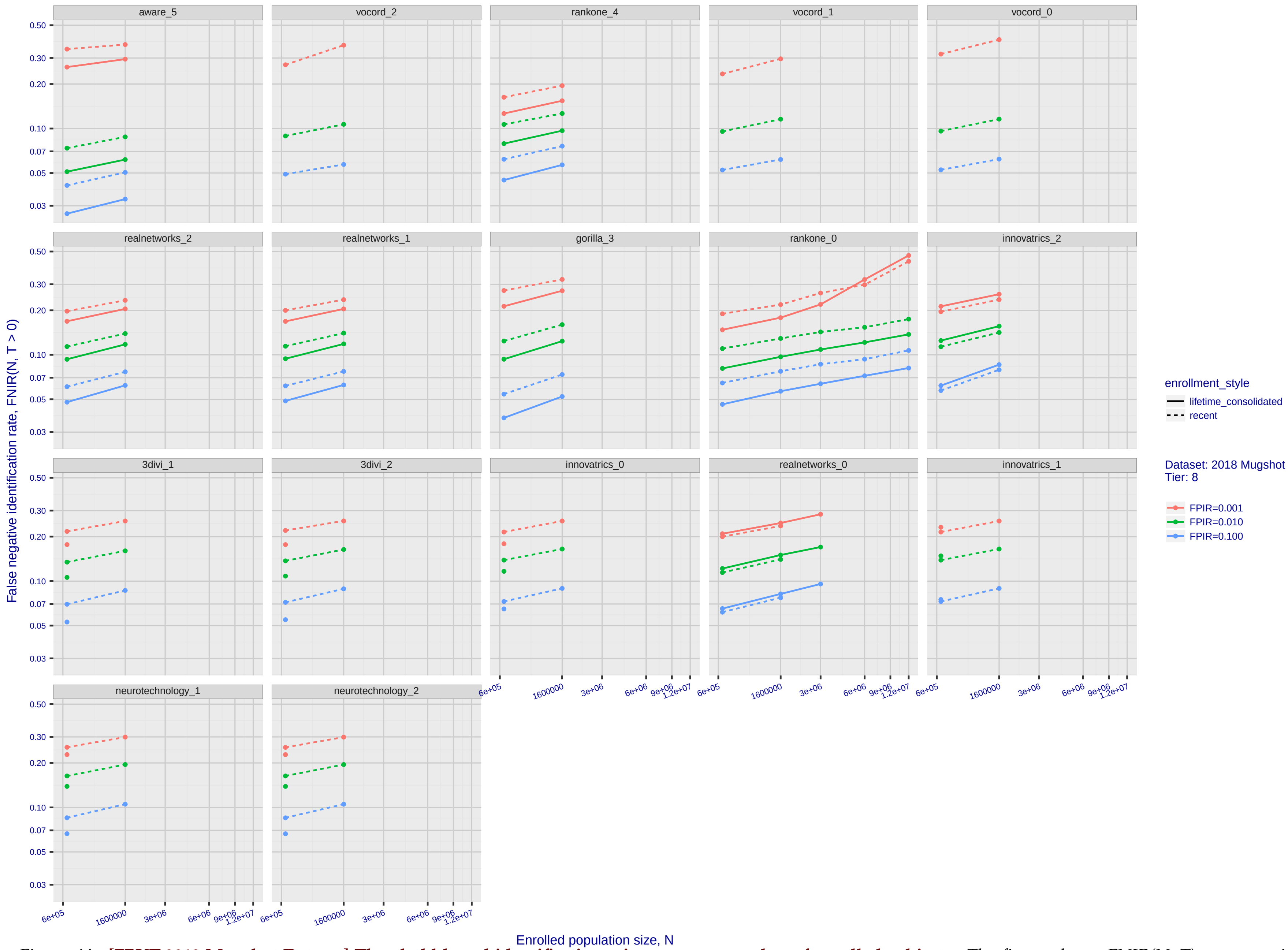

Figure 44: **[FRVT-2018 Mugshot Dataset] Threshold-based identification miss rates vs. number of enrolled subjects**. *The figure shows FNIR(N, T) across various gallery sizes when the threshold is set to achieve the given FPIRs. The rank criterion is irrelevant at high thresholds as mates are always at rank 1. The results are computed from the trials listed in rows 1-10 of Table 1. Less accurate algorithms were not run on large N, so results are missing. For clarity, results are sorted and reported into tiers spanning multiple pages. The tiering criteria is complicated: First paging by FNIR(N_b, 1, 0), then sorting by median FNIR(N_b, T), N_b = 640 000.*

FNIR(N, R, T) = False neg. identification rate
FPIR(N, T) = False pos. identification rate
N = Num. enrolled subjects
R = Num. candidates examined
T = Threshold
T = 0 → Investigation
T > 0 → Identification

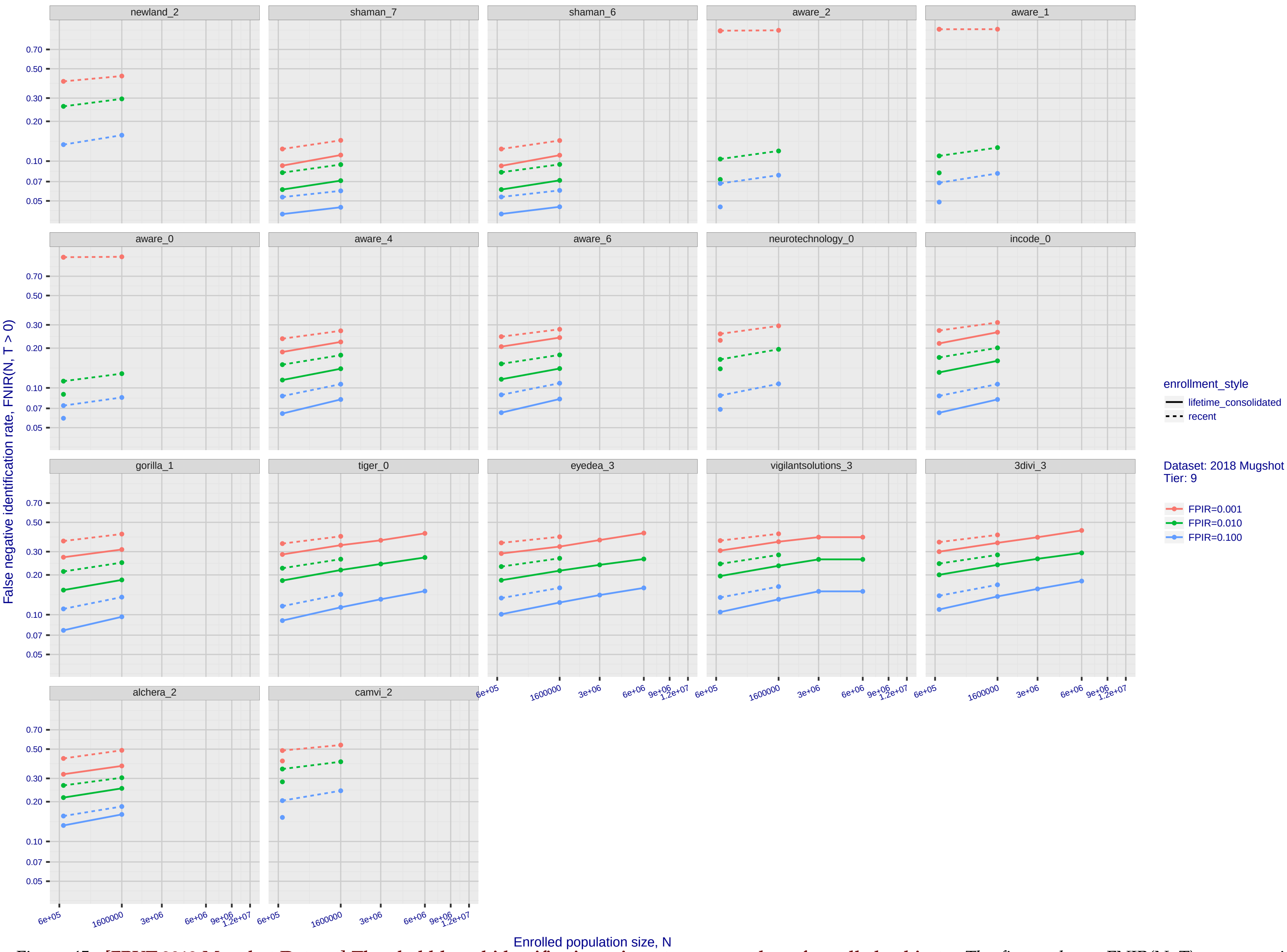

Figure 45: **[FRVT-2018 Mugshot Dataset] Threshold-based identification miss rates vs. number of enrolled subjects**. *The figure shows FNIR(N, T) across various gallery sizes when the threshold is set to achieve the given FPIRs. The rank criterion is irrelevant at high thresholds as mates are always at rank 1. The results are computed from the trials listed in rows 1-10 of Table 1. Less accurate algorithms were not run on large N, so results are missing. For clarity, results are sorted and reported into tiers spanning multiple pages. The tiering criteria is complicated: First paging by FNIR(N_b, 1, 0), then sorting by median FNIR(N_b, T), N_b = 640 000.*

This publication is available free of charge from: https://doi.org/10.6028/NIST.IR.8271

FNIR(N, R, T) = False neg. identification rate
FPIR(N, T) = False pos. identification rate
N = Num. enrolled subjects
R = Num. candidates examined
T = Threshold
T = 0 → Investigation
T > 0 → Identification

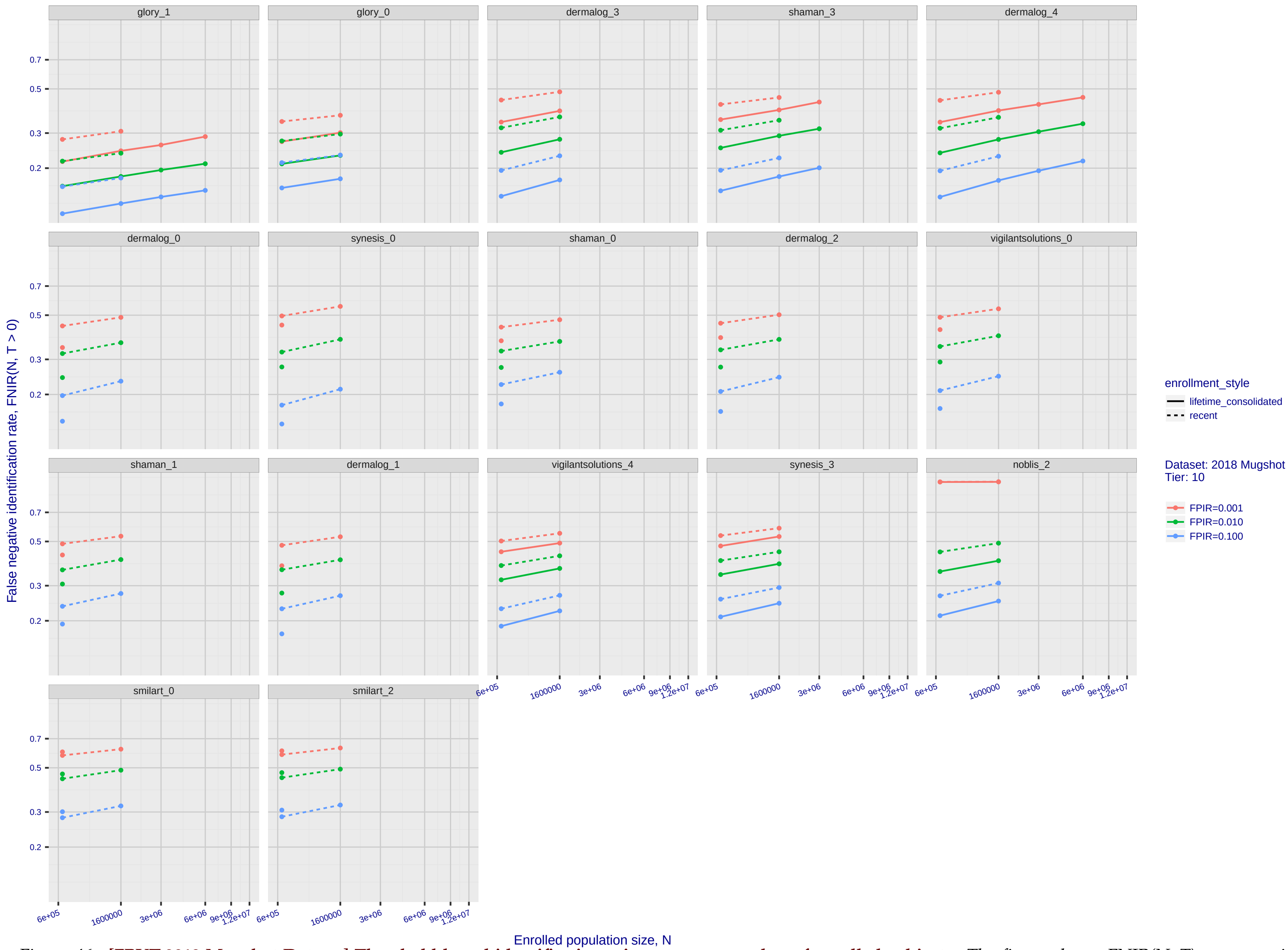

Figure 46: **[FRVT-2018 Mugshot Dataset] Threshold-based identification miss rates vs. number of enrolled subjects**. *The figure shows FNIR(N, T) across various gallery sizes when the threshold is set to achieve the given FPIRs. The rank criterion is irrelevant at high thresholds as mates are always at rank 1. The results are computed from the trials listed in rows 1-10 of Table 1. Less accurate algorithms were not run on large N, so results are missing. For clarity, results are sorted and reported into tiers spanning multiple pages. The tiering criteria is complicated: First paging by FNIR(N_b, 1, 0), then sorting by median FNIR(N_b, T), N_b = 640 000.*

2020/02/26
13:34:01

FNIR(N, R, T) = False neg. identification rate
FPIR(N, T) = False pos. identification rate
N = Num. enrolled subjects
R = Num. candidates examined
T = Threshold
T = 0 → Investigation
T > 0 → Identification

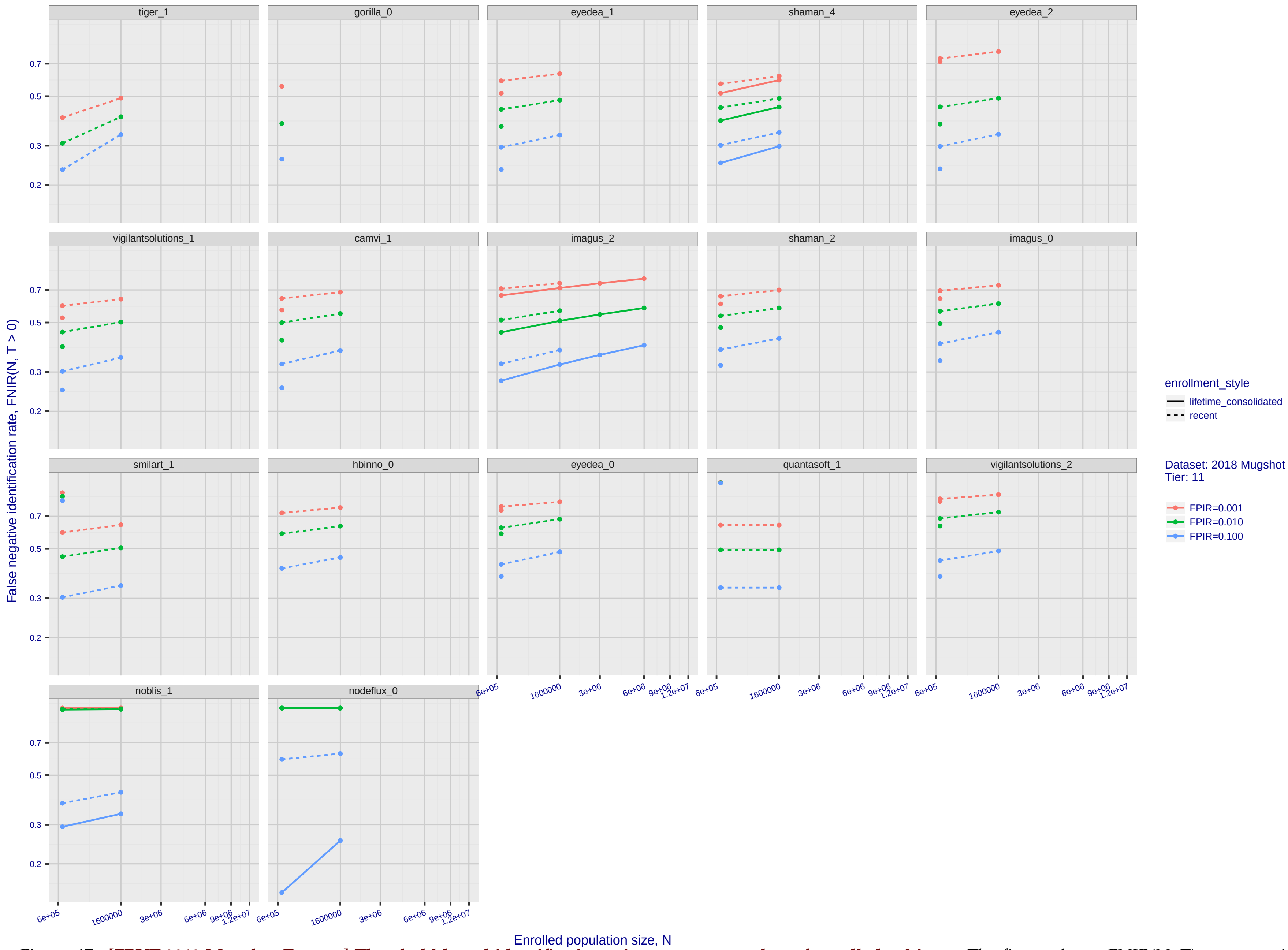

Figure 47: **[FRVT-2018 Mugshot Dataset] Threshold-based identification miss rates vs. number of enrolled subjects**. *The figure shows FNIR(N, T) across various gallery sizes when the threshold is set to achieve the given FPIRs. The rank criterion is irrelevant at high thresholds as mates are always at rank 1. The results are computed from the trials listed in rows 1-10 of Table 1. Less accurate algorithms were not run on large N, so results are missing. For clarity, results are sorted and reported into tiers spanning multiple pages. The tiering criteria is complicated: First paging by FNIR(N_b, 1, 0), then sorting by median FNIR(N_b, T), N_b = 640 000.*

FNIR(N, R, T) = False neg. identification rate
FPIR(N, T) = False pos. identification rate
N = Num. enrolled subjects
R = Num. candidates examined
T = Threshold
T = 0 → Investigation
T > 0 → Identification

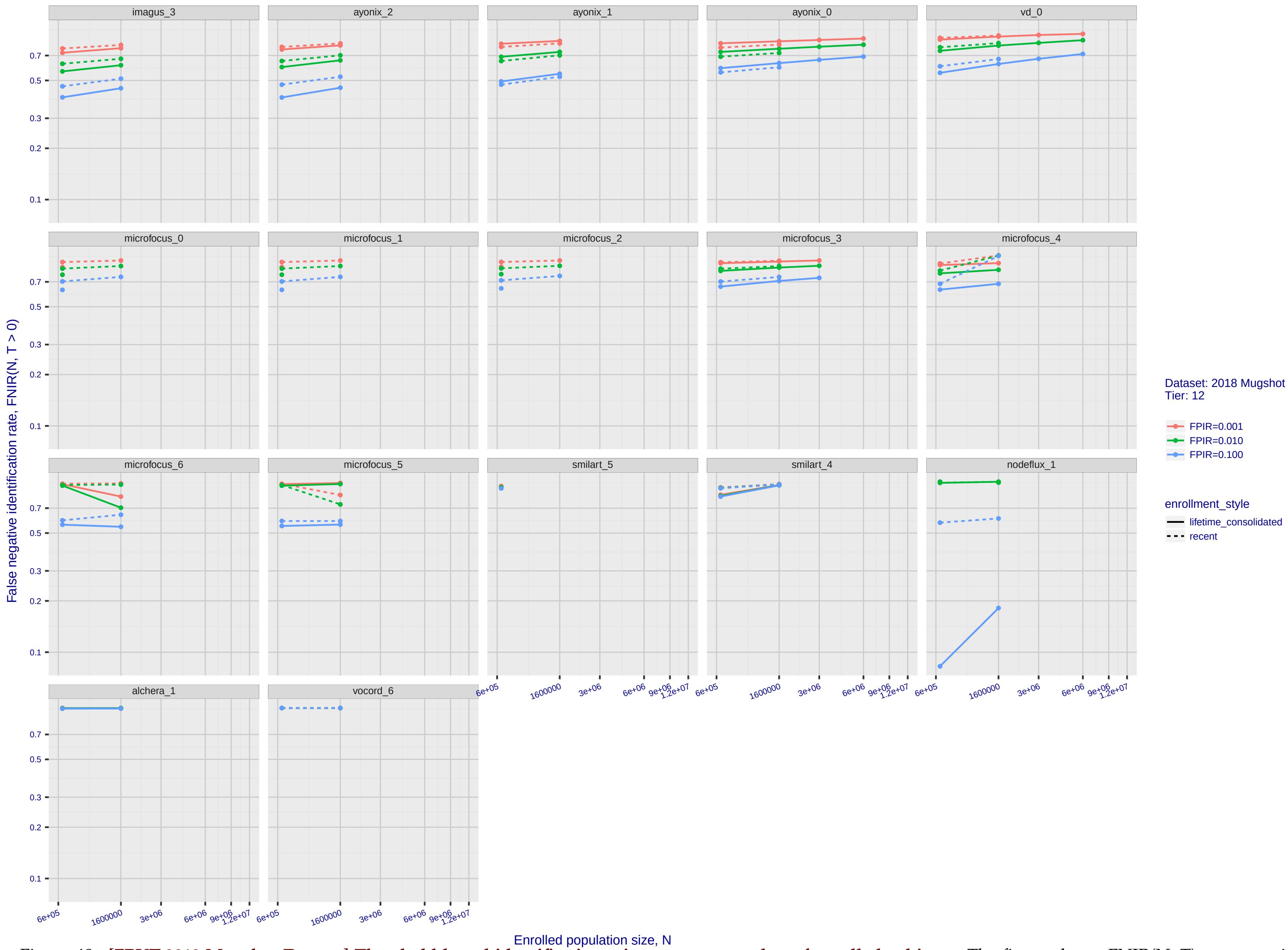

Figure 48: **[FRVT-2018 Mugshot Dataset] Threshold-based identification miss rates vs. number of enrolled subjects**. *The figure shows FNIR(N, T) across various gallery sizes when the threshold is set to achieve the given FPIRs. The rank criterion is irrelevant at high thresholds as mates are always at rank 1. The results are computed from the trials listed in rows 1-10 of Table 1. Less accurate algorithms were not run on large N, so results are missing. For clarity, results are sorted and reported into tiers spanning multiple pages. The tiering criteria is complicated: First paging by FNIR(N_b, 1, 0), then sorting by median FNIR(N_b, T), N_b = 640 000.*

2020/02/26	FNIR(N, R, T) =	False neg. identification rate	N = Num. enrolled subjects	T = Threshold	$T = 0 \rightarrow$ Investigation
13:34:01	FPIR(N, T) =	False pos. identification rate	R = Num. candidates examined		$T > 0 \rightarrow$ Identification

FNIR(N, R, T) = False neg. identification rate
FPIR(N, T) = False pos. identification rate
N = Num. enrolled subjects
R = Num. candidates examined
T = Threshold
T = 0 → Investigation
T > 0 → Identification

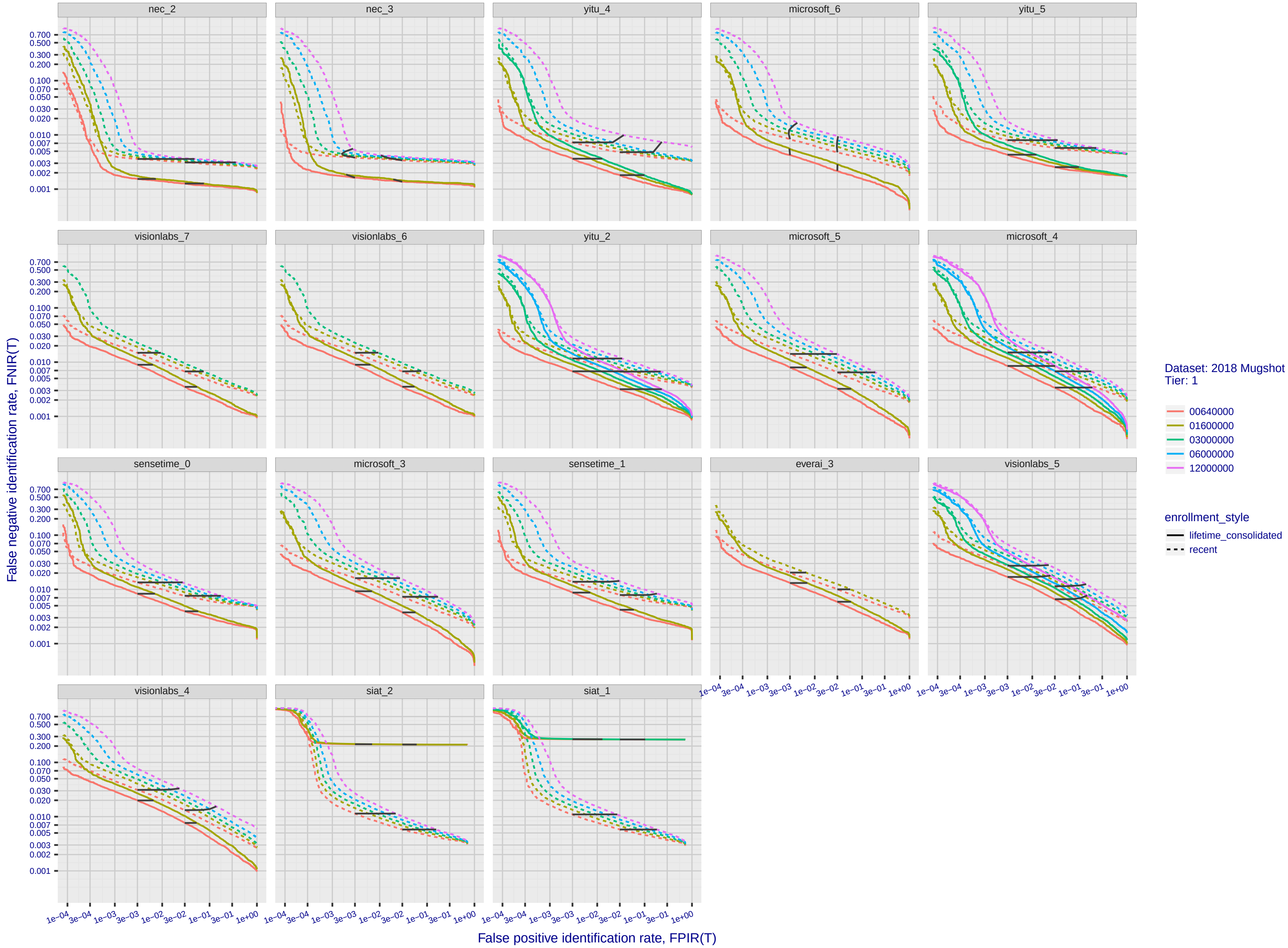

Figure 49: **[FRVT-2018 Mugshot Dataset] Identification miss rates vs. false positive rates**. *The figure shows miss rates FNIR(N, L, T) as a function of FPIR(N, T), with N ranging from 640 000 to 12 000 000 as noted in rows 1-10 of Table 1. These error tradeoff characteristics are useful for applications where a threshold must be elevated to limit false positives, such as when human reviewer labor is not matched to the volume of searches. Dark lines join points of equal threshold: If horizontal, FPIR(T) rises with N, and mate scores are independent of N. Other algorithms adjust scores in an attempt to make FPIR independent of N.*

This publication is available free of charge from: https://doi.org/10.6028/NIST.IR.8271

2020/02/26 13:34:01

FNIR(N, R, T) = False neg. identification rate
FPIR(N, T) = False pos. identification rate
N = Num. enrolled subjects
R = Num. candidates examined
T = Threshold
T = 0 → Investigation
T > 0 → Identification

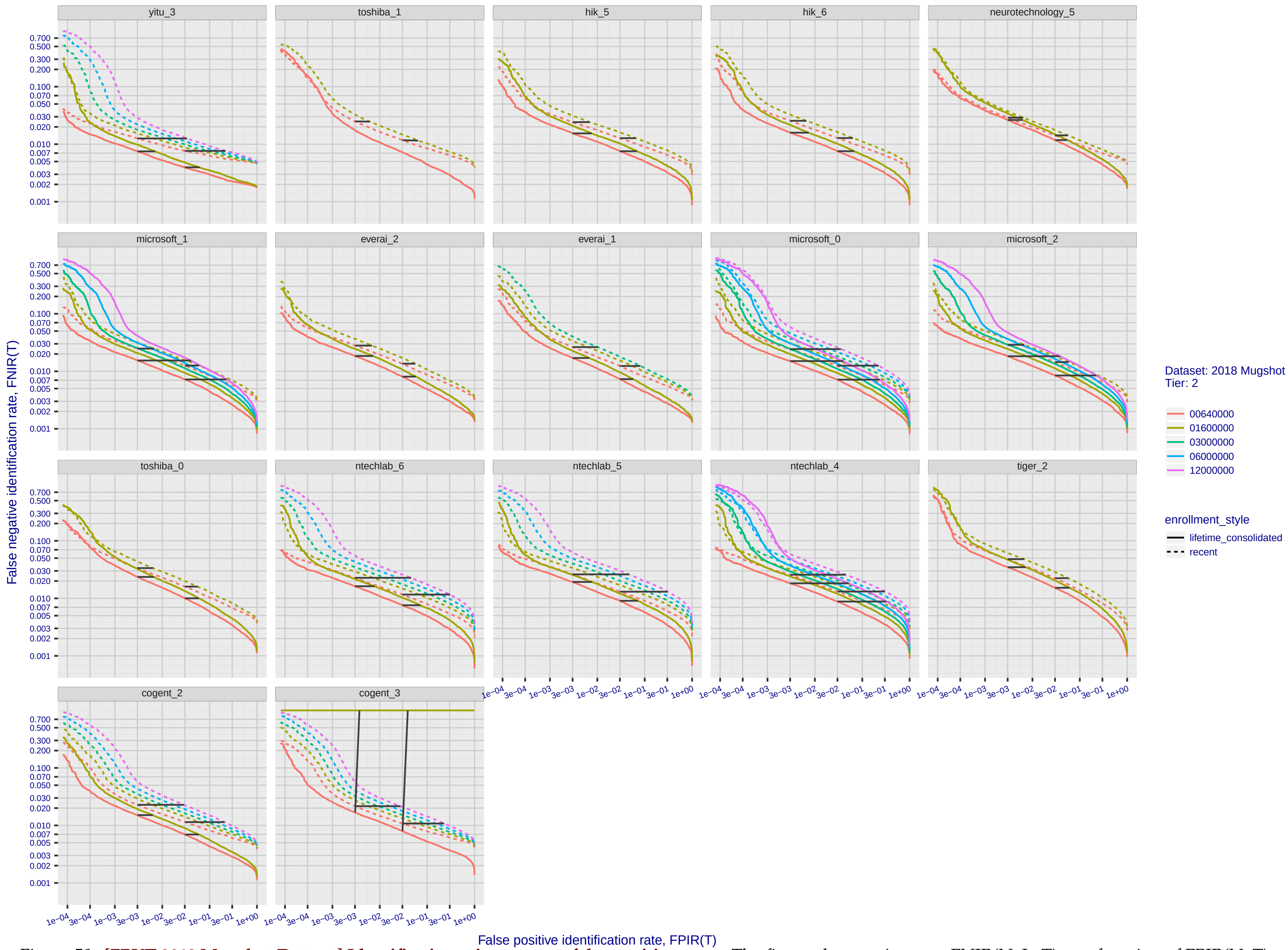

Figure 50: **[FRVT-2018 Mugshot Dataset] Identification miss rates vs. false positive rates**. *The figure shows miss rates FNIR(N, L, T) as a function of FPIR(N, T), with N ranging from 640 000 to 12 000 000 as noted in rows 1-10 of Table 1. These error tradeoff characteristics are useful for applications where a threshold must be elevated to limit false positives, such as when human reviewer labor is not matched to the volume of searches. Dark lines join points of equal threshold: If horizontal, FPIR(T) rises with N, and mate scores are independent of N. Other algorithms adjust scores in an attempt to make FPIR independent of N.*

FNIR(N, R, T) = False neg. identification rate
FPIR(N, T) = False pos. identification rate
N = Num. enrolled subjects
R = Num. candidates examined
T = Threshold
T = 0 → Investigation
T > 0 → Identification

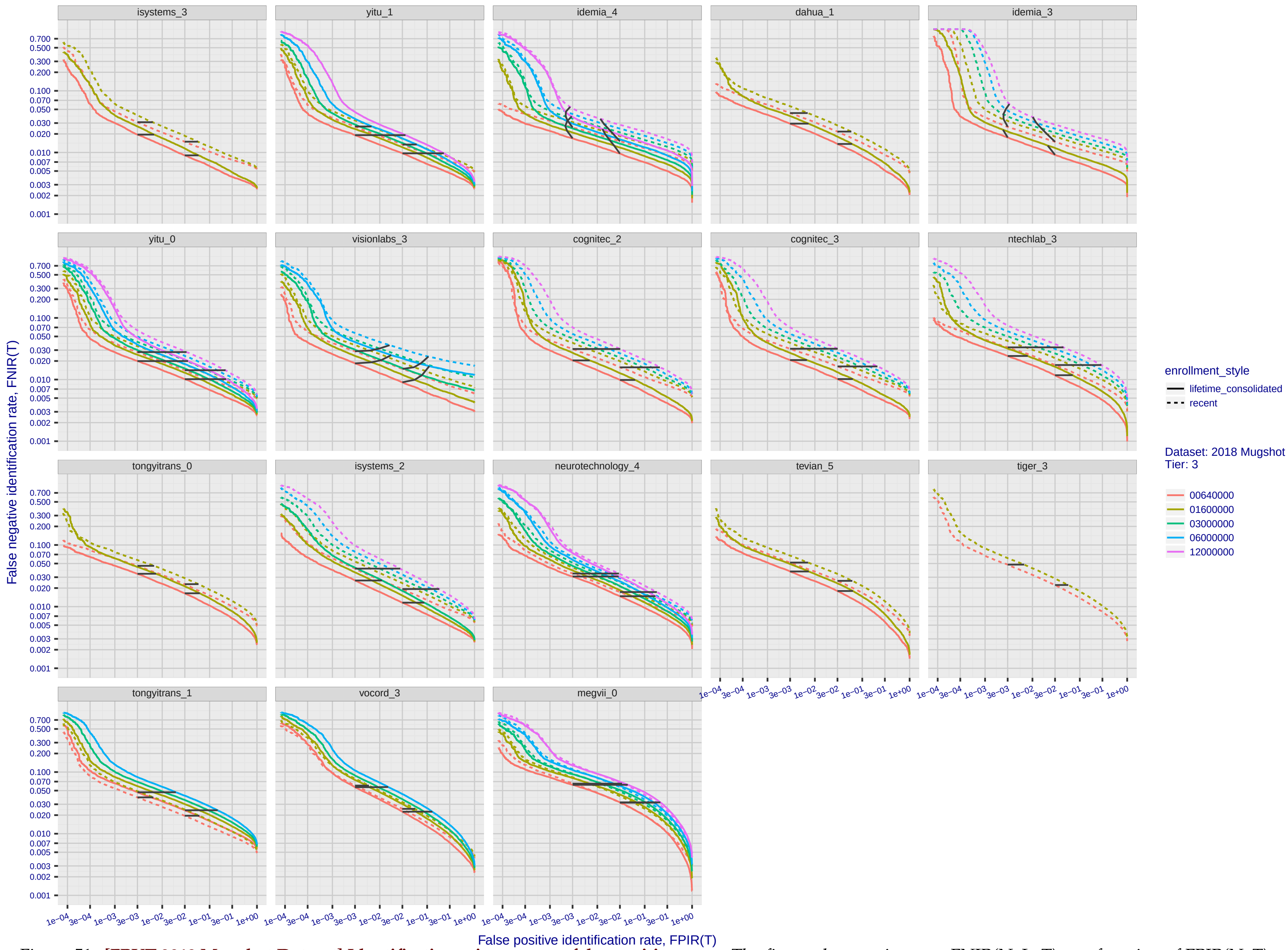

Figure 51: **[FRVT-2018 Mugshot Dataset] Identification miss rates vs. false positive rates**. *The figure shows miss rates FNIR(N, L, T) as a function of FPIR(N, T), with N ranging from 640 000 to 12 000 000 as noted in rows 1-10 of Table 1. These error tradeoff characteristics are useful for applications where a threshold must be elevated to limit false positives, such as when human reviewer labor is not matched to the volume of searches. Dark lines join points of equal threshold: If horizontal, FPIR(T) rises with N, and mate scores are independent of N. Other algorithms adjust scores in an attempt to make FPIR independent of N.*

FNIR(N, R, T) = False neg. identification rate
FPIR(N, T) = False pos. identification rate
N = Num. enrolled subjects
R = Num. candidates examined
T = Threshold
T = 0 → Investigation
T > 0 → Identification

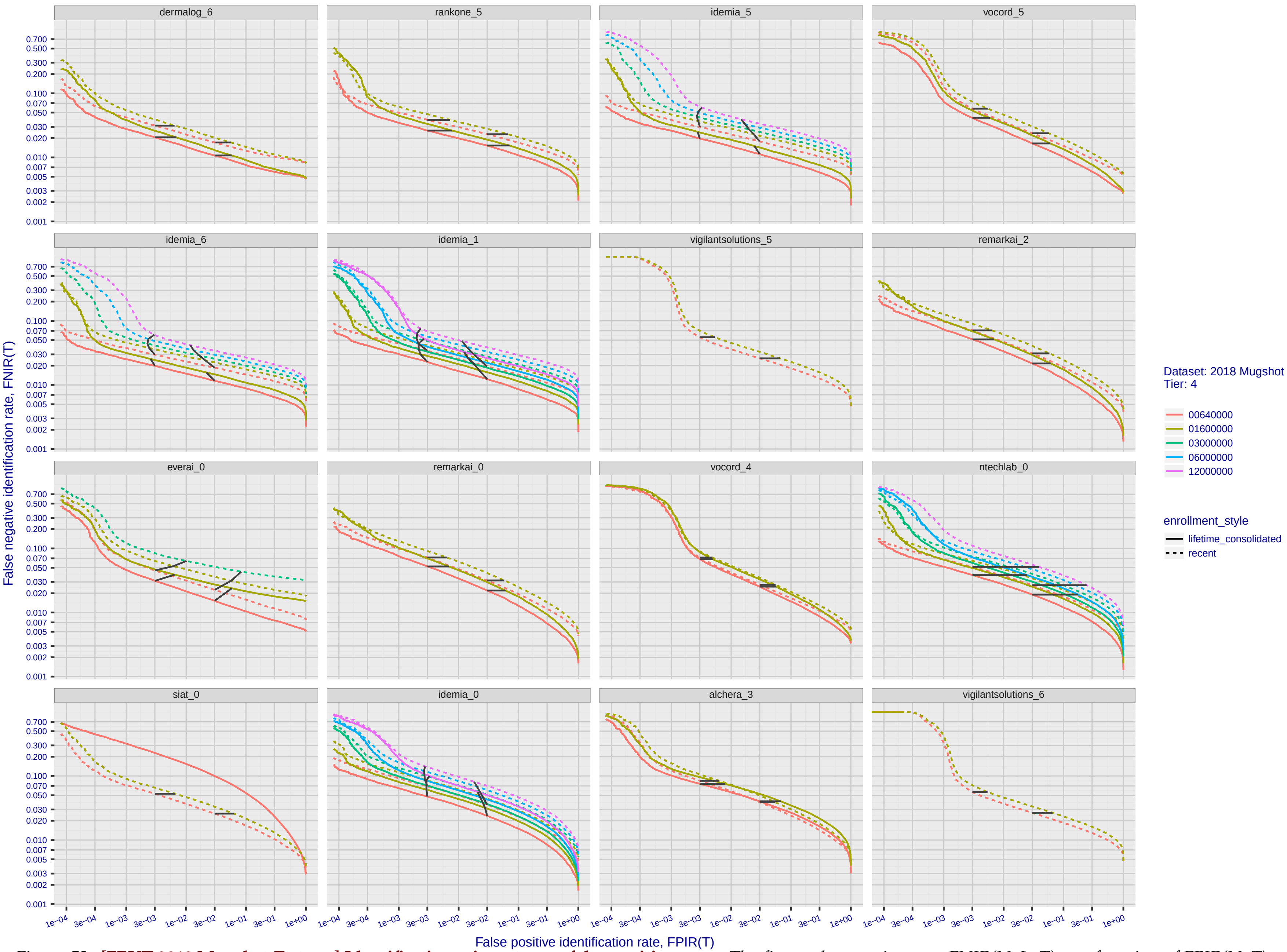

Figure 52: **[FRVT-2018 Mugshot Dataset] Identification miss rates vs. false positive rates**. *The figure shows miss rates FNIR(N, L, T) as a function of FPIR(N, T), with N ranging from 640 000 to 12 000 000 as noted in rows 1-10 of Table 1. These error tradeoff characteristics are useful for applications where a threshold must be elevated to limit false positives, such as when human reviewer labor is not matched to the volume of searches. Dark lines join points of equal threshold: If horizontal, FPIR(T) rises with N, and mate scores are independent of N. Other algorithms adjust scores in an attempt to make FPIR independent of N.*

2020/02/26
13:34:01

FNIR(N, R, T) = False neg. identification rate
FPIR(N, T) = False pos. identification rate
N = Num. enrolled subjects
R = Num. candidates examined
T = Threshold
T = 0 → Investigation
T > 0 → Identification

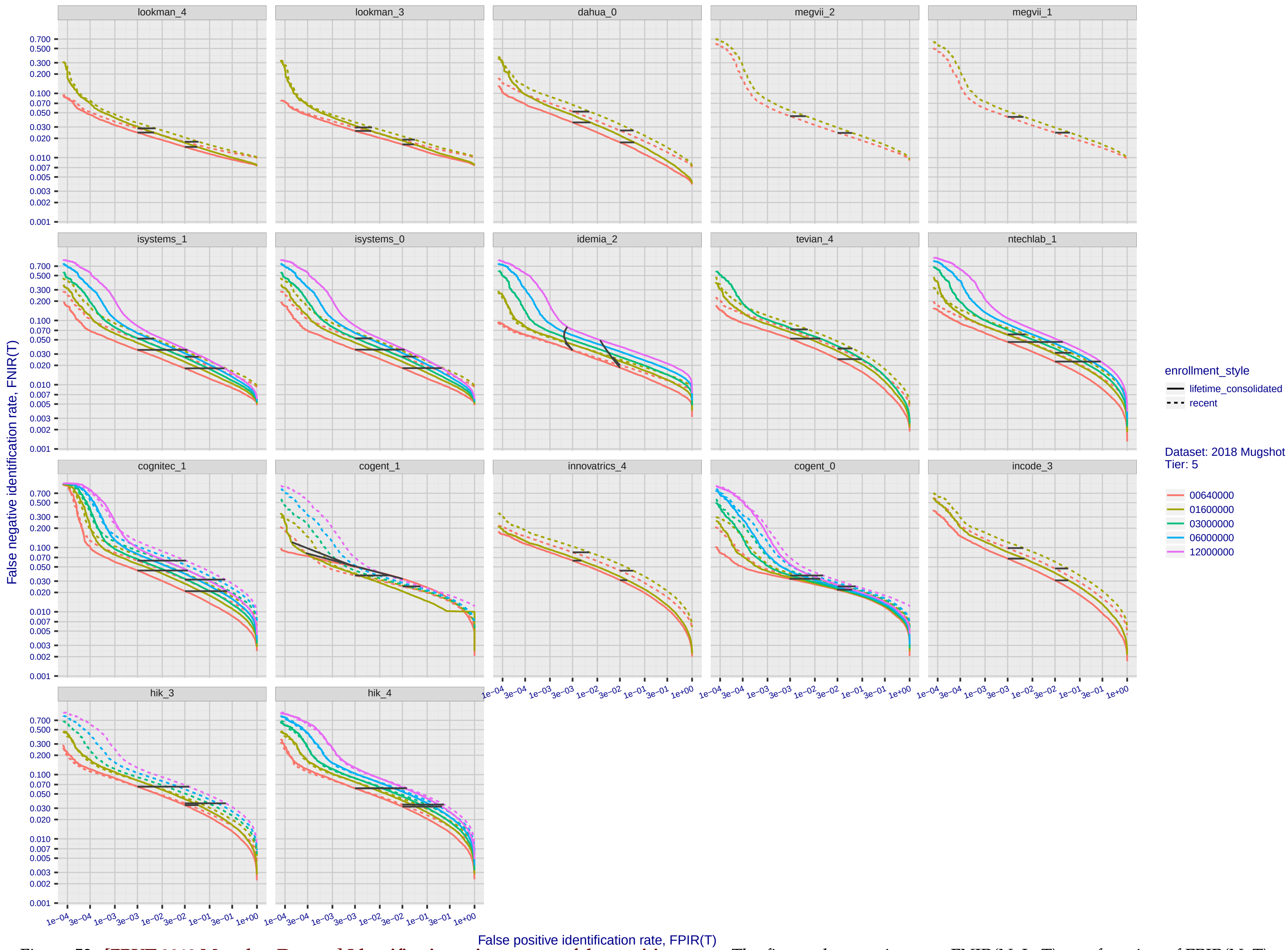

Figure 53: **[FRVT-2018 Mugshot Dataset] Identification miss rates vs. false positive rates**. *The figure shows miss rates FNIR(N, L, T) as a function of FPIR(N, T), with N ranging from 640 000 to 12 000 000 as noted in rows 1-10 of Table 1. These error tradeoff characteristics are useful for applications where a threshold must be elevated to limit false positives, such as when human reviewer labor is not matched to the volume of searches. Dark lines join points of equal threshold: If horizontal, FPIR(T) rises with N, and mate scores are independent of N. Other algorithms adjust scores in an attempt to make FPIR independent of N.*

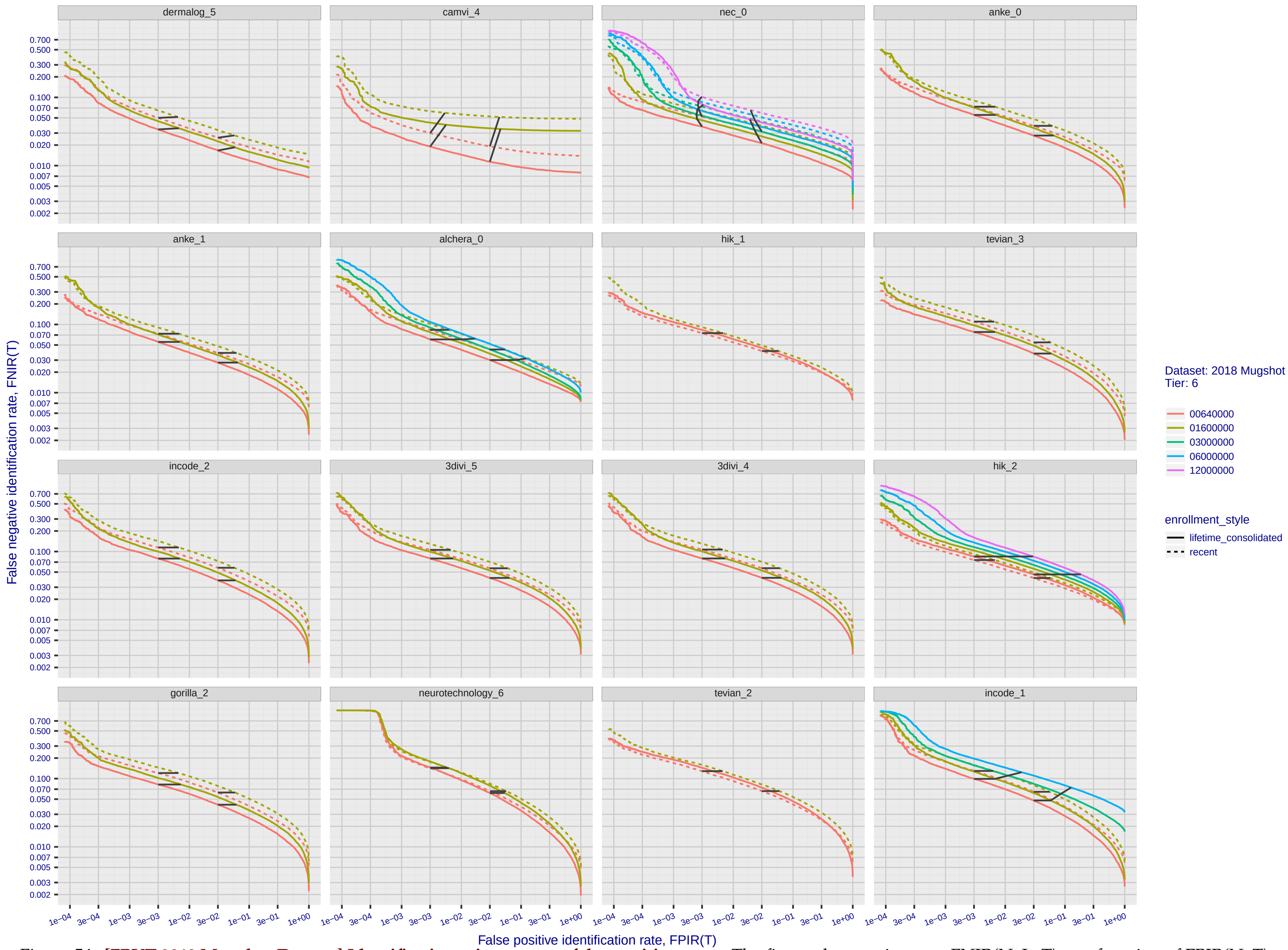

Figure 54: **[FRVT-2018 Mugshot Dataset] Identification miss rates vs. false positive rates**. *The figure shows miss rates FNIR(N, L, T) as a function of FPIR(N, T), with N ranging from 640 000 to 12 000 000 as noted in rows 1-10 of Table 1. These error tradeoff characteristics are useful for applications where a threshold must be elevated to limit false positives, such as when human reviewer labor is not matched to the volume of searches. Dark lines join points of equal threshold: If horizontal, FPIR(T) rises with N, and mate scores are independent of N. Other algorithms adjust scores in an attempt to make FPIR independent of N.*

This publication is available free of charge from: https://doi.org/10.6028/NIST.IR.8271

FNIR(N, R, T) = False neg. identification rate
FPIR(N, T) = False pos. identification rate
N = Num. enrolled subjects
R = Num. candidates examined
T = Threshold
T = 0 → Investigation
T > 0 → Identification

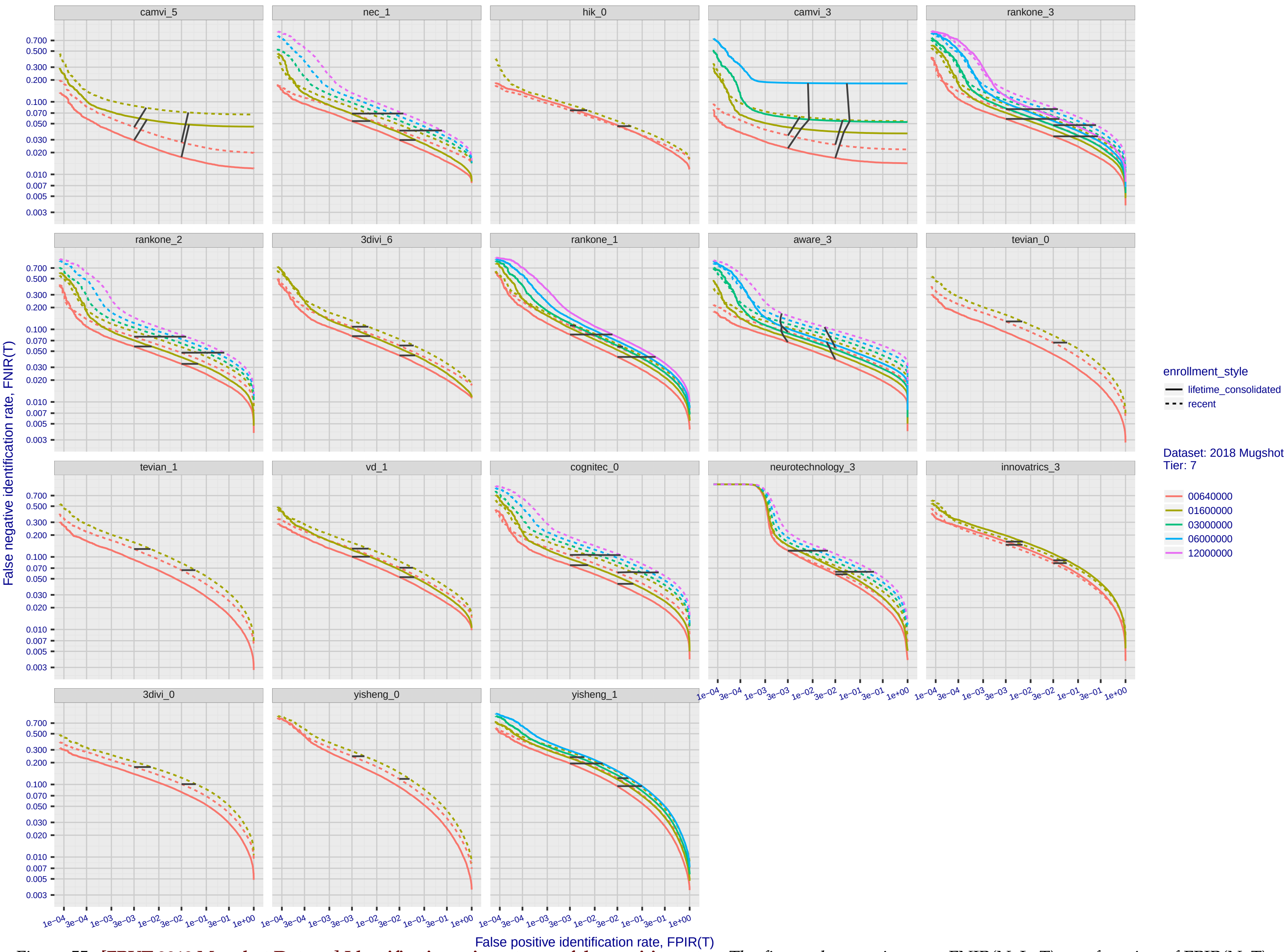

Figure 55: **[FRVT-2018 Mugshot Dataset] Identification miss rates vs. false positive rates**. *The figure shows miss rates FNIR(N, L, T) as a function of FPIR(N, T), with N ranging from 640 000 to 12 000 000 as noted in rows 1-10 of Table 1. These error tradeoff characteristics are useful for applications where a threshold must be elevated to limit false positives, such as when human reviewer labor is not matched to the volume of searches. Dark lines join points of equal threshold: If horizontal, FPIR(T) rises with N, and mate scores are independent of N. Other algorithms adjust scores in an attempt to make FPIR independent of N.*

This publication is available free of charge from: https://doi.org/10.6028/NIST.IR.8271

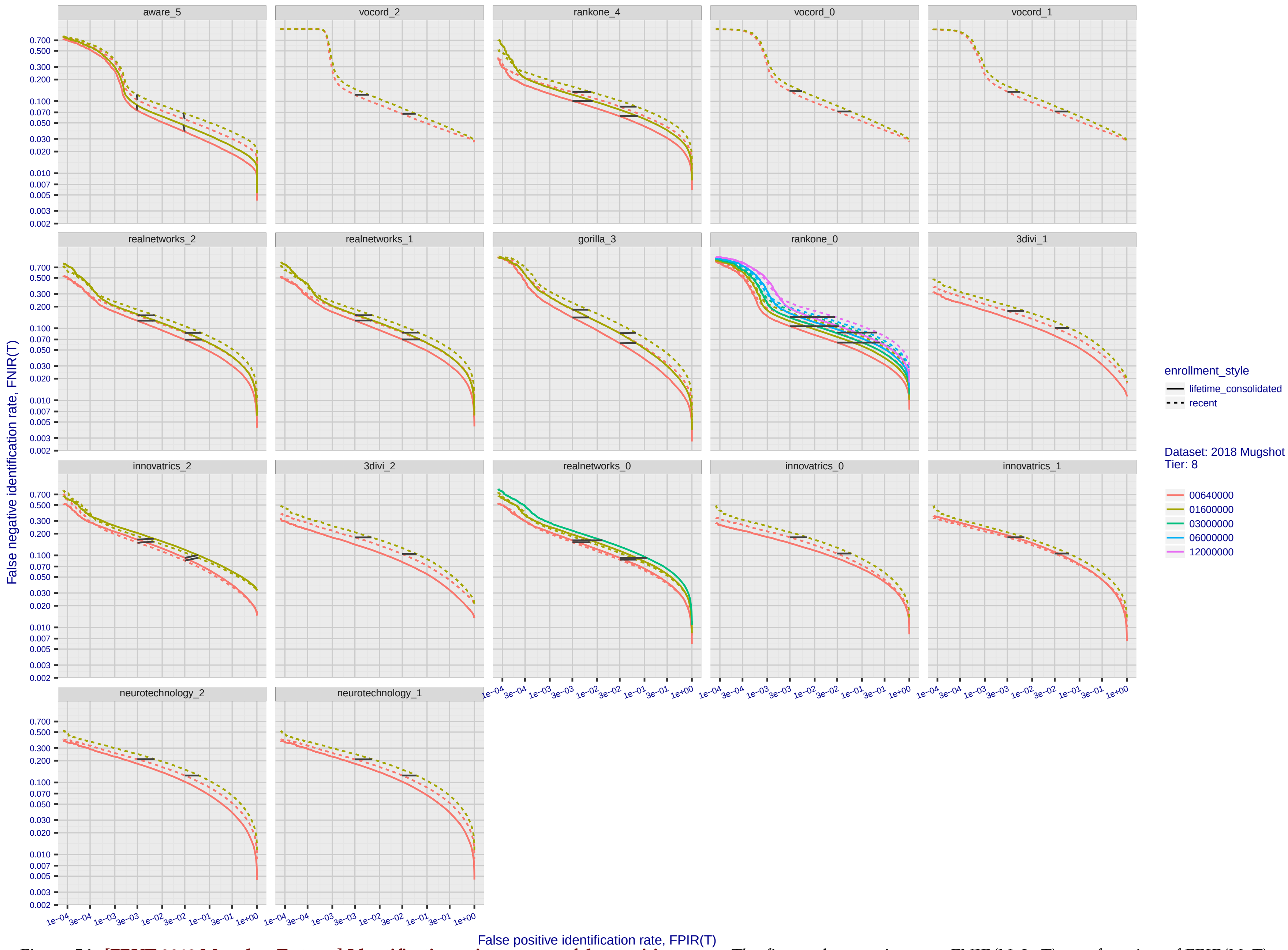

Figure 56: **[FRVT-2018 Mugshot Dataset] Identification miss rates vs. false positive rates**. *The figure shows miss rates FNIR(N, L, T) as a function of FPIR(N, T), with N ranging from 640 000 to 12 000 000 as noted in rows 1-10 of Table 1. These error tradeoff characteristics are useful for applications where a threshold must be elevated to limit false positives, such as when human reviewer labor is not matched to the volume of searches. Dark lines join points of equal threshold: If horizontal, FPIR(T) rises with N, and mate scores are independent of N. Other algorithms adjust scores in an attempt to make FPIR independent of N.*

FNIR(N, R, T) = False neg. identification rate
FPIR(N, T) = False pos. identification rate
N = Num. enrolled subjects
R = Num. candidates examined
T = Threshold
T = 0 → Investigation
T > 0 → Identification

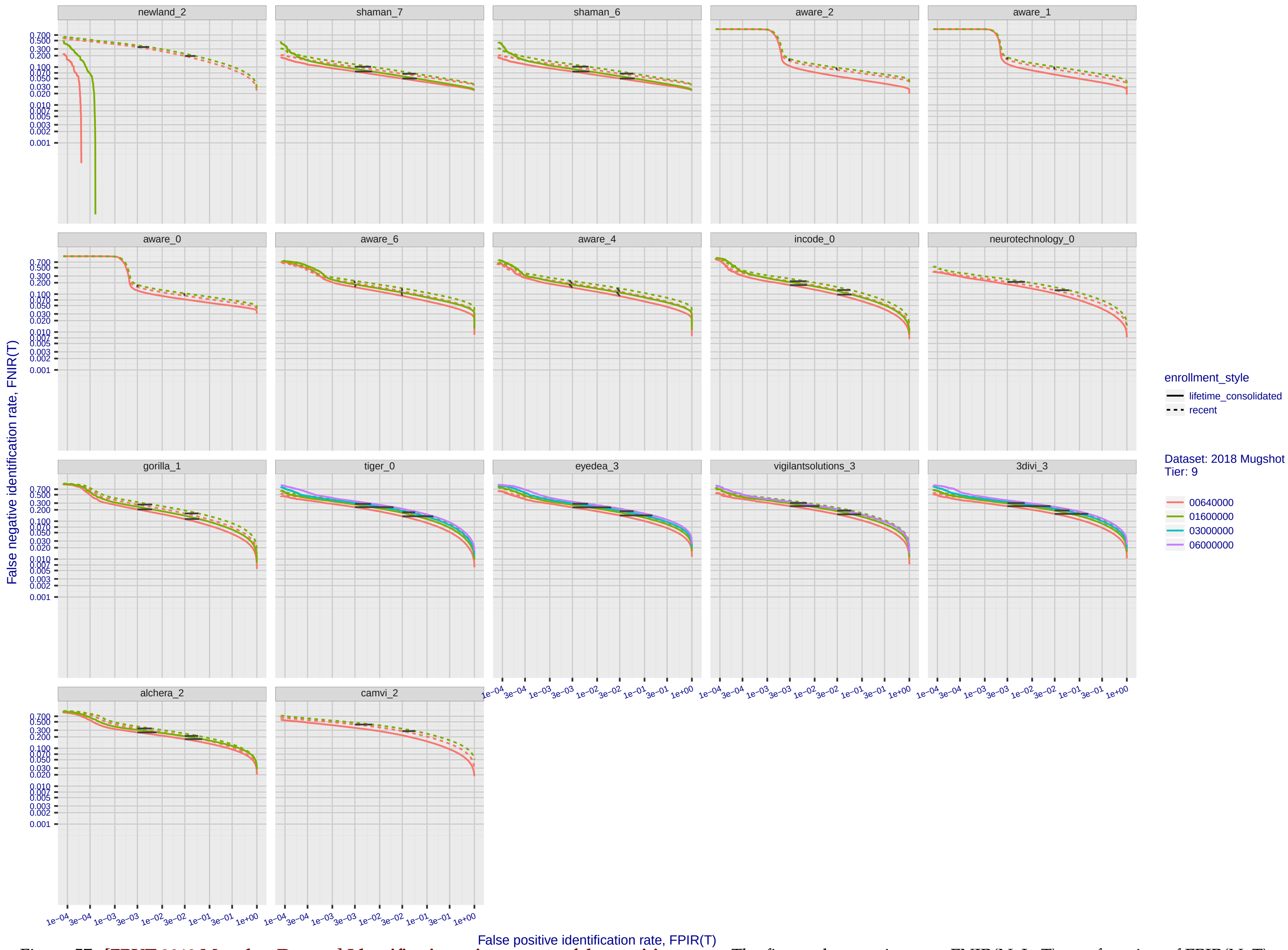

Figure 57: **[FRVT-2018 Mugshot Dataset] Identification miss rates vs. false positive rates**. *The figure shows miss rates FNIR(N, L, T) as a function of FPIR(N, T), with N ranging from 640 000 to 12 000 000 as noted in rows 1-10 of Table 1. These error tradeoff characteristics are useful for applications where a threshold must be elevated to limit false positives, such as when human reviewer labor is not matched to the volume of searches. Dark lines join points of equal threshold: If horizontal, FPIR(T) rises with N, and mate scores are independent of N. Other algorithms adjust scores in an attempt to make FPIR independent of N.*

This publication is available free of charge from: https://doi.org/10.6028/NIST.IR.8271

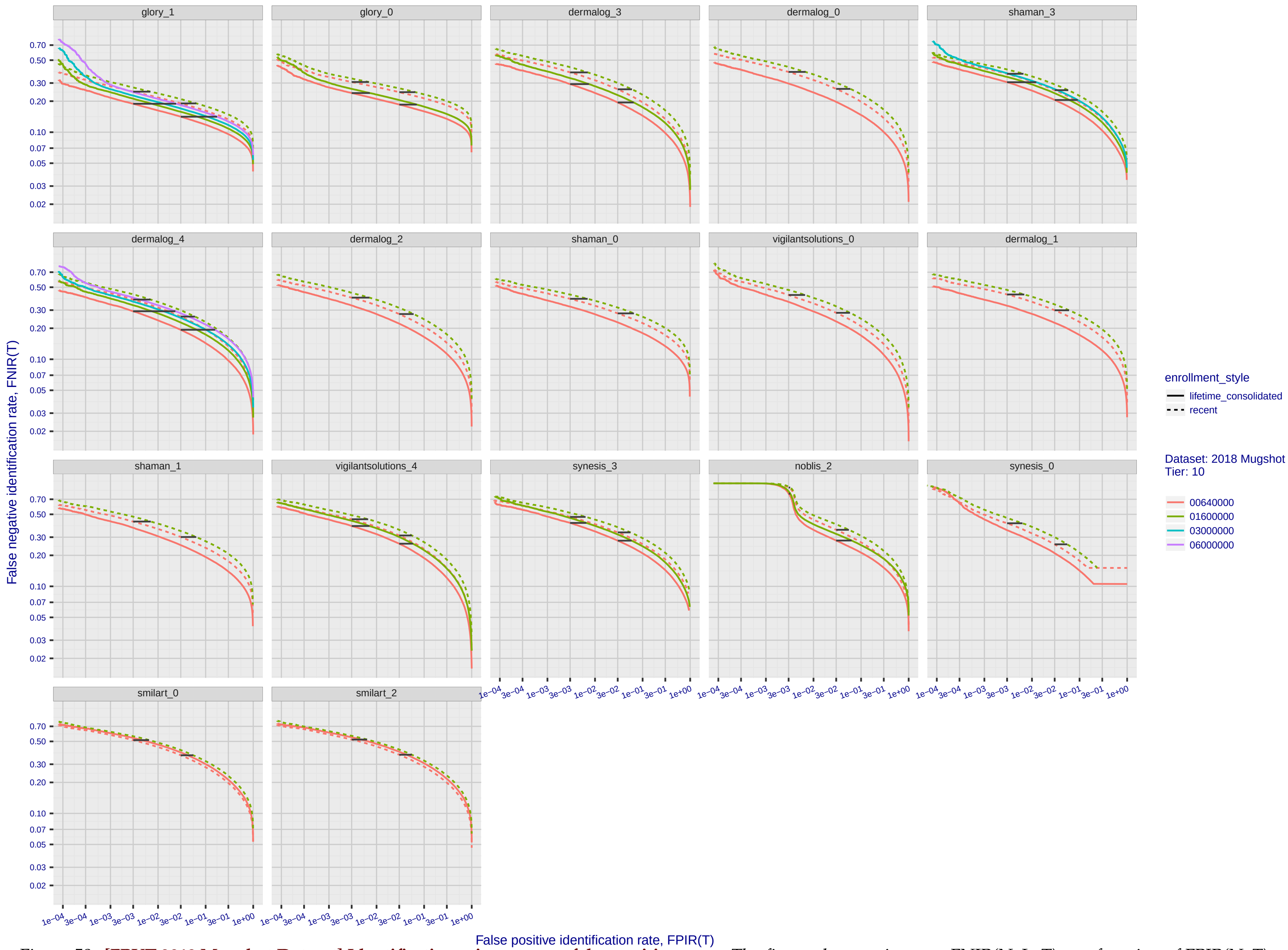

Figure 58: **[FRVT-2018 Mugshot Dataset] Identification miss rates vs. false positive rates**. *The figure shows miss rates FNIR(N, L, T) as a function of FPIR(N, T), with N ranging from 640 000 to 12 000 000 as noted in rows 1-10 of Table 1. These error tradeoff characteristics are useful for applications where a threshold must be elevated to limit false positives, such as when human reviewer labor is not matched to the volume of searches. Dark lines join points of equal threshold: If horizontal, FPIR(T) rises with N, and mate scores are independent of N. Other algorithms adjust scores in an attempt to make FPIR independent of N.*

FNIR(N, R, T) = False neg. identification rate
FPIR(N, T) = False pos. identification rate
N = Num. enrolled subjects
R = Num. candidates examined
T = Threshold
T = 0 → Investigation
T > 0 → Identification

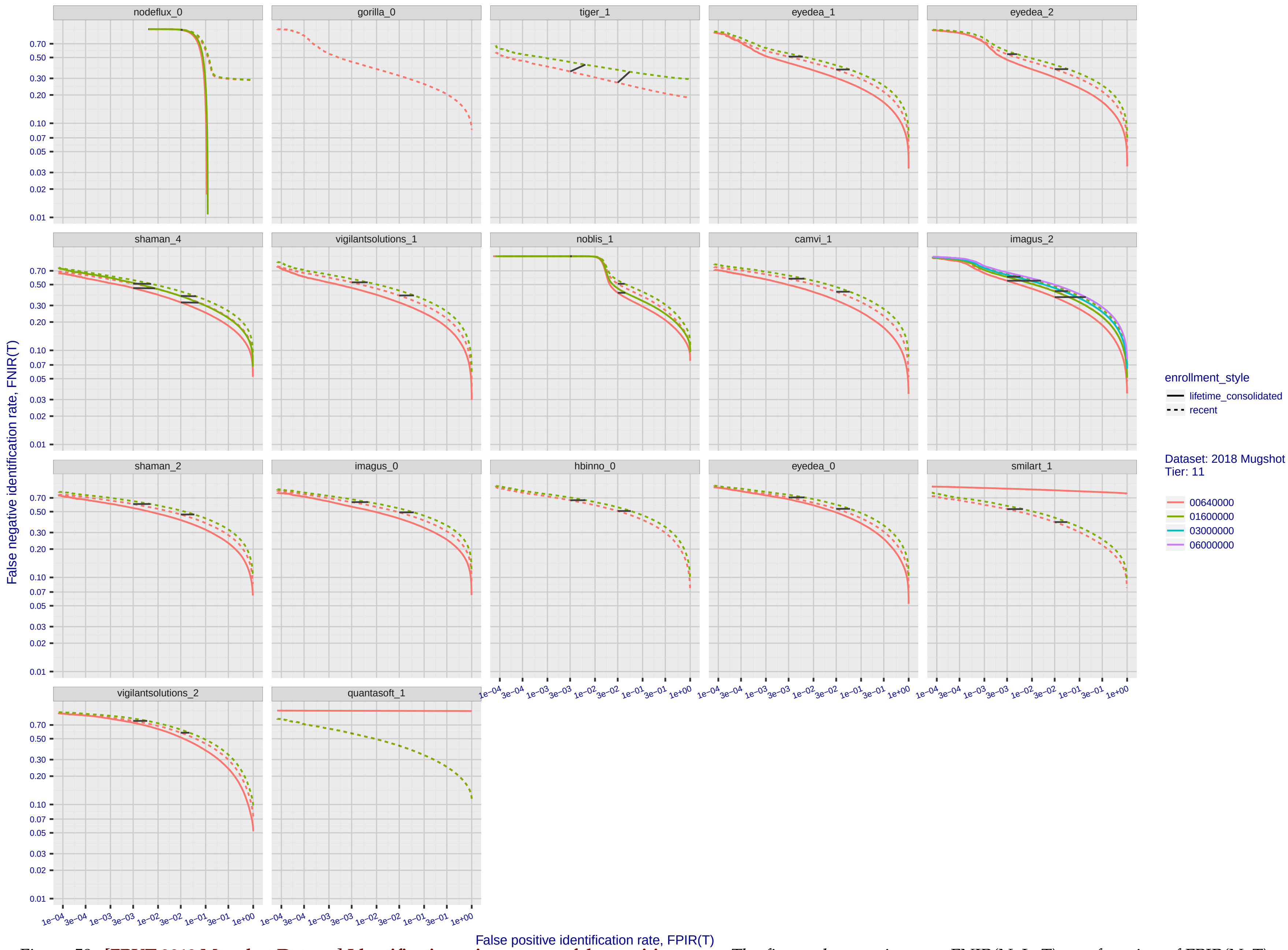

Figure 59: **[FRVT-2018 Mugshot Dataset] Identification miss rates vs. false positive rates**. *The figure shows miss rates FNIR(N, L, T) as a function of FPIR(N, T), with N ranging from 640 000 to 12 000 000 as noted in rows 1-10 of Table 1. These error tradeoff characteristics are useful for applications where a threshold must be elevated to limit false positives, such as when human reviewer labor is not matched to the volume of searches. Dark lines join points of equal threshold: If horizontal, FPIR(T) rises with N, and mate scores are independent of N. Other algorithms adjust scores in an attempt to make FPIR independent of N.*

FNIR(N, R, T) = False neg. identification rate
FPIR(N, T) = False pos. identification rate
N = Num. enrolled subjects
R = Num. candidates examined
T = Threshold
T = 0 → Investigation
T > 0 → Identification

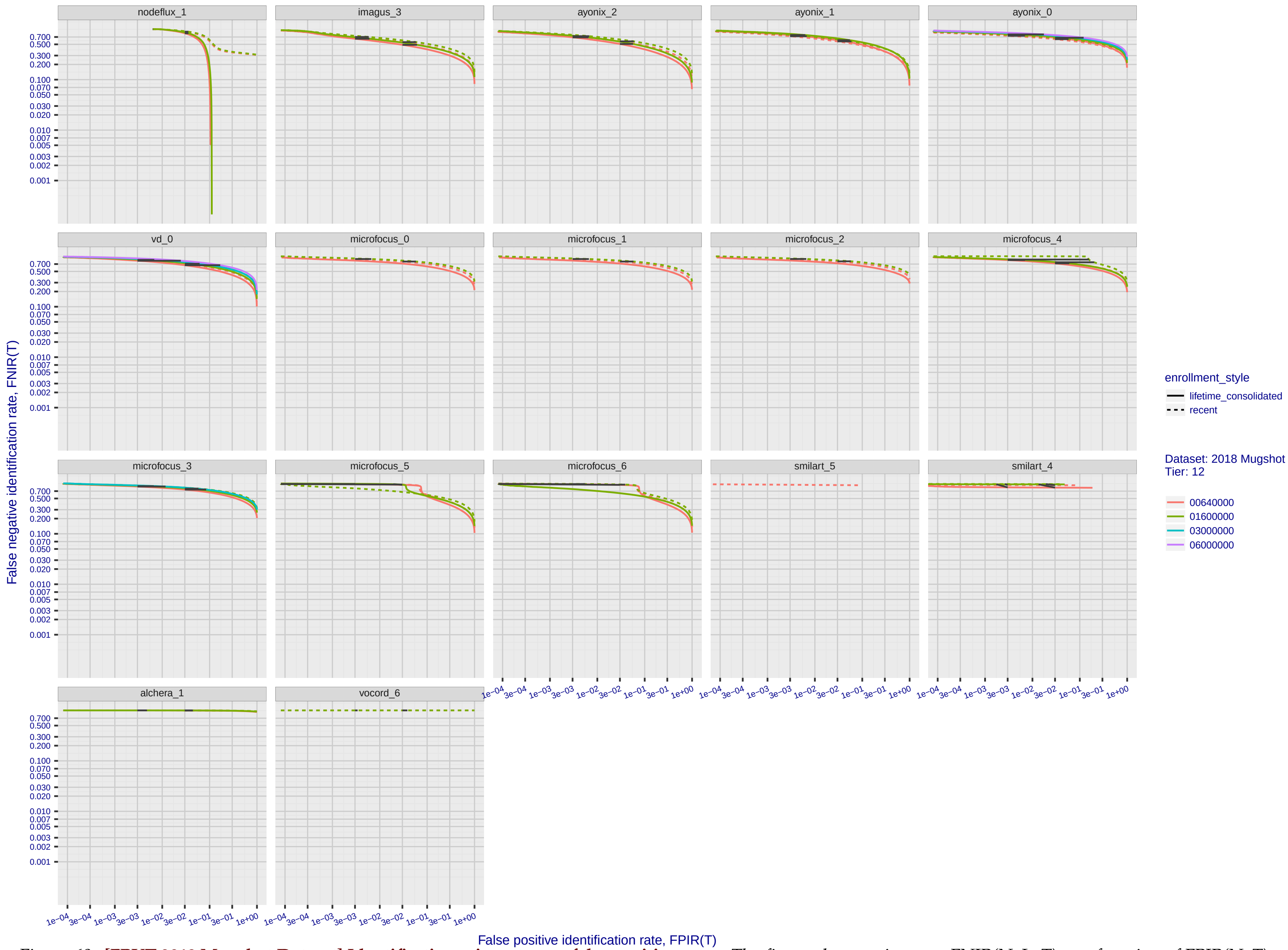

Figure 60: **[FRVT-2018 Mugshot Dataset] Identification miss rates vs. false positive rates**. *The figure shows miss rates FNIR(N, L, T) as a function of FPIR(N, T), with N ranging from 640 000 to 12 000 000 as noted in rows 1-10 of Table 1. These error tradeoff characteristics are useful for applications where a threshold must be elevated to limit false positives, such as when human reviewer labor is not matched to the volume of searches. Dark lines join points of equal threshold: If horizontal, FPIR(T) rises with N, and mate scores are independent of N. Other algorithms adjust scores in an attempt to make FPIR independent of N.*

Appendix B Effect of time-lapse: Accuracy after face ageing

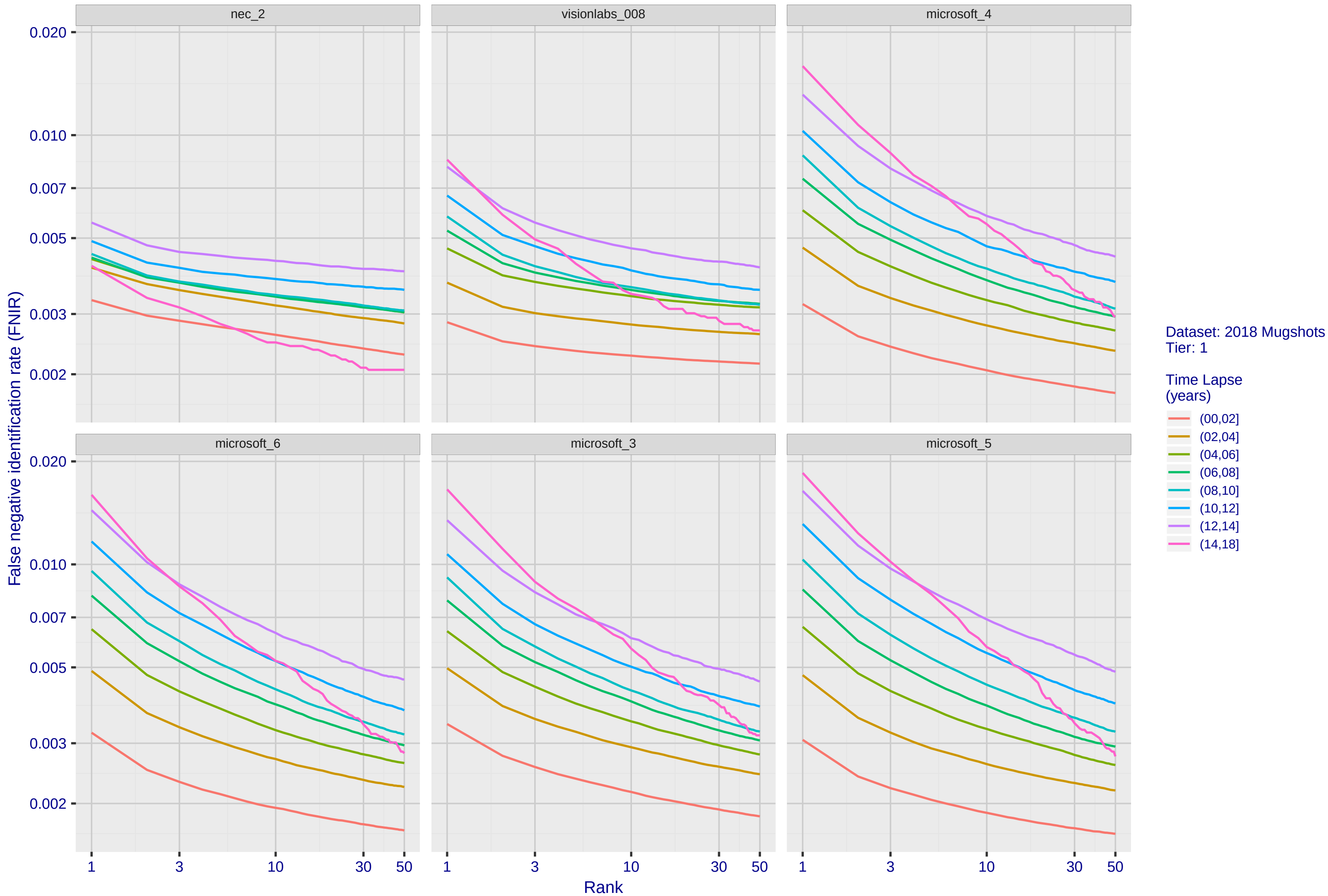

Figure 61: **[FRVT-2018 Mugshot Ageing Dataset] Identification miss rates vs. rank by time-elapsed**. *The oldest image of each individual is enrolled. Thereafter, all more recent images are searched. Miss rates are computed over all searches noted in row 17 of Table 1 and binned by number of years between search and initial enrollment.*

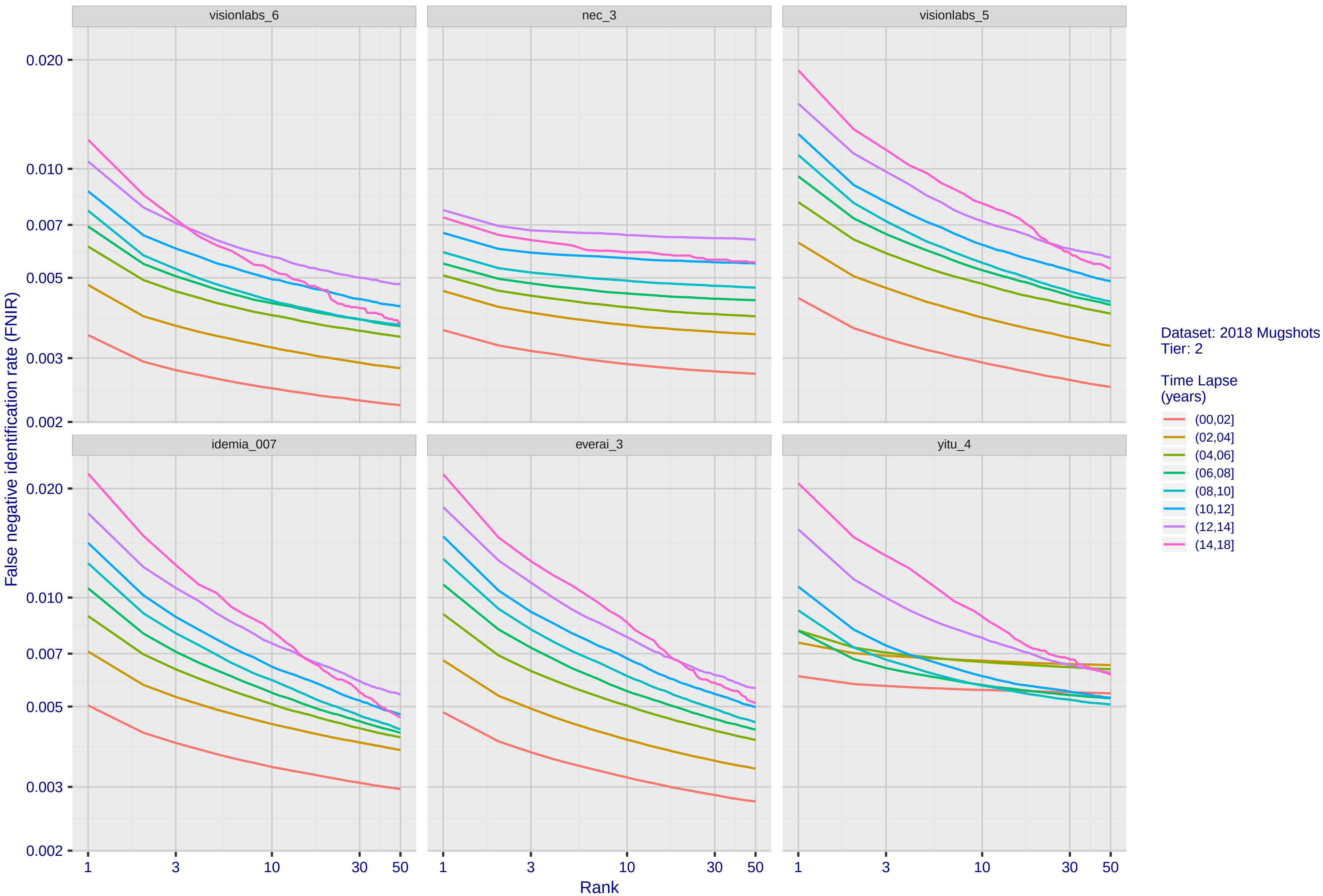

Figure 62: **[FRVT-2018 Mugshot Ageing Dataset] Identification miss rates vs. rank by time-elapsed**. *The oldest image of each individual is enrolled. Thereafter, all more recent images are searched. Miss rates are computed over all searches noted in row 17 of Table 1 and binned by number of years between search and initial enrollment.*

This publication is available free of charge from: https://doi.org/10.6028/NIST.IR.8271

FNIR(N, R, T) = False neg. identification rate
FPIR(N, T) = False pos. identification rate
N = Num. enrolled subjects
R = Num. candidates examined
T = Threshold
T = 0 → Investigation
T > 0 → Identification

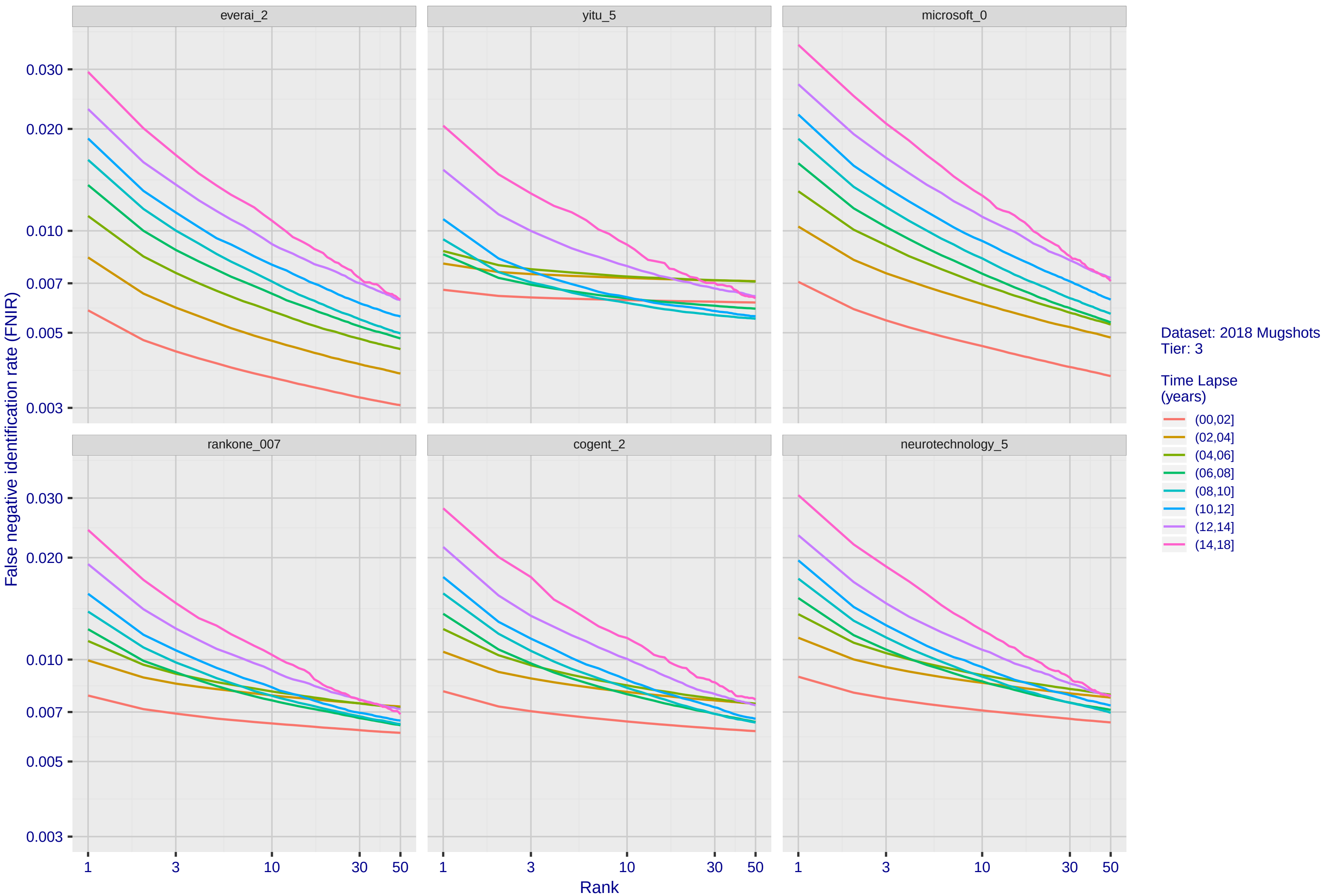

Figure 63: **[FRVT-2018 Mugshot Ageing Dataset] Identification miss rates vs. rank by time-elapsed**. *The oldest image of each individual is enrolled. Thereafter, all more recent images are searched. Miss rates are computed over all searches noted in row 17 of Table 1 and binned by number of years between search and initial enrollment.*

FNIR(N, R, T) = False neg. identification rate
FPIR(N, T) = False pos. identification rate
N = Num. enrolled subjects
R = Num. candidates examined
T = Threshold
T = 0 → Investigation
T > 0 → Identification

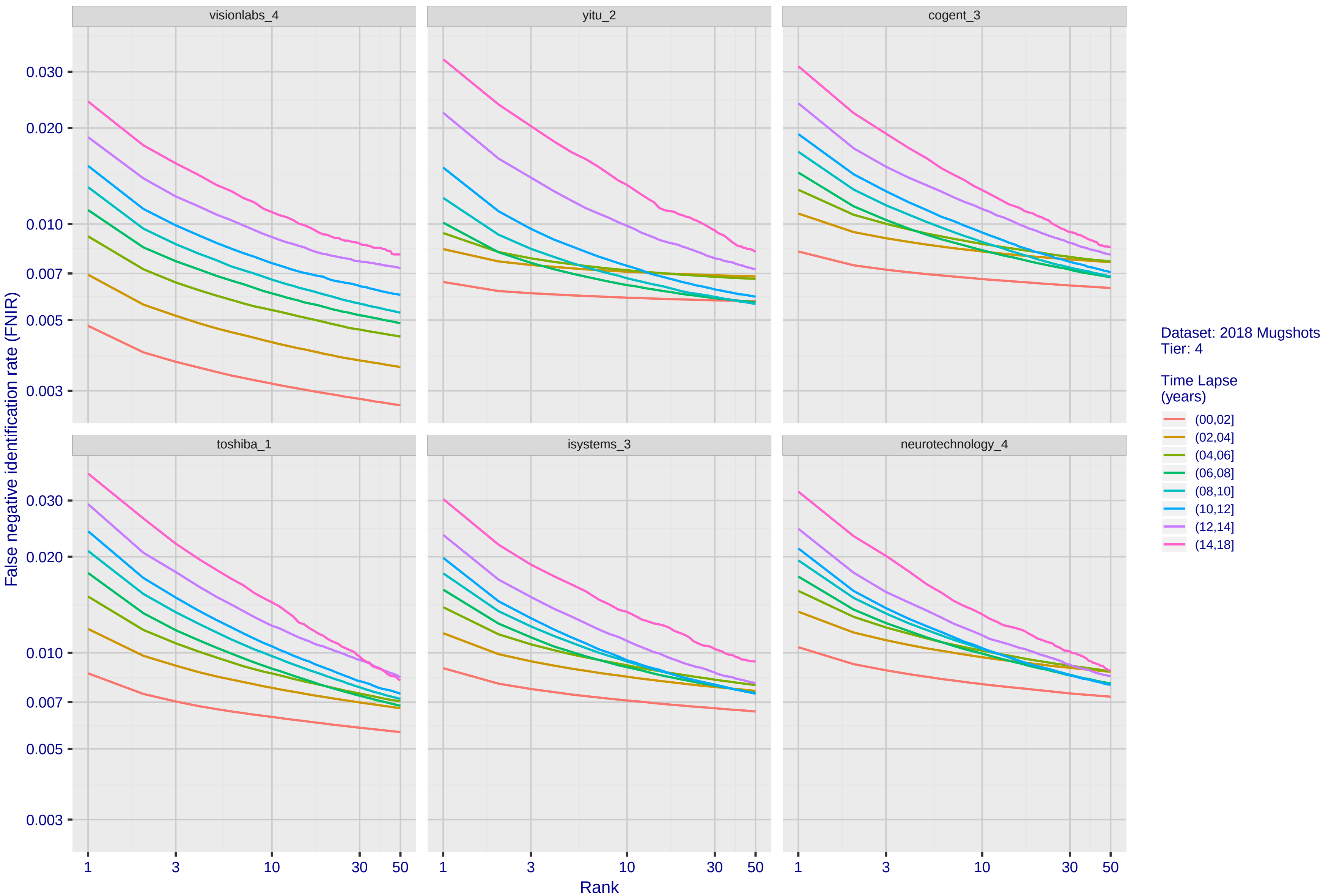

Figure 64: **[FRVT-2018 Mugshot Ageing Dataset] Identification miss rates vs. rank by time-elapsed**. *The oldest image of each individual is enrolled. Thereafter, all more recent images are searched. Miss rates are computed over all searches noted in row 17 of Table 1 and binned by number of years between search and initial enrollment.*

FNIR(N, R, T) = False neg. identification rate
FPIR(N, T) = False pos. identification rate
N = Num. enrolled subjects
R = Num. candidates examined
T = Threshold
T = 0 → Investigation
T > 0 → Identification

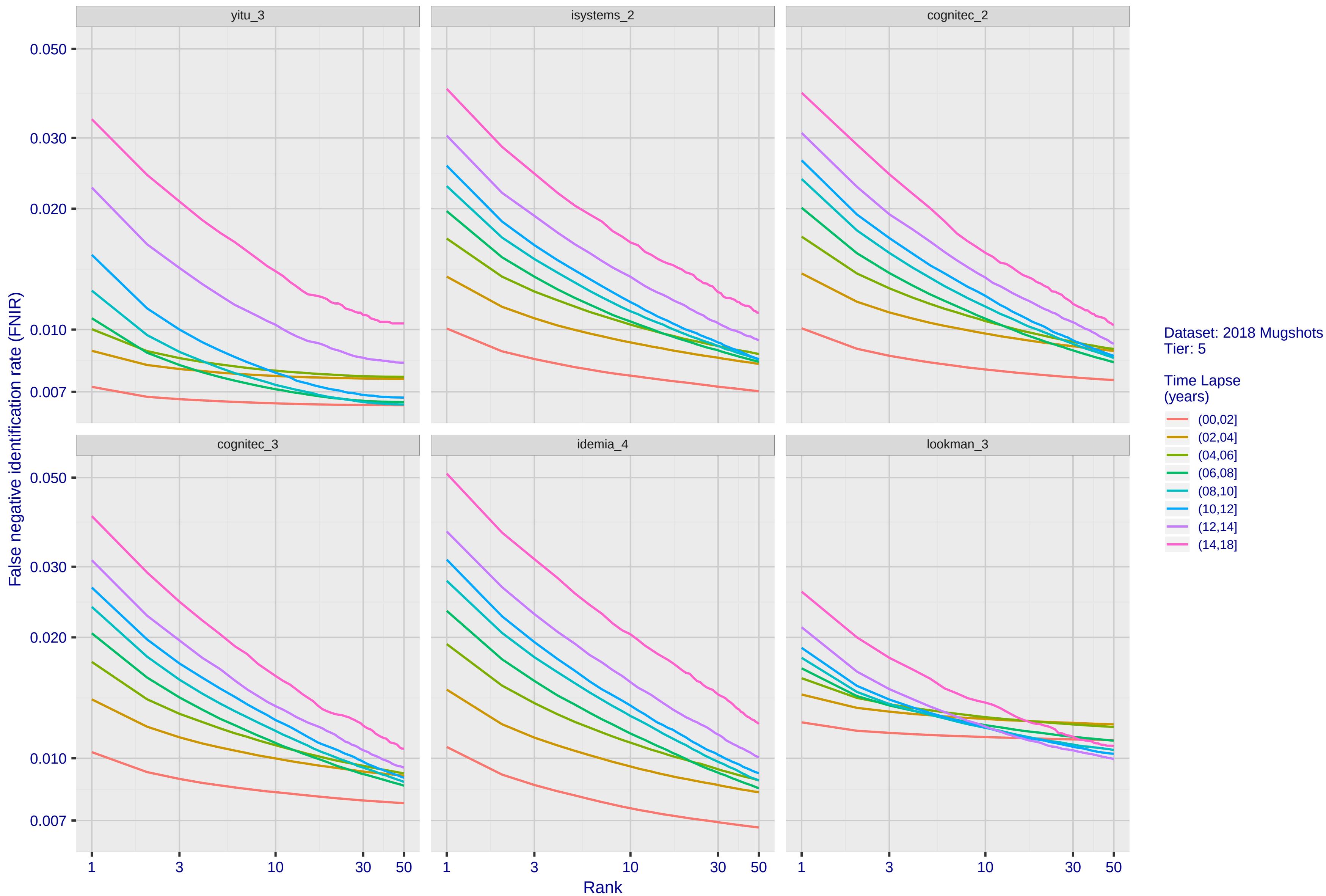

Figure 65: **[FRVT-2018 Mugshot Ageing Dataset] Identification miss rates vs. rank by time-elapsed**. *The oldest image of each individual is enrolled. Thereafter, all more recent images are searched. Miss rates are computed over all searches noted in row 17 of Table 1 and binned by number of years between search and initial enrollment.*

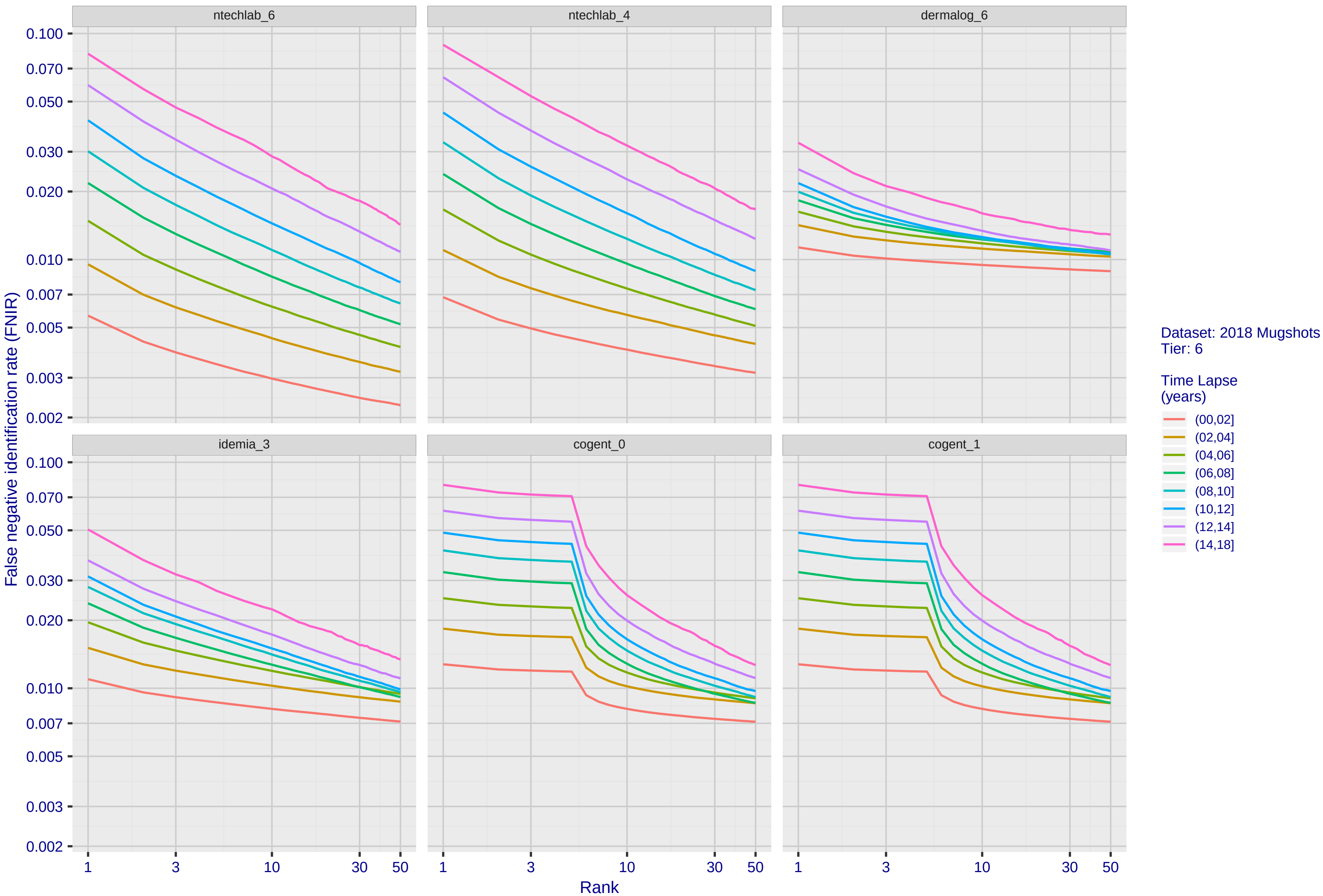

Figure 66: **[FRVT-2018 Mugshot Ageing Dataset] Identification miss rates vs. rank by time-elapsed**. *The oldest image of each individual is enrolled. Thereafter, all more recent images are searched. Miss rates are computed over all searches noted in row 17 of Table 1 and binned by number of years between search and initial enrollment.*

FNIR(N, R, T) = False neg. identification rate
FPIR(N, T) = False pos. identification rate
N = Num. enrolled subjects
R = Num. candidates examined
T = Threshold
T = 0 → Investigation
T > 0 → Identification

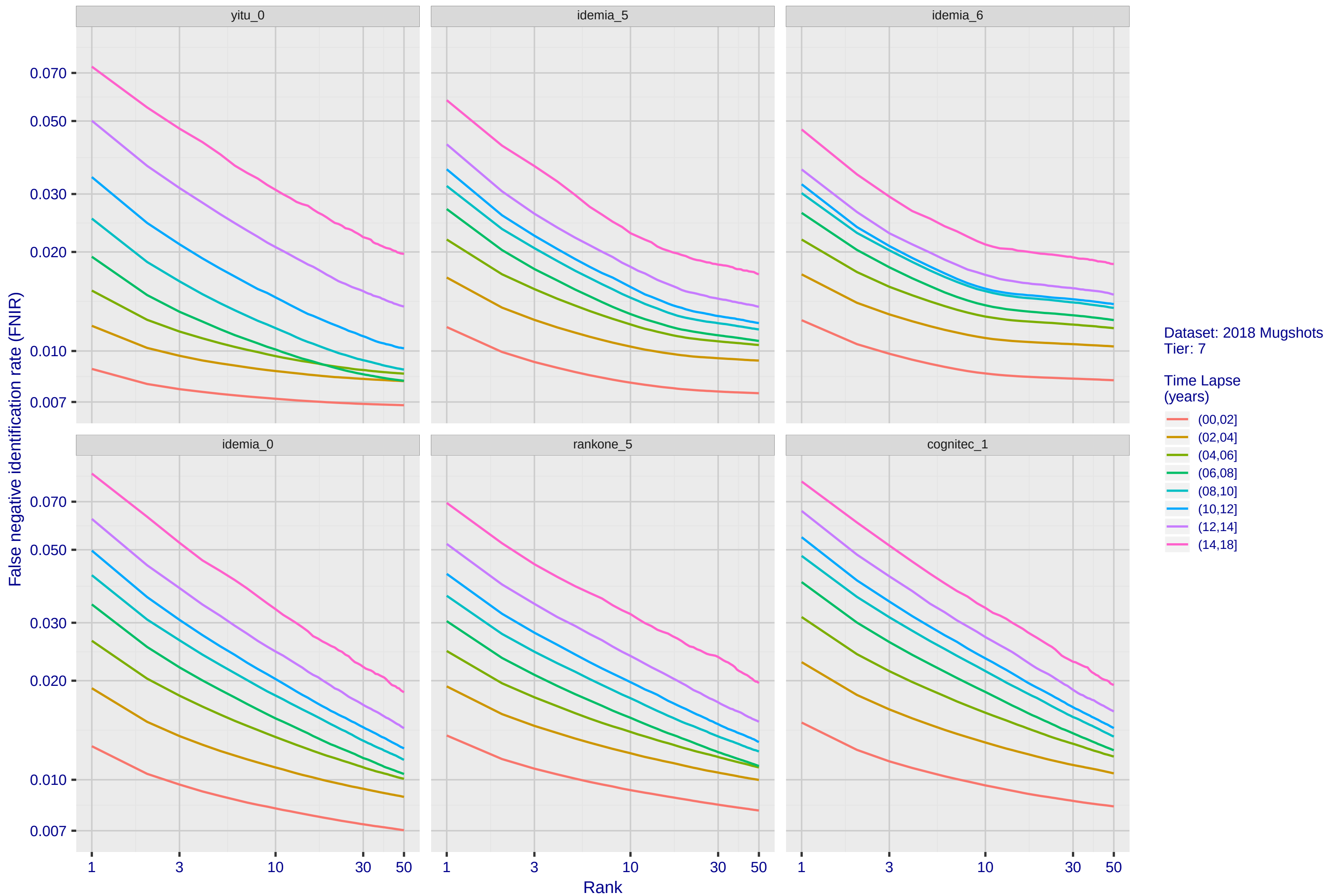

Figure 67: **[FRVT-2018 Mugshot Ageing Dataset] Identification miss rates vs. rank by time-elapsed**. *The oldest image of each individual is enrolled. Thereafter, all more recent images are searched. Miss rates are computed over all searches noted in row 17 of Table 1 and binned by number of years between search and initial enrollment.*

This publication is available free of charge from: https://doi.org/10.6028/NIST.IR.8271

FNIR(N, R, T) = False neg. identification rate
FPIR(N, T) = False pos. identification rate
N = Num. enrolled subjects
R = Num. candidates examined
T = Threshold
T = 0 → Investigation
T > 0 → Identification

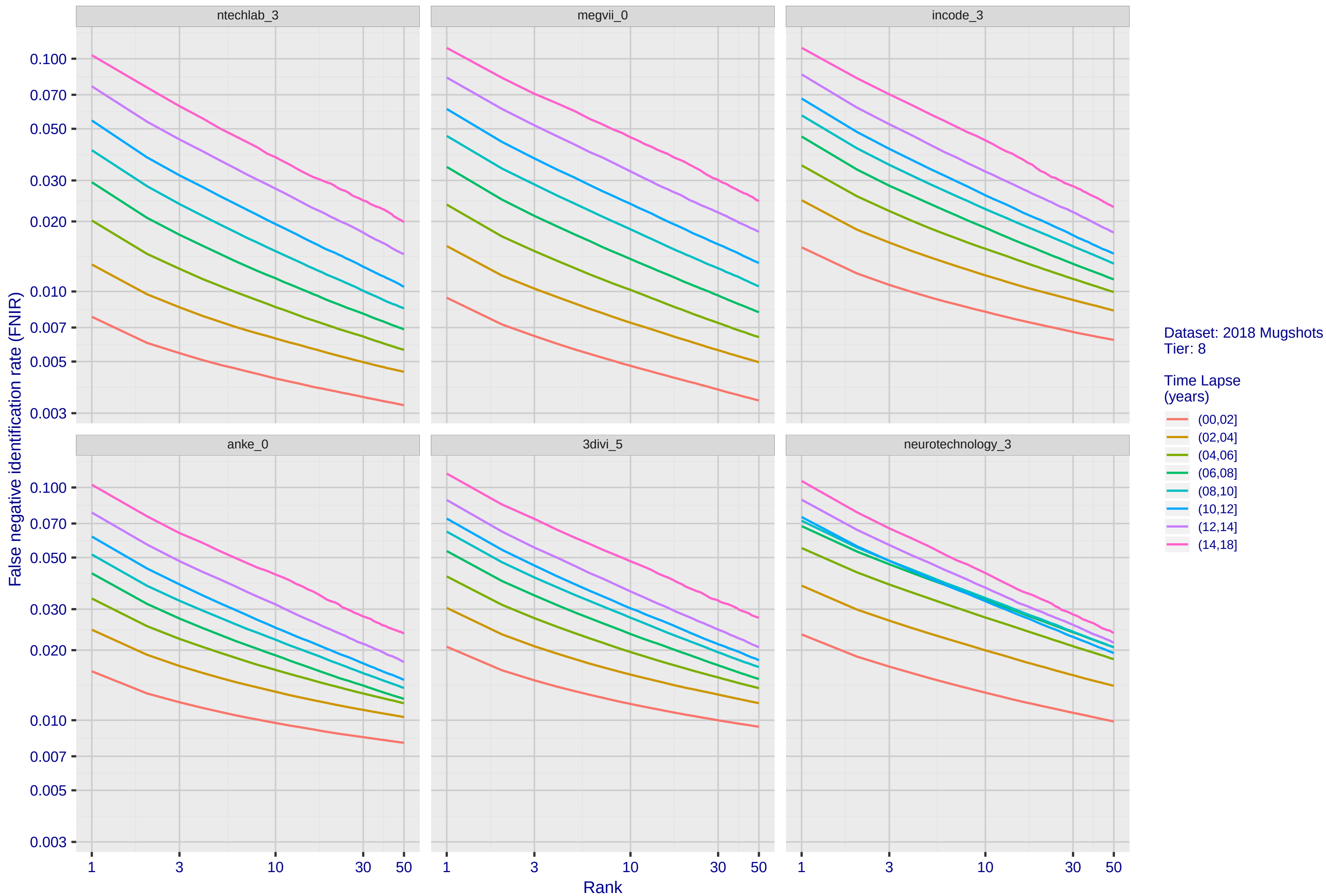

Figure 68: **[FRVT-2018 Mugshot Ageing Dataset] Identification miss rates vs. rank by time-elapsed**. *The oldest image of each individual is enrolled. Thereafter, all more recent images are searched. Miss rates are computed over all searches noted in row 17 of Table 1 and binned by number of years between search and initial enrollment.*

This publication is available free of charge from: https://doi.org/10.6028/NIST.IR.8271

2020/02/26 13:34:01

FNIR(N, R, T) = False neg. identification rate
FPIR(N, T) = False pos. identification rate
N = Num. enrolled subjects
R = Num. candidates examined
T = Threshold
T = 0 → Investigation
T > 0 → Identification

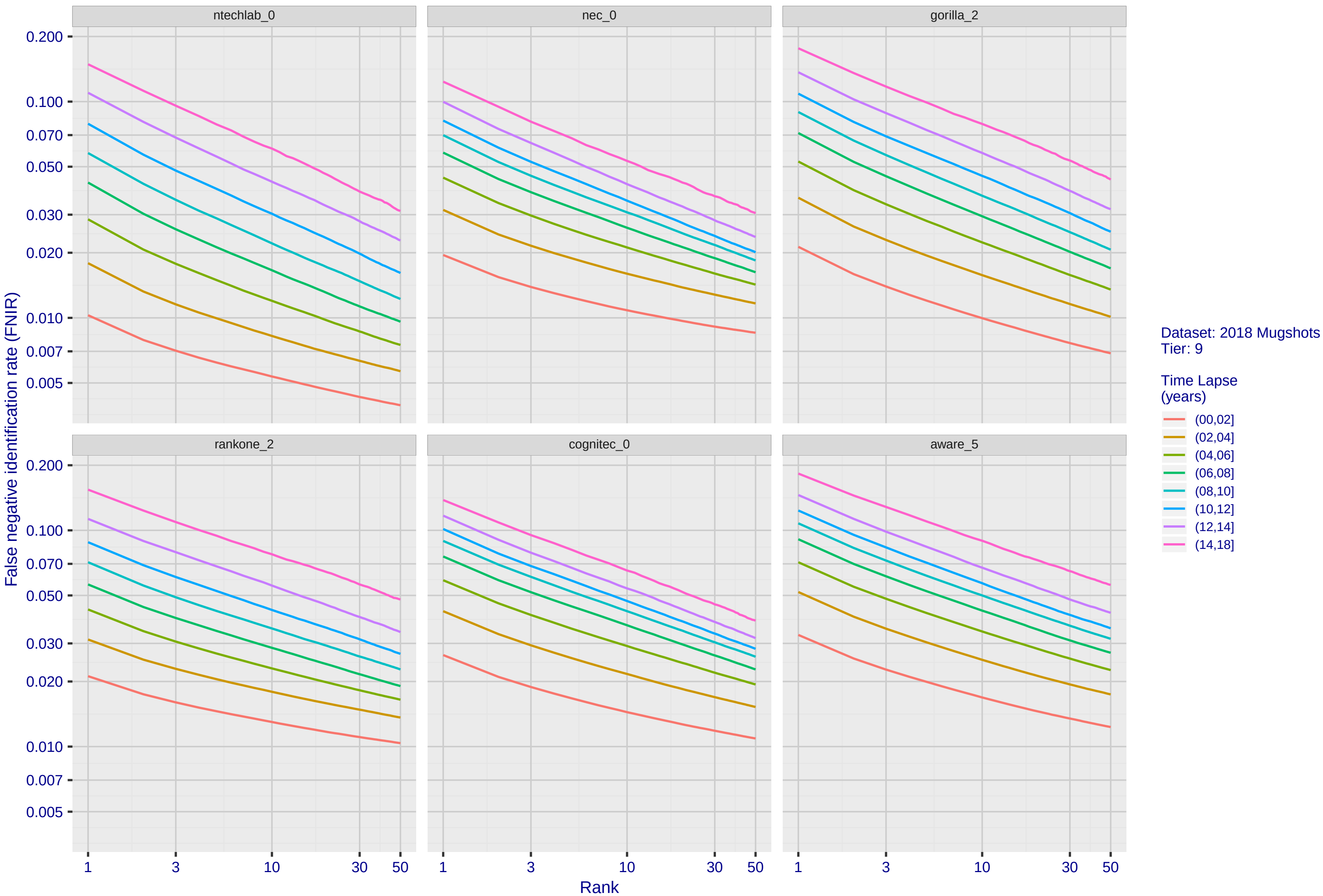

Figure 69: **[FRVT-2018 Mugshot Ageing Dataset] Identification miss rates vs. rank by time-elapsed**. *The oldest image of each individual is enrolled. Thereafter, all more recent images are searched. Miss rates are computed over all searches noted in row 17 of Table 1 and binned by number of years between search and initial enrollment.*

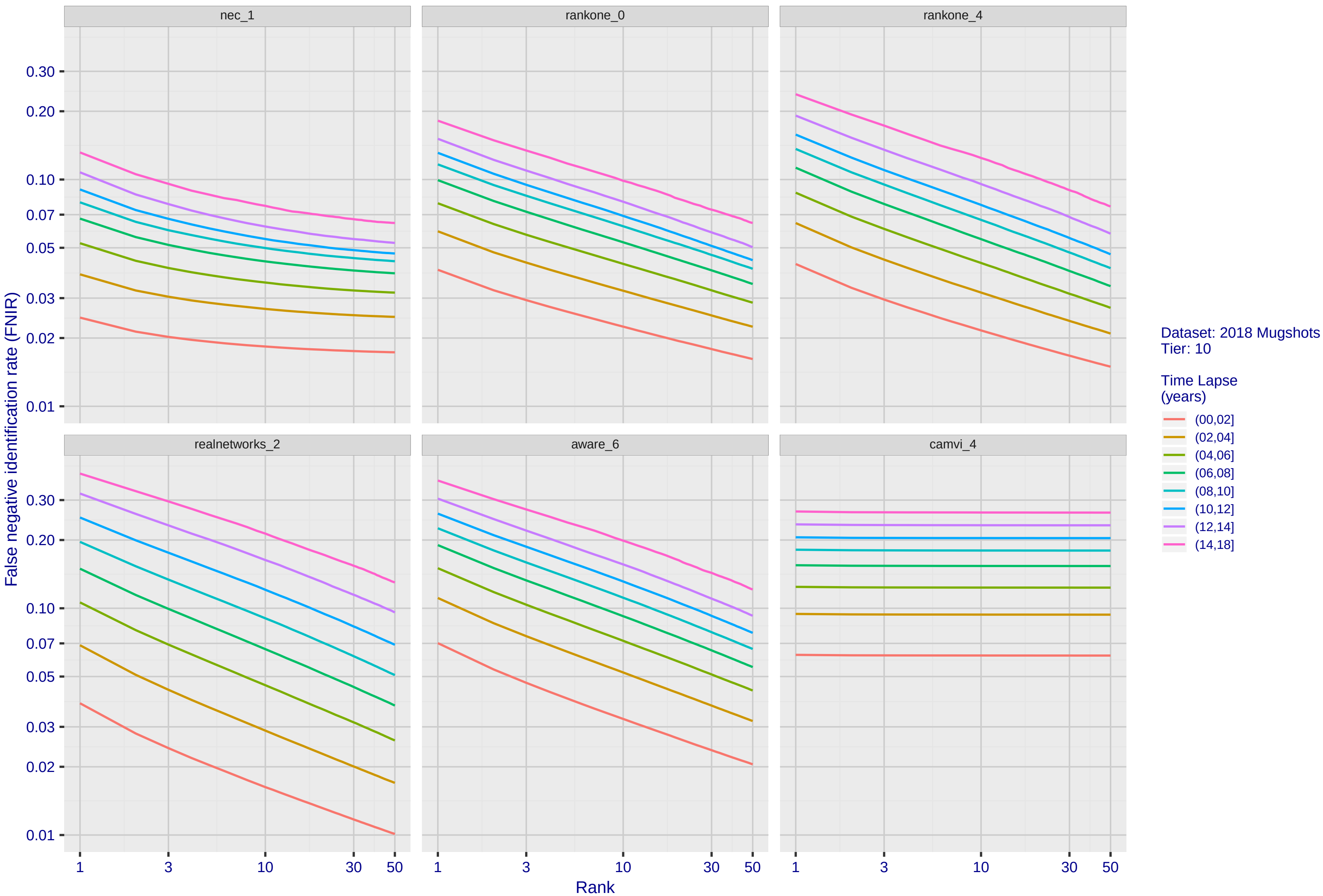

Figure 70: **[FRVT-2018 Mugshot Ageing Dataset] Identification miss rates vs. rank by time-elapsed**. *The oldest image of each individual is enrolled. Thereafter, all more recent images are searched. Miss rates are computed over all searches noted in row 17 of Table 1 and binned by number of years between search and initial enrollment.*

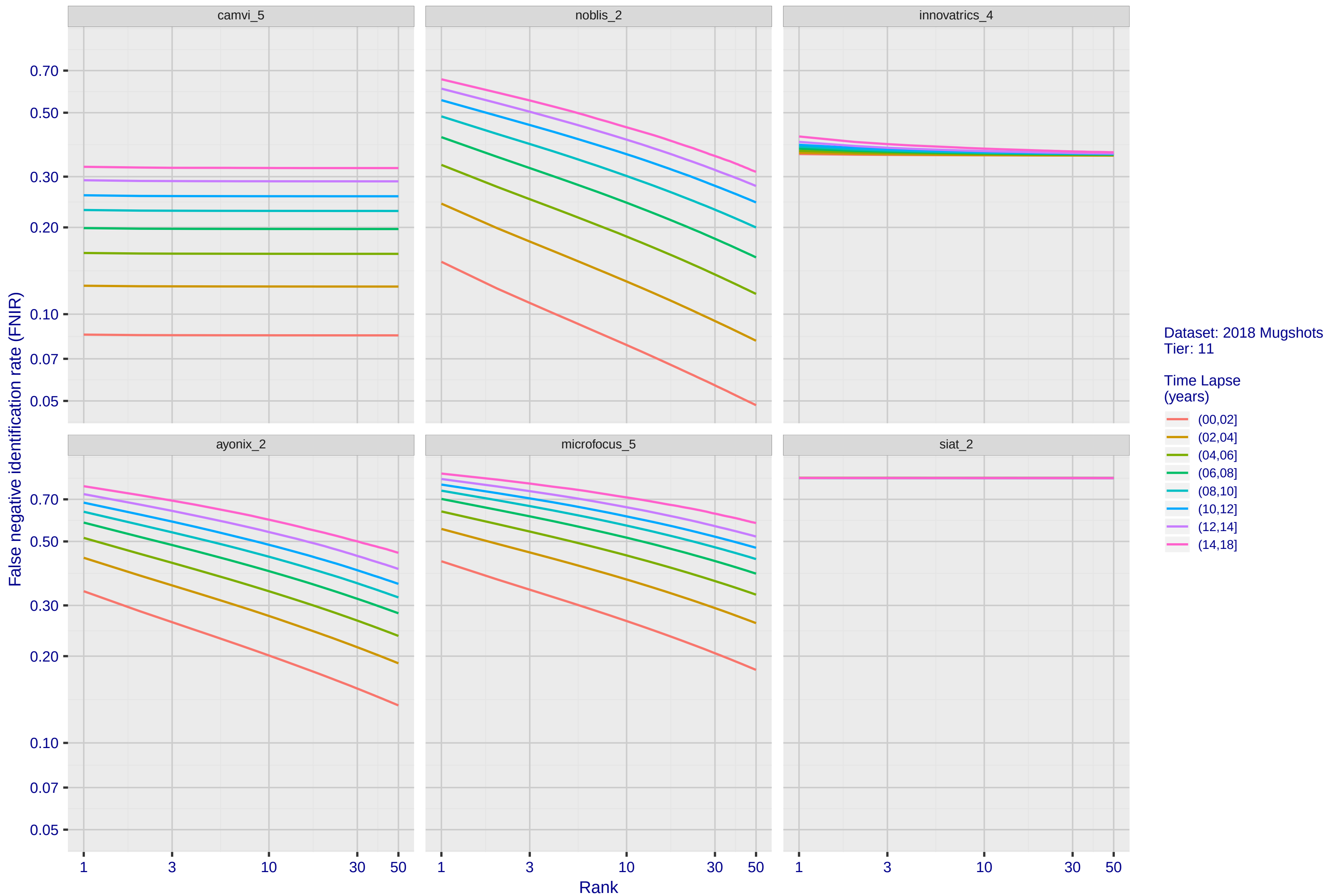

Figure 71: **[FRVT-2018 Mugshot Ageing Dataset] Identification miss rates vs. rank by time-elapsed**. *The oldest image of each individual is enrolled. Thereafter, all more recent images are searched. Miss rates are computed over all searches noted in row 17 of Table 1 and binned by number of years between search and initial enrollment.*

2020/02/26	FNIR(N, R, T) =	False neg. identification rate	N = Num. enrolled subjects	T = Threshold	$T = 0 \rightarrow$ Investigation
13:34:01	FPIR(N, T) =	False pos. identification rate	R = Num. candidates examined		$T > 0 \rightarrow$ Identification

FNIR(N, R, T) = False neg. identification rate
FPIR(N, T) = False pos. identification rate
N = Num. enrolled subjects
R = Num. candidates examined
T = Threshold
T = 0 → Investigation
T > 0 → Identification

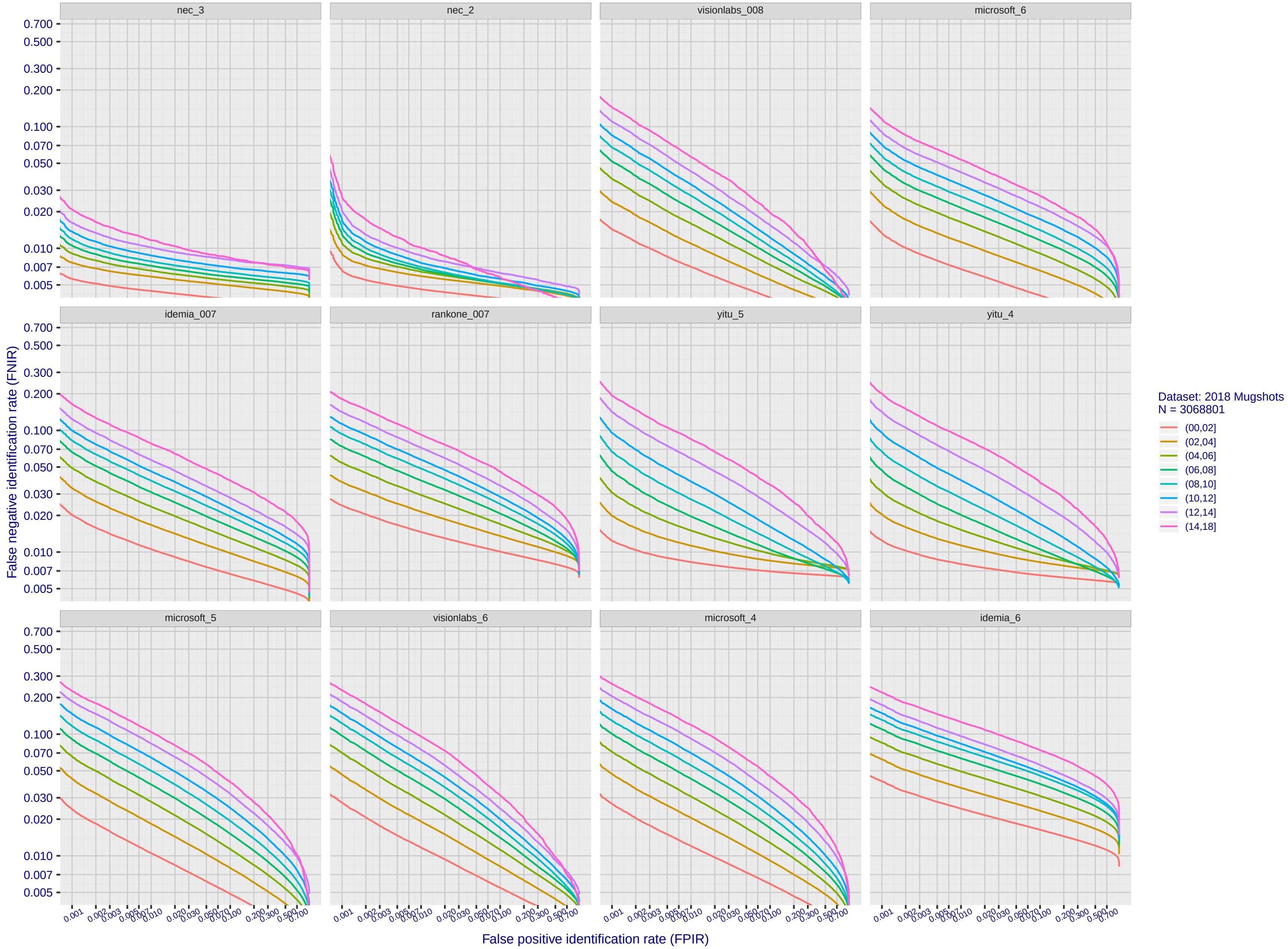

Figure 72: **[FRVT-2018 Mugshot Ageing Dataset] Identification miss rates vs. FPIR by time-elapsed**. *The oldest image of each individual is enrolled. Thereafter, all more recent images are searched. Miss rates are computed over all searches noted in row 17 of Table 1 and binned by number of years between search and initial enrollment. FPIR is computed from the same FRVT 2018 non-mates noted in row 3 of Table 1 with N = 3 000 000.*

FNIR(N, R, T) = False neg. identification rate
FPIR(N, T) = False pos. identification rate
N = Num. enrolled subjects
R = Num. candidates examined
T = Threshold
T = 0 → Investigation
T > 0 → Identification

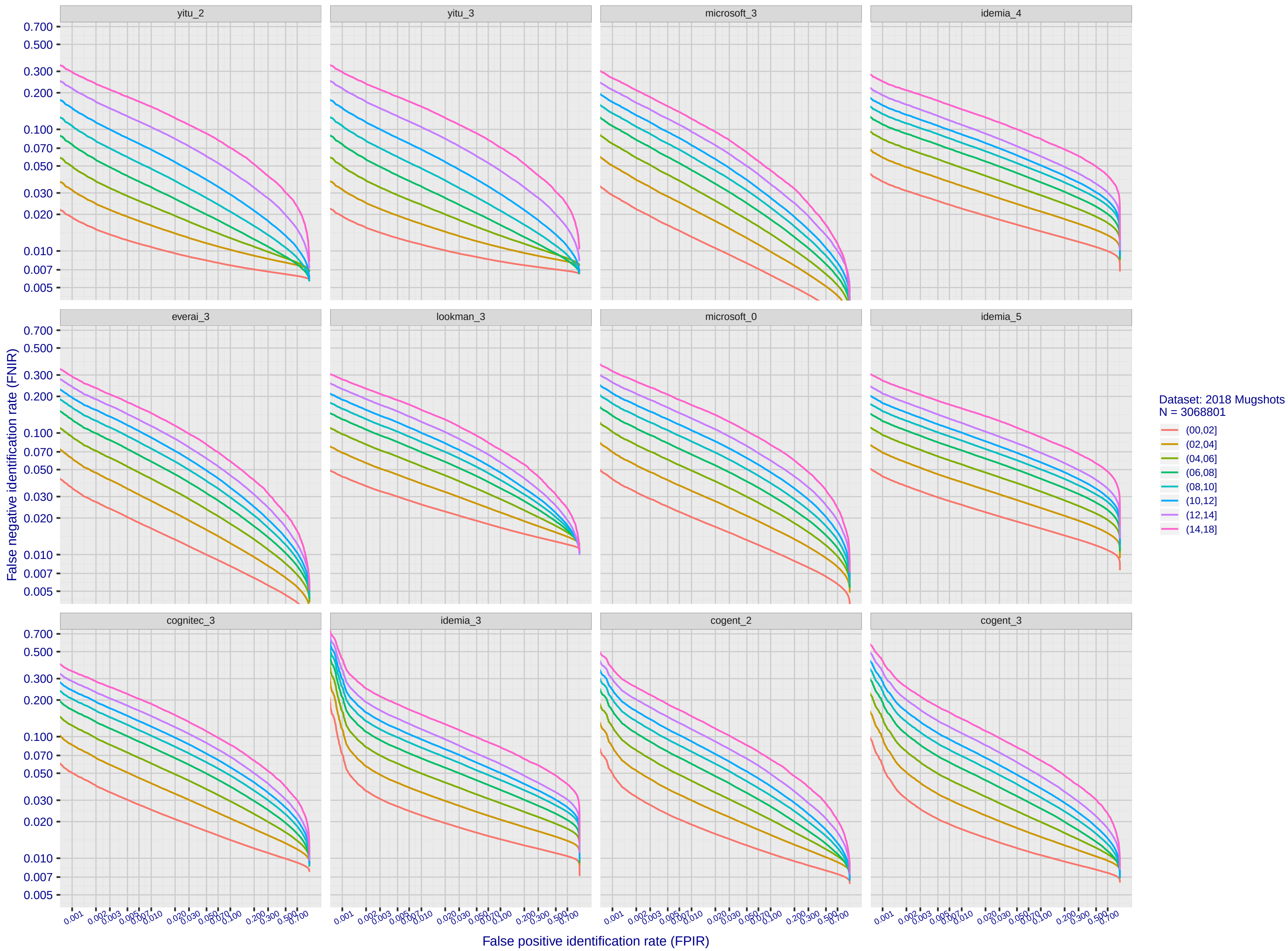

Figure 73: **[FRVT-2018 Mugshot Ageing Dataset] Identification miss rates vs. FPIR by time-elapsed**. *The oldest image of each individual is enrolled. Thereafter, all more recent images are searched. Miss rates are computed over all searches noted in row 17 of Table 1 and binned by number of years between search and initial enrollment. FPIR is computed from the same FRVT 2018 non-mates noted in row 3 of Table 1 with N = 3 000 000.*

This publication is available free of charge from: https://doi.org/10.6028/NIST.IR.8271

FNIR(N, R, T) = False neg. identification rate
FPIR(N, T) = False pos. identification rate
N = Num. enrolled subjects
R = Num. candidates examined
T = Threshold
T = 0 → Investigation
T > 0 → Identification

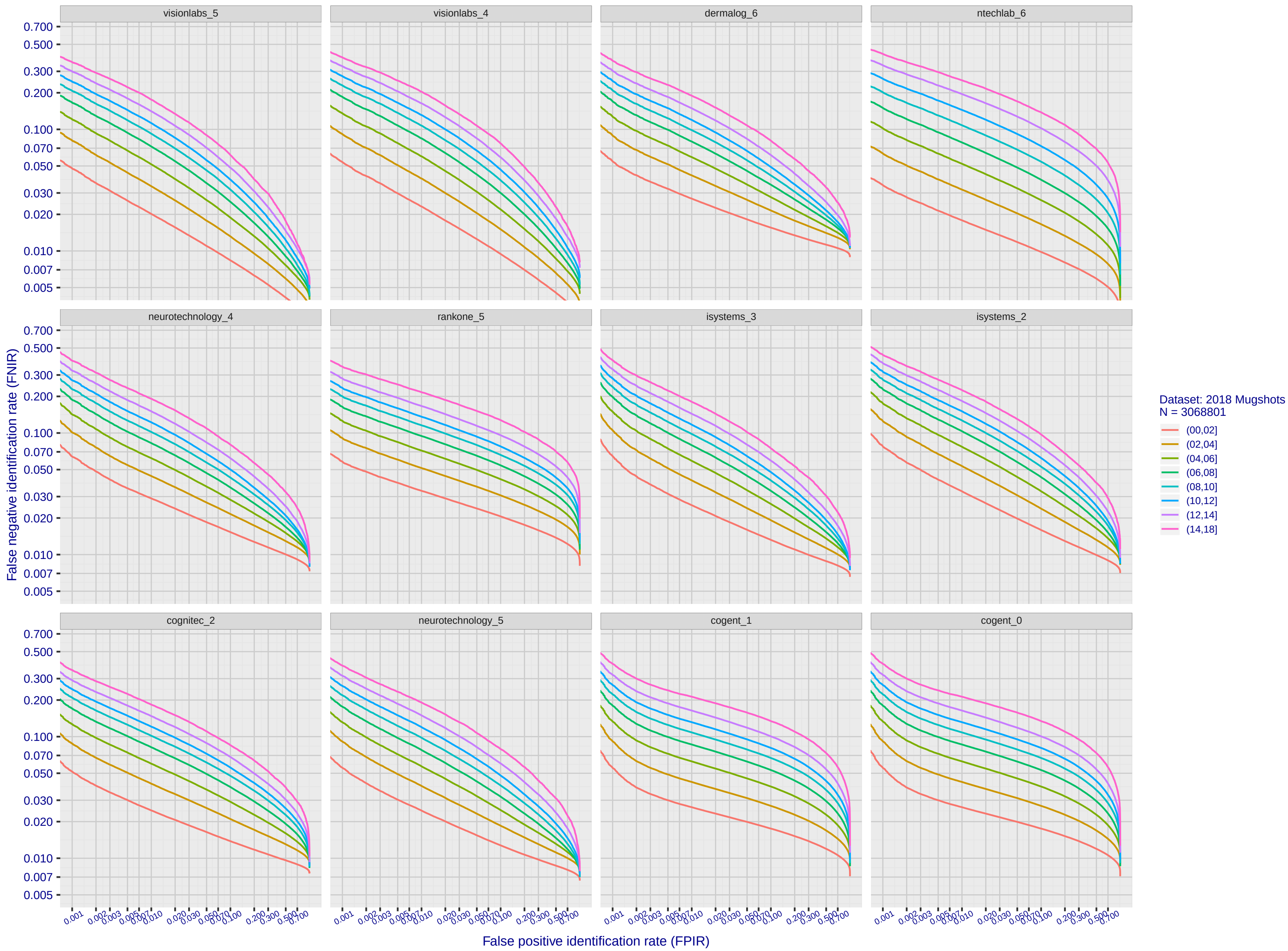

Figure 74: **[FRVT-2018 Mugshot Ageing Dataset] Identification miss rates vs. FPIR by time-elapsed**. *The oldest image of each individual is enrolled. Thereafter, all more recent images are searched. Miss rates are computed over all searches noted in row 17 of Table 1 and binned by number of years between search and initial enrollment. FPIR is computed from the same FRVT 2018 non-mates noted in row 3 of Table 1 with N = 3 000 000.*

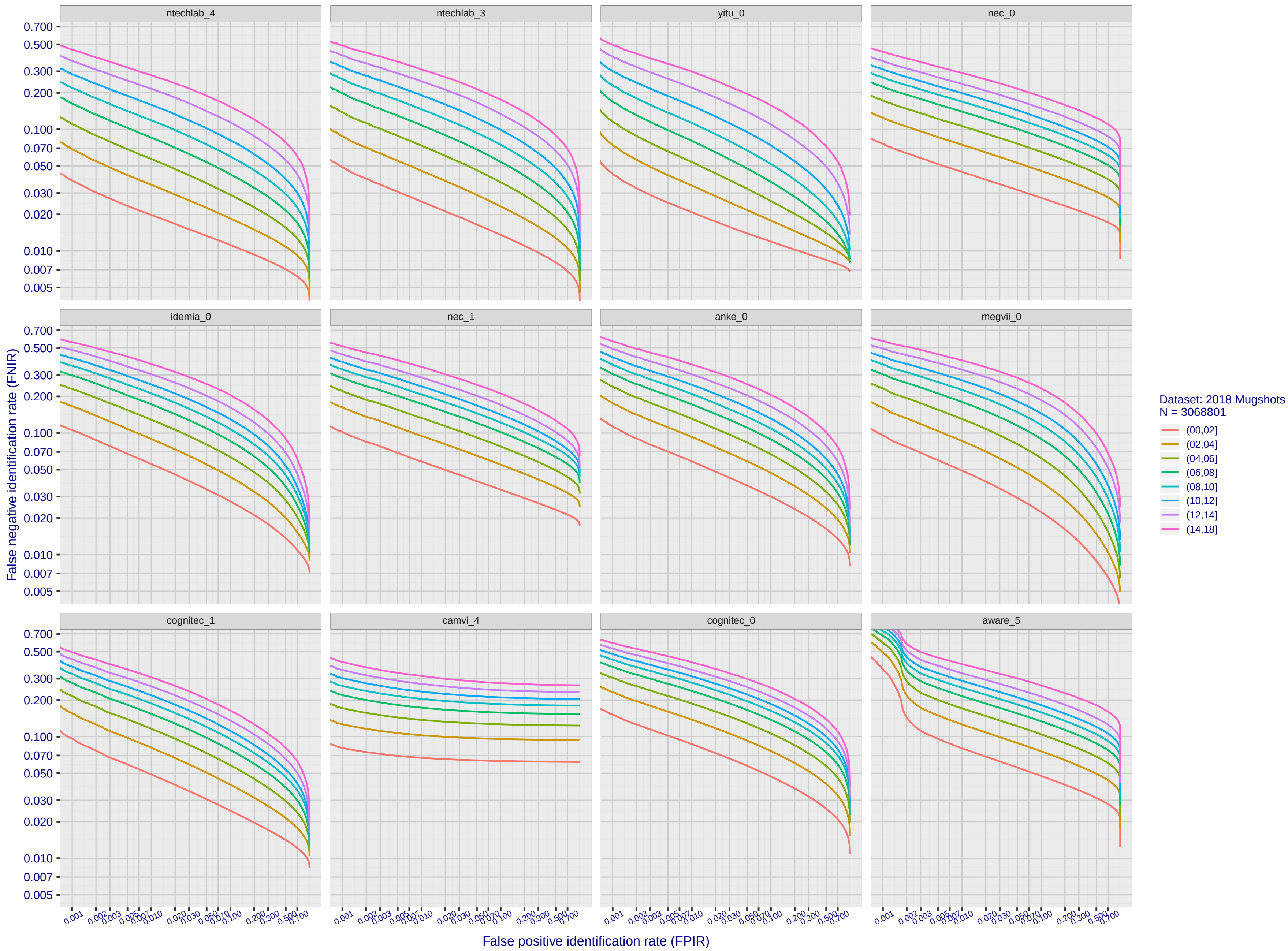

Figure 75: **[FRVT-2018 Mugshot Ageing Dataset] Identification miss rates vs. FPIR by time-elapsed**. *The oldest image of each individual is enrolled. Thereafter, all more recent images are searched. Miss rates are computed over all searches noted in row 17 of Table 1 and binned by number of years between search and initial enrollment. FPIR is computed from the same FRVT 2018 non-mates noted in row 3 of Table 1 with N = 3 000 000.*

2020/02/26
13:34:01

FNIR(N, R, T) = False neg. identification rate
FPIR(N, T) = False pos. identification rate
N = Num. enrolled subjects
R = Num. candidates examined
T = Threshold
T = 0 → Investigation
T > 0 → Identification

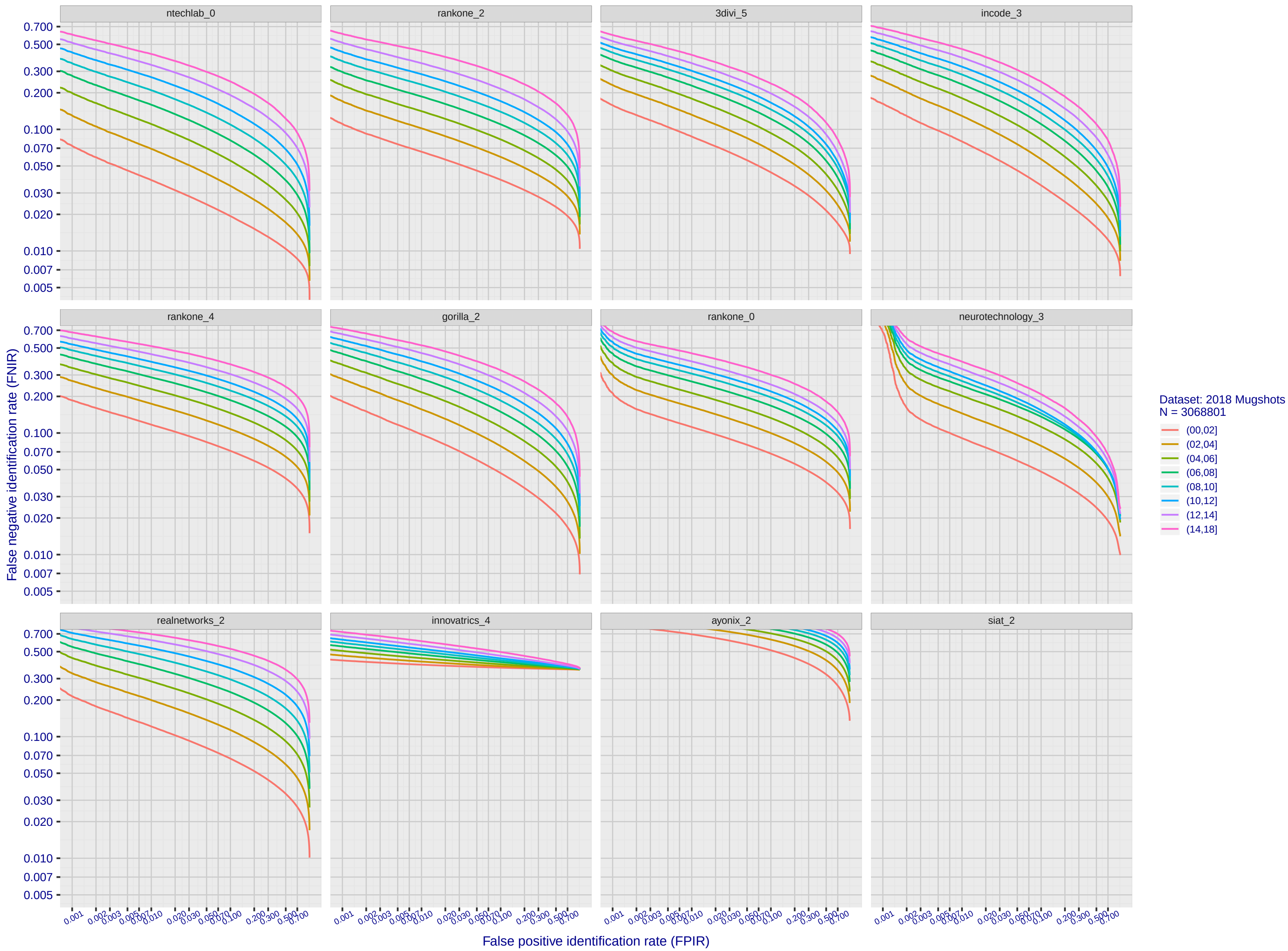

Figure 76: **[FRVT-2018 Mugshot Ageing Dataset] Identification miss rates vs. FPIR by time-elapsed**. *The oldest image of each individual is enrolled. Thereafter, all more recent images are searched. Miss rates are computed over all searches noted in row 17 of Table 1 and binned by number of years between search and initial enrollment. FPIR is computed from the same FRVT 2018 non-mates noted in row 3 of Table 1 with N = 3 000 000.*

This publication is available free of charge from: https://doi.org/10.6028/NIST.IR.8271

FNIR(N, R, T) = False neg. identification rate
FPIR(N, T) = False pos. identification rate
N = Num. enrolled subjects
R = Num. candidates examined
T = Threshold
T = 0 → Investigation
T > 0 → Identification

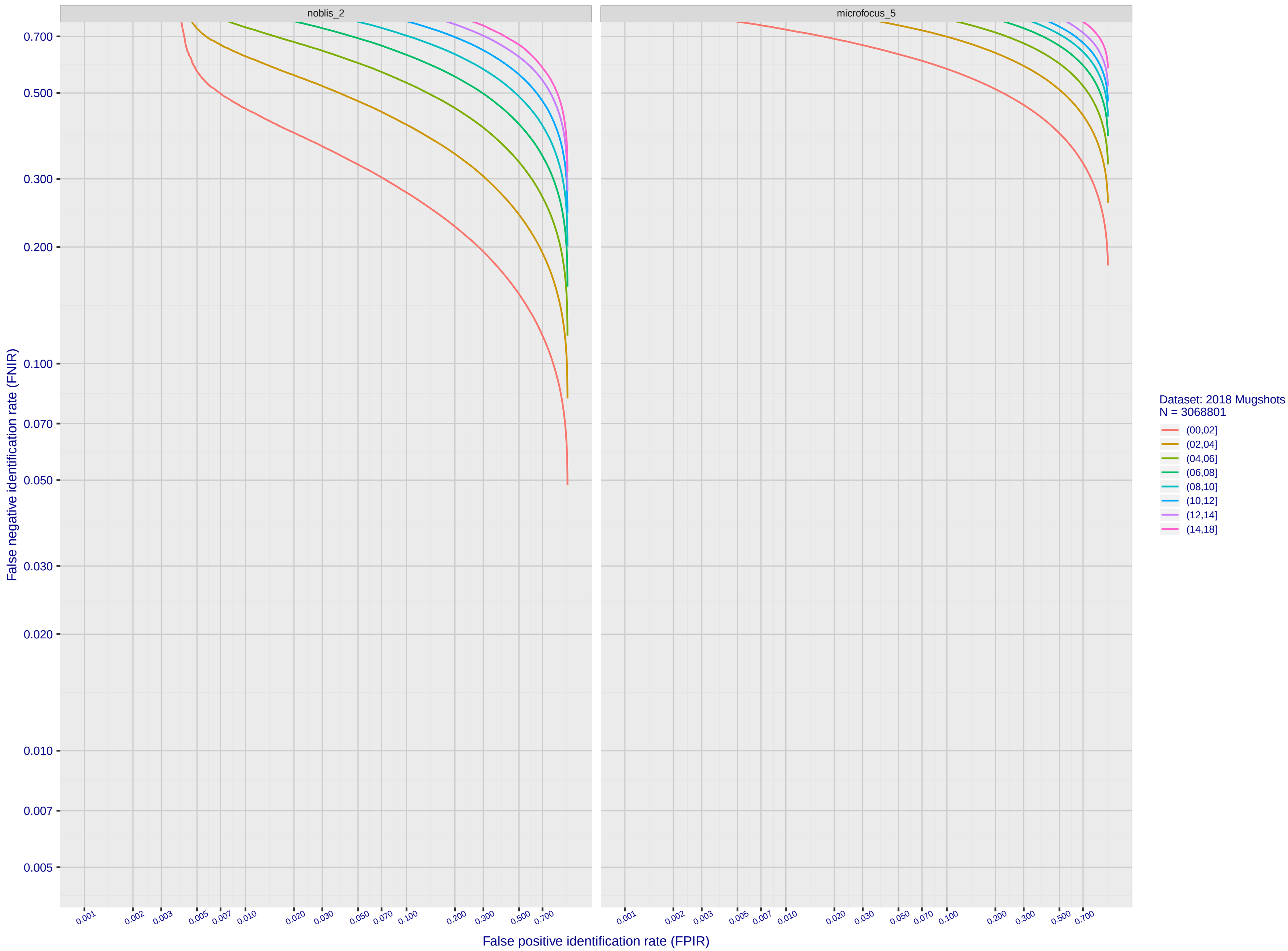

Figure 77: **[FRVT-2018 Mugshot Ageing Dataset] Identification miss rates vs. FPIR by time-elapsed**. *The oldest image of each individual is enrolled. Thereafter, all more recent images are searched. Miss rates are computed over all searches noted in row 17 of Table 1 and binned by number of years between search and initial enrollment. FPIR is computed from the same FRVT 2018 non-mates noted in row 3 of Table 1 with N = 3 000 000.*

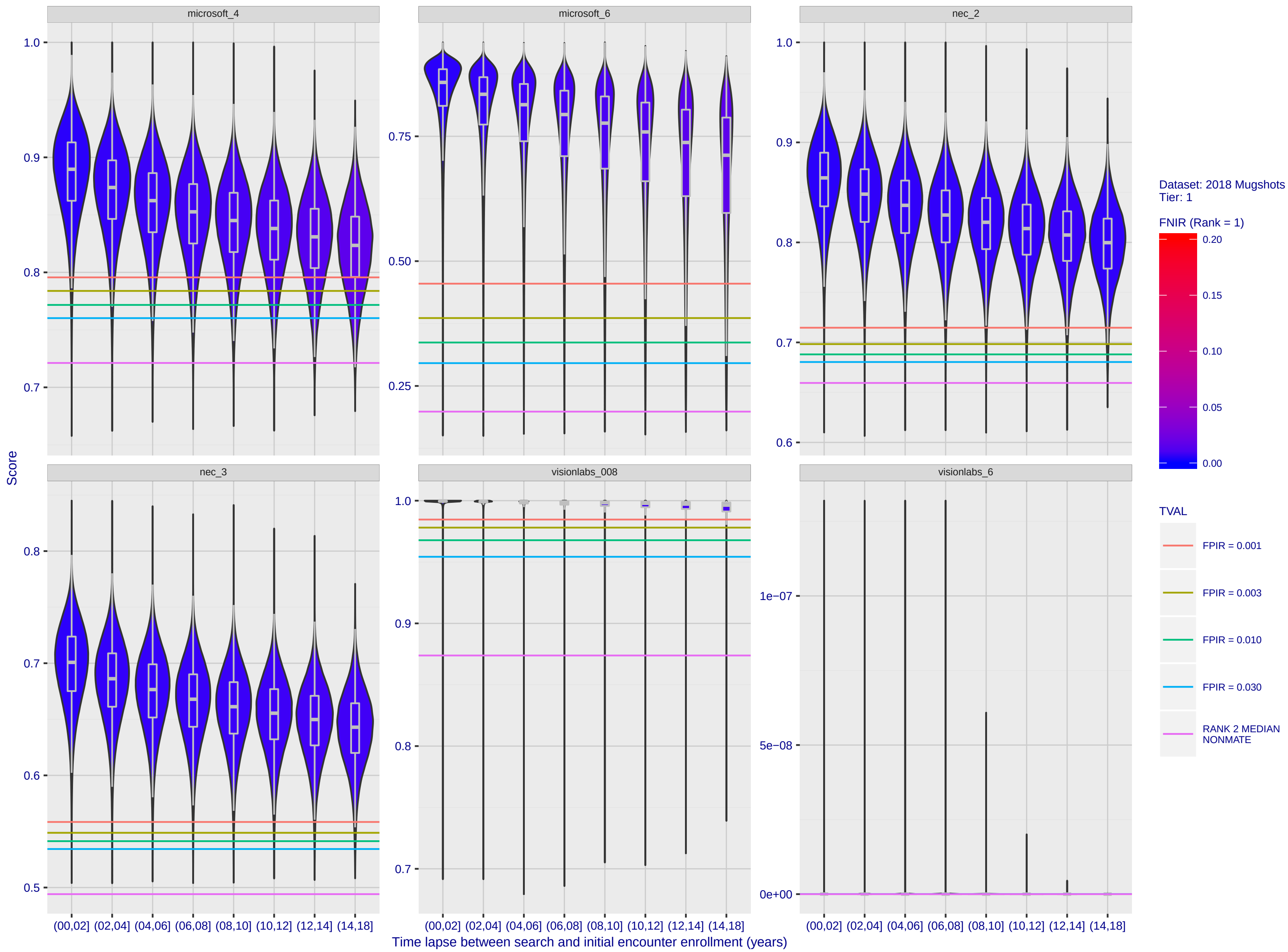

Figure 78: **[FRVT-2018 Mugshot Ageing Dataset] Native mate scores vs. time-elapsed**. *The oldest image of each individual is enrolled. Thereafter, all more recent images are searched. Mated score distributions are computed over all searches noted in row 17 of Table 1 binned by number of years between search and initial enrollment.*

FNIR(N, R, T) = False neg. identification rate
FPIR(N, T) = False pos. identification rate
N = Num. enrolled subjects
R = Num. candidates examined
T = Threshold
T = 0 → Investigation
T > 0 → Identification

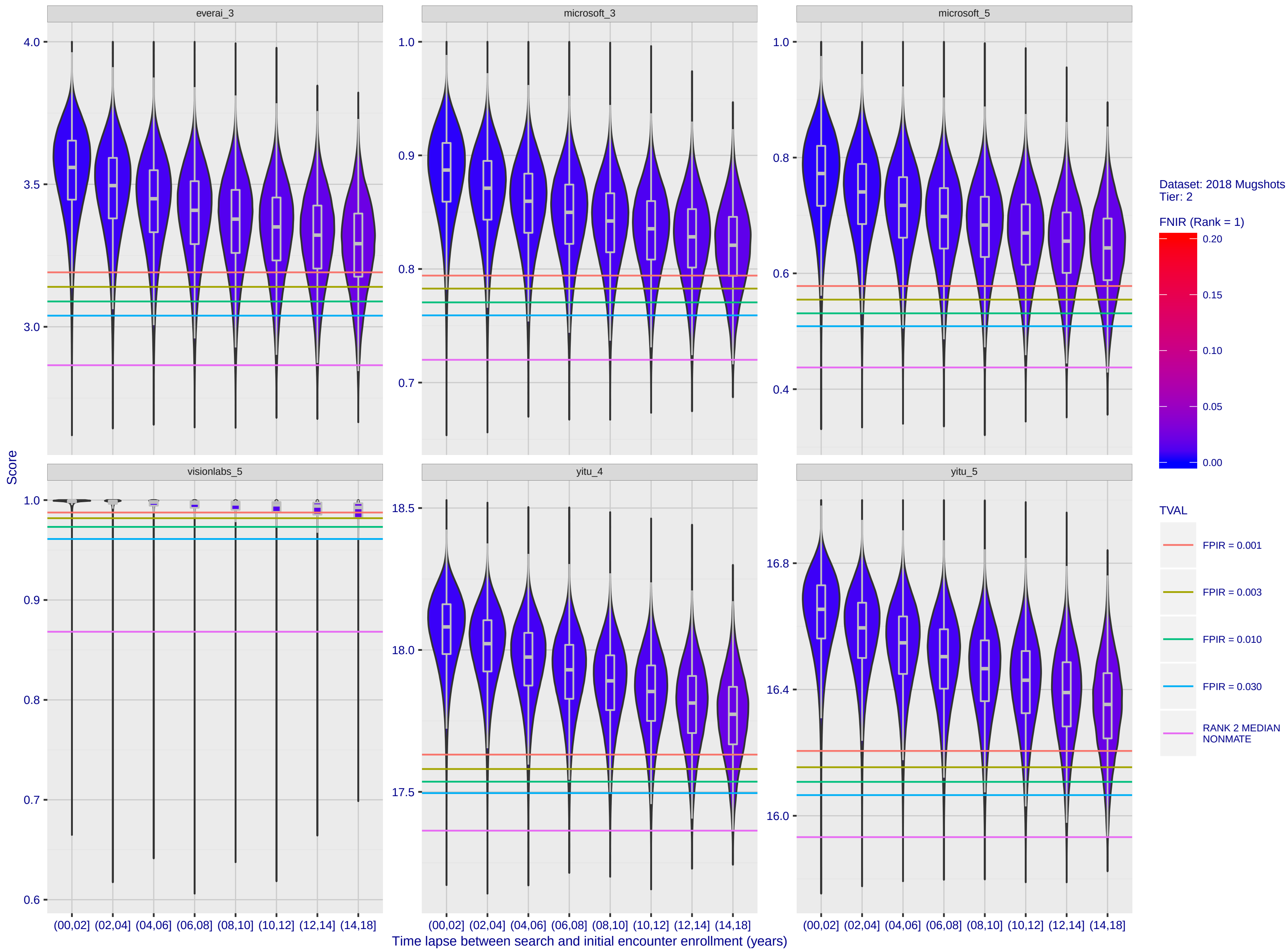

Figure 79: **[FRVT-2018 Mugshot Ageing Dataset] Native mate scores vs. time-elapsed**. *The oldest image of each individual is enrolled. Thereafter, all more recent images are searched. Mated score distributions are computed over all searches noted in row 17 of Table 1 binned by number of years between search and initial enrollment.*

FNIR(N, R, T) = False neg. identification rate
FPIR(N, T) = False pos. identification rate
N = Num. enrolled subjects
R = Num. candidates examined
T = Threshold
T = 0 → Investigation
T > 0 → Identification

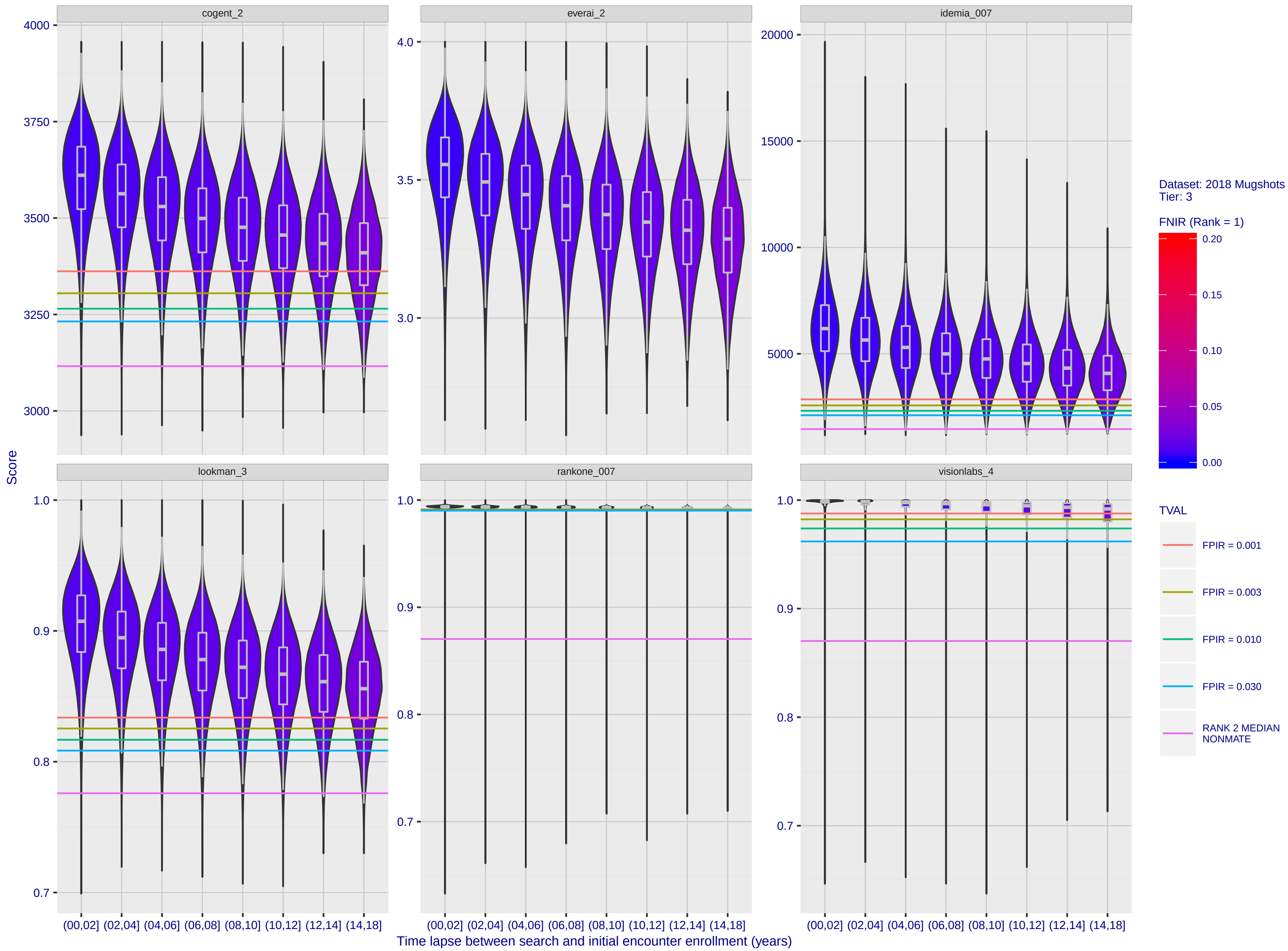

Figure 80: **[FRVT-2018 Mugshot Ageing Dataset] Native mate scores vs. time-elapsed**. *The oldest image of each individual is enrolled. Thereafter, all more recent images are searched. Mated score distributions are computed over all searches noted in row 17 of Table 1 binned by number of years between search and initial enrollment.*

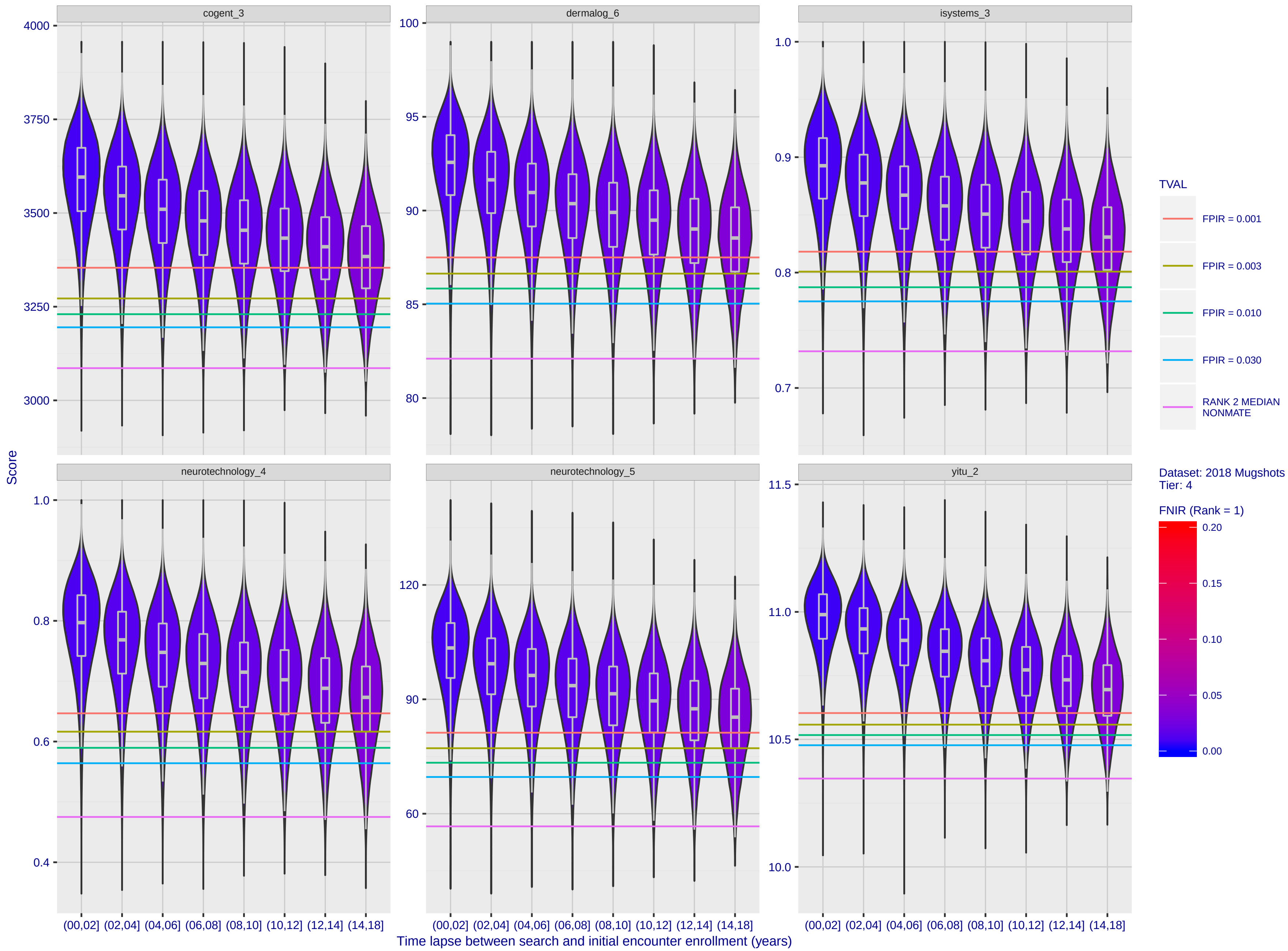

Figure 81: **[FRVT-2018 Mugshot Ageing Dataset] Native mate scores vs. time-elapsed**. *The oldest image of each individual is enrolled. Thereafter, all more recent images are searched. Mated score distributions are computed over all searches noted in row 17 of Table 1 binned by number of years between search and initial enrollment.*

FNIR(N, R, T) = False neg. identification rate
FPIR(N, T) = False pos. identification rate
N = Num. enrolled subjects
R = Num. candidates examined
T = Threshold
T = 0 → Investigation
T > 0 → Identification

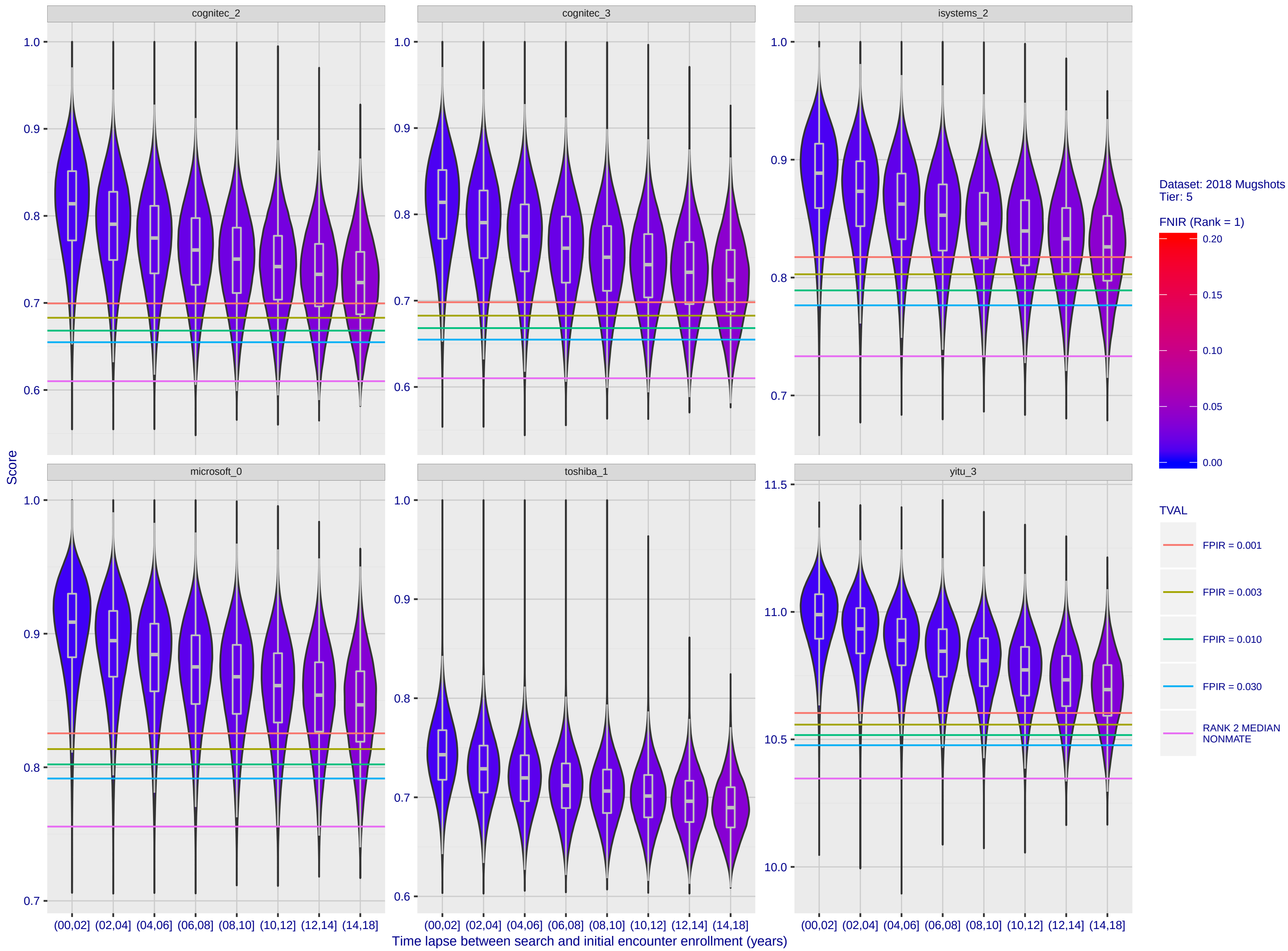

Figure 82: **[FRVT-2018 Mugshot Ageing Dataset] Native mate scores vs. time-elapsed**. *The oldest image of each individual is enrolled. Thereafter, all more recent images are searched. Mated score distributions are computed over all searches noted in row 17 of Table 1 binned by number of years between search and initial enrollment.*

This publication is available free of charge from: https://doi.org/10.6028/NIST.IR.8271

2020/02/26
13:34:01

FNIR(N, R, T) = False neg. identification rate
FPIR(N, T) = False pos. identification rate
N = Num. enrolled subjects
R = Num. candidates examined
T = Threshold
T = 0 → Investigation
T > 0 → Identification

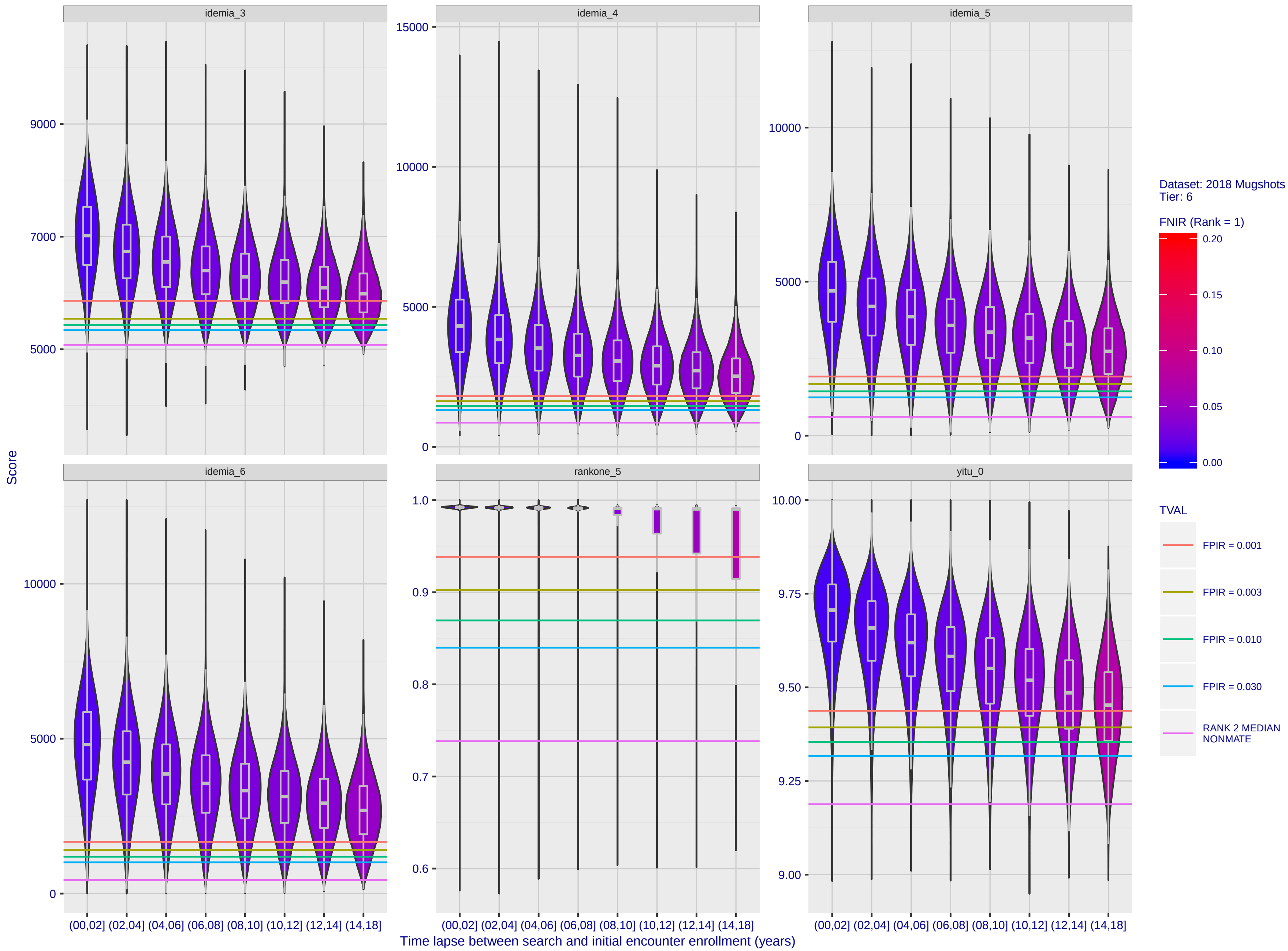

Figure 83: **[FRVT-2018 Mugshot Ageing Dataset] Native mate scores vs. time-elapsed**. *The oldest image of each individual is enrolled. Thereafter, all more recent images are searched. Mated score distributions are computed over all searches noted in row 17 of Table 1 binned by number of years between search and initial enrollment.*

2020/02/26
13:34:01

FNIR(N, R, T) = False neg. identification rate
FPIR(N, T) = False pos. identification rate
N = Num. enrolled subjects
R = Num. candidates examined
T = Threshold
T = 0 → Investigation
T > 0 → Identification

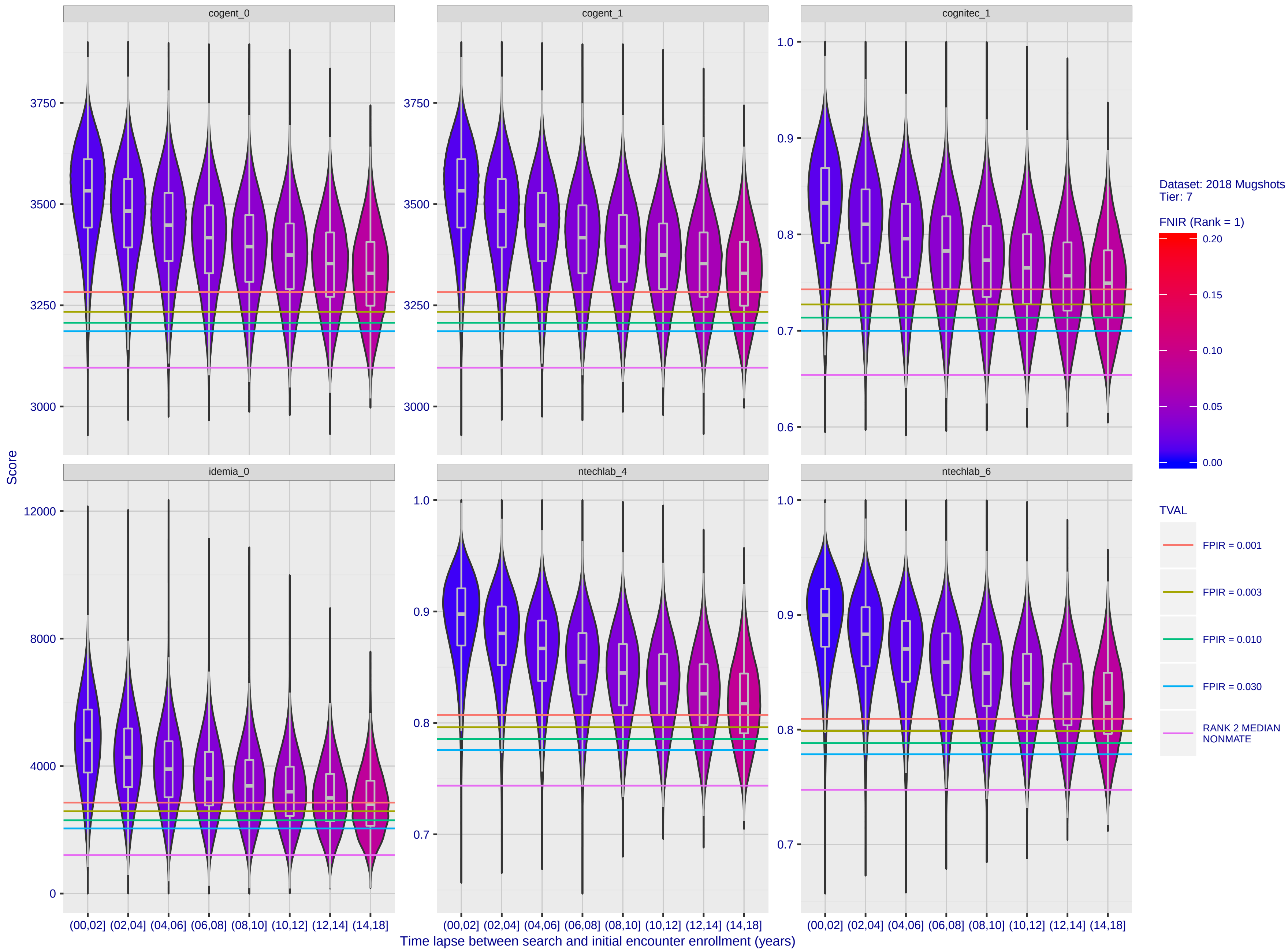

Figure 84: **[FRVT-2018 Mugshot Ageing Dataset] Native mate scores vs. time-elapsed**. *The oldest image of each individual is enrolled. Thereafter, all more recent images are searched. Mated score distributions are computed over all searches noted in row 17 of Table 1 binned by number of years between search and initial enrollment.*

FNIR(N, R, T) = False neg. identification rate
FPIR(N, T) = False pos. identification rate
N = Num. enrolled subjects
R = Num. candidates examined
T = Threshold
T = 0 → Investigation
T > 0 → Identification

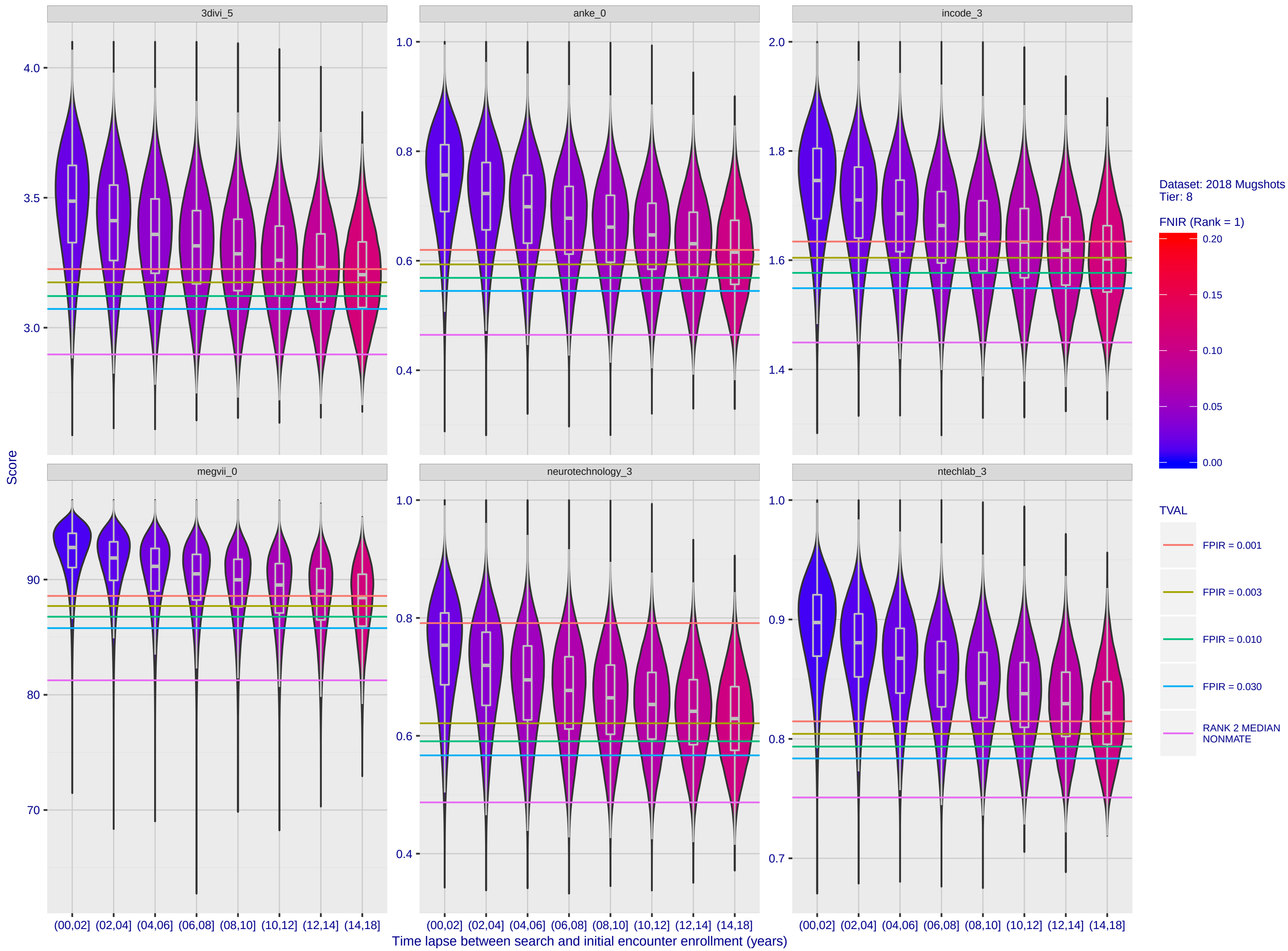

Figure 85: **[FRVT-2018 Mugshot Ageing Dataset] Native mate scores vs. time-elapsed**. *The oldest image of each individual is enrolled. Thereafter, all more recent images are searched. Mated score distributions are computed over all searches noted in row 17 of Table 1 binned by number of years between search and initial enrollment.*

FNIR(N, R, T) = False neg. identification rate
FPIR(N, T) = False pos. identification rate
N = Num. enrolled subjects
R = Num. candidates examined
T = Threshold
T = 0 → Investigation
T > 0 → Identification

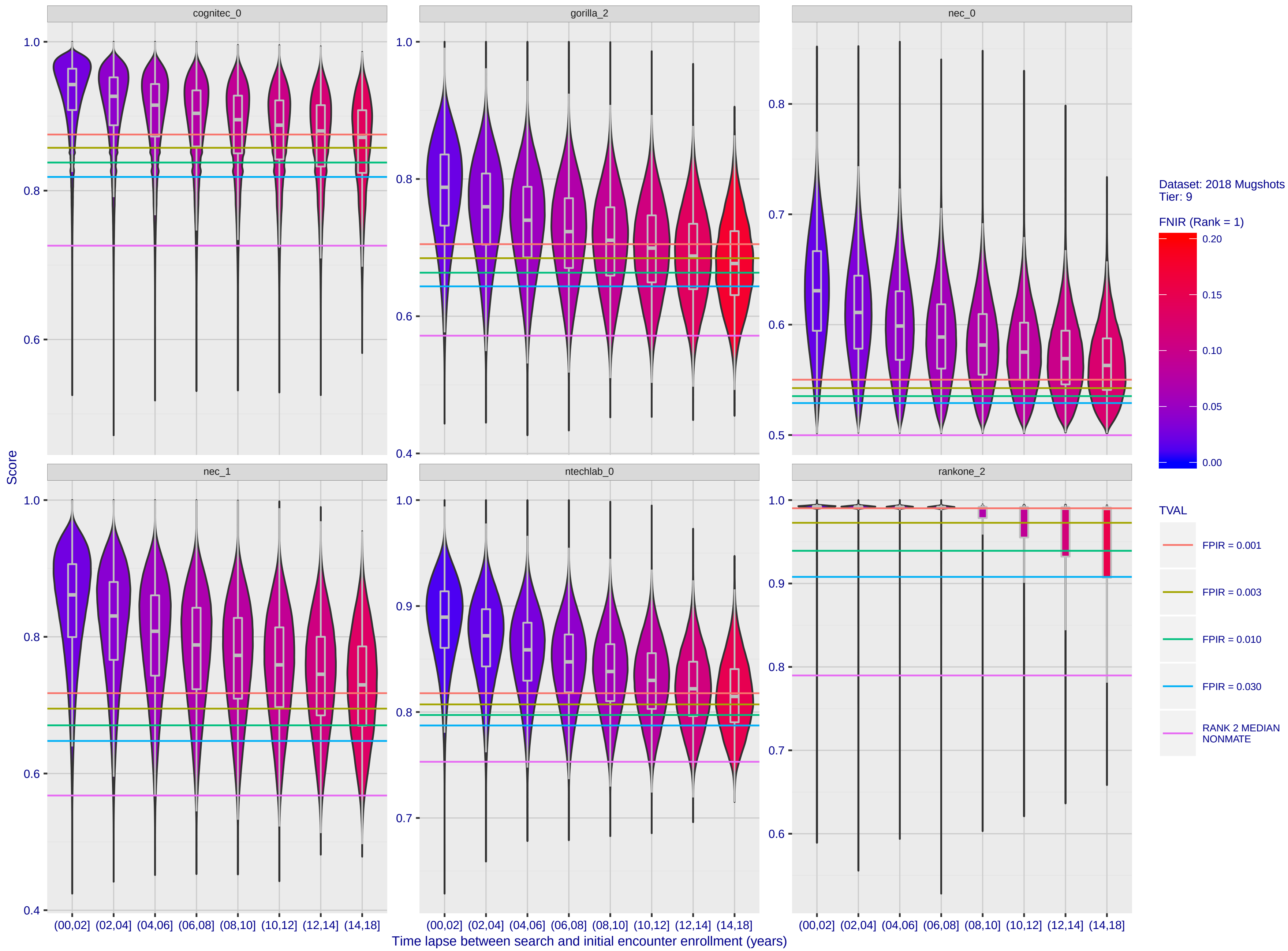

Figure 86: **[FRVT-2018 Mugshot Ageing Dataset] Native mate scores vs. time-elapsed**. *The oldest image of each individual is enrolled. Thereafter, all more recent images are searched. Mated score distributions are computed over all searches noted in row 17 of Table 1 binned by number of years between search and initial enrollment.*

This publication is available free of charge from: https://doi.org/10.6028/NIST.IR.8271

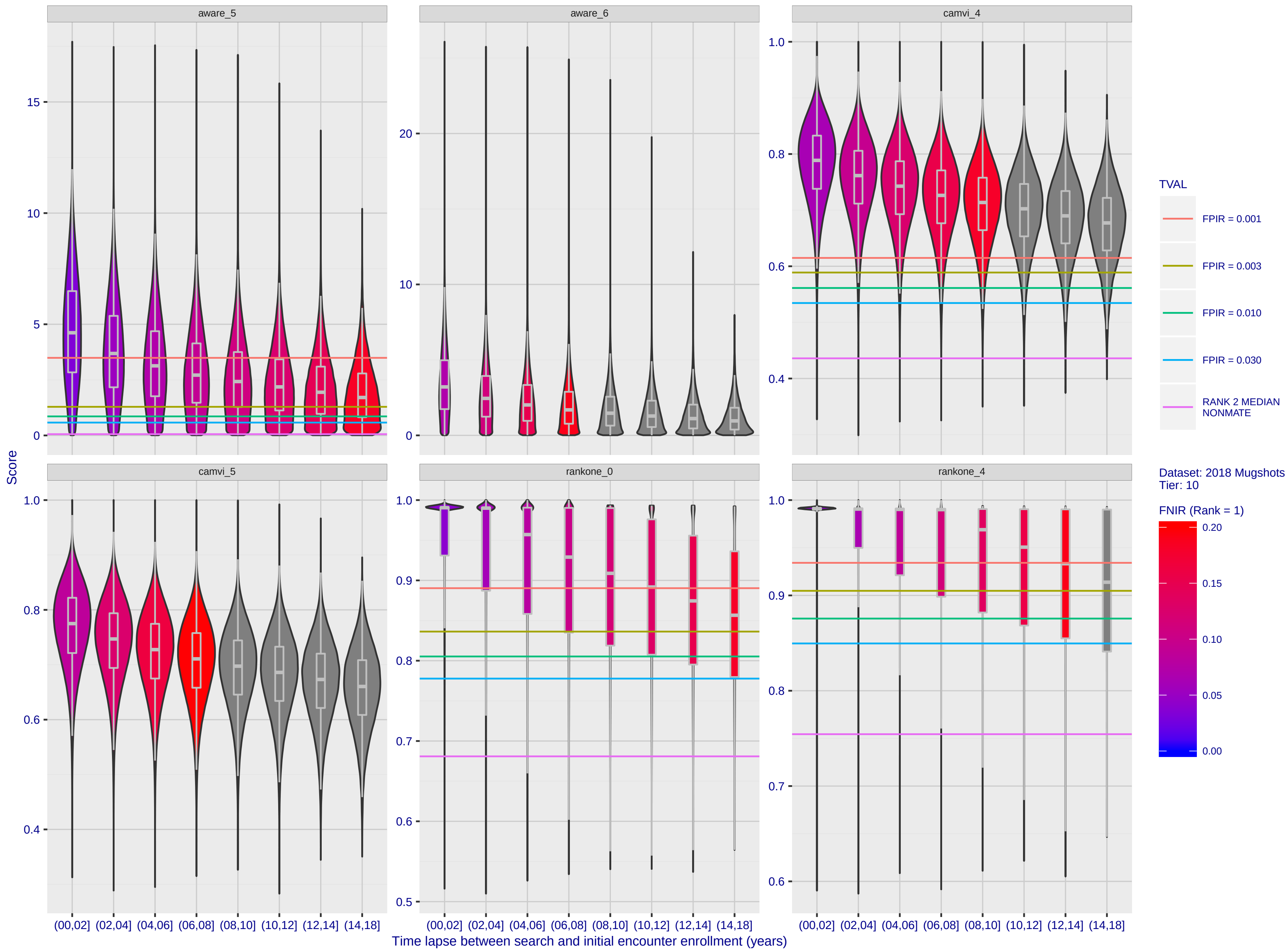

Figure 87: **[FRVT-2018 Mugshot Ageing Dataset] Native mate scores vs. time-elapsed**. *The oldest image of each individual is enrolled. Thereafter, all more recent images are searched. Mated score distributions are computed over all searches noted in row 17 of Table 1 binned by number of years between search and initial enrollment.*

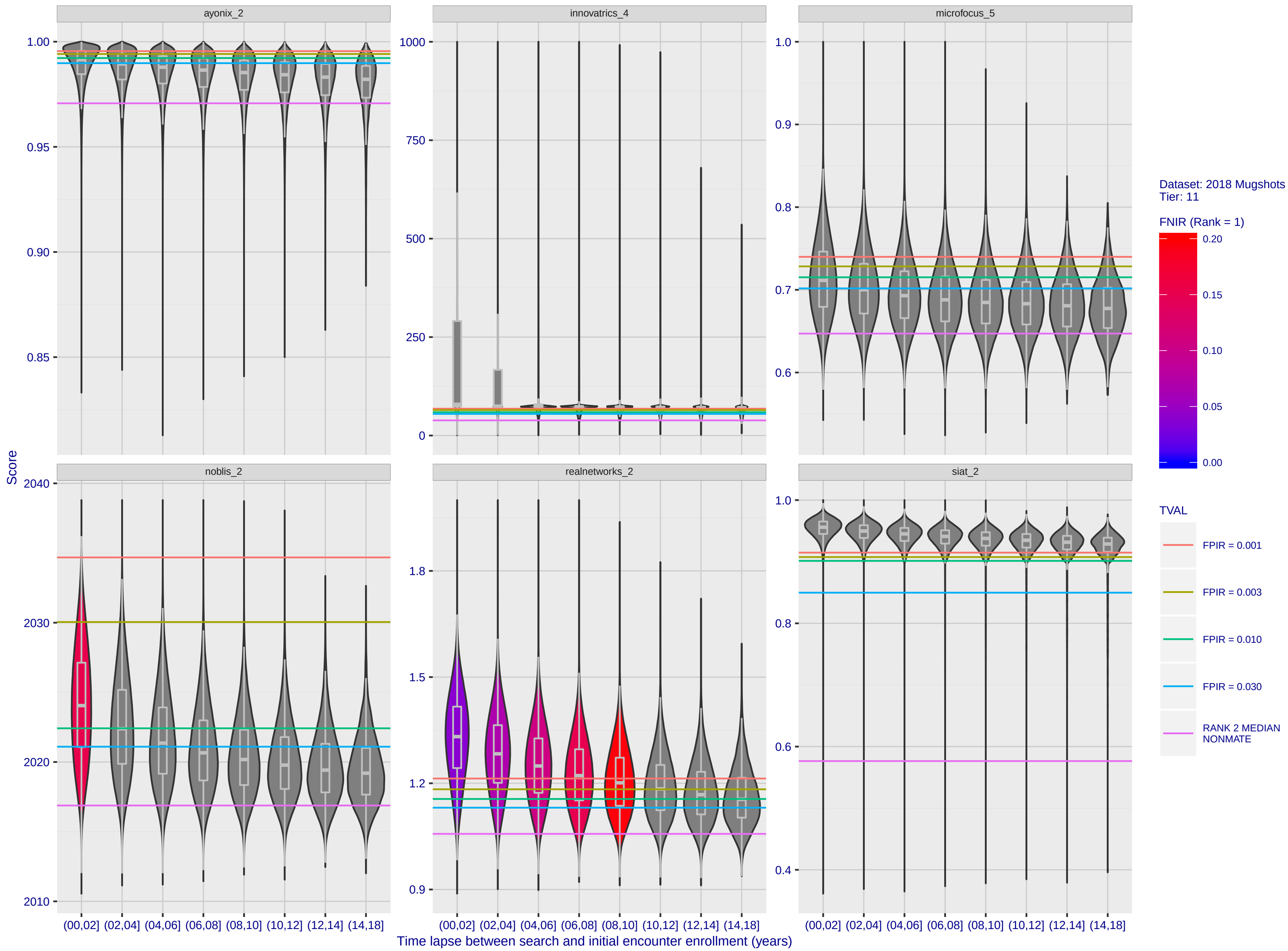

Figure 88: **[FRVT-2018 Mugshot Ageing Dataset] Native mate scores vs. time-elapsed**. *The oldest image of each individual is enrolled. Thereafter, all more recent images are searched. Mated score distributions are computed over all searches noted in row 17 of Table 1 binned by number of years between search and initial enrollment.*

Appendix C Effect of enrolling multiple images

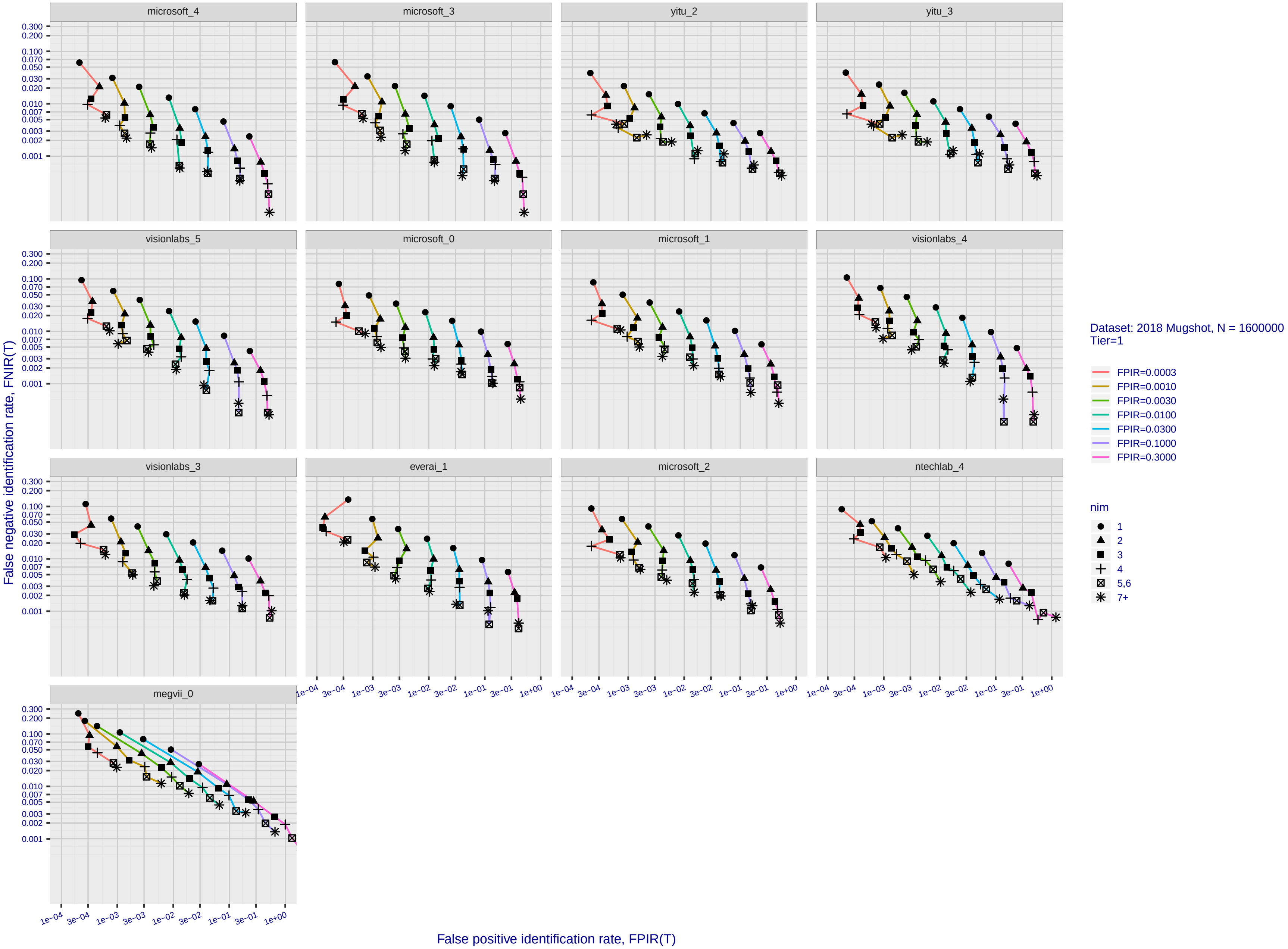

Figure 89: **[FRVT-2018 Mugshot Dataset] Effect of enrolling multiple images for each identity**. *The plot shows an identification miss rates vs. false positive rates, at seven operating thresholds. The enrolled population size is fixed. The images are enrolled with lifetime-consolidation - see section 2.2.*

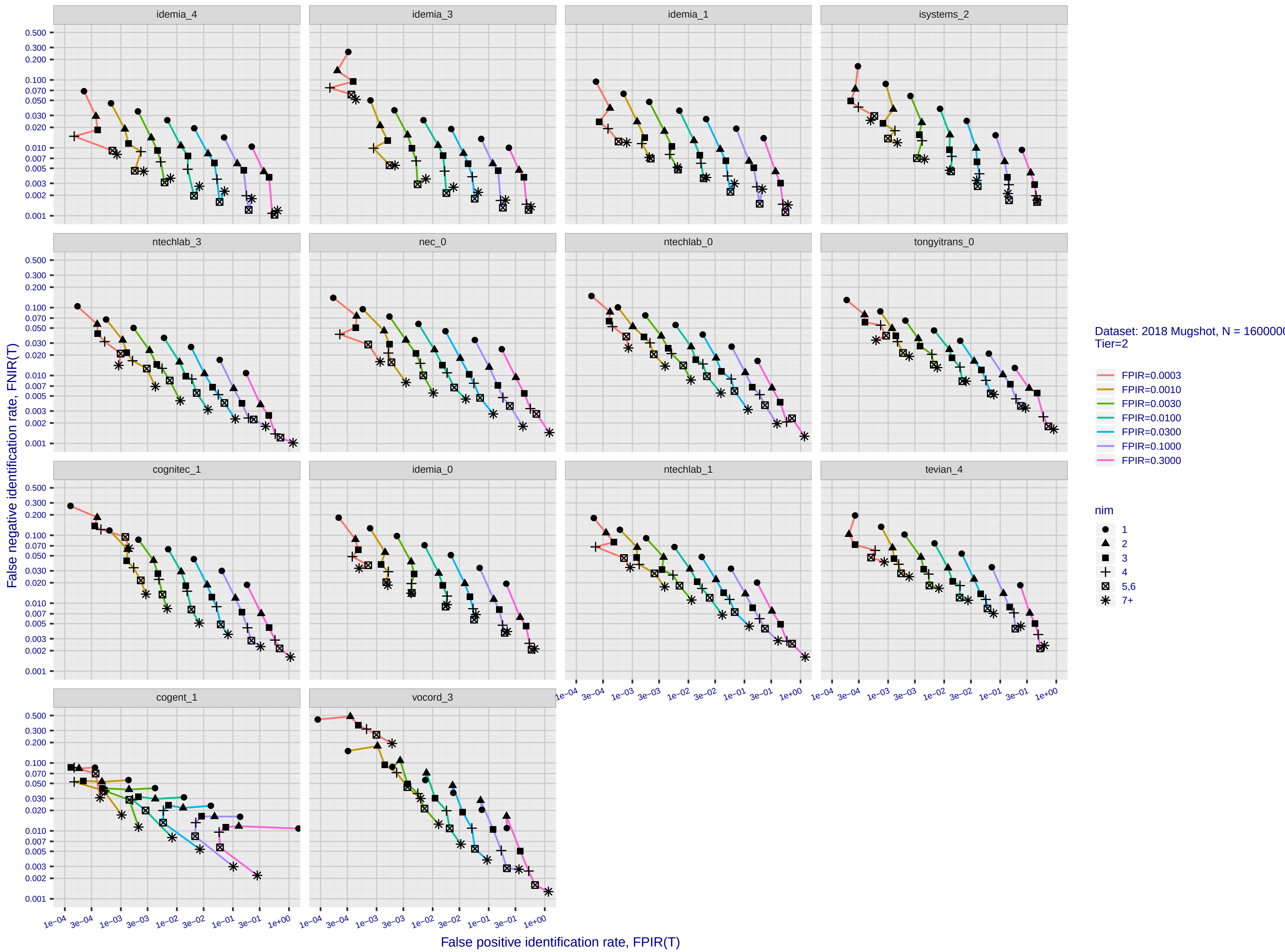

Figure 90: **[FRVT-2018 Mugshot Dataset] Effect of enrolling multiple images for each identity**. *The plot shows an identification miss rates vs. false positive rates, at seven operating thresholds. The enrolled population size is fixed. The images are enrolled with lifetime-consolidation - see section 2.2.*

FNIR(N, R, T) = False neg. identification rate
FPIR(N, T) = False pos. identification rate
N = Num. enrolled subjects
R = Num. candidates examined
T = Threshold
T = 0 → Investigation
T > 0 → Identification

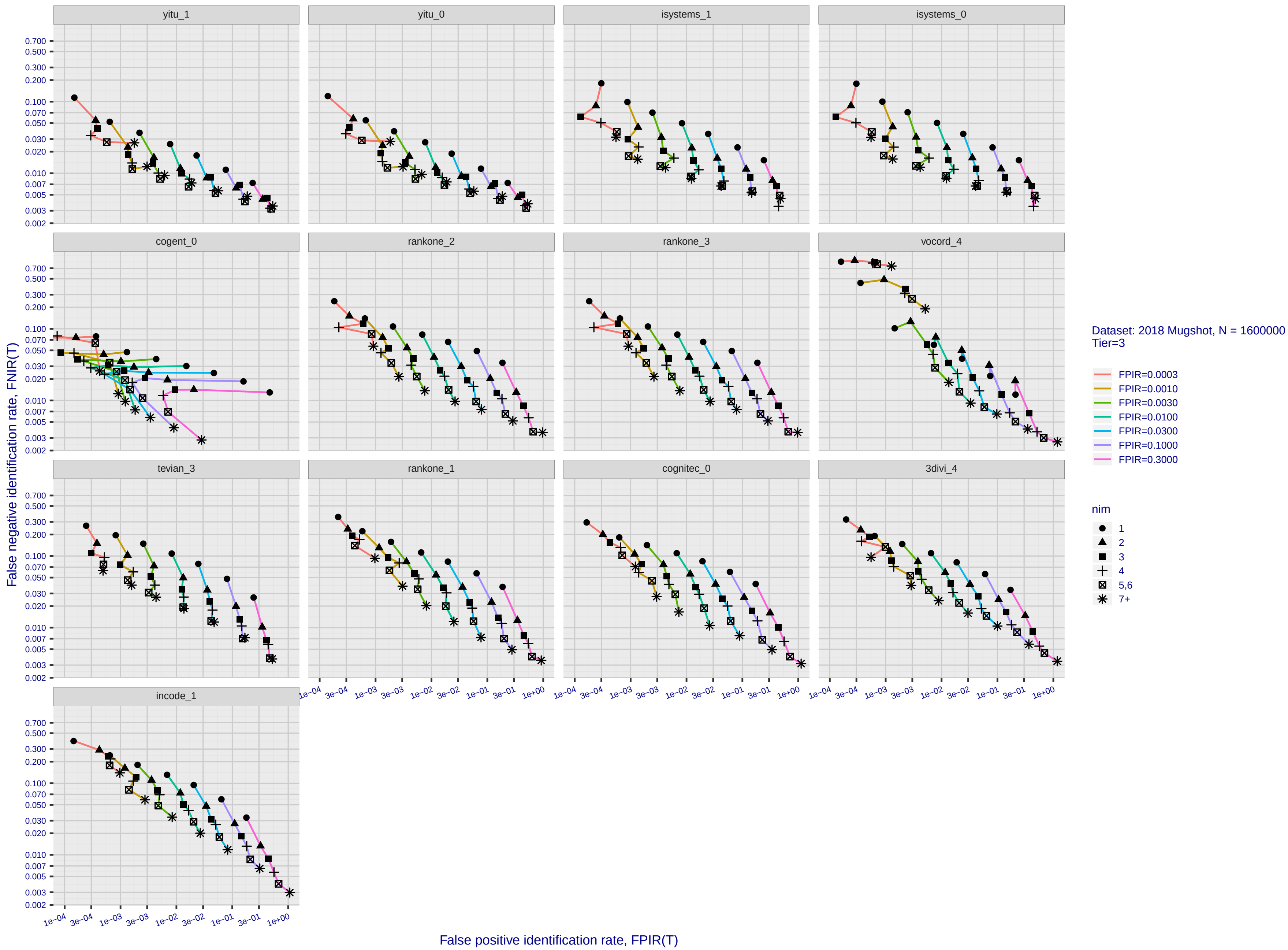

Figure 91: **[FRVT-2018 Mugshot Dataset] Effect of enrolling multiple images for each identity**. *The plot shows an identification miss rates vs. false positive rates, at seven operating thresholds. The enrolled population size is fixed. The images are enrolled with lifetime-consolidation - see section 2.2.*

This publication is available free of charge from: https://doi.org/10.6028/NIST.IR.8271

2020/02/26
13:34:01

FNIR(N, R, T) = False neg. identification rate
FPIR(N, T) = False pos. identification rate
N = Num. enrolled subjects
R = Num. candidates examined
T = Threshold
T = 0 → Investigation
T > 0 → Identification

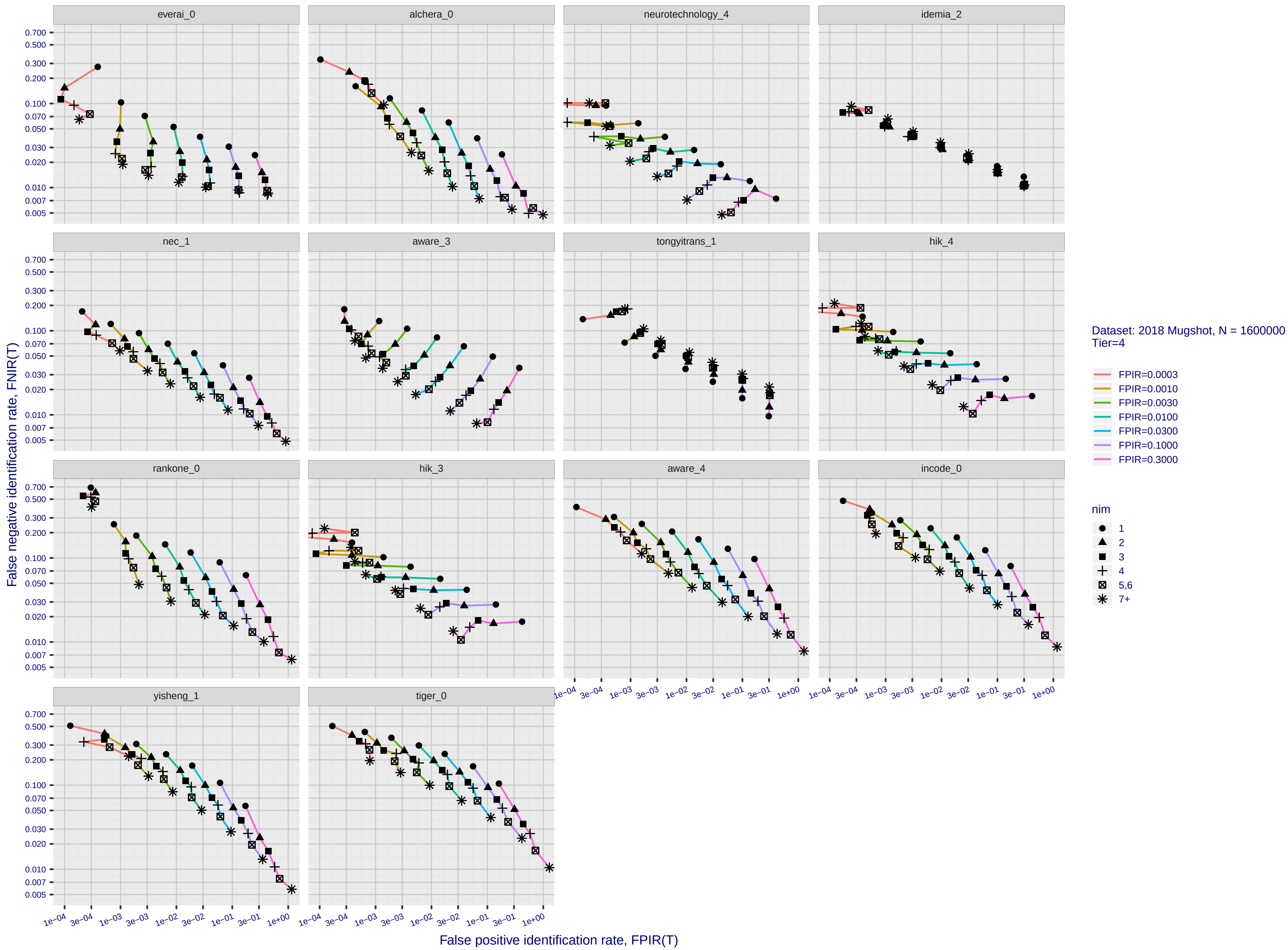

Figure 92: **[FRVT-2018 Mugshot Dataset] Effect of enrolling multiple images for each identity**. *The plot shows an identification miss rates vs. false positive rates, at seven operating thresholds. The enrolled population size is fixed. The images are enrolled with lifetime-consolidation - see section 2.2.*

FNIR(N, R, T) = False neg. identification rate
FPIR(N, T) = False pos. identification rate

N = Num. enrolled subjects
R = Num. candidates examined

T = Threshold

T = 0 → Investigation
T > 0 → Identification

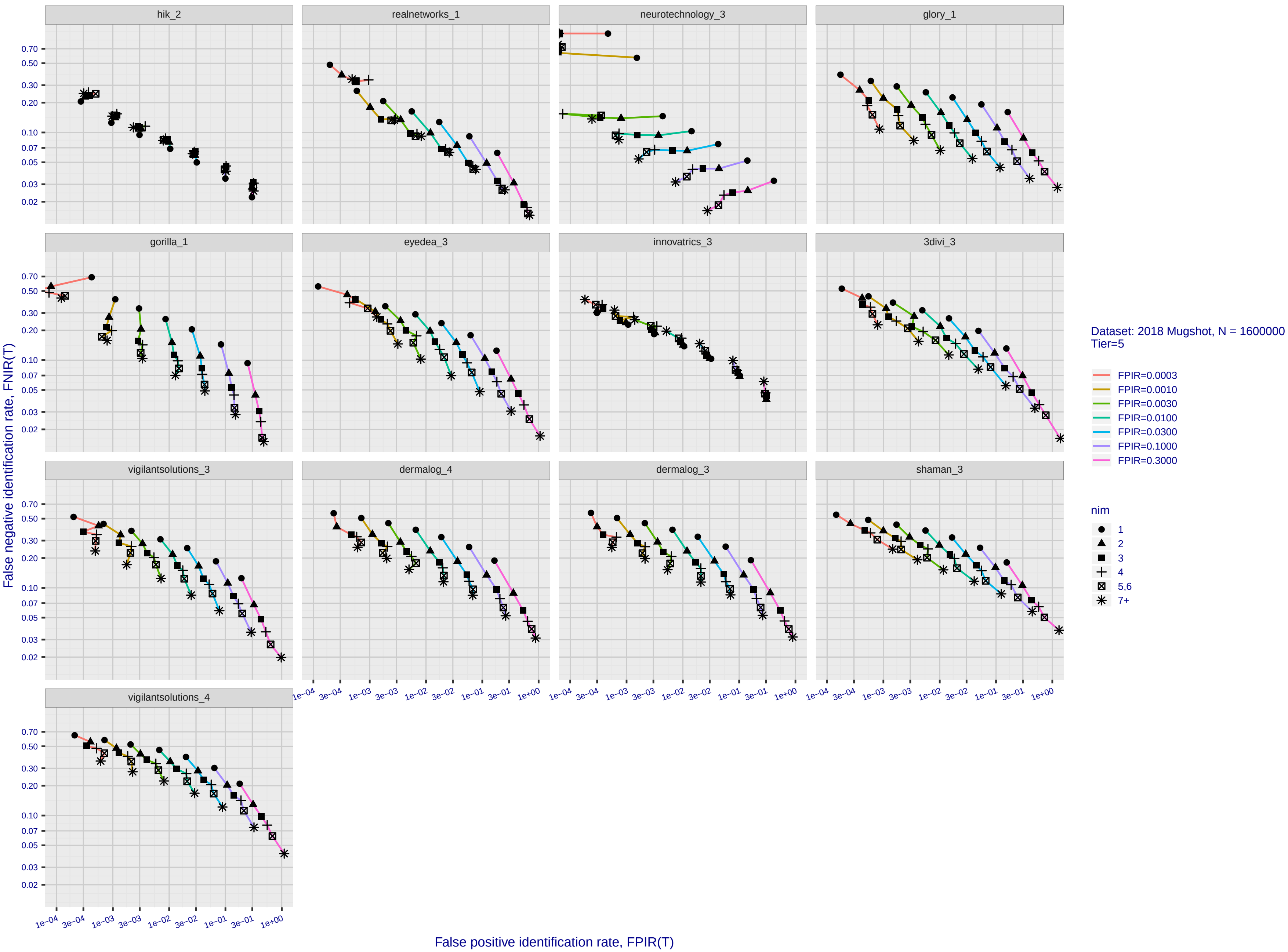

Figure 93: **[FRVT-2018 Mugshot Dataset] Effect of enrolling multiple images for each identity**. *The plot shows an identification miss rates vs. false positive rates, at seven operating thresholds. The enrolled population size is fixed. The images are enrolled with lifetime-consolidation - see section 2.2.*

This publication is available free of charge from: https://doi.org/10.6028/NIST.IR.8271

FNIR(N, R, T) = False neg. identification rate
FPIR(N, T) = False pos. identification rate
N = Num. enrolled subjects
R = Num. candidates examined
T = Threshold
T = 0 → Investigation
T > 0 → Identification

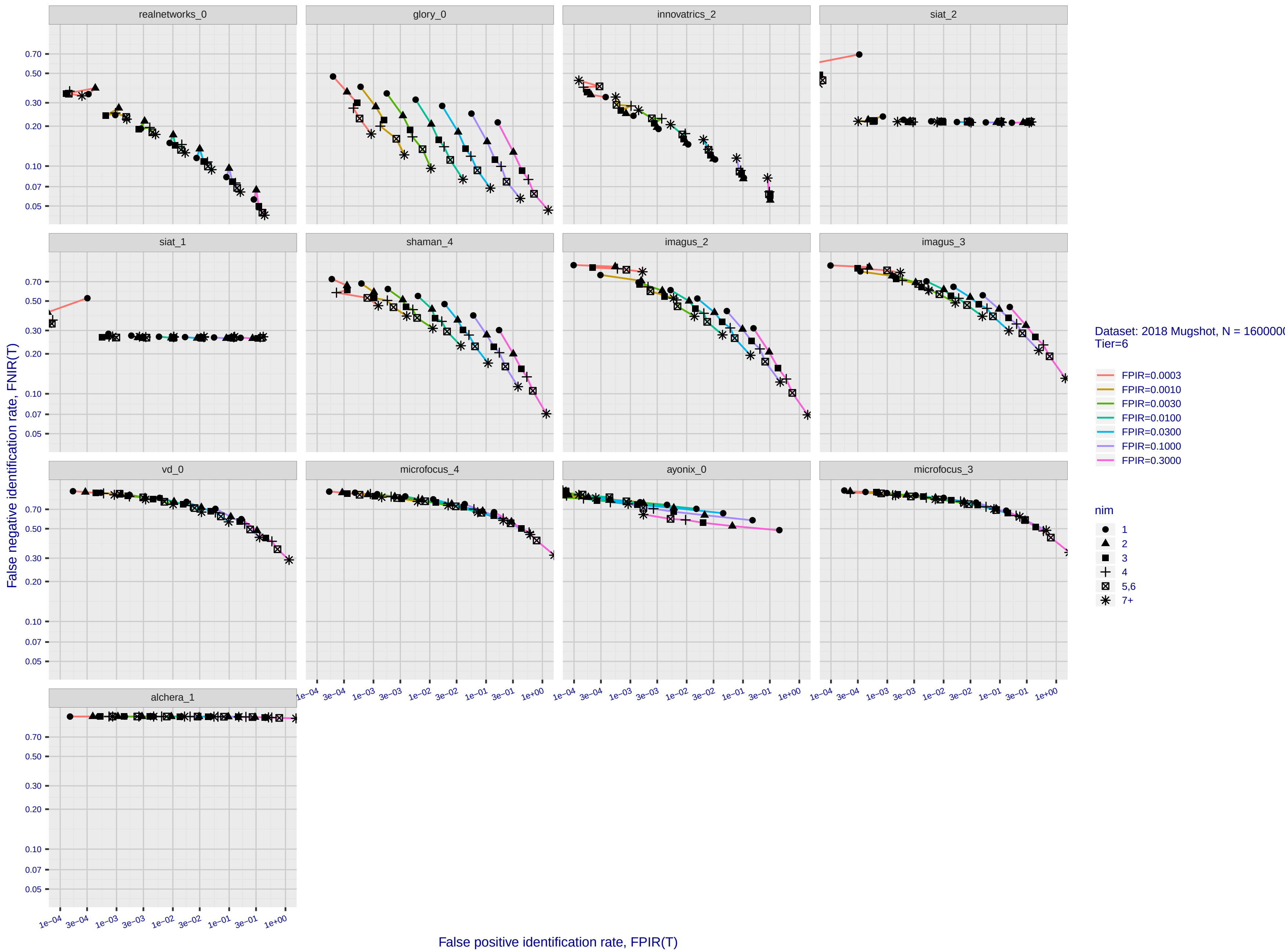

Figure 94: **[FRVT-2018 Mugshot Dataset] Effect of enrolling multiple images for each identity**. *The plot shows an identification miss rates vs. false positive rates, at seven operating thresholds. The enrolled population size is fixed. The images are enrolled with lifetime-consolidation - see section 2.2.*

Appendix D Accuracy with poor quality webcam images

2020/02/26	FNIR(N, R, T) =	False neg. identification rate	N = Num. enrolled subjects	T = Threshold	$T = 0 \rightarrow$ Investigation
13:34:01	FPIR(N, T) =	False pos. identification rate	R = Num. candidates examined		$T > 0 \rightarrow$ Identification

FNIR(N, R, T) = False neg. identification rate
FPIR(N, T) = False pos. identification rate
N = Num. enrolled subjects
R = Num. candidates examined
T = Threshold
T = 0 → Investigation
T > 0 → Identification

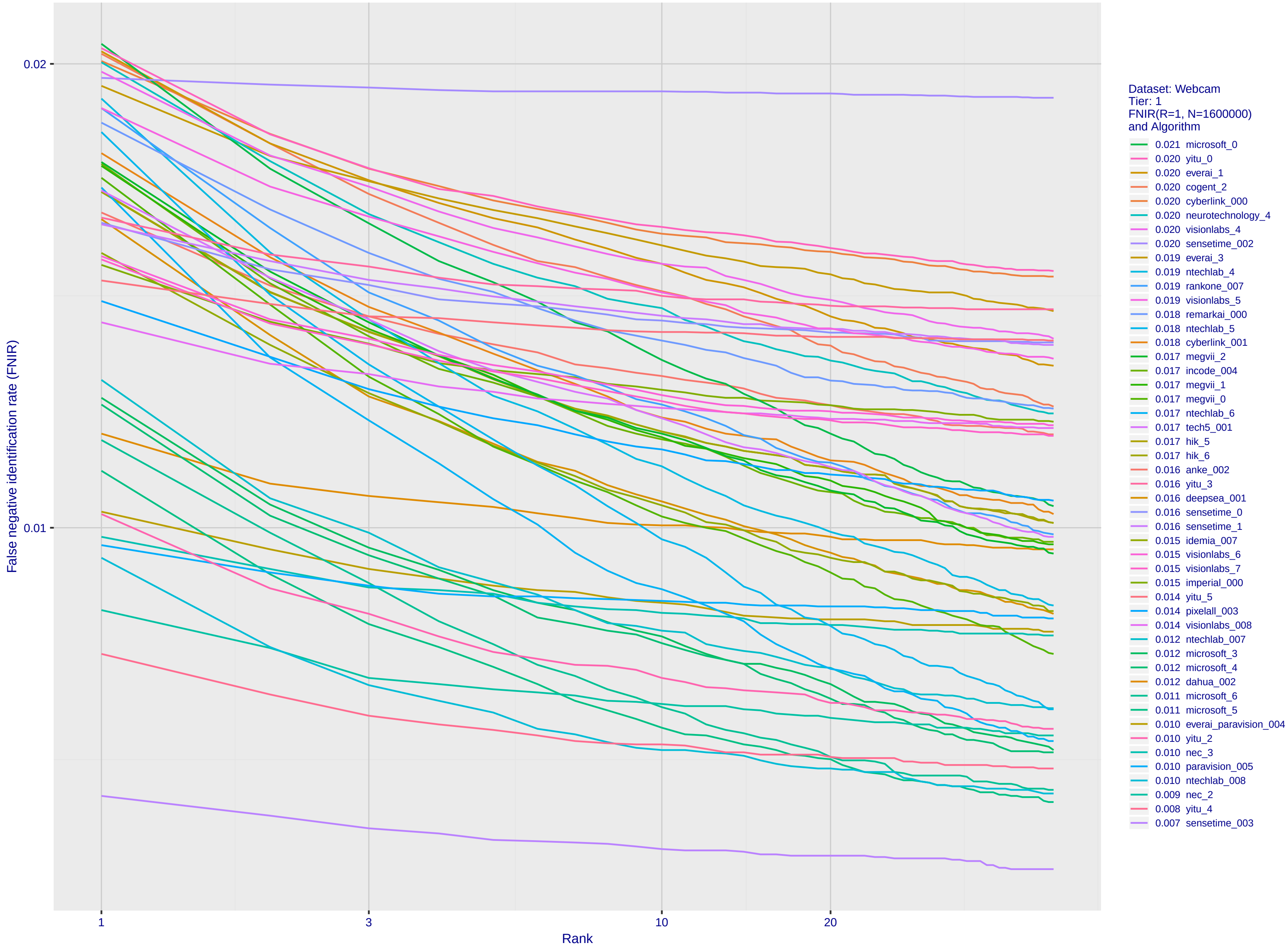

Figure 95: **[Webcam Dataset] Identification miss rates vs. rank**. *The results apply to cross-domain recognition in which webcams are searched against enrolled mugshots. The FNIR values are higher than those for mugshot-mugshot identification due to low image resolution, lighting and less constrained subject pose in webcam images - see Figure 4.*

FNIR(N, R, T) = False neg. identification rate
FPIR(N, T) = False pos. identification rate
N = Num. enrolled subjects
R = Num. candidates examined
T = Threshold
T = 0 → Investigation
T > 0 → Identification

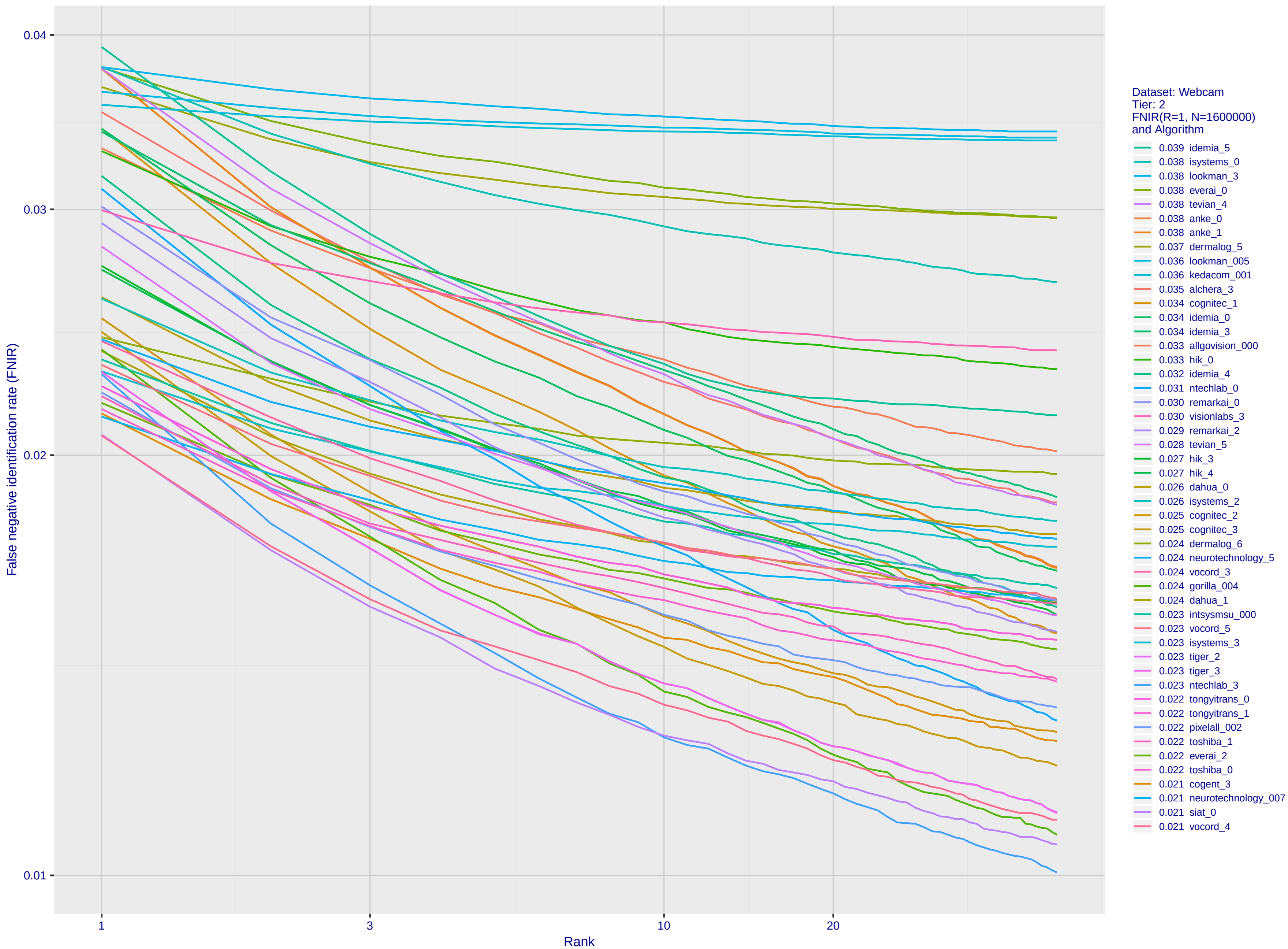

Figure 96: **[Webcam Dataset] Identification miss rates vs. rank**. *The results apply to cross-domain recognition in which webcams are searched against enrolled mugshots. The FNIR values are higher than those for mugshot-mugshot identification due to low image resolution, lighting and less constrained subject pose in webcam images - see Figure 4.*

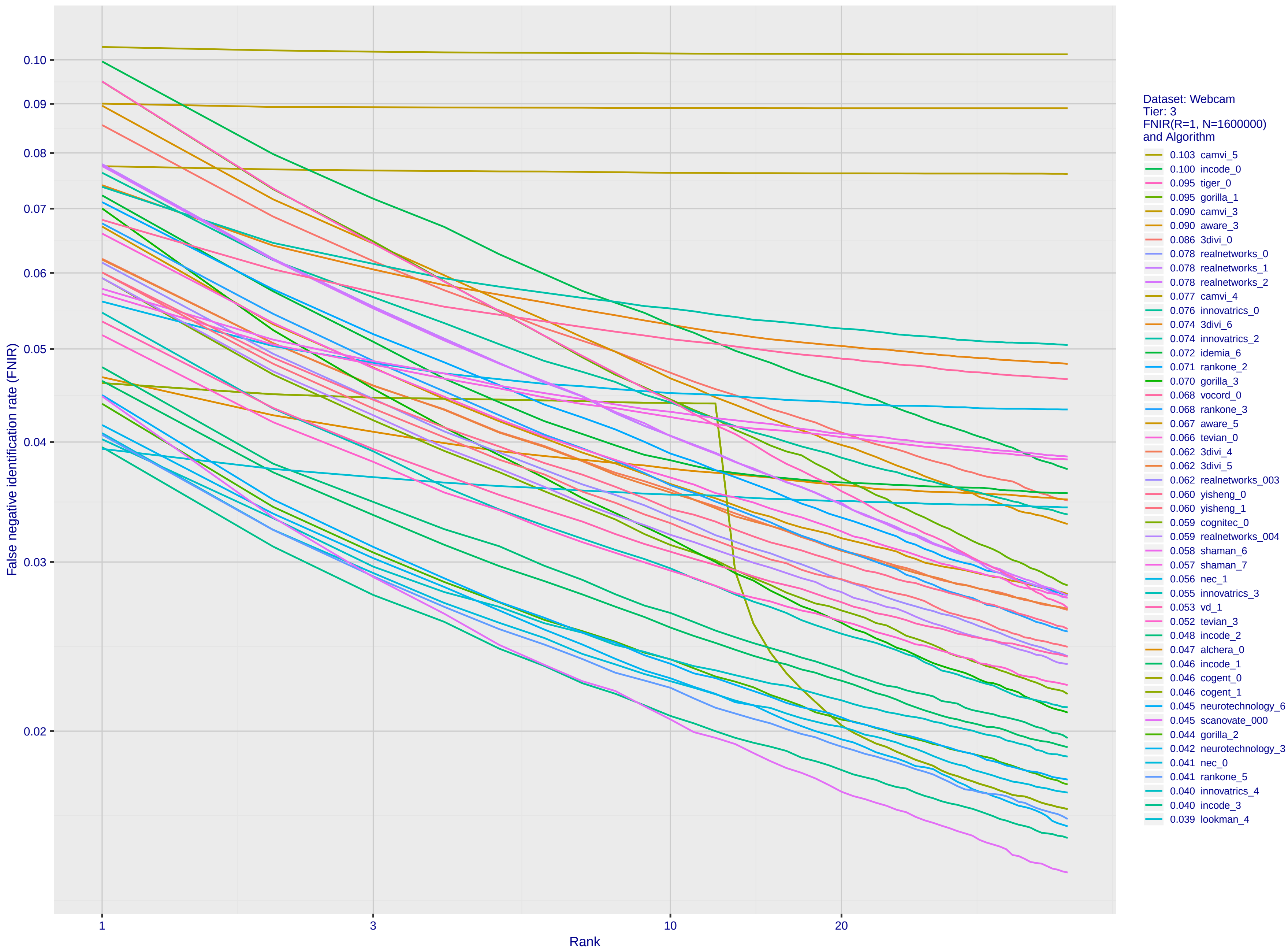

Figure 97: **[Webcam Dataset] Identification miss rates vs. rank**. *The results apply to cross-domain recognition in which webcams are searched against enrolled mugshots. The FNIR values are higher than those for mugshot-mugshot identification due to low image resolution, lighting and less constrained subject pose in webcam images - see Figure 4.*

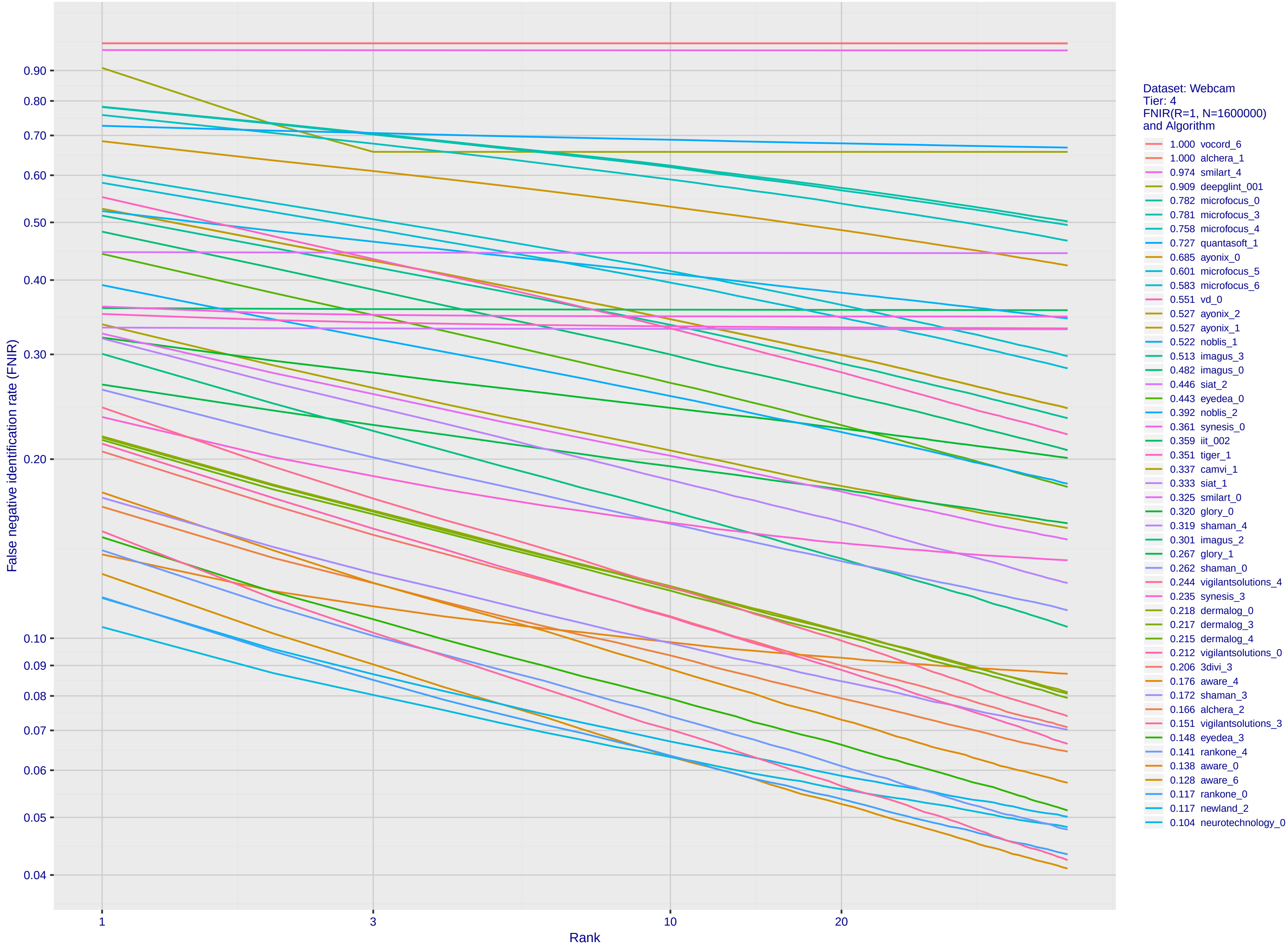

Figure 98: **[Webcam Dataset] Identification miss rates vs. rank**. *The results apply to cross-domain recognition in which webcams are searched against enrolled mugshots. The FNIR values are higher than those for mugshot-mugshot identification due to low image resolution, lighting and less constrained subject pose in webcam images - see Figure 4.*

2020/02/26	FNIR(N, R, T) =	False neg. identification rate	N = Num. enrolled subjects	T = Threshold	$T = 0 \rightarrow$ Investigation
13:34:01	FPIR(N, T) =	False pos. identification rate	R = Num. candidates examined		$T > 0 \rightarrow$ Identification

FNIR(N, R, T) = False neg. identification rate
FPIR(N, T) = False pos. identification rate
N = Num. enrolled subjects
R = Num. candidates examined
T = Threshold
T = 0 → Investigation
T > 0 → Identification

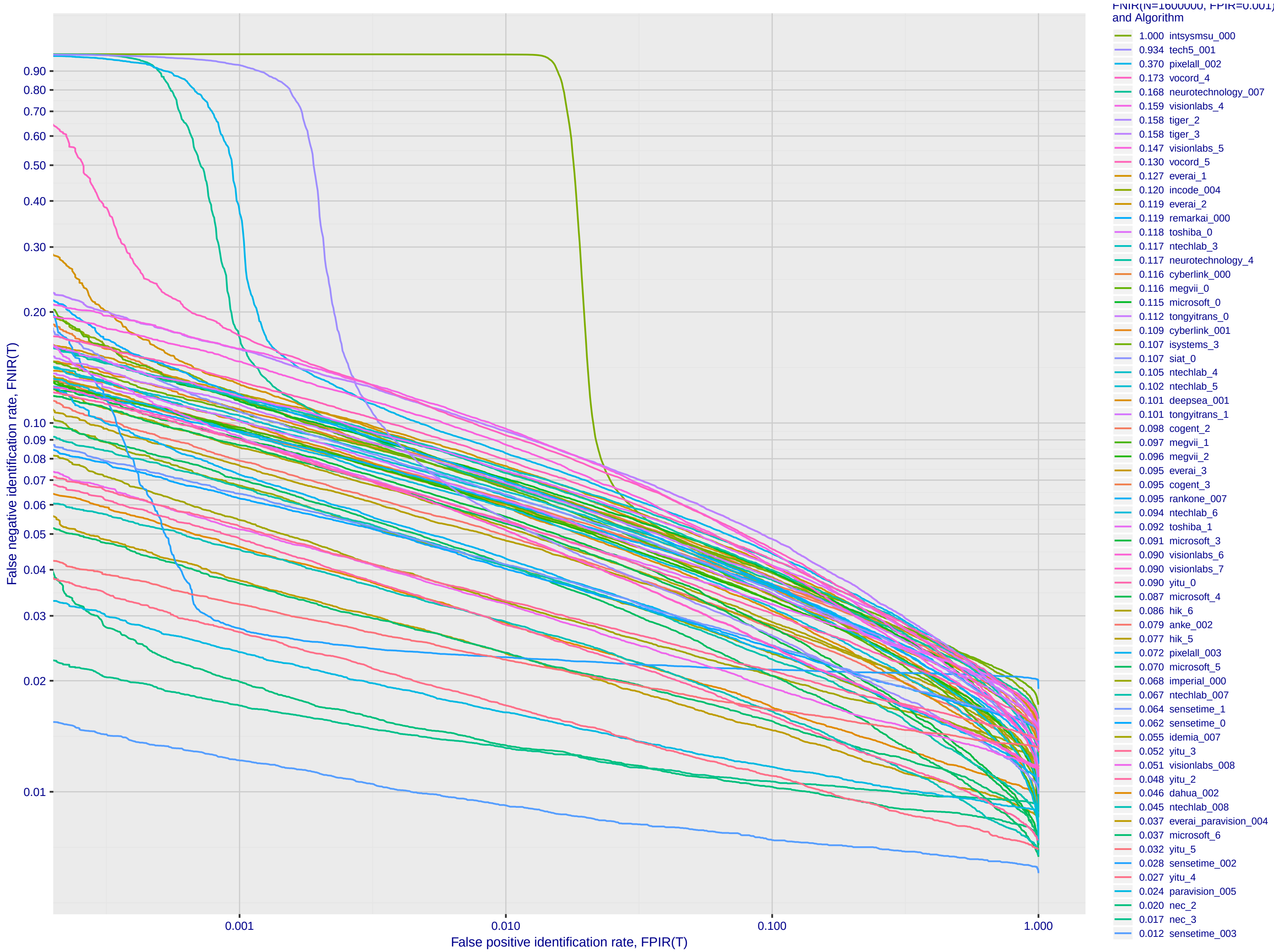

Figure 99: **[Webcam Dataset] Identification miss rates vs. false positive rates**. *The results apply to cross-domain recognition in which webcams are searched against enrolled mugshots. The FNIR values are higher than those for mugshot-mugshot identification due to low image resolution, lighting and less constrained subject pose in webcam images - see Figure 4.*

FNIR(N, R, T) = False neg. identification rate
FPIR(N, T) = False pos. identification rate
N = Num. enrolled subjects
R = Num. candidates examined
T = Threshold
T = 0 → Investigation
T > 0 → Identification

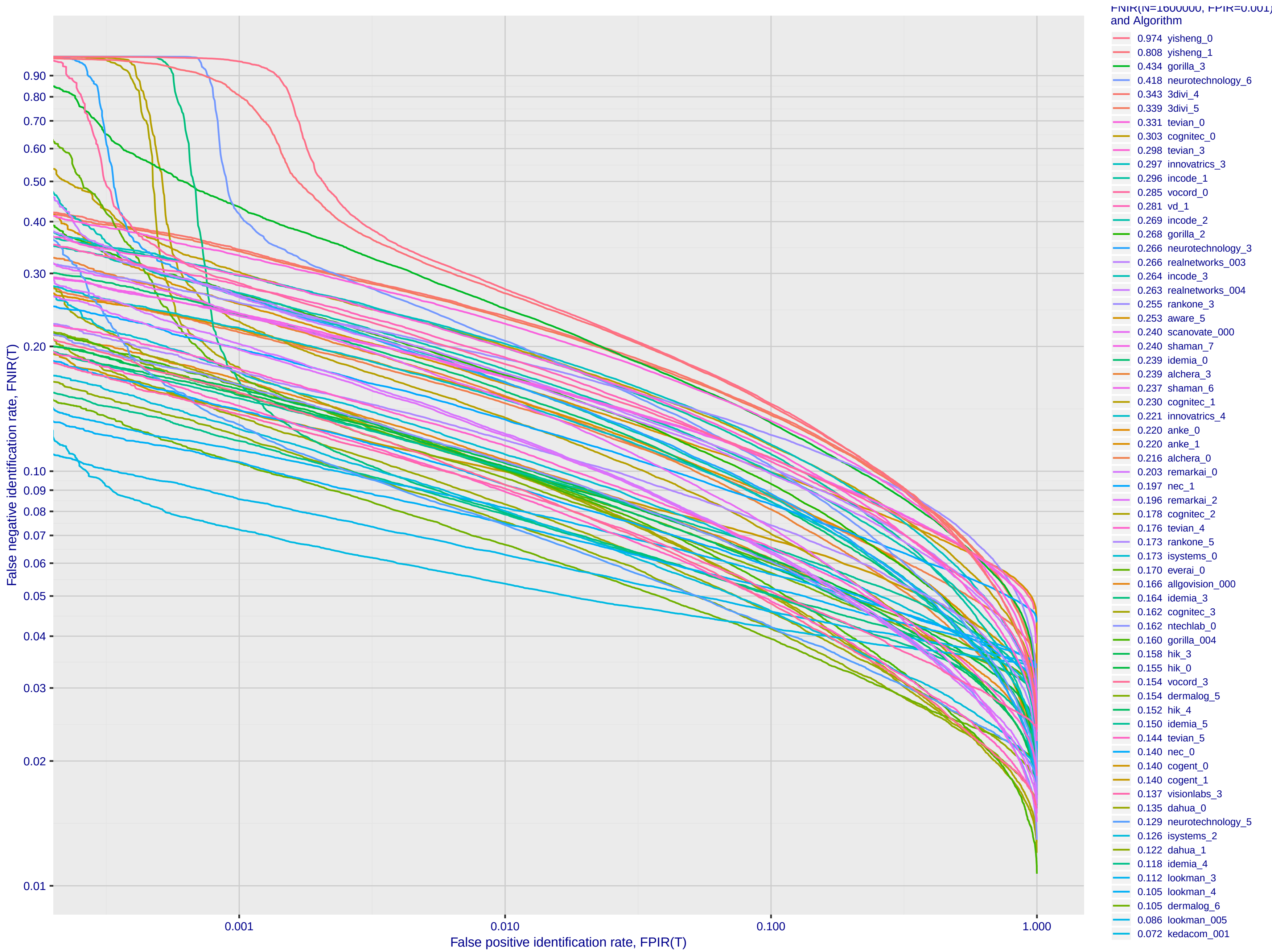

Figure 100: **[Webcam Dataset] Identification miss rates vs. false positive rates**. *The results apply to cross-domain recognition in which webcams are searched against enrolled mugshots. The FNIR values are higher than those for mugshot-mugshot identification due to low image resolution, lighting and less constrained subject pose in webcam images - see Figure 4.*

FNIR(N, R, T) = False neg. identification rate
FPIR(N, T) = False pos. identification rate
N = Num. enrolled subjects
R = Num. candidates examined
T = Threshold
T = 0 → Investigation
T > 0 → Identification

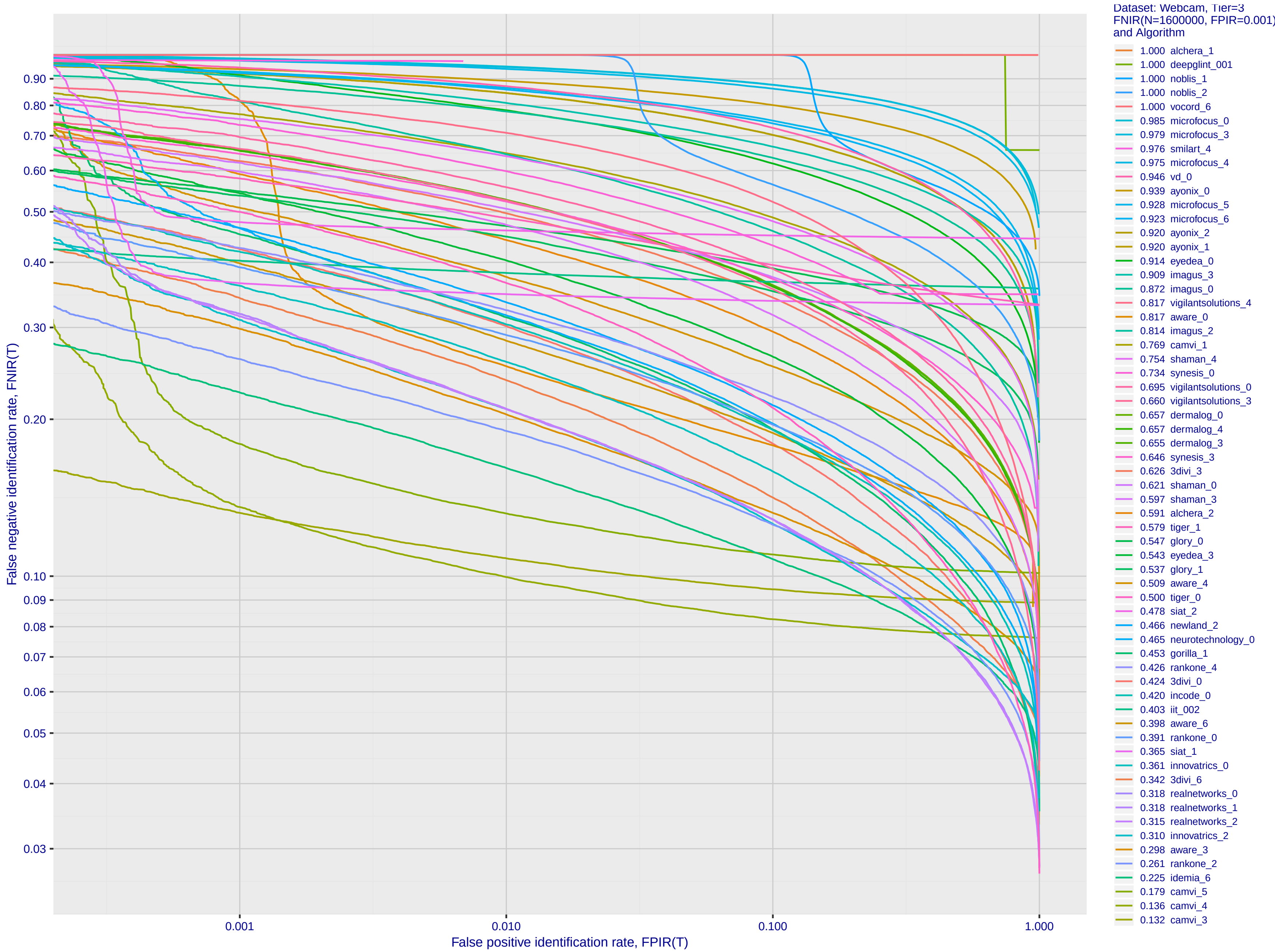

Figure 101: **[Webcam Dataset] Identification miss rates vs. false positive rates**. *The results apply to cross-domain recognition in which webcams are searched against enrolled mugshots. The FNIR values are higher than those for mugshot-mugshot identification due to low image resolution, lighting and less constrained subject pose in webcam images - see Figure 4.*

Appendix E Accuracy for profile-view to frontal recognition

Figures 102 - 104 gives accuracy results for searching 100 000 mated and 100 000 non-mated profile-view images against the same FRVT 2018 frontal enrollment dataset, N = 1 600 000, used in the main mugshot trials. This experiment corresponds to row-13 of Table 1. An example of profile-view image is given in Figure 5.

FNIR(N, R, T) = False neg. identification rate
FPIR(N, T) = False pos. identification rate
N = Num. enrolled subjects
R = Num. candidates examined
T = Threshold
T = 0 → Investigation
T > 0 → Identification

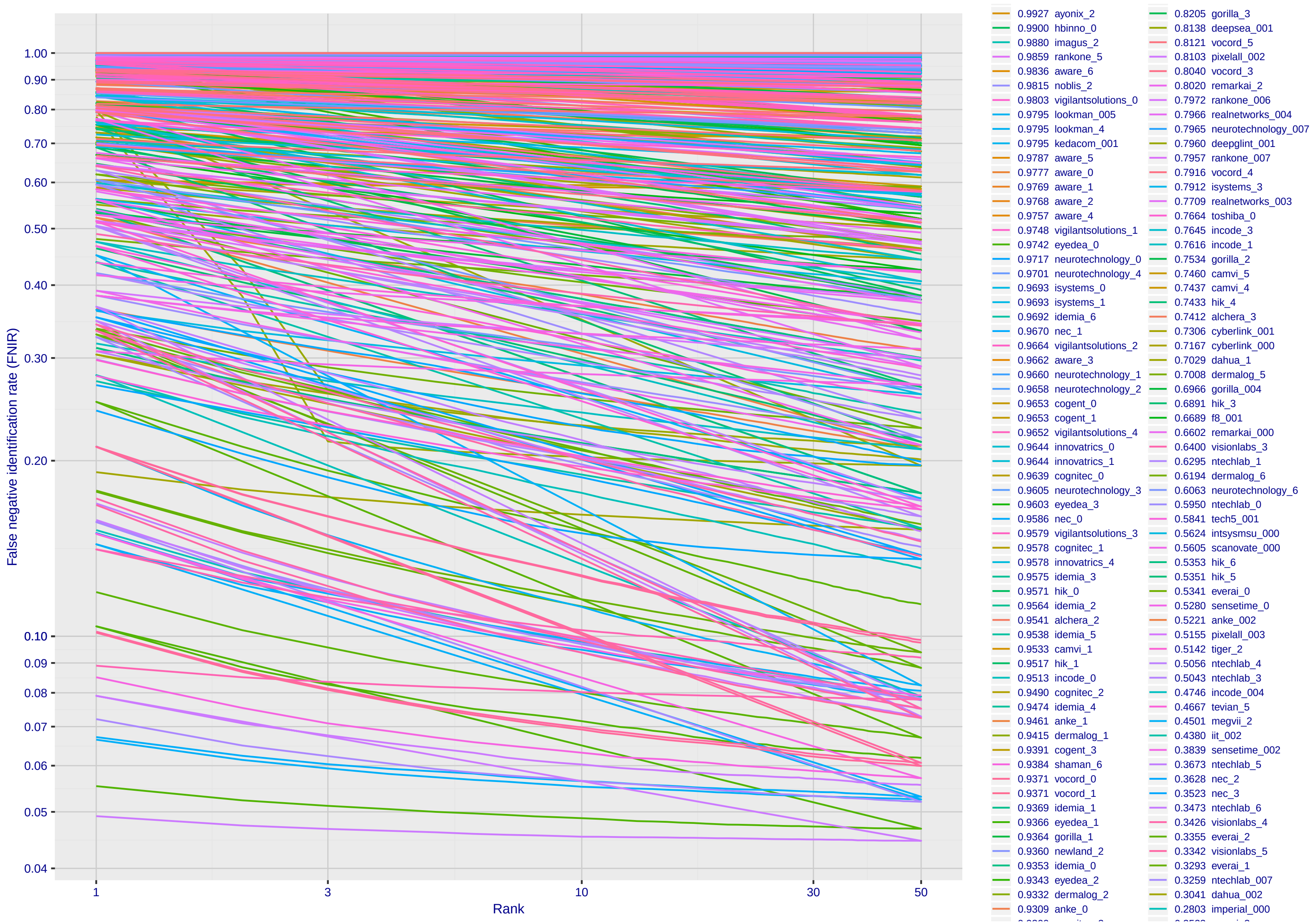

Figure 102: **[Mugshot and profile-view dataset] Rank-based accuracy**. *For some of the more accurate Phase 3 algorithms the figure plots error tradeoff characteristics for frontal and profile-view searches into an enrolled set of N = 1 600 000 frontal images. Note that some algorithms fail on profile-view images with FNIR → 1 - this evaluation did not ask developers to provide profile-view capability. Some algorithms, on the other hand, give FNIR approaching that for frontal-view searches using c. 2010 algorithms. The best result is that 91% of profile-view searches yield the correct mate at rank 1, and better than 94% in the top-50 candidates.*

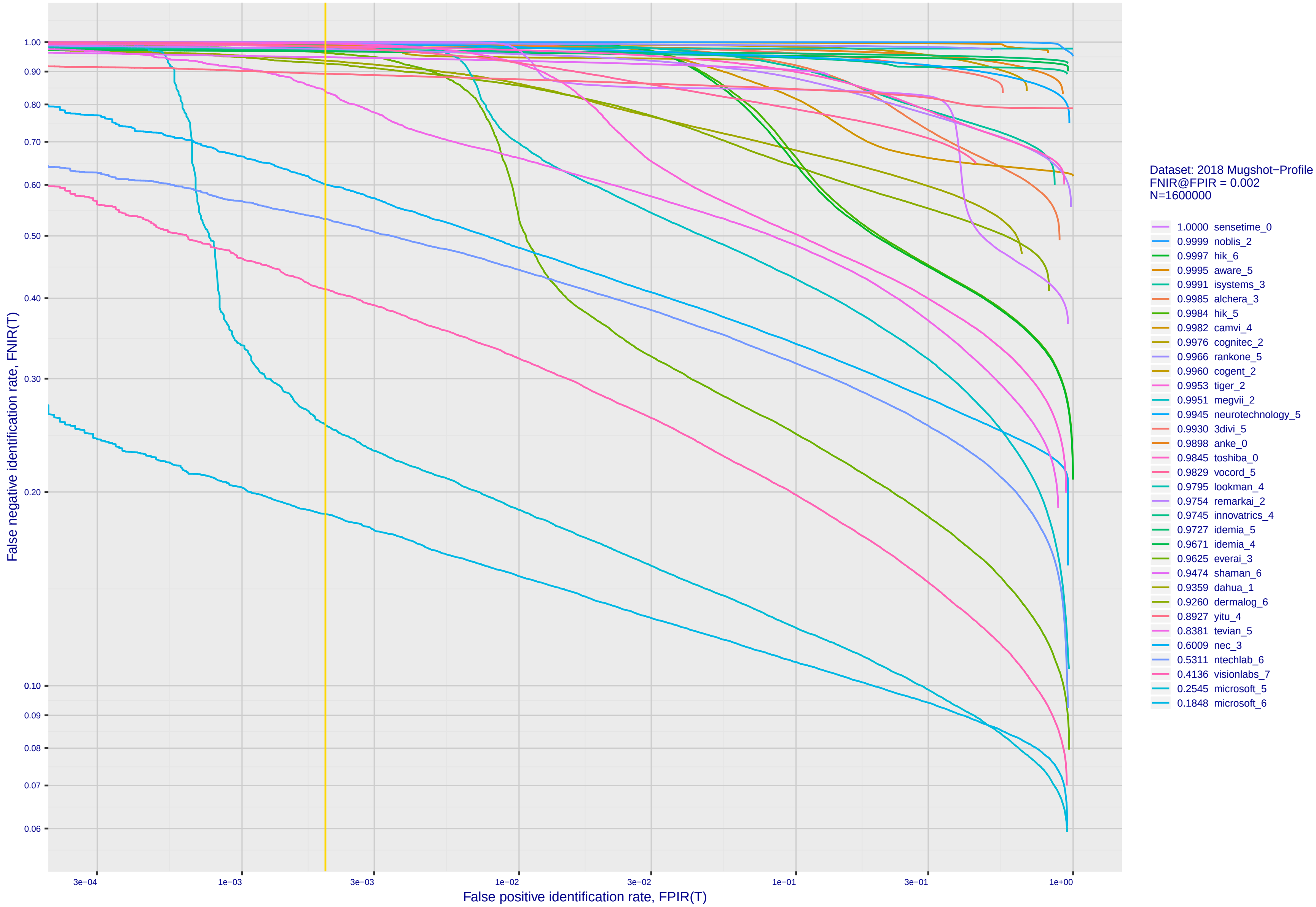

Figure 103: **[Mugshot and profile-view dataset] Threshold-based accuracy**. *For some of the more accurate Phase 3 algorithms the figure plots error tradeoff characteristics for frontal and profile-view searches into an enrolled set of N = 1 600 000 frontal images. Note that some algorithms fail on profile-view images with FNIR → 1 - this evaluation did not ask developers to provide profile-view capability. Some algorithms, on the other hand, give FNIR approaching that for frontal-view searches using c. 2010 algorithms.*

FNIR(N, R, T) = False neg. identification rate
FPIR(N, T) = False pos. identification rate
N = Num. enrolled subjects
R = Num. candidates examined
T = Threshold
T = 0 → Investigation
T > 0 → Identification

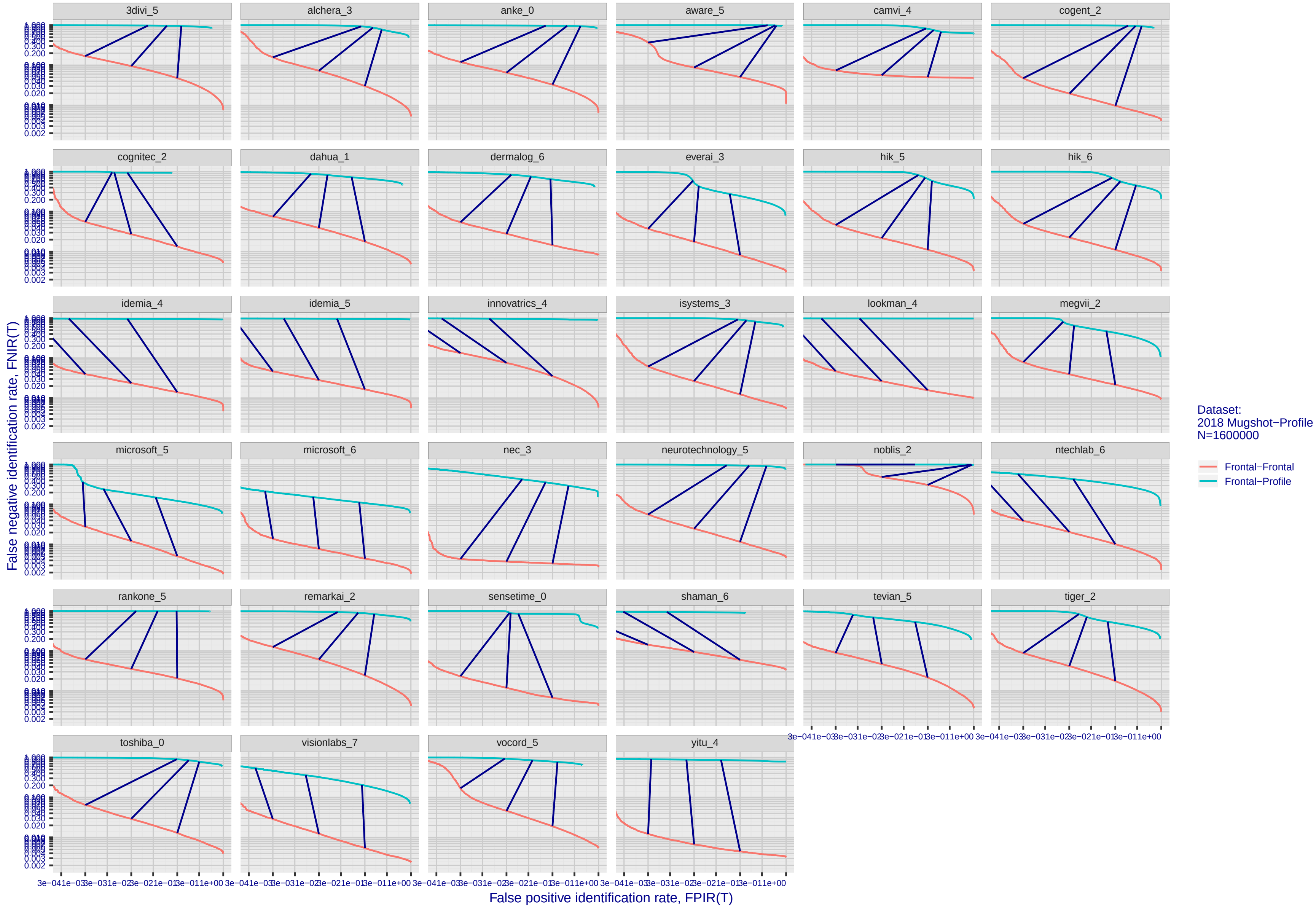

Figure 104: **[Mugshot and profile-view dataset] Speed-accuracy tradeoff**. *For some of the more accurate Phase 3 algorithms the figure plots error tradeoff characteristics for frontal and profile-view searches into an enrolled set of N = 1 600 000 frontal images. Some algorithms fail on profile-view images with FNIR → 1 - this evaluation did not ask developers to provide profile-view capability. Some algorithms, on the other hand, give FNIR approaching that for frontal-view searches using c. 2010 algorithms. Blue lines connect points of equal threshold from which it is evident that some algorithms would give markedly higher false positive outcomes if profile-view images were searched in a system configured for frontal searches. This would be a vulnerability in an access control system.*

Appendix F Search duration

As in and prior tests, this section documents search speeds spanning three orders of magnitude. In applications where search volumes are high enough, this will have implications for hardware requirements especially for large N or when search duration is appreciably larger than the time it takes to prepare a template from the search image(s). Further, given very large (and growing) operational databases, the scalability of algorithms is important. It has been reported previously [7] that search duration can scale sublinearly with enrolled population size N. Further there has been considerable recent research on indexing, exact [12] and approximate nearest neighbor search [1,12] and fast-search [13,15].

Figure 105 charts the search duration measurements presented earlier in Tables 2 - 5.

- ▷ Most algorithms scale linearly. For those in that category, there is a wide range in speed with search durations ranging from 82 milliseconds for a 12 million gallery (for NEC-3) to more than 40 seconds (for Yitu-3, Toshiba-2) and even higher for less accurate algorithms.
- ▷ Some developers (Camvi, Dermalog, EverAI, Innovatrics, and Visionlabs) provide algorithms whose template search durations grow logarithmically i.e. approximately $T(N) = a \log N$ with the constant a varying between implementations. In the figure this model is fit using the point $T(1) = 0$, and $T(640\,000)$. This very sublinear behaviour affords extremely fast search times in very large galleries. One caveat for the sublinear algorithms is that the fast-search data structures require considerable computation time - on the order of hours - for N in the millions, and this scales mildy super-linearly, i.e. $O(N^b), b > 1$. There are exceptions: the Camvi algorithms take minutes; and Innvovatrics' scale sublinearly.

2020/02/26	FNIR(N, R, T) =	False neg. identification rate	N = Num. enrolled subjects	T = Threshold	$T = 0 \rightarrow$ Investigation
13:34:01	FPIR(N, T) =	False pos. identification rate	R = Num. candidates examined		$T > 0 \rightarrow$ Identification

FNIR(N, R, T) = False neg. identification rate
FPIR(N, T) = False pos. identification rate
N = Num. enrolled subjects
R = Num. candidates examined
T = Threshold
T = 0 → Investigation
T > 0 → Identification

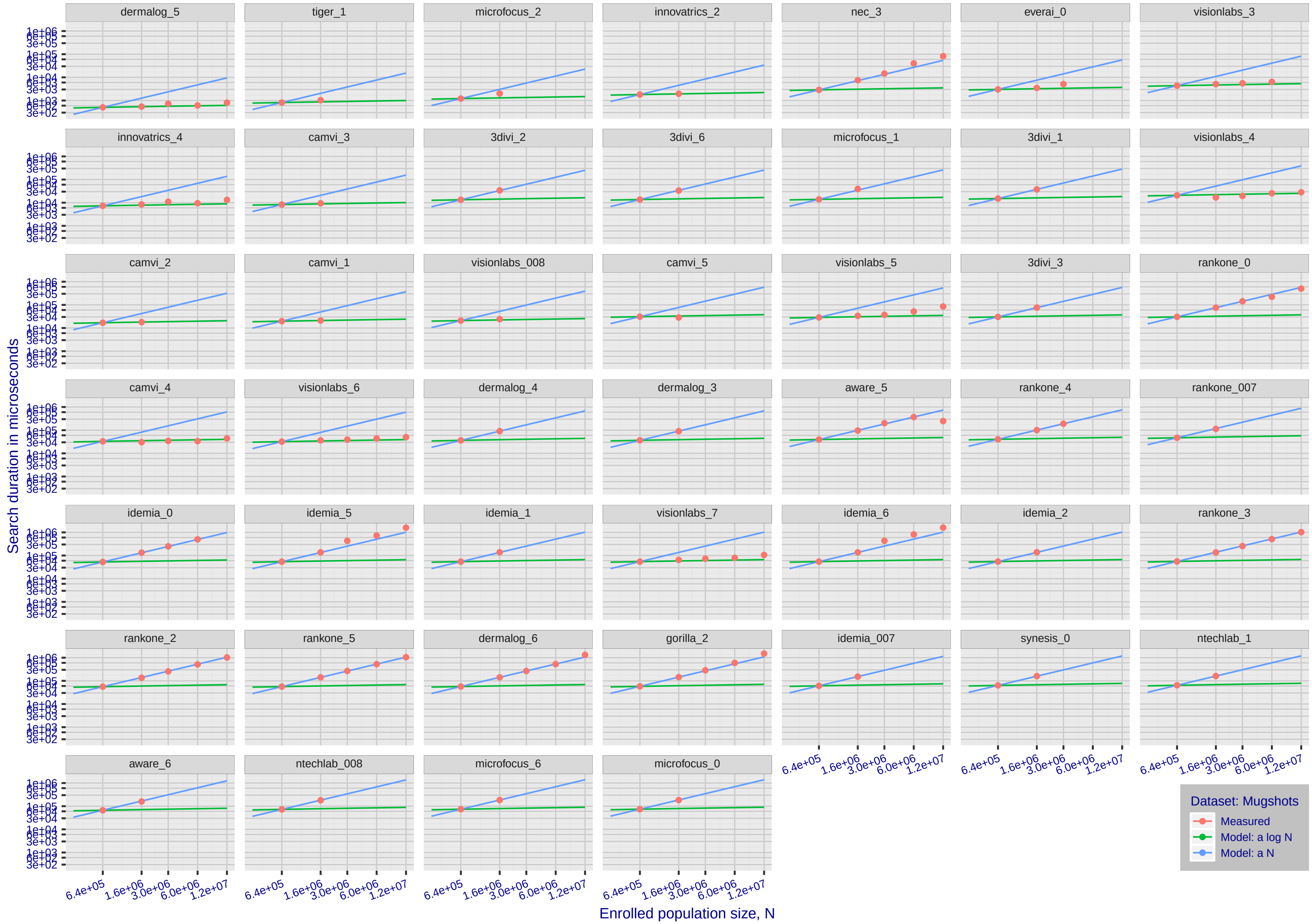

Figure 105: **[Mugshot Dataset] Search duration vs. enrolled population size**. *In red are the actual point durations measured on a single c. 2016 core. The blue shows linear growth from $N = 640\,000$. The green line shows logathmic growth from that point to $N = 1\,600\,000$. Note the sublinear growth from algorithms from Camvi, Dermalog, EverAI, Innovatrics, and Visionlabs. The tiger_1 algorithm is also sublinear, but inaccurate and inoperable at $N \geq 3000000$. This capability sometimes comes at the additional expense of converting a linear gallery data structure into whatever fast-search data structure is used. Note that search times are sometimes dominated by the template generation times shown in Table 16.*

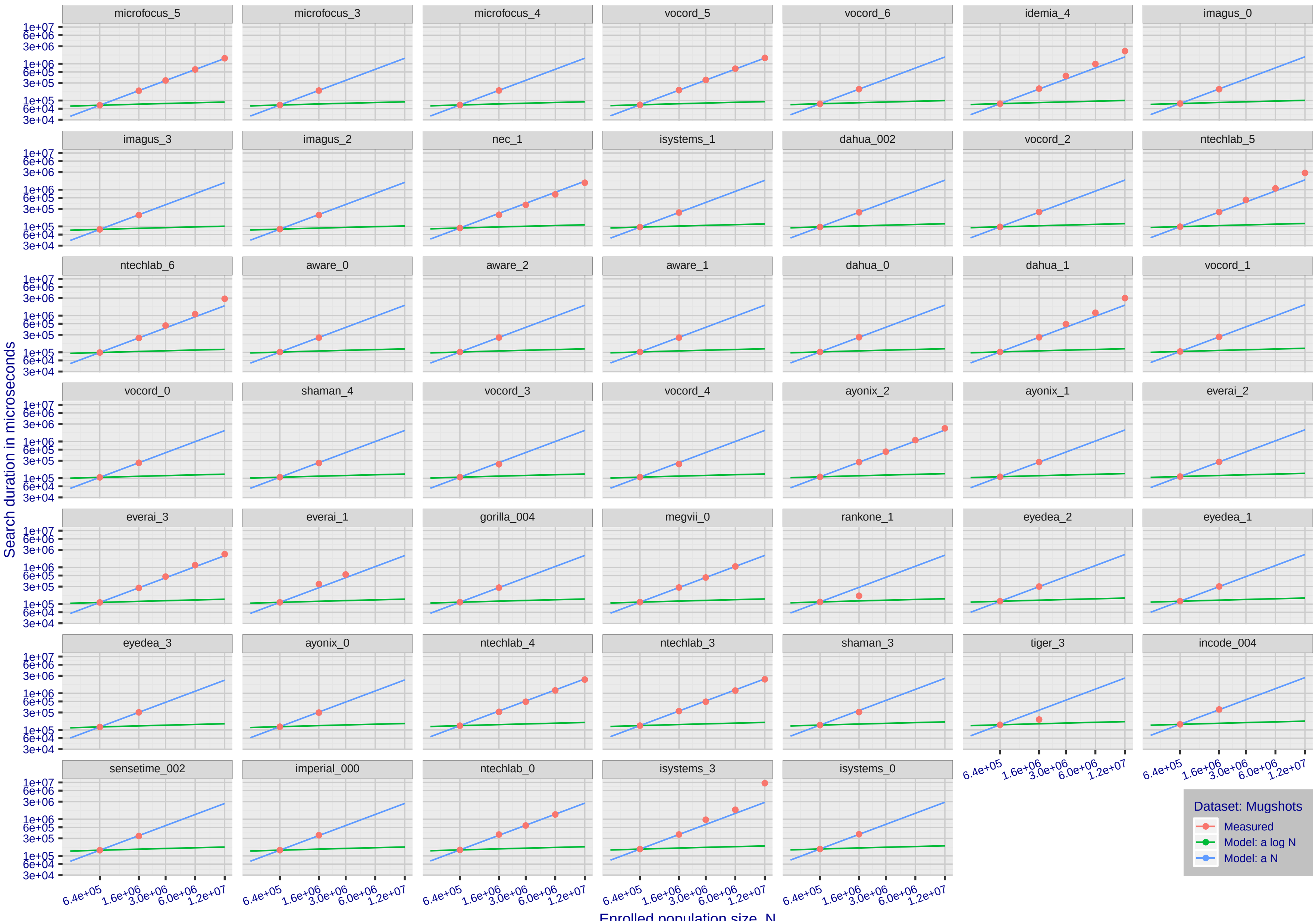

Figure 106: **[Mugshot Dataset] Search duration vs. enrolled population size**. *In red are the actual point durations measured on a single c. 2016 core. The blue shows linear growth from $N = 640\,000$. The green line shows logathmic growth from that point to $N = 1\,600\,000$. Note the sublinear growth from algorithms from Camvi, Dermalog, EverAI, Innovatrics, and Visionlabs. The tiger_1 algorithm is also sublinear, but inaccurate and inoperable at $N \geq 3000000$. This capability sometimes comes at the additional expense of converting a linear gallery data structure into whatever fast-search data structure is used. Note that search times are sometimes dominated by the template generation times shown in Table 16.*

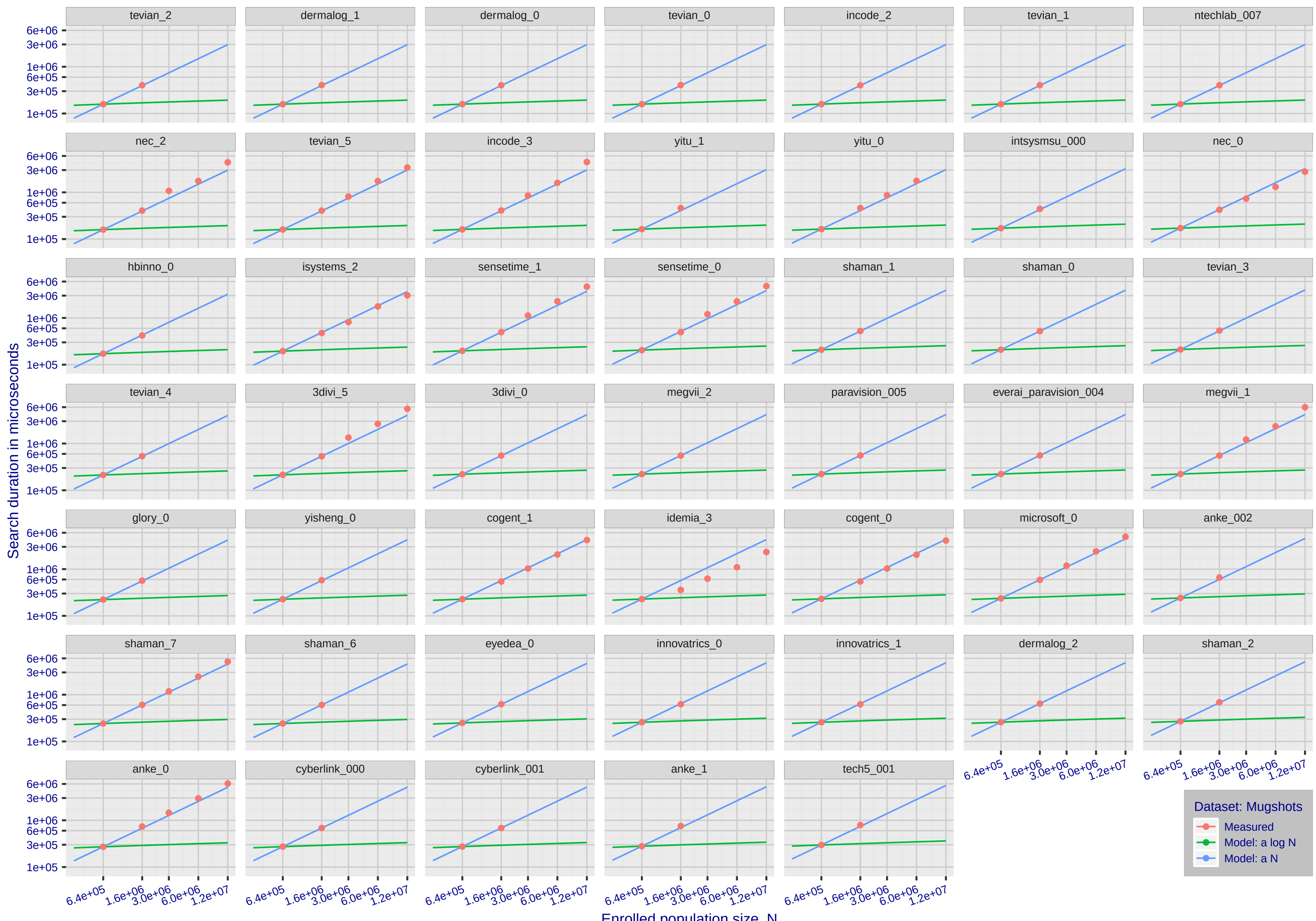

Figure 107: **[Mugshot Dataset] Search duration vs. enrolled population size**. *In red are the actual point durations measured on a single c. 2016 core. The blue shows linear growth from $N = 640\,000$. The green line shows logathmic growth from that point to $N = 1\,600\,000$. Note the sublinear growth from algorithms from Camvi, Dermalog, EverAI, Innovatrics, and Visionlabs. The tiger_1 algorithm is also sublinear, but inaccurate and inoperable at $N \geq 3000000$. This capability sometimes comes at the additional expense of converting a linear gallery data structure into whatever fast-search data structure is used. Note that search times are sometimes dominated by the template generation times shown in Table 16.*

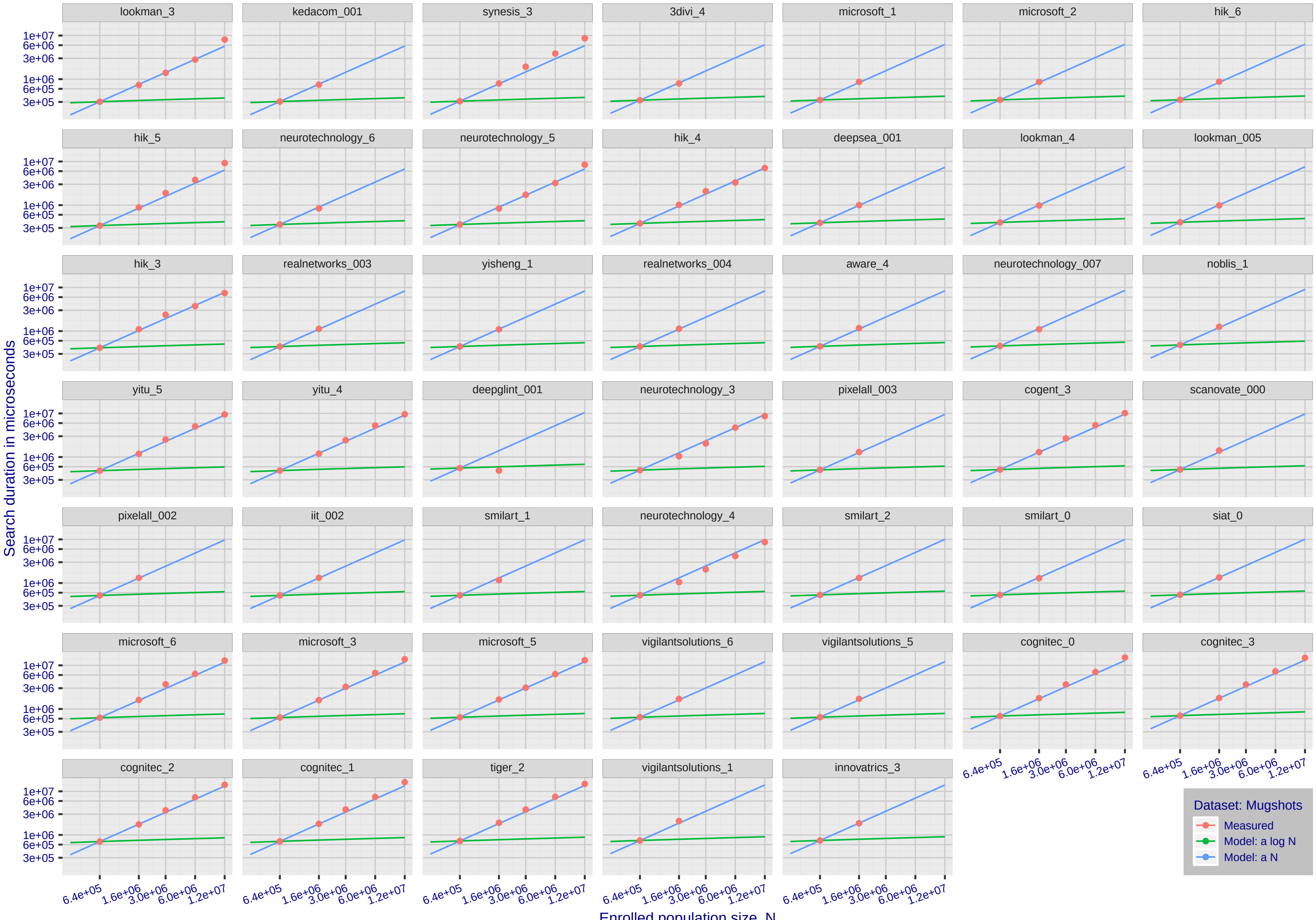

Figure 108: **[Mugshot Dataset] Search duration vs. enrolled population size**. *In red are the actual point durations measured on a single c. 2016 core. The blue shows linear growth from $N = 640\,000$. The green line shows logathmic growth from that point to $N = 1\,600\,000$. Note the sublinear growth from algorithms from Camvi, Dermalog, EverAI, Innovatrics, and Visionlabs. The tiger_1 algorithm is also sublinear, but inaccurate and inoperable at $N \geq 3000000$. This capability sometimes comes at the additional expense of converting a linear gallery data structure into whatever fast-search data structure is used. Note that search times are sometimes dominated by the template generation times shown in Table 16.*

This publication is available free of charge from: https://doi.org/10.6028/NIST.IR.8271

FNIR(N, R, T) = False neg. identification rate
FPIR(N, T) = False pos. identification rate
N = Num. enrolled subjects
R = Num. candidates examined
T = Threshold
T = 0 → Investigation
T > 0 → Identification

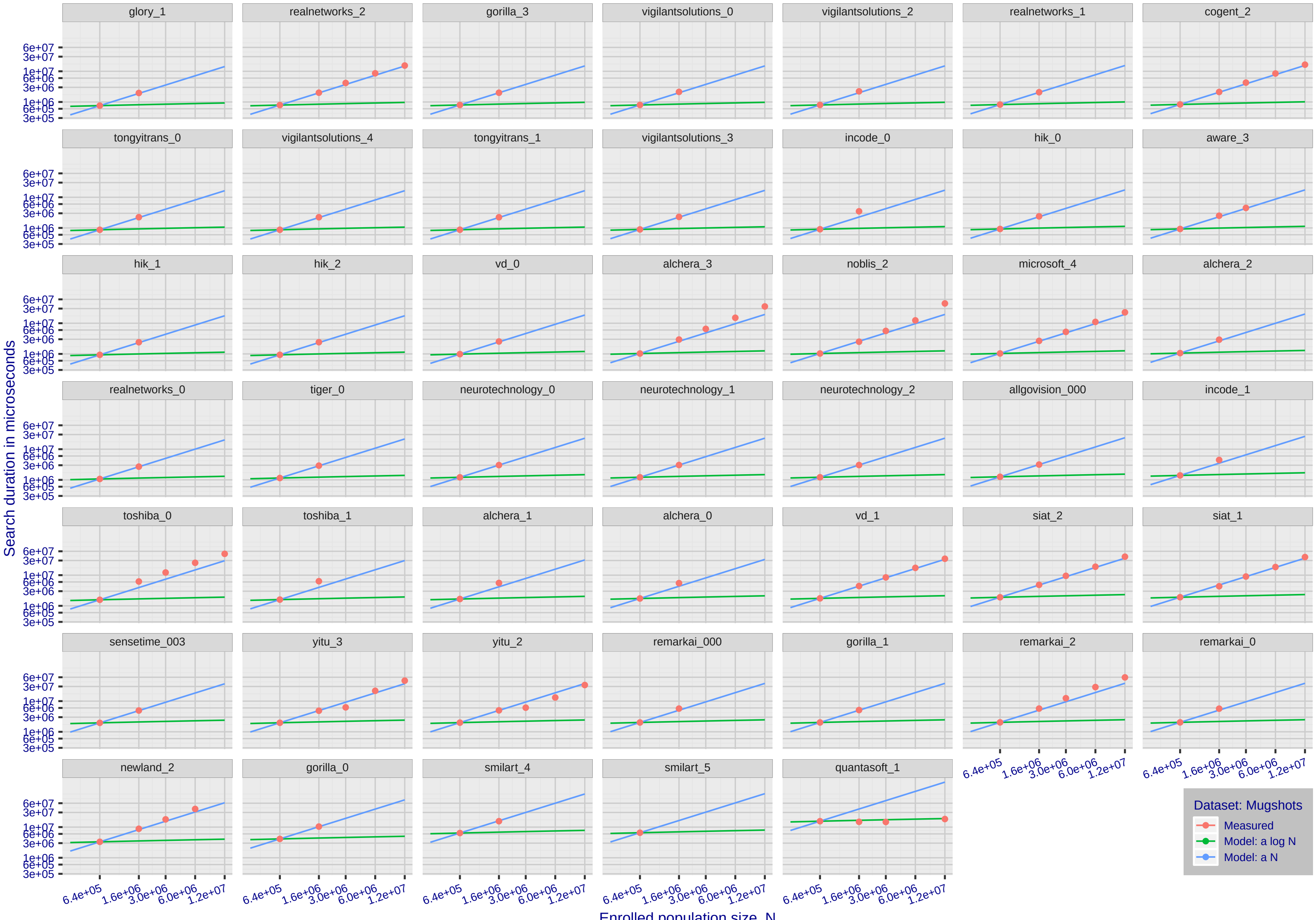

Figure 109: **[Mugshot Dataset] Search duration vs. enrolled population size**. *In red are the actual point durations measured on a single c. 2016 core. The blue shows linear growth from* $N = 640\,000$*. The green line shows logathmic growth from that point to* $N = 1\,600\,000$*. Note the sublinear growth from algorithms from Camvi, Dermalog, EverAI, Innovatrics, and Visionlabs. The tiger_1 algorithm is also sublinear, but inaccurate and inoperable at* $N \geq 3000000$*. This capability sometimes comes at the additional expense of converting a linear gallery data structure into whatever fast-search data structure is used. Note that search times are sometimes dominated by the template generation times shown in Table 16.*

Appendix G Gallery Insertion Timing

This publication is available free of charge from: https://doi.org/10.6028/NIST.IR.8271

FNIR(N, R, T) = False neg. identification rate
FPIR(N, T) = False pos. identification rate
N = Num. enrolled subjects
R = Num. candidates examined
T = Threshold
T = 0 → Investigation
T > 0 → Identification

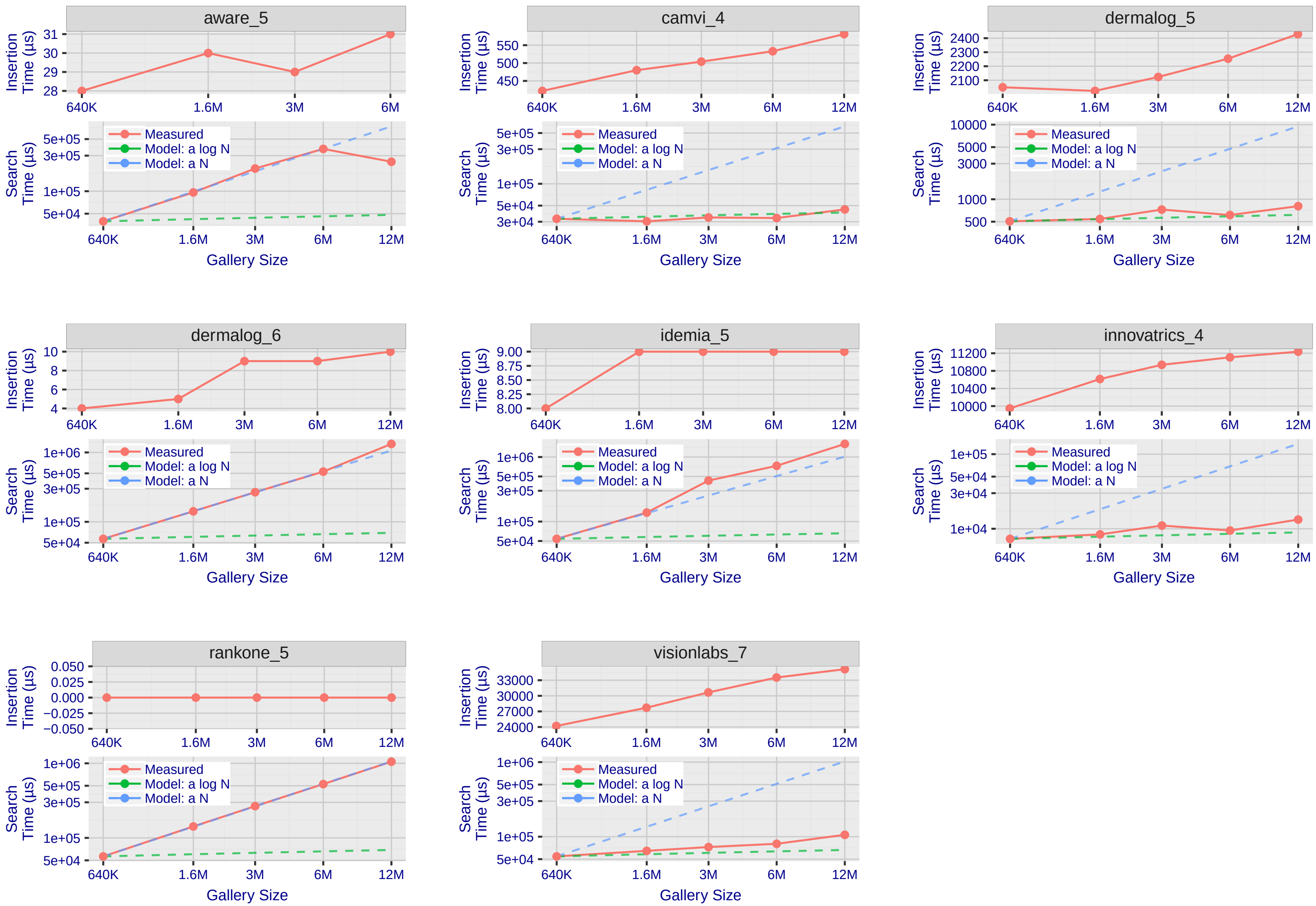

Figure 110: **[Mugshot Dataset] Gallery insertion duration vs. enrolled population size**. *This chart plots the time it takes to insert a single template into a finalized gallery, illustrated over increasing gallery sizes. For reference, search times on finalized galleries of corresponding sizes are plotted right underneath. Gallery insertion time plots were generated on algorithms that 1) successfully implemented gallery insertion with no errors and 2) that were run on galleries with N up to 12 000 000. Generally, only the more accurate algorithms were run on galleries with N up to 12 000 000.*

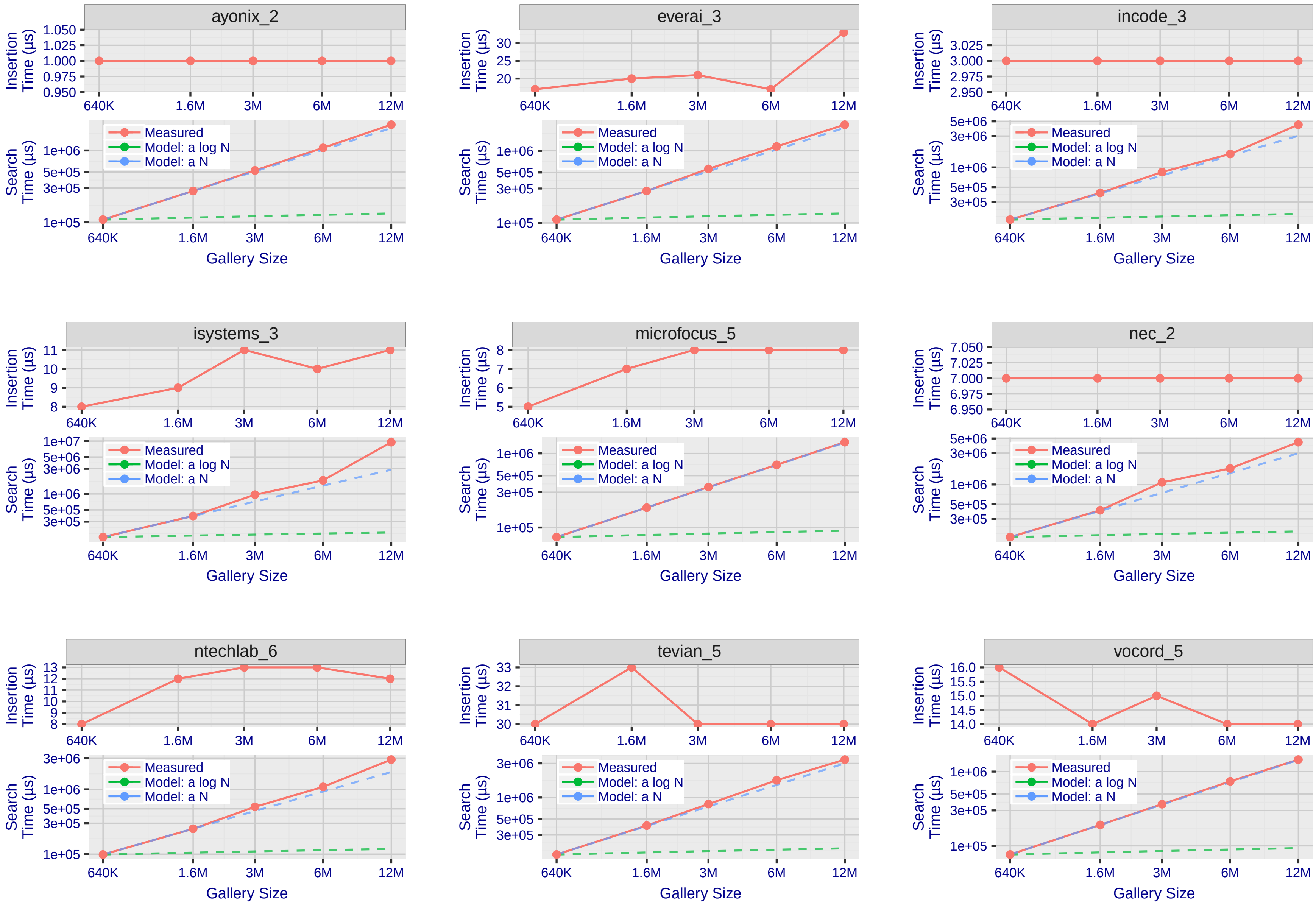

Figure 111: **[Mugshot Dataset] Gallery insertion duration vs. enrolled population size**. *This chart plots the time it takes to insert a single template into a finalized gallery, illustrated over increasing gallery sizes. For reference, search times on finalized galleries of corresponding sizes are plotted right underneath. Gallery insertion time plots were generated on algorithms that 1) successfully implemented gallery insertion with no errors and 2) that were run on galleries with N up to 12 000 000. Generally, only the more accurate algorithms were run on galleries with N up to 12 000 000.*

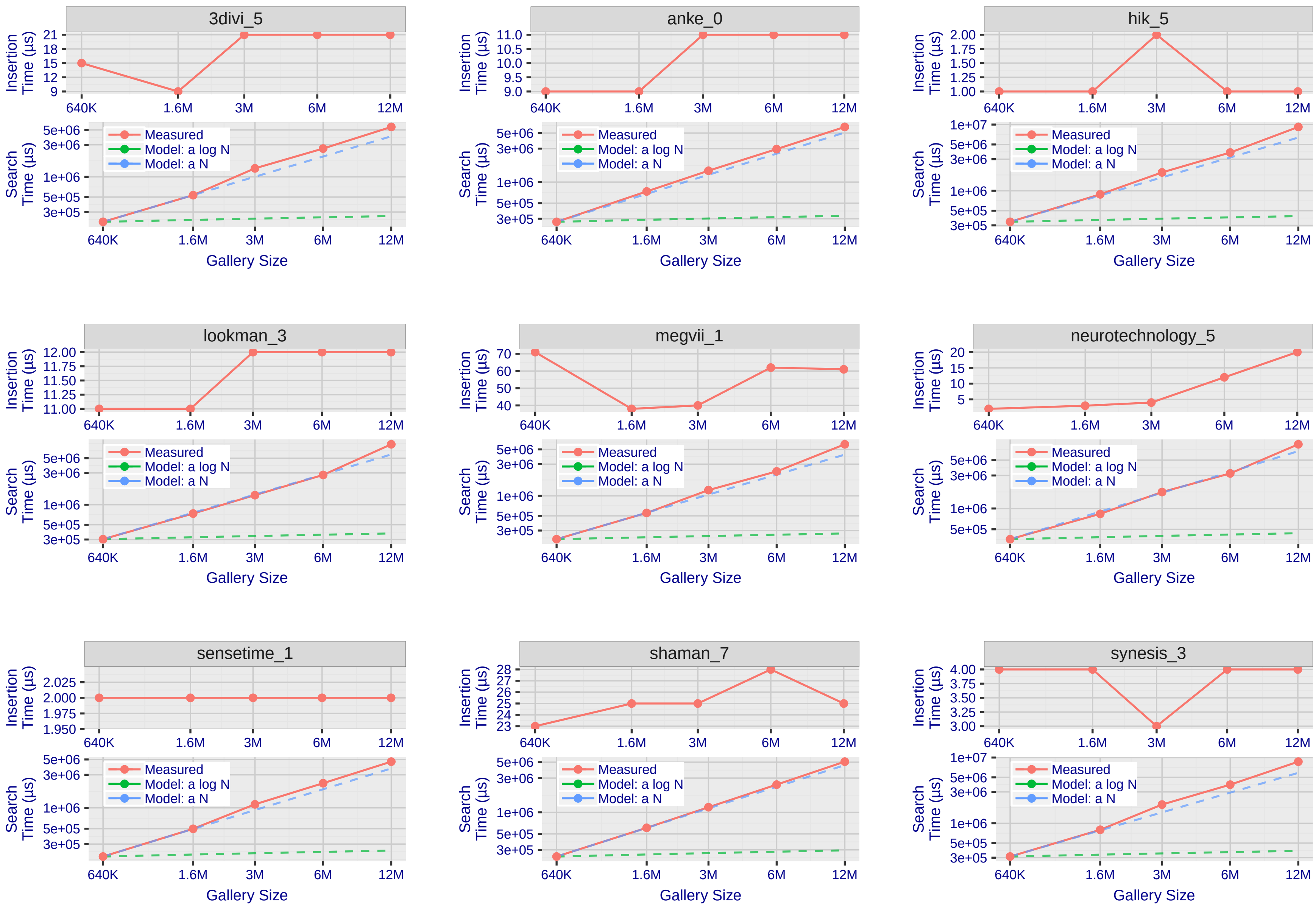

Figure 112: **[Mugshot Dataset] Gallery insertion duration vs. enrolled population size**. *This chart plots the time it takes to insert a single template into a finalized gallery, illustrated over increasing gallery sizes. For reference, search times on finalized galleries of corresponding sizes are plotted right underneath. Gallery insertion time plots were generated on algorithms that 1) successfully implemented gallery insertion with no errors and 2) that were run on galleries with N up to 12 000 000. Generally, only the more accurate algorithms were run on galleries with N up to 12 000 000.*

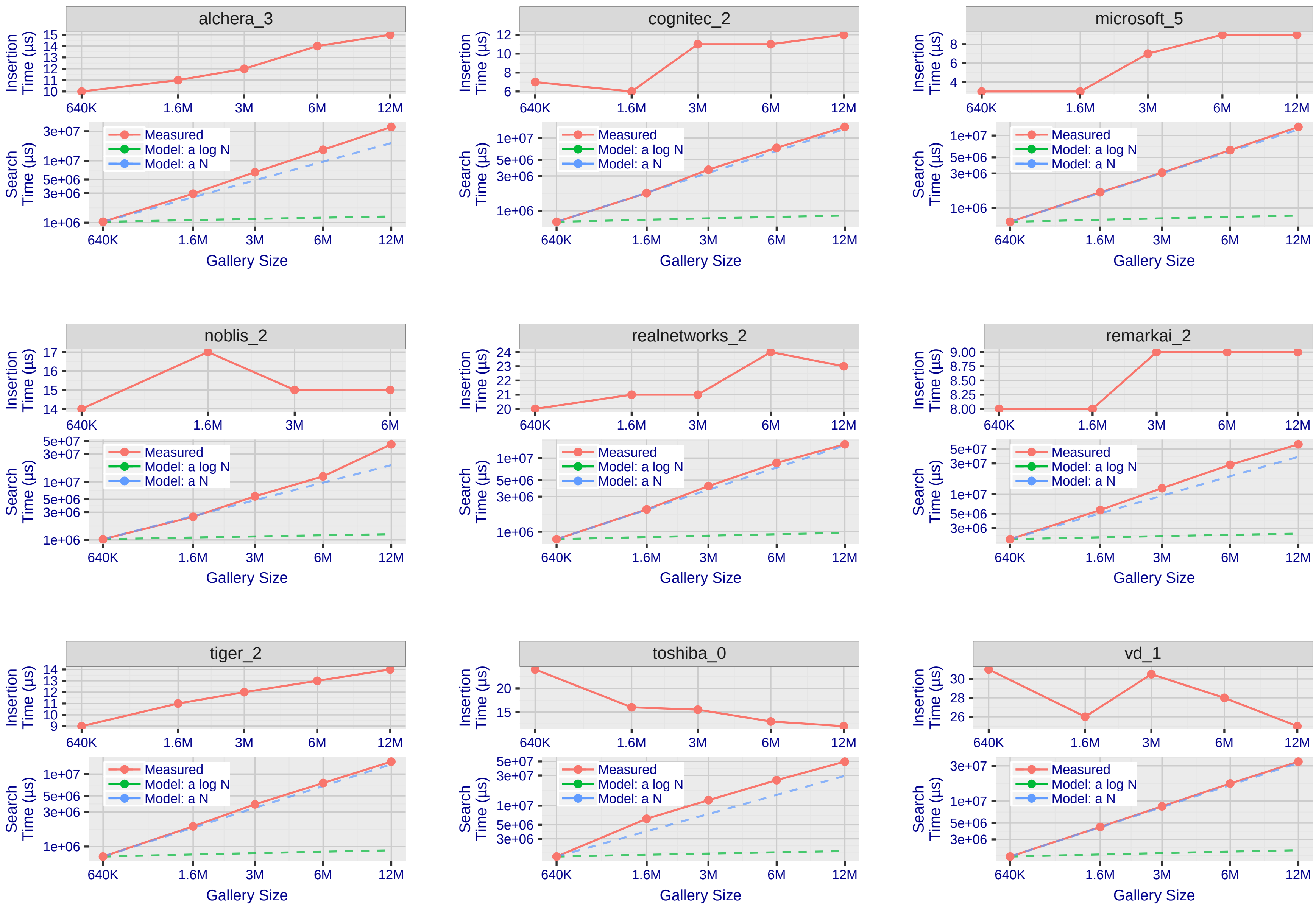

Figure 113: **[Mugshot Dataset] Gallery insertion duration vs. enrolled population size**. *This chart plots the time it takes to insert a single template into a finalized gallery, illustrated over increasing gallery sizes. For reference, search times on finalized galleries of corresponding sizes are plotted right underneath. Gallery insertion time plots were generated on algorithms that 1) successfully implemented gallery insertion with no errors and 2) that were run on galleries with N up to* 12 000 000. *Generally, only the more accurate algorithms were run on galleries with N up to* 12 000 000.

References

[1] Artem Babenko and Victor Lempitsky. Efficient indexing of billion-scale datasets of deep descriptors. In *The IEEE Conference on Computer Vision and Pattern Recognition (CVPR)*, June 2016.

[2] Blumstein, Cohen, Roth, and Visher, editors. *Random parameter stochastic models of criminal careers*. National Academy of Sciences Press, 1986.

[3] Thomas P. Bonczar and Lauren E. Glaze. Probation and parole in the united statesm 2007, statistical tables. Technical report, Bureau of Justice Statistics, December 2008.

[4] White D., Kemp R. I., Jenkins R., Matheson M, and Burton A. M. Passport officers errors in face matching. *PLoS ONE*, 9(8), 2014. e103510. doi:10.1371/journal. pone.0103510.

[5] P. Grother, G. W. Quinn, and P. J. Phillips. Evaluation of 2d still-image face recognition algorithms. NIST Interagency Report 7709, National Institute of Standards and Technology, 8 2010. http://face.nist.gov/mbe as MBE2010 FRVT2010.

[6] P. J. Grother, R. J. Micheals, and P. J. Phillips. Performance metrics for the frvt 2002 evaluation. In *Proceedings of Audio and Video Based Person Authentication Conference (AVBPA)*, June 2003.

[7] Patrick Grother and Mei Ngan. Interagency report 8009, performance of face identification algorithms. *Face Recognition Vendor Test (FRVT)*, May 2014.

[8] Patrick Grother, George Quinn, and Mei Ngan. Face in video evaluation (five) face recognition of non-cooperative subjects. Interagency Report 8173, National Institute of Standards and Technology, March 2017. https://doi.org/10.6028/NIST.IR.8173.

[9] Patrick Grother, George W. Quinn, and Mei Ngan. Face recognition vendor test - still face image and video concept, evaluation plan and api. Technical report, National Institute of Standards and Technology, 7 2013. http://biometrics.nist.gov/cs_links/face/frvt/frvt2012/NIST_FRVT2012_api_Aug15.pdf.

[10] K. He, X. Zhang, S. Ren, and J. Sun. Deep residual learning for image recognition. In *2016 IEEE Conference on Computer Vision and Pattern Recognition (CVPR)*, pages 770–778, June 2016.

[11] Gary B. Huang, Manu Ramesh, Tamara Berg, and Erik Learned-Miller. Labeled faces in the wild: A database for studying face recognition in unconstrained environments. Technical Report 07-49, University of Massachusetts, Amherst, October 2007.

[12] Masato Ishii, Hitoshi Imaoka, and Atsushi Sato. Fast k-nearest neighbor search for face identification using bounds of residual score. In *2017 12th IEEE International Conference on Automatic Face & Gesture Recognition (FG 2017)*, pages 194–199, Los Alamitos, CA, USA, May 2017. IEEE Computer Society.

[13] Jeff Johnson, Matthijs Douze, and Hervé Jégou. Billion-scale similarity search with gpus. *CoRR*, abs/1702.08734, 2017.

[14] Ira Kemelmacher-Shlizerman, Steven M. Seitz, Daniel Miller, and Evan Brossard. The megaface benchmark: 1 million faces for recognition at scale. *CoRR*, abs/1512.00596, 2015.

[15] Yury A. Malkov and D. A. Yashunin. Efficient and robust approximate nearest neighbor search using hierarchical navigable small world graphs. *CoRR*, abs/1603.09320, 2016.

[16] Joyce A. Martin, Brady E. Hamilton, Michelle J.K. Osterman, Anne K. Driscoll, , and Patrick Drake. National vital statistics reports. Technical Report 8, Centers for Disease Control and Prevention, National Center for Health Statistics, National Vital Statistics System, Division of Vital Statistics, November 2018.

[17] O. M. Parkhi, A. Vedaldi, and A. Zisserman. Deep face recognition. In *British Machine Vision Conference*, 2015.

[18] P. Jonathon Phillips, Amy N. Yates, Ying Hu, Carina A. Hahn, Eilidh Noyes, Kelsey Jackson, Jacqueline G. Cavazos, Géraldine Jeckeln, Rajeev Ranjan, Swami Sankaranarayanan, Jun-Cheng Chen, Carlos D. Castillo, Rama Chellappa, David White, and Alice J. O'Toole. Face recognition accuracy of forensic examiners, superrecognizers, and face recognition algorithms. *Proceedings of the National Academy of Sciences*, 115(24):6171–6176, 2018.

[19] Florian Schroff, Dmitry Kalenichenko, and James Philbin. Facenet: A unified embedding for face recognition and clustering. *CoRR*, abs/1503.03832, 2015.

[20] Jeroen Smits and Christiaan Monden. Twinning across the developing world. *PLOS ONE*, 6(9):1–5, 09 2011.

[21] Yaniv Taigman, Ming Yang, Marc'Aurelio Ranzato, and Lior Wolf. Deepface: Closing the gap to human-level performance in face verification. In *Proceedings of the 2014 IEEE Conference on Computer Vision and Pattern Recognition*, CVPR '14, pages 1701–1708, Washington, DC, USA, 2014. IEEE Computer Society.

[22] A. Towler, R. I. Kemp, and D White. *Unfamiliar face matching systems in applied settings*. Nova Science, 2017.

[23] Working Group 3. Ed. M. Werner. *ISO/IEC 19794-5 Information Technology - Biometric Data Interchange Formats - Part 5: Face image data*. JTC1 :: SC37, 2 edition, 2011. http://webstore.ansi.org.

[24] David White, James D. Dunn, Alexandra C. Schmid, and Richard I. Kemp. Error rates in users of automatic face recognition software. *PLoS ONE*, 10:1–14, October 2015.

[25] Bradford Wing and R. Michael McCabe. Special publication 500-271: American national standard for information systems data format for the interchange of fingerprint, facial, and other biometric information part 1. Technical report, NIST, September 2015. ANSI/NIST ITL 1-2015.

[26] Andreas Wolf. Portrait quality - (reference facial images for mrtd). Technical report, ICAO, April 2018.